1995 ANNUAL TROPICAL CYCLONE REPORT

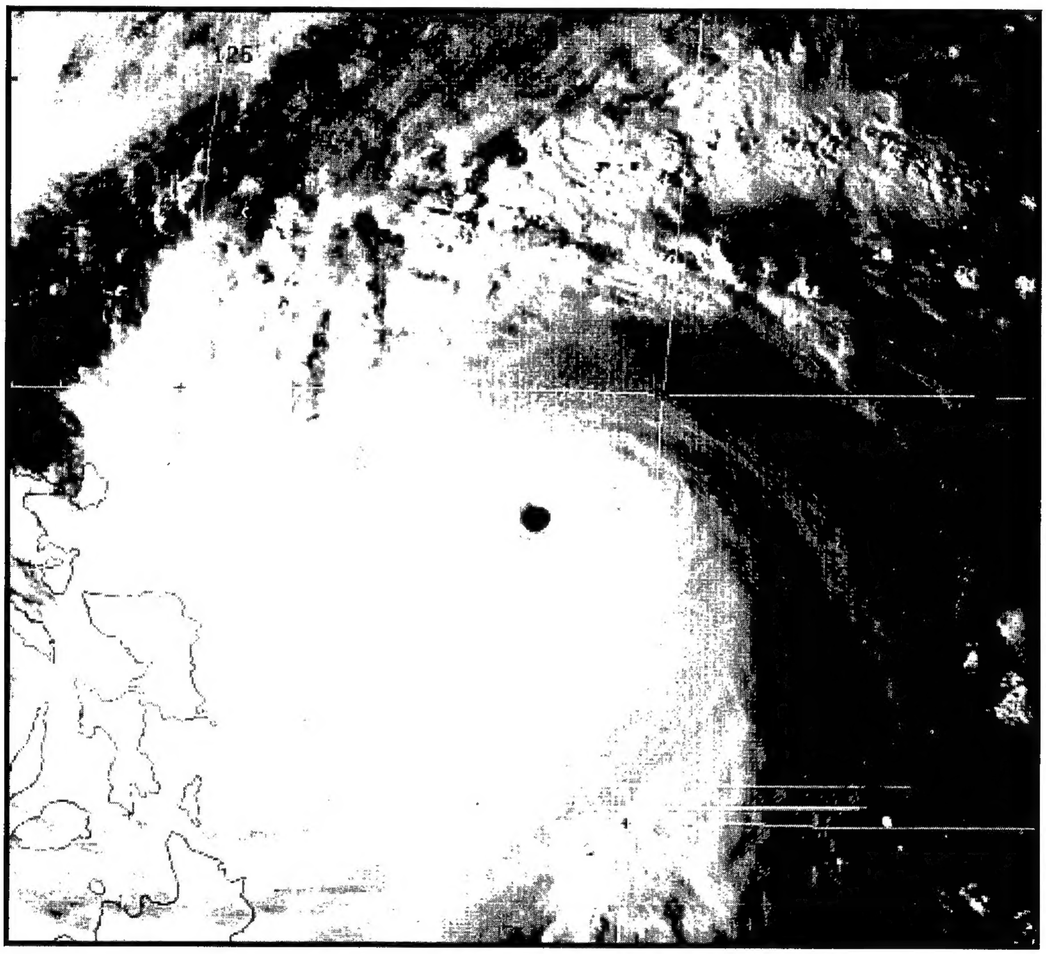

JOINT TYPHOON WARNING CENTER
GUAM, MARIANA ISLANDS

FRONT COVER: The most intense western North Pacific tropical cyclone of 1995, Super Typhoon Angela (29W), approaches the northern Philippine Islands. At the time of this image, Angela has a peak intensity of 155 knots (80 m/sec), an estimated minimum sea-level pressure of 879 millibars, and an 18 nautical mile diameter eye (010731Z November visible GMS imagery).

U. S. NAVAL PACIFIC METEOROLOGY AND OCEANOGRAPHY CENTER WEST
JOINT TYPHOON WARNING CENTER
PSC 489, BOX 12
FPO AP 96536-0051

JAMES F. ETRO

CAPTAIN, UNITED STATES NAVY
COMMANDING OFFICER

JOSEPH P. BASSI

LIEUTENANT COLONEL, UNITED STATES AIR FORCE
DIRECTOR, JOINT TYPHOON WARNING CENTER

Work on this report was supported in part by funds provided by the Office of Naval Research Grant N00014-91-J1721

STAFF

JOINT TYPHOON WARNING CENTER

	LCDR	MICHAEL D. ANGOVE	USN	TDO, DEPUTY DIRECTOR
*	LCDR	ERNEST P. PETZRICK	USN	TDO, DEPUTY DIRECTOR
	LCDR	ALEX J. DECARIA	USN	TDO
**	LCDR	STACY R. STEWART	USNR	TDO
	LT	STEVEN P. DUARTE	USN	TDO
	LT	MICHAEL S. KALAFSKY	USN	TDO
	CAPT	RICHARD A. ANSTETT	USAF	TDO
*	CAPT	DAN B. MUNDELL	USAF	TDO
	CAPT	WILLIAM J. CARLE	USAF	TDO
	CAPT	GARY B. KUBAT	USAF	TDO
*	AG1	SHISHMON D. BAILEY	USN	LPO, SAT FORECASTER
*	AG3	JASON E. ECCLES	USN	GRAPHICS, TDA
	AG3	ROBERT M. GIGUERE	USN	STATISTICS, TDA
	SRA	DAVID J. CORREA, JR.	USAF	TDA
*	SRA	JORDAN S. KELLY	USAF	TDA
*	SRA	VINCENT L. PETRASEK	USAF	TDA
	SRA	JEFFREY L. WILKERSON	USAF	TDA
	SRA	TIMOTHY C. WILLIAMS	USAF	TDA
	SRA	CLARK D. WILSON	USAF	TDA
*	A1C	SHAWN L. PETERSON	USAF	TDA

36 OSS/OSJ

	MAJ	ROGER T. EDSON	USAF	TECHNIQUE DEVELOPMENT
*	CAPT	ELIZABETH B. BORELLI	USAF	TDO, OIC USPACOM SAT NETWORK
	CAPT	JOHN A. RUPP	USAF	TDO, OIC USPACOM SAT NETWORK
	MSGT	TIMOTHY R. CRUME	USAF	SAT FORECASTER, NCOIC
*	TSGT	VINCENT T. AGUON	USAF	CHIEF INFORMATION MANAGEMENT
	TSGT	SHIRLEY A. BROWN	USAF	CHIEF INFORMATION MANAGEMENT
*	TSGT	SCOTT C. COPELAND	USAF	SAT FORECASTER
	TSGT	ZEFANIAS E. EBARLE	USAF	SAT FORECASTER
*	TSGT	HAROLD D. EIFERT	USAF	SAT FORECASTER
*	TSGT	MICHAEL S. GREHAN	USAF	SAT FORECASTER
	TSGT	DENNIS W. MILLER	USAF	SAT FORECASTER
	SSGT	MERRYRUTH I. DEOCARIZA	USAF	SAT FORECASTER
*	SSGT	RICHARD D. JACOBSEN	USAF	SAT FORECASTER
	SSGT	LINDA R. HAM	USAF	SAT FORECASTER
*	SSGT	JEWEL K. TAPPY	USAF	SAT FORECASTER
	SSGT	BRUCE W. WOFFORD	USAF	SAT FORECASTER
	SRA	SEAN M. MCDUNN	USAF	DATA DEVELOPMENT

ATCR STAFF

LT	ERIC J. TREHUBENKO	USN	TDO, EDITOR, BEST TRACK OFFICER
CAPT	PAUL H. LEWIS	USAF	TDO, STATISTICS OFFICER
MR	FRANK H. WELLS	USN	TECHNICAL EDITOR
AG2	DARIN L. WARD	USN	LPO, TDA, GRAPHICS
AG3	CHRISTOPHER CROSS	USN	GRAPHICS, TDA
AG3	ANDRES G. GRANT	USN	GRAPHICS, TDA

UNIVERSITY OF GUAM / JTWC RESEARCH LIAISON

DR	MARK A. LANDER	TROPICAL CYCLONE RESEARCH, TECHNICAL WRITING
MR	CHARLES P. GUARD	TROPICAL CYCLONE RESEARCH, TECHNICAL WRITING

* TRANSFERRED DURING 1995

** ACTIVE DUTY TRAINING

FOREWORD

The Annual Tropical Cyclone Report is prepared by the staff of the Joint Typhoon Warning Center (JTWC), a combined Air Force/Navy organization operating under the command of the Commanding Officer, U.S. Naval Pacific Meteorology and Oceanography Center West (NAVPACMETOCCEN WEST)/Joint Typhoon Warning Center, Guam. The JTWC was founded 1 May 1959 when the U.S. Commander-in-Chief Pacific (USCINCPAC) forces directed that a single tropical cyclone warning center be established for the western North Pacific region. The operations of JTWC are guided by USCINCPAC Instruction 3140.1W.

The mission of JTWC is multifaceted and includes:

1. Continuous monitoring of all tropical weather activity in the Northern and Southern Hemispheres, from 180° east longitude westward to the east coast of Africa, and the prompt issuance of appropriate advisories and alerts when tropical cyclone development is anticipated.

2. Issuance of warnings on all significant tropical cyclones in the above area of responsibility.

3. Determination of requirements for tropical cyclone reconnaissance and assignment of appropriate priorities.

4. Post-storm analysis of significant tropical cyclones occurring within the western North Pacific and North Indian Oceans.

5. Cooperation with the Naval Research Laboratory, Monterey, California on evaluation of tropical cyclone models and forecast aids, and the development of new techniques to support forecast requirements.

Special thanks to: the men and women of the Alternate Joint Typhoon Warning Center for standing in for JTWC as needed; Fleet Numerical Meteorology and Oceanography Center (FLENUMETOCCEN) for their operational support; the Naval Research Laboratory for its dedicated research; the Air Force Global Weather Central (AFGWC) and National Oceanic and Atmospheric Administration (NOAA) National Environmental Satellite, Data, and Information Service (NESDIS) for satellite support; the 36th Communications Squadron's Defense Meteorological Satellite Program (DMSP) Site 18 at Nimitz Hill, Guam; and the Operations and Equipment Support departments of NAVPACMETOCCEN WEST, Guam for their high quality support; all the men and women of the ships and facilities ashore throughout the JTWC area of responsibility (AOR), and especially on Guam, who took the observations that became the basis for our analyses, forecasts and postanalyses; CDR. Lester E. Carr III and Dr. Russell L. Elsberry for their efforts at the Naval Postgraduate School and publication of the Systematic and Integrated Approach to Tropical Cyclone Track Forecasting Part II ; the personnel at the Navy Publications and Printing Service Branch Office, Pearl Harbor; Dr. Robert F. Abbey Jr. and the Office of Naval Research for their support to the University of Guam (UOG) for the JTWC Research Liaisons to JTWC; the UOG Research Liaisons for their contributions to this publication; Dr. Mark Lander for his training efforts, suggestions and valuable insights, and Mr. Charles P. Guard for his support and data collection efforts; Dr. Jeff Hawkins, Chris Veldon, Samuel Chang and Roger Weldon for their tireless efforts to get the most possible out of remote sensing technologies; Capt Carl Davis for his assistance in obtaining the satellite imagery for the northern Indian Ocean tropical cyclones; Mr. John "Jack" Beven for his efforts to include ground truth in his Weekly Tropical Cyclone Summaries; and, AG2 Darin Ward, AG3 Andres Grant, and AG3 Chris Cross for their excellent desktop publishing and graphics assistance.

EXECUTIVE SUMMARY

Although 1995 was an average year with respect to the number of significant tropical cyclones (TCs) in the western North Pacific, it challenged the Joint Typhoon Warning Center (JTWC) with a variety of types. Highlights include the very small, or "midget", Typhoon Mark, forming at an uncharacteristically high latitude; Tropical Storm Colleen, which transitioned from a subtropical "Kona" storm to a tropical storm; and Super Typhoon Angela, which hammered the island of Luzon in the Philippines with their strongest winds in three decades.

Less than half of the western North Pacific significant TCs reached typhoon intensity or greater during 1995. A total of 599 warnings were issued on these — the lowest number of warnings in seven years. The larger number of poorly defined, or "low end" systems contributed to some large initial position errors and larger than normal mean 24-hour forecast errors when compared with the 10-year average. In contrast, the forecast errors at 48 and 72 hours were normal with respect to the 10-year averages.

JTWC continued to outperform the majority of the objective forecast guidance available to support its warnings in 1995. This appears to be due, in part, to the aggressive application of CDR Lester E. Carr III and Dr. Russell L. Elsberry's Techniques detailed in <u>Systematic and Integrated Approach to Tropical Cyclone Track Forecasting</u> (NPS-MR-94-002 December 1994).

Fifty-four warnings were issued on the four significant tropical cyclones which occurred in the North Indian Ocean during 1995, and only 245 warnings were issued on the 22 significant tropical cyclones in the Southern Hemisphere. JTWC forecast errors in the Northern Indian Ocean were comparable to the 19-year average and the lowest ever for the 15 years in the Southern Hemisphere.

Several exciting tools were made available to the JTWC during 1995, contributing to improved gradient- and upper-level analyses. These tools ranged from improved data availability and display, to improved satellite reconnaissance capabilities within JTWC's Area of Responsibility. Summarized below, they are discussed in greater detail within the report.

Improvements to scatterometer data display and availability by both Naval Oceanographic Office and NOAA have aided in positioning of TCs, as well as defining wind-field structure.

The addition of water vapor imagery and water vapor-derived wind vectors have made significant impact on the TDO's upper-level wind analysis — helping to define upper-level structure and aiding in intensity forecasts.

The addition of Naval Pacific Meteorology and Oceanography Detachment Diego Garcia, to the DMSP Tropical Cyclone Reporting Network has resulted in a significant increase in the number of fixes taken for TCs in the Indian Ocean — increasing TDO confidence in TC location and movement in this data-sparse region.

The JTWC is now receiving METEOSAT 5 imagery from Naval European Meteorology and Oceanography Center (NEMOC), Rota, Spain. These images are remapped from a normal polar to a mercator projection at NEMOC and then automatically forwarded via File Transfer Protocol (FTP) to the JTWC, where they are animated. This new capability, coupled with the additional fix support from Diego Garcia, allows the JTWC to truly MET Watch the Western Indian Ocean for the first time in history.

We at JTWC are looking forward to making use of these tools in 1996 and the development of even more exciting techniques.

TABLE OF CONTENTS

1. OPERATIONAL PROCEDURES

1.1 GENERAL

The Joint Typhoon Warning Center (JTWC) provides a variety of routine products and services to the organizations within its area of responsibility (AOR), including:

1.1.1 SIGNIFICANT TROPICAL WEATHER ADVISORY — Issued daily or more frequently as needed, to describe all tropical disturbances and their potential for further development during the advisory period. Separate bulletins are issued for the western Pacific and the Indian oceans.

1.1.2 TROPICAL CYCLONE FORMATION ALERT — Issued in a specified area when synoptic, satellite, or other germane data indicate that the development of a significant tropical cyclone is likely within 24 hours.

1.1.3 TROPICAL CYCLONE/ TROPICAL DEPRESSION WARNING — Issued periodically throughout each day to provide forecasts of position, intensity, and wind distribution for tropical cyclones in JTWC's AOR.

1.1.4 PROGNOSTIC REASONING MESSAGE — Issued with warnings for tropical storms, typhoons, and super typhoons in the western North Pacific to discuss the rationale for the content of the specific JTWC warning.

1.1.5 PRODUCT CHANGES — The contents and availability of the above JTWC products are set forth in USCINCPACINST 3140.1W. Changes to USCINCPACINST 3140.1W and JTWC products and services are proposed and discussed at the annual U.S. Pacific Command (PACOM) Tropical Cyclone Conference.

1.2 DATA SOURCES

1.2.1 COMPUTER PRODUCTS — Numerical and statistical guidance are available from the USN Fleet Numerical Meteorology and Oceanography Center (FLENUMETOCCEN) at Monterey, California. FLENUMETOCCEN supplies JTWC with analyses and prognoses, from 0000Z and 1200Z synoptic data, at the surface, 850-mb, 700-mb, 500-mb, 400-mb, and 200-mb levels. The charts provided include: deep-layer-mean winds, wind shear, geopotential height-change, surface pressure, streamlines, and sea surface temperature, as well as many other routine products. These products, along with selected ones from the National Centers for Environmental Prediction (NCEP) Suitland, the European Centre for Medium-Range Weather Forecasts (ECMWF), and the Japanese Meteorological Agency (JMA) are received as electronic files via networked computers, and by computer modem connections on government and commercial telephone lines as a backup method for the network. Additionally, selected computer generated products are received via the PC-Based Weather Facsimile (PCGRAFAX) System.

1.2.2 CONVENTIONAL DATA — These data sets are comprised of land and shipboard surface observations, enroute meteorological observations from commercial and military aircraft (AIREPS) recorded within six hours of synoptic times, and cloud-motion winds derived from satellite data. The conventional data are hand- and computer-plotted, and hand-analyzed in the tropics for the surface/gradient and 200-mb levels. These analyses are prepared twice daily from 0000Z and 1200Z synoptic data.

1.2.3 SATELLITE RECONNAISSANCE — Meteorological satellite imagery recorded at USAF/USN ground sites and USN ships supply day and night coverage in JTWC's AOR. Interpretation of this satellite data provides tropical cyclone positions and estimates of current and forecast intensities (Dvorak, 1984). The USAF tactical satellite sites and Air Force Global Weather Central (AFGWC) currently receive and analyze special sensor microwave/imager (SSM/I) data to provide locations of tropical cyclones of which the center is obscured by cirrus clouds, and estimates of 35-kt (18 m/sec) wind radii near tropical cyclones.

In addition, scatterometry data are retrieved over the computer network from the Naval Oceanographic Office (NAVOCEANO) (high resolution, small area depictions), and the Oceanic Sciences Branch (OSB), National Oceanic and Atmospheric Administration (NOAA) (lower resolution, large area depictions). This scatterometry data provides tropical cyclone positions and a graphical representation of the wind profile surrounding a tropical cyclone. It is also used in the twice daily surface/gradient hand-analysis performed at JTWC. Use of satellite reconnaissance is discussed further in section 2.3 Satellite Reconnaissance Summary.

1.2.4 RADAR RECONNAISSANCE — Land-based radar observations are used to position tropical cyclones. Once a well-defined tropical cyclone moves within range of land-based radar sites, radar reports are invaluable for determination of position, movement, and, in the case of Doppler radar, storm structure and wind information. JTWC's use of radar reports during 1994 is discussed in section 2.4 Radar Reconnaissance Summary.

1.2.5 AIRCRAFT RECONNAISSANCE — Until the summer of 1987, dedicated aircraft reconnaissance was used routinely to locate and determine the wind structure of tropical cyclones. Now, aircraft fixes are only rarely available from transiting jet aircraft or from weather reconnaissance aircraft involved in research missions.

1.2.6 DRIFTING METEOROLOGICAL BUOYS — In 1989, the Commander, Naval Meteorology and Oceanography Command (COMNAVMETOCCOM) put its Integrated Drifting Buoy Plan (1989-1994) into action to meet USCINCPACFLT requirements that included tropical cyclone warning support. In 1995, 30 drifting buoys were deployed in the western North Pacific by a Naval Oceanographic Office-contracted C-130 aircraft. Of the 30 buoys, 24 were Compact Meteorological and Oceanographic Drifters (CMOD) with temperature and pressure sensors and six were Wind Speed and Direction (WSD) drifters with wind speed and direction, temperature and pressure. The drifters were evenly split by type over two deployments - the first in June followed by the second in September. The purpose of the split deployment was to overlap the expected three month lifespans of the CMOD buoys in order to provide continuous coverage during the peak of the western North Pacific tropical cyclone season.

1.2.7 AUTOMATED METEOROLOGICAL OBSERVING STATIONS (AMOS) — Through a cooperative effort between the COMNAVMETOCCOM, the Department of the Interior, and NOAA/NWS to increase data available for tropical analysis and forecasting, a network of 20 AMOS stations is being installed in the Micronesian Islands (see Tables 1-1 and 1-2). Previous to this effort, two sites were installed in the Northern Mariana Islands at Saipan and Rota through a joint venture between the Navy and NOAA/NWS. The site at Saipan relocated to Tinian in 1992. Since September of 1991, the capability to transmit data via Service ARGOS and NOAA polar orbiting satellites has

Table 1-1 AUTOMATED METEOROLOGICAL OBSERVING STATIONS SUMMARY

Site	Location	Call sign	ID#	System	Installed
Saipan*	15.2°N, 145.7°E	15D151D2	-----	ARC	1986
Rota	14.2°N, 145.2°E	15D16448	91221	ARC	1987
Faraulep**	8.1°N, 144.6°E	FARP2	52005	C-MAN/ARGOS	1988
Enewetak	11.4°N, 162.3°E	ENIP2	91251	C-MAN/ARGOS	1989
Ujae***	8.9°N, 165.7°E	UJAP2	91365	C-MAN	1989
Pagan	18.1°N, 145.8°E	PAGP2	91222	C-MAN/ARGOS	1990
Kosrae	5.4°N, 163.0°E	KOSP2	91355	C-MAN/ARGOS	1990
Mili	6.1°N, 172.1°E	MILP2	91377	C-MAN	1990
Oroluk	7.6°N, 155.2°E	ORKP2	91343	C-MAN	1991
Pingelap	6.2°N, 160.7°E	PIGP2	91352	C-MAN/ARGOS	1991
Ulul	8.4°N, 149.4°E	NA	91328	C-MAN/ARGOS	1992
Tinian*	15.0°N, 145.6°E	15D151D2	91231	ARC	1992
Satawan	6.1°N, 153.8°E	SATP2	91338	C-MAN/ARGOS	1993
Ulithi	9.9°N, 139.7°E	NA	91204	C-MAN/ARGOS	1995
Ngulu	8.3°N, 137.5°E	NA	91411	C-MAN/ARGOS	1995

* Saipan site relocated to Tinian and commissioned on 1 June 1992.

** The prototype site on Faraulep was destroyed on 28 November 1991 by Super Typhoon Owen.

*** Ujae site was destroyed on 18 November 1992 by Super Typhoon Gay.

ARC = Automated Remote Collection system (via GOES West)

C-MAN = Coastal-Marine Automated Network (via GOES West or GMS)

ARGOS = Service ARGOS data collection (via NOAA's TIROS-N)

Table 1-2 PROPOSED AUTOMATED METEOROLOGICAL OBSERVING STATIONS

Site	Location	Installation	Delayed
Pulusuk	6.5°N, 149.5°E	1993	Yes*
Faraulep	8.6°N, 144.6°E	1994	Yes**
Eauripik	6.7°N, 143.0°E	1994	Yes**
Maloelap	8.7°N, 171.2°E	1994	Yes
Utirik	11.2°N, 169.7°E	1994	Yes
Satawal	7.4°N, 147.0°E	1995	Yes
Ujelang	9.8°N, 161.0°E	1995	Yes
Ebon	4.6°N, 168.7°E	1995	Yes
Maug	20.0°N, 145.2°E	1996	No

* Runway construction

** Testing of GMS transmission packages

been available as a backup to regular data transmission to the Geostationary Operational Environmental Satellite (GOES) West, and more recently for sites to the west of Guam, to the Japanese Geostationary Meteorological Satellite (GMS). Upgrades to existing sites are also being accomplished as the opportunity arises to enable access to the ARGOS. JTWC receives data from all AMOS sites via the AWN under the KWBC bulletin headers SMPW01, SIPW01 and SNPW01 (SXMY10 for Tinian and Rota).

1.3 TELECOMMUNICATIONS

Telecommunications support for the NPMOCW/JTWC is provided by the Naval Telecommunications Area Master Station, Western Pacific (NTWP) and their Base Communications Department. The NPMOCW/JTWC telecommunications link to NTWP is a new fiber optic cable which incorporates stand-by redundancy features. Connectivity includes "switched" secure and non-secure voice, facsimile, data services, and dedicated audio and digital circuits to NTWP. Telecommunications connectivity and the basic system configurations which are available to JTWC follow.

1.3.1 AUTOMATED DIGITAL NETWORK (AUTODIN) — AUTODIN currently supports the message requirements for JTWC, with the process of converting to the new Defense Messaging System (DMS) in progress. A personal computer (PC) system running the "Gateguard" software application provides transmit and receive message capabilities. Secure connectivity is provided by a dial-up Secure Telephone Unit-III path with NTWP.

The Gateguard system is used to access the AUTODIN/DMS network for dissemination of warnings, alerts, related bulletins, and messages to Department of Defense (DoD) and U.S. Government installations. Message recipients can retransmit these messages for further dissemination using the Navy Fleet Broadcasts, Coast Guard continuous wave (CW) Morse code, and text to voice broadcasts.

AUTODIN/DMS messages are also relayed via commercial telecommunications routes for delivery to non-DoD users. Inbound message traffic for JTWC is received via AUTODIN/DMS addressed to NAVPACMETOCCEN WEST GU//JTWC//.

1.3.2 AUTOMATED WEATHER NETWORK (AWN) — The AWN provides weather data over the Pacific Meteorological Data System (PACMEDS). JTWC uses two PC systems which run the Windows based WINDS/AWNCOM software application package to interface with a dedicated 1.2 kb/sec (kilo-bits per second) PACMEDS circuit. These PC systems provide JTWC the PACMEDS transmit and receive capabilities needed to effectively store and manipulate large volumes of alphanumeric meteorological data available from reporting stations throughout JTWC's AOR. The AWN also allows JTWC access to data which are available on the Global Telecommunications System (GTS). JTWC's AWN station identifier is PGTW.

1.3.3 AUTOMATED WEATHER DISTRIBUTION SYSTEM (AWDS) — The AWDS consists of two dual monitor workstations which communicate with a UNIX based communications/data server via a private Local Area Network (LAN). The server's data connectivity is provided by two dedicated long-haul data circuits. The AWDS provides JTWC with additional transmit and receive access to alphanumeric AWN data at Tinker AFB using a dedicated 9.6 kb/sec circuit. Access to satellite imagery and computer graphics from Air Force Global Weather Center (AFGWC) is provided by another dedicated 9.6 kb/sec circuit.

AWDS current configuration should be upgraded in the summer of 1996 to include improved workstation performance, and integration into NPMOCW's LAN backbone which has access to the Defense Information Systems Network's (DISN), Non-secure Internet Protocol (IP) Router Network's (NIPRNET) Wide Area Network (WAN). The LAN and WAN connectivity will allow JTWC to send and receive products among other AWDS systems. AWDS IP address information should be available third quarter 1996. Send email requests to jtops@npmocw.navy.mil for more information.

1.3.4 DEFENSE SWITCHED NETWORK (DSN) — DSN is a worldwide, general purpose, switched telecommunications network for the DoD. The network provides a rapid and vital voice and data link for JTWC to communicate tropical cyclone information with DoD installations and civilian agencies.

JTWC utilizes DSN to access DSN based users, FTS2000, SprintNET networks for commercial or non-DoD based users, and local commercial long distance carriers for voice and data requirements. These requirements include the pulling of Naval Oceanography Data Distribution System (NODDS) data, accessing Air Force Dial-In System (AFDIS), transmitting and receiving facsimile products, and as an alternate route for sending and receiving data to support the Automated Tropical Cyclone Forecast (ATCF) system requirements.

The DSN and commercial telephone numbers for JTWC are (671) 349-5240 or 349-4224. Note: the DSN area code for Pacific is 315.

1.3.5 TACTICAL ENVIRONMENTAL SUPPORT SYSTEM (3) (TESS(3)) — The TESS(3) is connected by NIPRNET WAN to FNMOC. NIPRNET connectivity is provided by a dedicated virtual switched data services 56 kb/sec packet switched data link. FNMOC's supercomputer generated gridded fields are pushed to the TESS(3) using NIPRNET, allowing for local value added tailoring of analyses and prognoses. The TESS(3) provides connectivity through NIPRNET to all COMNAVMETOCCOM (CNMOC) Centers world-wide.

1.3.6 NIPRNET—DISN's NIPRNET has replaced the DDN MILNET computer communications network, providing a much needed boost in throughput speed needed in the transfer of large data and image files. NIPRNET has links or gateways to the non-DoD Internet, allowing data to be pulled and pushed from Internet based World Wide Web (WWW) and File Transfer Protocol (FTP) servers. This capability has enhanced JTWC's ability to exchange data with the Internet based research community.

JTWC's products are currently available to users of the DISN based Secret IP Router Network (SIPRNET) using WWW browser software. JTWC's SIPRNET homepage address can be obtained by contacting JTWC's Operations Officer. Plans are to have an operational NIPRNET/Internet based WWW server in place by third quarter 1996.

JTWC's Internet email server's IP address is 192.231.128.1 and the email address is jtops@npmocw.navy.mil.

1.3.7 TELEPHONE FACSIMILE — TELEFAX provides the capability to rapidly scan and transmit, or receive, documents over commercial telephone lines or DSN. TELEFAX is used to disseminate tropical cyclone advisories and warnings to key agencies on Guam and, in special situations, to DoD, other U.S. Government agencies, and the other Micronesian Islands. Inbound documents for JTWC are received at (671) 349-6143, (671) 349-6101, or (671) 349-4032.

1.3.8 LOCAL USER TERMINAL (LUT) — JTWC uses a LUT, provided by the Naval Oceanographic Office, as the primary means of

receiving real-time data from drifting meteorological buoys and ARGOS-equipped AMOS via the polar orbiting TIROS-N satellites.

1.4 DATA DISPLAYS

1.4.1 AUTOMATED TROPICAL CYCLONE FORECAST (ATCF) SYSTEM — The ATCF is an advanced software program that assists the Typhoon Duty Officer (TDO) in the preparation, formatting, and dissemination of JTWC's products. It cuts message preparation time and reduces the number of corrections. The ATCF automatically displays: the working and objective best tracks; forecasts of track, intensity, and wind distribution; and, information from computer generated forecast aids and products from other agencies. It also computes the myriad of statistics calculated by JTWC. Links have been established through a Local Area Network (LAN) to the NAVPACMETOCCEN WEST Operations watch team to facilitate the generation of tropical cyclone warning graphics for the fleet facsimile broadcasts, for NAVPACMETOCCEN WEST's local metwatch program, and for warning products for Micronesia. A module permits satellite reconnaissance fixes to be input from 36 OSS/OSJ into the LAN.

1.4.2 TESS(3) receives, processes, stores, displays and prints copies of FLENUMETOCCEN data and environmental products. It also ingests and displays satellite imagery from the Naval Meteorological Data Receiver-Recorder Set (SMQ-11) and other TESS(3) sets worldwide.

1.4.3 AWDS functions are similar to those of the TESS(3), but the environmental products and satellite global data base imagery are produced by AFGWC.

1.4.4 NAVAL OCEANOGRAPHIC DATA DISTRIBUTION SYSTEM (NODDS) — NODDS is a personal computer (PC)-based system that uses a telephone modem to download, store and display environmental and satellite data base products from FLENUMETOCCEN.

1.4.5 NAVAL SATELLITE DISPLAY SYSTEM - GEOSTATIONARY (NSDS-G) — The NSDS-G is NAVPACMETOCCEN WEST's primary geostationary imagery processing and display system. It can be used to process high resolution geostationary imagery for analysis of tropical cyclone positions and intensity estimates for the western Pacific Ocean should the the Meteorological Imagery, Data Display, and Analysis System (MIDDAS - see Chapter 2) fail.

1.4.6 PC-BASED WEATHER FACSIMILE (PCGRAFAX) SYSTEM — PCGRAFAX is a microcomputer-based system that receives, stores and displays analog and digital facsimile products that are transmitted over high frequency (HF) radio.

1.4.7 SATELLITE WEATHER DATA IMAGING SYSTEM (SWDIS) — The SWDIS (also known as the M-1000) is a PC-based system that interfaces with the LAN to retrieve, store, and display various products such as: geostationary satellite imagery from other NSDS-G sites at Rota (Spain), Pearl Harbor (Hawaii), or Norfolk (Virginia), scatterometer data from NAVOCEANO and NOAA, and composites of global geostationary satellite imagery from the Internet. The SWDIS has proven instrumental in providing METEOSAT reduced-resolution coverage of tropical cyclones over the western Indian Ocean.

1.5 ANALYSES

The JTWC TDO routinely performs manual streamline analyses of composite surface/gradient-level (3000 ft (914 m)) and upper-tropospheric (centered on the 200-mb level) data for 0000Z and 1200Z daily. Computer analyses of the surface, 925-, 850-, 700-, 500-, 400-, and

200-mb levels, deep-layer-mean winds, frontal boundaries depiction, 1000-200 mb/400-200 mb/and 700-400 mb wind shear, 500 mb and 700 mb 24-hour height change, and a variety of other meteorological displays come from the 0000Z and 1200Z FLENUMETOCCEN data bases. Additional sectional charts at intermediate synoptic times and auxiliary charts, such as station-time plot diagrams, time-height cross section charts and pressure-change charts, are analyzed during periods of significant tropical cyclone activity.

1.6 FORECAST PROCEDURES

1.6.1 INITIAL POSITIONING — The warning position is the best estimate of the center of the surface circulation at synoptic time. It is estimated from an analysis of all fix information received from one hour before to one and one-half hours after that synoptic time. The analysis is aided by a computer-generated objective best track scheme that weights fix information based on its statistical accuracy. The TDO includes synoptic observations and other information to adjust the position, testing consistency with the past direction, speed of movement and the influence of the different scales of motions. If the fix data are not available due to reconnaissance platform malfunction or communication problems, or are considered unrepresentative, synoptic data and/or extrapolation from previous fixes are used.

1.6.2 TRACK FORECASTING — In preparing the JTWC official forecast, the TDO evaluates a wide variety of information, and employs a number of objective and subjective techniques. Because tropical cyclone track forecasting has and continues to require a significant amount of subjective input from the TDO, detailed aspects of the forecast-development process will vary somewhat from TDO to TDO, particularly with respect to the weight given to any of the available guidance. JTWC uses a standardized, three-phase tropical cyclone motion forecasting process to improve not only track forecast accuracy, but also intensity forecast accuracy and forecast-to-forecast consistency.

1.6.2.1 Field Analysis Phase — Navy Operational Global Atmospheric Prediction System (NOGAPS) analyses and prognoses at various levels are evaluated for position, development, and movement of not only the tropical cyclone, but also relevant synoptic features such as: 1) subtropical ridge circulations, 2) mid-latitude short/long-wave troughs and associated weaknesses in the subtropical ridge, 3) monsoon surges, 4) influences of cyclonic cells in the Tropical Upper-Tropospheric Trough (TUTT), 5) other tropical cyclones, and 6) the distribution of sea surface temperature. This process permits the TDO to develop an initial impression of the environmental steering influences to which the tropical cyclone is and will be subjected to as depicted by NOGAPS. The NOGAPS analyses are then compared to the hand-plotted and analyzed charts prepared by the TDO and to the latest satellite imagery in order to determine how well the NOGAPS-initialization process has conformed to the available synoptic data, and how well the resultant analysis fields agree with the synoptic situation inferred from the imagery. Finally, the TDO compares both the computer and hand-analyzed charts to monthly climatology in order to make a preliminary determination of to what degree the tropical cyclone is, and will continue to be, subjected to a climatological or nonclimatological synoptic environment. Noting latitudinal and longitudinal displacements of subtropical ridge and long-wave midlatitude features is of particular importance, and will partially determine the relative weights given to climatologically- or dynamically-based objective forecast guidance.

1.6.2.2 Objective Techniques Analysis Phase — By applying the guidance of the "Systematic and Integrated Approach to Tropical Cyclone

Forecasting,"(Carr and Elsberry, 1994) the TDO can relate the latest set of guidance given by JTWC's suite of objective techniques with the NOGAPS model prognoses and currently observed meteorological conditions. This allows the TDO to evaluate the objective techniques guidance to the following principles.

First, the degree to which the current situation is considered to be, and will continue to be, climatological is further refined by comparing the forecasts of the climatology-based objective techniques, dynamically-based techniques, and past motion of the present storm. This assessment partially determines the relative weighting given the different classes of objective techniques.

Second, the spread of the set of objective forecasts, when plotted, is used to provide a measure of the predictability of subsequent motion, and the advisability of including a moderate probability alternate forecast scenario in the prognostic reasoning message or warning (outside the western North Pacific). The directional spread of the plotted objective techniques is typically small well-before or well-after recurvature (providing high forecast confidence), and is typically large near the decision-point of recurvature or non-recurvature, or during a quasi-stationary or erratic movement phase. A large spread increases the likelihood of alternate forecast scenarios.

1.6.2.3 Construct Forecast Phase — The TDO then constructs the JTWC official forecast giving due consideration to the: 1) extent to which the synoptic situation is, and is expected to remain, climatological; 2) past statistical performance of the various objective techniques on the current storm; and, 3) known properties of individual objective techniques given the present synoptic situation or geographic location. The following guidance for weighting the objective techniques is applied:

a) Weight persistence strongly in the first 12 to 24 hours of the forecast period.

b) Give significant weight to the last JTWC forecast at all forecast times, unless there is significant evidence to warrant a departure (also consider the latest forecasts from regional warning centers, if applicable).

c) Apply the "Systematic and Integrated Approach," (Carr and Elsberry, 1994) using conceptual models of recurring, dynamically-related meteorological patterns with the traits of the numerical and objective aid guidance associated with the specific synoptic situation.

1.6.3 INTENSITY FORECASTING — The empirically derived Dvorak (1984) technique is used as a first guess for the intensity forecast. The TDO then adjusts the forecast after evaluating climatology and the synoptic situation. An interactive conditional climatology scheme allows the TDO to define a situation similar to the system being forecast in terms of location, time of year, current intensity, and intensity trend. Synoptic influences such as the location of major troughs and ridges, and the position and intensity of the TUTT all play a large part in intensifying or weakening a tropical cyclone. JTWC incorporates a checklist into the intensity forecast procedure. Such criteria as upper-level outflow patterns, neutral points, sea-surface temperatures, enhanced monsoonal or cross-equatorial flow, and vertical wind shear are evaluated for their tendency to enhance or inhibit normal development, and are incorporated into the intensity forecast process. In addition to climatology and synoptic influences, the first guess is modified for interactions with land, with other tropical cyclones, and with extratropical features. Climatological and statistical methods are also used to assess the potential for rapid intensification (Mundell, 1990).

1.6.4 WIND-RADII FORECASTING — Since the loss of dedicated aircraft reconnaissance in 1987, JTWC has turned to other data sources for determining the radii of winds around tropical cyclones. The determination of wind radii fore-

casts is a three-step process:

a) First, low-level satellite drift winds, scatterometer and microwave imager 35-kt wind speed analysis (see Chapter 2), and synoptic data are used to derive the current wind distribution.

b) Next the first guess of the radii is determined from statistically-derived empirical wind radii models. JTWC currently used three models: the Tsui model, the Huntley model, and the Martin-Holland model. The latter model uses satellite-derived parameters to determine the size and shape of the wind profile associated with a particular tropical cyclone. The Martin-Holland model also incorporates latitude and speed of motion to produce an asymmetrical wind distribution. These models provide wind distribution analyses and forecasts that are primarily influenced by the intensity forecasts. The analyses are then adjusted based on the actual analysis from step a), and the forecasts are adjusted appropriately.

c) Finally, synoptic considerations, such as the interaction of the cyclone with mid-latitude high pressure cells, are used to fine-tune the forecast wind radii.

1.6.5 EXTRATROPICAL TRANSITION — When a tropical cyclone moves into the mid-latitudes, it often enters an environment that is detrimental to the maintenance of the tropical cyclone's structure and energy-producing mechanisms. The effects of cooler sea surface temperatures, cooler and dryer environmental air, and strong vertical wind shear all act to convert the tropical cyclone into an extratropical cyclone. JTWC indicates that this conversion process is occurring by stating that the tropical cyclone is "becoming extratropical." JTWC will indicate that the conversion is expected to be complete by stating that the system has become "extratropical." When a tropical cyclone is forecast to become extratropical, JTWC coordinates the transfer of responsibility with the appropriate regional NAVPACMETOCCEN, which assumes warning responsibility for the extratropical system.

1.6.6 TRANSFER OF WARNING RESPONSIBILITY — JTWC coordinates the transfer of warning responsibility for tropical cyclones entering or exiting its AOR. For tropical cyclones crossing 180° E longitude in the North Pacific Ocean, JTWC coordinates with the Central Pacific Hurricane Center (CPHC), Honolulu via the Naval Western Oceanography Center (NAVPACMETOCCEN), Pearl Harbor, Hawaii. For tropical cyclones crossing 180° E longitude in the South Pacific Ocean, JTWC coordinates with the NAVPACMETOCCEN, which has responsibility for the eastern South Pacific. Whenever a tropical cyclone threatens Guam, files are electronically transferred from JTWC to the Alternate Joint Typhoon Warning Center (AJTWC) collocated with NAVPACMETOCCEN. In the event that JTWC should become incapacitated, the AJTWC assumes JTWC's functions. Assistance in determining satellite reconnaissance requirements, and in obtaining the resultant data, is provided by the weather unit supporting the 15th Air Base Wing, Hickam AFB, Hawaii.

1.7 WARNINGS

JTWC issues two types of warnings: Tropical Cyclone Warnings and Tropical Depression Warnings.

1.7.1 TROPICAL CYCLONE WARNINGS — These are issued when a closed circulation is evident and maximum sustained 1-minute winds are forecast to reach 35 kt (18 m/sec) within 48 hours, or when the tropical cyclone is in such a position that life or property may be endangered within 72 hours.

Each Tropical Cyclone Warning is numbered sequentially and includes the following information: the current position of the surface center; an estimate of the position accuracy and

the supporting reconnaissance (fix) platform(s); the direction and speed of movement during the past six hours (past 12 hours in the Southern Hemisphere); and the intensity and radial extent of over 35-, 50-, and 100-kt (18-, 26-, and 51-m/sec) surface winds, when applicable. At forecast intervals of 12, 24, 36, 48, and 72 hours (12, 24, and 48 hours in the Southern Hemisphere, (72 hours as required)), information on the tropical cyclone's anticipated position, intensity and wind radii is provided. Vectors indicating the mean direction and mean speed between forecast positions are included in all warnings. In addition, a 3-hour extrapolated position is provided in the remarks section.

Warnings in the western North Pacific and North Indian Oceans are issued every six hours (unless an amendment is required), valid at standard times: 0000Z, 0600Z, 1200Z and 1800Z (at a minimum every 12 hours: 0000Z, 1200Z or 0600Z, 1800Z in the Southern Hemisphere). All warnings are released to the communications network no earlier than synoptic time and no later than synoptic time plus two and one-half hours, so that recipients are assured of having all warnings in hand by synoptic time plus three hours (0300Z, 0900Z, 1500Z and 2100Z). By area, the warning bulletin headers are: WTIO31-35 PGTW for northern latitudes from 35° to 100° east longitude, WTPN31-36 PGTW for northern latitudes from 100° to 180° east longitude, WTXS31-36 PGTW for southern latitudes from 35° to 135° east longitude, and WTPS31-35 PGTW for southern latitudes from 135° to 180° east longitude.

1.7.2 TROPICAL DEPRESSION WARNINGS — These are issued only for western North Pacific tropical depressions that are not expected to reach the criteria for Tropical Cyclone Warnings, as mentioned above. The depression warning contains the same information as a Tropical Cyclone Warning except that the Tropical Depression Warning is issued every 12 hours (unless an amendment is required) at standard synoptic times and extends in 12-hour increments only through 36 hours.

Both Tropical Cyclone and Tropical Depression Warning forecast positions are later verified against the corresponding best track positions (obtained during detailed post-storm analyses) to determine the most probable path and intensity of the cyclone. A summary of the verification results for 1995 is presented in Chapter 5, Summary of Forecast Verification.

1.8 PROGNOSTIC REASONING MESSAGES

These plain language messages provide meteorologists with the rationale for the JTWC forecasts for tropical cyclones in the western North Pacific Ocean. They also discuss alternate forecast scenarios, if changing conditions indicate such potential. Prognostic reasoning messages (WDPN31-36 PGTW) are prepared to complement tropical cyclone (but not tropical depression) warnings. In addition to these messages, prognostic reasoning information may be provided in the remarks section of a warning message.

1.9 TROPICAL CYCLONE FORMATION ALERTS

Tropical Cyclone Formation Alerts are issued whenever interpretation of satellite imagery and other meteorological data indicates that the formation of a significant tropical cyclone is likely. These alerts will specify a valid period, usually not exceeding 24 hours, and must either be canceled, reissued, or superseded by a warning prior to expiration. By area, the Alert bulletin headers are: WTIO21-25 PGTW for northern latitudes from 35° to 100°E longitude, WTPN21-26 PGTW for northern latitudes from 100° to 180°E longitude, WTXS21-26 PGTW for southern latitudes from 35° to 135°E longitude, and WTPS21-25 PGTW for southern latitudes from 135° to 180°E longitude.

1.10 SIGNIFICANT TROPICAL WEATHER ADVISORIES

This product contains a description of all tropical disturbances in JTWC's AOR and their potential for further (tropical cyclone) development. In addition, all tropical cyclones in warning status are briefly discussed and referenced.

Two separate messages are issued daily, and each is valid for a 24-hour period. The Significant Tropical Weather Advisory for the Western Pacific Ocean is issued by 0600Z. The Significant Tropical Weather Advisory for the Indian Ocean is issued by 1800Z. These are reissued whenever the situation warrants. For each suspect area, the words "poor", "fair", or "good" are used to describe the potential for development. "Poor" will be used to describe a tropical disturbance in which the meteorological conditions are currently unfavorable for development. "Fair" will be used to describe a tropical disturbance in which the meteorological conditions are becoming more favorable for further development (i.e. improving), but significant development has not commenced. "Good" will be used to describe the potential for development of a disturbance covered by an Alert. By area, the advisory bulletin headers are: ABPW10 PGTW for northern latitudes from 100° to 180°E longitude and southern latitudes from 135° to 180°E longitude and ABIO10 PGTW for northern latitudes from 35° to 100°E longitude and southern latitudes from 35° to 135°E longitude.

Intentionally left blank

2. RECONNAISSANCE AND FIXES

2.1 GENERAL

JTWC depends primarily on two reconnaissance platforms, satellite and radar, to provide necessary, accurate and timely meteorological information in support of advisories, alerts and warnings. When available, synoptic and aircraft reconnaissance data are also used to supplement the above. As in past years, the optimal use of all available reconnaissance resources to support JTWC's products remains a primary concern. Weighing the specific capabilities and limitations of each reconnaissance platform, and the tropical cyclone's threat to life and property, both afloat and ashore, continues to be an important factor in careful product preparation.

2.2 RECONNAISSANCE AVAILABILITY

2.2.1 SATELLITE — Interpretation of satellite imagery by analysts at Air Force/Navy ground sites and on Navy ships yields tropical cyclone positions, estimates of the current intensity, and 24-hr forecast intensity. Additional positioning and surface wind estimation information are available for analysis where DMSP SSM/I and ERS-1 scatterometer are received and displayed.

2.2.2 RADAR — Interpretation of land-based radar, which remotely senses and maps precipitation within tropical cyclones, provides positions in the proximity (usually within 175 nm (325 km) of radar sites in the Kwajalein, Guam, Japan, South Korea, China, Taiwan, Philippine Islands, Hong Kong, Thailand, India and Australia. Where Doppler radars are located, such as the WSR-88D on Guam, measurements of radial velocity are also available, and observations of the tropical cyclone's horizontal velocity field and wind structure integrated in the vertical are possible within the radar volume.

2.2.3 AIRCRAFT — No weather reconnaissance aircraft fixes were received at JTWC in 1995.

2.2.4 SYNOPTIC — JTWC also determines tropical cyclone positions based on the analysis of conventional surface/gradient-level synoptic data. These positions are an important supplement to fixes provided by analysts using data from remote sensing platforms, and become most valuable in situations where neither satellite, radar, nor aircraft fixes are available or representative.

2.3 SATELLITE RECONNAISSANCE SUMMARY

The Air Force provides satellite reconnaissance support to JTWC through the DMSP Tropical Cyclone Reporting Network (DMSP Network), which consists of several tactical sites and a centralized facility. The personnel of the Satellite Operations (hereafter referred to as Sat Ops) at 36 OSS/OSJ, collocated with JTWC at Nimitz Hill, Guam, coordinate required tropical cyclone reconnaissance support with the following units:

Unit	Call sign
15 OSS/OSW, Hickam AFB, Hawaii	PHIK
18 OSS/OSW, Kadena AB, Japan	RODN
607 COS/DOW, Osan AB, Republic of Korea	RKWU
Air Force Global Weather Central, Offutt AFB, Nebraska	KGWC
NPMOD DGAR, Diego Garcia	FJDG

The DMSP Network sites provide a combined coverage from polar orbiting satellites that includes most of the western North Pacific, from near the international date line westward into the South China Sea. The Naval Pacific Meteorology and Oceanography Detachment at Diego Garcia furnishes fixes through interpretation of high resolution NOAA and DMSP polar

orbiting satellite imagery that covers the central Indian Ocean, and Navy ships equipped for direct satellite readout contribute supplementary support. Also, civilian contractors with the U.S. Army at Kwajalein Atoll supplement Sat Ops satellite coverage with fixes on tropical cyclones in the Marshall Islands and east of the date line.

Additionally, mosaics developed from DMSP satellite imagery are available from the AFGWC via AWDS. These mosaics are used to metwatch the areas not included in the coverage of DMSP Network tactical sites. They provide JTWC forecasters with the time-delayed capability to “see” what AFGWC’s satellite image analysts have been fixing. Also available are three-hourly METEOSAT-5 infrared images from NEMOC via JTWC'S M1000, allowing forecasters to animate these regions.

Sat Ops also uses high resolution geostationary imagery to support the reconnaissance mission. Animation of images is invaluable for determining the location and motion of cloud system centers, particularly in the formative stages. Animation is also valuable in assessing changes in the environment that affect tropical cyclone behavior. Sat Ops is able to process high resolution digital geostationary data through its MIDDAS, and the Navy’s Geostationary Satellite Receiving System (GSRS). The MIDDAS consists of a network of three microcomputers, advanced graphics software, and large screen work stations that process and display geostationary imagery, NOAA High Resolution Picture Transmission (HRPT) and TIROS Operational Vertical Sounder (TOVS) data, and DMSP imagery.

In support of JTWC, AFGWC analyzes stored imagery from both the DMSP and NOAA spacecraft. These imagery are recorded and stored onboard the spacecraft for later relay to a command readout site which in turn passes the data via a communication satellite to AFGWC. This enables AFGWC to obtain the global coverage needed to monitor all tropical cyclones worldwide several times a day.

The hub of the DMSP Network is Sat Ops, which is responsible for coordinating satellite reconnaissance requirements with JTWC and tasking the individual network sites for the necessary tropical cyclone fixes, current intensity estimates, and SSM/I-derived surface winds. Sat Ops monitors all suspect areas defined by the JTWC using geostationary METSAT data. When a warning is in effect, two sites will be tasked if possible for all passes falling within the "warning window" of 1 hour prior to and 1.5 hours after warning time. It also supplies independent assessments of the same data to provide TDOs a measure of confidence in the location and intensity information.

The DMSP Network provides JTWC with several products and services. The main service is to monitor the AOR for indications of tropical cyclone development. If development is suspected, JTWC is notified. Once JTWC issues either a TCFA or a warning, the DMSP Network provides tropical cyclone positions and current intensity estimates, with a forecast intensity estimate implied from the code (Dvorak 1975, 1984) shown in Figure 2-1. Each satellite-derived tropical cyclone position is assigned a Position Code Number (PCN), which is a measure of positioning confidence. The PCN is determined by a combination of 1) the availability of visible landmarks in the image that can be used as references for precise gridding, and 2) the degree of organization of the tropical cyclone’s cloud system (Table 2-1). Once the tropical cyclone’s intensity reaches 50 kt (26 m/sec), the DMSP Network analyzes the distribution of SSM/I-derived 35-kt (18-m/sec) winds in the rain-free areas near the tropical cyclone.

Sat Ops provides at least one estimate of the tropical cyclone’s current intensity every 6 hours once JTWC is in alert or warning status. Current intensity estimates are made using the Dvorak technique for both visible and enhanced infrared imagery. For the intensity analysis of mature tropical cyclones, the enhanced infrared

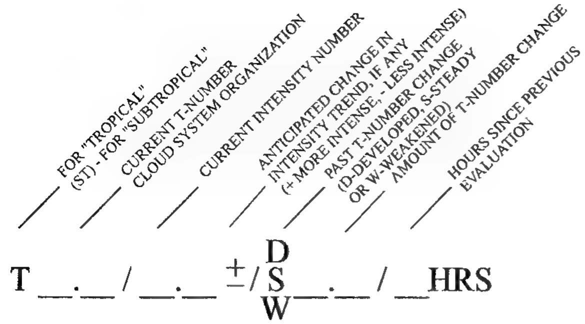

Example: T 3.5 / 4.5+ /W1.5 / 24 HRS

Figure 2-1 Dvorak code for communicating estimates of current and forecast intensity derived from satellite data. In the example, the current "T-number" is 3.5, but the current intensity is 4.5. The cloud system has weakened by 1.5 "T-numbers" since the evaluation conducted 24 hours earlier. The plus (+) symbol indicates an expected reversal of the weakening trend or very little further weakening of the tropical cyclone during the next 24-hour period.

technique is preferred due to its objectivity; however, daily use of the visible technique adds a measure of consistency and helps resolve ambiguities in the enhanced infrared techniques. The standard relationship between tropical cyclone "T-number", maximum sustained surface wind speed, and minimum sea-level pressure (Atkinson and Holliday, 1977) for the Pacific is shown in Table 2-2. For subtropical cyclones, intensity estimates are made using the Hebert and Poteat (1975) technique.

Table 2-1 POSITION CODE NUMBER (PCN)

PCN	METHOD FOR CENTER DETERMINATION/ GRIDDING
1	EYE/GEOGRAPHY
2	EYE/EPHEMERIS
3	WELL DEFINED CIRCULATION CENTER/GEOGRAPHY
4	WELL DEFINED CIRCULATION CENTER/EPHEMERIS
5	POORLY DEFINED CIRCULATION CENTER/GEOGRAPHY
6	POORLY DEFINED CIRCULATION CENTER/EPHEMERIS

2.3.1 SATELLITE PLATFORM SUMMARY— Figure 2-2 shows the operational status of polar orbiting spacecraft. Data were received from four DMSP spacecraft during 1995. Of these, F10 and F11 provided only SSM/I imagery. F12 produced only Operational Line Scan (OLS). F13 was launched in Mar of 1995 and became fully operational in May. F8 remained in standby mode. Of the TIROS-N spacecraft, NOAA 12 was fully operational. NOAA-14 was launched in December 1994 and became operational in April, 1995. NOAA-10 was deactivated in March and NOAA-11 failed in April. NOAA-9 remained in standby mode.

Table 2-2 ESTIMATED MAXIMUM SUSTAINED WIND SPEED (KT)AS A FUNCTION OF DVORAK CURRENT AND FORECAST INTENSITY NUMBER AND MINIMUM SEA-LEVEL PRESSURE (MSLP)

T-NUMBER	ESTIMATED WIND SPEED-KT	(M/SEC)	MSLP(MB) (PACIFIC)
0.0	<25	<(13)	- - - -
0.5	25	(13)	- - - -
1.0	25	(13)	- - - -
1.5	25	(13)	- - - -
2.0	30	(15)	1000
2.5	35	(18)	997
3.0	45	(23)	991
3.5	55	(28)	984
4.0	65	(33)	976
4.5	77	(40)	966
5.0	90	(46)	954
5.5	102	(53)	941
6.0	115	(59)	927
6.5	127	(65)	914
7.0	140	(72)	898
7.5	155	(80)	879
8.0	170	(87)	858

2.3.2 STATISTICAL SUMMARY — During 1995, fix and intensity information from the DMSP Network was the primary input to JTWC's warnings and postanalyses. JTWC received at least 7949 satellite fixes — 4802 covered tropical cyclones in the western North Pacific, 367 in the North Indian Ocean, and 1813 in the Southern Hemisphere. The geostationary platform was the source of 65 percent of the fixes and 35 percent were from polar orbiters. A comparison of all satellite fixes with only their corresponding best track positions is shown in Table 2-3.

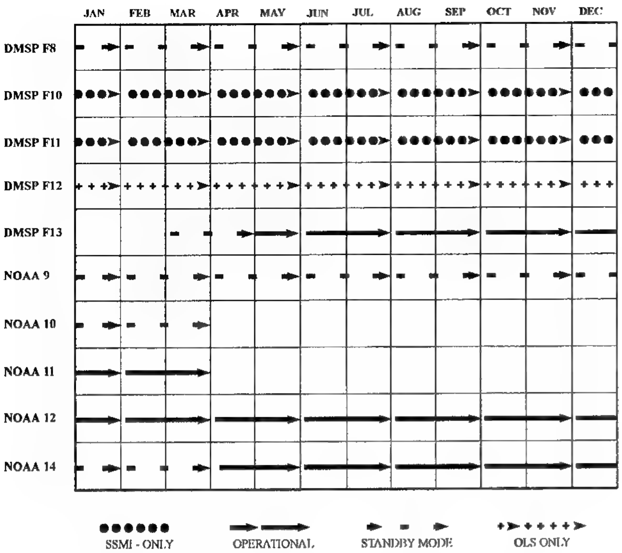

Figure 2-2 Polar orbiting spacecraft status for 1995

2.3.3 APPLICATION OF NEW TECHNOLOGY — Sat Ops continued to make use of the real-time direct transmissions of SSM/I data received, processed and displayed by the Air Force's Mark IVB tactical terminals for surface wind speed estimation. These data were routinely used to identify areas of 35-kt winds, particularly surrounding tropical cyclones. Time-late SSM/I data, stored on board the DMSP spacecraft for later reception, processing and forwarding from FNMOC to be displayed on the MISTIC II, provided coverage over the JTWC's entire AOR. These time-late SSM/I data were used by analysts at AFGWC to develop 35-kt wind envelope bulletins for tropical cyclone warning support.

2.3.4 FUTURE OF SATELLITE RECONNAISSANCE — Sat Ops remains committed to improving support to the PACOM tropical cyclone warning system. The most significant improvement planned in 1996 is the availability of data from more satellite platforms. AFGWC is planning a new capability to include the use of data from more Geostationary satellites in providing fix support. This capability allows for better metwatch and fix support over the entire JTWC AOR. Internal projects include the verification of SSM/I data related to position estimates of tropical cyclones in a highly sheared environment.

2.4 RADAR RECONNAISSANCE SUMMARY

Of the 34 significant tropical cyclones in the western North Pacific during 1995, 12 passed within range of land-based radar with sufficient precipitation and organization to be fixed. A total of 292 land-based radar fixes were logged at JTWC. As defined by the World Meteorological Organization (WMO), the accuracy of these fixes falls within three categories: good [within 10 km (5 nm)], fair [within 10 - 30 km (5 - 16 nm)], and poor [within 30 - 50 km (16 - 27 nm)]. Of the 264 radar fixes encoded in this manner, 62 were good, 138 fair, and 92 poor. The radar network provided timely and accurate fixes which allowed JTWC to better track and forecast tropical cyclone movement. In addition to fixes, the Andersen AFB (Guam) WSR-88D radar supplied meteorologists with a look into the vertical and horizontal structure of precipitation and winds in tropical cyclones passing near the island.

In the Southern Hemisphere, two radar reports were logged for tropical cyclones. No radar fixes were received for the North Indian Ocean.

2.5 TROPICAL CYCLONE FIX DATA

Table 2-4a delineates the number of fixes per platform for each individual tropical cyclone for the western North Pacific. Totals and percentages are also indicated. Similar information is provided for the North Indian Ocean in Table 2-4b, and for the South Pacific and South Indian Ocean in Table 2-4a.

Table 2-3 MEAN DEVIATION(NM) OF ALL DMSP NETWORK DERIVED TROPICAL CYCLONE POSITIONS FROM JTWC BEST TRACK POSITIONS (NUMBER OF CASES IN PARENTHESES)

NORTHWEST PACIFIC OCEAN

PCN	1985-1994 AVERAGE		1995 AVERAGE	
1&2	14.0	(6980)	14.5	(561)
3&4	23.1	(6604)	27.4	(601)
5&6	39.5	(16253)	50.8	(1823)
Totals	29.9	(29837)	39.3	(2985)

NORTH INDIAN OCEAN

PCN	1985-1994 AVERAGE		1995 AVERAGE	
1&2	12.5	(149)	15.8	(15)
3&4	32.4	(130)	24.9	(31)
5&6	38.5	(1348)	37.3	(162)
Totals	35.6	(1627)	33.9	(208)

WESTERN SOUTH PACIFIC AND SOUTH INDIAN OCEAN

PCN	1985-1994 AVERAGE		1995 AVERAGE	
1&2	15.7	(2521)	15.5	(181)
3&4	26.2	(2104)	25.9	(132)
5&6	39.7	(9273)	33.7	(712)
Totals	33.3	(13898)	29.4	(1025)

Table 2-4a 1995 NORTHWEST PACIFIC OCEAN FIX PLATFORM SUMMARY

TROPICAL CYCLONE	SATELLITE	RADAR	SYNOPTIC	AIRCRAFT	TOTAL
01W TD	24	0	0	0	24
02W TS CHUCK	77	0	0	0	77
03W TS DEANNA	135	0	4	0	139
04W TS ELI	74	1	0	0	75
05W TY FAYE	204	65	6	0	275
06W TS UNNAMED	54	0	2	0	56
07W TY GARY	55	25	3	0	83
08W TY HELEN	109	13	13	0	135
09W TS IRVING	47	11	0	0	58
10W TS JANIS	113	0	12	0	125
11W TD	8	0	0	0	8
12W STY KENT	106	8	0	0	114
13W TY LOIS	85	0	0	0	85
14W TY MARK	44	0	0	0	44
15W TS NINA	78	0	5	0	83
16W TD	21	0	0	0	21
17W STY OSCAR	112	22	0	0	134
18W TY POLLY	169	0	0	0	169
19W STY RYAN	155	86	1	0	242
20W TY SIBYL	119	14	13	0	146
21W TD	45	0	0	0	45
22W TD	38	0	0	0	38
23W TD	23	0	0	0	23
24W TY TED	76	0	0	0	76
25W TS VAL	85	0	2	0	87
26W STY WARD	156	20	0	0	176
27W TY YVETTE	76	0	0	0	76
28W TY ZACK	162	5	7	0	174
29W STY ANGELA	234	10	0	0	244
30W TS BRIAN	51	0	1	0	52
31W TS COLLEEN	33	0	0	0	33
32W* TD	41	2	0	0	43
34W TD	61	0	0	0	61
35W TS DAN	102	0	1	0	103
Totals	2972	282	70	0	3324
Percentage of Total	89%	9%	2%	0%	100%

* Regenerated

Table 2-4b 1995 NORTH INDIAN OCEAN FIX PLATFORM SUMMARY

TROPICAL CYCLONE	SATELLITE	RADAR	SYNOPTIC	AIRCRAFT	TOTAL
01B	39	0	1	0	40
02A	40	0	0	0	40
03B	55	0	1	0	56
04B	79	0	1	0	80
Totals	213	0	3	0	216
Percentage of Total	99%	0%	1%	0%	100%

Table 2-4c 1995 SOUTH PACIFIC AND SOUTH INDIAN OCEANS FIX PLATFORM SUMMARY

TROPICAL CYCLONE	SATELLITE	RADAR	SYNOPTIC	AIRCRAFT	TOTAL
01P Vania	78	0	0	0	78
02S Albertine	73	0	0	0	73
03S Annette	70	0	0	0	70
04P ----	13	0	0	0	13
05P William	14	0	0	0	14
06S Bentha	24	0	0	0	24
07S Christelle	22	0	2	0	24
08S Dorina	82	0	0	0	82
09S Fodah	18	0	0	0	18
10S Gail	44	0	0	0	44
11S Heida	55	0	0	0	55
12S Bobby	71	0	0	0	71
13S Ingrid	38	0	2	0	40
14P Violet	46	0	0	0	46
15P Warren	29	2	0	0	31
16S Josta	28	0	0	0	28
17S Kylie	51	0	2	0	53
18P ----	5	0	0	0	5
19S Marlene	102	0	0	0	102
20S ----	33	0	0	0	33
21S Chloe	63	0	0	0	63
22P Agnes	86	0	0	0	86
Totals	1045	2	6	0	1053
Percentage of Total	99%	<1%	<1%	0%	100%

Intentionally left blank

3. SUMMARY OF WESTERN NORTH PACIFIC AND NORTH INDIAN OCEAN TROPICAL CYCLONES

3.1 WESTERN NORTH PACIFIC OCEAN TROPICAL CYCLONES

For the western North Pacific (WNP), 1995 included five super typhoons, 10 lesser typhoons, 11 tropical storms and eight tropical depressions (Table 3-1). The calendar-year total of 34 significant tropical cyclones[1] (TCs) in the WNP was three above the long-term (36-year) average. The year's total of 26 TCs of at least tropical storm intensity was two below the long-term average (Figure 3-1).

---

[1]Postanalysis indicated that Tropical Depression 33W was the regeneration of Tropical Depression 32W, and the two best tracks were combined as one.

Table 3-1 WESTERN NORTH PACIFIC SIGNIFICANT TROPICAL CYCLONES FOR 1995

Tropical Cyclone		Period of Warning	NUMBER OF WARNINGS ISSUED	Estimated Maximum Surface Winds KT	Estimated Maximum Surface Winds M/SEC	Estimated MSLP (MB)
01W	TD	08 JAN	3	30	15	1000
02W	TS CHUCK	28 MAY - 01 JUN	12	35	18	1002
03W	TS DEANNA	01 JUN - 09 JUN	30	45	23	991
04W	TS ELI	04 JUN - 08 JUN	13	40	21	994
05W	TY FAYE	16 JUL - 24 JUL	36	105	54	938
06W	TS UNNAMED	26 JUL - 29 JUL	10	35	18	996
07W	TY GARY	29 JUL - 31 JUL	12	65	33	976
08W	TY HELEN	07 AUG - 12 AUG	23	70	36	972
09W	TS IRVING	17 AUG - 20 AUG	15	60	31	980
10W	TS JANIS	21 AUG - 26 AUG	22	55	28	984
11W	TD	22 AUG - 23 AUG	2	25	13	1002
12W	STY KENT	26 AUG - 01 SEP	24	140	72	898
13W	TY LOIS	26 AUG - 30 AUG	18	65	33	976
14W	TY MARK	30 AUG - 02 SEP	15	95	49	949
15W	TS NINA	02 SEP - 07 SEP	20	45	23	991
16W	TD	09 SEP - 11 SEP	4	30	15	1000
17W	STY OSCAR	11 SEP - 18 SEP	26	140	72	898
18W	TY POLLY	14 SEP - 21 SEP	31	90	46	954
19W	STY RYAN	15 SEP - 24 SEP	36	130	67	910
20W	TY SIBYL	28 SEP - 03 OCT	24	95	49	949
21W	TD	28 SEP - 29 SEP	3	25	13	1002
22W	TD	01 OCT - 02 OCT	6	30	15	1000
23W	TD	05 OCT - 06 OCT	2	25	13	1002
24W	TY TED	09 OCT - 13 OCT	19	70	36	962
25W	TS VAL	09 OCT - 14 OCT	19	45	23	991
26W	STY WARD	16 OCT - 22 OCT	25	140	72	898
27W	TY YVETTE	23 OCT - 26 OCT	14	65	33	976
28W	TY ZACK	25 OCT - 01 NOV	31	120	62	922
29W	STY ANGELA	25 OCT - 06 NOV	49	155	80	879
30W	TS BRIAN	01 NOV - 04 NOV	13	50	26	987
31W	TS COLLEEN	12 NOV - 13 NOV	5	35	18	996
32W	TD 32 & 33	02 DEC - 04 DEC	6	30	15	1000
34W	TD	08-11 DEC/13-14 DEC	11	30	15	1000
35W	TS DAN	26 DEC - 31 DEC	20	55	28	984

The year of 1995 was the first since 1988 during which the number of TCs of at least tropical-storm intensity was below normal. Likewise, the total of 15 typhoons was below the long-term average of 18. Since 1959, twelve years (1969, 1970, 1973-1980, 1983, and 1988) have had 15 or less typhoons (Table 3-2). Most of the years with a low number of typhoons occurred during an eight-year run from 1973-1980. Despite the low number of typhoons during 1995, the year's total of five super typhoons was one above average (Figure 3-2).

Twenty-nine of the 34 significant TCs in the WNP during 1995 originated in the low-level monsoon trough or near-equatorial trough.

Table 3-2 DISTRIBUTION OF WESTERN NORTH PACIFIC TROPICAL CYCLONES FOR 1959 - 1995

YEAR	JAN	FEB	MAR	APR	MAY	JUN	JUL	AUG	SEP	OCT	NOV	DEC	TOTALS
1959	0	1	1	1	0	1	3	8	9	3	2	2	31
	000	010	010	100	000	001	111	512	423	210	200	200	17 7 7
1960	1	0	1	1	1	3	3	9	5	4	1	1	30
	001	000	001	100	010	210	210	810	041	400	100	100	19 8 3
1961	1	1	1	1	4	6	5	7	6	7	2	1	42
	010	010	100	010	211	114	320	313	510	322	101	100	20 11 11
1962	0	1	0	1	3	0	8	8	7	5	4	2	39
	000	010	000	100	201	000	512	701	313	311	301	020	24 6 9
1963	0	0	1	1	0	4	5	4	4	6	0	3	28
	000	000	001	100	000	310	311	301	220	510	000	210	19 6 3
1964	0	0	0	0	3	2	8	8	[illegible]	7	6	2	44
	000	000	000	000	201	200	611	350	521	331	420	101	26 13 5
1965	2	2	1	1	2	4	6	7	9	3	2	1	40
	110	020	010	100	101	310	411	322	531	201	110	010	21 13 6
1966	0	0	0	1	2	1	4	9	10	4	5	2	38
	000	000	000	100	200	100	310	531	532	112	122	101	20 10 8
1967	1	0	2	1	1	1	8	10	8	4	4	1	41
	010	000	110	100	010	100	332	343	530	211	400	010	20 15 6
1968	0	1	0	1	0	4	3	8	4	6	4	0	31
	000	001	000	100	000	202	120	341	400	510	400	000	20 7 4
1969	1	0	1	1	0	0	3	3	6	5	2	1	23
	100	000	010	100	000	000	210	210	204	410	110	010	13 6 4
1970	0	1	0	0	0	2	3	7	4	6	4	0	27
	000	100	000	000	000	110	021	421	220	321	130	000	12 12 3
1971	1	0	1	2	5	2	8	5	7	4	2	0	37
	010	000	010	200	230	200	620	311	511	310	110	000	24 11 2
1972	1	0	1	0	0	4	5	5	6	5	2	3	32
	100	000	001	000	000	220	410	320	411	410	200	210	22 8 2
1973	0	0	0	0	0	0	7	6	3	4	3	0	23
	000	000	000	000	000	000	430	231	201	400	030	000	12 9 2
1974	1	0	1	1	1	4	5	7	5	4	4	2	35
	010	000	010	010	100	121	230	232	320	400	220	020	15 17 3
1975	1	0	0	1	0	0	1	6	5	6	3	2	25
	100	000	000	001	000	000	010	411	410	321	210	002	14 6 5
1976	1	1	0	2	2	2	4	4	5	0	2	2	25
	100	010	000	110	200	200	220	130	410	000	110	020	14 11 0
1977	0	0	1	0	1	1	4	2	5	4	2	1	21
	000	000	010	000	001	010	301	020	230	310	200	100	11 8 2
1978	1	0	0	1	0	3	4	8	4	7	4	0	32
	010	000	000	100	000	030	310	341	310	412	121	000	15 13 4
1979	1	0	1	1	2	0	5	4	6	3	2	3	28
	100	000	100	100	011	000	221	202	330	210	110	111	14 9 5
1980	0	0	1	1	4	1	5	3	7	4	1	1	28
	000	000	001	010	220	010	311	201	511	220	100	010	15 9 4
1981	0	0	1	1	1	2	5	8	4	2	3	2	29
	000	000	100	010	010	200	230	251	400	110	210	200	16 12 1
1982	0	0	3	0	1	3	4	5	6	4	1	1	28
	000	000	210	000	100	120	220	500	321	301	100	100	19 7 2
1983	0	0	0	0	0	1	3	6	3	5	5	2	25
	000	000	000	000	000	010	300	231	111	320	320	020	12 11 2

TABLE CONTINUED ON TOP OF NEXT PAGE

Table 3-2 (CONTINUED FROM PREVIOUS PAGE)

YEAR	JAN	FEB	MAR	APR	MAY	JUN	JUL	AUG	SEP	OCT	NOV	DEC	TOTALS
1984	0	0	0	0	0	2	5	7	4	8	3	1	30
	000	000	000	000	000	020	410	232	130	521	300	100	16 11 3
1985	2	0	0	0	1	3	1	7	5	5	1	2	27
	020	000	000	000	100	201	100	520	320	410	010	110	17 9 1
1986	0	1	0	1	2	2	2	5	2	5	4	3	27
	000	100	000	100	110	110	200	410	200	320	220	210	19 8 0
1987	1	0	0	1	0	2	4	4	7	2	3	1	25
	100	000	000	010	000	110	400	310	511	200	120	100	18 6 1
1988	1	0	0	0	1	3	2	5	8	4	2	1	27
	100	000	000	000	100	111	110	230	260	400	200	010	14 12 1
1989	1	0	0	1	2	2	6	8	4	6	3	2	35
	010	000	000	100	200	110	231	332	220	600	300	101	21 10 4
1990	1	0	0	1	2	4	4	5	5	5	4	1	31
	100	000	000	010	110	211	220	500	410	230	310	100	21 9 1
1991	0	0	2	1	1	1	4	8	6	3	6	0	32
	000	000	110	010	100	100	400	332	420	300	330	000	20 10 2
1992	1	1	0	0	0	3	4	8	5	6	5	0	33
	100	010	000	000	000	210	220	440	410	510	311	000	21 11 1
1993	0	0	2	2	1	2	5	8	5	6	4	3	38
	000	000	011	002	010	101	320	611	410	321	112	300	21 9 8
1994	1	0	1	0	2	2	9	9	8	7	0	2	41
	001	000	100	000	101	020	342	630	440	511	000	110	21 15 5
1995	1	0	0	0	1	2	3	7	7	8	2	3	34
	001	000	000	000	010	020	210	421	412	512	020	012	15 11 8
(1959-1995)													
MEAN	0.6	0.3	0.6	0.8	1.3	2.2	4.7	6.6	5.9	4.9	3.0	1.5	32.3
CASES	22	10	23	27	46	79	168	238	212	177	107	54	1129

The criteria used in Table 3-2 are as follows:
1) If a tropical cyclone was first warned on during the last two days of a particular month and continued into the next month for longer than two days, then that system was attributed to the second month.
2) If a tropical cyclone was warned on prior to the last two days of a month, it was attributed to the first month, regardless of how long the system lasted.
3) If a tropical cyclone began on the last day of the month and ended on the first day of the next month, that system was attributed to the first month. However, if a tropical cyclone began on the last day of the month and continued into the next month for only two days, then it was attributed to the second month.

TABLE 3-2 LEGEND

Total for the month/year → 34
Typhoons → 15
Tropical Storms → 11
Tropical Depressions → 8

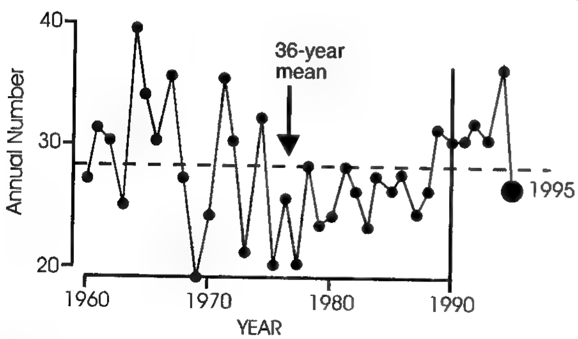

Figure 3-1 Tropical cyclones of tropical storm or greater intensity in the western North Pacific (1960-1995).

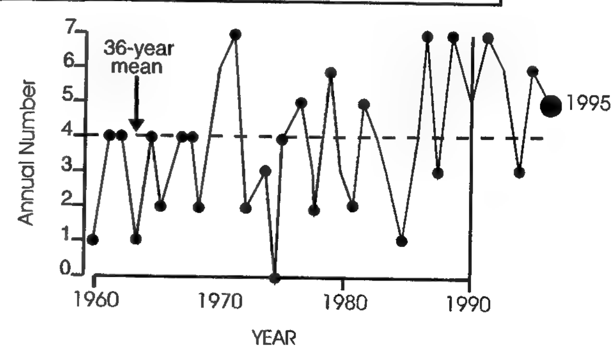

Figure 3-2 Number of western North Pacific super typhoons (1960-1995).

Three — Typhoon Mark (14W), Tropical Depression 22W, and Tropical Storm Brian (30W) — formed at relatively high latitude in association with cold-core cyclonic vortices in the tropical upper tropospheric trough (TUTT). Small-sized Tropical Depression 11W formed from a mesoscale convective system (MCS) that was located to the north of Tropical Storm Janis (10W), and Tropical Storm Colleen (31W) formed from a subtropical cyclone near the

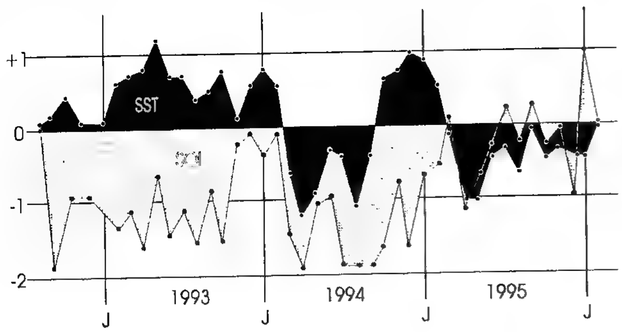

Figure 3-3 Anomalies from the monthly mean for eastern equatorial Pacific Ocean sea surface temperature (black) in degrees Celsius and the Southern Oscillation Index (SOI) (shaded) for the period 1993 through 1995. (Adapted from Climate Prediction Center 1995).

international date line. There were two TCs in the WNP during 1995 that originated east of the international date line — Tropical Depression 01W and Tropical Storm Colleen (31W) — which became significant TCs when they entered the JTWC's area of responsibility. Historically, about one significant TC per year named by the Central Pacific Hurricane Center (CPHC) or the National Hurricane Center (NHC) moves into the WNP.

This year marked the end of a prolonged period of the warm phase of the El Niño/Southern Oscillation (ENSO). Large-scale atmospheric and oceanic circulation anomalies indicative of the warm phase of ENSO (e.g., consistently warmer than normal sea surface temperature (SST) over much of the eastern equatorial Pacific, a strongly negative Southern Oscillation Index (SOI), and a penetration of monsoon westerlies in the WNP far to the east of normal), rapidly returned to near normal, or even reversed during the first half of 1995. By July of 1995, the SST along the equator in the central and eastern Pacific had become colder than normal (Figure 3-3), the SOI had risen to near zero (Figure 3-3), and low-level easterly wind anomalies replaced westerly wind anomalies in the low latitudes of the WNP (Figures 3-4 and 3-5). Based on these Pacific basin SST patterns and the distribution of wind and surface pressure in the tropics of the Pacific

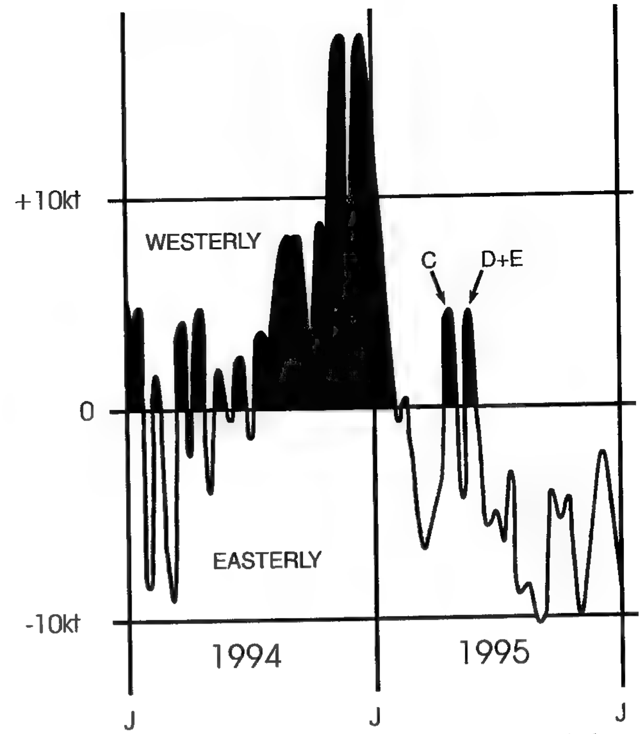

Figure 3-4 Time series of the daily low-level wind along the equator at 150°E during 1994 and 1995. Westerly winds are black, easterlies are shaded. The C indicates the time of formation of Chuck (02W), and the D and E indicates the time of formation of Deanna (03W) and Eli (04W). The winds were adapted from the Climate Prediction Center (1994, 1995).

basin, the U.S. Climate Analysis Center (along with other international meteorological centers) officially declared that the warm phase of ENSO was over. In some respects (e.g., the cooling of the equatorial sea surface, and the anomalously strong low-level easterly winds in the low latitudes of the WNP) the climatic anomalies of the Pacific basin during most of 1995 were consistent with those expected during a cold phase of ENSO, sometimes referred to as La Niña, or El Viejo.

During the first few months of 1995, when ENSO-related low-level westerly winds still dominated equatorial latitudes of the WNP, the year's first two significant TCs — Tropical Depression 01W in January and Chuck (02W) in April — formed at a low latitude (5° N) and east of 160° E. During most of May, a very weak monsoon trough stretched across Micronesia, but no significant TCs formed in it

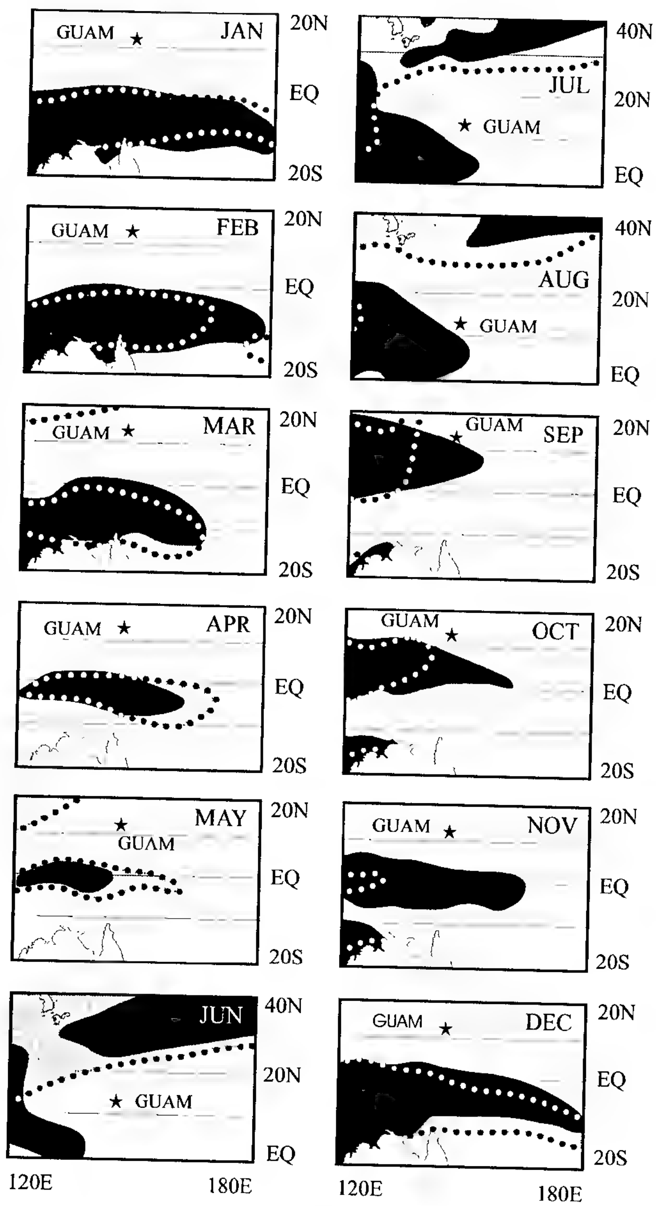

Figure 3-5 Comparison between climatological (black) and analyzed (shaded) mean monthly winds with a westerly component for the western North Pacific in 1995. For June, July, and August the area of coverage is shifted northward to include the subtropics of the North Pacific. For reference, the star indicates the location of Guam. The outline of Australia appears in the lower left of each panel except for June, July, and August where the Korean Peninsula and Japan appear in the upper left. The climatology is adapted from Sadler et al. (1987). The 1995 monthly mean winds were adapted from the Climate Prediction Center (1995) and the Australian Bureau of Meteorology (1995).

until very late in the month when two relatively small and weak TCs — Deanna (03W) and Eli (04W) — developed. As they moved northward during early June, the weak monsoon trough across Micronesia was replaced by low-level easterlies, and southwesterly winds became restricted to the South China Sea, within a narrow band south of the mei-yu trough (Figures 3-5 and 3-6a).

The annual mean genesis location (Figure 3-7a) was west of normal — the first such occurrence since 1990. The annual mean genesis location of tropical cyclones that form in the WNP is highly dependent upon the status of ENSO, and tends to be to the east of normal during El Niño years and west of normal during La Niña years. During 1995, six TCs formed east of 160°E (Figure 3-7b), but most formed in the Philippine Sea (west of 140°E) and eight formed in the South China Sea, resulting in a westward displacement of the annual mean genesis location.

The low-level wind of the tropical Pacific in 1995 was dominated by easterly flow. As a consequence, the summer monsoon circulation of the WNP was weak — in stark contrast to the very active summer monsoon of 1994. During June, July and August of 1995, low-level easterly wind flow was unusually persistent in the low latitudes of the WNP (Figure 3-8a), and the normal southwest monsoon of the Philippine Sea (Figure 3-6b) (with its episodic extensions further eastward) was replaced by mean monthly easterly flow. Also, during these months, the axis of the low-level subtropical ridge was displaced approximately 5° equatorward of normal. Corresponding anomalies in the upper troposphere consisted of westerly wind anomalies over the low latitudes of the WNP (Figure 3-8b). Low-level easterly anomalies coupled with upper tropospheric westerly anomalies resulted in strong westerly shear over the deep tropics of the WNP. This may be related to the large number of weak and poorly defined TCs during much of the year (Figure 3-9). The synoptic

(a)

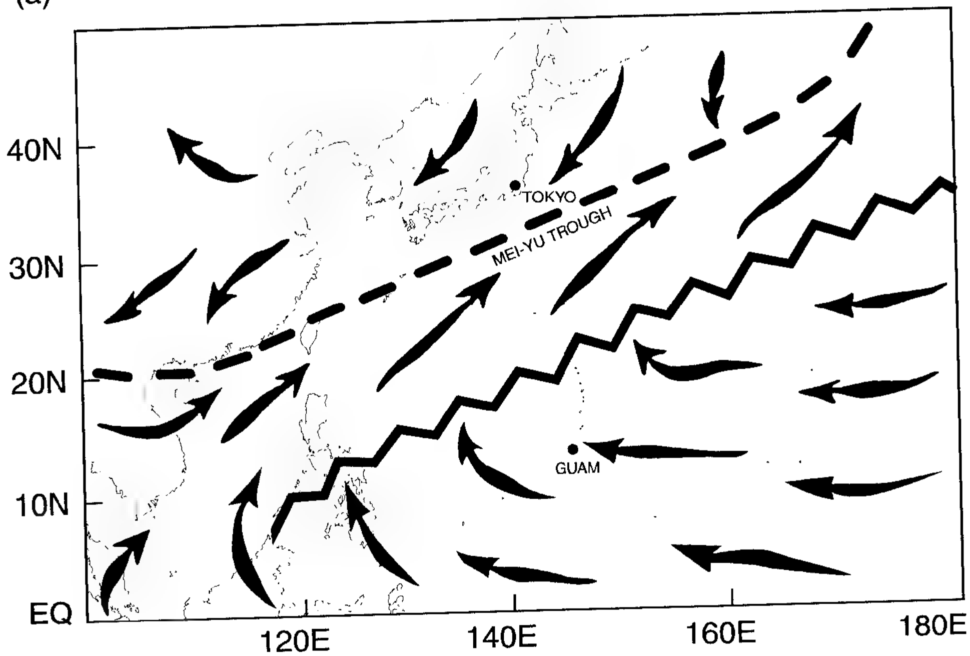

Figure 3-6a The low-level circulation during the summer in the tropics of the western North Pacific. Schematic example of the low-level circulation associated with dominant easterly flow in low latitudes and southwesterlies restricted to the South China Sea and to the south of the mei-yu trough.

(b)

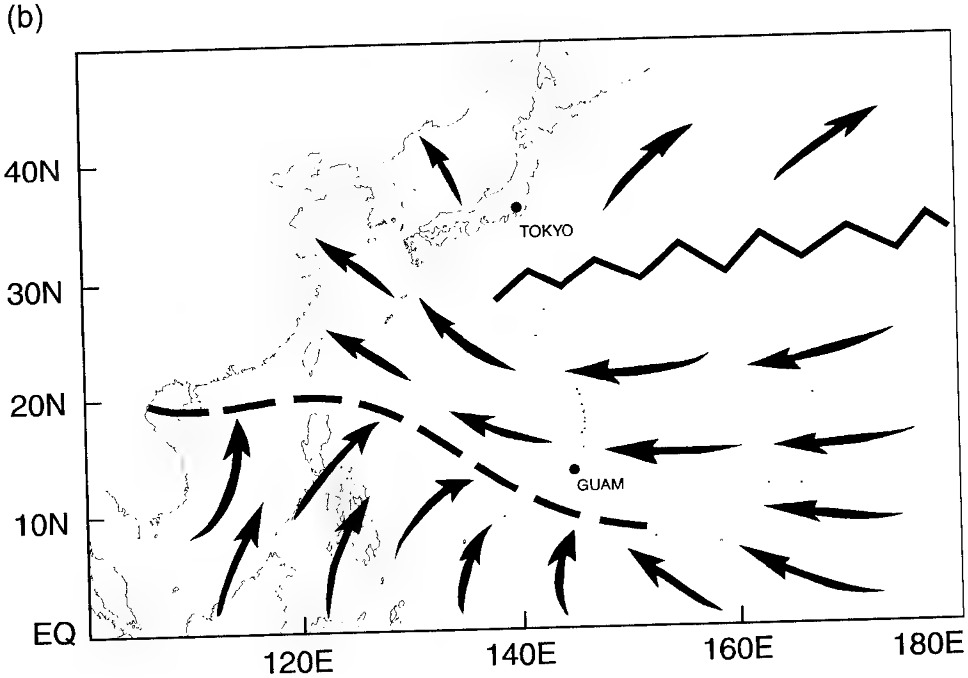

Figure 3-6b The low-level circulation during the summer in the tropics of the western North Pacific - the long-term average. Bold zig-zag lines indicate ridge axes, and bold dashed lines indicate trough axes. Arrows indicate low-level wind direction.

(c)

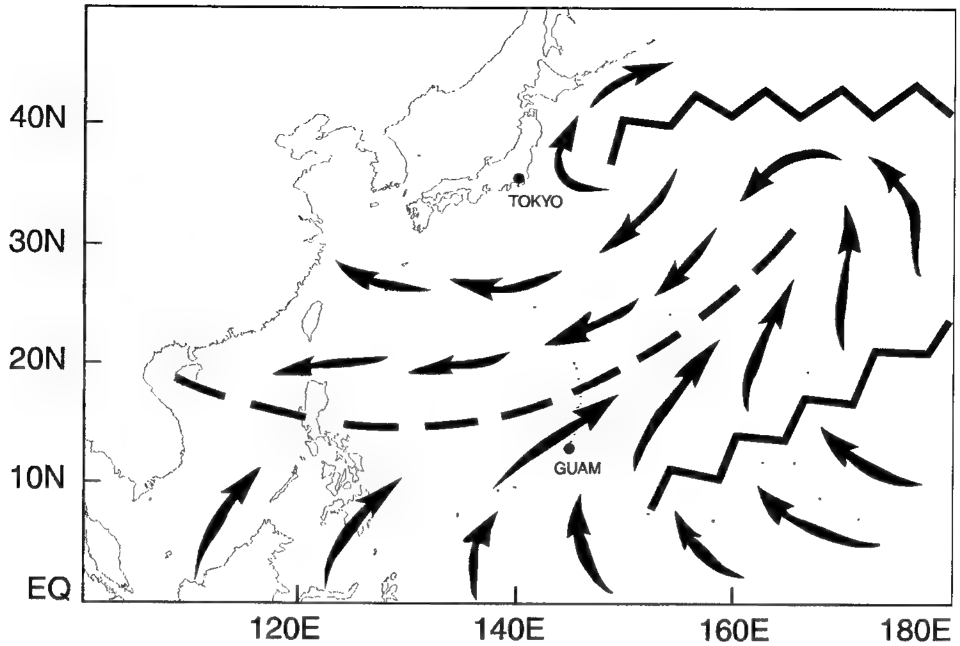

Figure 3-6c The low-level circulation during the summer in the tropics of the western North Pacific. A schematic example of the low-level circulation associated with a reverse-oriented monsoon trough.

(d)

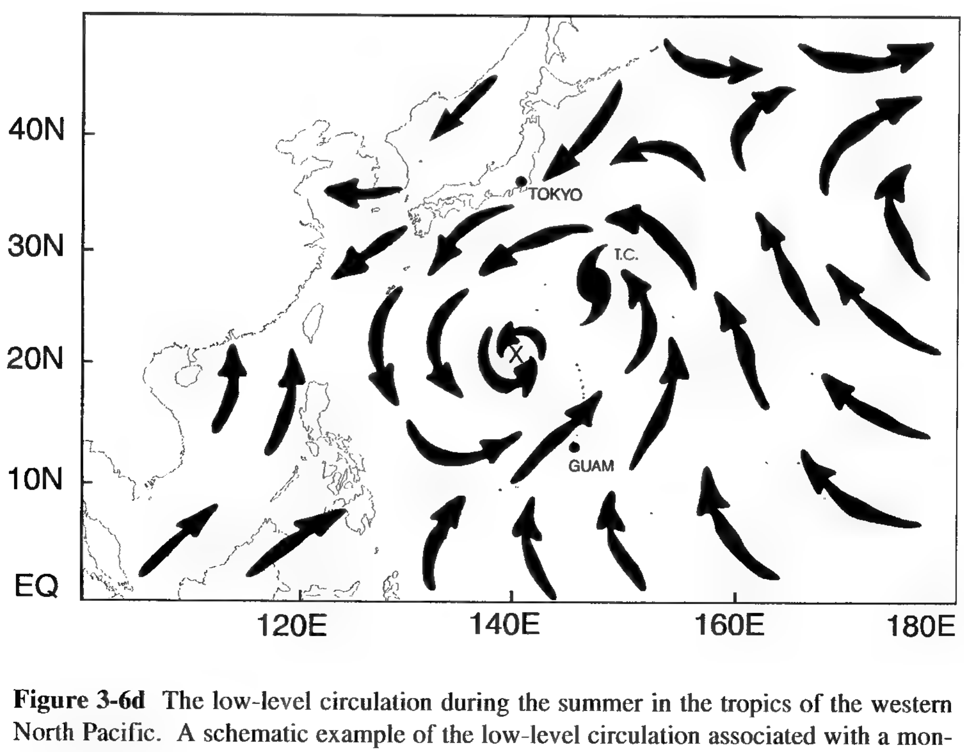

Figure 3-6d The low-level circulation during the summer in the tropics of the western North Pacific. A schematic example of the low-level circulation associated with a monsoon gyre ("x" = gyre center, a tropical cyclone is shown within the circulation of the gyre).

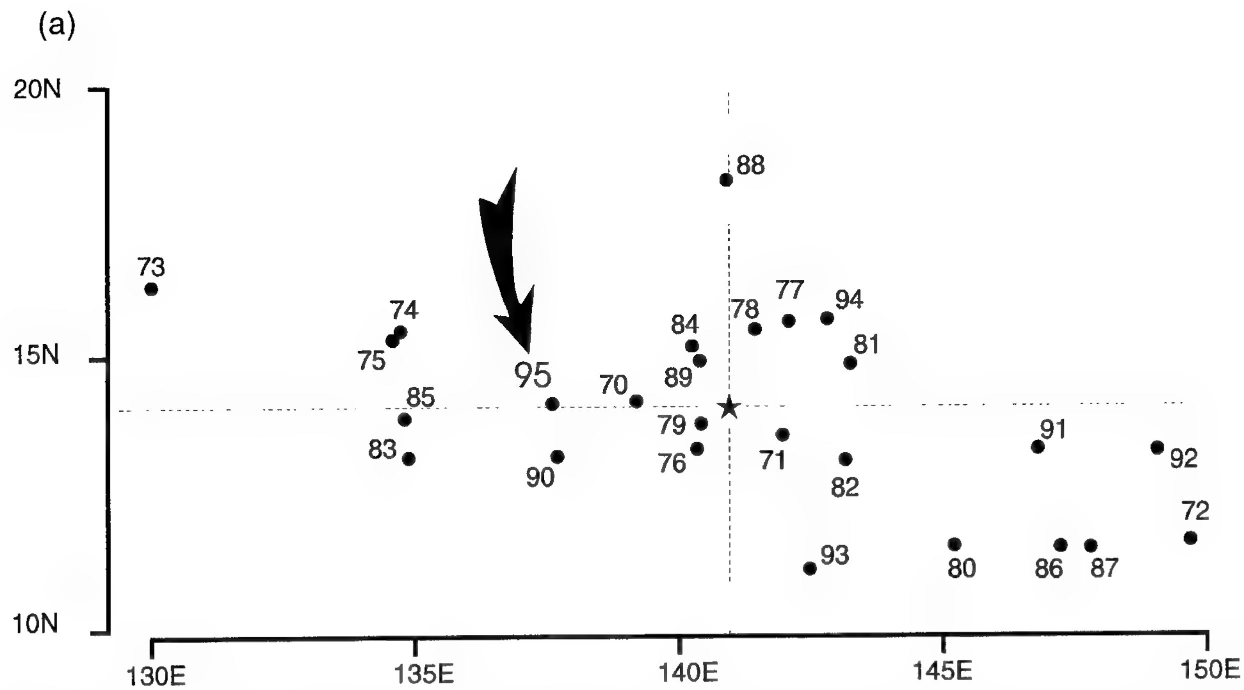

Figure 3-7a Mean annual genesis locations for the period 1970-1995. 1995's location is indicated by the arrow. The star lies at the intersection of the 26-year average latitude and longitude of genesis. For statistical purposes, genesis is defined as the first 25 kt (13 m/sec) intensity on the best track.

regime that dominated most of the middle and latter half of 1995 featured low-level winds with an easterly component that converged at low-latitude, while westerly winds aloft carried the cirrus generated by mesoscale convective systems (MCSs) eastward. Throughout Micronesia, MCSs grew and decayed at the 12-18 hour mesoscale life cycle along the convergence zone and in association with TUTT cells. With few exceptions, tropical cyclone formation was confined to the South China Sea and the Philippine Sea from May through the end of the year. Only two relatively active monsoon episodes were noted during 1995: a reverse-oriented monsoon trough (e.g., Figure 3-c) formed during mid-September and a large monsoon gyre (e.g., Figure 3-6d) formed during mid-October. Neither of these events brought exceptionally strong southwesterly monsoon winds into the tropical WNP, but each did briefly shift the southwest monsoon eastward.

During mid-September, a reverse-oriented monsoon trough formed. Its axis stretched from the South China Sea eastward across Luzon and the Philippine Sea, and then northeastward to the northeast of Guam. This episode of a reverse-oriented monsoon trough saw the simultaneous development of three TCs along its axis — Oscar (17W), Polly (18W), and Ryan (19W). When the monsoon trough axis acquires a reverse orientation, TCs along it tend to move on north-oriented tracks. An unusual type of north-oriented track — the "S" track — is almost always associated with reverse orientation of the monsoon trough axis (Lander 1996). Consistent with Lander's findings, Polly and Ryan moved on unusual north-oriented "S"-shaped tracks. After Oscar, Polly and Ryan recurved into the mid-latitudes during the latter half of September, easterly winds returned to most of the WNP basin.

In the mean, during October, the axis of the monsoon trough extended across Luzon and into the Philippine Sea to the southwest of Guam. This is where it remained for most of the month with one major exception: during

(b)

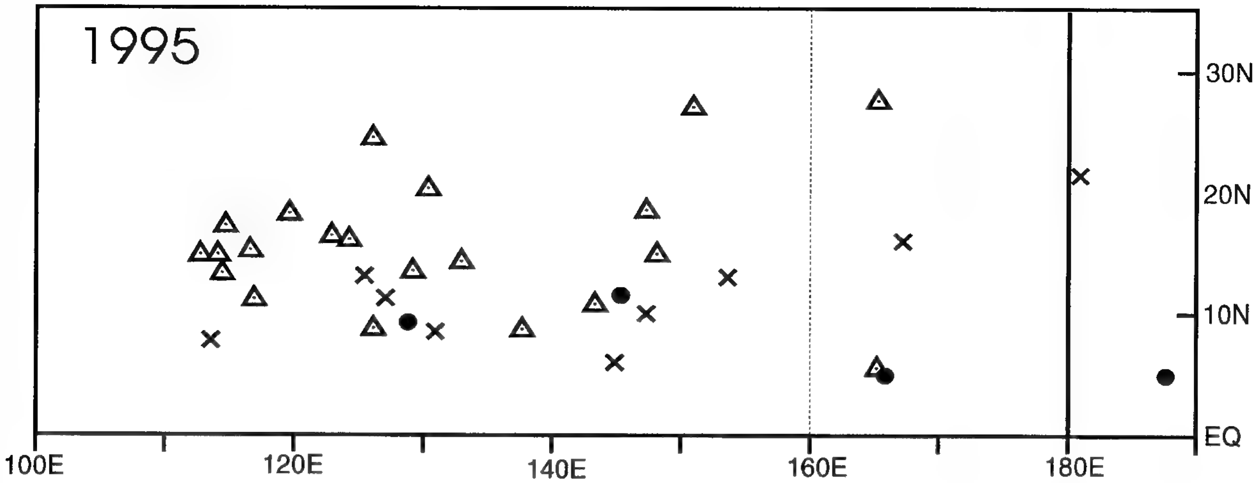

Figure 3-7b Point of formation of significant tropical cyclones in 1995 as indicated by the initial intensity of 25 kt (13 m/sec) on the best track. The symbols indicate: solid dots = 01 January to 15 July; open triangles = 16 July to 15 October; and, X = 16 October to 31 December.

mid-October a large monsoon gyre formed in the Philippine Sea. Tropical Storm Val (25W) interacted with this monsoon gyre. After the monsoon gyre dissipated in the latter half of October, the monsoon trough axis became re-established across the Philippine Sea from Luzon to the southwest of Guam. During the latter half of October, all TCs, except the TUTT-related Brian (30W), formed near, or west, of Guam.

During November 1995, easterly winds returned to the entire deep tropics of the WNP. In what is normally the month of farthest eastward extension of monsoonal westerly winds at low latitudes, the winds along the equator during November 1995 were easterly from the international date line to the Philippines. Tropical cyclone formation during November was restricted to the South China Sea and near the Philippines, with the exception of Colleen (31W) which developed from a cut-off low at relatively high latitude near the international date line. Easterly wind anomalies continued during December, and only one named tropical cyclone — Dan (35W) — formed near the Philippines.

The tracks of the tropical cyclones which formed in the WNP during 1995 indicate a high number of TCs (eight) in the South China Sea, and several (six) with very short tracks. Of the 34 TCs: seven (20%) were straight moving, six (18%) were recurvers, five (15%) moved on north-oriented tracks, and sixteen (47%) were designated as "other" (Table 3-3). Of the five TCs which moved on north-oriented tracks during 1995, two underwent "S" motion. Eight of the sixteen "other" storms remained in or near the South China Sea. Two of the five tropical cyclones which moved on north-oriented tracks occurred in association with September's episode of reverse orientation of the monsoon trough.

An illustration of all the tropical cyclone activity in the western North Pacific and North Indian Oceans is provided in Figure 3-10. Table 3-4 includes: a climatology of typhoons, and tropical storms and typhoons for the WNP for the period 1945-1959 and 1960-1995; and a summary of warning days. Table 3-5 is a summary of the TCFA's for the WNP for 1976-1995. Composite best tracks for the WNP tropical cyclones are provided for the periods: 01 January to 01 September (Figure 3-11), 21 August to 14 October (Figure 3-12), and 05

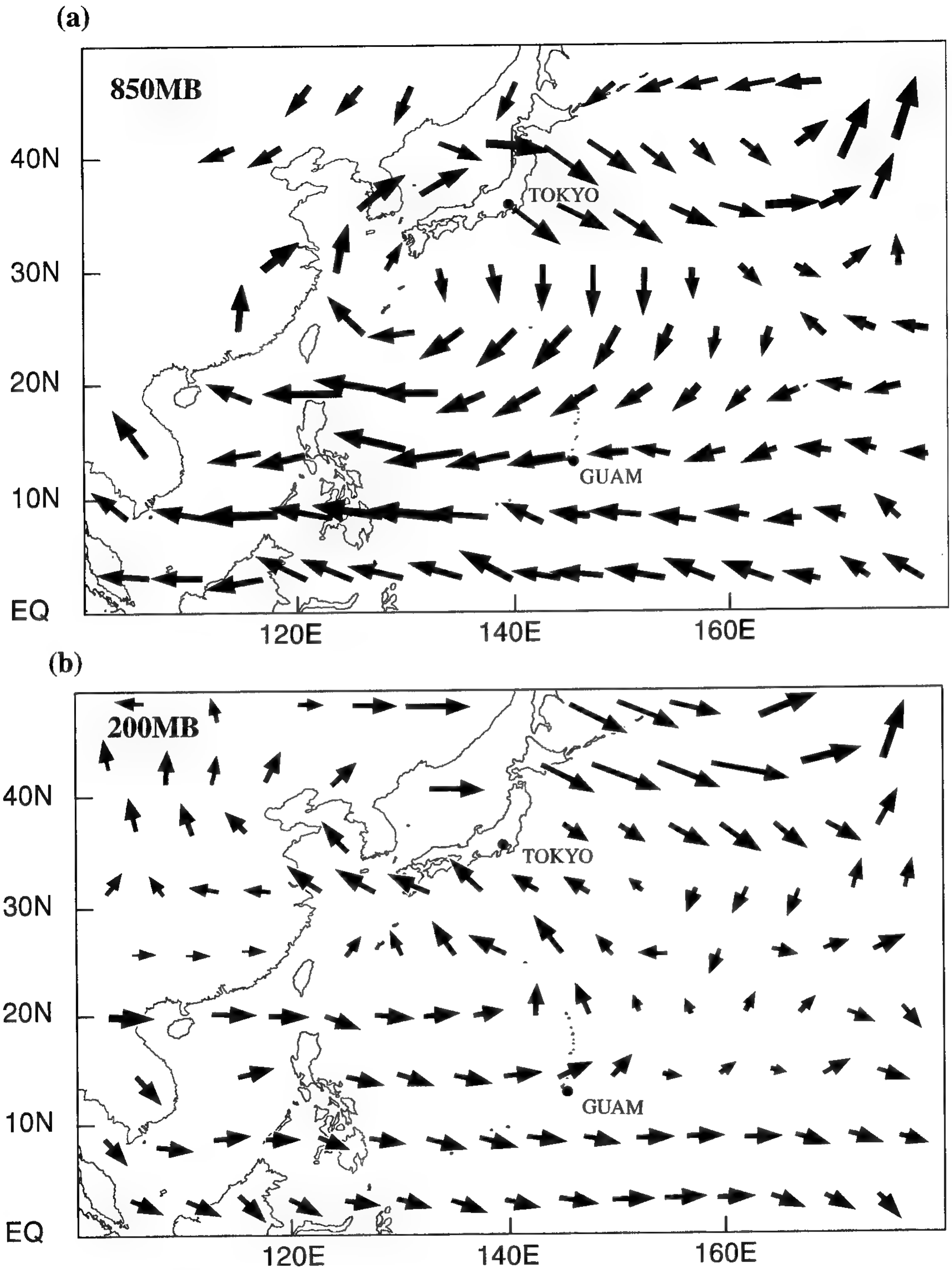

Figure 3-8a,b August wind anomalies: (a) 850 mb, and (b) 200 mb. Arrows indicate wind direction and arrow lenth is proportional to wind speed. In (a) the longest arrows indicate wind anomalies of approximately 10 kt (5 m/sec); in (b) the longest arrows indicate wind anomalies of approximately 30 kt (15 m/sec). The low-lattitude westerly wind anomalies at 200 mb and the low-lattitude easterly wind anomalies at 850 mb are both approximately 10 kt (5 m/sec) — the dicrepency of arrow length is due to the fact that the 200 mb arrows are scaled approximately one-third the length of the 850 mb wind arrows. The locations of Guam and Tokyo are indicated (wind anomalies are adapted from the Climate Prediction Center 1995).

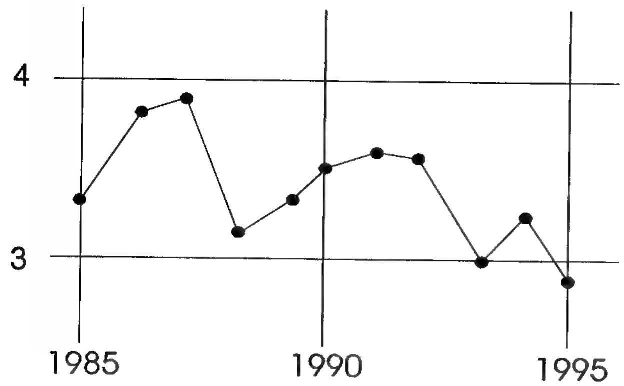

Figure 3-9 Average annual intensity of all tropical cyclones for each year from 1985 to 1995. Intensity units are based upon the following categories: 1 = 25-44 kt; 2 = 45-63 kt; 3 = 64-80 kt; 4 = 81-95 kt; 5 = 96-115 kt; 6 = 116-135 kt; and, 7 = > 135 kt. Categories 3 through 7 are indentical to Categories 1 through 5 on the Saffir-Simpson Hurricane Scale (Simpson 1974).

October to 31 December (Figure 3-13).

The year that saw the end of prolonged El Niño conditions, 1995 can be summarized as a year with a weak monsoon, many weak and poorly defined tropical cyclones, and a westward shift of the formation region of tropical cyclones in the WNP.

3.1.1 MONTHLY ACTIVITY SUMMARY

JANUARY

Tropical Depression 01W occurred in January in the near-equatorial trough. January TCs are most properly considered to be late-season storms, born in atmospheric conditions that evolved during November and December of the previous calendar year.

FEBRUARY

The month with the lowest average number of TCs in the WNP is February. In keeping with climatology, there were no significant TCs in the WNP basin during February 1995.

MARCH

Climatology shows a small increase (over February) in the number of tropical cyclones in the WNP during March. TCs occurring during March are related to the status of ENSO and during El Niño years there tends to be an increased number of early season (March through June) TCs. Consistent with the demise of El Niño conditions during 1995, there were no significant TCs in the WNP basin during March.

APRIL

One TC — **Chuck (02W)** — was active during April. The tropical disturbance from which this first named tropical cyclone of 1995 developed formed in the Marshall Islands at the end of the month. Chuck was a named TC for only two days and peaked at 35 kt (18 m/sec).

MAY

During the first week of May, the remnants of Chuck drifted toward the Mariana Islands bringing Guam about one-quarter of its rainfall for the month of May. The tropical disturbances that became Deanna (03W) and Eli (04W) formed in a weak monsoon trough that stretched across Micronesia during late May. They did not become named TCs until early June.

JUNE

Deanna (03W) was a relatively weak TC that crossed the central Philippines on 02 June. It stalled in the South China Sea for about two days, and then accelerated toward the northeast as it came under the steering influence of strong southwesterly flow to the south of the axis of the mei-yu trough. Deanna merged with the mei-yu cloud band as it moved rapidly northeastward through the Ryukyu island chain. **Eli (04W)**, also a weak tropical cyclone, passed very close to Guam on 04 June. The system turned northward, and dissipated over open water southeast of Japan.

JULY

July 1995 was a relatively quiet month in

the WNP with only three named TCs active during the month. Forming at mid-month, **Faye (05W)** was the first TC of 1995 to become a typhoon. Reaching typhoon intensity on 19 July, Faye tied the record for the latest date for the occurrence of a typhoon in the WNP. Moving on a north-oriented track through the East China Sea, Faye made landfall on the southern coast of Korea, and was one of the most intense TC to strike the Korean peninsula in many years.

In postanalysis, Tropical Depression 06W (TD 06W) was upgraded to **Tropical Storm 06W** based upon scatterometer data from the European Space Agency's remote sensing (ERS-1) satellite. These data indicated that an area of 35 kt (18 m/sec) wind speed accompanied TD 06W as it moved northward just off the east coast of Luzon on 28 July. Tropical Storm 06W merged with Tropical Storm Gary (07W) during a time when both of these TCs were embedded within the circulation of a larger monsoon depression, and while both were affected by the island of Luzon.

Gary (07W) merged with Tropical Storm 06W during a time when both of these TCs were embedded within the circulation of a large monsoon depression near the island of Luzon. Forming in the South China Sea, Gary made landfall in southeastern China very close to the city of Shantou. Based upon ship reports received in the Weekly Tropical Cyclone Summaries compiled by Mr. Jack Beven of the National Hurricane Center, and upon delayed reports of typhoon intensity wind speeds experienced in the city of Shantou, Gary was upgraded from a tropical storm to a typhoon in post-analysis.

AUGUST

The pace of TC formation picked up during August with a total of seven significant TCs active during the month. Originating near Guam during the first week of August, the tropical disturbance that became **Helen (08W)** was slow to develop, taking six days to reach tropical storm intensity. Helen skirted northern Luzon and reached a peak intensity of 70 kt (36 m/sec) just before making landfall east of Hong Kong. Helen was upgraded to typhoon intensity in postanalysis based on data obtained from Hong Kong. A week later, **Irving (09W)** formed in the South China Sea. Irving was very small, and isolated in an otherwise relatively cloud-free region of the South China Sea, it maintained a very small CDO under which microwave imagery indicated the presence of an eye.

During the middle of August, a weak monsoon trough extended into the Philippine Sea. Forming in this monsoon trough, **Janis (10W)** moved northwestward and merged with **Tropical Depression 11W** (TD 11W formed in association with a TUTT-induced area of convection to the north of Janis). In an unusual case of TC merger, the larger Janis lost much of its deep convection and became less organized as it merged with the smaller TD 11W. Subsequent to the merger, all deep convection was lost, but later regenerated as the system moved northward east of Shanghai. Moving eastward across the Yellow Sea, Janis made landfall in central Korea near Seoul. Heavy rain and winds associated with Janis had a significant impact on South Korea.

As Janis was undergoing recurvature, two tropical disturbances formed in the monsoon trough simultaneously: **Kent (12W)** in the Philippine Sea, and **Lois (13W)** in the South China Sea. Kent was the first of five super typhoons to occur in 1995. It rapidly intensified as it approached the Luzon Strait. Basco, Batan Island (WMO 98135), which was briefly in the northern part of Kent's eye, observed a peak wind gust of 140 kt, and a minimum sea-level pressure of 928 mb. Hourly radar images from Kaohsiung, Taiwan showed concentric eyewalls that persisted for at least 22 hours. Kent continued on a west-northwest track and made landfall in China, just east of Hong Kong. Lois became

a typhoon as it was passing over the southern end of Hainan Island in the South China Sea and later made landfall in northern Vietnam. Lois was one of an unusually large number of TCs (eight) that formed in the South China Sea during 1995.

At the end of August, **Mark (14W)** formed at a relatively high latitude. Mark was a small sized TC that moved northeastward for most of its track. It did not reach peak intensity until the first day of September.

SEPTEMBER

September was more active than August , with a total of nine significant TCs: eight that formed during the month and one — Mark — that was still active from August. On the first day of the month, Mark was moving in excess of 20 kt (37 km/hr) toward the polar front. While passing over increasingly cooler sea surface temperatures, it acquired a well-defined eye and reached a peak estimated intensity of 95 kt (49m/sec) as it tracked northeastward from 35°N to 37°N.

During the first week of September, two relatively weak TCs— **Nina (15W)** and **Tropical Depression 16W** (TD 16W) — formed in a weak monsoon trough, crossed the Philippines, and entered the South China Sea. Nina ultimately made landfall in Southern China. TD 16W made landfall in Vietnam, and survived its passage across Southeast Asia and entered the Bay of Bengal, where it regenerated and became **Tropical Cyclone 01B**.

During mid September, the first of two relatively active monsoon episodes during 1995 occurred. A reverse-oriented monsoon trough (Lander 1996) formed, its axis stretching from the South China Sea eastward across Luzon and the Philippine Sea, and then northeastward to the northeast of Guam. This episode of a reverse-oriented monsoon trough saw the simultaneous development of three TCs along its axis — Oscar (17W), Polly (18W), and Ryan (19W).

Oscar (17W) became a very large TC. It also became very intense, reaching a peak intensity of 140 kt (72 m/sec). Oscar posed a serious threat to Tokyo and the southeastern coast of Japan, however, it recurved enough eastward to give only a glancing blow to extreme southeastern Honshu; the eye remained offshore as it passed about 100 nm (185 km) southeast of Tokyo. Oscar's rapid speed of translation — in excess of 40 kt (75 km/hr) — helped to spare Japan the full effects of the typhoon's highest winds. Nevertheless, heavy rain and high winds were responsible for loss of life and some minor damage in Japan.

Like many other tropical cyclones that form within (or move into) a reverse-oriented monsoon trough, **Polly (18W)** underwent unusual motion: an "S"-shaped track. Polly reached peak intensity of 90 kt (46 m/sec) before it turned to the north-northeast on the final leg of its "S" track. The extratropical remains of Polly, possessing a well-defined low-level circulation, moved across the international date line on 24 September.

Ryan (19W) was the first TC on JTWC's records to both form and attain super typhoon intensity within the South China Sea. As was also the case with Polly (18W), Ryan moved on an "S"-shaped track. Ryan passed through the southern islands of the Ryukyu chain, and made landfall in southwestern Japan. On 22 September, Ryan passed near the Taiwanese island of Lanyu (WMO 46762) where a peak wind gust of 166 kt (85.3 m/sec) tied the strongest wind gust ever recorded in a typhoon. The other event occurred at Miyako Jima (WMO 47927) in September 1966 near the eye of Typhoon Cora.

After the reverse-oriented monsoon trough of mid-September migrated out of the tropics, a near-equatorial trough was re-established across Micronesia during the final week of September. **Sibyl (20W)** and **Tropical Depression 21W** (TD 21W) formed in this trough. Sibyl reached its peak intensity of 95 kt (49 m/sec) as it crossed the Visayan Islands. Later, it tracked

over metro-Manila and entered the South China Sea, where it slowly weakened before making landfall east of the Luichow peninsula in southern China. The tropical disturbance that became TD 21W crossed the Philippines on 25 September, and on 28 September, as this tropical disturbance neared the coast of Vietnam, the deep convection consolidated near the low-level circulation center, and it became TD 21W. The system made landfall on the coast of Vietnam and dissipated.

An unusual TC — **Tropical Depression 22W** (TD 22W) — formed at the end of the month and continued into October. TD 22W formed at a relatively high latitude (30°N) near the international date line. It was a very small TC — the smallest TC in the WNP warned on by the JTWC during 1995.

OCTOBER

October was a month of above normal TC activity in the WNP basin: eight TCs formed during the month and two — TD 22W and Sibyl (20W) — formed in September, but were active until 04 October. The first TC that formed during October was **Tropical Depression 23W** (TD 23W). The tropical disturbance that became TD 23W originated over the Philippines and briefly became a tropical depression with maximum winds of 25 kt (13 m/sec) as it moved westward over the South China Sea. **Ted (24W)** developed east of the Philippines in the near-equatorial trough. After moving through the islands of the central Philippines as a tropical disturbance, Ted became a typhoon in the South China Sea when south of Hainan Island. As Ted passed into the Gulf of Tonkin, a gust of 111 kt (55 m/sec) was observed at the top (100 m above sea level) of an oil rig. Ted eventually dissipated over the mountains of southern China.

In the mean, during October, the axis of the monsoon trough extended across Luzon and into the Philippine Sea to the southwest of Guam. This is where it remained for most of the month with one major exception: during mid-October a large monsoon gyre formed in the Philippine Sea. **Tropical Storm Val (25W)** interacted with this monsoon gyre: Val orbited from the eastern side of the gyre to its northern side. Eventually, all of Val's deep convection was sheared away, and it merged with the monsoon gyre. The merged vortex drifted to the west-southwest and slowly dissipated. After the monsoon gyre dissipated in the latter half of October, the monsoon trough axis became re-established across the Philippine Sea from Luzon to the southwest of Guam. During the latter half of October, all TCs — Ward (26W), Yvette (27W), Zack (28W), and Angela (29W) — except the TUTT-related Brian (30W), formed near, or west, of Guam.

The fourth of five super typhoons during 1995, **Ward (26W)** formed as a small TC east of Guam. Moving rather quickly at 17 kt (32 km/hr) toward the west, Ward passed between the islands of Rota and Saipan, or about 70 nm (130 km) to the north of Guam, during the night of 17 October. While approaching its point of recurvature, Ward also intensified, and attained its peak intensity of 140 kt (72 m/sec).

Yvette (27W) was one of seven TCs during 1995 that passed over the Philippines with an intensity of 35 kt (18 m/sec) or greater. Like many other TCs during 1995, Yvette did not develop significantly until it had tracked westward, to near the Philippines where it finally became a tropical storm. After crossing the Philippines, Yvette moved westward over the South China Sea where it reached typhoon intensity just before making landfall along the coast of Vietnam.

Originating from a tropical disturbance in the eastern Caroline Islands, **Zack (28W)** did not significantly intensify for nearly six days. As was the case with Sibyl (20W), Zack intensified as it crossed the Visayan Islands. But, unlike Sibyl (which weakened over the South China Sea after crossing the Philippines), Zack intensified significantly, peaking at an intensity of 120 kt (62 m/sec).

Angela (29W) was the most intense typhoon of 1995, and it was the most intense typhoon to hit the Philippines since Typhoon Joan (1970). First striking southern Luzon, it moved westward and crossed the metro-Manila area. More than 600 people perished in the Philippines as a result of Angela. At its various stages of development, Angela followed Typhoon Zack (28W) nearly 4000 nm (7400 km) across the western North Pacific. Like many of the 1995 tropical cyclones, Angela was slow to develop, but ultimately, it became one of the most intense typhoons of the decade when it peaked at an intensity of 155 kt (80 m/sec).

During the final days of October, **Brian (30W)** formed in direct association with a TUTT cell. Typical of such TCs, Brian was small and embedded in the easterly wind flow on the southwestern quadrant of the low-level subtropical high. It recurved and became absorbed into the cloud band of an advancing cold front.

NOVEMBER

Easterly wind anomalies related to La Niña dominated the tropics of the WNP during November and, as a consequence, November was very quiet. As November began, Brian was recurving, and only one tropical cyclone — Colleen (31W) — formed during the month. On the final day of the month, a tropical disturbance that would become Tropical Depression 32W formed near the Philippines.

Colleen (31W) developed in an unusual manner for a TC in the WNP. The disturbance that became Colleen was a cut-off low that formed in the subtropics to the northwest of Hawaii — a classic "Kona" low. Drifting toward the southwest, the "Kona" low crossed the international date line into JTWC's area of responsibility, where it acquired persistent central convection and became a tropical storm. Colleen was a tropical storm for only six hours, and dissipated after a short life about 420 nm (800 km) east-southeast of Wake Island.

DECEMBER

Three significant TCs formed in the WNP during December — Tropical Depression 32/33W, Tropical Depression 34W, and Tropical Storm Dan. The tropical disturbance that became **Tropical Depression 32W** (TD 32W) formed near the Philippines on the last day of November. As it drifted toward the central Philippines on 02 December, it intensified and was upgraded by the JTWC to TD 32W. Deep convection moving northward along a shear line was originally thought to be TD 32W. After this convection dissipated, a new area of persistent deep convection formed over the central Philippines and it was, at the time, upgraded to Tropical Depression 33W. TD 33W dissipated as it moved westward toward the South China Sea. Postanalysis indicated that TD 33W was the regeneration of Tropical Depression 32W, and the two best tracks were combined as one.

On 07 December, satellite imagery and synoptic data showed that a low-level circulation center was associated with an area of persistent deep convection northwest of Borneo. Based on ship reports indicating wind speeds of 30 kt (15 m/sec) near the low-level circulation center, this system was upgraded to **Tropical Depression 34W** (TD 34W). Wind speeds of 40 kt (21 m/sec) were occurring throughout much of the South China Sea to the north of TD 34W as a manifestation of a surge in the northeast monsoon. TD 34W formed from processes that produce TC twins during times of enhanced equatorial westerly winds (Lander 1990) and it was the Northern Hemisphere twin to Tropical Cyclone Frank (03S) in the Southern Hemisphere. TD 34W dissipated over water near 7°N 109°E.

Dan (35W) was the last significant TC to occur in the WNP during 1995. Like many other TCs during 1995, Dan did not develop until it had tracked westward to near the Philippines. During December 1995, strong tradewinds dominated the tropics of the WNP. A persistent tradewind convergence zone devel-

oped along 5°N, extending from 170°W to 140°E. Several tropical disturbances formed in the convergence zone and moved across the southern islands of Micronesia. These disturbances, coupled with the penetration of shear lines into low latitudes, produced heavier than normal rainfall across Guam and the Northern Mariana Islands. One of these disturbances became Dan. Dan reached a peak intensity of 55 kt (28 m/sec), and early on 30 December, it began to accelerate toward the northeast. Moving to the northeast in excess of 30 kt (55 km/hr), the last TC warning of 1995 was issued on Dan, valid at 310600Z, when the system transitioned into an extratropical low.

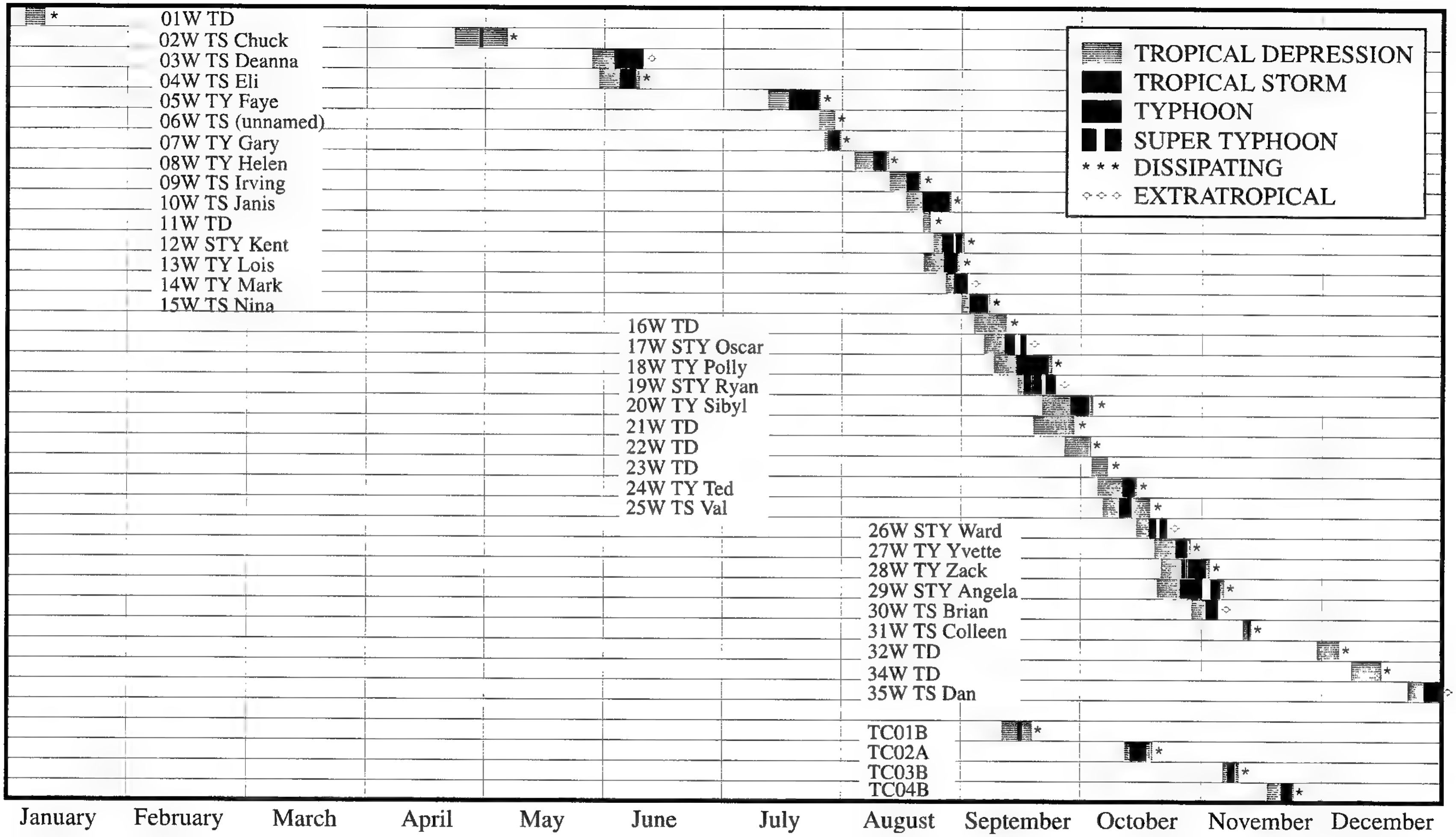

Figure 3-10 Chronology of western North Pacific and North Indian Ocean tropical cyclones for 1995.

Table 3-3 Individual 1978-1995 tropical cyclone (TC) track types. The observed track classes are defined as straight moving (SM), Recurving (R), North-oriented (NO), "S"-track (S), and OTHER. Further subdivisions of the OTHER category are indicated by icons: SCS = TC remained in or near South China Sea for its whole life; A = TC formed over open Pacific and died over water after a short track; B= TC made many loops and meanders but made little overall forward progress; C = TC formed in Mei-yu cloud band and tracked rapidly to the northeast; D = TC formed in the lee of Taiwan during conditions of monsoonal southerwesterly flow and tracked northward then westward around the top of Taiwan to make landfall on the China coast. Note: the subdivisions within the OTHER category are not mutually exclusive: for example, a South China Sea TC (SCS) might also have looped and meandered (B).

YEAR	SM	R	NO	"S"	OTHER	SCS	A	B	C	D
1978	5	10	9	1	7	4	3	-	-	-
1979	10	12	2	-	4	2	1	1	1	-
1980	10	7	5	1	6	5	1	1	-	-
1981	11	7	4	1	6	2	2	1	-	1
1982	9	5	6	1	7	3	1	2	2	-
1983	11	5	4	-	4	4	-	1	-	-
1984	6	5	7	4	8	5	3	1	-	-
1985	7	3	3	6	8	5	2	1	-	-
1986	9	12	2	-	3	1	1	1	1	-
1987	8	2	9	-	5	2	3	-	-	-
1988	9	4	7	1	5	2	-	1	2	1
1989	15	5	5	4	6	3	3	-	-	-
1990	8	11	1	4	7	5	1	-	-	1
1991	11	14	2	-	4	3	1	1	-	-
1992	8	11	5	4	4	3	1	2	-	-
1993	15	10	4	-	8	2	6	-	-	-
1994	15	5	6	8	5	4	1	-	-	-
1995	7	6	3	2	16	8	6	2	-	-
Total:	174	134	84	37	113	61	36	15	6	3
Avg:	9.7	7.4	4.7	2.0	6.3	3.4	2.0	0.8	0.3	0.2

Table 3-4 WESTERN NORTH PACIFIC TROPICAL CYCLONES

TYPHOONS

(1945 - 1959)

	JAN	FEB	MAR	APR	MAY	JUN	JUL	AUG	SEP	OCT	NOV	DEC	TOTALS
MEAN	0.3	0.1	0.3	0.4	0.7	1.0	2.9	3.1	3.3	2.4	2.0	0.9	16.4
CASES	5	1	4	6	10	15	29	46	49	36	30	14	245

(1960 - 1995)

	JAN	FEB	MAR	APR	MAY	JUN	JUL	AUG	SEP	OCT	NOV	DEC	TOTALS
MEAN	0.3	0.1	0.2	0.4	0.7	1.1	2.8	3.5	3.4	3.4	1.7	0.7	18.3
CASES	10	2	8	15	25	38	98	122	120	118	61	24	641

TROPICAL STORMS AND TYPHOONS

(1945 - 1959)

	JAN	FEB	MAR	APR	MAY	JUN	JUL	AUG	SEP	OCT	NOV	DEC	TOTALS
MEAN	0.4	0.1	0.5	0.5	0.8	1.6	2.9	4.0	4.2	3.3	2.7	1.2	22.2
CASES	6	2	7	8	11	22	44	60	64	49	41	18	332

(1960 - 1995)

	JAN	FEB	MAR	APR	MAY	JUN	JUL	AUG	SEP	OCT	NOV	DEC	TOTALS
MEAN	0.5	0.3	0.5	0.6	1.1	1.9	4.3	5.7	5.2	4.5	2.7	1.7	28.7
CASES	19	9	17	22	39	67	152	201	182	156	94	44	1004

Table 3-5 TROPICAL CYCLONE FORMATION ALERTS FOR THE WESTERN NORTH PACIFIC OCEAN FOR 1976-1995

YEAR	INITIAL TCFAS	TROPICAL CYCLONES WITH TCFAS	TOTAL TROPICAL CYCLONES	PROBABILITY OF TCFA WITHOUT WARNING*	PROBABILITY OF TCFA BEFORE WARNING
1976	34	25	25	26%	100%
1977	26	20	21	23%	95%
1978	32	27	32	16%	84%
1979	27	23	28	15%	82%
1980	37	28	28	24%	100%
1981	29	28	29	3%	96%
1982	36	26	28	28%	93%
1983	31	25	25	19%	100%
1984	37	30	30	19%	100%
1985	39	26	27	33%	96%
1986	38	27	27	29%	100%
1987	31	24	25	23%	96%
1988	33	26	27	21%	96%
1989	51	32	35	37%	91%
1990	33	30	31	9%	97%
1991	37	29	31	22%	94%
1992	36	32	32	20%	100%
1993	50	35	38	30%	92%
1994	50	40	40	20%	100%
1995	54	33	34	19%	97%
(1976-1995)					
MEAN:	35	26	28	22%	95%
TOTALS:	691	526	533		

* Percentage of initial TCFA's not followed by warnings.

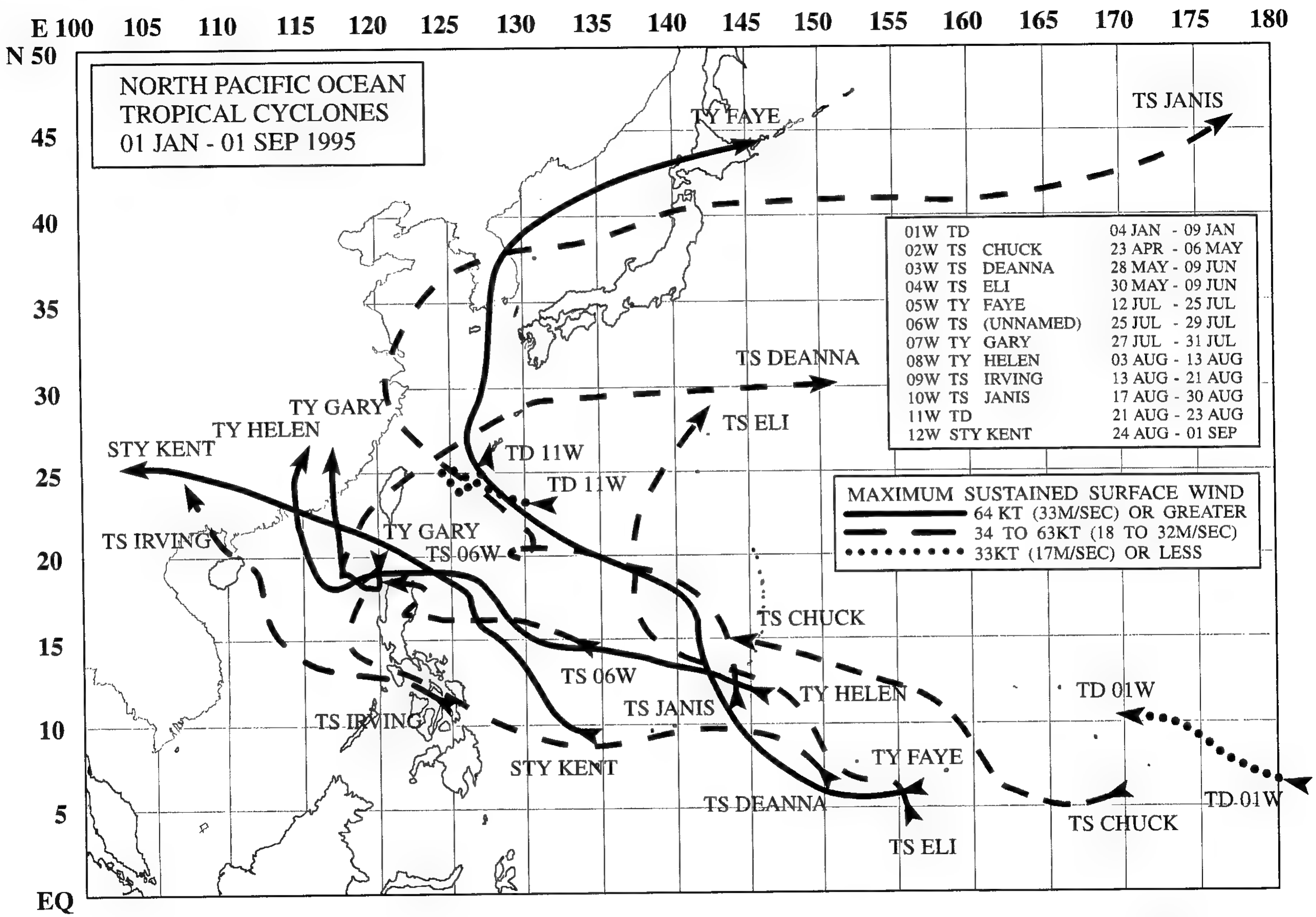

Figure 3-11 Composite best tracks for the North West Pacific Ocean tropical cyclones for the period 01 January to 01 September 1995.

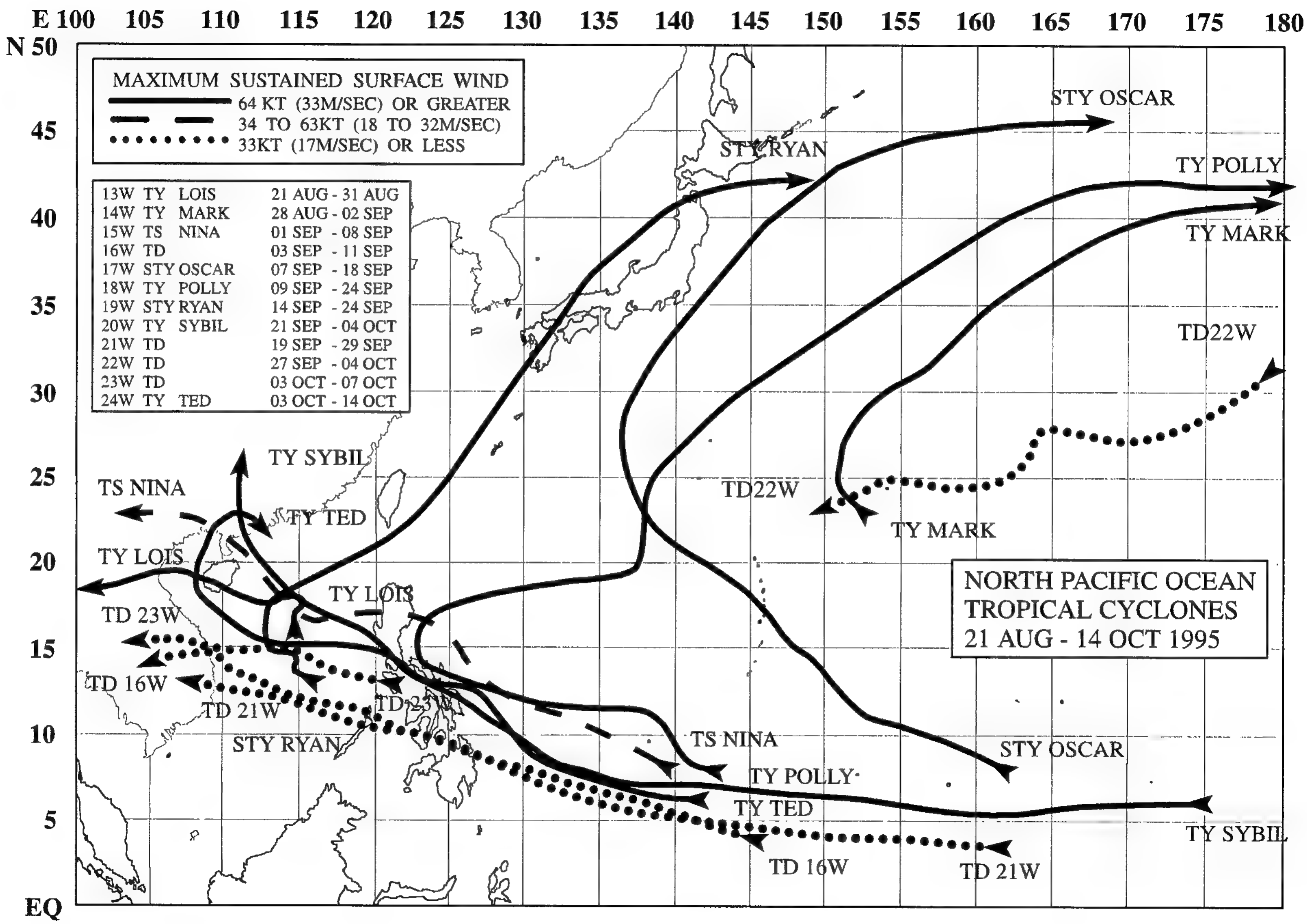

Figure 3-12 Composite best tracks for the North West Pacific Ocean tropical cyclones for the period 21 August to 14 September 1995.

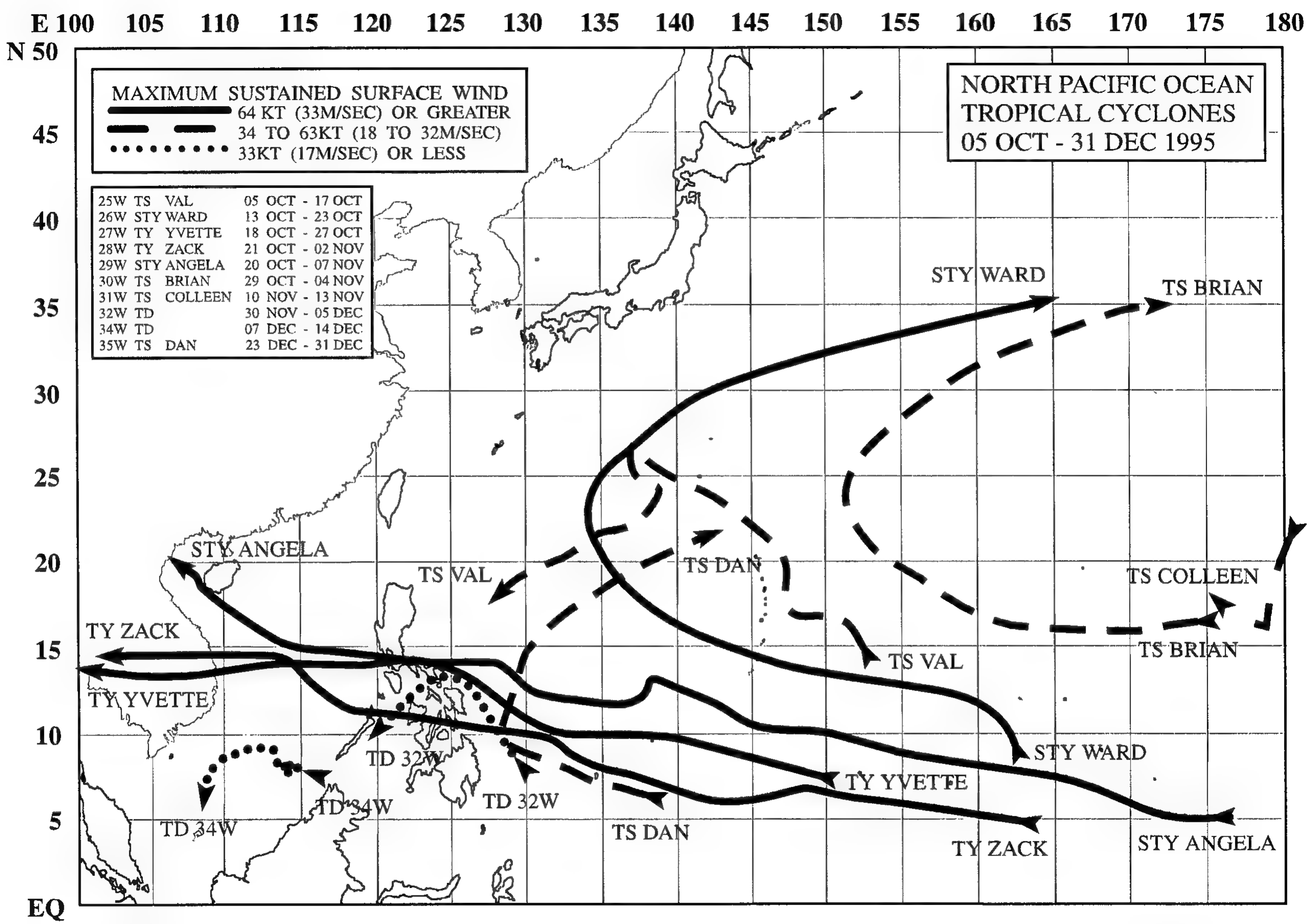

Figure 3-13 Composite best tracks for the North West Pacific Ocean tropical cyclones for the period 05 October to 31 December 1995.

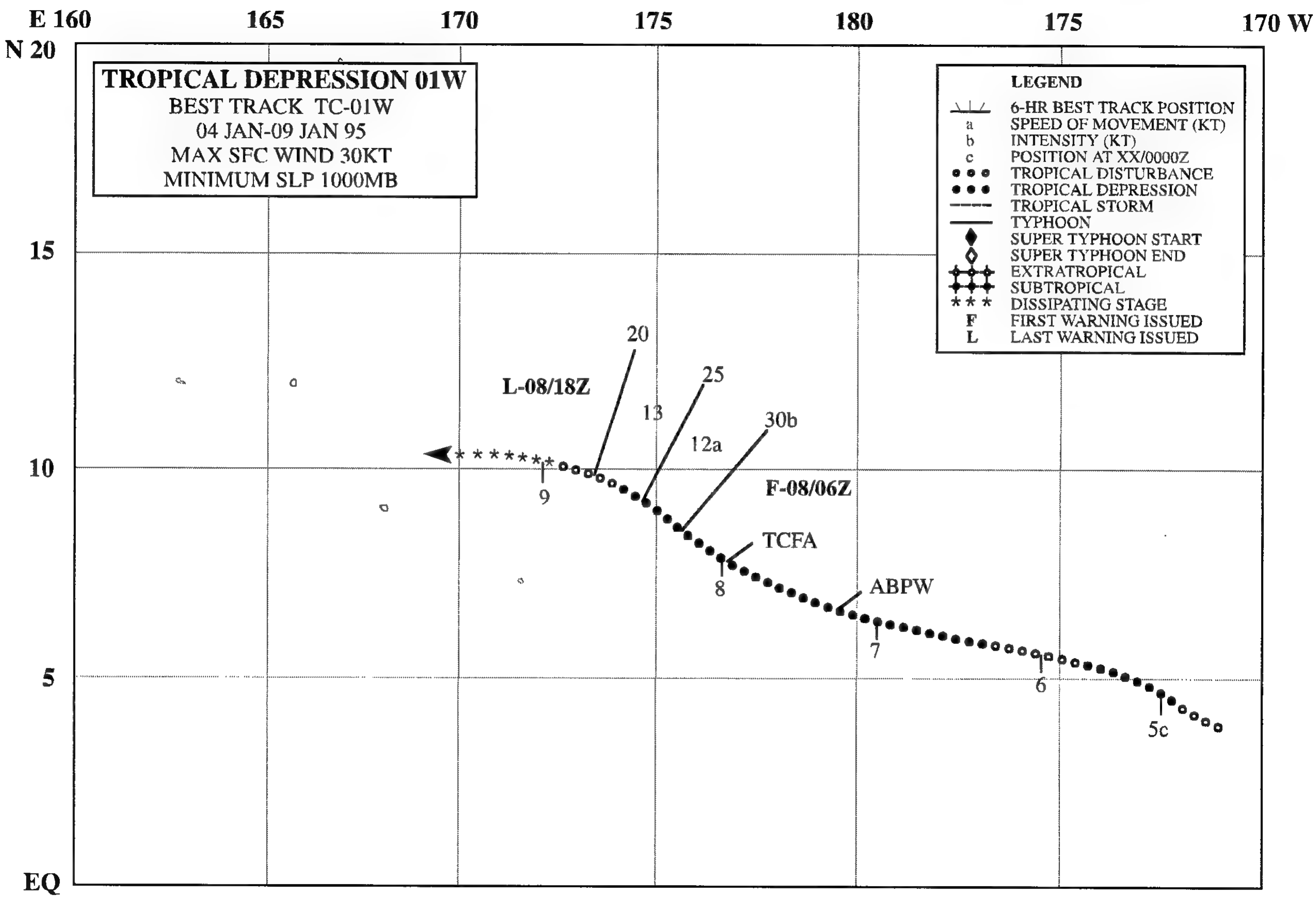
TROPICAL DEPRESSION 01W
BEST TRACK TC-01W
04 JAN-09 JAN 95
MAX SFC WIND 30KT
MINIMUM SLP 1000MB
LEGEND
6-HR BEST TRACK POSITION
a SPEED OF MOVEMENT (KT)
b INTENSITY (KT)
c POSITION AT XX/0000Z
TROPICAL DISTURBANCE
TROPICAL DEPRESSION
TROPICAL STORM
TYPHOON
SUPER TYPHOON START
SUPER TYPHOON END
EXTRATROPICAL
SUBTROPICAL
DISSIPATING STAGE
F FIRST WARNING ISSUED
L LAST WARNING ISSUED
E 160
165
170
175
180
175
170 W
N 20
15
10
5
EQ
L-08/18Z
F-08/06Z
TCFA
ABPW
20
13
25
12a
30b
9
8
7
6
5c

TROPICAL DEPRESSION 01W

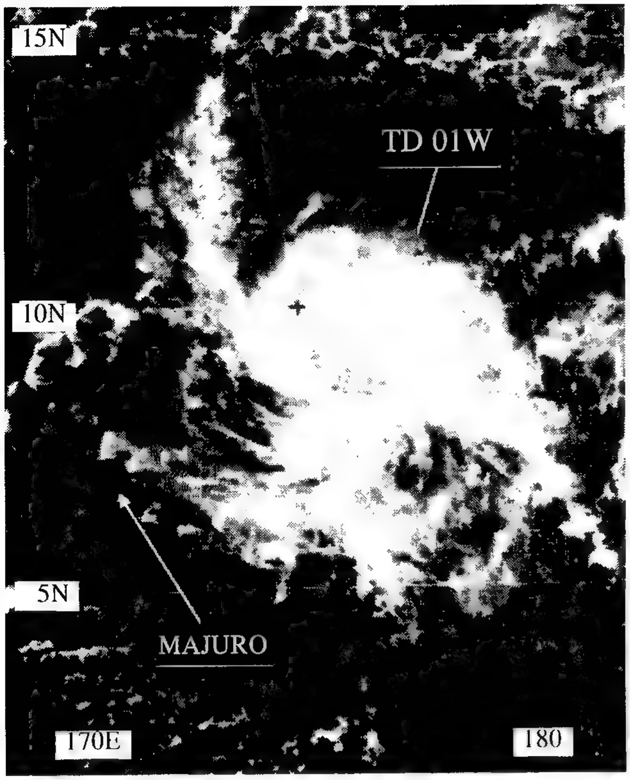

Figure 3-01-1 Tropical Depression 01W shortly before the time of the first warning (080331Z January visible GMS imagery).

I. HIGHLIGHTS

The first significant tropical cyclone of 1995 in the western North Pacific, Tropical Depression 01W formed east of the international date line, moved westward, and dissipated in the Marshall Islands after only a brief life span. This tropical depression formed at the eastern reaches of the near-equatorial trough of the Northern Hemisphere at a time when the axis of this trough had extended far to the east of its typical climatological position — a large scale circulation anomaly associated with the warm phase of El Niño/Southern Oscillation (ENSO) conditions in the tropical Pacific.

II. TRACK AND INTENSITY

The tropical disturbance that became Tropical Depression 01W was first detected east of the international date line, and was first mentioned on the 040600Z January Significant Tropical Weather Advisory as a low-level cyclonic circulation that was a Northern Hemisphere twin to another cyclonic circulation that was located in the Southern Hemisphere. This Advisory stated:

"[an] area of convection . . . is now located near 10°S 180°. . . . A flare up of convection is [located] on the northern side of the low-level circulation. A "twin" low-level circulation exists in the Northern Hemisphere near 5°N 175°W and the two may be enhancing each other . . ."

During the next few days, the tropical disturbance in the Northern Hemisphere moved westward, crossed the international date line and entered the western North Pacific basin. As this tropical disturbance approached the Marshall Island group in the early morning hours of 08 January, a major flare-up of a very cold topped mesoscale convective system (MCS) occurred near the low-level circulation center, and this event, coupled with a twenty-four hour pressure fall of 2 mb at Majuro (WMO 91366),

prompted the JTWC to issue a Tropical Cyclone Formation Alert at 072300Z. During the day on 08 January, the deep convection of the MCS collapsed, leaving behind well-defined cyclonically curved low-level cloud lines accompanying a curved band of deep convection on the northern side of the low-level circulation center (Figure 3-01-1). Based upon these improvements in organization, the first warning valid at 080600Z January on Tropical Depression 01W was issued.

Synoptic data from the Marshall Islands at 081200Z January, indicated that Tropical Depression 01W was not well developed at the surface. The Prognostic Reasoning message that accompanied the 081200Z warning included commentary on the implications of the synoptic reports in the Marshall Islands:

"Tropical Depression 01W . . . is weak, with the primary cyclonic circulation existing in the midlevels of the troposphere. Synoptic reports from the eastern Marshall Islands do not yet support a well defined low-level vortex. . . ."

When the first-light visual satellite imagery and synoptic data on the morning of 09 January did not show evidence of a low-level circulation center, the 081800Z warning on Tropical Depression 01W was amended at 082153Z to become the final warning.

III. DISCUSSION

Tropical Depression 01W formed in a low-level wind pattern associated with the twin-trough pattern that is commonly observed during the simultaneous occurrence of tropical cyclones on both sides of the equator (Figure 3-01-2). The twin near-equatorial troughs and the equatorial low-level westerly winds associated with Tropical Depression 01W and its accompanying unnamed southern twin, were located well to the east of their typical climatological position. Beginning in October of 1994 and extending into January of 1995, low-level westerly winds had persisted to the east of the international date line at low latitudes. This eastward push of monsoonal westerlies was associated with a warm phase (i.e., El Niño conditions) of the ENSO that had dominated the climate of the Pacific basin for all of 1994. El Niño continued to affect the large-scale wind flow of the tropical Pacific during early 1995, but it later waned, and easterly winds began to dominate the low-level flow in the deep tropics of the western North Pacific basin for much of the rest of 1995.

IV. IMPACT

No reports of significant damage or fatalities were received.

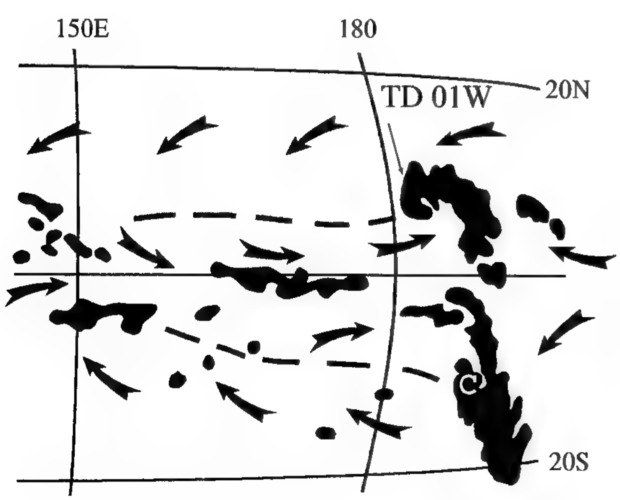

Figure 3-01-2 Cloud silhouettes based on the 070231Z January infrared GMS imagery show patterns typical of the distribution of deep convection within the twin-trough pattern of the low-level monsoon flow. The low-level winds are indicated by arrows, the trough axes by large dashed lines, and the twin cyclones are located in the cloudiness at the eastern ends of the trough axes.

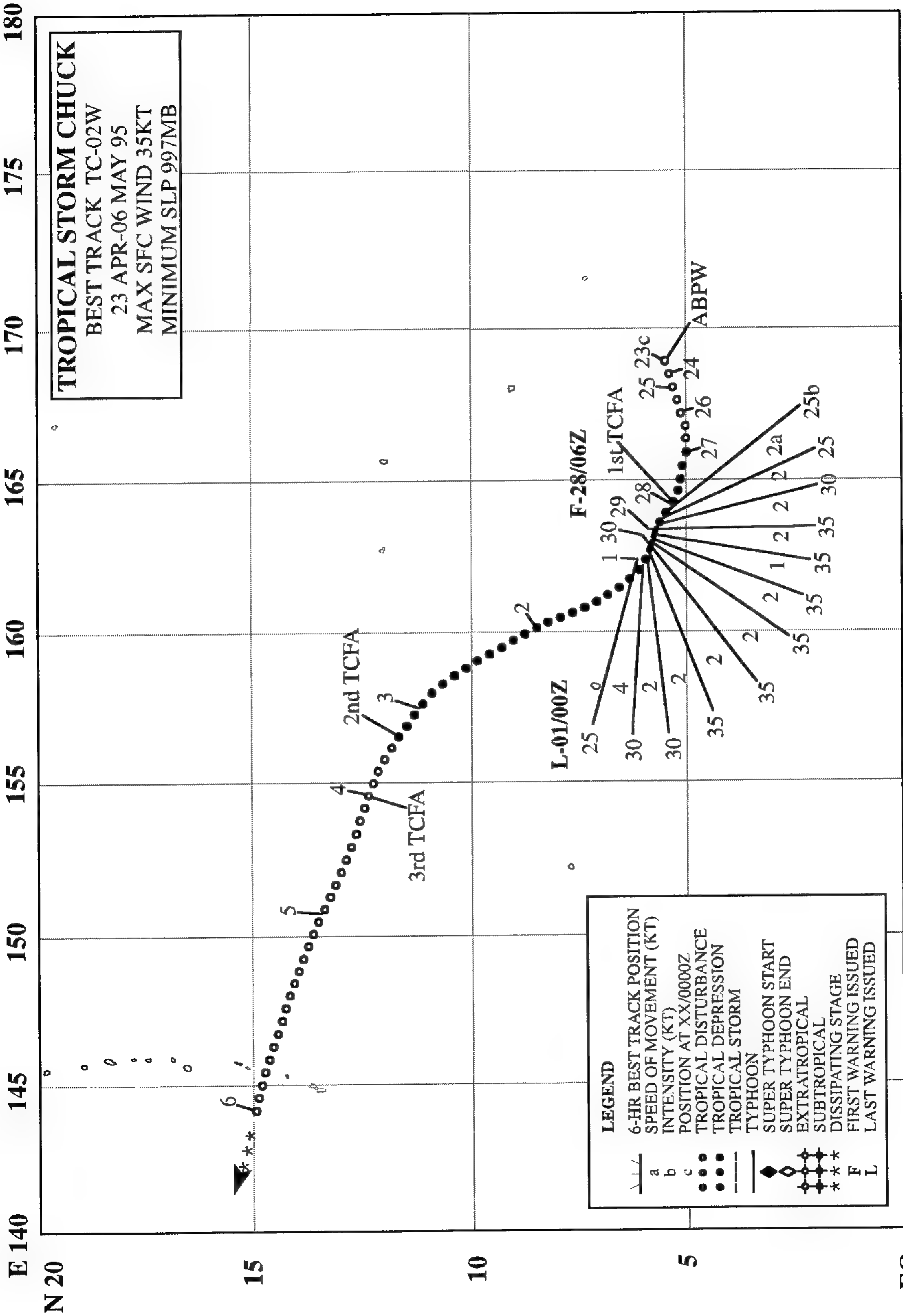
TROPICAL STORM CHUCK
BEST TRACK TC-02W
23 APR-06 MAY 95
MAX SFC WIND 35KT
MINIMUM SLP 997MB
LEGEND
6-HR BEST TRACK POSITION
SPEED OF MOVEMENT (KT)
INTENSITY (KT)
POSITION AT XX/0000Z
TROPICAL DISTURBANCE
TROPICAL DEPRESSION
TROPICAL STORM
TYPHOON
SUPER TYPHOON START
SUPER TYPHOON END
EXTRATROPICAL
SUBTROPICAL
DISSIPATING STAGE
FIRST WARNING ISSUED
LAST WARNING ISSUED
ABPW
1st TCFA
2nd TCFA
3rd TCFA
F-28/06Z
L-01/00Z
E 140
145
150
155
160
165
170
175
180
N 20
15
10
5
EQ

TROPICAL STORM CHUCK (02W)

I. HIGHLIGHTS

After Tropical Depression 01W dissipated in January, tropical cyclone activity was confined to the Southern Hemisphere until Tropical Storm Chuck (02W) formed in the Northern Hemisphere during late April. The first named tropical cyclone of 1995 in the western North Pacific basin, Chuck formed in a near-equatorial trough in the Marshall Islands. Chuck was a named tropical cyclone for only two days and peaked at 35 kt (18 m/sec) (Figure 3-02-1). While slowly dissipating, the remnants of Chuck drifted toward the Mariana Islands bringing Guam about one quarter of its rainfall for the month of May, a dry season month.

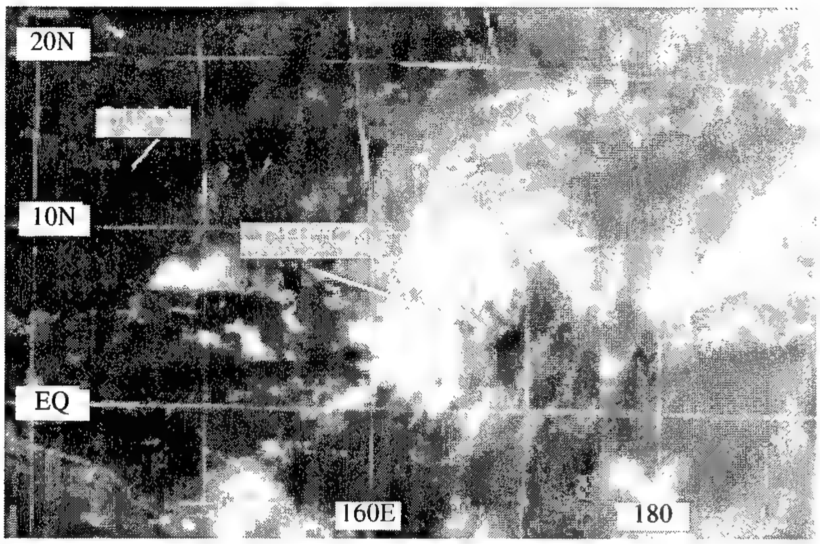

Figure 3-02-1 Tropical Storm Chuck (02W) at peak intensity (291833Z April visible GMS imagery).

II. TRACK AND INTENSITY

Beginning on or about 20 April, low-level westerly monsoonal winds became established along the equator between about 150°E to 170°E. Twin near-equatorial troughs bounded these low-level westerlies, and twin (i.e., one north, and the other south, of the equator) low-level cyclonic circulations persisted equatorward of 10° at about 170°E (e.g., see Figure 3-02-2). This synoptic pattern persisted for several days, and at 230600Z April, an area of deep convection associated with a weak low-level circulation located near 6°N 168°E was first mentioned on JTWC's Significant Tropical Weather Advisory. For several more days, this tropical disturbance drifted slowly westward, and did not show any signs of intensification. On 28 April, satellite data and synoptic reports indicated that the system was intensifying, and a Tropical Cyclone Formation Alert (TCFA) was issued at 272200Z. Remarks on this TCFA included:

"The tropical disturbance near Kosrae in the Marshall Islands has gradually become better organized over the past 24 hours. Synoptic data from Kosrae and the NOAA vessel 'Discoverer' now indicate that a well-defined circulation is present at the surface. The Discoverer reported light winds near the center of the disturbance, but 25 kt [13 m/sec] west-southwesterly sustained winds south of the center . . ."

Based upon these reports and synoptic reports from other ships and islands in the area, and indications on satellite imagery of increased organization of the deep convection, the tropical disturbance near

Kosrae was upgraded to Tropical Depression 02W at 280600Z April. Eighteen hours later, with improved organization observed in satellite imagery, Tropical Depression 02W was upgraded to Tropical Storm Chuck at 290000Z.

At 291200Z, satellite imagery indicated that Chuck was being affected by westerly vertical wind shear, and the low-level circulation center became displaced to the west of the deep convection. The intensity remained at 35 kt (18 m/sec) until 301200Z April, when Chuck was downgraded to a tropical depression. The downgrade to tropical depression was based upon the loss of clear indications from synoptic reports of the existence of a well-defined low-level circulation center, and on evidence from satellite imagery that the deep convection had become displaced even further to the east-northeast of the estimated low-level center position. At 010000Z May, Tropical Depression 02W (Chuck) was completely sheared, with the deep convection displaced 135 nm (250 km) to the east of the very weak low-level circulation center, and a final warning was issued.

For the next six days the remnants of Chuck drifted west northwestward toward the Mariana Islands. At 030600Z, a second TCFA was issued when low-level cloud lines better defined the remnants of Chuck on satellite imagery. The deep convection, however was still displaced well to the east of the low-level circulation center. A third TCFA was issued at 040130Z May in order to adjust the coordinates of the alert area to account for a more westward motion of the tropical disturbance. At 042230Z, the TCFA was cancelled when satellite imagery indicated that the weak low-level circulation center had become further displaced from the deep convection. The remnants of Chuck drifted westward and passed to the north of Guam on 06 May.

III. DISCUSSION

Chuck was the last tropical cyclone to form in the western North Pacific in association with low-level monsoonal winds that were displaced well eastward of normal in association with a waning El Niño event. After Chuck, which first attained an estimated intensity of 25 kt (13 m/sec) at 166°E, no significant tropical cyclones in the western North Pacific basin of monsoon origin would form east of 160°E. Three tropical cyclones — Tropical Depression 22W, Tropical Storm Brian and Tropical Storm Colleen formed east of 160°E, but these were not of monsoon origin.

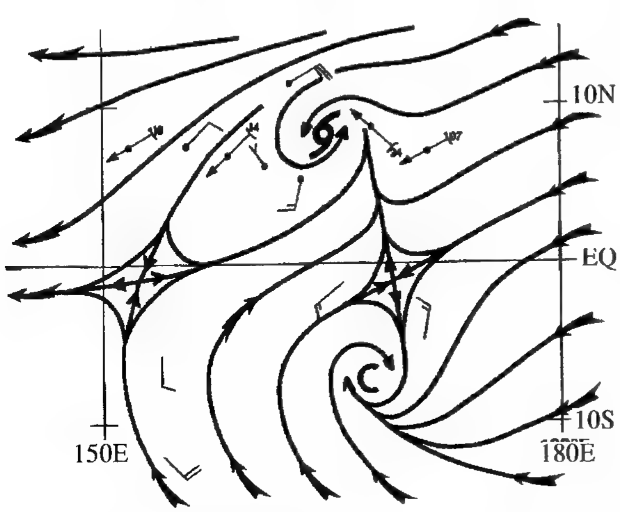

Figure 3-02-2 Surface/gradient streamline analysis for 290000Z April shows Tropical Storm Chuck (02W) and a twin cyclonic circulation to the south. Gradient wind reports are indicated by arrows and surface winds by wind barbs. All reports are in knots.

IV. IMPACT

The passage of Chuck (and later, its remnants) across much of Micronesia did not result in any known incidences of significant damage or injury. On the positive side, the remnants of Chuck contributed some much needed dry season rainfall to some of the Mariana Islands. On the islands of Guam and Rota, 25% (1.5 inches) of May's rainfall occurred during a 24 hour period as the remnants of Chuck neared and passed north of these islands.

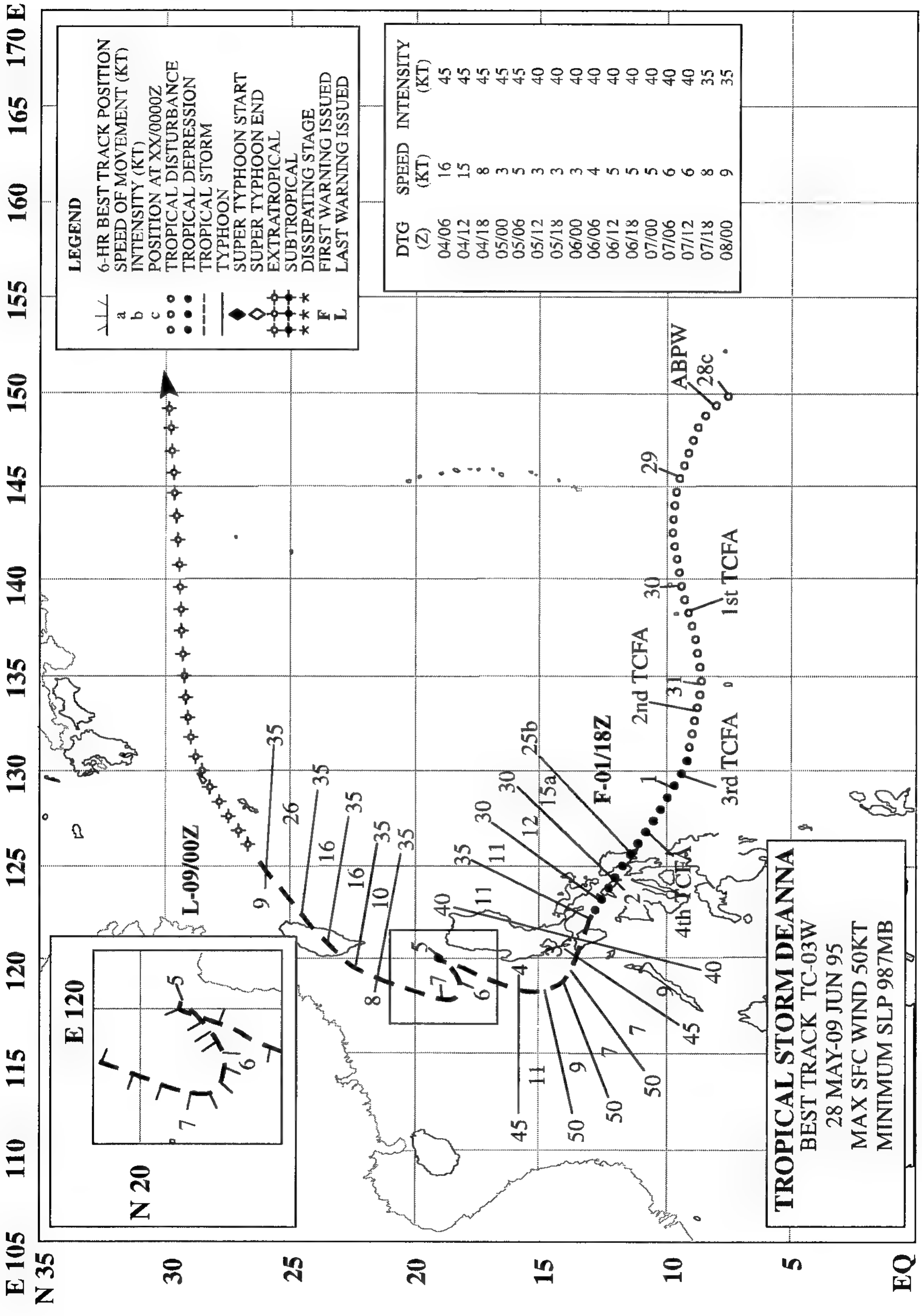

TROPICAL STORM DEANNA
BEST TRACK TC-03W
28 MAY-09 JUN 95
MAX SFC WIND 50KT
MINIMUM SLP 987MB
LEGEND
6-HR BEST TRACK POSITION
SPEED OF MOVEMENT (KT)
INTENSITY (KT)
POSITION AT XX/0000Z
TROPICAL DISTURBANCE
TROPICAL DEPRESSION
TROPICAL STORM
TYPHOON
SUPER TYPHOON START
SUPER TYPHOON END
EXTRATROPICAL
SUBTROPICAL
DISSIPATING STAGE
FIRST WARNING ISSUED
LAST WARNING ISSUED
DTG (Z) | SPEED (KT) | INTENSITY (KT)
04/06 | 16 | 45
04/12 | 15 | 45
04/18 | 8 | 45
05/00 | 3 | 45
05/06 | 5 | 45
05/12 | 3 | 40
05/18 | 3 | 40
06/00 | 3 | 40
06/06 | 4 | 40
06/12 | 5 | 40
06/18 | 5 | 40
07/00 | 5 | 40
07/06 | 6 | 40
07/12 | 6 | 40
07/18 | 8 | 35
08/00 | 9 | 35
L-09/00Z
F-01/18Z
ABPW
1st TCFA
2nd TCFA
3rd TCFA
4th TCFA
E 120
N 20
E 105
N 35
170 E
EQ

TROPICAL STORM DEANNA (03W)

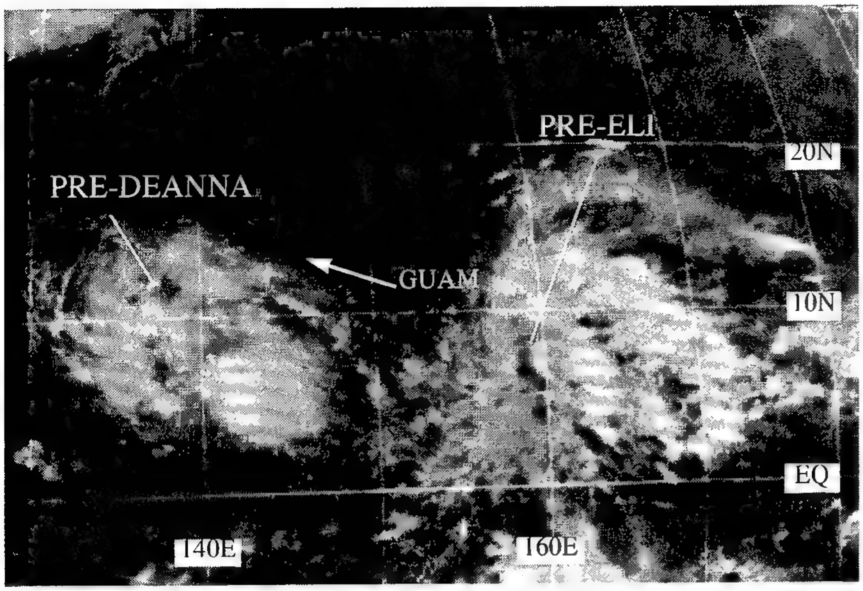

Figure 3-03-1 The tropical disturbances that became Deanna (03W) and Eli (04W) are found along a weak monsoon trough that stretched across Micronesia during late May (301332Z May infrared GMS imagery).

I. HIGHLIGHTS

Tropical Storm Deanna formed in a weak monsoon trough that stretched across Micronesia during late May. Deanna was a relatively weak tropical cyclone that crossed the central Philippines, stalled in the South China Sea for about two days, and then accelerated toward the northeast as it came under the steering influence of strong southwesterly flow to the south of the axis of the mei-yu trough. Deanna merged with the mei-yu cloud band as it moved rapidly northeastward through the Ryukyu island chain.

II. TRACK AND INTENSITY

During the last week of May, there were two tropical disturbances located along a weak monsoon trough that stretched east-west across Micronesia (Figure 3-03-1). The westernmost of the two became Deanna (03W), while the easternmost became Eli (04W). The tropical disturbance that became Deanna was first mentioned on the 280600Z May Significant Tropical Weather Advisory when satellite and synoptic data indicated that a weak low-level cyclonic circulation center had formed in an extensive area of persistent deep convection in the Caroline Islands. Over the next three days, this disturbance moved westward, just south of 10°N, and passed 240 nm (445 km) south of Guam on the evening of 29 May. During the daylight hours of 30 May, satellite imagery indicated that a broad area of persistent convection was consolidating near the island of Yap. Based upon the imagery, and lowered sea-level pressure at Yap (WMO 91413), a Tropical Cyclone Formation Alert (TCFA) was issued at 300730Z May. The tropical disturbance continued moving westward toward the central Philippines, however, on 31 May, it appeared that it had become less organized, and thus the TCFA was cancelled at 310600Z May. Reasons cited for cancellation of the TCFA included:

"... Satellite imagery and synoptic data from Yap and Koror indicate that the tropical disturbance east of Mindanao has a weak cyclonic circulation near the surface. Winds and pressure trends at Yap and Koror do not indicate that a tropical cyclone is developing at the present time. The disturbance appears to be primarily a mid-level feature with active unorganized convection. The long-term outlook favors very slow intensification. ..."

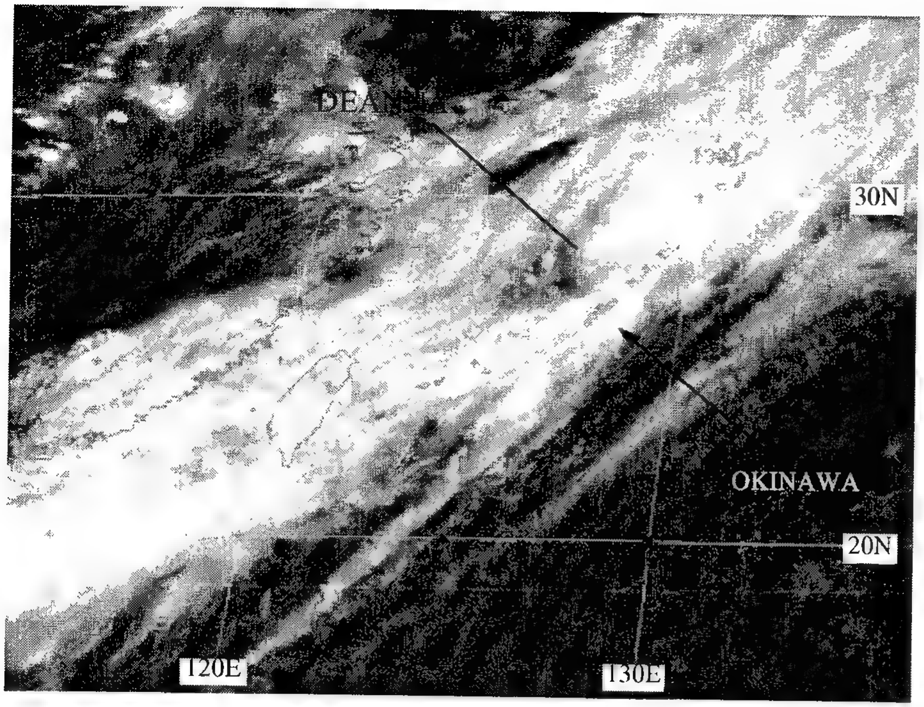

Figure 3-03-2 Absorbed into the mei-yu cloud band, the remnants of Deanna race northeastward (090424Z June visible GMS imagery.)

As the system approached Mindanao, satellite imagery and synoptic data once again indicated that intensification was taking place. A TCFA was issued at 312200Z May. The tropical disturbance now began to track toward the islands of the central Philippines. Evidence of further intensification was lacking, but further development was considered possible, so another TCFA was issued at 011500Z June. Shortly thereafter, satellite imagery showed an increase in the amount of deep convection near the estimated position of the low-level circulation center, and the JTWC issued the first warning on Tropical Depression 03W valid at 011800Z June.

Tropical Depression 03W moved rapidly through the islands of the central Philippines. Tropical Depression 03W was upgraded to Tropical Storm Deanna at 021200Z June based on satellite intensity estimates and synoptic data.

On 03 June, Deanna entered the South China Sea where it slowed and turned toward the north. It is here also, while southwest of Luzon, that Deanna reached its peak intensity of 50 kt (26 m/sec). Subsequently, a slight weakening occurred as Deanna moved slowly northward. On 05 June, Deanna stalled northwest of Luzon, and began a very slow drift back toward the southwest. At this time, northeasterly vertical shear caused the low-level circulation center to become partially exposed on the northeastern side of the deep convection. On 07 June, Deanna resumed a slow north-northeastward movement toward Taiwan. On 08 June, Deanna began to increase its speed of translation as it neared Taiwan. The low-level circulation center became fully exposed and the system was downgraded to tropical depression intensity at 080000Z. (In postanalysis, however, it was determined that Deanna retained tropical storm intensity through 09 June based on a 49-kt 925-mb report from Kadena (WMO 47931) at 290000Z and later a 35-kt surface wind from the buoy (WMO 21004) near 29°N, 135°E at 091800Z). On 09 June, Deanna was absorbed into the mei-yu cloud band, (Figure 3-03-2), although it retained a distinct circulation center. The final warning was issued at 090000Z June when it was deemed that the rapidly moving low pressure system along the mei-yu cloud band (that had been Deanna) had become extratropical. The remnants of Deanna retained gale force winds for 18 hours following the final warning.

III. DISCUSSION

NEXRAD observed wind profile as pre-Deanna passed south of Guam

On the evening of 29 May, the tropical disturbance that became Deanna passed 240 nm (445 km) south of Guam. At this time, Guam was experiencing heavy showers and gusty easterly winds. The vertical wind profile over Guam at this time (obtained from Guam's NEXRAD) (Figure 3-03-3) shows three characteristics that are typical of the vertical wind profiles obtained within the vicinity of tropical cyclones:

1) A peak wind velocity in the lowest levels of the troposphere (2000 to 5000 ft).

2) A relatively deep unidirectional wind flow— in this case, deep easterly — through at least 35,000 ft.

3) Evidence of upper-level outflow (winds directed away from the tropical cyclone) restricted to 40,000 feet and higher.

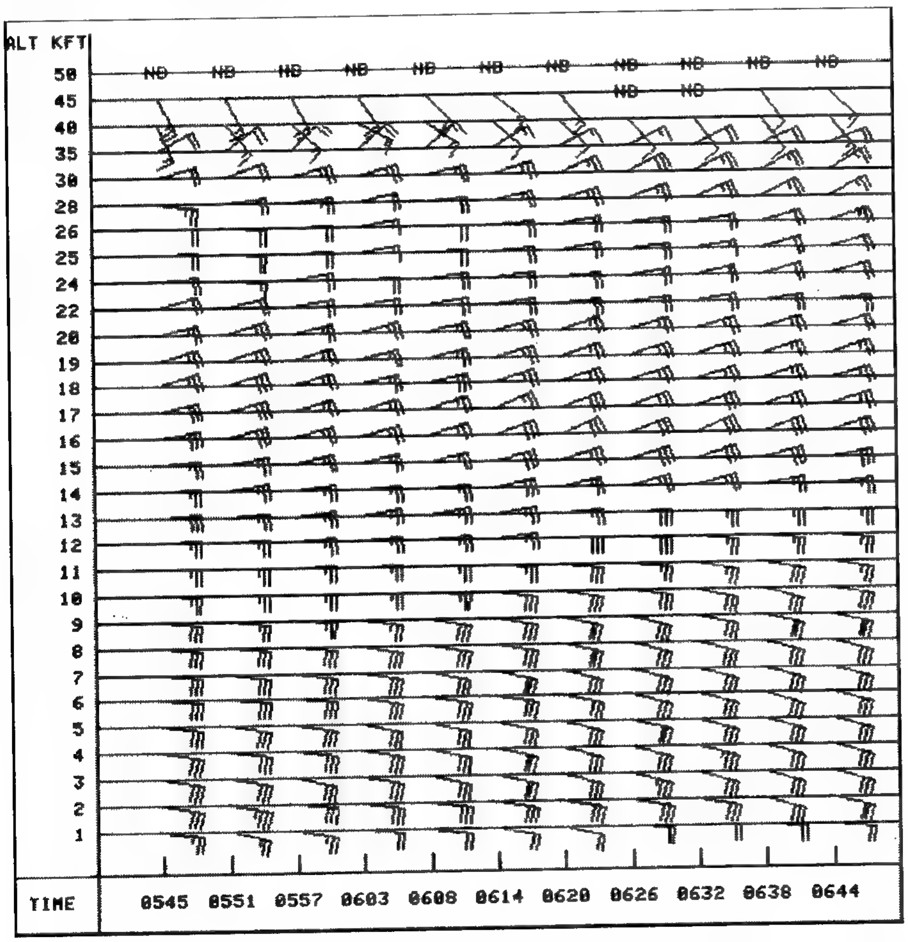

Figure 3-03-3 Vertical wind profile over Guam from the NEXRAD for the period 290545Z to 290644Z May reflects the passage of Deanna to the south.

IV. IMPACT

Heavy rains associated with Tropical Storm Deanna caused mudslides near Mayon Volcano, located in southeastern Luzon. These mudslides buried 140 homes; it is not known if there were any associated injuries or deaths. No additional reports of damage or injuries were received.

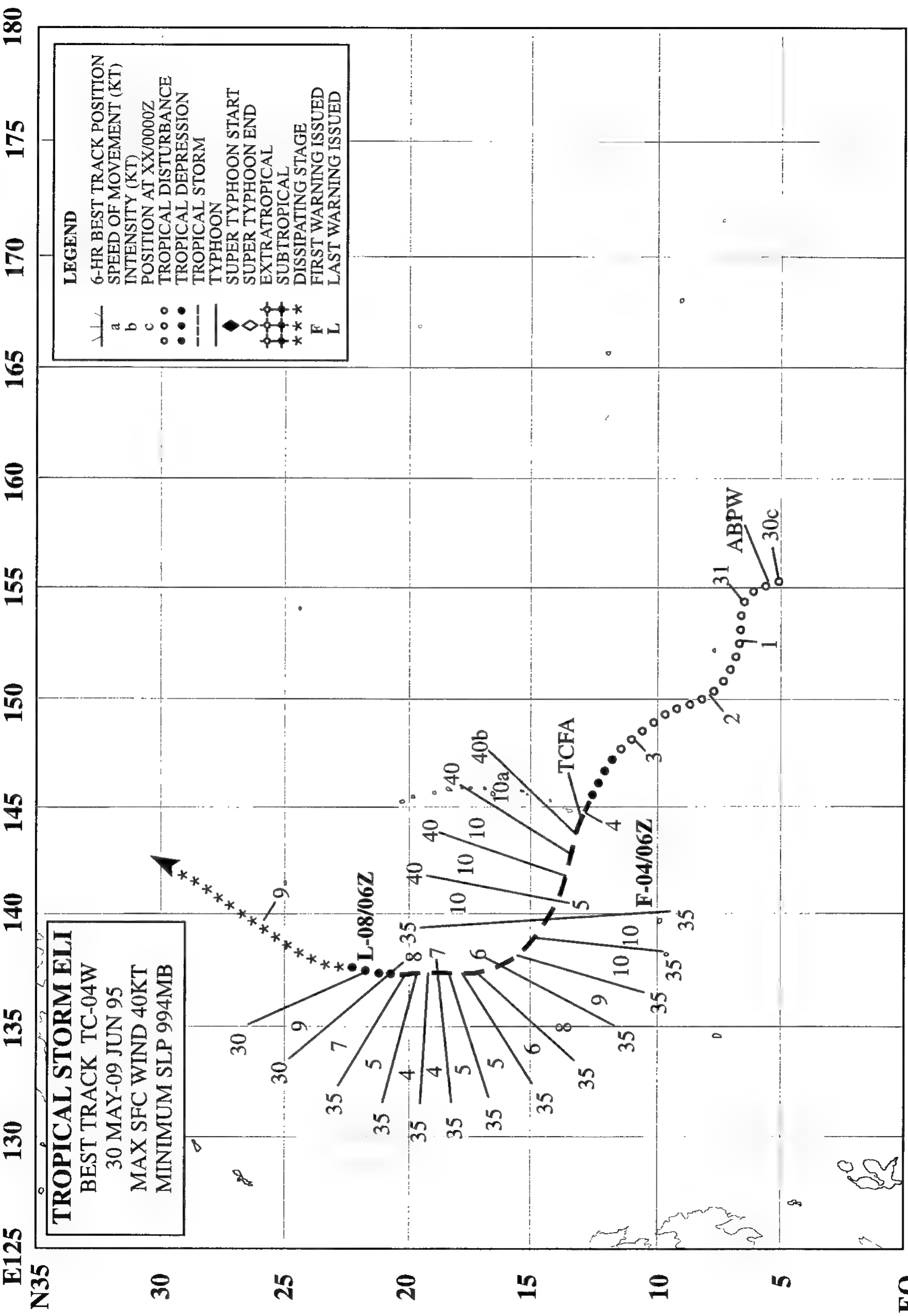
TROPICAL STORM ELI
BEST TRACK TC-04W
30 MAY-09 JUN 95
MAX SFC WIND 40KT
MINIMUM SLP 994MB
LEGEND
a 6-HR BEST TRACK POSITION
b SPEED OF MOVEMENT (KT)
c INTENSITY (KT)
POSITION AT XX/0000Z
TROPICAL DISTURBANCE
TROPICAL DEPRESSION
TROPICAL STORM
TYPHOON
SUPER TYPHOON START
SUPER TYPHOON END
EXTRATROPICAL
SUBTROPICAL
DISSIPATING STAGE
F FIRST WARNING ISSUED
L LAST WARNING ISSUED
ABPW
TCFA
F-04/06Z
L-08/06Z
E125
130
135
140
145
150
155
160
165
170
175
180
N35
30
25
20
15
10
5
EQ

TROPICAL STORM ELI (04W)

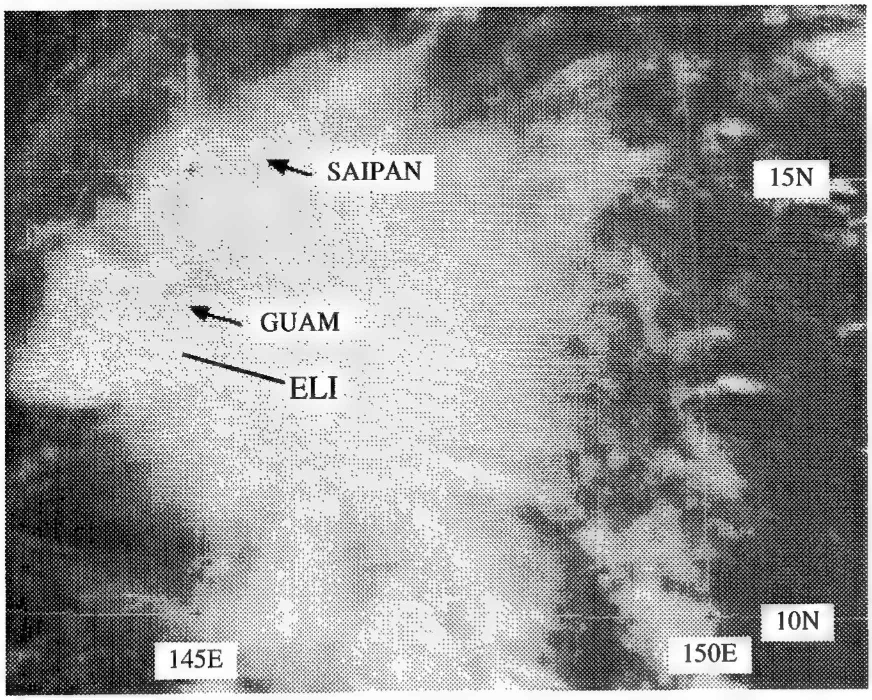

Figure 3-04-1 Eli at minimal tropical storm intensity passes south of Guam (032331Z June visible GMS imagery).

I. HIGHLIGHTS

Forming in a weak monsoon trough that stretched across Micronesia during late May, Eli was a relatively weak tropical cyclone that passed very close to Guam, turned northward, and then dissipated over open water southeast of Japan. While passing south of Guam on 04 June, Eli came within range of Guam's NEXRAD (see discussion section).

II. TRACK AND INTENSITY

During the last week of May, two tropical disturbances formed in a weak monsoon trough that stretched east-west across Micronesia (see Figure 3-03-1 of Deanna's summary). The westernmost of the two became Deanna (03W), while the easternmost became Eli (04W). The Significant Tropical Weather Advisory was reissued at 300800Z May to included the tropical disturbance that became Eli. Comments on this advisory included:

". . . A broad area of convection has persisted for 24 hours near 6°N 160°E. This broad area of convection, around 900 nm [1700 km] in diameter, is the third in a series of circulation areas associated with the establishment of the first monsoon trough of the '95 WNP season. This area is expected to continue to organize and develop over the next 72 hours. . . ."

This tropical disturbance continued moving northwestward through the Caroline Islands toward Guam. On the morning of 04 June, satellite imagery, Doppler radar (NEXRAD), and synoptic data from Guam, indicated that this disturbance had intensified. At 040230Z June, a Tropical Cyclone Formation Alert was issued, followed by the first warning on Tropical Depression 04W at 040600Z June. Based upon 34-kt wind observations received after the fact from Guam's commercial port, it was determined in postanalysis that Tropical Depression 04W had reached tropical storm intensity as it passed south of Guam on 04 June (Figure 3-04-1). In real time, Tropical Depression 04W was not upgraded to Tropical Storm Eli until 070000Z, when satellite intensity estimates increased to tropical

storm intensity. Earlier satellite intensity estimates remained at tropical depression intensity due to the appearance of westerly wind shear aloft on the cloud system and a lack of organized low-level cloud lines to define a circulation center.

At 080300Z June, Tropical Storm Eli was downgraded to a tropical depression in response to satellite imagery that indicated increasing northerly wind shear on the system. The final warning was issued shortly thereafter, at 080600Z, when satellite imagery indicated that the organization of the system had further deteriorated. In postanalysis, the intensity was held at 30 kt (15 m/sec) through 090000Z based on synoptic data.

III. DISCUSSION

NEXRAD observations of Eli as it passed south of Guam

On the morning of 04 June, the tropical disturbance that became Eli passed 30 nm (55 km) south of Guam. During the day, the wind speeds on Guam increased as the sea-level pressure fell. Position and intensity estimates made from satellite imagery did not agree with the synoptic reports from Guam. The location of the low-level circulation center as diagnosed from satellite and as determined from NEXRAD products differed by 90 nm (170 km). Guam's NEXRAD provided crucial information that allowed for a more accurate estimate of position of the low-level circulation center. The curved paths of the rainfall on the NEXRAD three-hour precipitation product (Figure 3-04-2) implied a circulation center was located near the heaviest band of rain located about 30 nm south southwest of Guam. In fact, for a few hours (centered at 040000Z), the NEXRAD generated alerts on mesocyclones forming near the downstream end of the curved rain band.

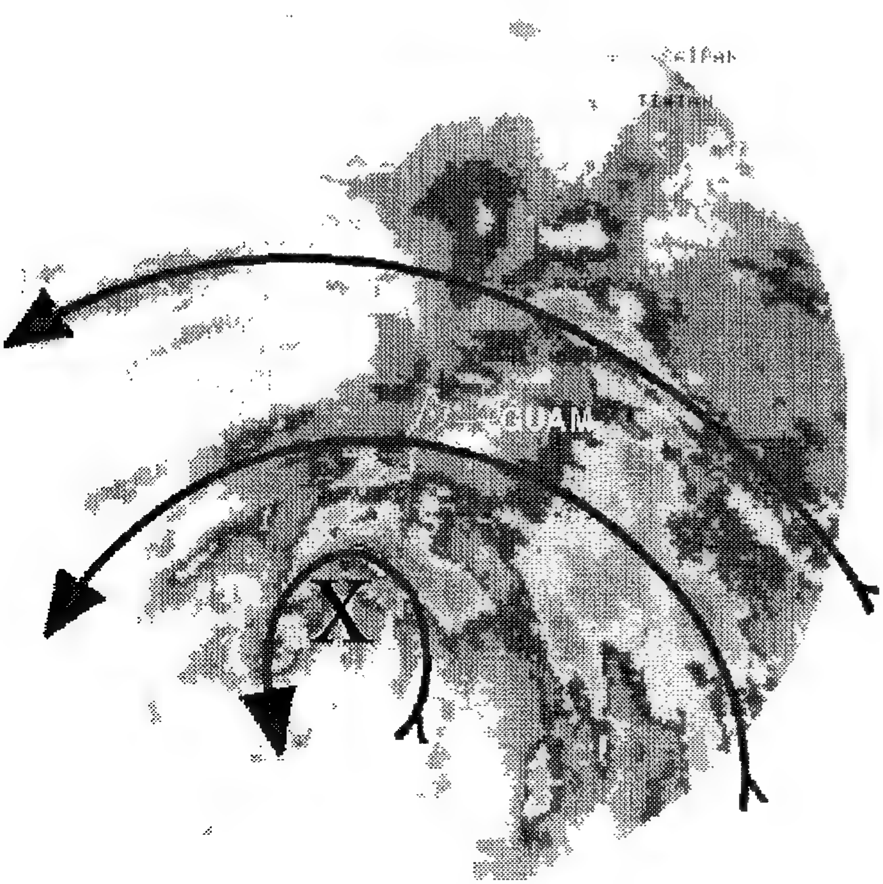

Figure 3-04-2 NEXRAD three-hour integrated rainfall total ending at 040100Z June. Shaded regions depicting the total rainfall over a three-hour period exhibit curved paths that imply a center about 30 nm southwest of Guam. The NEXRAD was producing mesocyclone alerts at the location marked with an "X".

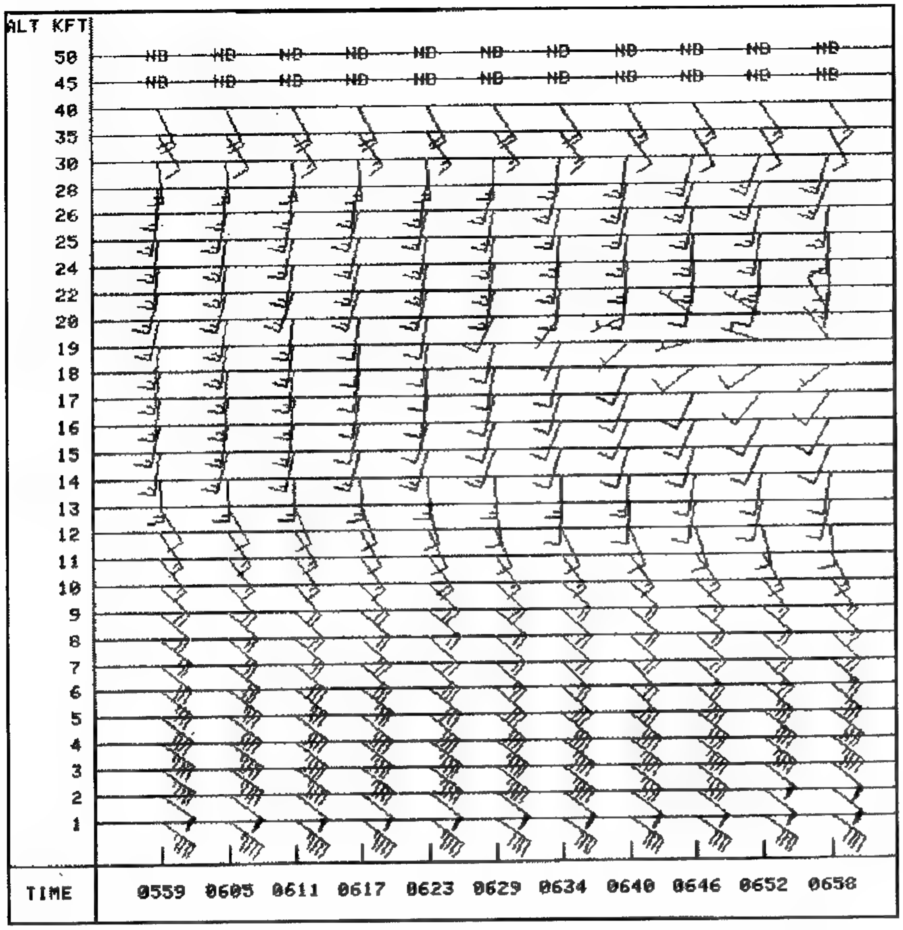

Figure 3-04-3 NEXRAD velocity azimuth display wind profile for the period 040559Z to 040658Z June shows the maximum winds associated with Eli are located at 2,000 to 3,000 feet.

The NEXRAD vertical wind profiles over Guam during the afternoon of 04 June (Figure 3-04-3) showed a peak wind velocity in the lowest levels (2,000 to 3,000 feet) of the troposphere. The 50-kt winds at 2,000 feet were reflected in a peak wind gust to 48 kt (25 m/sec) at Guam's commercial port.

In addition, the synoptic reports and information from Guam's NEXRAD suggest that Eli's wind distribution most probably featured a large asymmetry, with highest winds on the northeastern side and a very small region of light westerly wind close to the small low-level cyclonic vortex located at the western edge of the primary rain band.

IV. IMPACT

The two to three inches of rain that fell on Guam in association with Eli comprised roughly one-third of the total precipitation on Guam during an otherwise relatively dry month of June. No reports of damage or injuries were received.

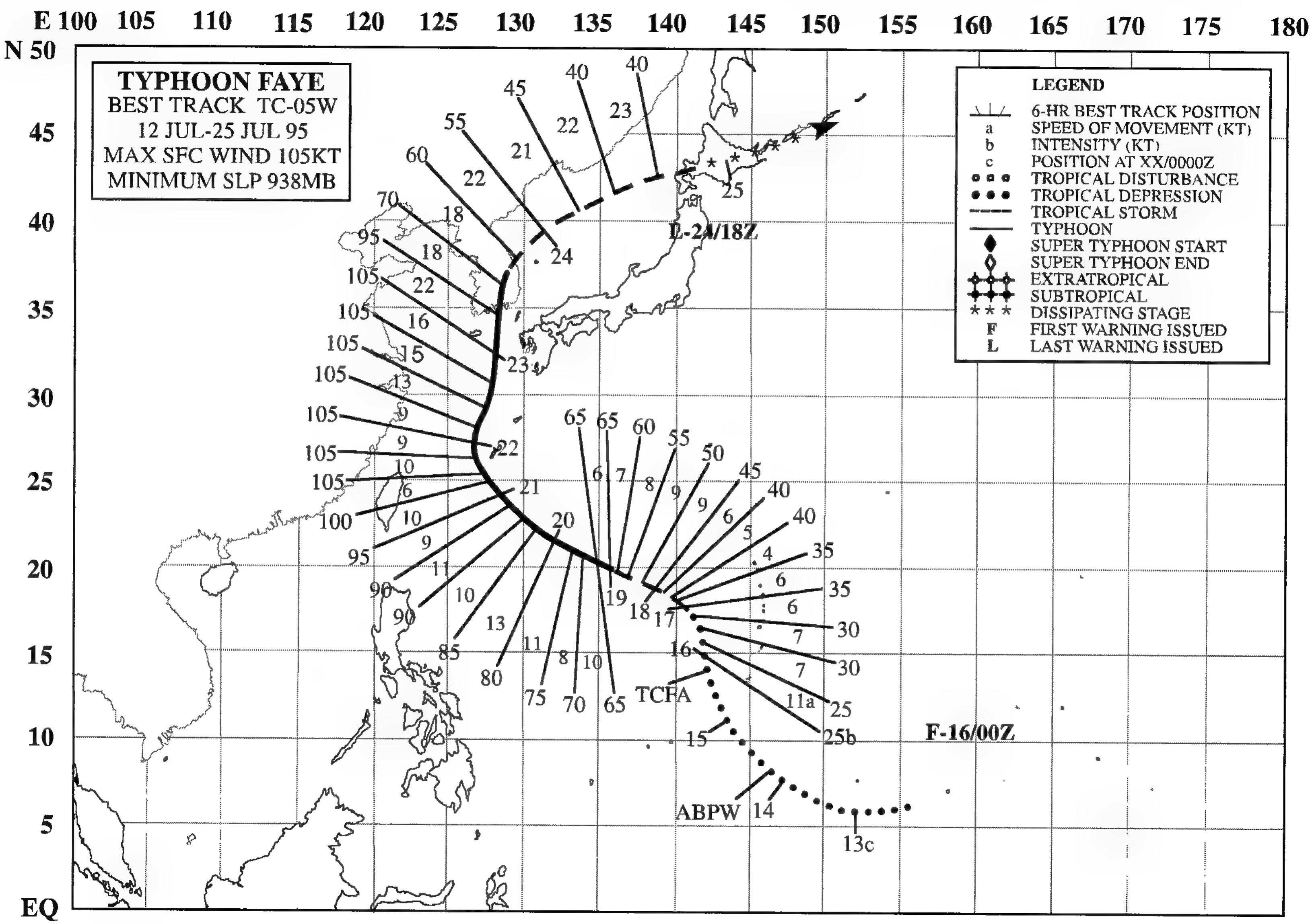
TYPHOON FAYE
BEST TRACK TC-05W
12 JUL-25 JUL 95
MAX SFC WIND 105KT
MINIMUM SLP 938MB
LEGEND
6-HR BEST TRACK POSITION
a SPEED OF MOVEMENT (KT)
b INTENSITY (KT)
c POSITION AT XX/0000Z
TROPICAL DISTURBANCE
TROPICAL DEPRESSION
TROPICAL STORM
TYPHOON
SUPER TYPHOON START
SUPER TYPHOON END
EXTRATROPICAL
SUBTROPICAL
DISSIPATING STAGE
F FIRST WARNING ISSUED
L LAST WARNING ISSUED
L-24/18Z
F-16/00Z
TCFA
ABPW
E 100 105 110 115 120 125 130 135 140 145 150 155 160 165 170 175 180
N 50 45 40 35 30 25 20 15 10 5 EQ

TYPHOON FAYE (05W)

I. HIGHLIGHTS

Faye (05W) was the first tropical cyclone of 1995 to become a typhoon. Reaching typhoon intensity on 19 July, Faye tied the record for the latest date for the occurrence of a typhoon in the western North Pacific. Moving on a north-oriented track through the East China Sea, Faye made landfall on the southern coast of Korea, and was one of the most intense tropical cyclones to strike the Korean peninsula in many years.

II. TRACK AND INTENSITY

During the first week of July, most of the deep convection in the tropics of the western North Pacific was located near the Philippines and over the South China Sea. Throughout Micronesia, amounts of deep convection were relatively low, the low-level winds were predominantly from the east, and the upper-level winds were predominantly from the west (creating a zone of high vertical wind shear within which isolated mesoscale convective systems grew and decayed). Toward the end of the second week of July, an area of persistent deep convection was located in the Caroline Islands. On 14 July, synoptic data indicated that a low-level circulation center accompanying this area of deep convection was located about 300 nm (550 km) south-southeast of Guam, prompting its first mention on the 140600Z July Significant Tropical Weather Advisory. During the next 24 hours, this weak low-level circulation turned toward the north-northwest and passed about 180 nm (330 km) to the west of Guam. Late on 15 July, satellite imagery and radar data from Guam indicated that the organization of the system was improving. A Tropical Cyclone Formation Alert was issued at 151730Z.

On the morning of 16 July, visible satellite imagery indicated that the system had a well-defined low-level circulation center associated with its small area of deep convection. This prompted the JTWC to issue the first warning on Tropical Depression 05W, valid at 160000Z. Despite numerical guidance (i.e., NOGAPS) that indicated that the system would not deepen, the relatively small-sized tropical cyclone continued to intensify and, on the warning valid at 170600Z, Tropical Depression 05W was upgraded to Tropical Storm Faye. In keeping with indications of northeasterly shear on the system, and with NOGAPS not indicating deepening, Faye was not forecast to reach typhoon intensity.

Faye continued to intensify as it moved northwestward toward Okinawa. It was upgraded to a typhoon on the warning valid at 191200Z. After passing to the southwest of Okinawa on 21 July, Faye turned to the north and intensified. It reached its peak intensity of 105 kt (54 m/sec) at 211200Z as it was moving northward (Figure 3-05-1). Now on a north-oriented track, Faye maintained its intensity of 105 kt (54 m/sec) for the next 36 hours. It began to weaken after 230000Z, while accelerating toward Korea. Shortly after 230600Z, Faye made landfall on the south coast of Korea with an intensity of 95 kt (49 m/sec) (Figure 3-05-2). Weakening rapidly over the Korean peninsula, Faye was downgraded to a tropical storm on the warning valid at 240000Z after it had recurved and entered the Sea of Japan. In postanalysis it was downgraded to a tropical storm about nine hours earlier, while it was over the mountains of Korea. Moving rapidly across the Sea of Japan, Faye continued to weaken, and the final warning was issued, valid at 241800Z, shortly before it made landfall on the west coast of Hokkaido.

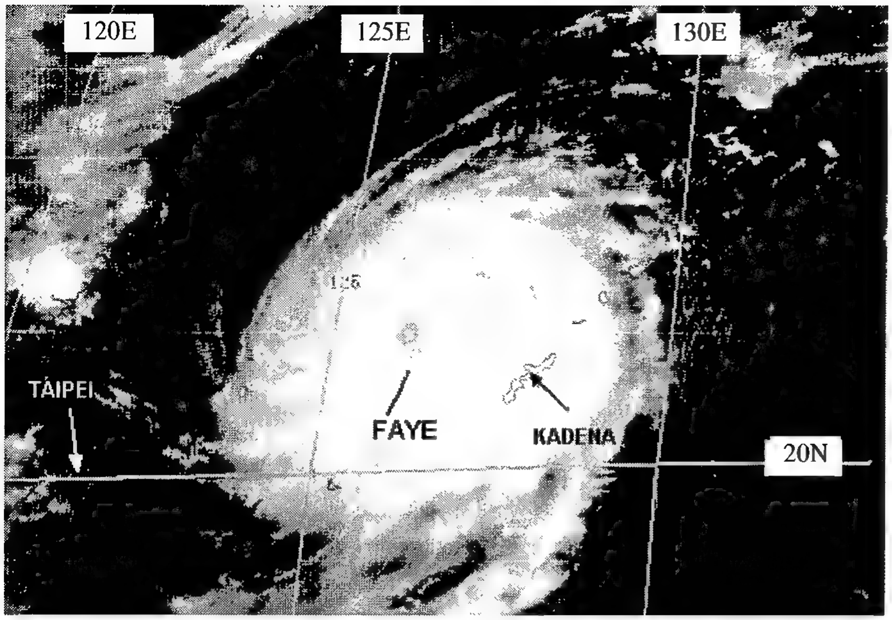

Figure 3-05-1 Faye at peak intensity of 105 kt (54 m/sec) (212331Z July visible GMS imagery).

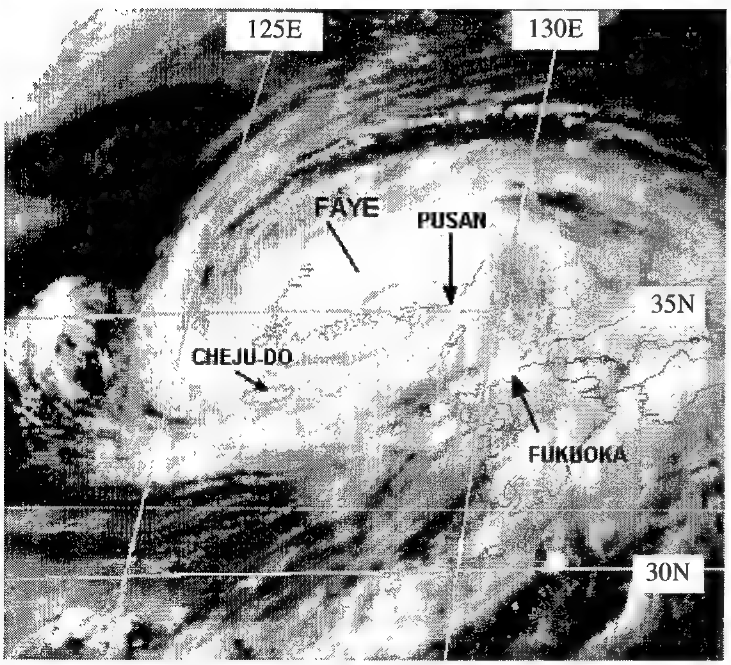

Figure 3-05-2 Faye makes landfall on the southern coast of Korea (230831Z July visible GMS imagery).

III. DISCUSSION

a. *A late date for the first typhoon*

Faye became a typhoon on 19 July, tying the latest date in the year for a tropical cyclone to become a typhoon in the western North Pacific. In the 37-year period 1959-1995, only one other year — 1977 — had such a late date of record for the first tropical cyclone of typhoon intensity. Other years during which the first typhoon intensity was recorded in July (but before 19 July) include 1973 (07 July), 1983 (11 July), and 1984 (02 July). Note: the latest occurrence of typhoon intensity during what might be considered the most active part of the year in the western North Pacific was 01 August 1975, not counting the occurrence of a typhoon during January of that year.

b. *Forecast performance*

The JTWC's mean track forecast errors for Faye (91 nm, 194 nm, and 348 nm at 24, 48, and 72 hours respectively) were close to their long-term averages. During the period 21 through 23 July, however, Faye underwent a synoptic-scale meander along its north-oriented track that led to track forecasts with some large errors. By 220000Z, Faye had passed to the west of Okinawa and began to head to the north-northeast. At 221200Z it appeared that Faye had begun its recurvature to the northeast, and a significant track change was forecast, bringing Faye along an accelerating recurve trajectory that skirted along the southeastern coast of Japan (Figure 3-05-3). This was in sharp contrast to earlier track forecasts that had Faye tracking northward toward the coast of southern Korea. Soon after 221200Z, Faye's track began to shift back to a more northward direction, and the next warning, valid at 221800Z indicated that Faye would pass approximately 35 nm (65 km) to the east of Pusan, Korea — the 24-hour forecast position on this warning was nearly 240 nm (450 km) to the northwest of the 24-hour forecast position given on the previous warning. Faye's meandering track caused the JTWC to incur some large forecast errors.

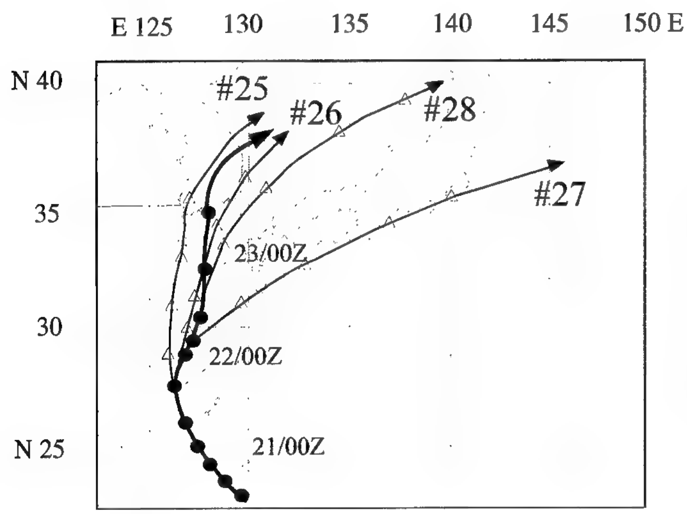

Figure 3-05-3 A synoptic-scale meander in Faye's track prompts dramatic changes in the forecast track. The final best track is indicated by the thick black line that connects large black dots at six hour intervals. The thin lines connecting the open triangles indicate the forecast track of the indicated warning. Open triangles are at 12-hour intervals.

IV. IMPACT

As Faye approached Okinawa, aircraft from Kadena Air Force Base were evacuated to Guam and other locations. Kadena reported gales and gusts over 50 kt throughout the evening of 21 July as Faye passed about 120 nm (220 km) to the southwest.

On the afternoon of 23 July, the USNS Wilkes (an oceanographic survey ship operated by the Commander, Military Sealift Command for the Commander, Naval Meteorology and Oceanography Command) was overtaken by Typhoon Faye, and probably experienced eye passage. During its encounter with Faye, the Wilkes reported winds of 70-80 kt (36-41 m/sec) and a minimum sea level pressure of 965 mb. At approximately 230530Z July, the master of Wilkes judged that the ship was in the eye of Faye. Damage to the Wilkes caused by Typhoon Faye included: broken wires, lights, and chemical containers; numerous holes in the deck; crane cradle torn loose; VHF and INMARSAT antennae damaged; salt water contamination of oil in all deck machinery; and damage to scientific equipment stowed on weather decks. Personnel casualties were limited to only one minor head laceration.

In the East China Sea, the cargo ship Far East Beauty sank with two Chinese crewmen reported dead and three others missing. In Korea, Faye was described as the worst typhoon to hit the Korean peninsula in 37 years. It capsized dozens of small boats, overturned cars, uprooted trees, and disrupted train

service. At least 14 people were reported killed and 21 others were missing. Nine people died and three were missing after high surf swept a bus off of a coastal highway. The 140,000-ton tanker Sea Prince ran aground and leaked oil into the sea around Yochon, one of many small islands off the coast of Yosu on the southern tip of South Korea. In southern Japan, the typhoon disrupted air travel and caused power outages, but no injuries or deaths were reported. U.S. military bases in South Korea and Japan reported no significant damage.

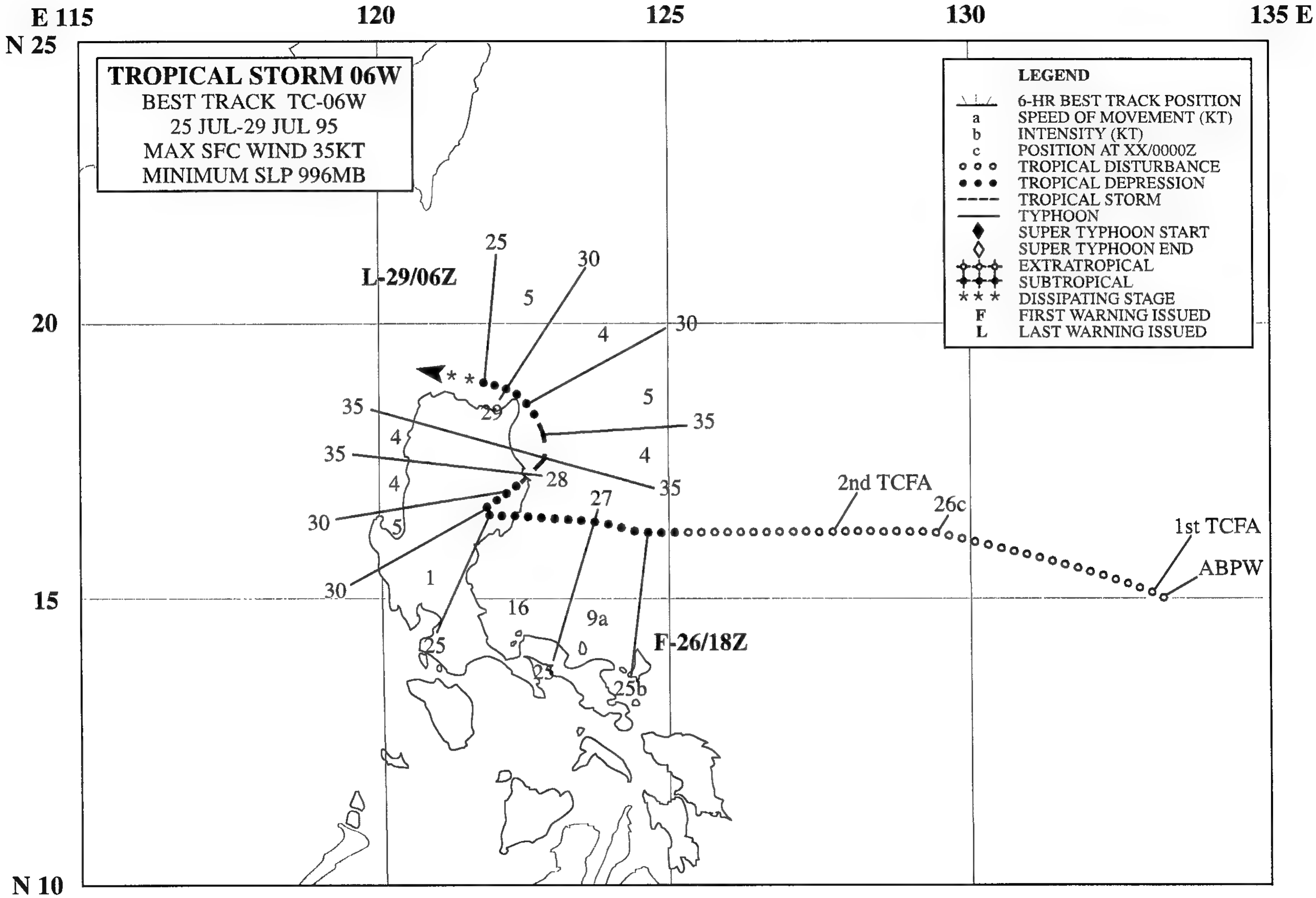
E 115
120
125
130
135 E
N 25
20
15
N 10
TROPICAL STORM 06W
BEST TRACK TC-06W
25 JUL-29 JUL 95
MAX SFC WIND 35KT
MINIMUM SLP 996MB
LEGEND
6-HR BEST TRACK POSITION
a SPEED OF MOVEMENT (KT)
b INTENSITY (KT)
c POSITION AT XX/0000Z
TROPICAL DISTURBANCE
TROPICAL DEPRESSION
TROPICAL STORM
TYPHOON
SUPER TYPHOON START
SUPER TYPHOON END
EXTRATROPICAL
SUBTROPICAL
DISSIPATING STAGE
F FIRST WARNING ISSUED
L LAST WARNING ISSUED
L-29/06Z
F-26/18Z
1st TCFA
ABPW
2nd TCFA
26c
25b
9a

TROPICAL STORM 06W

I. HIGHLIGHTS

In postanalysis, Tropical Depression 06W was upgraded to tropical storm intensity based upon scatterometer data from the European Space Agency's remote sensing (ERS-1) satellite. These data indicated that an area of 35 kt (18 m/sec) wind speed accompanied Tropical Depression 06W as it moved northward just off the east coast of Luzon on 28 July. Conventional visible and infrared satellite imagery also supported the post-event upgrade. Tropical Storm 06W merged withTropical Storm Gary (07W) during a time when both of these tropical cyclones were embedded within the circulation of a larger monsoon depression, and while both were affected by the island of Luzon.

II. TRACK AND INTENSITY

The tropical disturbance that became Tropical Storm 06W began as a large area of disturbed weather near the Mariana Islands. This tropical disturbance was first mentioned on the 230600Z July Significant Tropical Weather Advisory. Moving westward as a large weak monsoon depression, the convection in this tropical disturbance expanded as it approached the Philippines. On 25 July, a smaller area of deep convection, within the confines of the larger monsoon depression, became focused near a poorly defined low-level circulation center. A Tropical Cyclone Formation Alert (TCFA) was issued at 250800Z July based upon expectations that this area of deep convection would continue to develop and become a significant tropical cyclone within 24 hours. When the system failed to intensify, a second TCFA was issued at 260800Z. The first warning on 06W, valid at 261800Z, was issued by JTWC when the amount of deep convection increased and lines of deep convective cloud began to exhibit increased cyclonic curvature.

On 27 July, 06W moved ashore on the east coast of the island of Luzon. At this time, the synoptic situation became more complex, as the larger scale circulation of the monsoon depression, within which 06W was embedded, began to be affected by the island of Luzon. In addition to Tropical Storm 06W, there was evidence that a second circulation was forming in the South China Sea just off the northwest corner of Luzon. This second circulation became Typhoon Gary (07W). In response to a surge in the southwest monsoon, coupled with an interaction with the developing Gary (07W), 06W stalled over land on the eastern side of Luzon, and then moved northeastward back over water.

As visible satellite imagery became available on the morning of 28 July, it indicated that the low-level circulation center of Tropical Storm 06W had moved back over water east of Luzon. At 280000Z, JTWC relocated the center of 06W. During the daylight hours of 28 July, the well-defined, exposed, low-level circulation center of 06W (Figure 3-06-1) moved northward, over water, east of Luzon (it was at this time that scatterometer winds obtained from the ERS-1 satellite indicated that the wind speeds associated with 06W had reached tropical storm intensity — see the discussion section for more details). For several hours, later in the day, a circular area of deep convection developed in association with the low-level circulation center (Figure 3-06-2). During the night of 28 July, and into the morning of 29 July, the convection associated with 06W moved on a cyclonically curved track around the northeastern coast of Luzon, and was absorbed into cloud bands associated with the developing Gary (07W). The Prognostic Reasoning Message accompanying the 290000Z July warning stated:

". . . 06W is becoming more disorganized as the circulation to the west of Luzon (Tropical Depression 07W) becomes more dominant. Synoptic data around Luzon also shows the western circulation [TD 07W] affecting most of the monsoon flow over this region. However, synoptic data . . . still

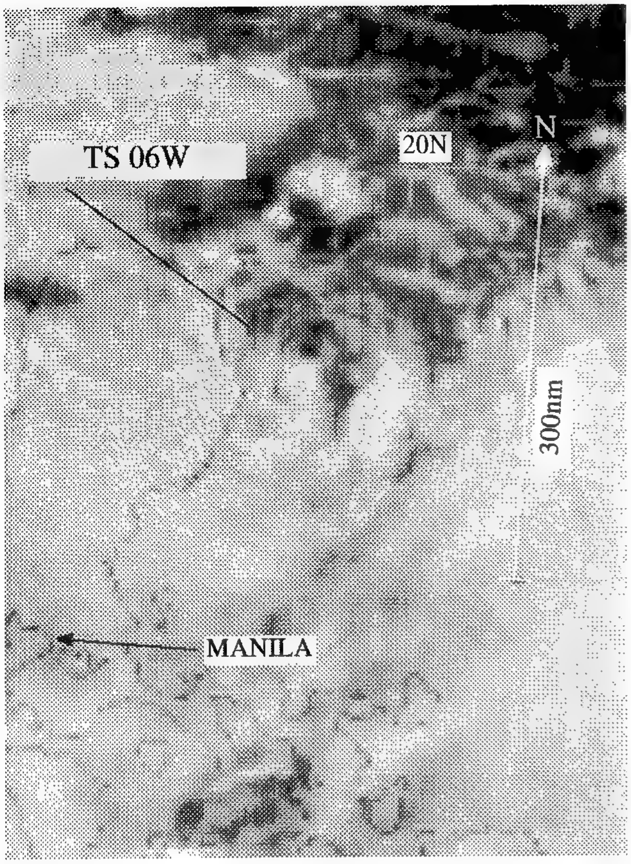

Figure 3-06-1 The well-defined and tightly wrapped low-level cloud lines of the exposed circulation of Tropical Storm 06W are seen just east of Luzon (280031Z July visible GMS imagery).

support a 999 mb circulation just north of the island of Luzon. . . ."

The final warning on Tropical Storm 06W was issued at 290600Z when, according to remarks on the warning:

". . . Latest satellite and synoptic data reveal that the surface circulation that was once ....06W has become completely entrained into the large circulation of TD 07W . . ."

III. DISCUSSION

TD 06W— an unnamed tropical storm

While 06W was moving northward, over water east of Luzon on 28 July (see Figures 3-06-1 and 3-06-2), the scatterometer aboard the ERS-1 spacecraft obtained a pass directly over the circulation center (Figure 3-06-3). Wind speeds of 35 kt (18 m/sec) were indicated by the scatterometer in the vicinity of 06W. In postanalysis, these scatterometer-derived wind speeds, and also synoptic data supporting an estimated central sea-level pressure of 996 mb, were used to upgrade the estimated peak intensity of 06W to 35 kt (18 m/sec). Figure 3-06-3 is a classic example of the wind direction algorithm used to process the scatterometer data failing on its first guess. This resulted in all the wind directions being plotted 180° out of phase — e.g. the wind field that curves anticyclonically is in reality cyclonically curved.

Over the past several years, the JTWC has been receiving and evaluating unconventional sources of remotely sensed marine wind speeds (e.g., the scatterometer-derived winds, and the SSM/I wind speeds). These scatterometer winds, from JTWC's perspective, are sufficiently accurate to be a useful tool in diagnosing the structure of the low-level wind field within and near tropical cyclones.

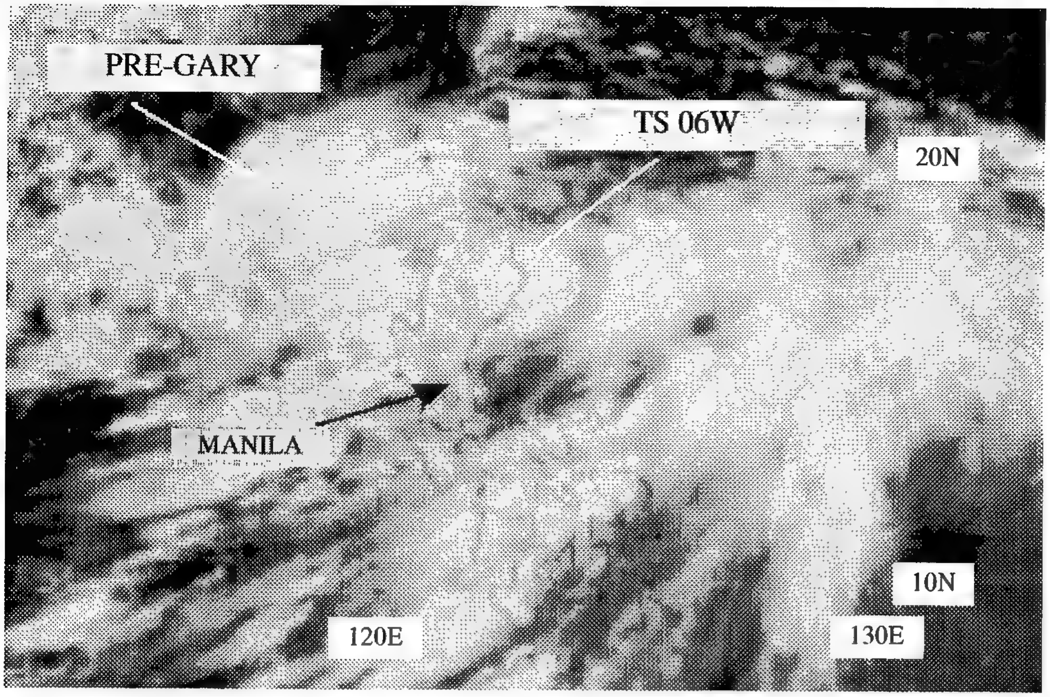

Figure 3-06-2 Deep convection has formed at the center of Tropical Storm 06W. Gary (07W) can be seen forming northwest of Luzon (280424Z July visible GMS imagery).

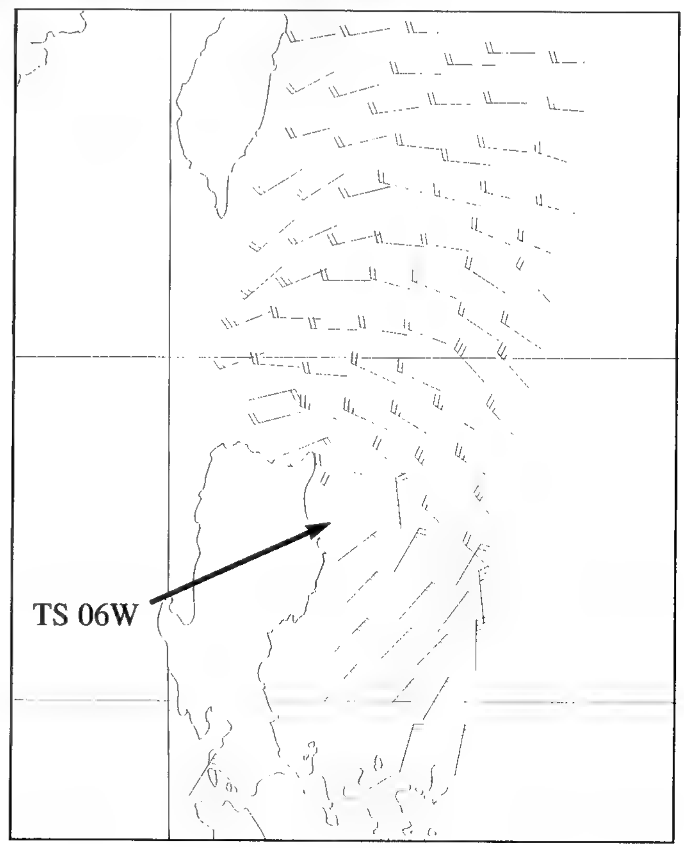

20N

15N

120E

Figure 3-06-3 Scatterometer-derived wind speeds in a swath that passed over 06W (280214Z July ERS-1 scatterometer-derived marine surface wind speeds). The 35-kt (18-m/sec) wind speeds define the center of TS 06W. (The wind direction algorithm's first guess resulted in all the wind directions being 180 degrees in error).

IV. IMPACT

No reports of damage or injuries were received.

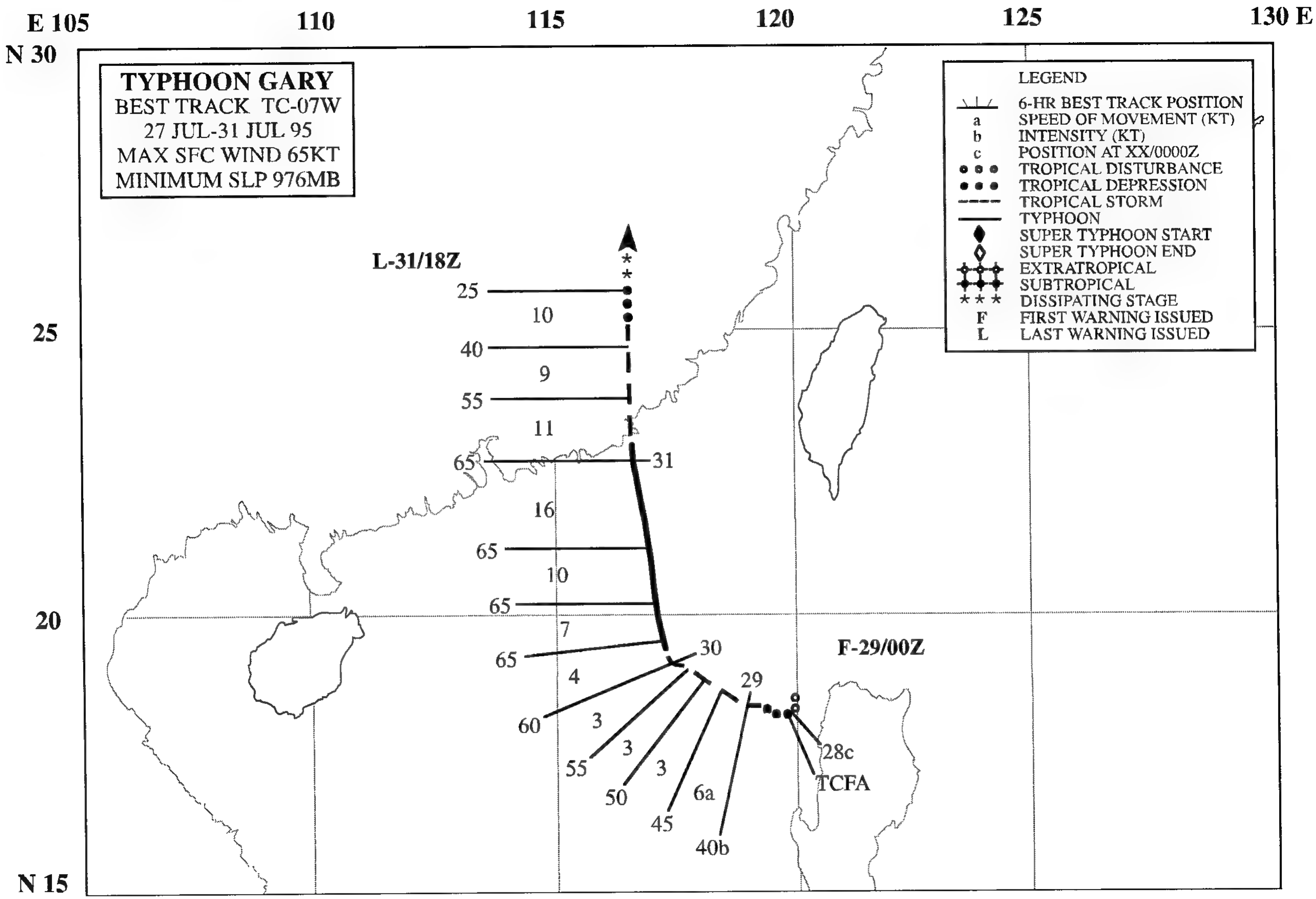
E 105
110
115
120
125
130 E
N 30
25
20
N 15
TYPHOON GARY
BEST TRACK TC-07W
27 JUL-31 JUL 95
MAX SFC WIND 65KT
MINIMUM SLP 976MB
LEGEND
6-HR BEST TRACK POSITION
a SPEED OF MOVEMENT (KT)
b INTENSITY (KT)
c POSITION AT XX/0000Z
TROPICAL DISTURBANCE
TROPICAL DEPRESSION
TROPICAL STORM
TYPHOON
SUPER TYPHOON START
SUPER TYPHOON END
EXTRATROPICAL
SUBTROPICAL
DISSIPATING STAGE
F FIRST WARNING ISSUED
L LAST WARNING ISSUED
L-31/18Z
F-29/00Z
25
10
40
9
55
11
65
31
16
65
10
65
7
65
30
4
60
3
55
3
50
3
45
6a
40b
29
28c
TCFA

TYPHOON GARY (07W)

I. HIGHLIGHTS

Gary (07W) merged with Tropical Storm 06W during a time when both of these tropical cyclones were embedded within the circulation of a large monsoon depression near the island of Luzon (see also the summary of Tropical Storm 06W). Gary made landfall in southeastern China very close to the city of Shantou. Based upon ship reports received in a delayed mode on the Weekly Tropical Cyclone Summaries compiled by Mr. Jack Beven of the National Hurricane Center, and upon delayed reports of typhoon intensity wind speeds experienced in the city of Shantou that accompanied severe damage to a newly constructed sea wall, Gary was upgraded from a tropical storm to a typhoon in post-analysis.

II. TRACK AND INTENSITY

During the last week of July, a monsoon depression moved westward over the Philippine Islands. There were multiple low-level circulation centers in this monsoon depression — one of these became Tropical Storm 06W, and another became Typhoon Gary (07W).

As early as 270600Z July, when Tropical Depression 06W was making landfall on the island of Luzon, it was noted in the remarks section of JTWC's second warning for Tropical Depression 06W that a secondary circulation may be forming off the west coast of Luzon. On 28 July, as Tropical Storm 06W moved northward just east of Luzon, a Tropical Cyclone Formation Alert was issued at 280230Z July indicating the possibility of further development of the circulation west of Luzon. The Prognostic Reasoning Message that accompanied the 281200Z July warning on 06W included the following synoptic discussion:

"... Infrared satellite imagery shows a broad region of convection that extends from 112°E to 135°E. Synoptic data indicate there are two distinct circulations in this region of convection ... 06W is a well-defined [low-level circulation center] ... just east of Luzon with minimum sea-level pressure estimated at 996 mb.... The second circulation evident in this broad region of convection is west of the island of Luzon, and the possibility exists for this area to also develop into a significant tropical cyclone ..."

On the morning of 29 July, satellite imagery indicated that the circulation west of Luzon had become more organized. It was upgraded to Tropical Depression 07W at 290000Z. At 290600Z, Tropical Storm 06W was entrained into the circulation of Tropical Depression 07W — the final warning was thus issued on 06W, and 07W continued to move slowly westward in the South China Sea. At 291200Z, Tropical Depression 07W was upgraded to Tropical Storm Gary. The Prognostic Reasoning Message accompanying this warning included the following synoptic discussion:

"... Tropical Depression 07W has intensified and has been upgraded to Tropical Storm Gary. Gary is tracking slowly to the north-northwest in the South China Sea. Satellite imagery indicates that the system has become more organized [and has absorbed] the remnants of former Tropical Depression 06W... Intensity estimates are based upon a combination of satellite analysis and ... a 40 kt [21 m/sec] ship observation near the system center. ..."

On 30 July, Gary accelerated northward and intensified. Shortly before 310600Z July, Gary made landfall near the city of Shantou in southeastern China (Figure 3-07-1). In real time, the peak intensity was estimated to be 60 kt (31 m/sec), however, in postanalysis, it was determined that Gary most prob-

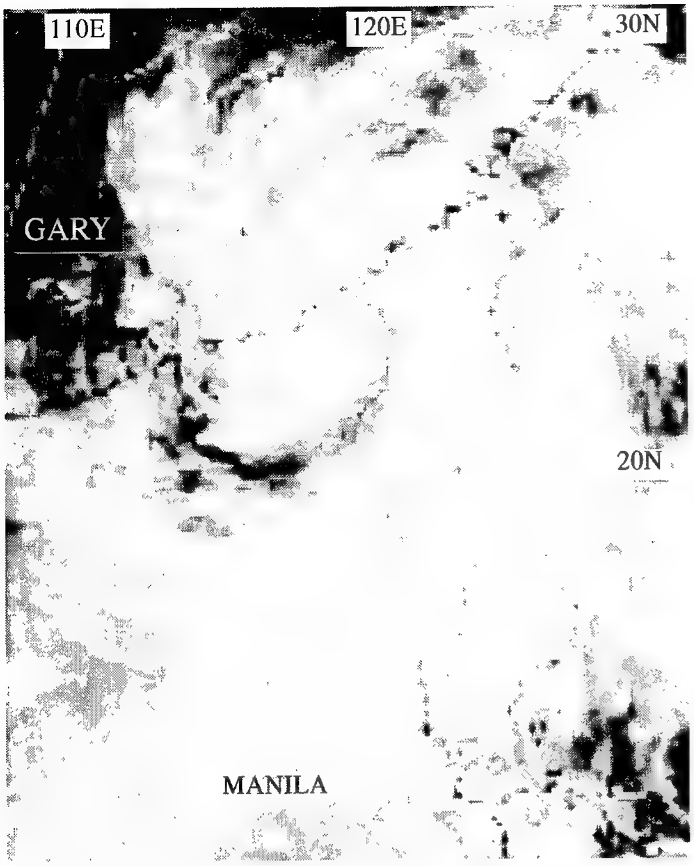

Figure 3-07-1 Gary becomes a typhoon shortly before making landfall near the city of Shantou (302331Z July visible GMS imagery).

ably became a typhoon a day earlier at 300600Z. Gary was well inland in southeastern China when JTWC issued the final warning valid at 311800Z July.

III. DISCUSSION

Island effects

The complex behavior of Tropical Storm 06W and the developing Gary (07W) while they were near the island of Luzon presented a unique forecasting challenge. Initially, as Tropical Storm 06W approached the Philippines, it was thought that it would pass across the islands into the South China Sea, and then intensify. When it stalled over Luzon, and a second circulation appeared to be forming off of the northwest coast of Luzon, it became unclear which circulation would dominate, or whether two would form and undergo a binary interaction.

A case can be made that TD 07W developed from a lee side low that formed off the northwest coast of Luzon as the center of the monsoon depression moved across the central Philippines. Another interesting feature to note is the binary interaction — at close range, and ending in merger — that 06W and 07W underwent for approximately 30 hours (Figure 3-06-2a,b). The after the fact upgrade to typhoon intensity at 300600Z was based on a 62 kt (32 m/sec) ship report that appeared in Mr. Jack Beven's Weekly Tropical Cyclone Summary #208. Gary appeared to have maintained minimal typhoon intensity until making landfall near Shantou a day later.

IV. IMPACT

A newly constructed sea wall was seriously damaged as Gary made landfall near the city of Shantou along the southeastern coast of China. No other reports of significant damage or serious injuries were received.

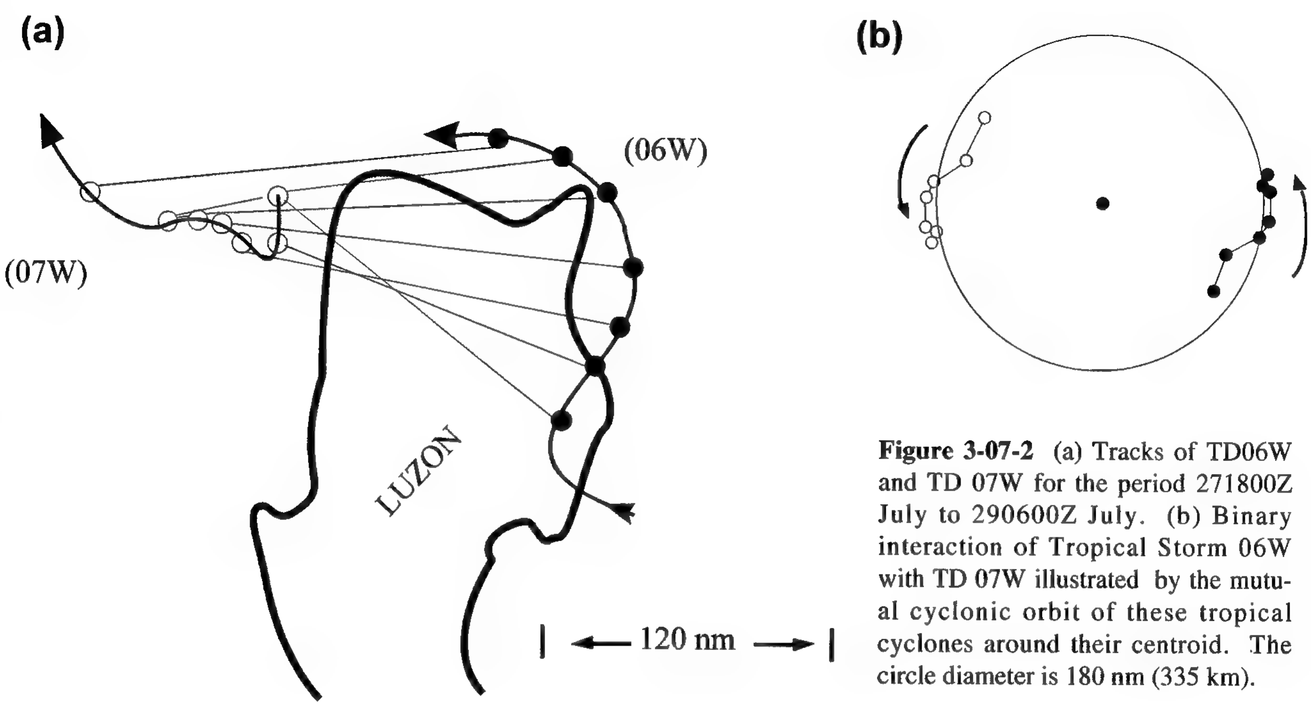

Figure 3-07-2 (a) Tracks of TD06W and TD 07W for the period 271800Z July to 290600Z July. (b) Binary interaction of Tropical Storm 06W with TD 07W illustrated by the mutual cyclonic orbit of these tropical cyclones around their centroid. The circle diameter is 180 nm (335 km).

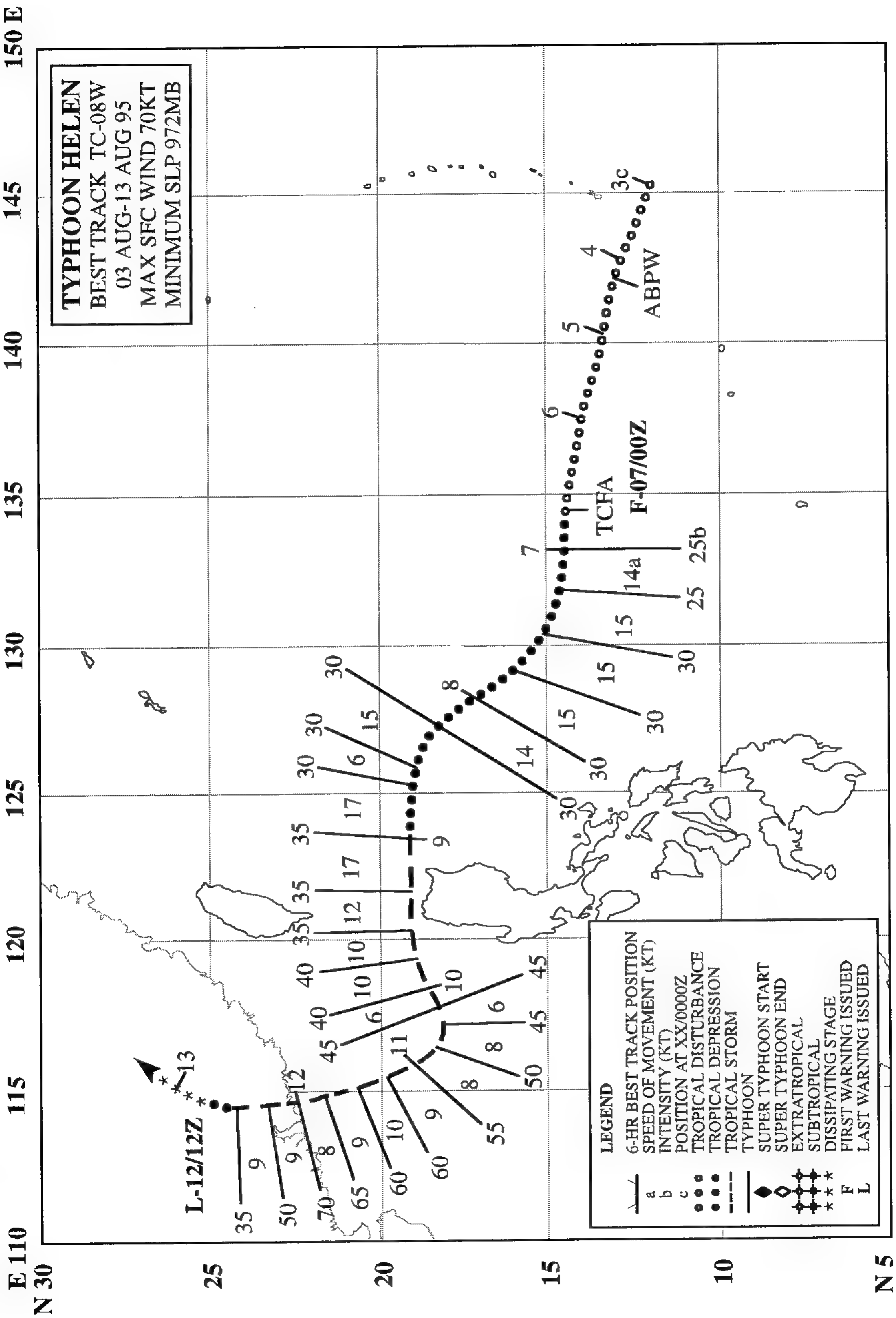
TYPHOON HELEN
BEST TRACK TC-08W
03 AUG-13 AUG 95
MAX SFC WIND 70KT
MINIMUM SLP 972MB
LEGEND
6-HR BEST TRACK POSITION
SPEED OF MOVEMENT (KT)
INTENSITY (KT)
POSITION AT XX/0000Z
TROPICAL DISTURBANCE
TROPICAL DEPRESSION
TROPICAL STORM
TYPHOON
SUPER TYPHOON START
SUPER TYPHOON END
EXTRATROPICAL
SUBTROPICAL
DISSIPATING STAGE
FIRST WARNING ISSUED
LAST WARNING ISSUED
TCFA
F-07/00Z
L-12/12Z
ABPW
E 110
115
120
125
130
135
140
145
150 E
N 30
25
20
15
10
N 5

TYPHOON HELEN (08W)

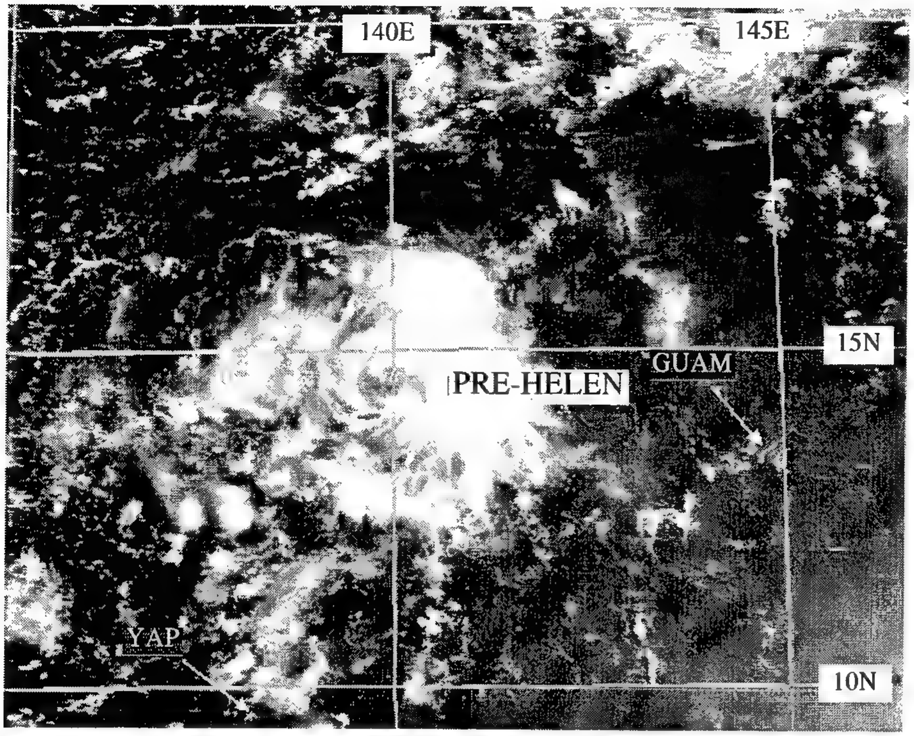

Figure 3-08-1 This vortical cloud pattern was observed about 300 nm (550 km) to the west of the region where, a day earlier, a large MCS had grown and collapsed. Appearing well-organized, it later dissipated, and new deep convection in the pre-Helen tropical disturbance developed further to the south and west (050131Z August visible GMS imagery).

I. HIGHLIGHTS

Helen (08W) was upgraded to typhoon intensity in postanalysis based on data obtained from the Royal Observatory Hong Kong. Originating near Guam, the tropical disturbance that became Helen was slow to develop, taking six days to reach tropical storm intensity. Helen skirted northern Luzon and, after moving into the South China Sea, dipped toward the west-southwest for a day prior to turning to the north-northwest and intensifying. Helen reached a peak intensity of 70 kt (36 m/sec) just before making landfall east of Hong Kong.

II. TRACK AND INTENSITY

Despite the persistent easterly low-level winds that dominated the western North Pacific through early August, a weak low-level cyclonic circulation developed to the south of Guam on 03 August. Scatterometer data from the ERS-1 satellite indicated that the surface circulation had an intensity of 15 kt (8 m/sec). For the next three days, the disturbance moved to the west-northwest and remained poorly organized. A large mesoscale convective system (MCS) that formed over Guam on 04 August, collapsed by the early morning of 05 August and left behind a well-defined, but short-lived, vortical cloud pattern (Figure 3-08-1). The vortical cloud pattern dissipated by the evening of 05 August, and one can not establish a direct link between it and the subsequent development of Helen (see the discussion section for more details on the generation of mid-tropospheric vortices by MCSs and their possible association with tropical cyclogenesis).

Organized convection began to persist by 06 August and a Tropical Cyclone Formation Alert was issued valid at 061830Z. The first warning on Tropical Depression 08W was issued, valid at 070000Z, as the tropical disturbance intensified. During the evening of 07 August, TD 08W turned to the north-

west, as monsoon winds to its southwest strengthened and deepened. On 08 August, the tropical depression turned to the west in response to easterly wind flow south of the mid-tropospheric subtropical ridge. Based on intensity estimates made from satellite imagery, Tropical Depression 08W was upgraded to Tropical Storm Helen on the warning valid at 090000Z. On 09 August, Helen moved westward about 30 nm (55 km) north of Luzon. After the system cleared the northwest tip of Luzon and entered the South China Sea, it slowed and took a dip to the west-southwest for about 24 hours.

At approximately 101800Z, Helen turned abruptly to the north-northwest and accelerated to an average speed of 9 kt (17 km/hr). This turn was most probably due to the modification of the steering flow by the deepening southerly flow of a surging monsoon to the southwest of the tropical cyclone. Such sudden track changes that are caused by the interaction of a tropical cyclone with the monsoon flow are described by Carr and Elsberry (1994).

Helen intensified after turning to the north-northwest (Figure 3-08-2). During postanalysis, wind observations from Waglan Island (WMO 45007), which were obtained from the Royal Observatory in Hong Kong, revealed that Helen reached typhoon intensity before making landfall in southern China early on 12 August (for further details about the postanalysis upgrade of Helen to typhoon intensity see the discussion section). The JTWC issued the final warning valid at 121200Z as Helen dissipated over the mountains of southern China.

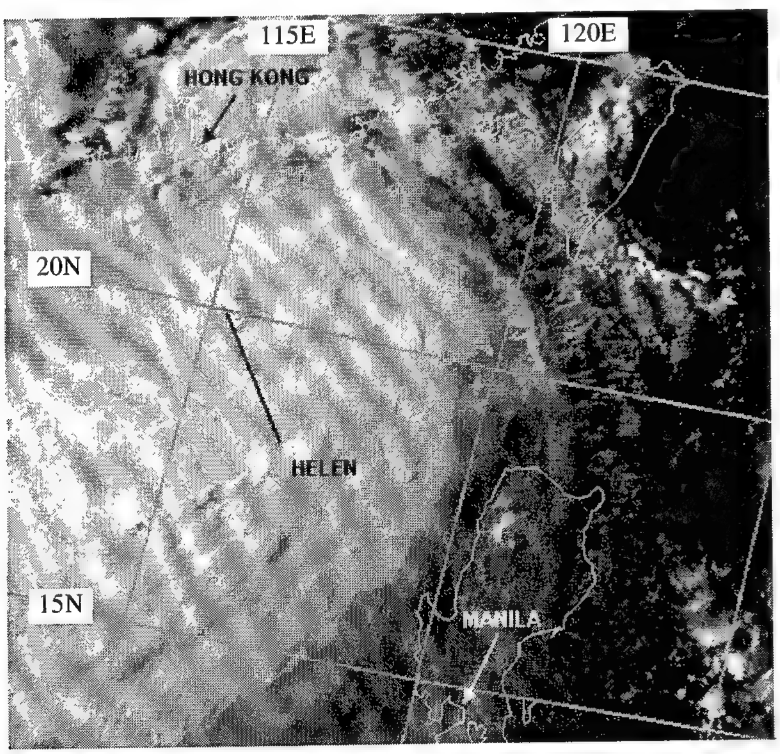

Figure 3-08-2 An intensifying Tropical Storm Helen is located about 150 nm (275 km) south of Hong Kong. The intensity is estimated to be 60 kt (31 m/sec) (110854Z August visible DMSP imagery).

III. DISCUSSION

a. *On the use of microwave imagery to modify the Dvorak intensity estimate*

Between 110000Z and 120000Z, most of the satellite intensity estimates for Helen made by applying Dvorak's techniques to visible (e.g., Figure 3-08-2) and infrared satellite imagery had a magnitude of T3.0 (45 kt) to T3.5 (55 kt), while analysts at the AFGWC assigned it a T4.0 (65 kt). The higher T number assigned to Helen by the AFGWC was based upon additional information about the structure of the tropical cyclone as revealed by microwave imagery. Able to see through the overlying cirrus with

the microwave sensor, they noted a well-developed circular eye and wall cloud. Thus, the AFGWC analysts upped their intensity estimates by one-half a T number to arrive at the T4.0 estimate for the 111525Z and 120230Z DMSP satellite fixes. Confirmation of Helen's typhoon status was later obtained from wind observations at Waglan Island where one-minute average sustained winds were 65 kt (33 m/sec) at 111740Z. Seventy-five knot (39 m/sec) gusts were recorded at 111751Z and 120158Z. These winds were recorded on the west side of Helen while it was moving at 9 kt (17 km/hr) toward the north. Allowing for the speed of translation, the final best track intensity was adjusted to 70 kt (36 m/sec).

b. *JTWC forecast performance*

JTWC track forecasts for Helen were very good at the longer time periods. Average forecast errors were 122 nm (226 km), 172 nm (319 km), and 117 (217 km) for 24, 48, and 72 hours. While NOGAPS handled the transition from westward to northward motion in the South China Sea on 11 August quite well, it indicated the northward turn earlier than actually observed. According to Carr (personal communication), this is a common NOGAPS trait. JTWC intensity forecasts were also very good, with an average error of 10 kt (5 m/sec) or less at all forecast periods. The largest intensity forecast errors were produced during the 10 August period, where the intensity was under-forecast by as much as 30 kt (15 m/sec).

c. *Tropical cyclogenesis initiated by a mesoscale convective system*

A recent hypothesis concerning the mechanism of TC genesis is that TCs originate from a mid-level cyclonic vortex that is the product of a mesoscale convective system (MCS). Bartels and Maddox (1990) and Frank and Chen (1991) have provided theoretical and observational evidence that the formation of a mid-tropospheric mesoscale vortex is favored in the large stratiform-rain region of a mature MCS. It has been further proposed that the mid-level mesoscale cyclonic vortices formed via this mechanism can develop into tropical cyclones (e.g., Frank and Chen 1991; Zehr 1992; and Emanuel 1992). The problem lies in linking such mid-level mesoscale vortices to the generation of a surface circulation with organized deep convection. Zehr (1992) postulates a two-stage process whereby a mid-level mesoscale vortex generated by an MCS becomes a TC. In the first stage, a mature MCS creates a mid-level mesoscale vortex which persists after the MCS collapses. The second stage occurs when the remnant mid-level mesoscale vortex works its way to the surface and becomes the site for renewed deep convection resulting in the creation of a TC.

That mid-tropospheric mesoscale vortices are produced during the life cycle of both continental and maritime MCSs is beyond dispute. The results of the TCM-92 and TCM-93 field experiments (Mckinley and Elsberry 1993) and of the TEXMEX field experiment (Bister and Emanuel 1995) confirmed the generation of mid-level mesoscale vortices by tropical maritime MCSs. There remains some controversy as to how the mid-level vortex produced by MCS works its way into the low levels; although Zehr (1992), and Bister and Emanuel (1995), have shown convincing observational evidence that the mesoscale vortices created during the life cycle of an MCS have later become the site of TC development. In Helen's case, there is insufficient evidence to determine if the well-defined mesoscale vortex that appears in Figure 3-08-1 played a direct role in Helen's development. At best, the formation of this mesoscale vortex is a good example Stage One of Zehr's two-stage pathway to tropical cyclogenesis (i.e., the formation of a mid tropospheric mesoscale vortex by an MCS). However, since this well-defined mesoscale vortex dissipated, it is difficult to establish a direct link between it and Helen's subsequent development.

IV. IMPACT

Twenty-three deaths were reported by the Chinese media. In Hong Kong, one person was reported killed and two were reported missing. Although Waglan Island reported sustained (one-minute average) winds of 65 kt (33 m/sec) with gusts to 75 kt (39 m/sec) between 111740Z and 111751Z August (see Figure 3-08-3), winds were weaker over Hong Kong proper. Helen caused about 100 landslides and deposited about 24 inches (600 mm) of rain on Hong Kong during its four days of influence. Damage was slight as implied by a small number of insurance claims.

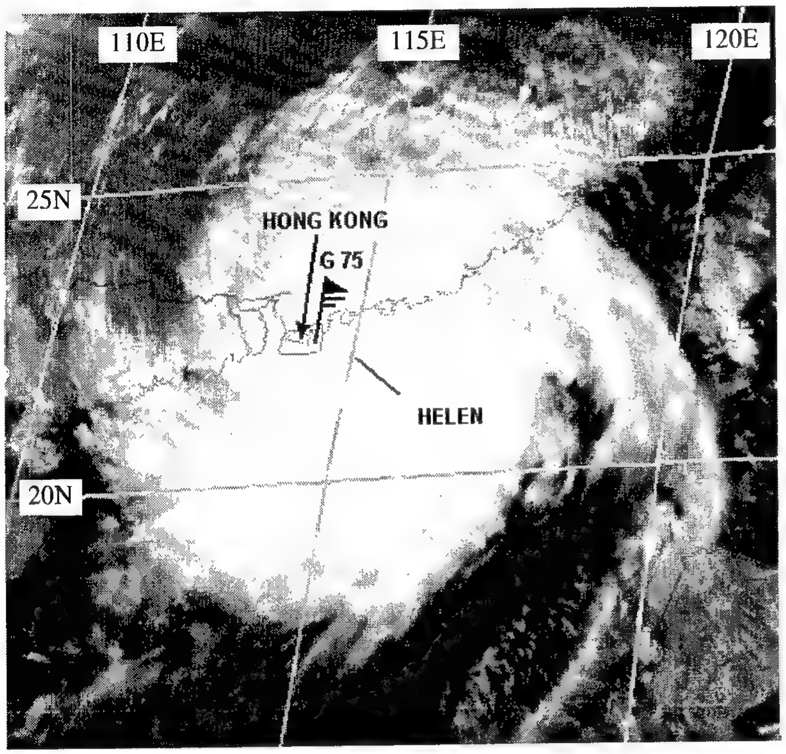

Figure 3-08-3 Typhoon Helen brushes by to the east of Waglan Island, Hong Kong (120131Z August visible GMS imagery). The 120000Z 65 kt (33 m/sec) one-minute averaged sustained wind and the peak 75 kt (39 m/sec) wind gust observed at Waglan Island are indicated (wind data courtesy of the Royal Observatory Hong Kong).

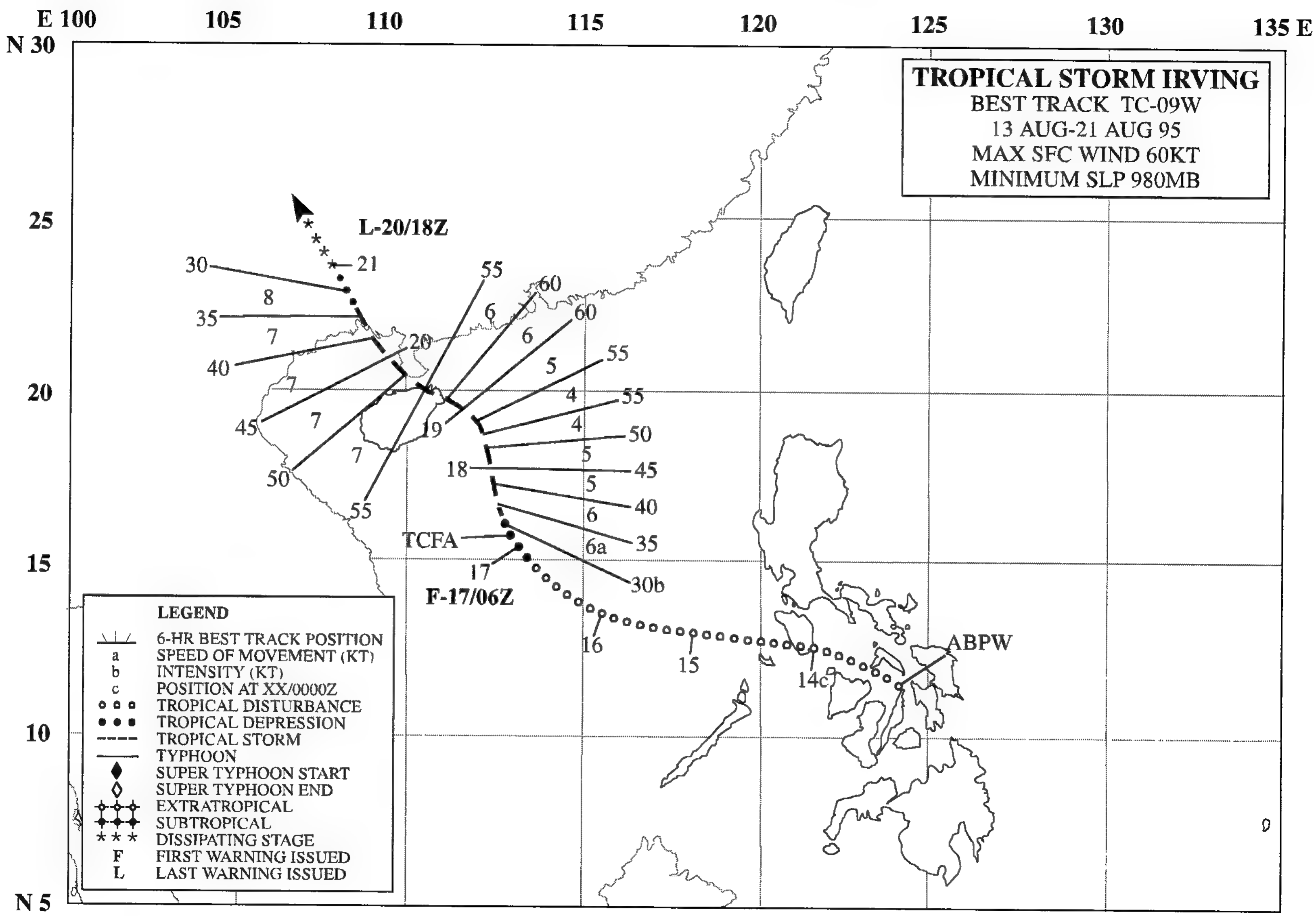

TROPICAL STORM IRVING
BEST TRACK TC-09W
13 AUG-21 AUG 95
MAX SFC WIND 60KT
MINIMUM SLP 980MB
E 100
105
110
115
120
125
130
135 E
N 30
25
20
15
10
N 5
L-20/18Z
F-17/06Z
TCFA
ABPW
LEGEND
6-HR BEST TRACK POSITION
a SPEED OF MOVEMENT (KT)
b INTENSITY (KT)
c POSITION AT XX/0000Z
TROPICAL DISTURBANCE
TROPICAL DEPRESSION
TROPICAL STORM
TYPHOON
SUPER TYPHOON START
SUPER TYPHOON END
EXTRATROPICAL
SUBTROPICAL
DISSIPATING STAGE
F FIRST WARNING ISSUED
L LAST WARNING ISSUED

TROPICAL STORM IRVING (09W)

I. HIGHLIGHTS

The second of eight tropical cyclones to form in, or near, the South China Sea during 1995, Irving was very small. Isolated in an otherwise relatively cloud free region of the South China Sea, Irving maintained a very small CDO under which microwave imagery indicated the presence of an eye.

II. TRACK AND INTENSITY

As Tropical Storm Helen (08W) was moving inland over southern China, an area of deep convection associated with the monsoon trough consolidated near the central Philippines on 12 August. On 13 August, synoptic data indicated that a weak low-level circulation center accompanied this tropical disturbance, which was mentioned on the 130600Z August Significant Tropical Weather Advisory. For the next few days, the tropical disturbance moved slowly westward in the South China Sea and showed no signs of further intensification. Visible satellite imagery obtained at first light on the morning of 17 August revealed increased organization of the convective cloud lines, and JTWC issued a Tropical Cyclone Formation Alert at 170100Z. Later that afternoon, visible satellite imagery indicated a further increase in the definition of the low-level circulation center, and the JTWC issued the first warning on Tropical Depression 09W, valid at 170600Z. The deep convection of Tropical Depression 09W rapidly consolidated into a small area very close to the low-level circulation center while, at the same time, other areas of deep convection away from the low-level circulation center subsided. The formation of this small CDO led to the upgrade of Tropical Depression 09W to tropical storm intensity at 171200Z August.

As Irving moved northward toward Hainan Island, it retained its small CDO. Microwave imagery at 172121Z (Figure 3-09-1) indicated the presence of an eye. A visible image two hours later showed that the eye was obscured (Figure 3-09-2). The intensity estimates of Irving gradually increased (based on its persistent CDO, more

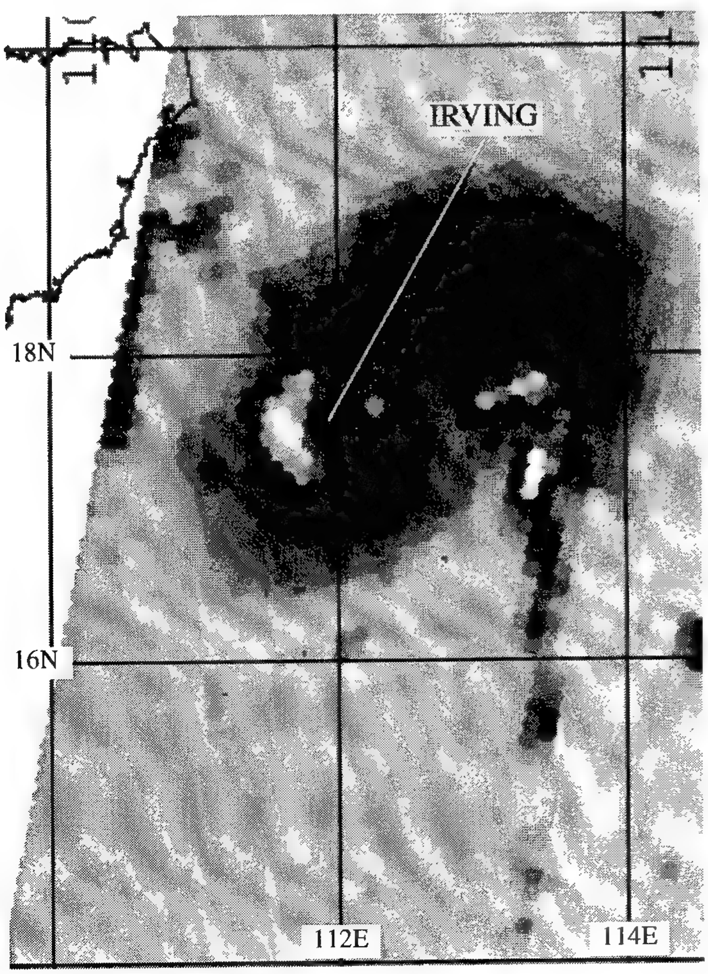

Figure 3-09-1 A small eye is revealed by microwave imagery under the dense cirrus overcast of Irving's small CDO (172121Z August SSM/I 85 GHz DMSP imagery).

tightly curved low-level cloud lines, and better organized cirrus outflow streamers), and at 190000Z it peaked at 60 kt (31 m/sec) (Figure 3-09-3). Moving northwestward, Irving grazed the northeastern tip of Hainan island, crossed the southern end of the Luichow peninsula, and moved inland into southern China near the city of Quinzhou on 20 August. The JTWC issued the final warning, valid at 201800Z August, as Irving dissipated over land.

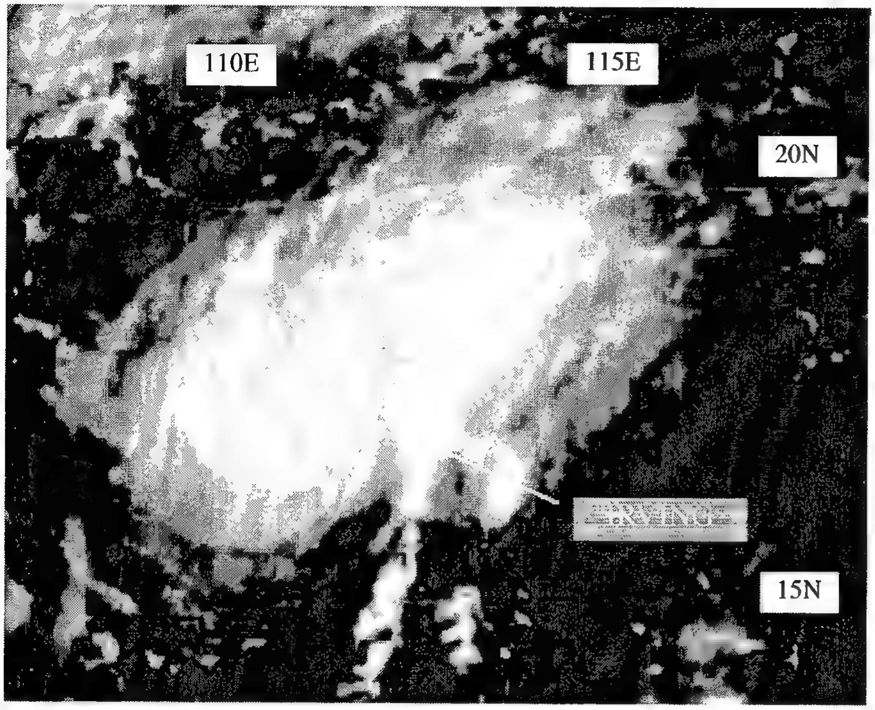

Figure 3-09-2 Cirrus overcast obscures the small eye that appears in Figure 3-09-1 (172331Z August visible GMS imagery).

III. DISCUSSION

a. *Tropical cyclone size: the "midget" tropical cyclone*

Tropical Storm Irving was one of the smallest tropical cyclones of 1995 — only Tropical Depression 22W was smaller. In fact, from the perspective of the size of Irving's satellite-observed cloud shield (including the CDO and curved cirrus outflow streamers), there are few tropical cyclones in recent years that have been as small. Since 1990, only Cecil (1990), Ellie (1991), Zelda (1991), and Ofelia (1993) have been of similar size.

Tropical cyclones of very small size have caught the attention of forecasters and researchers for many years. The terminology used to address very small tropical cyclones still has not been resolved. One of the first written studies of very small typhoons was by Arakawa (1952). Arakawa wrote of very small typhoons that had struck Japan by complete surprise. He called such typhoons, Mame-Taifu (literally, "bean" typhoon; figuratively "midget" typhoon). Dr. C.E. Palmer, one of the meteorologists working in the Marshall Islands during the years of atomic testing by the United States, corresponded with Arakawa on his (Palmer's) observations of very small storms of typhoon intensity occurring in the Marshalls. During September 1966, a reconnaissance flight passed through an extremely intense, but incredibly small hurricane (Inez) in the Caribbean. This hurricane was so small that two scientists working with the data from the flight into Inez (Hawkins and Rubsam 1967) proposed that such storms be called "micro-hurricanes". However, the preferred designation for very small tropical cyclones in the western North Pacific remains Arakawa's "midget".

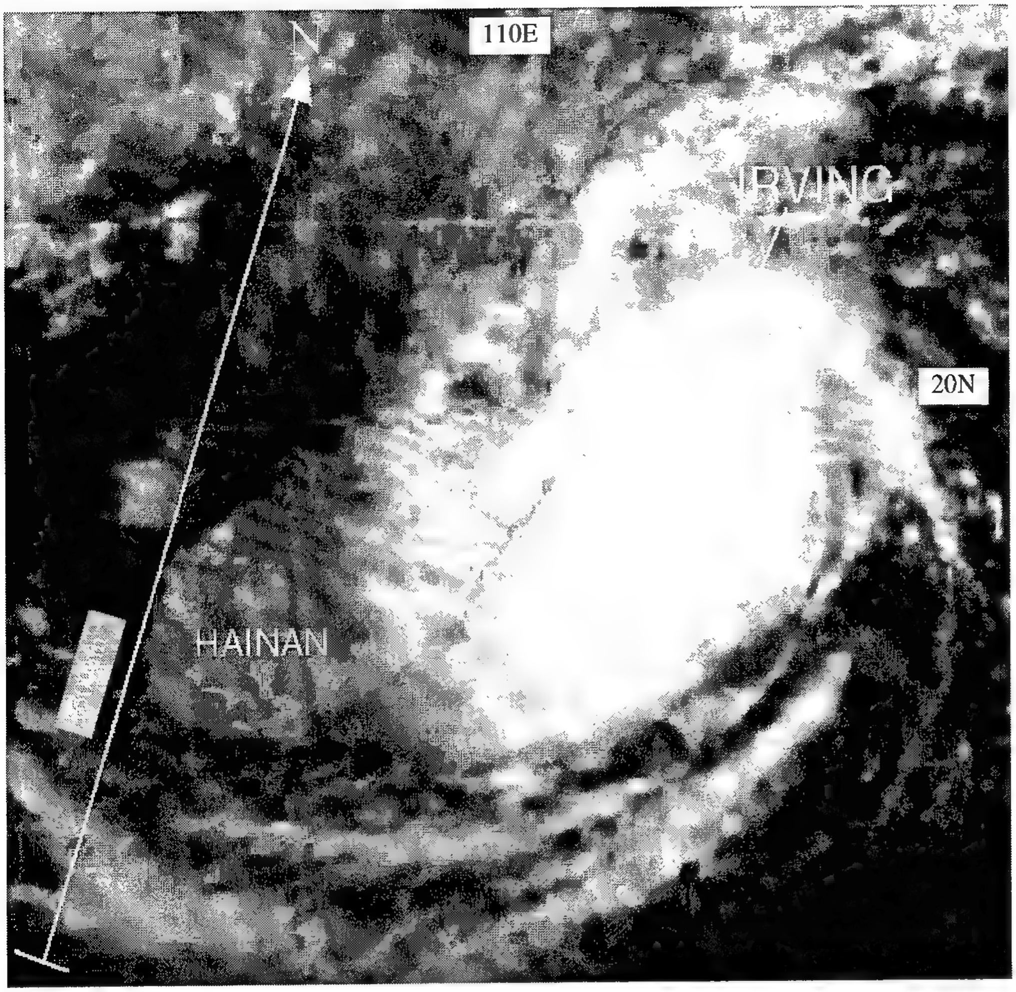

Figure 3-09-3 Tropical Storm Irving at its peak intensity of 60 kt (31 m/sec) (190231Z August visible GMS imagery).

Tropical cyclone size is a very difficult parameter to objectively measure. Brand (1972) classified a tropical cyclone as "very small" if the mean radius to the outer-most closed isobar (ROCI) was two degrees (120 nm, 222 km) of great circle arc (GCA) or smaller. Both the terms "very small" and the term "midget" are used on JTWC bulletins and in the research community, however, the term "midget" is nowhere officially defined (see Appendix A, where herein the size categories of tropical cyclones are: very small, small, average, large, and very large — and are based upon the ROCI). Determining the mean ROCI of tropical cyclones is difficult. This is especially true of tropical cyclones in the western North Pacific that are embedded within larger monsoonal low pressure areas, and where synoptic reports are sparse. After examining recent "midget" tropical cyclones, Guard and Lander (1995) suggest that the satellite cloud signature be used as the primary tool to identify "midget" tropical cyclones. Cloud features used to identify a midget tropical cyclone include:

(1) a CDO, or eyewall plus eye, that does not exceed 90 nm in diameter,

(2) no bands of deep convection more than 120 nm from the low-level center,

(3) a conspicuous lack of low-level cloud lines away from the cover of the central cirrus canopy,

(4) central convection that is often isolated in an otherwise relatively cloud free region,

(5) anticyclonically curved cirrus outflow streamers may be well-organized, but do not extend more than 180 nm from the central convection in any direction.

In addition to the aforementioned satellite-observed characteristics, a structural characteristic found by Lander and Guard (1996) to be typical of the midget tropical cyclone is a rapid drop-off of the wind from the radius of maximum wind outward.

Typical of many "midget" tropical cyclones, Irving lacked peripheral rainbands, and synoptic data indicated that the highest winds were concentrated extremely close to the center. In fact, while it was over the South China Sea, if it were not for detection by satellite, it is doubtful that this tropical cyclone would have ever been detected. Even with detection of Irving by satellite, its intensity was difficult to diagnose. The rapid, and early, formation of Irving's CDO — and its very small size — did not lend itself well to Dvorak enhanced infrared analysis, which requires that the intensity of a tropical cyclone must have become at least 55 kt (28 m/sec) 12 hours before the embedded center technique can be applied. Microwave imagery showing a cirrus covered eye embedded in Irving's small CDO was helpful in supporting the warning intensity of 60 kt (31 m/sec).

b. *Inability of numerical models to analyze and maintain midget tropical cyclones*

Because of their very small size, "midget" tropical cyclones tend not to be analyzed by numerical products. Further, a "midget" tropical cyclone tends to weaken in the forecast and lose its identity as a distinct vortex. These shortcomings of the dynamic guidance are reflected in the following excerpts from the Deputy Director's unofficial log during the development of Irving:

"...Warning # 01: 170900 . . . [Irving] should continue to [intensify] in the forecast period. NOGAPS does not have the circulation. . . ."

"...Warning # 02: 171500 . . . Aids are confusing showing a scatter from west to north. NGPS has no vortex to track. . . ."

"...Warning # 03: 172100 . . . NOGAPS model progs are now in fairly good agreement. N to NNWward, slow. . . . However it [NOGAPS] doesn't hold the circulation. NGPS therefore still having problems. . . ."

IV. IMPACT

No reports of significant damage or injuries were received.

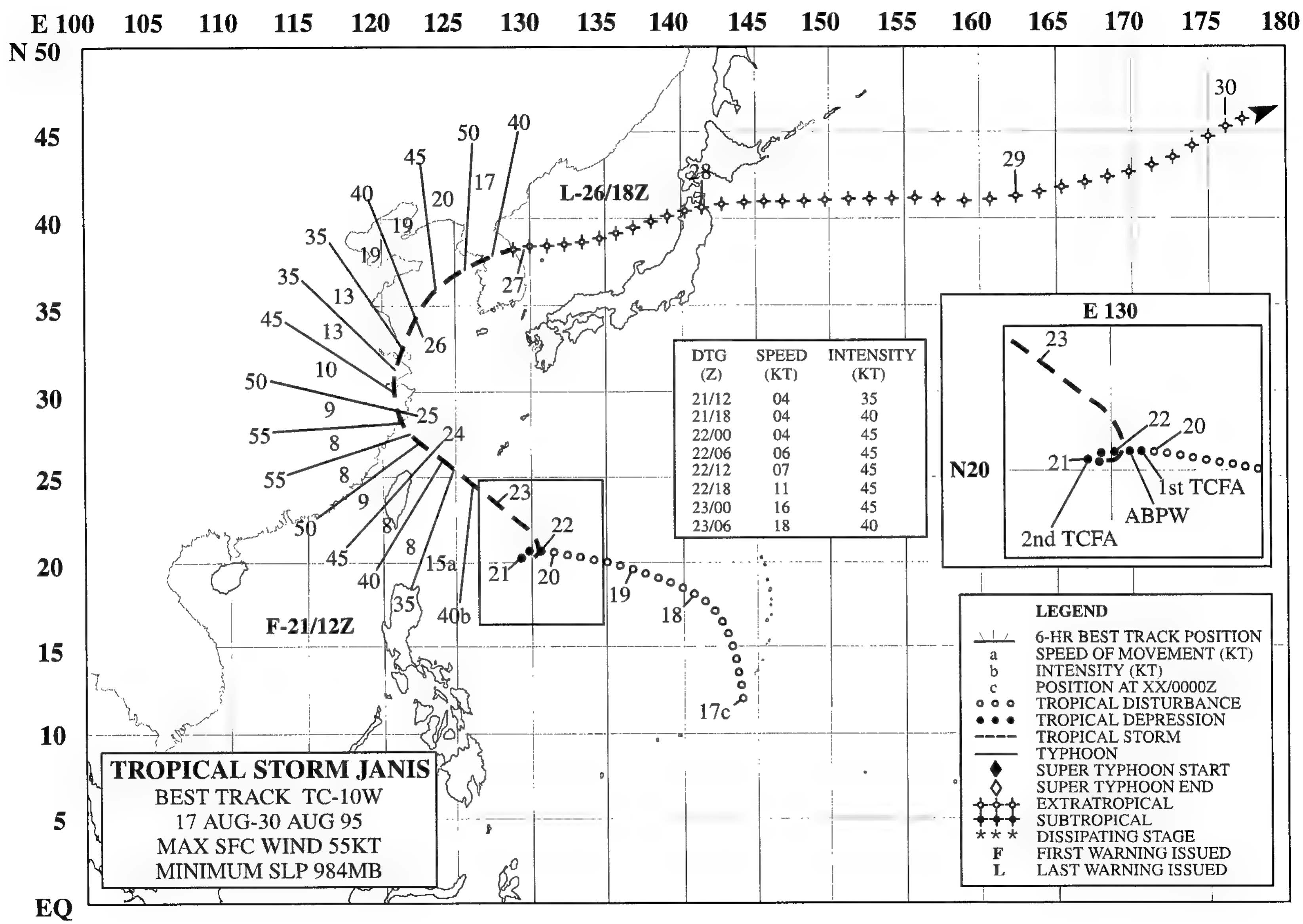

DTG (Z)	SPEED (KT)	INTENSITY (KT)
21/12	04	35
21/18	04	40
22/00	04	45
22/06	06	45
22/12	07	45
22/18	11	45
23/00	16	45
23/06	18	40

TROPICAL STORM JANIS (10W)

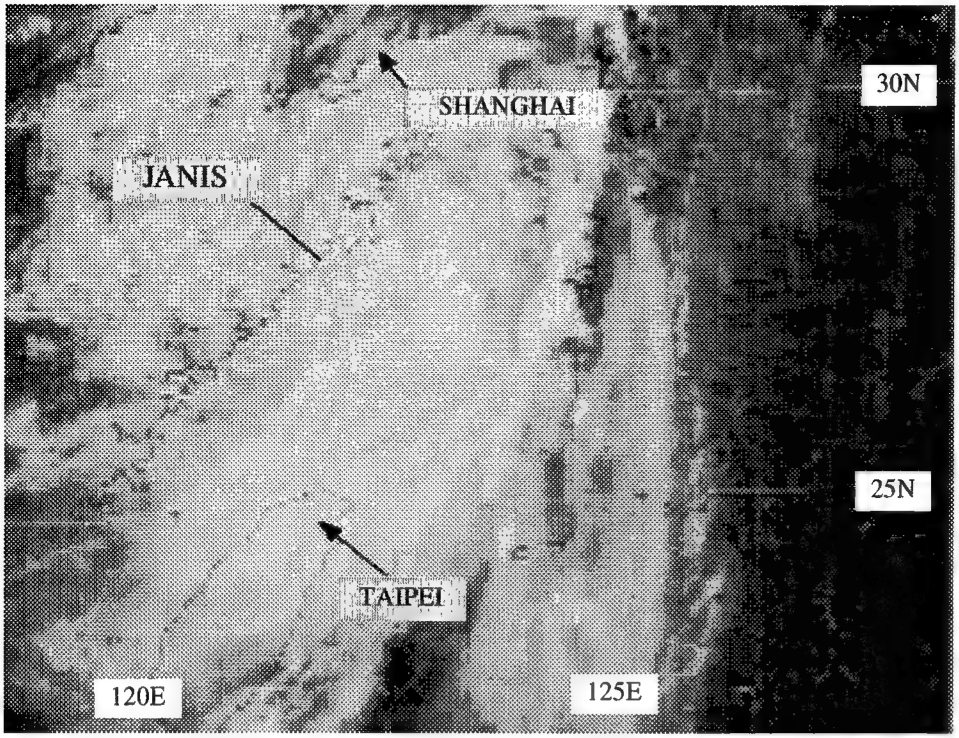

Figure 3-10-1 Janis makes landfall in eastern China shortly after attaining its peak intensity of 55 kt (28 m/sec) (250031Z August visible GMS imagery).

I. HIGHLIGHTS

Forming in a monsoon trough that extended from Asia into the Philippine Sea, Janis moved northwestward and merged with Tropical Depression 11W. In an unusual case of tropical cyclone merger, the larger Janis actually lost much of its deep convection and became less organized as it merged with the smaller Tropical Depression 11W. Subsequent to the merger, all deep convection was lost, but later regenerated as the system moved northward east of Shanghai (Figure 3-10-1). Moving eastward across the Yellow Sea, Janis made landfall in central Korea near Seoul. Heavy rain and winds associated with Janis had a significant impact on South Korea.

II. TRACK AND INTENSITY

During the second week of August, there was relatively little deep convection throughout the tropics of the western North Pacific. On or about 16 August, deep convection had increased across the Philippine Sea and eastward into Micronesia. Several clusters of enhanced convection were distributed along this cloud band in a complex association with a chain of TUTT cells to the north. The tropical disturbance that became Janis had a rather ambiguous start. The first mention of the tropical disturbance that most probably became Janis appeared on the 180600Z August Significant Tropical Weather Advisory. This tropical disturbance moved northwestward and slowly became better organized. The following excerpts from the Deputy Directors' unofficial log provide an insight into the techniques and thought processes used by JTWC forecasters to construct the sequence of warnings on Janis (note the use of concepts developed by Carr and Elsberry (1994) in their systematic approach to tropical cyclone forecasting):

"[Tropical Cyclone Formation Alert] TCFA #1 [issued at 200330Z August], circulation around 21N 132E, Broad area of deepening convection starting to show cyclonic turning."

"TCFA #2, [issued at 210300Z August] Two distinct circulation centers: 19N 133E and 20N 129E. Broad circulation, [it] remains unclear which of these will [develop]. BUT one of them will."

"Warning #01: 21/12Z: Dvorak 2.0 and synoptic obs of 20 and 25 knots about the circulation center near 20.4N 129.9E prompts this warning [on Tropical Depression 10W]. NOGAPS anal indicates model has fair to good initialization despite not having the circulation. 700 and 500 mb indicates slow westward motion through 24-36 hours followed by increasing northward motion out to 72 hours. Models indicate building of the ridge, already analyzed, to the SE of the circulation. Appears to be a classic N2 [see discussion of the Systematic Approach] and forecasting a north-oriented track after about 24 hours of slow westward drift, while consolidating. Intensification 1T/day. Everything looks favorable; in addition there is a TUTT cell to NW that should support outflow on NE quadrant of the TC."

"Warning #02: 21/18Z: [Upgraded to TS (JANIS) based on synoptic and satellite data. Still N2 forecasting very slow westward drift while system consolidates followed by northward acceleration at 36 - 48 hours."

"Warning #03: 22/00Z: NOGAPS 21/12Z continues to build ridge from south along east side of storm up to the [subtropical ridge]. Modifying the [subtropical ridge] in classic N2 and north-oriented motion. However the model does not build very strong [outer wind] asymmetries . . . as expected. This may be a factor of large TC actual size, but NOGAPS not hanging onto the vortex yet. Still forecasting for slow westward now for 12-24 hours, followed by acceleration to northward. Okinawa in danger. Intensification remains 1T/day. NOTE: [Mesoscale Convective Complex] developing about 350 nm NNW of Janis. This is [associated with] the TUTT cell, but may . . . support cyclogenesis. Issuing TCFA on it. Potentially 11W."

"Warning #05: 22/12Z: TS Janis has slowly moved back to the east as it undergoes binary interaction with TD 11W. Intensification is stalling but that should be temporary. Forecasting for slow ENEward motion followed by . . . NWward track thru period. This places Okinawa directly in the path of Janis."

"Warning #07: 23/00Z RELOCATED: Janis absorbed TD 11W but did not execute as long a ENEward track as forecasted. Janis is now tracking NWward at about 16 knots. NOGAPS no longer supports north-oriented pattern. NWward steering asymmetries are evident early in prog series and weaken thru 72 hours. Now forecasting for a more classic recurver scenario. NWward track thru 48 hours followed by recurvature towards Korea. Intensification should resume but current rate does not support 1T/day. Forecast TY by 25/00Z with 75 knots at 72 hours off the southern coast of Korea."

"Warning #09: 23/12Z: Janis is tracking Nward at 13 knots and intensifying slowly. NOGAPS fields do not clearly [indicate] the steering flow . . . 500 mb 20 knot, Nward asymmetries are evident thru 48 hours. By 72 hours only a small finger of 20 knot [wind extends] north towards the storm circulation. This could indicate northward motion and weakening, OR the storm could move over China and dissipate. Forecast is similar to previous: NWward out to 25/00Z followed by recurvature towards Korea. [However] losing confidence in this philosophy. System may go over land in China and dissipate."

On 25 August, Janis made landfall in eastern China near Wenzhou. Moving northward over land, the system weakened. Approximately six hours after passing near or over Shanghai, Janis turned to the northeast and moved into the Yellow Sea; its intensity had fallen to 35 kt (18 m/sec). Once over water

again, Janis began to re-intensify as it turned more eastward and accelerated toward the Korean peninsula. Janis made landfall near Seoul at approximately 261500Z. Peak winds at the time of landfall were estimated to have been 50 kt (26 m/sec). The JTWC issued the final warning valid at 261800Z as Janis became extratropical while passing over the mountains of Korea. The system continued as an extratropical low — with gales — as it crossed the Sea of Japan.

III. DISCUSSION

a. *The "Systematic Approach" to tropical cyclone track forecasting*

As seen in some of the Deputy Director's log entries listed above, the rationale for the forecast is couched in terms of a forecast scheme developed by Carr and Elsberry (1994). Carr and Elsberry developed what they term "a systematic and integrated approach to tropical cyclone track forecasting" (hereafter referred to as the "Systematic Approach"). The "Systematic Approach" is intended to address some deficiencies in the current forecasting process. It employs two important knowledge bases: (1) a comprehensive set of conceptual models (Part I) to assist the forecaster in characterizing the tropical cyclone environment; and, (2) a compilation (Part II) of the traits and biases of the numerical tropical cyclone prediction models organized in accordance with the conceptual model knowledge base. The conceptual models developed in Part I relate tropical cyclone motion to tropical cyclone structure (both intensity and size); and, most importantly, to tropical cyclone/environment transformations, by which environmental patterns (and thus the attendant steering) may be significantly altered by the presence of the tropical cyclone.

The set of conceptual models is organized into three general groups that are further organized into two subsets based on scale: synoptic patterns (classifications of the large-scale environment surrounding the tropical cyclone based on the existence and orientation of various synoptic features such as cyclones, anticyclones, ridges, and troughs); and, synoptic regions (identification of smaller areas within the synoptic patterns where certain characteristic directions of environmental steering may be expected to occur).

JTWC forecasters have begun to use and evaluate Carr and Elsberry's "Systematic Approach". The comment, "modifying the [subtropical ridge] in classic N2 and north-oriented motion", that appeared in the log entry concerning Warning #3 is based upon use of the "Systematic Approach". The N2 pattern is a specific environmental flow pattern identified by Carr and Elsberry (Figure 3-10-2) that is associated with north-oriented motion. Carr and Elsberry's scheme is still in the process of development, but it is also being used by JTWC forecaster's even as the knowledge base is established and refined; thus, a

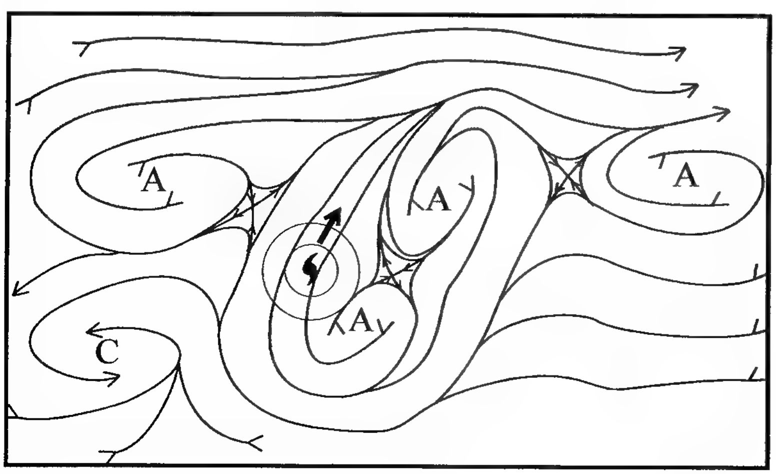

Figure 3-10-2 Schematic illustration of the wind flow at the 500-mb level in the synoptic pattern N2 that is favorable for north-oriented tropical cyclone motion. (Adapted from Carr and Elsberry, 1994).

healthy feedback between the JTWC and the research community has been established. The reader is referred to Carr and Elsberry (1994) for a complete treatment of the "Systematic Approach".

b. *Tropical cyclone merger*

Janis merged with Tropical Depression 11W. Tropical cyclone merger is one possible outcome of the mutual interaction of spatially proximate tropical cyclones. The interaction of two adjacent tropical cyclones is often referred to as the Fujiwhara effect after the pioneering laboratory and observational studies of Fujiwhara (1921, 1923, and 1931). Fujiwhara demonstrated that the relative motion of two adjacent cyclonic vortices was composed of cyclonic orbit around their centroid, coupled with a mutual attraction. The rate of orbit steadily increases as the vortices spiral inward toward one another and eventually the two vortices coalesce into one vortex located at the centroid (i.e., the geographical mid-point between the two tropical cyclones).

The observed behavior of two adjacent tropical cyclones usually differs from the classical Fujiwhara effect in several aspects. Prominent among these is the usual failure of tropical cyclones to merge. Because of these differences, the interaction between two tropical cyclones is usually called binary interaction. Lander and Holland (1993) developed a generalized model of binary interaction, and showed that the classical Fujiwhara model of converging cyclonic rotation about a centroid followed by merger is rarely observed. Rather, the most common outcome of binary interaction is a mutual cyclonic orbit of the centroid by each tropical cyclone at a fairly constant separation distance followed by a sudden escape wherein the mutual cyclonic orbit ceases and the tropical cyclones move apart.

Though less frequent, the merger of two tropical cyclones usually involves the destruction (i.e. loss of deep convection) of one member of the binary pair. The remnants of the destroyed tropical cyclone are

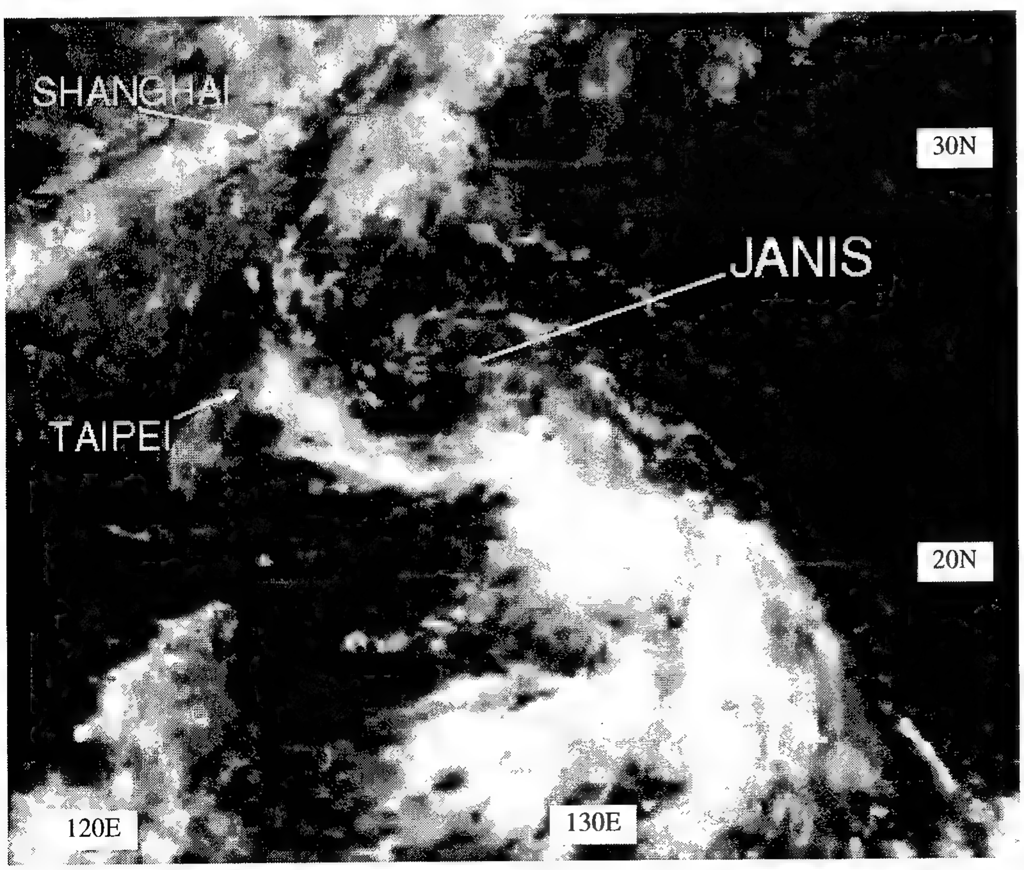

Figure 3-10-3 After Janis had absorbed the circulation of Tropical Depression 11W, the amount of deep convection near the center of the combined vortex decreased considerably (230231Z August visible GMS imagery).

then swept into the circulation of the remaining one. The merger of Janis with Tropical Depression 11W was somewhat unusual in that, as the merger was taking place, each system lost much of its deep convection, and in the case of the larger and better organized Janis, the deep convection also lost much of its organization. Ultimately, Tropical Depression 11W was absorbed into the larger circulation of Janis, but after the merger, most of the deep convection was lost in the combined vortex (Figure 3-10-3). Later, convection became reestablished near the low-level circulation center (Figure 3-10-4).

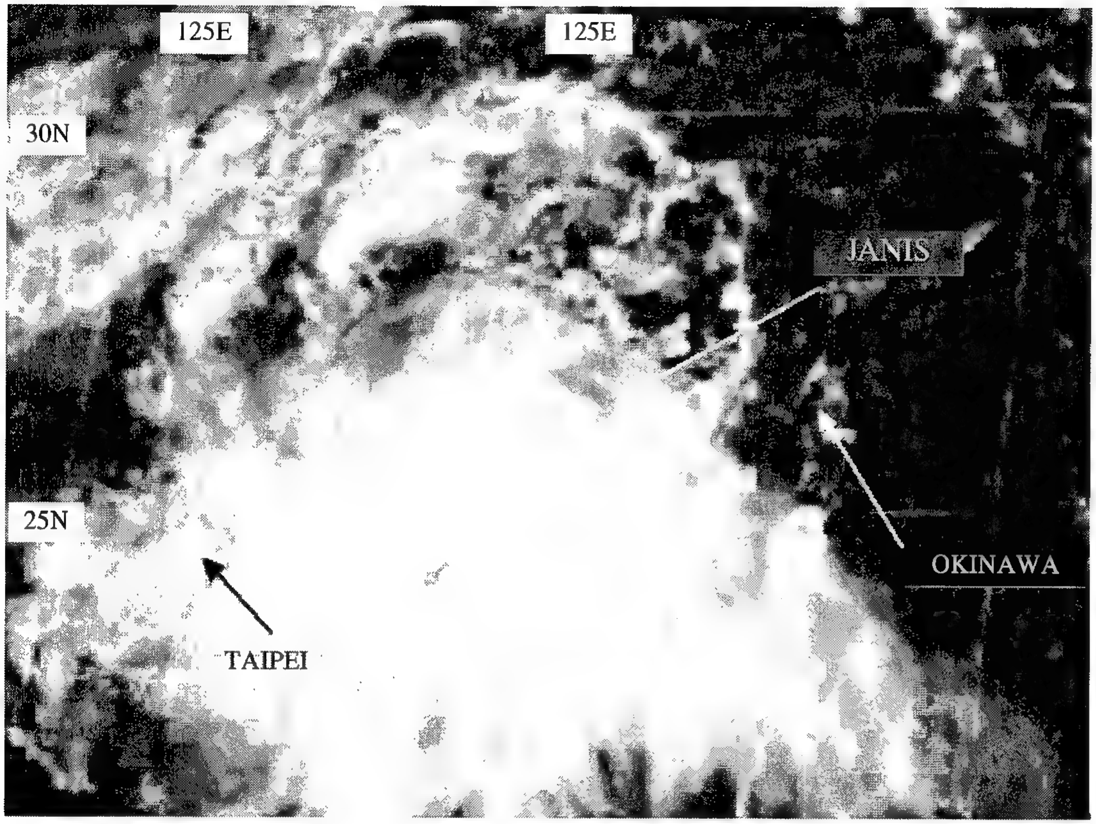

Figure 3-10-4 Deep convection became reestablished near the center of Janis approximately 24 hours after its merger with Tropical Depression 11W (232331Z August visible GMS imagery).

IV. IMPACT

After brushing past Shanghai, Janis turned eastward, crossed the Yellow Sea (Figure 3-10-5), and then made landfall in Korea just north of Seoul. At Osan Air Base, a wind gust of 52 kt (27 m/sec) broke the standing record of 51 kt (26 m/sec) recorded in 1968. The record wind, accompanied by heavy rain, forced the evacuation of two fighter squadrons, uprooted hundreds of trees, knocked down power lines, and left more than 65 buildings without power for more than 12 hours. Elsewhere in Korea, reports of 45 people dead and nine missing were received. Thirty of those killed were crushed by landslides. The rest died when they were swept away by strong currents in streams or struck by lightning. One person died when a train derailed on a bridge over a swollen river. Torrential rains associated with Janis left more than 22,000 people homeless and caused damage in South Korea totaling about $US 428.5 million, the largest rain related disaster in the nation's history. As Janis passed over northern Japan, wind gusts in the high 40s were recorded at many stations. No reports of significant damage or injuries were received from Japan.

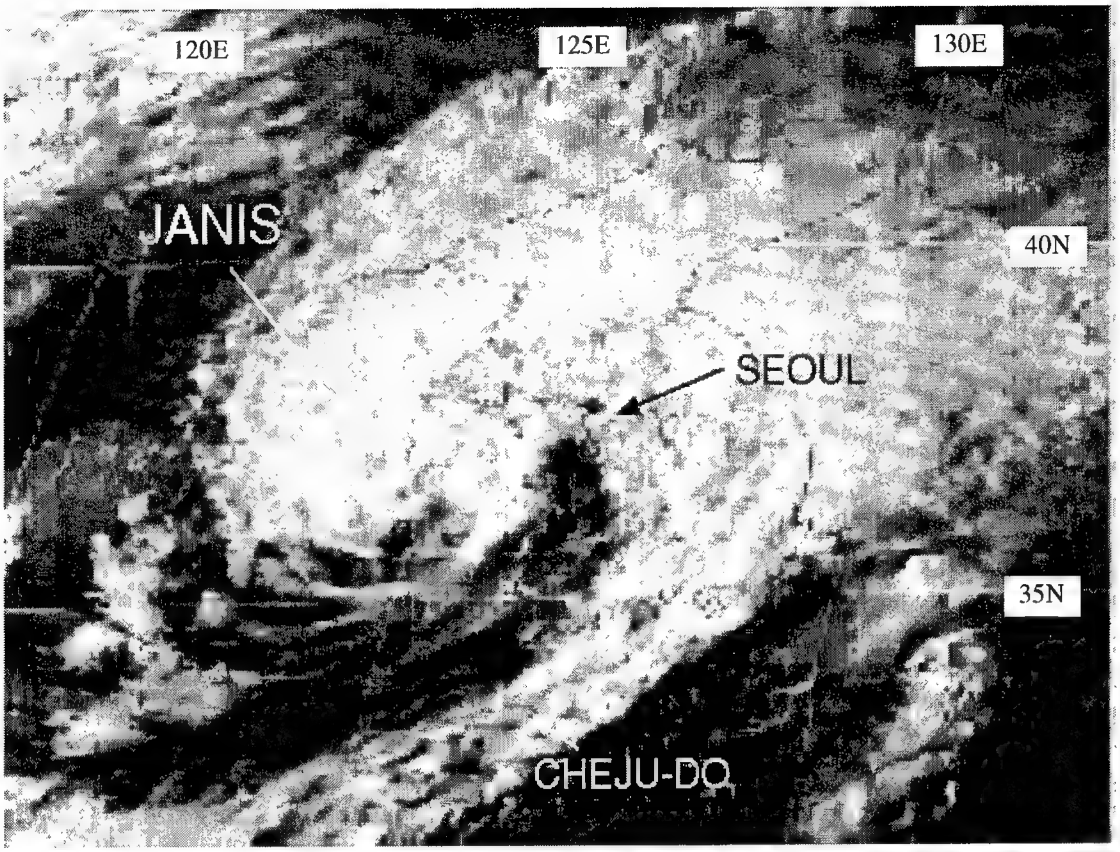

Figure 3-10-5 Janis closes in on the Korean peninsula (260831Z August visible GMS imagery).

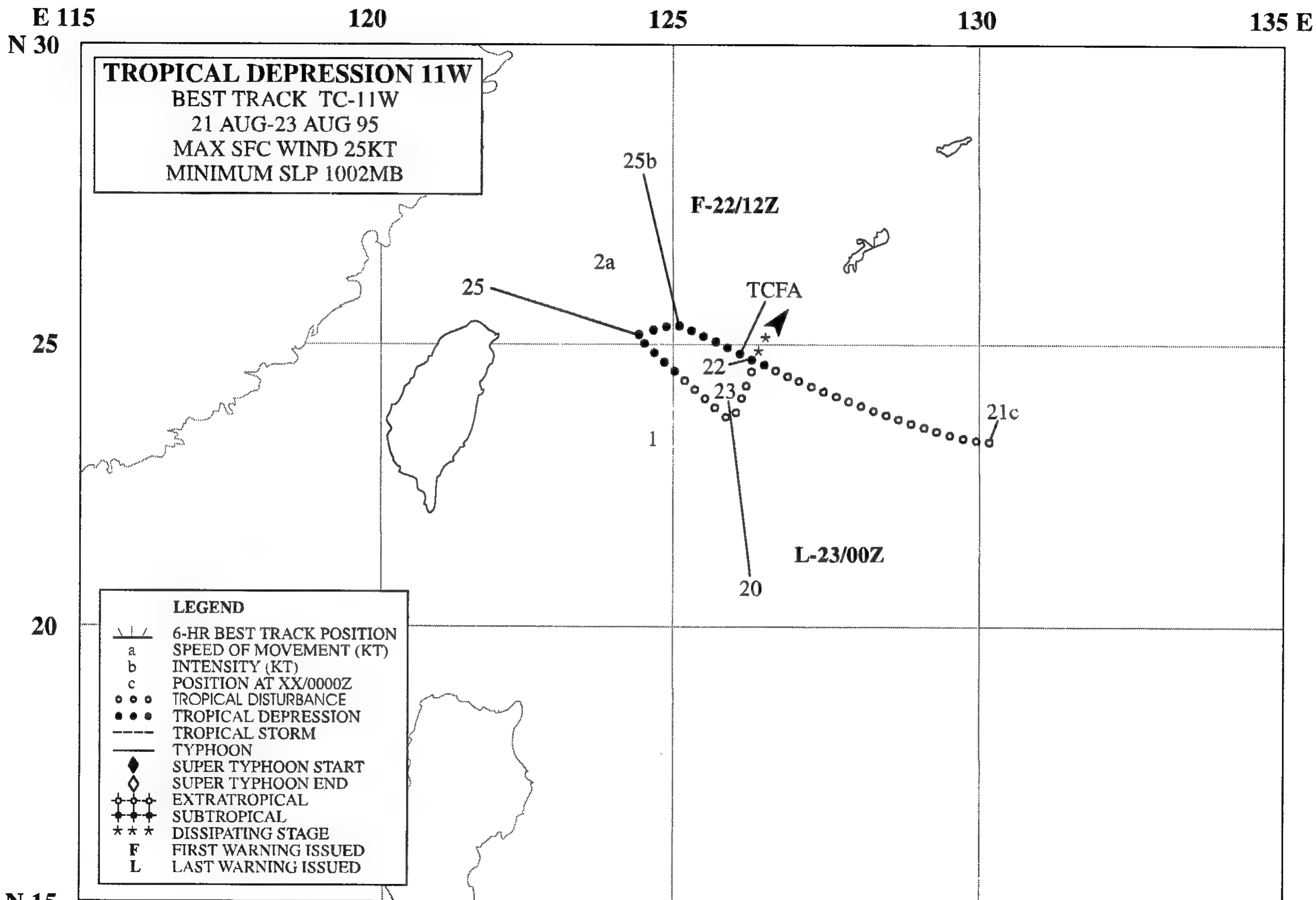
E 115
120
125
130
135 E
N 30
25
20
N 15
TROPICAL DEPRESSION 11W
BEST TRACK TC-11W
21 AUG-23 AUG 95
MAX SFC WIND 25KT
MINIMUM SLP 1002MB
25b
F-22/12Z
2a
25
TCFA
22
23
1
21c
L-23/00Z
20
LEGEND
6-HR BEST TRACK POSITION
a SPEED OF MOVEMENT (KT)
b INTENSITY (KT)
c POSITION AT XX/0000Z
TROPICAL DISTURBANCE
TROPICAL DEPRESSION
TROPICAL STORM
TYPHOON
SUPER TYPHOON START
SUPER TYPHOON END
EXTRATROPICAL
SUBTROPICAL
DISSIPATING STAGE
F FIRST WARNING ISSUED
L LAST WARNING ISSUED

TROPICAL DEPRESSION (11W)

I. HIGHLIGHTS

Forming in association with a TUTT-induced area of convection to the north of Tropical Storm Janis (10W), Tropical Depression 11W eventually merged with Janis (see Janis' summary for more details on the merger).

II. TRACK AND INTENSITY

On August 20, an area of persistent deep convection became established to the north of the area of convection associated with the developing Janis (10W). This area of deep convection (pre-TD 11W) appeared to be directly related to a TUTT cell that had moved westward into the southern Ryukyu Islands. This area of persistent deep convection became better organized (e.g., cyclonically curved bands of deep convection, low-level cloud lines suggesting the formation of a low-level circulation center, and a wide band of anticyclonically curved cirrus outflow to the north) in satellite imagery (Figure 3-11-1). Synoptic data also indicated the formation of a low-level circulation center separate from, and to the north of, Janis. A Tropical Cyclone Formation Alert (TCFA) was issued on this area at 220330Z August.

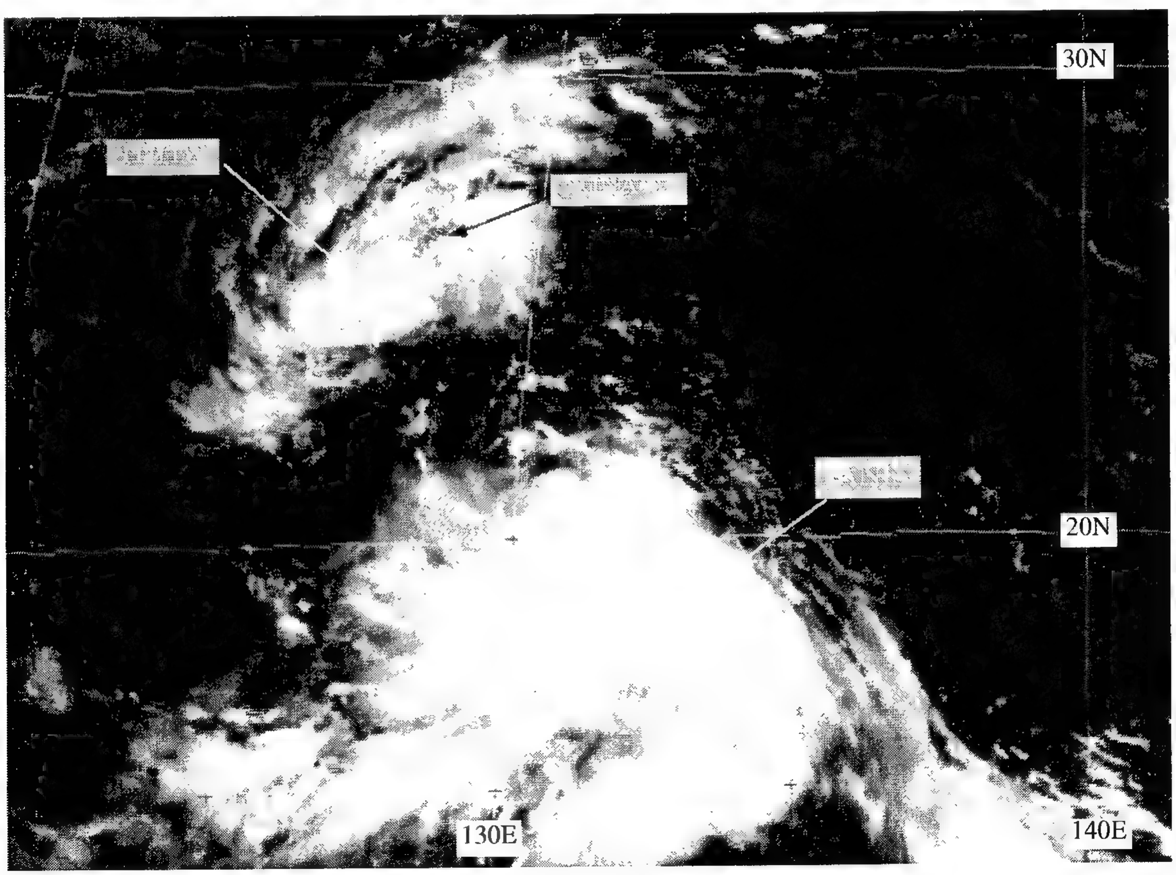

Figure 3-11-1 Tropical Depression 11W as it orbits Tropical Storm Janis (10W) in a binary interaction that will culminate in the merger of these two tropical cyclones (212331Z August visible GMS imagery).

From the beginning, the JTWC anticipated that this system would be absorbed into the larger circulation of Janis (10W). Remarks on the TCFA included:

"... conditions are currently favorable for separate development of this system, re-absorption of this [system] into Janis (10W) is the favored scenario ..."

Remarks on the Prognostic Reasoning message that accompanied the 221200Z warning on Janis (10W) included:

"... there is some evidence of binary interaction [of Janis] with the tropical disturbance near Okinawa. This may cause Janis to remain stationary, or undergo erratic motion over the next 12-24 hours ..."

The first warning on Tropical Depression 11W was issued valid at 221200Z August based upon satellite imagery and synoptic data that clearly indicated that a separate low-level circulation center, possessing 25 kt (13 m/sec) maximum sustained wind, had formed in the southern Ryukyu Islands. During the subsequent 12 to 18 hours, Tropical Depression 11W executed a counter-clockwise loop, and its deep convection collapsed as it merged with the low-level circulation center of Janis. The JTWC issued the final warning valid at 230000Z for Tropical Depression 11W.

III. DISCUSSION

Tropical Depression 11W merged with Tropical Storm Janis (10W). For more details of the merger of these two tropical cyclones see the discussion section of Janis' narrative.

IV. IMPACT

No reports of significant damage or injuries were received.

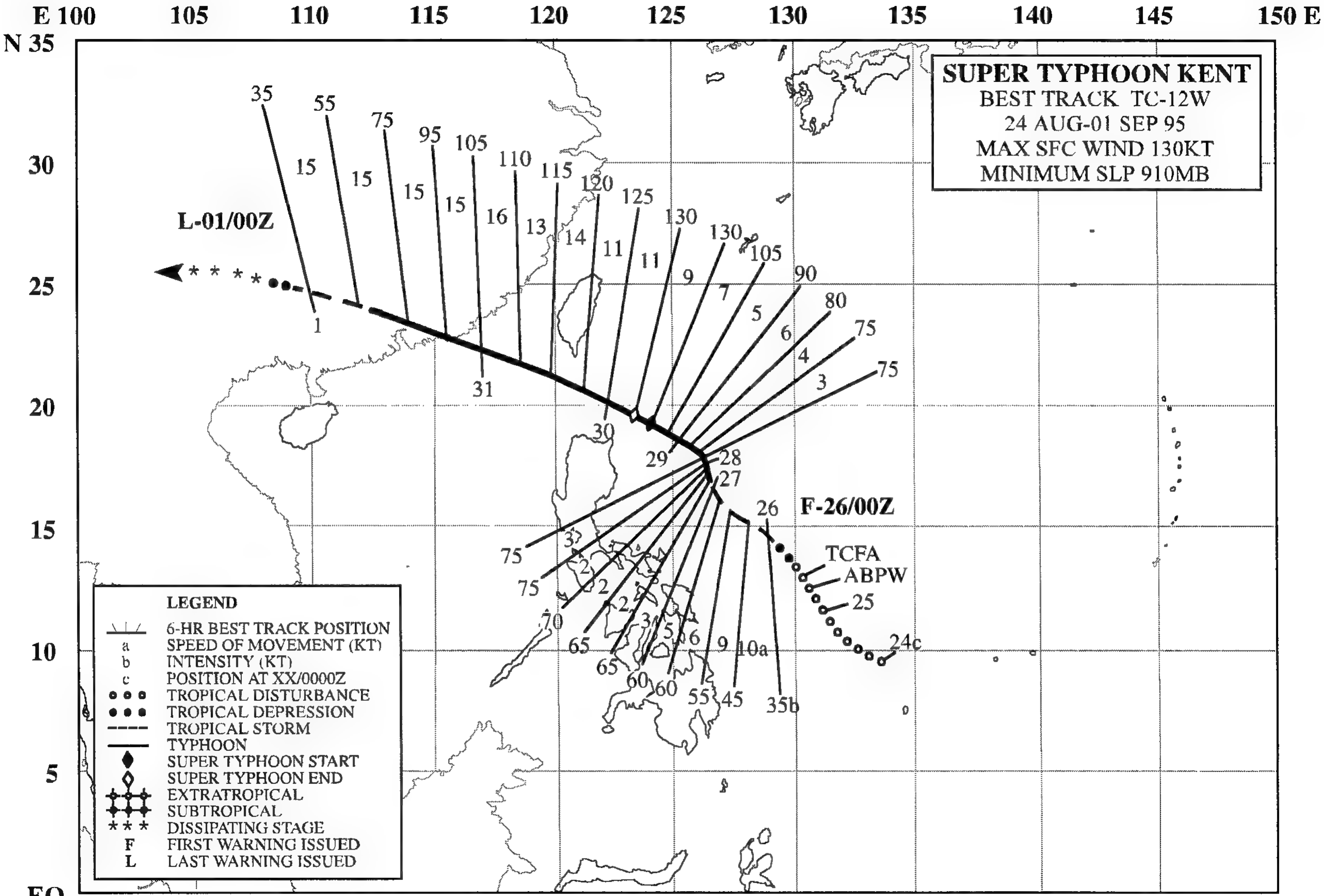
SUPER TYPHOON KENT
BEST TRACK TC-12W
24 AUG-01 SEP 95
MAX SFC WIND 130KT
MINIMUM SLP 910MB
LEGEND
a SPEED OF MOVEMENT (KT)
b INTENSITY (KT)
c POSITION AT XX/0000Z
6-HR BEST TRACK POSITION
TROPICAL DISTURBANCE
TROPICAL DEPRESSION
TROPICAL STORM
TYPHOON
SUPER TYPHOON START
SUPER TYPHOON END
EXTRATROPICAL
SUBTROPICAL
DISSIPATING STAGE
F FIRST WARNING ISSUED
L LAST WARNING ISSUED
L-01/00Z
F-26/00Z
TCFA
ABPW
E 100
105
110
115
120
125
130
135
140
145
150 E
N 35
30
25
20
15
10
5
EQ

SUPER TYPHOON KENT (12W)

I. HIGHLIGHTS

Kent was one of seven tropical cyclones and one of three typhoons to develop in August. It was also the first of five super typhoons to occur in 1995. Kent formed in the Philippine Sea and, after slow development, it rapidly intensified as it approached the Luzon Strait. Basco, Batan Island (WMO 98135), which was briefly in the northern part of Kent's eye, observed a peak wind gust of 140 kt, and a minimum sea-level pressure of 928 mb. Hourly radar images from Kaohsiung, Taiwan showed concentric eyewalls that persisted for at least 22 hours. Kent continued on a west-northwest track and made landfall in China, just east of Hong Kong.

II. TRACK AND INTENSITY

The tropical disturbance that became Kent was first mentioned on the 250600Z August Significant Tropical Weather Advisory when satellite imagery indicated increased organization in an area of deep convection, located north-northwest of Palau. Scatterometer data from the ERS-1 satellite (which was not available to the JTWC in real time) revealed that, 24 hours earlier, this disturbance was accompanied by a low-level cyclonic vortex with a maximum intensity of 15 kt (8 m/sec). The disturbance moved to the northwest, and its satellite signature continued to improve. A Tropical Cyclone Formation Alert was issued by the JTWC at 251130Z. At 260000Z, Dvorak intensity estimates reached 35 kt (18 m/sec) and the first warning on Tropical Storm Kent was issued, valid at 260000Z. The tropical cyclone intensified at a greater-than-normal rate (i.e., greater than one "T" number per day), and at 270600Z, Kent was upgraded to a typhoon. After becoming a typhoon, Kent's rate of intensification slowed, as did its speed of translation. During its 48-hour period (261800Z to 281800Z) of slow (5 kt, or less) forward motion, satellite imagery (Figure 3-12-1) revealed restricted outflow of the cirrus to the northwest of the system.

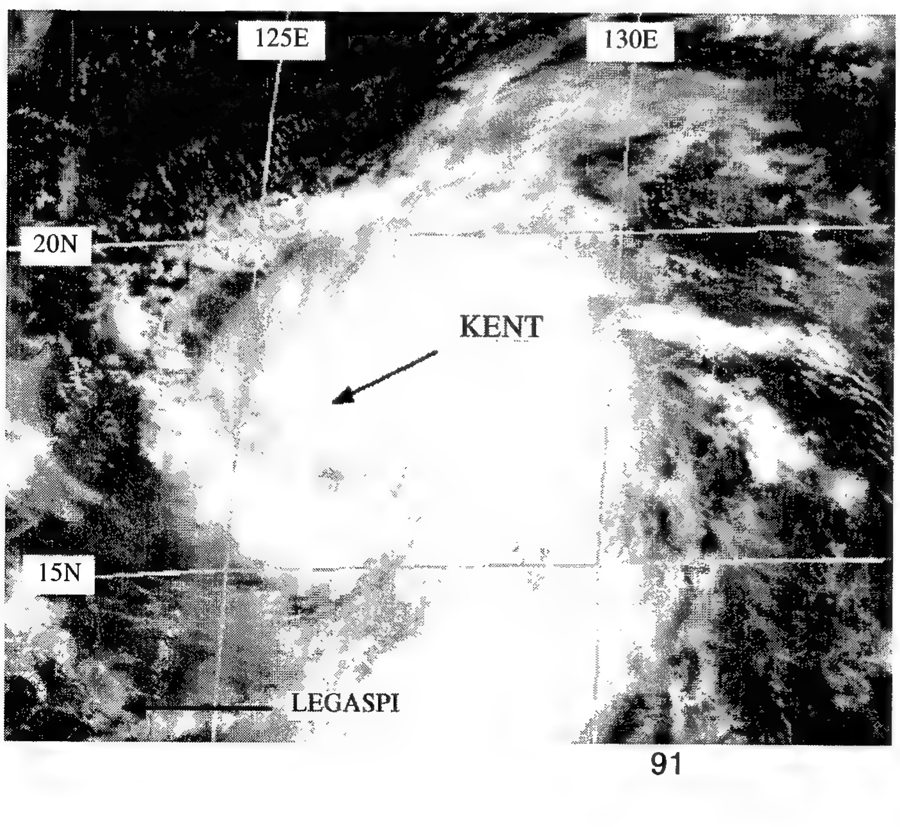

Figure 3-12-1 Kent with an intensity of 75 kt (39 m/sec) when 270 nm (510 km) east of Luzon (272331Z August visible GMS imagery).

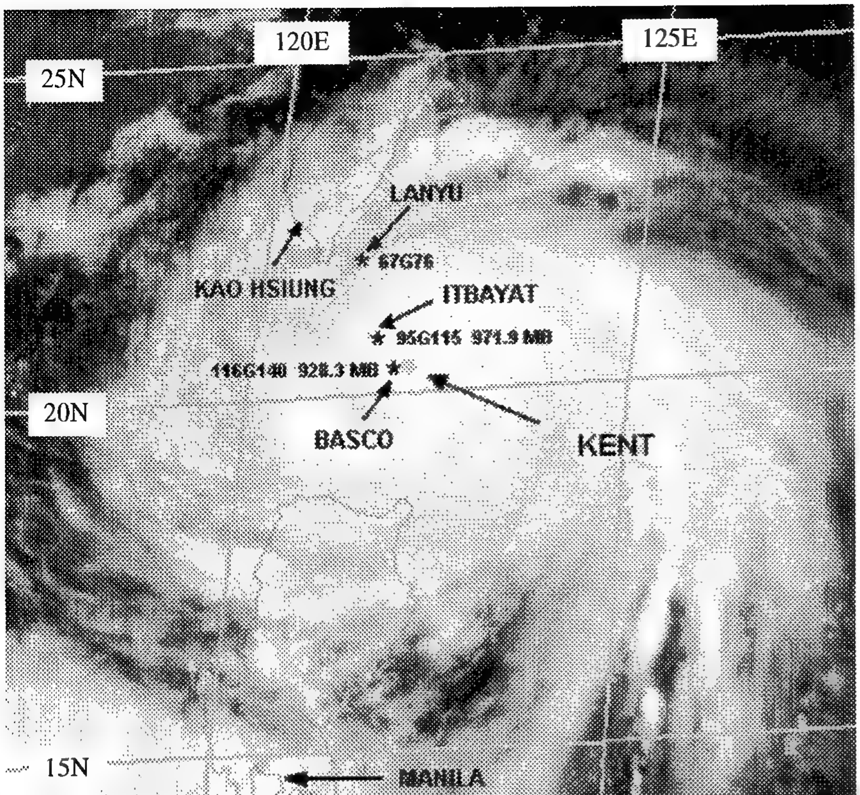

Figure 3-12-2 Kent nears Basco, with sustained winds estimated at 125 kt (64 m/sec). Maximum observed winds and minimum sea-level pressures are indicated for Basco and Itbayat Island during peak conditions (292331Z August visible GMS imagery).

On 28 August, Kent developed a banding-type eye, and remained at 75 kt (39 m/sec) intensity until 281800Z, when it began to intensify. Kent reached its peak intensity of 130 kt (67 m/sec) at 291200Z. At 300100Z, the center of Kent's eye passed south of Basco. Satellite imagery (Figure 3-12-2) and radar imagery (Figure 3-12-3a-h) are available for this time period. Kent's passage over Basco afforded an opportunity for ground validation of the satellite-derived intensity. Kent's intensity (satellite-derived and ground-truth), and its structure as revealed by radar during its passage over Basco, are described more fully in the discussion section.

On 30 August, Kent began to weaken slowly. At the same time, it began to accelerate on its west-northwest track toward the China mainland (Figure 3-12-4). Kent made landfall at 310700Z approximately 50 nm (95 km) northeast of central Hong Kong. The final warning was issued, valid at 010000Z September, as Kent dissipated while passing over the rugged terrain of south central China.

III. DISCUSSION

a. *The passage of Kent over Basco*

The passage of the eye of Kent just south of the Philippine meteorological station at Basco, Batan Island (WMO 98135), allowed for an excellent comparison between actual measured winds and the estimated winds given by the application of Dvorak's techniques to a very intense typhoon. At the time of the satellite image (292331Z) in Figure 3-12-2, Basco was entering the western wall cloud of the eye of Kent. The application of the digital Dvorak (DD) algorithm (see Oscar's (17W) summary for an in-depth discussion of the DD algorithm) to the 292331Z infrared image yielded an intensity estimate of T 6.1. This corresponds to a sustained 1-minute wind speed of 117 kt (60 m/sec) and a minimum sea-level pressure of 926 mb. The DD estimates of Kent's intensity during the six hours prior to its closest point of approach to Basco averaged approximately T6.5, which yields an equivalent 1-minute wind speed of approximately 130 kt (67 m/sec) and a minimum sea level pressure of 910 mb.

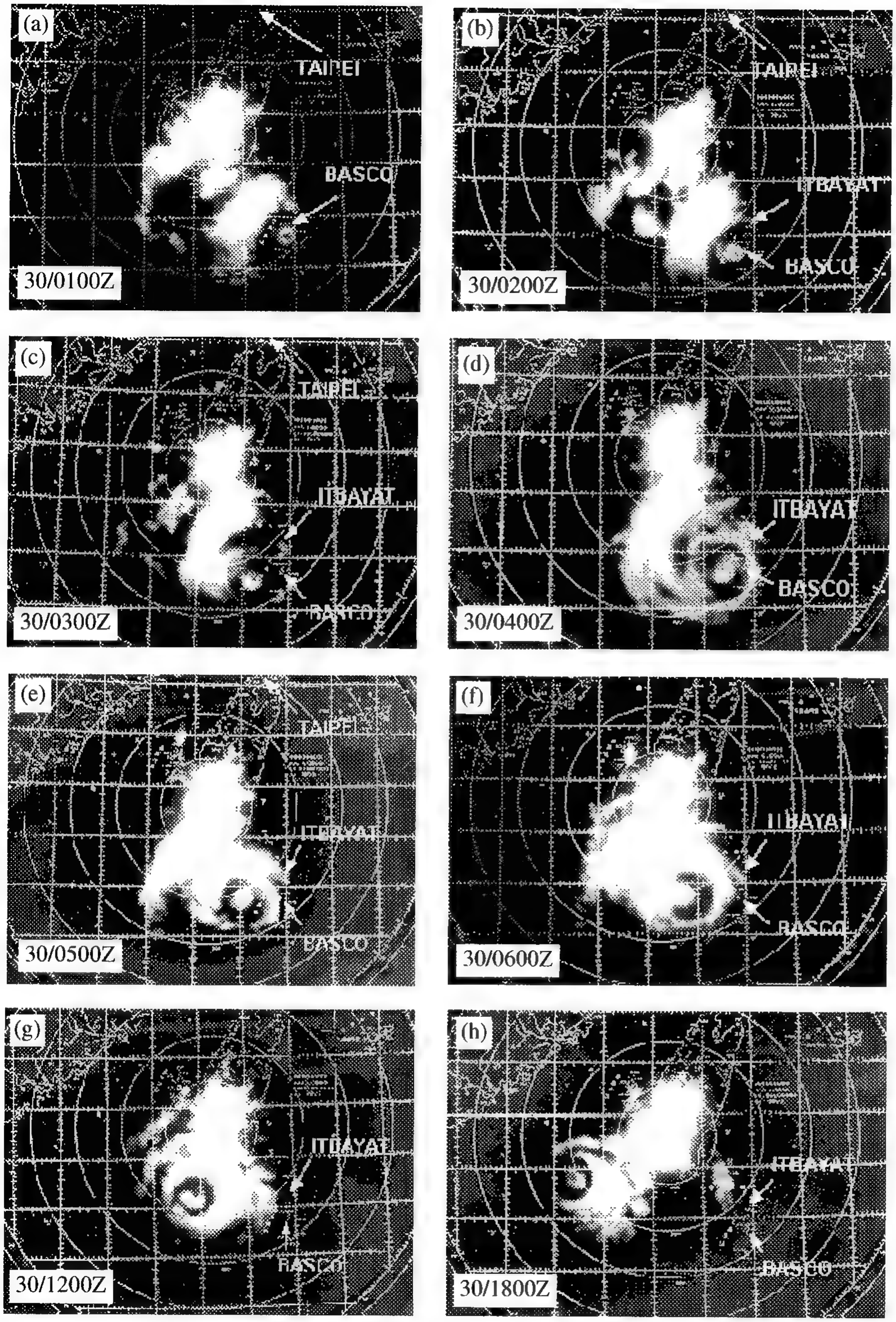

Figure 3-12-3 Radar images from the Kaohsiung radar show the concentric eye-walls of Kent. Images (a) through (f) are hourly, and (g) and (h) are 6-hourly. (Radar images courtesy of the Central Weather Bureau, Taiwan).

For the purposes of postanalysis, research, and development of a high-confidence tropical cyclone intensity data base at the University of Guam, several international meteorological agencies have generously provided landfall/eye passage maximum wind information to researchers there. For Kent, critical data were provided by the Philippine Atmospheric, Geophysical, and Astronomical Services Administration (PAGASA), the Royal Observatory Hong Kong, and the Central Weather Bureau,

Taiwan. These agencies report sustained winds as a 10-minute average, and when necessary for comparison with the JTWC, a conversion is made to the equivalent 1-minute sustained average. Critical wind and pressure data measured at various island locations that were affected by Kent have been superimposed on the satellite imagery of Figure 3-12-2. Table 3-12-1 summarizes the wind and pressure data recorded during Kent's passage over Basco.

The following conclusions can be drawn concerning Kent's passage over Basco: (1) the center of the eye may not have gone directly over Basco (the Kaohsiung radar images indicate that the center of the eye passed approximately 5 nm (10 km) south of Basco), but it did enter the northern edge of the eye given Basco's reported brief period (15 minutes) of lighter winds; (2) using the Atkinson/Holliday (A&H) wind-pressure relationship, the minimum sea-level pressure recorded at Basco of 928 mb corresponds to a sustained 1-minute wind speed of 114 kt (59 m/sec); (3) allowing for the fact the pressure in the exact center of the eye may have been approximately 10 mb lower (i.e., 918 mb), the corresponding sustained wind on the A&H scale would rise to 123 kt (63 m/sec); and, (4) the peak gust of 140 kt (72 m/sec) measured at Basco supports a sustained over-water 1-minute sustained wind of at least 115 kt (59 m/sec). The best-track indicates an intensity of 125 kt (64 m/sec) at 300000Z (and a gradual weakening trend) 50 minutes prior to Basco's peak gust and one hour prior to the minimum recorded sea-level pressure there. The peak wind and minimum sea-level pressure recorded at Basco are consistent with the intensity estimates from satellite imagery yielded by the DD algorithm.

b. *Radar depiction of Kent*

Radar images from Kaohsiung, Taiwan, (Figure 3-12-3a-h) indicated that Kent had concentric eye walls for at least 22 hours. Each hourly radar image from 300100Z to 302300Z (not all of these are shown in Figure 3-12-3a-h) shows an inner eyewall surrounded by an outer eyewall. The diameter of each eye appears to remain the same each hour, although the inner eye occasionally became open in one quadrant and the reflectivity appeared to fluctuate within the inner eyewall. The inner eye also appeared to wobble within the clear region separating the two eyewalls. The diameter of the inner eye was approximately 9 nm (17 km). The diameter of the outer eye fluctuated from 50-70 nm (93-130 km). There was no indication, however, that the inner eye disappeared or that as the outer eyewall shrank and replaced the inner eyewall (as in the eyewall replacement process described by Willoughby (1982, 1990)). A similar occurrence is discussed in the 1994 Annual Tropical Cyclone Report concerning Typhoon Gladys. In both cases, the inner and outer eye appeared to conserve their general characteristics for nearly a day.

IV. IMPACT

Damage at Basco (WMO 98135) was estimated at US$2 million, and at Itbayat (WMO 98132) US$50,000. Considerable flooding occurred on Luzon. In Pampanga province, 50 nm (95 km) north of Manila, 65,000 people were reported to have fled as heavy rains created mudflows from the slopes of Mount Pinatubo that buried entire communities. Five deaths were reported in Luzon. In southern China, Kent destroyed banana plantations and sunk many fishing boats. Thirty people were reported dead in Guangdong province, and 17 lost their lives in Hainan. Kent caused an estimated US$87 million in damage in China. Hong Kong was spared serious damage.

Table 3-12-1 Information about the eye passage of Super Typhoon Kent at Basco (WMO 98135). MWBE is the maximum sustained wind direction/speed/gust prior to eye passage; MWDE is the peak gust during eye passage; MSLP is the minimum sea-level pressure at eye passage; MWAE is the maximum sustained wind direction/speed/gust after eye passage. Sustained winds are one-minute averages. Time of occurrence is given below the meteorological information.

MWBE(kt)	MWDE(kt)	MSLP(mb)	MWAE(kt)
020/116/140	40	928.3	120/M/140
30/0050Z	30/0100Z	30/0100Z	30/0110Z

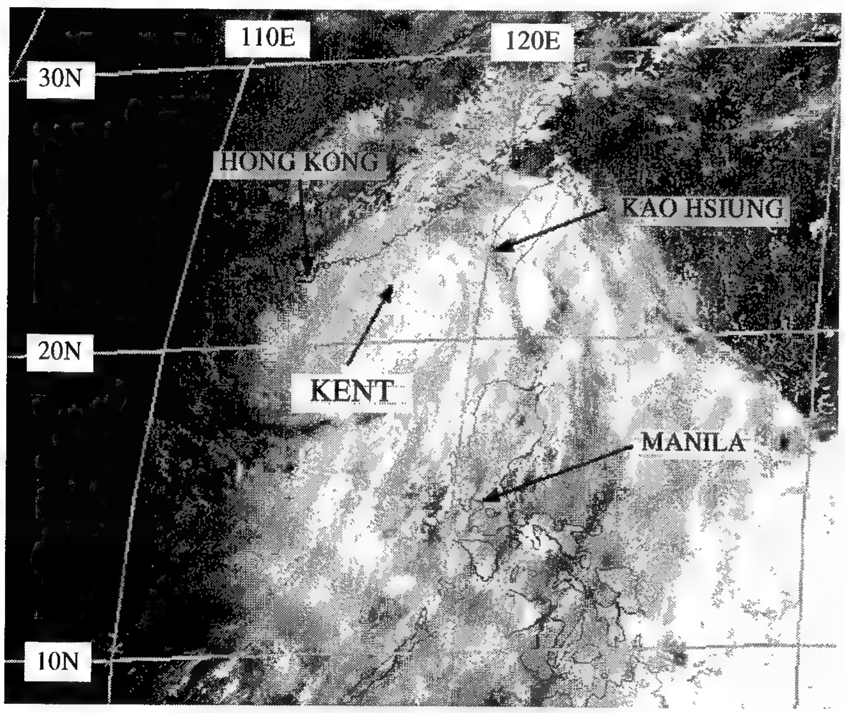

Figure 3-12-4 Kent with an intensity of 105 kt (54 m/sec) when located about 175 nm (325 km) east of Hong Kong (302231Z August visible GMS imagery).

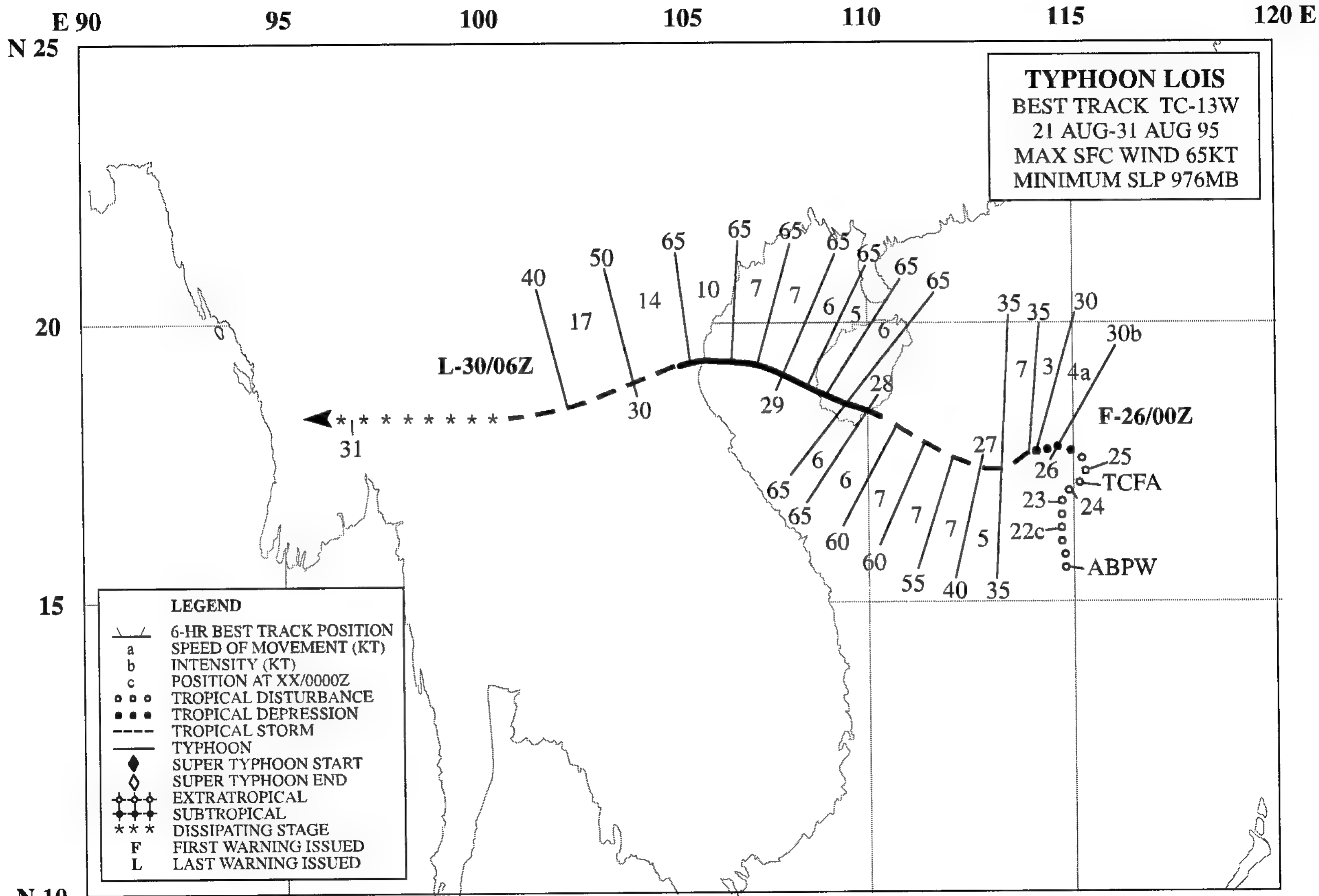
TYPHOON LOIS
BEST TRACK TC-13W
21 AUG-31 AUG 95
MAX SFC WIND 65KT
MINIMUM SLP 976MB
LEGEND
6-HR BEST TRACK POSITION
a SPEED OF MOVEMENT (KT)
b INTENSITY (KT)
c POSITION AT XX/0000Z
TROPICAL DISTURBANCE
TROPICAL DEPRESSION
TROPICAL STORM
TYPHOON
SUPER TYPHOON START
SUPER TYPHOON END
EXTRATROPICAL
SUBTROPICAL
DISSIPATING STAGE
F FIRST WARNING ISSUED
L LAST WARNING ISSUED
F-26/00Z
L-30/06Z
TCFA
ABPW
E 90
95
100
105
110
115
120 E
N 25
20
15
N 10

TYPHOON LOIS (13W)

I. HIGHLIGHTS

As Typhoon Kent (12W) was developing east of the Philippines and Tropical Storm Janis (10W) was crossing the southwestern Ryukyu Islands, Lois formed in the South China Sea. This was one of only three occasions during 1995 that the JTWC was simultaneously warning on three tropical cyclones in the western North Pacific. Lois was one of an unusually large number of tropical cyclones that formed in the South China Sea during 1995.

II. TRACK AND INTENSITY

On 21 August, synoptic data indicated the presence of a weak cyclonic circulation center near 15°N 115°E that accompanied an area of deep convection. This tropical disturbance was first mentioned on the 210600Z August Significant Tropical Weather Advisory. For two days, the disturbance drifted slowly to the north, and its deep convection became better organized. Beginning on 23 August, the disturbance moved toward the northeast, possibly in response to a surge in the southwest monsoon that flowed past the pre-Lois disturbance northeastward to the circulation of Janis (10W). A Tropical Cyclone Formation Alert was issued at 240830Z when the system appeared to be improving in organization. On 25 August, the long fetch of southwesterly monsoon flow began to weaken between pre-Lois and Janis (10W) as the axis of the subtropical ridge began to build between these two systems (see the discussion section for a more detailed discussion of the effects of the monsoon flow on the motion of Lois). As the subtropical ridge strengthened to its north, the pre-Lois tropical disturbance responded with a slow counterclockwise turn to the west. Based upon intensity estimates of 25 kt (13 m/sec) made from satellite imagery, the first warning on Tropical Depression 13W was issued valid at 260000Z. The system was upgraded to tropical storm intensity twelve hours later. South of a strengthening subtropical ridge, Lois moved on a generally westward track. At 280000Z, Lois was upgraded to a typhoon, just as it touched the southern coastline of Hainan Island. Crossing the southern edge of Hainan Island, Lois passed close to the city of Yaxian (WMO 59948) where a minimum sea-level pressure of 981.9 mb was reported. Lois then spent a day crossing the Gulf of Tonkin (Figures 3-13-1 and 3-13-2), before moving ashore at 291600Z in a sparsely populated area of Vietnam. Bach Longvi, Vietnam (WMO 48839), reported a minimum sea-level pressure of 989.9 mb at 291800Z. Continuing westward, the system dissipated over the mountains of Laos, prompting the JTWC to issue the final warning, valid at 300600Z.

III. DISCUSSION

Influence of the southwest monsoon on tropical cyclone motion

Lois' northeastward motion during the period of its formation (23 through 24 August) was typical of that seen whenever a tropical cyclone is affected by deep southwesterly monsoonal winds that flow past that tropical cyclone to another tropical cyclone downstream. In the case of Lois, as Tropical Storm Janis (10W) crossed the region of Taiwan and the Ryukyu Islands, the southwest monsoon in the South China Sea extended to the north-northeast, linking with the circulation of Janis (10W) (Figure 3-13-3). A case can be made that the pre-Lois tropical disturbance moved northeastward in response to the monsoonal flow that had extended toward Janis (10W). By 26 August, Janis (10W) was recurving into mid-latitudes, and a ridge became established between it and Lois that severed the northeastward extension

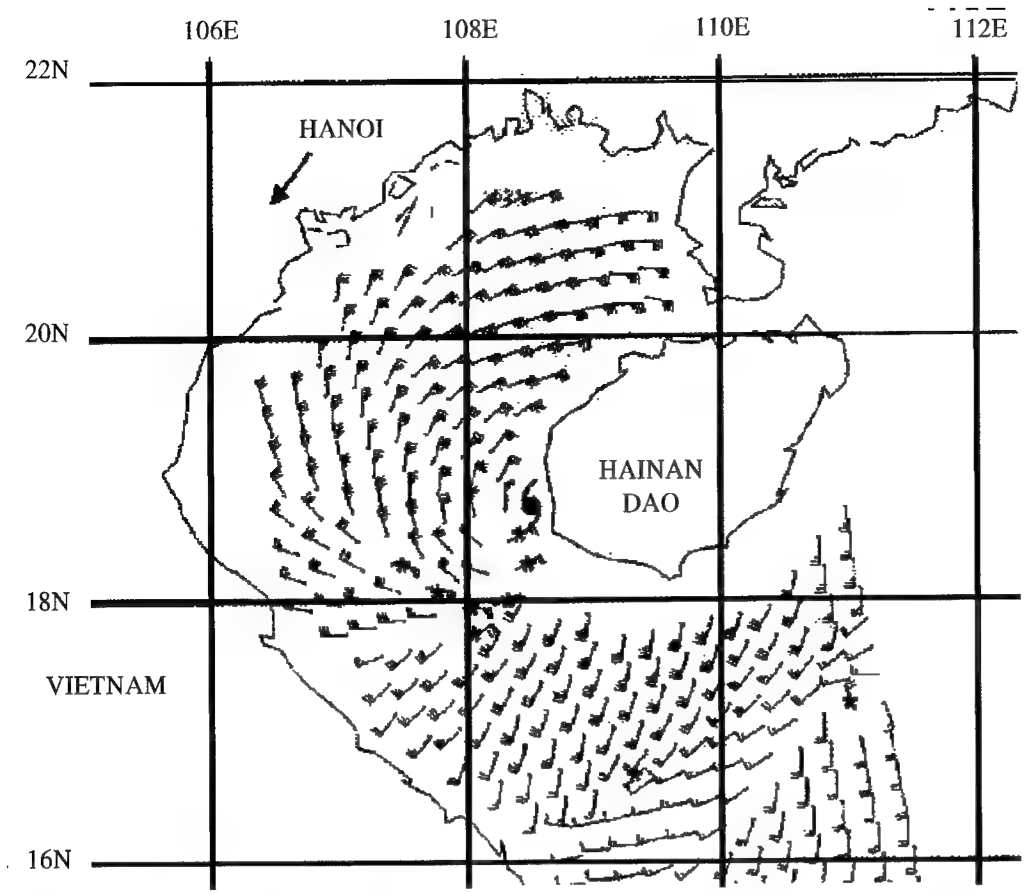

Figure 3-13-1 The surface wind field of Lois as it moves from Hainan Island into the Gulf of Tonkin as derived from the scatterometer aboard the ERS-1 spacecraft. Wind barbs that are 180 degrees in error are marked with an asterisk. Typhoon symbol marks the interpolated location of Lois (281500Z August ERS-1 scatterometer-derived marine surface winds).

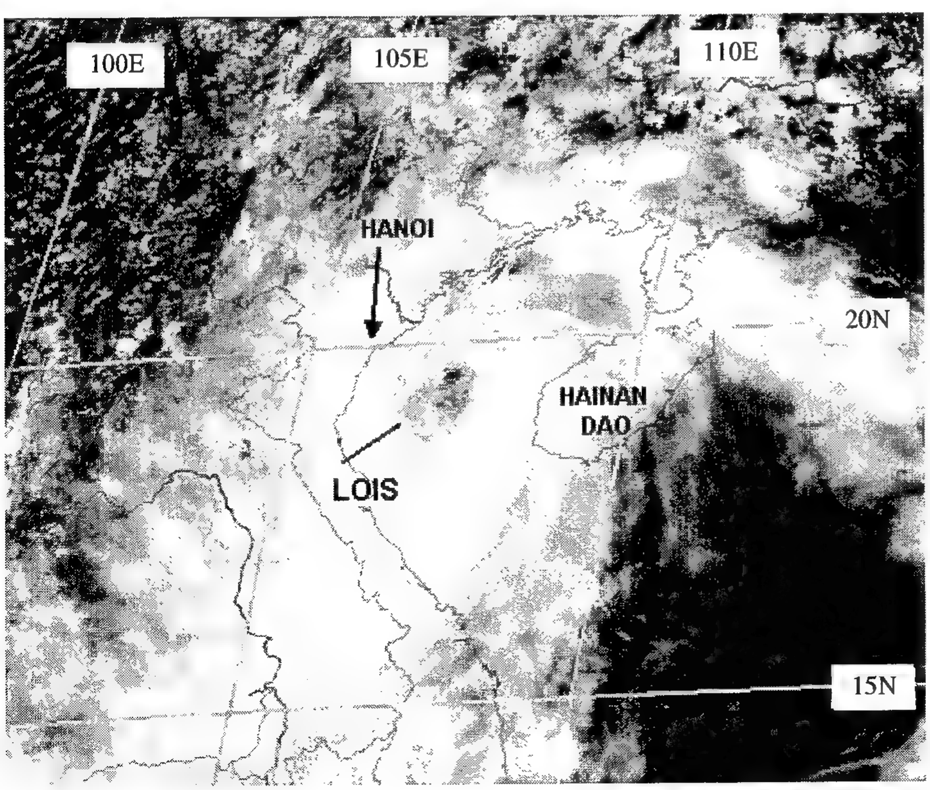

Figure 3-13-2 Typhoon Lois in the Gulf of Tonkin with a large 60 nm (110 km) diameter eye (290531Z August visible GMS imagery).

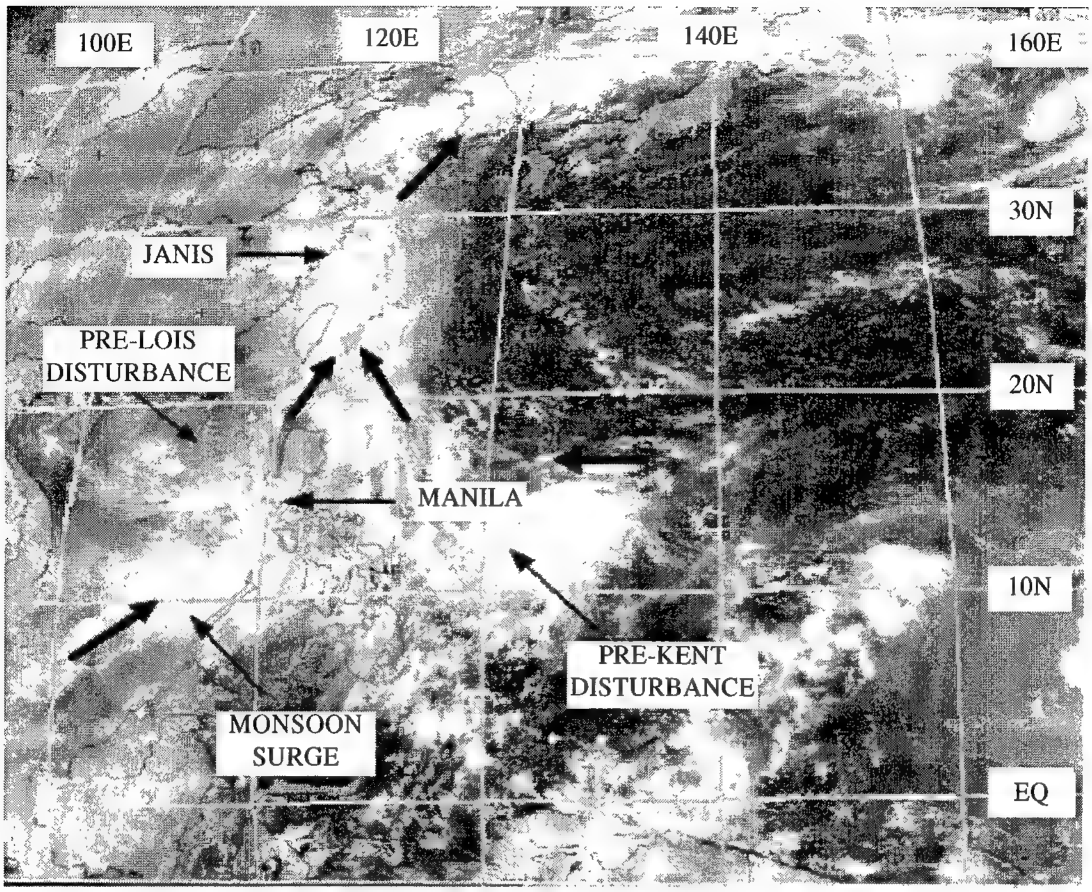

Figure 3-13-3 The southwest monsoon extends beyond the pre-Lois tropical disturbance and continues northeastward across the Philippines, then north-northeastward into Janis' circulation (242331Z August visible GMS imagery). Bold arrows depict the low-level wind flow. The locations of Janis (10W), pre-Kent (12W), and of pre-Lois are indicated.

of the southwest monsoon. In response to easterly flow south of the strengthening ridge, Lois turned toward the west.

IV. IMPACT

No reports of damage or injuries were received from China. In Vietnam, 45,000 acres of rice fields were reported flooded, with a total loss of the rice crop in nearly ten percent of the flooded acres. One hundred houses were destroyed and 2000 other homes were damaged in the province of Thanh Hoa, the hardest hit province. No reports of deaths or injuries in Vietnam were received at the JTWC.

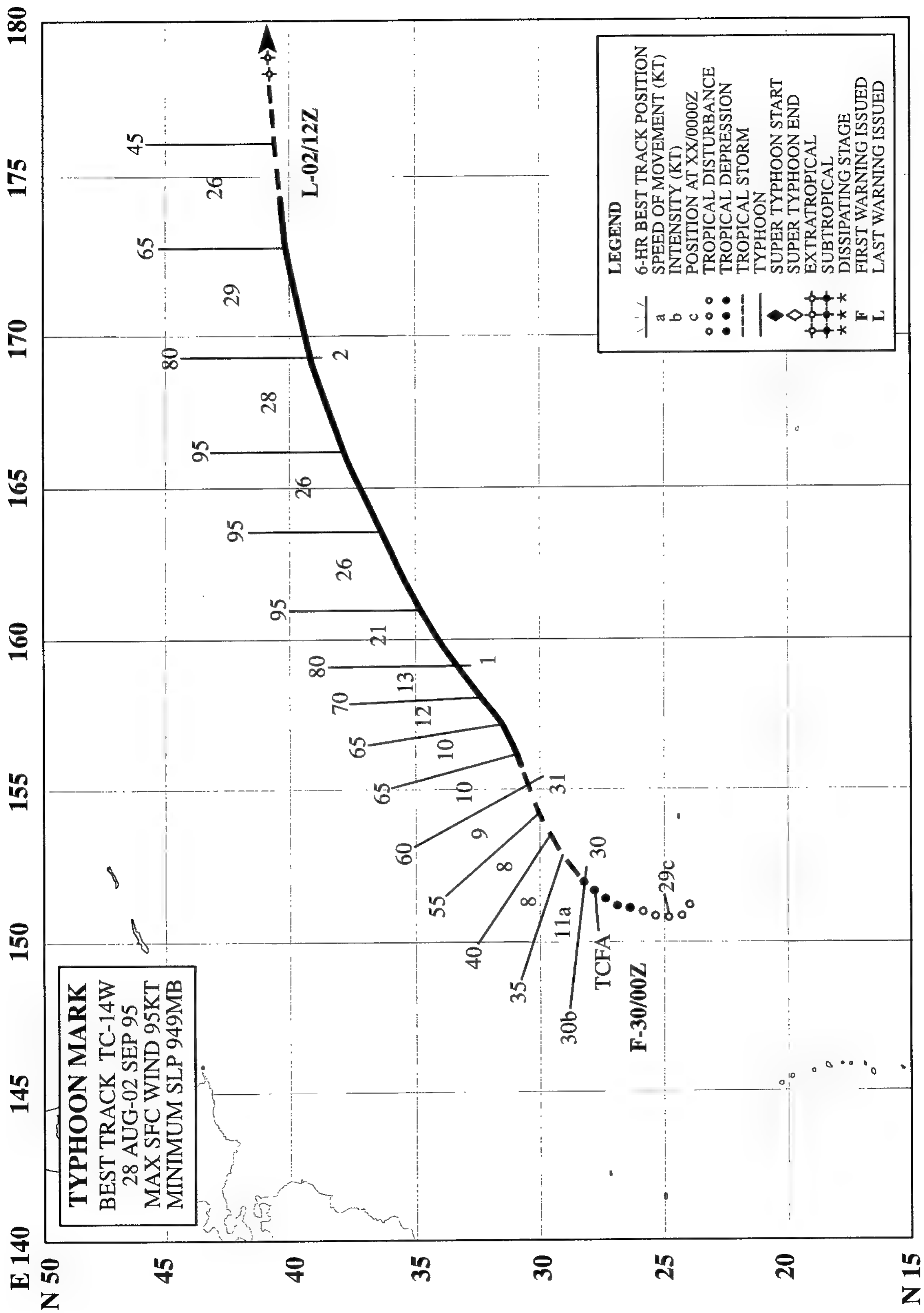
TYPHOON MARK
BEST TRACK TC-14W
28 AUG-02 SEP 95
MAX SFC WIND 95KT
MINIMUM SLP 949MB
LEGEND
6-HR BEST TRACK POSITION
SPEED OF MOVEMENT (KT)
INTENSITY (KT)
POSITION AT XX/0000Z
TROPICAL DISTURBANCE
TROPICAL DEPRESSION
TROPICAL STORM
TYPHOON
SUPER TYPHOON START
SUPER TYPHOON END
EXTRATROPICAL
SUBTROPICAL
DISSIPATING STAGE
FIRST WARNING ISSUED
LAST WARNING ISSUED
F-30/00Z
L-02/12Z
TCFA
E 140
145
150
155
160
165
170
175
180
N 50
45
40
35
30
25
20
N 15

TYPHOON MARK (14W)

I. HIGHLIGHTS

Forming at a relatively high latitude, Mark was a very small sized tropical cyclone that moved northeastward for most of its track. While moving in excess of 20 kt (37 km/hr) toward the polar front, and while passing over increasingly cooler sea surface temperatures, Mark acquired a well-defined eye and reached a peak estimated intensity of 95 kt (49m/sec) as it tracked northeastward from 35°N to 37°N. The relatively high peak intensity attained by Mark was somewhat of a surprise, given the synoptic situation.

II. TRACK AND INTENSITY

The tropical disturbance that became Mark was first detected on the northeastern side of a westward moving TUTT cell. Visible satellite imagery obtained shortly after sunrise on 30 August showed cyclonically curved low-level cloud lines wrapping beneath an area of deep convection. This disturbance was located north-northwest of Minami Tori Shima in a data-poor region in the subtropics of the western North Pacific. Based upon the aforementioned indications on satellite imagery of the development of a low-level circulation center associated with this tropical disturbance, a Tropical Cyclone Formation Alert was issued at 292200Z August. Shortly thereafter, at 300000Z August, the first warning was issued. The prognostic reasoning message accompanying this first warning stated:

"Tropical Depression 14W has formed north of Minami Tori Shima . . . the initial disturbance was spawned from a tropical upper tropospheric trough (TUTT) cell . . . [deep] convection [has] developed rapidly over an 18 hour period."

Additional comments included:

"Due to the relatively high latitude at which 14W formed, and its proximity to the baroclinic zone to the northeast, 14W is not expected to intensify much past minimal tropical storm [intensity] before it undergoes extratropical transition."

Tropical depression 14W was upgraded to Tropical Storm Mark at 300600Z August based upon indications from satellite imagery of further intensification. Mark was already moving to the northeast at a relatively high latitude (approximately 30°N), and significant further intensification was not anticipated. On the evening of 31 August, a small ragged eye appeared within the small CDO, and Mark was upgraded to a Typhoon at 310600Z August. Mark was now north of 30°N and moving northeastward at 10 kt. A frontal system was approaching from the west, and JTWC forecasters expected Mark to accelerate, interact with the approaching front, and undergo extratropical transition within 36 to 48 hours.

During the subsequent 24 hours, Mark continued to move northeastward while remaining ahead of the approaching front. In a surprising structural evolution, during the morning of 01 September, the very small sized Typhoon Mark developed a small well-defined eye (Figure 3-14-1a,b). During the evening and night of 01 September, the cloud-top temperatures of the wall cloud surrounding Mark's well-defined eye cooled, and the estimated intensity peaked at 95 kt (49 m/sec) at 010600Z September. While Mark retained its peak intensity during the period 010600Z to 011800Z September, its speed of translation increased from 20 kt to 31 kt (37 to 57 km/hr). This rapid speed of translation delayed Mark's entrainment into the frontal system approaching from the west. On 02 September, the typhoon began to experience vertical wind shear from the west, and Mark was downgraded to a tropical storm late in the day. At 021200Z September, the JTWC issued the final warning on Tropical Storm Mark based upon its acquisition of extratropical characteristics.

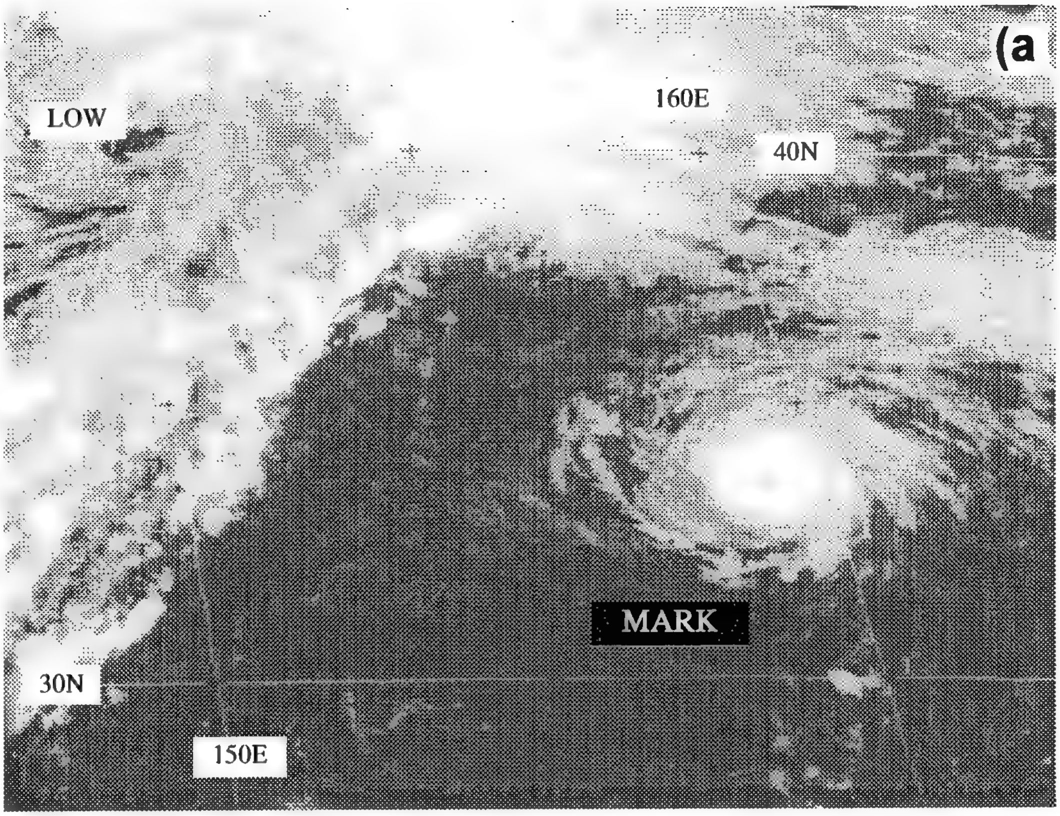

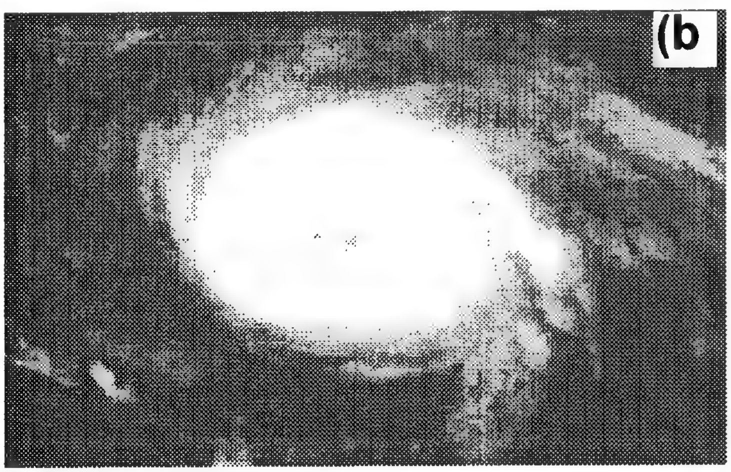

Figure 3-14-1 (a) Typhoon Mark intensifies as it moves rapidly northeastward in the warm sector of an approaching mid-latitude low-pressure system. (b) An expanded image of Typhoon Mark at the same picture time as in (a). (Both images are 010031Z September visible GMS imagery).

III. DISCUSSION

a. *Formation and development at high latitude*

Relatively few tropical cyclones (TCs) form in the western North Pacific poleward of 25°N — during the 21-year period 1970 to 1990 only twenty-four of 585 tropical cyclones (4%) that formed in the western North Pacific first attained 25 kt (12 m/sec) intensity at, or north, of 25°N. Mark first attained 25 kt intensity at 27°N. It became a tropical storm at 29°N, a typhoon at 31°N, and reached its peak intensity of 95 kt (49 m/sec) at 35°N. The sea surface temperature at the point where Mark's intensity peaked was approximately 24°C (Figure 3-14-2).

The synoptic conditions under which TCs form at very high latitude include:

1) formation in the mei-yu front,

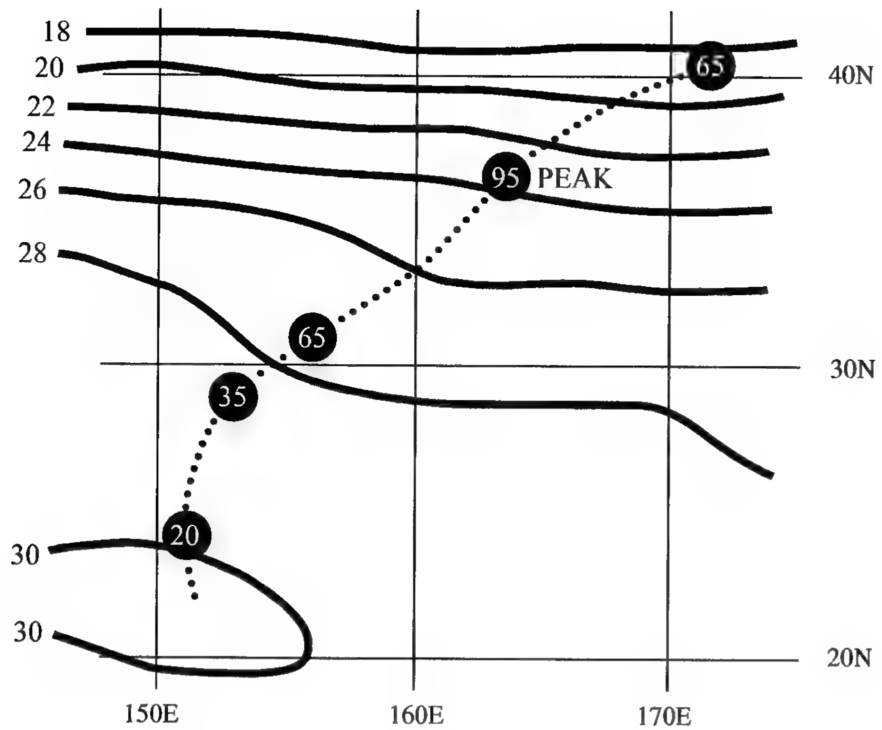

Figure 3-14-2 Selected threshold intensities (in kt) of Mark (white numbers within the black circles) along Mark's track (dotted line) superimposed on the NOGAPS sea surface temperature analysis (°C) of 02 September.

2) formation at the northeastern reaches of a reverse-oriented monsoon trough,
3) formation in association with a TUTT cell, and
4) formation at the base of a mid-latitude trough.

Mark formed in association with a TUTT cell. On 28 August, the tropical disturbance that became Mark was located in the northeastern quadrant of a TUTT cell that was centered at about 20°N over the Mariana Islands . The pre-Mark disturbance moved northward, intensified and approached the polar frontal boundary which then stretched east-west along approximately 35°N. Mark reached its peak intensity while traveling northeastward at a relatively high speed of translation, and while in the warm sector of an eastward moving mid-latitude low-pressure system (Figure 3-14-1a).

b. *Small size*

Like most TCs that form at high latitude in association with TUTT cells, Mark was a very small tropical cyclone. The diameter of its cloud shield was about 100 nm (185 km), and it encompassed a very small eye whose diameter fluctuated within a range from 5 (9 km) to 10 nm (18 km) on satellite imagery. As with many very small tropical cyclones, the intensity forecasts were quite poor: on the first eight warnings (issued at six-hour intervals from 300000Z August to 311800Z August), the 24-hour intensity was under-forecast by anywhere from 20 to 40 kt (21 m/sec); and, the 48-hour intensity was under-forecast by as much as 65 kt (33 m/sec).

IV. IMPACT

For its entire track, Mark remained far at sea, and no reports of significant damage were received.

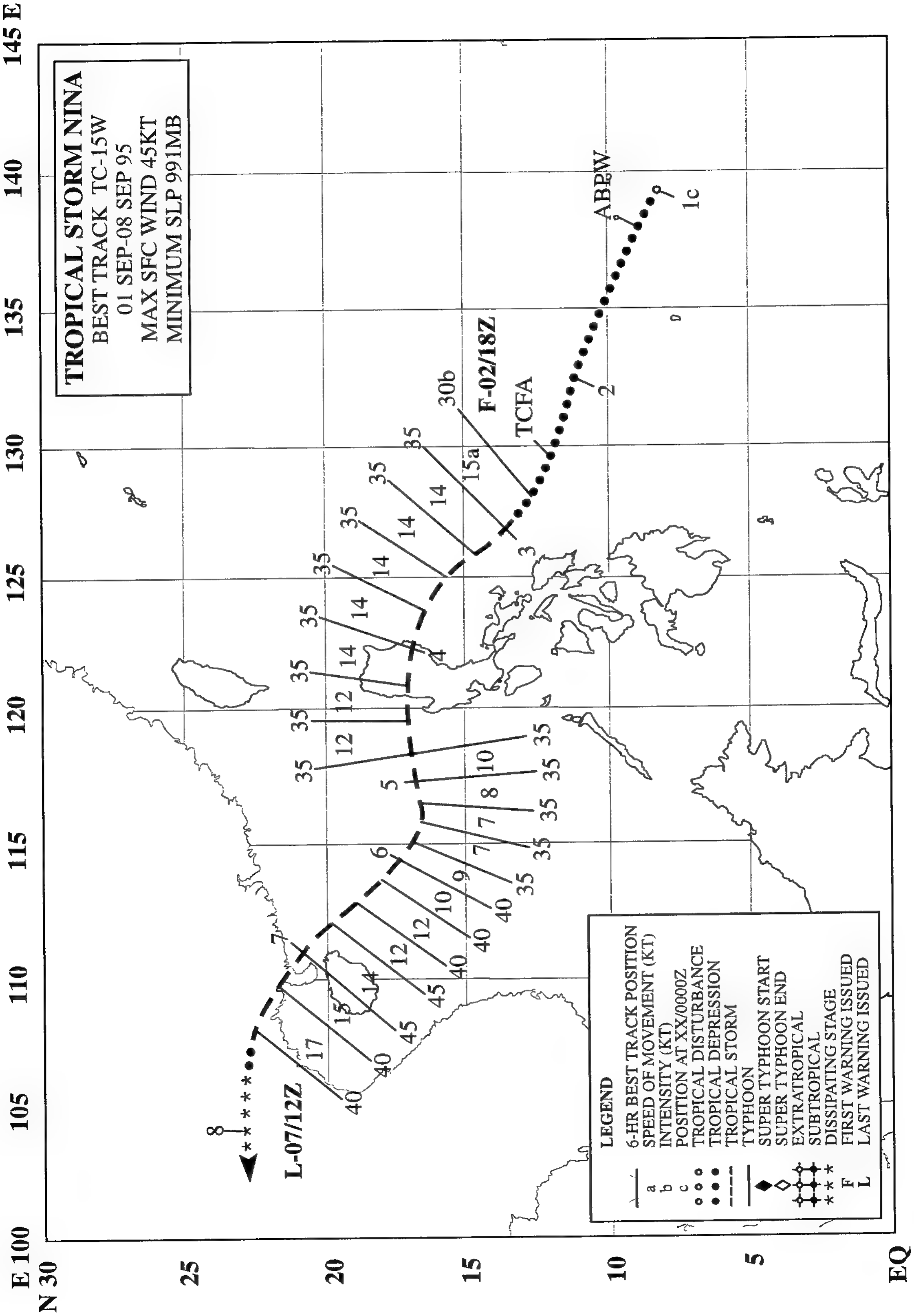
TROPICAL STORM NINA
BEST TRACK TC-15W
01 SEP-08 SEP 95
MAX SFC WIND 45KT
MINIMUM SLP 991MB
LEGEND
a 6-HR BEST TRACK POSITION
b SPEED OF MOVEMENT (KT)
c INTENSITY (KT)
POSITION AT XX/0000Z
TROPICAL DISTURBANCE
TROPICAL DEPRESSION
TROPICAL STORM
TYPHOON
SUPER TYPHOON START
SUPER TYPHOON END
EXTRATROPICAL
SUBTROPICAL
DISSIPATING STAGE
F FIRST WARNING ISSUED
L LAST WARNING ISSUED
ABPW
TCFA
F-02/18Z
L-07/12Z
E 100
105
110
115
120
125
130
135
140
145 E
N 30
25
20
15
10
5
EQ

TROPICAL STORM NINA (15W)

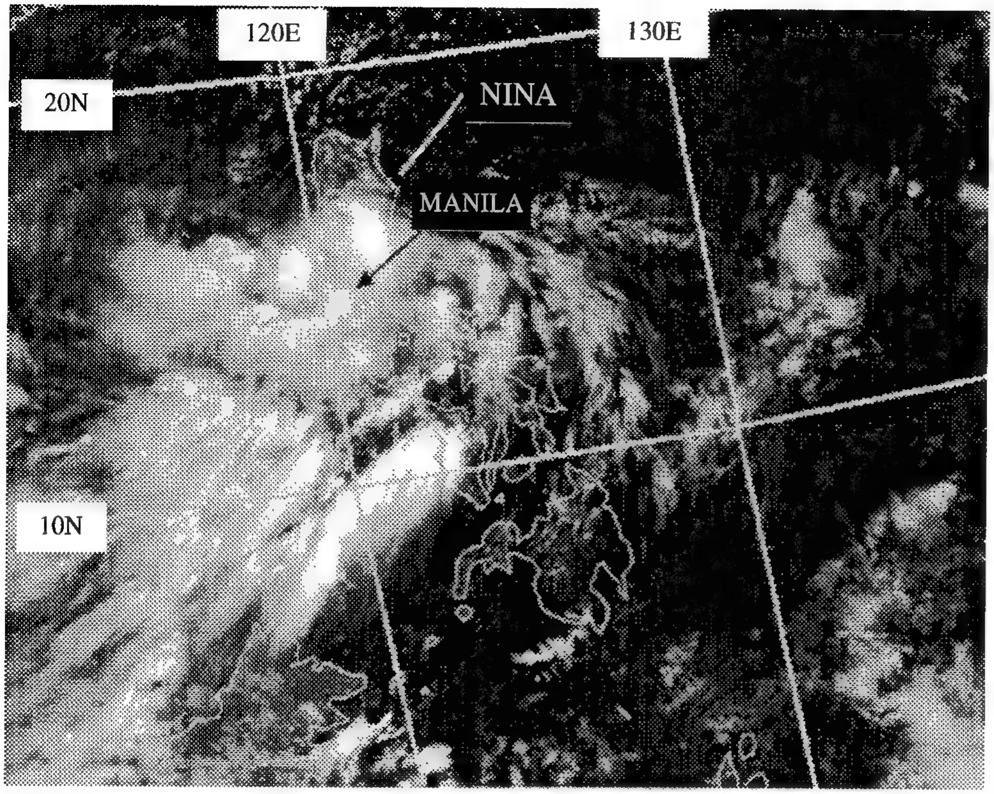

Figure 3-15-1 Tropical Storm Nina just after making landfall on eastern Luzon (040107Z September visible DMSP imagery).

I. HIGHLIGHTS

Nina was one of seven tropical cyclones during 1995 that passed over the Philippines with an intensity of 35 kt (18 m/sec) or greater. Reaching a peak intensity of only 45 kt (23 m/sec), it was one of several slow developing and low-intensity tropical cyclones — a signature characteristic of 1995.

II. TRACK AND INTENSITY

On the afternoon of 01 September, an area of deep convection was first mentioned on the Significant Tropical Weather Advisory, valid at 010600Z. This area, located approximately 400 nm (740 km) south-southwest of Guam, moved rapidly to the northwest. As the disturbance crossed the 130°E meridian, low-level southwesterly monsoon winds increased across the southern Philippines and merged with the disturbance. Based on an increase in the amount of deep convection and improvements in organization, the JTWC issued a Tropical Cyclone Formation Alert valid at 021630Z September. The first warning on Tropical Depression 15W followed, valid at 021800Z. Only six hours after the first warning, TD 15W was upgraded to Tropical Storm Nina.

Moving northwestward at 14 kt (26 km/hr), Nina made landfall on the east coast of Luzon shortly before 040000Z. Nina was poorly organized as it crossed Luzon (Figure 3-15-1), and though satellite intensity estimates indicated 35 kt (18 m/sec), no landfall wind reports were available from PAGASA that indicated more than 15 kt (8 m/sec). The lowest sea-level pressure recorded in the Philippines during Nina's passage was 1003 mb.

Nina slowly intensified once it entered the South China Sea. Under the influence of strong upper-level northeasterly flow, the system was sheared, with most of the deep convection located on the south side (Figure 3-15-2). On the morning of 06 September, Nina's movement changed from westward to northwestward. The system continued on a northwestward track until it made landfall at 070300Z on the Luichow peninsula in southern China. The peak intensity of 45 kt (23 m/sec) was attained eight hours before landfall. The final warning, valid at 071200Z, was issued by the JTWC as Nina dissipated near the China-Vietnam border.

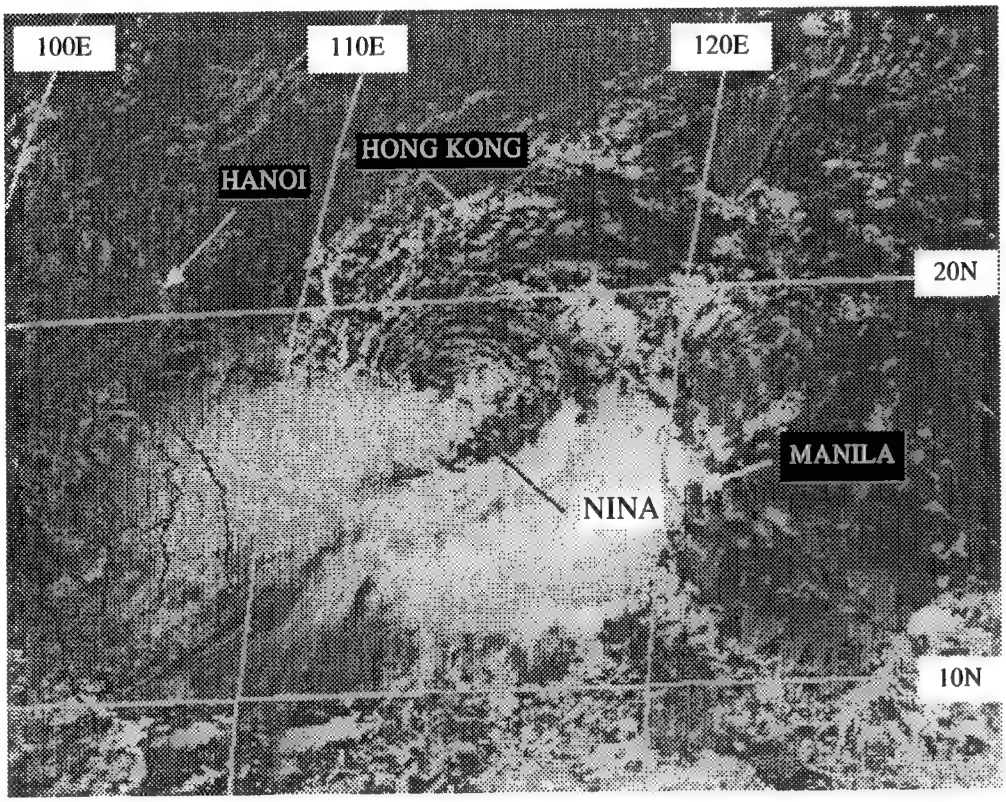

Figure 3-15-2 Thirty-six hours after exiting the Philippines, Tropical Storm Nina, with 40 kt (21 m/sec) one-minute sustained winds, is becoming better organized despite apparent manifestations of northeasterly shear (e.g., the low-level circulation center is partially exposed on the northeastern side of an area of deep convection) (052331Z September visible GMS imagery).

III. DISCUSSION

a. *Another low end tropical cyclone during 1995*

During 1995, a large proportion of the year's tropical cyclones were weak. Of the 34 significant tropical cyclones only 26 were tropical storms or typhoons, and eight never made it past tropical depression intensity. Of the 26 tropical cyclones that intensified beyond the tropical depression stage, 11 were tropical storms and 15 were typhoons. In all, 19 (56%) of the significant tropical cyclones of 1995 did not mature to become typhoons. The long term annual distribution of tropical cyclones in the western North Pacific stratified by intensity is: 18 typhoons, 10 tropical storms, and three tropical depressions. Thus, of the long-term annual average of 31 significant tropical cyclones in the western North Pacific, a total of 13 (42%) do not mature to become typhoons. The higher proportion of low-end tropical cyclones during 1995 is consistent with the persistent easterly wind flow at low latitudes, and the resulting westward shift of the leading edge of the monsoon trough and the westward shift of the mean genesis latitude.

b. *Dvorak T numbers too low*

From 06-08 September, the Dvorak T-number values were consistently 1.5 to 2.0 T-numbers too low for the observed maximum wind speeds. This result is typical when the Dvorak techniques are applied to tropical cyclones (such as Nina) that possess the characteristics of a monsoon depression. Many tropical cyclones that form in the western North Pacific start out as monsoon depressions. The lack of significant central deep convection within the light-wind core of the typical monsoon depression renders Dvorak's satellite intensity estimation techniques largely inapplicable. Many monsoon depressions that form in the western North Pacific develop peripheral gales before they acquire persistent central deep convection. Persistent central deep convection in the core of a monsoon depression marks its transition into a conventional tropical cyclone to which Dvorak's technique applies.

IV. IMPACT

In the Philippines, at least 50 people perished due to floods and mudslides. Several villages in the Pampanga Province (about 50 nm (95 km) north of Manila) were buried under lahars surging off the slopes of Mount Pinatubo. No reports of damage or injuries in China were received at the JTWC.

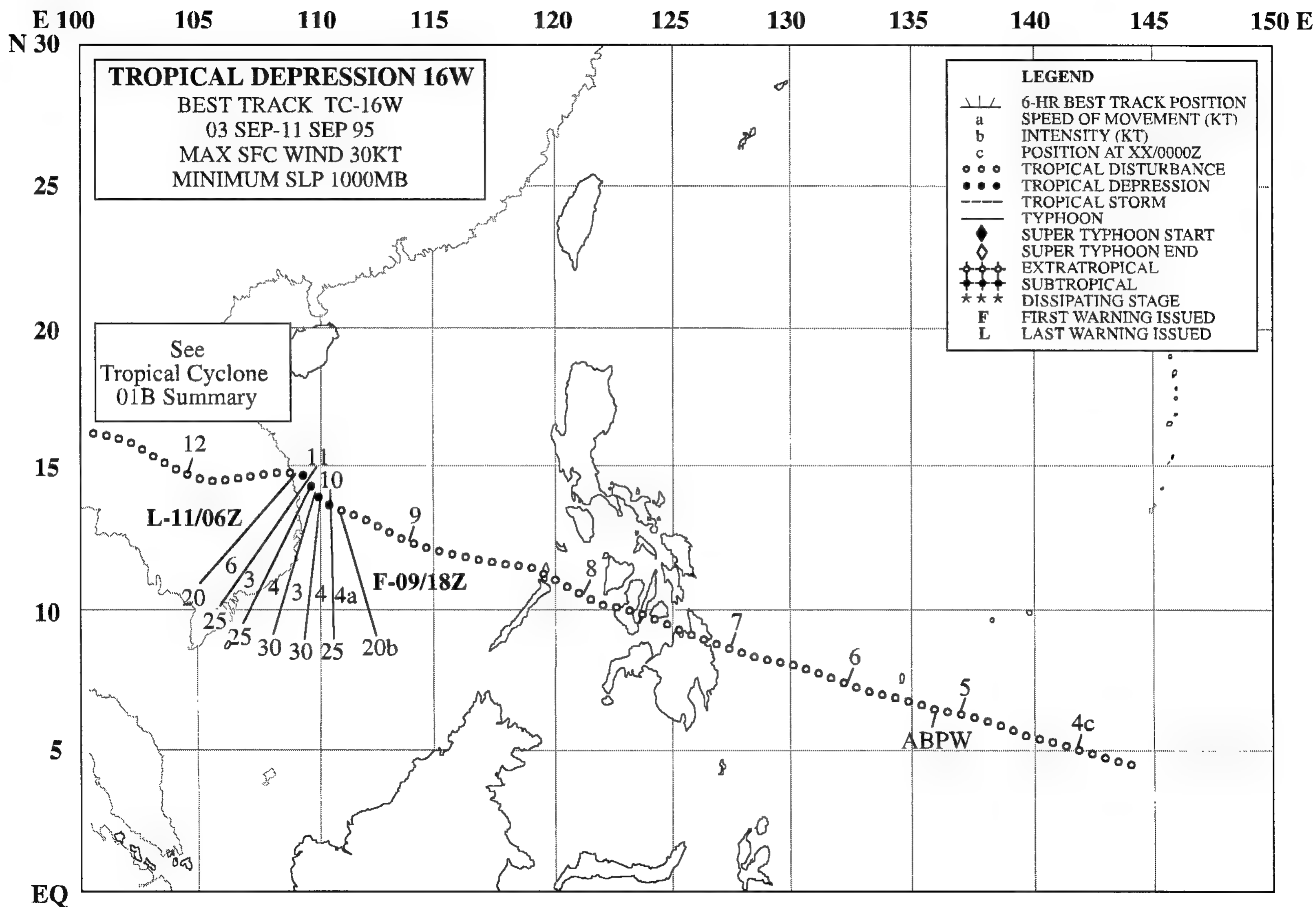
TROPICAL DEPRESSION 16W
BEST TRACK TC-16W
03 SEP-11 SEP 95
MAX SFC WIND 30KT
MINIMUM SLP 1000MB
See
Tropical Cyclone
01B Summary
LEGEND
6-HR BEST TRACK POSITION
a SPEED OF MOVEMENT (KT)
b INTENSITY (KT)
c POSITION AT XX/0000Z
TROPICAL DISTURBANCE
TROPICAL DEPRESSION
TROPICAL STORM
TYPHOON
SUPER TYPHOON START
SUPER TYPHOON END
EXTRATROPICAL
SUBTROPICAL
DISSIPATING STAGE
F FIRST WARNING ISSUED
L LAST WARNING ISSUED
E 100
105
110
115
120
125
130
135
140
145
150 E
N 30
25
20
15
10
5
EQ
L-11/06Z
F-09/18Z
ABPW
12
11
10
9
8
7
6
5
4c
6
3
4
3
4
4a
20
25
25
30
30
25
20b

TROPICAL DEPRESSION (16W)

I. HIGHLIGHTS

Tropical Depression 16W (TD 16W) followed three days behind Tropical Storm Nina (15W) on an almost parallel track, approximately 5 degrees latitude further to the south. Although their tracks were similar, TD 16W failed to develop into a significant tropical cyclone until just prior to making landfall on the Vietnam coast. The remains of TD 16W continued westward across Southeast Asia to form Tropical Cyclone 01B in the Bay of Bengal.

II. TRACK AND INTENSITY

The tropical disturbance that would eventually become Tropical Depression 16W (TD 16W) was first identified on satellite imagery as a large area of enhanced convection centered near 5°N 145°E on 03 September. Similar to other disturbances during this period, the system was slow to develop as it tracked slowly westward under persistent upper-level easterly shear. By 050600Z September, when it was first discussed on the Significant Tropical Weather Advisory, a well-defined low-level circulation still could not be readily identified on visual satellite imagery although it could be inferred from the gradient wind flow over Yap (WMO 91413) and Koror (WMO 91408). The disturbance continued to track westward for the next five days across the southern Philippine Islands and into the South China Sea with little sign of development. At 081200Z satellite imagery indicated the convective organization had improved and synoptic data indicated several 20-25 kt (10-13 m/sec) wind reports along the outer periphery of the convective area. During this time, however, the 200 mb analysis continued to show 25-35 kt (13-18 m/sec) easterly winds in the vicinity of the disturbance. The first warning for TD 16W was finally issued at 091800Z when scatterometer data from 091512Z and nearby ship reports indicated 25 kt (13 m/sec) winds near the circulation center. TD 16W reached a maximum intensity of 30 kt (15 m/sec) just prior to reaching the coast of Vietnam (Figure 3-16-1). The final warning for this system was issued at 110600Z after TD 16W had made landfall. The remains of TD 16W continued to move slowly

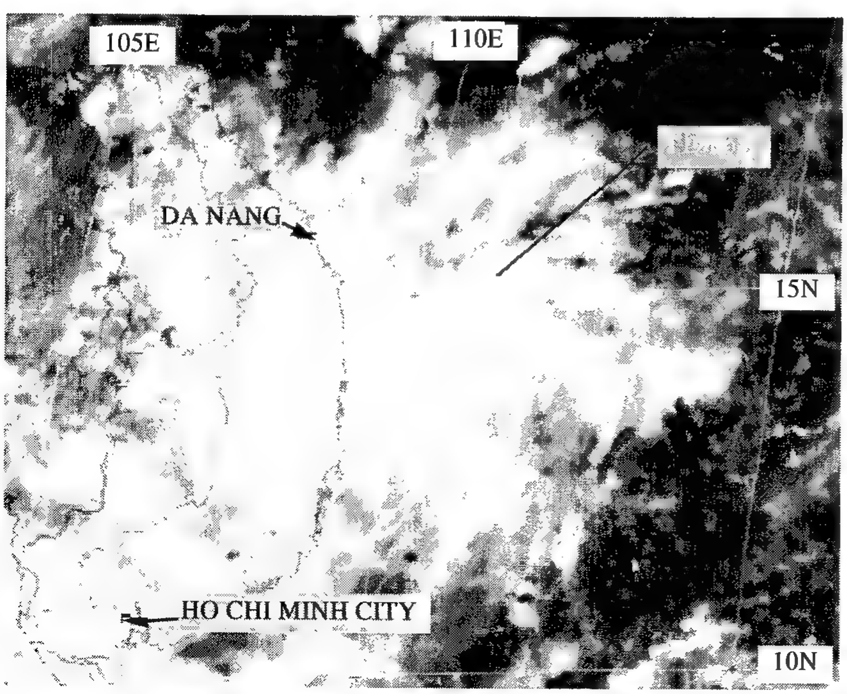

Figure 3-16-1 Tropical Depression 16W approaches the coast of Vietnam (100631Z September visible GMS imagery).

westward across Southeast Asia where it eventually became Tropical Cyclone 01B in the Bay of Bengal.

III. DISCUSSION

Eleven tropical cyclones formed in the western North Pacific during the nearly seven week period between 26 July and 10 September. Of these, eight formed in either the Philippine Sea or the South China Sea and were straight movers — presumably related to a strong dominant ridge (Figure 3-16-2) over the East China Sea and a monsoon flow that generally only extended as far east as the Philippine Islands. Typical of 1995, seven of the eight were relatively weak systems (one tropical depression, four tropical storms, and two minimal typhoons). TD 16W was the last of this series of weak systems.

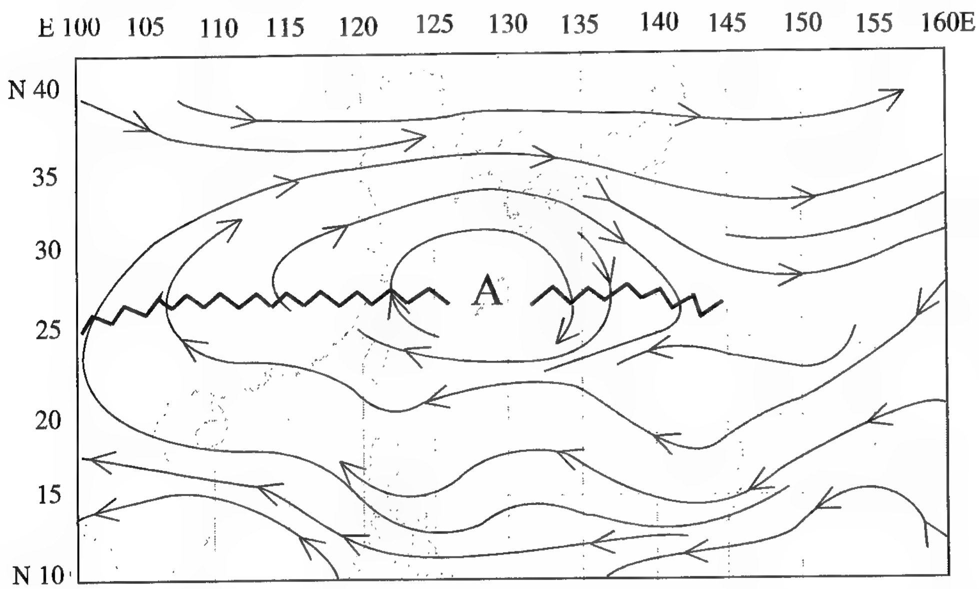

Figure 3-16-2 A strong subtropical ridge dominates the synoptic scale steering flow in the western North Pacific (091200Z September 500-mb NOGAPS streamline analysis).

Situated within the equatorial trough, the disturbance that was to become TD 16W fell under the influence of a strong upper-level ridge situated over the East China Sea and eastern China throughout most of its life. This dominant flow served to steer the cyclone on a mostly westward track under moderate to strong easterly shear. It was not until the disturbance moved into the South China Sea and under the influence of southwest monsoon flow, that development occurred. After TD 16W, the dominant ridge moved back into China (Figure 3-16-3) while the monsoon pushed east of the Philippines, and a series of more intense recurving tropical cyclones developed.

IV. IMPACT

No reports were received of significant damage or fatalities in Vietnam. However, news releases dated 07 September from the Mindanao Islands in the Philippines reported numerous homes damaged. The damage was initially attributed to a surprise eruption of a volcano. Later reports attributed the damage to mudslides from the collapse of a volcanic wall due to heavy rains in the area. Postanalysis shows that these heavy rains were probably associated with the disturbance that would eventually become TD 16W.

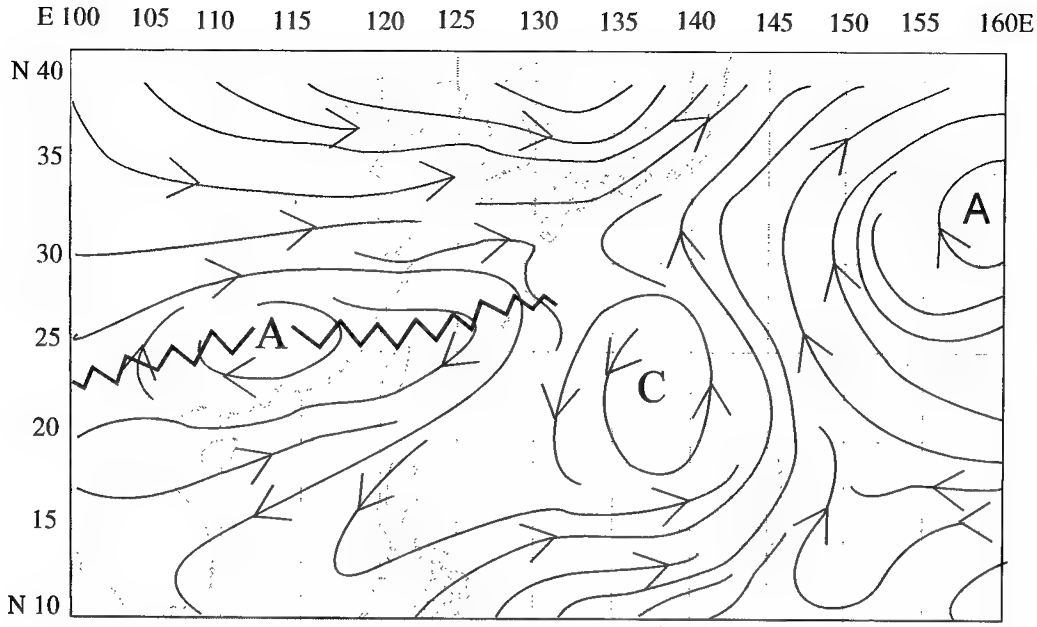

Figure 3-16-3 By mid-September, the subtropical ridge had receded westward into China, allowing a series of more intense recurving tropical cyclones to form (150000Z September 500-mb NOGAPS streamline analysis).

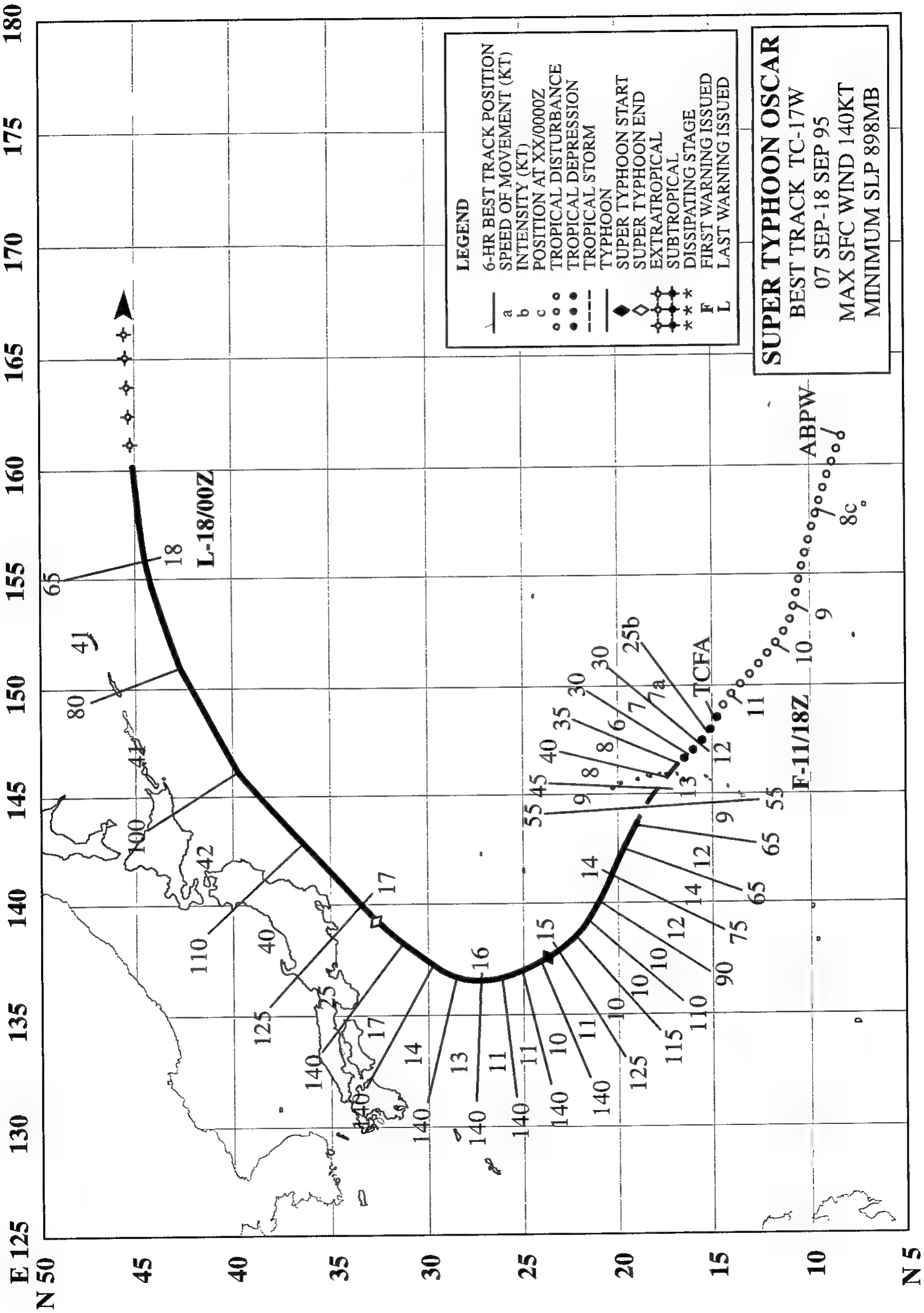
LEGEND
6-HR BEST TRACK POSITION
SPEED OF MOVEMENT (KT)
INTENSITY (KT)
POSITION AT XX/0000Z
TROPICAL DISTURBANCE
TROPICAL DEPRESSION
TROPICAL STORM
TYPHOON
SUPER TYPHOON START
SUPER TYPHOON END
EXTRATROPICAL
SUBTROPICAL
DISSIPATING STAGE
FIRST WARNING ISSUED
LAST WARNING ISSUED
SUPER TYPHOON OSCAR
BEST TRACK TC-17W
07 SEP-18 SEP 95
MAX SFC WIND 140KT
MINIMUM SLP 898MB
L-18/00Z
F-11/18Z
TCFA
ABPW

SUPER TYPHOON OSCAR (17W)

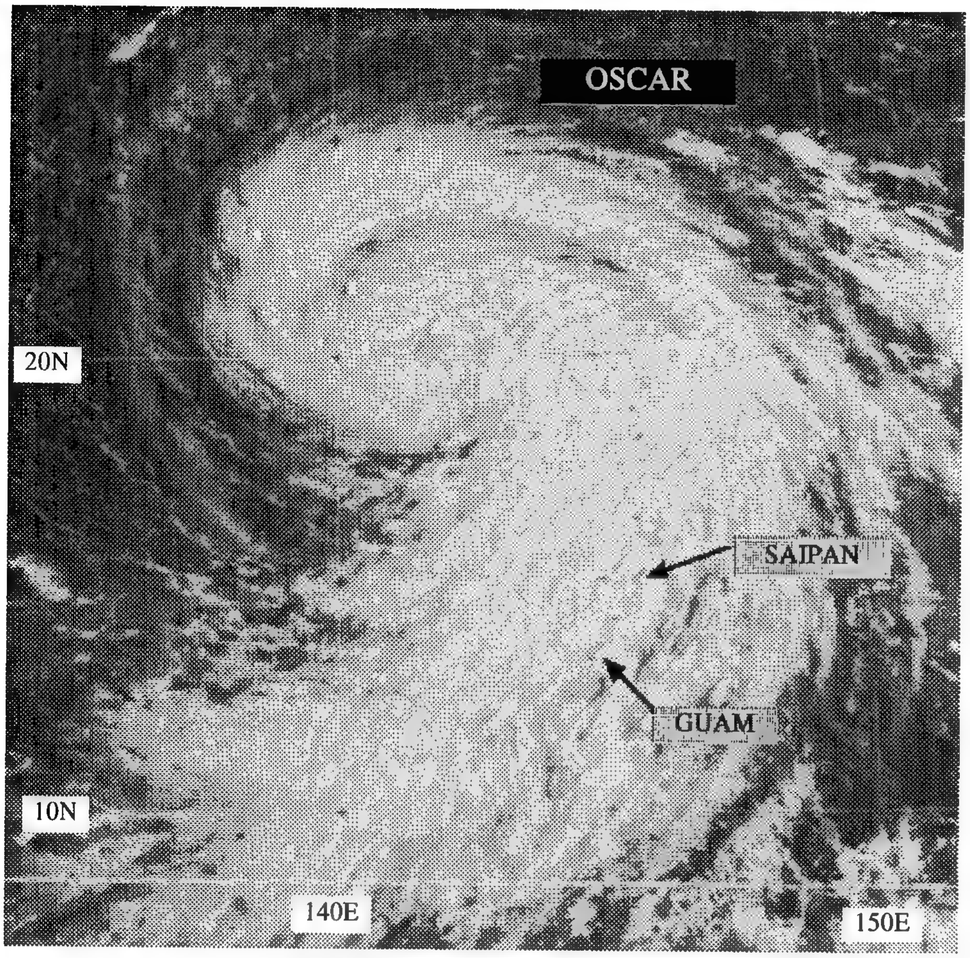

Figure 3-17-1 As Oscar becomes a typhoon, its cloud system covers a large area of the Pacific near the Mariana Islands (132131Z September visible GMS imagery).

I. HIGHLIGHTS

Forming at the eastern end of a monsoon trough which later became reverse-oriented, Oscar became a large tropical cyclone (Figure 3-17-1). Oscar also became a very intense tropical cyclone (Figure 3-17-2), reaching a peak intensity of 140 kt (72 m/sec). When the typhoon passed through the point of recurvature, it posed a serious threat to Tokyo and the southeastern coast of Japan. However, it turned far enough eastward to give only a glancing blow to extreme southeastern Honshu; the eye remained offshore as it passed about 100 nm (185 km) southeast of Tokyo. Oscar's rapid speed of translation — in excess of 40 kt (75 km/hr) — helped to spare Japan the full effects of the typhoon's highest winds. Nevertheless, heavy rain and high winds were responsible for loss of life, and some minor damage in Japan.

II. TRACK AND INTENSITY

Prior to the formation of Oscar, Tropical Storm Nina (15W) moved through the South China Sea. The southwest monsoon was well-established across the South China Sea, but extended only as far east as the Philippines. Elsewhere in the tropics, low-level winds were light, sea-level pressure was slightly above normal, and deep convection was scattered in disorganized clusters throughout Micronesia. Then,

on 07 September, the amount of deep convection began to increase in a broad area bounded by the equator and 20°N from 140°E to 170°E. A tropical disturbance was first mentioned on the 070600Z September Significant Tropical Weather Advisory: synoptic data indicated that a weak low-level cyclonic circulation center accompanied an area of convection near 8°N 163°E. By 11 September, the monsoon trough axis had lifted northward and extended past Guam to about 150°E. For the first time during 1995, Guam experienced monsoonal low-level southwesterly wind. At the eastern reaches of this monsoon trough (about 200 nm northeast of Guam), deep convection began to organize around a low-level circulation center, prompting the JTWC to issue a Tropical Cyclone Formation Alert at 111430Z. The JTWC issued the first warning, valid at 111800Z on Tropical Depression 17W. This was based on increased amounts of deep convection, the improved organization of the lines of deep convection and the pattern of the cirrus outflow. The island of Guam lay under one of the bands of deep convection. Lowering sea-level pressure, heavy rains, and gusty westerly winds confirmed the development of Tropical Depression 17W.

During the next two days, Oscar intensified, becoming a tropical storm at 121200Z, a typhoon at 131200Z, and a super typhoon at 150600Z. Even more noteworthy than the fairly rapid intensification of Oscar was its large size (Figures 3-17-1 and 3-17-2) (see the discussion section for comments on Oscar's large size). Near its point of recurvature, Oscar's radius of gales reached outward to 335 nm (620 km).

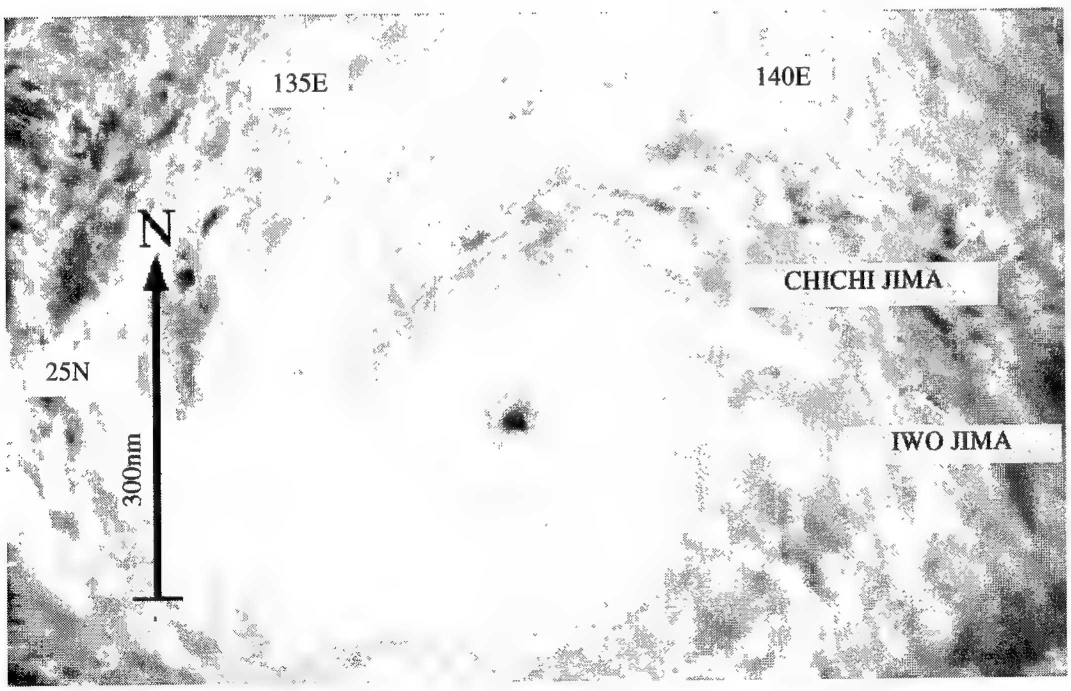

Figure 3-17-2 Oscar reaches its peak intensity of 140 kt (72 m/sec) (150730Z September visible GMS imagery).

Oscar reached its point of recurvature at 160000Z September when it was about 500 nm (925 km) southwest of Tokyo. At this point, forecast guidance and the synoptic situation suggested that Oscar would accelerate rapidly to the northeast and pass very close to Tokyo. During this very critical period, the JTWC forecasts were for landfall near Tokyo. Not until 170000Z did the official forecast take Oscar offshore about 90 nm (170 km) east-southeast of Tokyo. The following chronology of comments on JTWC warnings leading up to Oscar's closest point of approach (CPA) to Tokyo was extracted from the JTWC Deputy Director's unofficial electronic logbook:

"Warning #14 (15/0000Z): TY Oscar continues NWward 320 @ 09 knots. Forecasting super TY around 16/12Z. Track forecast follows the NO [north-oriented] pattern with slow turn NEward. This is the first forecast that makes landfall on Japan. Tokyo/Yokosuka around 17/06Z."

"Warning #19 (16/0600Z): STY Oscar's course has become more northward indicating the slow turn to the NEward track is occurring. (005@11 KTS). System will pass very close to Tokyo around 17/06. In fact, forecasting for landfall on Tokyo at 17/06Z."

"Warning #23 (17/0000Z): Oscar turned sharper to the right than forecasted. Now forecasting for about 60 nm's off the coast around 17/03Z."

"Warning #25 (17/1800Z): Tracking 046 @ 46 knots rapidly transitioning to ET [extratropical]."

The final warning, valid at 180000Z, was issued by the JTWC when Oscar was deemed to have transitioned into a vigorous extratropical low moving rapidly eastward along 45°N.

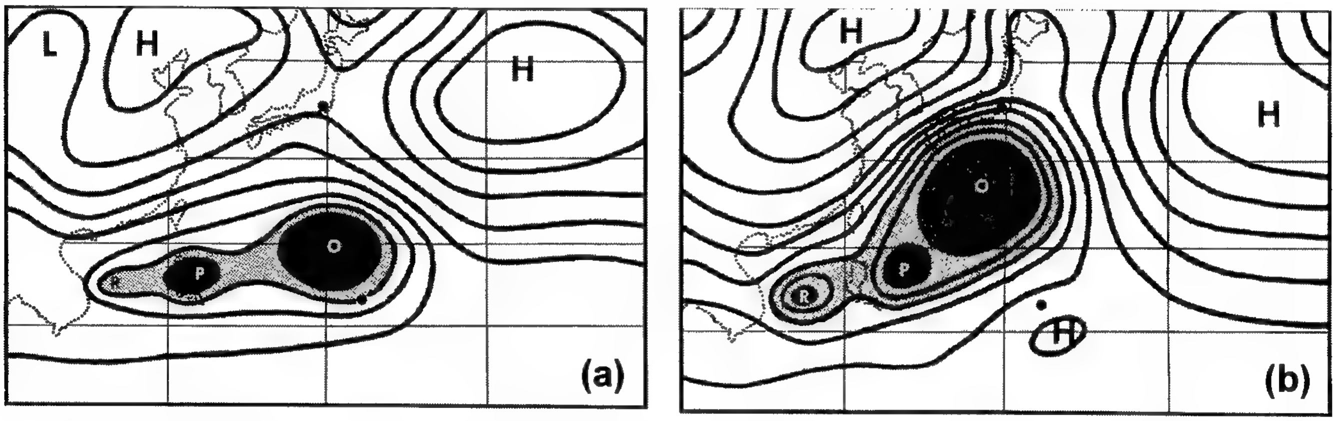

Figure 3-17-3 Sea-level pressure (SLP) analysis over the western North Pacific basin at 140000Z September (a), and 160000Z September (b). Three tropical cyclones — Oscar (O), Polly (18W) (P), and Ryan (19W) (R)— formed simultaneously along a reverse-oriented monsoon trough. Oscar's large size is indicated by its large average radius of outermost closed isobar which has a value of approximately 500 nm in (b). Solid lines are isobars at 2 mb intervals. In (a), the shaded region shows where SLP is lower than 1006 mb, the black areas are below 1004 mb. In (b), the shaded region shows where SLP is lower than 1006 mb, the black areas are below 1002 mb. The 1002 mb isobar in (b) is the outermost closed isobar of Oscar at that time.

III. DISCUSSION

a. *Development in a reverse-oriented monsoon trough.*

Oscar was the first of three tropical cyclones — the other two were Polly (18W) and Ryan (19W) — to develop along the axis of a reverse-oriented monsoon trough that stretched from the South China Sea east-northeastward into the Pacific Ocean north of Guam (Figure 3-17-3a). Oscar was the eastern-most tropical cyclone of the three. For a more detailed discussion of the reverse-oriented monsoon trough within which Oscar, Polly (18W) and Ryan (19W) developed, and its association with unusual motion of Polly and Ryan, see the discussion section in Polly's (18W) summary.

b. *Largest TC of 1995*

Super Typhoon Oscar was the largest tropical cyclone of 1995. Using the mean radius to the outermost closed isobar (ROCI) as a measure of Oscar's size, the system reached the threshold of the "very large" size category used by the JTWC (see Appendix A). At its largest, the mean ROCI was about 8° of great circle arc (GCA) (Figure 3-17-3b). Interestingly, the large expanse of cyclonically curved low-level wind flow surrounding Oscar, and the extensive amounts of cyclonically curved lines of low-level

cumulus and deep convection surrounding Oscar (e.g., see Figure 3-17-2), extend significantly beyond the mean ROCI.

Tropical cyclone size is a very difficult parameter to objectively measure. Merrill (1984) classified a tropical cyclone as "small" if the mean ROCI was three degrees (180 nm, 335 km) GCA, or smaller; as "medium" if the mean ROCI was between three to five degrees GCA (180 nm to 300 nm ; 335 km to 555 km), and as "large" if the mean ROCI was greater than five degrees GCA (greater than 300 nm, 555 km). The Japan Meteorological Agency recognizes two additional size categories — "very small" and "ultra large" — that mesh neatly with Merrill's scheme (See Table 3-17-1). The definitions of size used herein (see Appendix A) have been adapted by a mesh of the JMA size categories with those of Merrill.

Table 3-17-1 Categories of tropical cyclone size based upon the average radius of the outermost closed isobar.

SIZE CATEGORY	RADIUS OF OUTERMOST CLOSED ISOBAR (Degrees)	Nautical Miles
VERY SMALL	<2	<120
SMALL	2-3	120-180
AVERAGE	3-6	181-360
LARGE	6-8	361-480
VERY LARGE	>8	>480

c. *High speed of translation east of Japan*

While passing close to the eastern shores of the Japanese main island of Honshu, Oscar's speed of translation increased to values in excess of 40 kt (75 km/hr). The result of this rapid translation was a drastic reduction of the radial extent of high wind speeds to the left of Oscar's track, sparing Japan the full effects of Oscar's highest winds. A reasonable first approximation of the wind asymmetries in a tropical cyclone is to simply add the speed of translation to the vortex intensity on the right side — the so called dangerous semicircle — and to subtract the speed of translation from the vortex intensity on the left side, or weak semicircle. NEXRAD cross sections of tropical cyclones passing near Guam (see the discussion section of Super Typhoon Ward (25W)), and other composites of tropical cyclone wind structure show that this simple picture of tropical cyclone wind distribution is reasonable in the tropics. As tropical cyclones recurve into mid latitudes, it is not clear that the wind asymmetries are so simple. Indeed, the concepts of the "dangerous semicircle", where the vortex intensity is enhanced by the addition of translation, and the weak semicircle, where the vortex winds are reduced by the speed of translation are still valid to a large extent. However, as the case with Oscar shows, there are some fundamental properties of fast moving recurving tropical cyclones that need to be clarified.

There are insufficient data to allow one to accurately determine the wind distribution in Oscar as it sped past Japan, but one can analytically derive two possible wind distributions given two different interpretations of the warning intensity. If the intensity of a tropical cyclone is considered to be representative of the peak winds in the dangerous semicircle, one must subtract twice the translation speed from this wind in order to obtain the highest wind on the left side (given a uniform steering flow). In Oscar's case, if the peak winds were 120 kt on the right side of the storm, then, given its 40-kt translation speed, the peak winds on the left side could have been only 40 kt (i.e., 120 kt minus 80 kt). Mathematically, the shape of the isotachs surrounding a tropical cyclone with such a wind distribution will be bean-shaped (Figure 3-17-4). Given the warning radius of 50 kt winds of 220 nm (410 km) on the right side of Oscar, it is possible that 50 kt winds extended only 40 nm (75 km) to the left of Oscar's track in two lobes northwest and southwest of the center (Figure 3 -17-4).

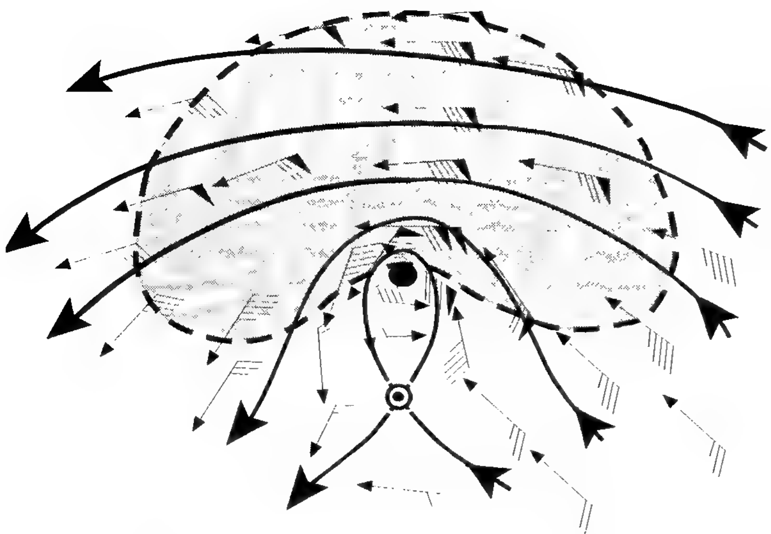

Figure 3-17-4 The analytical wind distribution for a tropical cyclone that is composed of an 80 kt symmetric vortex embedded in a 40 kt unidirectional steering flow. Large dot shows the cyclone center, solid lines are streamlines, and the dotted line shows the area of winds of 50 kt or greater.

If the intensity of a tropical cyclone is considered to be the intensity of the symmetrical portion of the tropical cyclone wind field (i.e., the translation speed is not considered), then the isotachs are shaped as above, only now the peak wind in the dangerous semicircle of a 120 kt tropical cyclone is 160 kt (i.e., 120 kt plus 40 kt), and in the weak semicircle (i.e., to the left of the track) it is only 80 kt. Now, given the warning radius of 50 kt winds of 220 nm (410 km) on the right side of Oscar, wind speeds of 50 kt (26 m/sec) extend 60 nm (110 km) directly to the left of the track, and nearly 100 nm to the left of the track in two lobes to the northwest and southwest. The wind distribution of a tropical cyclone that is rapidly accelerating following recurvature, and that is becoming extratropical is certainly a topic worthy of further study. This topic is of interest especially since the Dvorak technique does not explicitly address translational effects on intensity and wind distribution.

d. *Time series of the "digital Dvorak" (DD) number*

One of the utilities installed in the MIDDAS satellite image processing equipment is an automated routine for computing Dvorak "T" numbers for tropical cyclones that possess eyes. The routine, developed by Zehr (personal communication), adapts the rules of the Dvorak technique as subjectively applied to enhanced infrared imagery (Dvorak 1984) in order to arrive at an objective T number, or "digital Dvorak" T number (hereafter referred to as DD numbers). Infrared imagery is available hourly from the GMS satellite, and hourly DD numbers were calculated for several of the typhoons of 1995 (including Oscar).

The DD numbers presented herein are experimental, and methods for incorporating them into operational practice are being explored. In some cases, the DD numbers differ substantially from the warning intensity and also from the subjectively determined T numbers obtained from application of Dvorak's technique. The output of the DD algorithm, when performed hourly, often undergoes rapid and large fluctuations. The fluctuations of the DD numbers may lay the ground work for future modifications to the current methods of estimating tropical cyclone intensity from satellite imagery. The discussion of the behavior of the time series of the DD numbers for Oscar, and for some of the other typhoons of 1995 (e.g., see the summaries of Polly (18W), Ryan (19W), Ward (26W), and Angela (29W)), is intended to highlight certain aspects of the DD time series that may prove to have important research and/or warning implications.

In Oscar's case, the DD numbers rise steadily from values in the low fives beginning at 141630Z

September to a peak in the mid-sevens within a period of a few hours either side of 151230Z September (Figure 3-17-5). Thereafter, the DD numbers fall quite steadily, and drop below T 4.0 after 0630Z on September 17. Compared with both the warning intensity, and the final best track intensity, one can see that the DD number and the warning intensity (converted to a T number) rise in tandem. As the DD numbers began to fall, the warning intensity did not reflect this fall, but remained consistently higher. Part of the reason for this is the requirement in Dvorak's scheme that the current intensity (i.e., real-time warning intensity) be held one T number higher than the diagnosed (or data) T number when that diagnosed T number is falling.

On a final note, notice that in the case of Oscar, the time series of the DD numbers is well-behaved: they steadily rise to a peak, and then steadily fall after the peak is reached. The hour- to-hour variation is within a few tenths of a T number, and few large fluctuations are noted. Also, the warning intensity and the DD numbers are consistent (as described in the previous paragraph). This is not always the case: for Super Typhoon Ryan (19W), there were large short-term variations, and the DD numbers were not consistent with the best track intensity (see the discussion section in Ryan's summary).

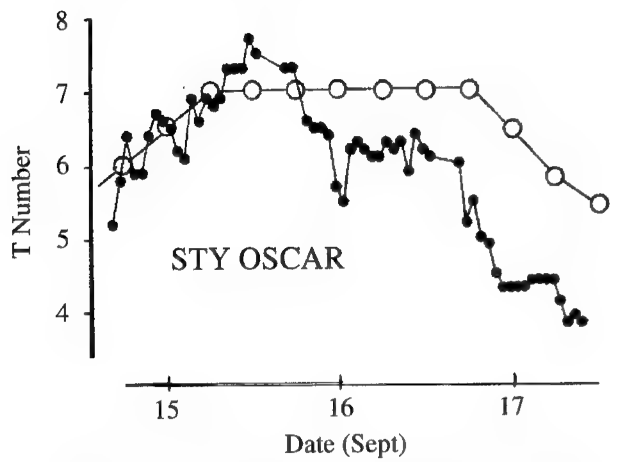

Figure 3-17-5 Hourly time series of the DD number obtained for Oscar during the period 141630Z September through 170930Z September (black dots), versus the final best track warning intensity (open circles).

IV. IMPACT

Sustained winds of typhoon intensity were recorded at exposed locations along the east coast of the Boso peninsula southeast of Tokyo. Winds at Narita airport and in the city of Tokyo did not exceed 50 kt (26 m/sec) sustained. The eye of Oscar passed near or over the island of Hachicho-Jima (WMO 47678) located about 90 nm (170 km) south of Tokyo; minimum sea-level pressure recorded was 938 mb.

Strong wind gusts and heavy rains associated with Oscar caused rail, air and ferry services to be suspended throughout the Kanto Plain. Press reports indicate that Oscar caused three deaths on land in Japan with six missing and feared dead in incidents at sea. Approximately 50 people were injured by falling debris (tiles blowing off roofs, and falling branches). Overall, only minor property damage was reported.

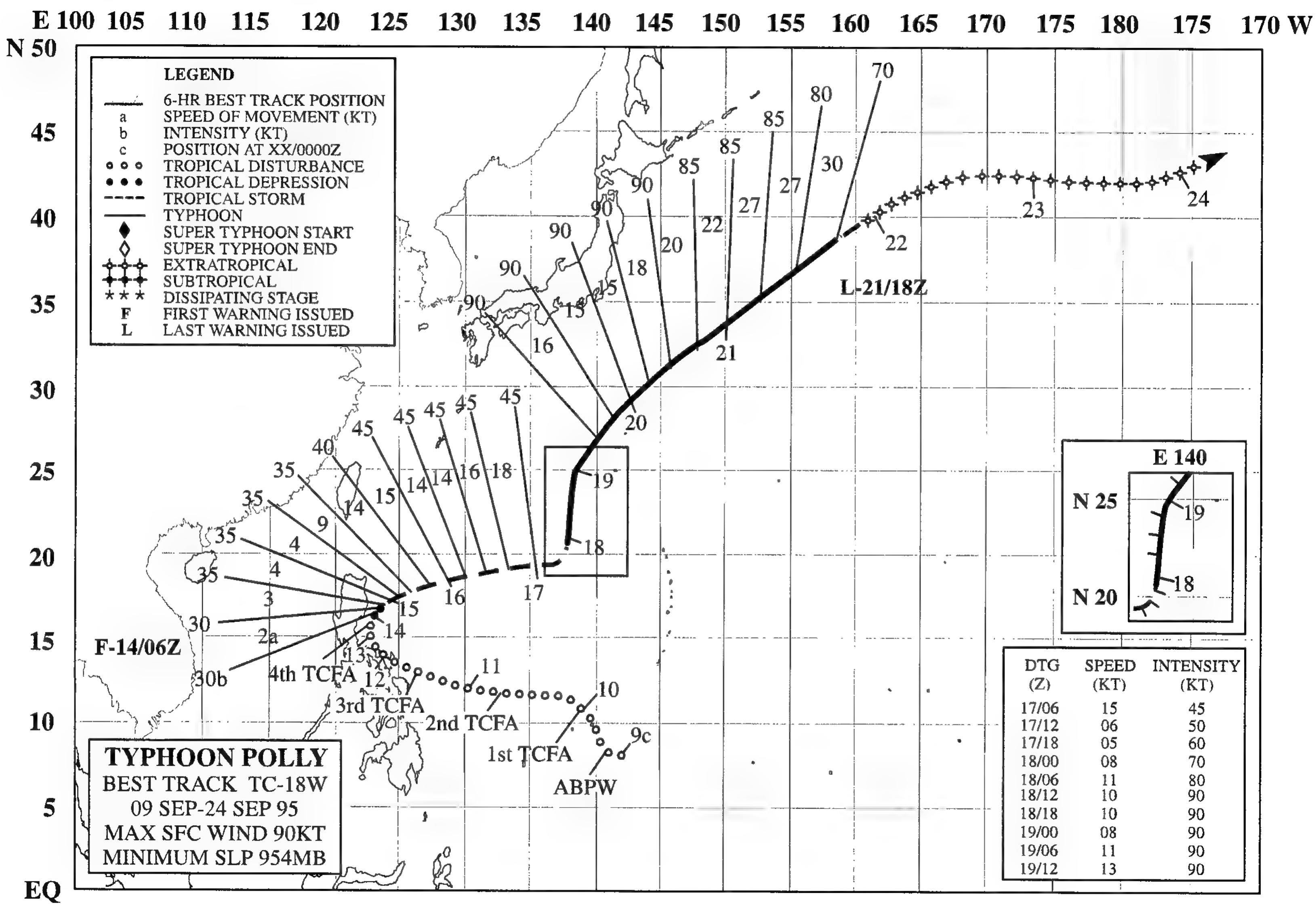

DTG (Z)	SPEED (KT)	INTENSITY (KT)
17/06	15	45
17/12	06	50
17/18	05	60
18/00	08	70
18/06	11	80
18/12	10	90
18/18	10	90
19/00	08	90
19/06	11	90
19/12	13	90

TYPHOON POLLY (18W)

I. HIGHLIGHTS

Polly developed in a reverse-oriented monsoon trough that extended from the South China Sea east-northeastward to just beyond Guam. Like many other tropical cyclones that form within, or move into, a reverse-oriented monsoon trough, Polly underwent unusual motion: an "S" shaped track. Two other tropical cyclones — Oscar (17W) and Ryan (19W) — also developed in this reverse-oriented monsoon trough; and, along with Polly, formed a SW-NE chain of tropical cyclones.

II. TRACK AND INTENSITY

The tropical disturbance that became Typhoon Polly can be traced back to a large area of deep convection centered south of Guam late on 08 September. It was first mentioned on the 090600Z Significant Tropical Weather Advisory when satellite imagery and synoptic data indicated the presence of a low-level cyclonic circulation center associated with this tropical disturbance. This disturbance moved westward for three days and then slowed as it neared Luzon. The first of four Tropical Cyclone Formation Alerts (TCFA) was issued on this disturbance at 100100Z as satellite imagery indicated improving organization of the system's deep convection and cirrus outflow, and synoptic data indicated that the sea level pressure near the center was falling. A second TCFA was issued at 102000Z when synoptic data indicated that the low-level circulation center had moved out of the area delineated by the first TCFA.

The pre-Polly tropical disturbance was slow to develop, as its deep convection failed to consolidate around a distinct center. Instead, the deep convection became more widespread and oriented east-west along the axis of the monsoon trough. Moving steadily westward, the low-level circulation center once again moved out of the area delineated by the TCFA, so a third TCFA was issued at 111330Z. The disturbance had shown little sign of further development, other than synoptic data that indicated that the central SLP had fallen to near 1004 mb. At 120600Z, the third TCFA was cancelled, as synoptic data indicated that the central sea level pressure had risen from 1004 mb to 1006 mb. At this time, the pre-Polly tropical disturbance had moved to a position just east of Luzon, where it had slowed and turned northward. A fourth TCFA was issued on this tropical disturbance at 132330Z, when satellite imagery indicated consolidation of deep convection near a low-level circulation center, and synoptic data indicated that the central SLP had fallen to 1000 mb. At this time, the large circulation of the developing Oscar (17W) was located about 1200 nm (2200 km) east-northeast of the pre-Polly tropical disturbance. Perhaps in response to deep monsoonal southwesterly flow south of the monsoon trough axis, the pre-Polly tropical disturbance began to move very slowly northeastward. The first warning on Tropical Depression 18W was issued at 140600Z when satellite imagery indicated a well-defined low-level circulation center accompanied by an area of persistent deep convection.

Polly was upgraded to a tropical storm at 141800Z as the amount of deep convection increased near the low-level circulation center, and the organization of the deep convection and cirrus outflow improved. With the very large Oscar to its northeast (Figure 3-18-1), Polly began to track east-northeastward. With little further intensification, Polly continued to move east-northeastward for approximately two days until late on 17 September when it made an abrupt turn to the north and began to intensify more rapidly. On the morning of 18 September, Polly was upgraded to a typhoon. Polly reached peak intensity of 90 kt (46 m/sec) at 181200Z (Figure 3-18-2). At 190000Z, Polly turned to the north-northeast on the final leg of its "S" track. With a remarkably stable satellite signature (i.e., a nearly con-

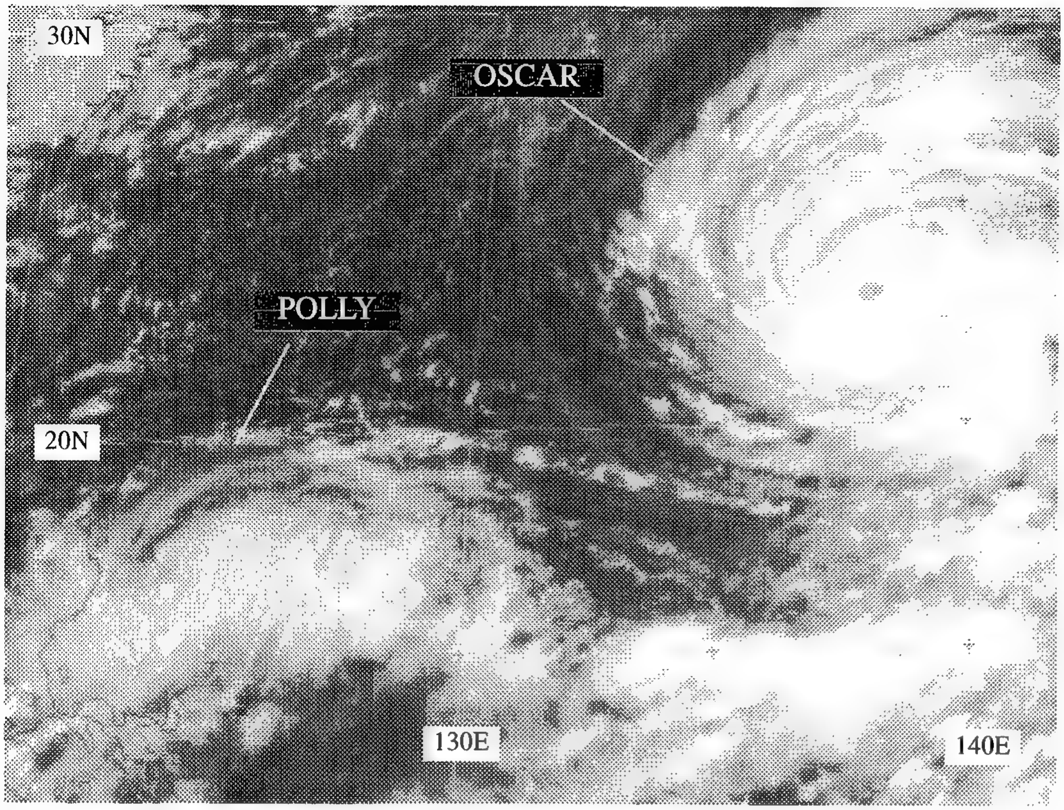

Figure 3-18-1 Polly's deep convection begins to consolidate around its low-level circulation center as it begins to move toward the east-northeast under the steering influence of south-westerly monsoonal flow and Oscar's large circulation (142331Z September visible GMS imagery).

stant Dvorak satellite intensity estimate of T 5.0), Polly's intensity remained at 90 kt (46 m/sec) for the 48-hour period 181200Z through 201200Z. After 201200Z, Polly increased its speed of translation to 30 kt (55 km/hr) as it moved northeastward into the mid latitudes. The final warning was issued on Polly, valid at 211800Z, when it appeared that it would become fully extratropical within six hours. The extratropical remains of Polly, possessing a well-defined low-level circulation, moved across the international date line on 24 September (Figure 3-18-3).

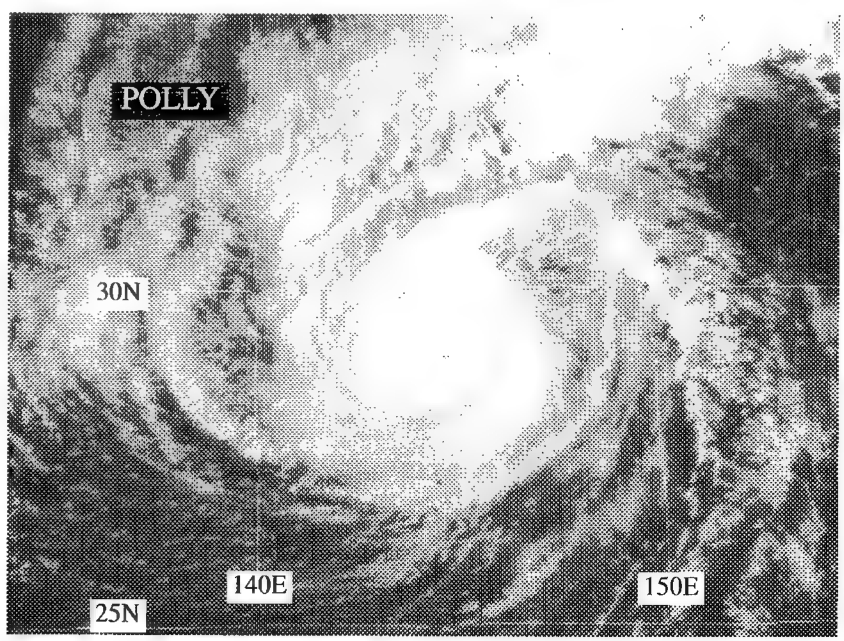

Figure 3-18-2 Polly at peak intensity of 90 kt (46 m/sec) (192224Z September visible GMS imagery).

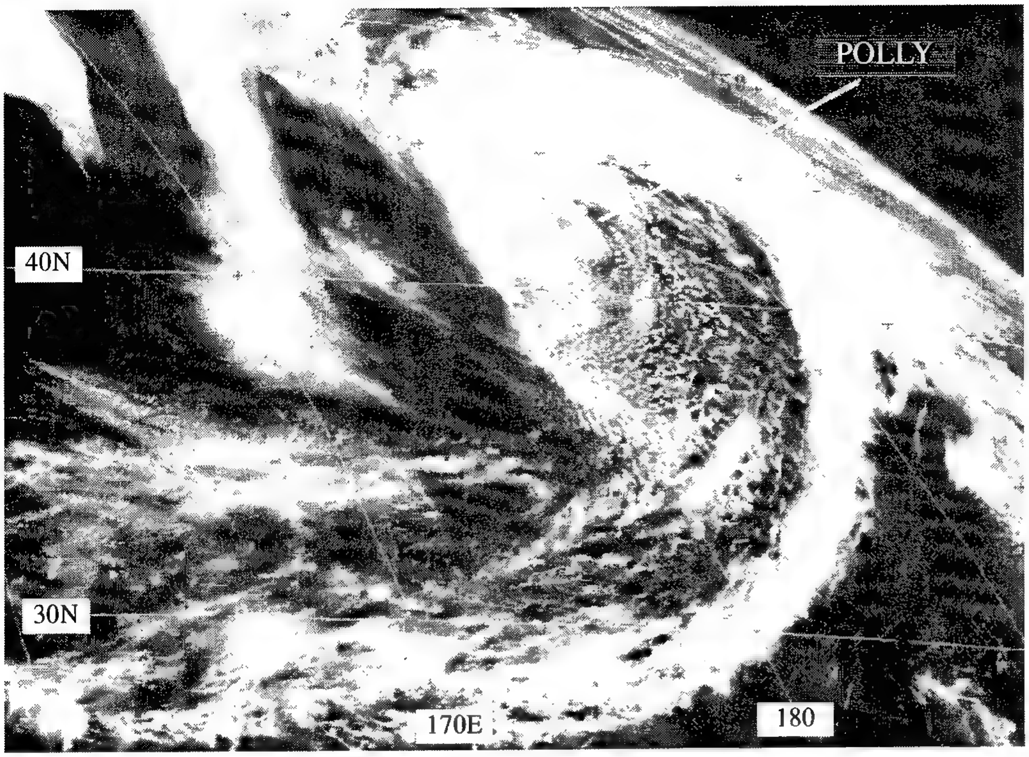

Figure 3-18-3 After the transition to an extratropical low, the well-defined low-level circulation — the remnants of Polly — crossed the international date line on a track towards the Gulf of Alaska (232331Z September visible GMS imagery).

III. DISCUSSION

a. *Unusual "S" motion*

During much of 1995 the low-level flow of the tropical Pacific was dominated by anomalous easterly low-level wind flow. As a consequence, the summer monsoon circulation of the western North Pacific was very weak. During June, July and August of 1995, low-level easterly wind flow dominated the low latitudes of the western North Pacific, and the normal southwest monsoon of the Philippine sea (with episodic extensions further eastward) was replaced by mean monthly easterly flow.

Only two relatively active monsoon episodes were noted during 1995: a reverse-oriented monsoon trough formed during mid-September and a large monsoon gyre formed during mid-October. The reverse-oriented monsoon trough of September stretched from the South China Sea eastward across Luzon and the Philippine Sea, and then northeastward to the northeast of Guam. This episode of reverse-oriented monsoon trough formation was associated with the simultaneous development of three tropical cyclones along the trough axis — Oscar (17W), Polly, and Ryan (19W).

When the monsoon trough axis acquires a reverse-orientation, TCs along it tend to move on north-oriented tracks. One unusual type of north-oriented track — the "S" track — is almost always associated with reverse orientation of the monsoon trough axis (Lander 1996). Consistent with Lander's findings, Polly and Ryan (19W) moved on unusual north-oriented "S"-shaped tracks.

Though not perfectly "S"-shaped, Polly's track nonetheless featured the requisite characteristics to be considered an example of "S" motion, as defined by Lander (1996). The "S" track — a specific variant of north-oriented motion — features eastward movement at low latitude, a later bend to the north or northwest, and then eventually northeastward motion as the system enters the mid-latitude westerlies. As was the case with Polly, a tropical cyclone undergoing "S" motion often intensifies after making its first bend to the north.

b. *Time series of Digital Dvorak (DD) numbers*

In Polly's case, there was a long period of time (181200Z to 210600Z) during which the warning intensity held steady at 85 to 90 kt (44 to 46 m/sec) — an intensity corresponding to a T 5.0 on Dvorak's scale. DD numbers were obtained during much of Polly's period of stable warning intensity. Unlike the DD number time series for Oscar (17W) (refer to the discussion section in Oscar's (17W) summary), the DD numbers for Polly showed a larger degree of short-term fluctuations (Figure 3-18-4). Nonetheless, the warning intensity represents an average value around which the DD numbers scatter. This is not the case with the next tropical cyclone — Ryan (19W) — in the three-TC (Polly, Oscar, Ryan) outbreak (refer to the discussion section in Ryan's summary).

IV. IMPACT

Polly affected the Volcano Islands where Iwo Jima reported a peak gust of 52 kt (27 m/sec) at 190424Z September, with nearby Chichi Jima reporting a minimum pressure of 987.8 mb at 1800Z the same day. Polly passed 130 nm (240 km) and 65 nm (120 km) to the northwest of these islands respectively. No reports of injuries or damage were received.

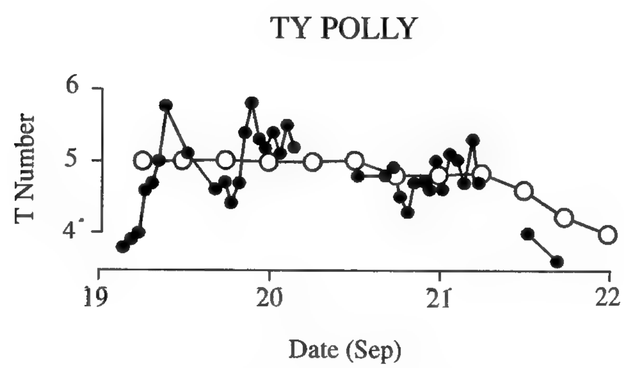

Figure 3-18-4 The hourly time series of the DD numbers obtained for Polly during the period 19 - 22 September (black dots), versus the final best track intensity (open circles). Ordinate labels are placed at 0000Z for the indicated date.

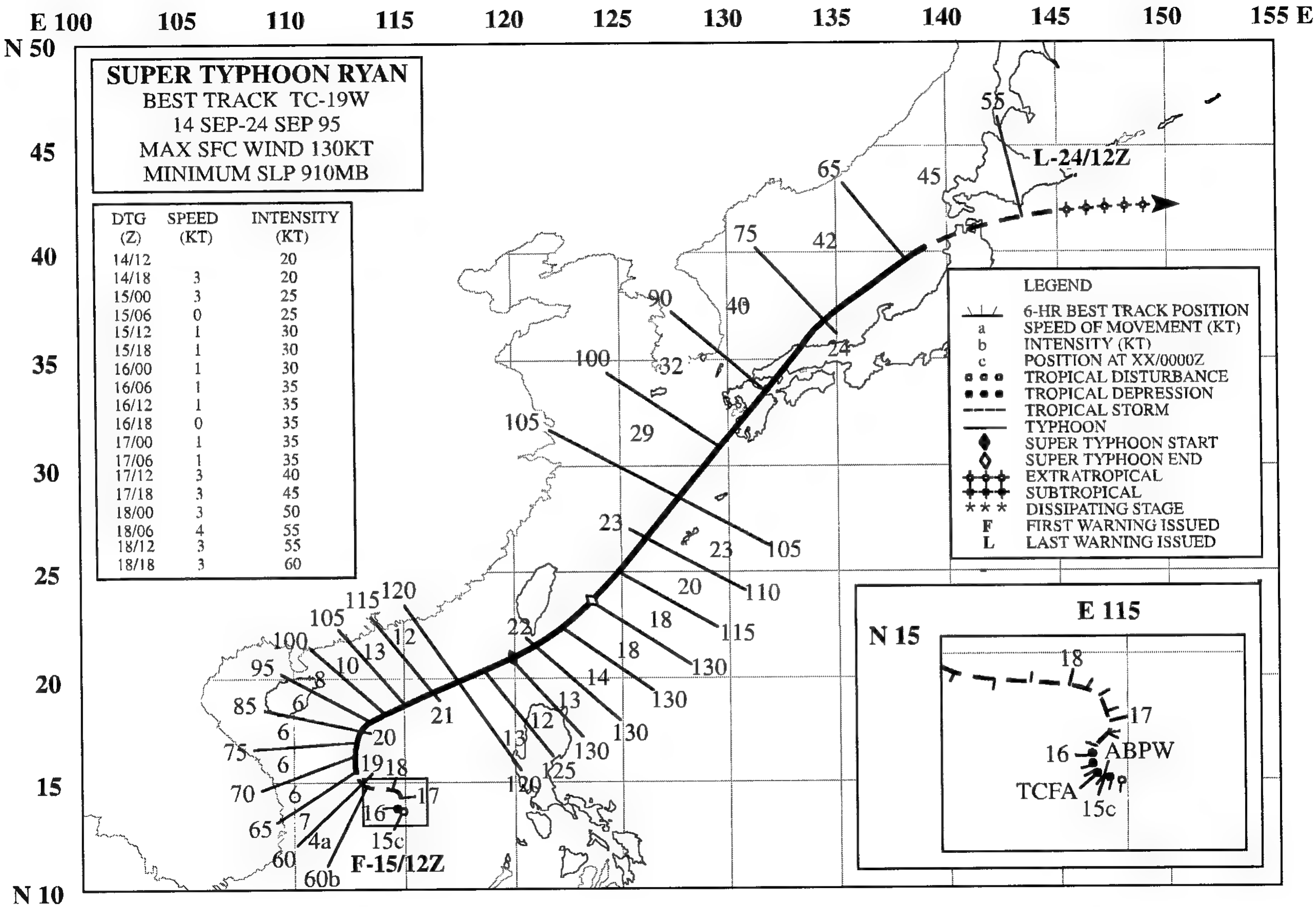

DTG (Z)	SPEED (KT)	INTENSITY (KT)
14/12		20
14/18	3	20
15/00	3	25
15/06	0	25
15/12	1	30
15/18	1	30
16/00	1	30
16/06	1	35
16/12	1	35
16/18	0	35
17/00	1	35
17/06	1	35
17/12	3	40
17/18	3	45
18/00	3	50
18/06	4	55
18/12	3	55
18/18	3	60

SUPER TYPHOON RYAN (19W)

I. HIGHLIGHTS

Ryan was the first tropical cyclone on JTWC's records to both form and attain super typhoon intensity within the South China Sea. Located along the axis of a reverse-oriented monsoon trough, Ryan underwent unusual motion: an "S"-shaped track. Two other tropical cyclones — Oscar (17W) and Polly (18W) — also developed in this reverse-oriented monsoon trough and, along with Ryan, formed a SW-NE chain of tropical cyclones. Estimates of Ryan's intensity based upon Digital Dvorak (DD) numbers exhibited some unusually large and rapid fluctuations. Ryan passed through the southern islands of the Ryukyu chain, and made landfall in southwestern Japan.

II. TRACK AND INTENSITY

On 13 September, the axis of the monsoon trough extended eastward from Southeast Asia across the South China Sea to Luzon, and from there, east-northeastward to Oscar (17W) in the northern Mariana Islands. Westward from Oscar (17W), and along the trough axis, lay the tropical disturbance that became Polly (18W) (then east of Luzon), and (in the South China Sea) the tropical disturbance that became Ryan. The pre-Ryan tropical disturbance was first mentioned on the 130600Z September Significant Tropical Weather Advisory based upon 24 hours of persistent deep convection associated with a weak low-level circulation center. Over the next two days, the sea-level pressure (SLP) slowly fell in the pre-Ryan tropical disturbance. At 151000Z September a Tropical Cyclone Formation Alert was issued based primarily on synoptic reports that indicated that the central SLP had fallen to 1002 mb within a well-defined low-level cyclonic circulation. The JTWC issued the first warning on Tropical Depression 19W valid at 151200Z.

Improvements in the organization of its deep convection resulted in an upgrade of Tropical Depression 19W to Tropical Storm Ryan at 160000Z. During the period 16 through 19 September, Ryan moved very slowly northward and then very slowly westward. After making a turn toward the north early on 19 September, Ryan was upgraded to a typhoon at 190600Z. On the morning of 20 September, the typhoon turned to the east-northeast, accelerated, and continued to intensify (Figure 3-19-1). Ryan attained its peak intensity of 130 kt (67 m/sec) at 211800Z as it swept around the southern tip of Taiwan, whereafter, it accelerated further, made a slight left turn, passed near (or over) Ishigaki Shima (WMO 47918) (see impact section), and then moved northeastward toward Japan.

Ryan made landfall on the Japanese island of Kyushu late on 23 September. Its landfall intensity was just under 100 kt (51 m/sec). After crossing Kyushu, Ryan tracked across the westernmost portion of the Japanese main island of Honshu and entered the Sea of Japan. Encountering strong deep layer westerly wind flow, Ryan weakened as it turned toward the east on the last leg of its "S" track, and passed over the northern tip of Honshu between 0600Z and 1200Z on 24 September. Under the influence of shear in the westerly wind flow at the higher latitudes, Ryan continued to weaken and began to transition to an extratropical cyclone. The final warning was issued valid at 240600Z.

III. DISCUSSION

a. *First super typhoon to form in the South China Sea*

Since the JTWC was established in 1959, there have been no super typhoons (130 kt (67 m/sec), or greater) in the South China Sea (although there have been super typhoons in the Philippine Sea that have moved into the South China Sea at lesser intensities). During the period 1945 to 1959, before the

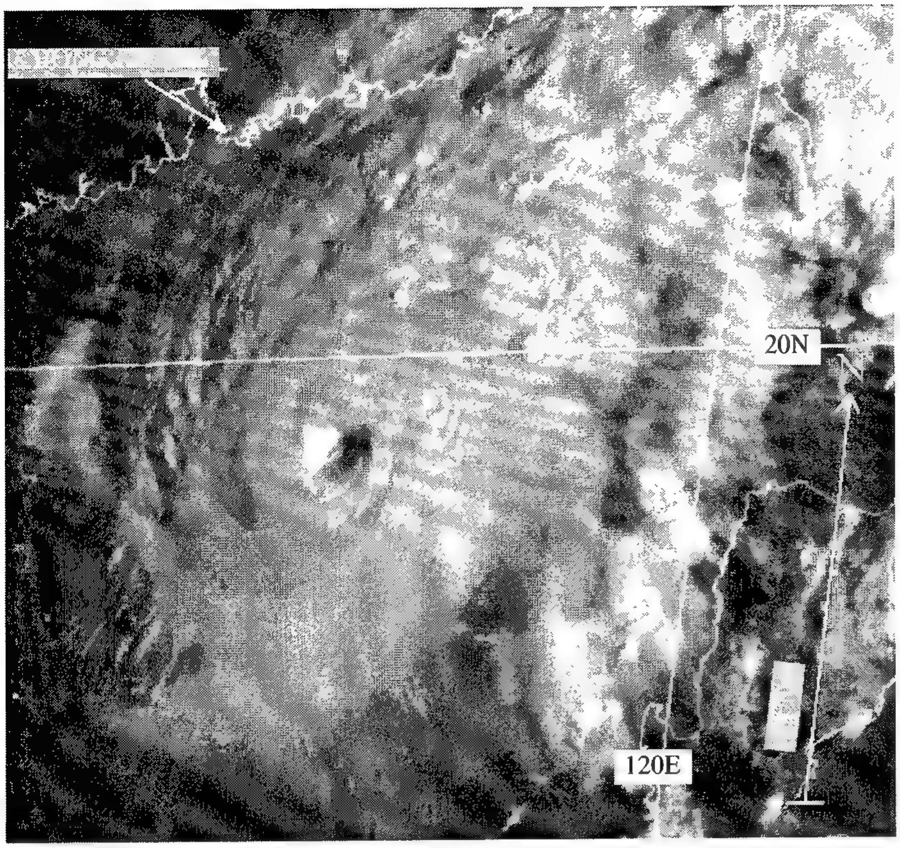

Figure 3-19-1 Ryan at 115 kt (59 m/sec) continues to intensify and will reach super typhoon intensity in 18 hours. The low sun angle in this image accentuates the cloud top topography (202332Z September visual GMS imagery).

JTWC was established, tropical cyclones in the western North Pacific were nonetheless reconnoitered by Air Force and Navy aircraft. During these years, two typhoons — Gloria (1952) and Betty (1953) — were reported to have attained super typhoon intensity after crossing the Philippines and while over the South China Sea. In the case of these two typhoons, it is difficult to assess the reliability of the reconnaissance reports of super typhoon intensity.

In the case of Gloria (1952) a Navy reconnaissance flight departed from Sangley Point at 222055Z December 1952, and made two eye fixes, one at 222309Z and the other at 230400Z. During the first pass through the eye, the crew estimated the maximum surface wind to be 110 kt (57 m/sec) in the northwest quadrant of the system accompanied by an estimated minimum sea-level pressure (SLP) in the eye of 982 mb. On the second pass through the eye, the maximum estimated surface wind was 130 kt (67 m/sec) in the southeastern quadrant accompanied by an estimated minimum SLP in the eye of 983 mb. The Atkinson/Holliday wind-pressure relationship (currently used as a baseline by the JTWC) requires a minimum SLP of 910 mb for a wind intensity of 130 kt (67 m/sec); conversely, a minimum SLP of 982 mb corresponds to a maximum wind speed of 55 kt (28 m/sec). In the case of Betty (1953), a Navy reconnaissance flight estimated the surface winds to be 130 kt (67 m/sec) in the left forward quadrant of the system. The lowest "observed" SLP (most probably obtained from a dropsonde) was 988.6 mb; however, owing to severe turbulence, the aircraft was unable to penetrate the eye.

Historical reconnaissance reports during the early years of record frequently have large mismatches between the minimum SLP and the associated maximum wind speed. Such large mismatches (as was the case with Gloria) render the data suspect. This is typical of historical reports during the early years of tropical cyclone reconnaissance.

Returning now to the case of Ryan, It must be noted that its super typhoon intensity was diagnosed from satellite using the techniques developed by Dvorak (1975, 1984), and one could raise questions as to the accuracy of its peak intensity estimate. Dvorak's techniques have been in use now for two decades, and for the most part, have been proven to be reasonable from coincident aircraft and land-falling "ground truth" measurements. There are occasional outliers from Dvorak intensity estimates, and examples have been pointed out in past Annual Tropical Cyclone Reports (e.g., see the summaries of Seth and John in the 1994 ATCR). Given that there may be a significant level of uncertainty of tropical cyclone intensity as estimated from satellite imagery, the least that can be said of Ryan is that during the past two decades of intensity estimation by satellite (accompanied by aircraft reconnaissance until 1987), no typhoon has ever been estimated to have attained super typhoon intensity while in the South China Sea.

b. *Ryan's north-oriented motion*

The north-oriented track was first recognized by the Japan Meteorological Agency (JMA) (1976). Lander (1996) further elaborated on the characteristics of north-oriented tracks. One particular type of north-oriented motion described by Lander was the "S" track. "S" motion is north-oriented motion of a TC that features eastward motion at low latitude, a later bend to the north or northwest, and then eventually northeastward motion as the TC enters the mid-latitude westerlies.

Twenty-five of 37 cases (68%) of observed "S" motion during the years 1978 through 1995 occurred when tropical cyclones undergoing "S" motion were located along the axis of a reverse-oriented monsoon trough. The "S" motion of Ryan — and also that of Polly (18W) — occurred when these tropical cyclones were located along the axis of a reverse-oriented monsoon trough. During 1995, the tracks of Ryan, and Polly (18W) were the only "S" tracks; and they comprised two of only five north-oriented tracks during the year (see Table 3-1).

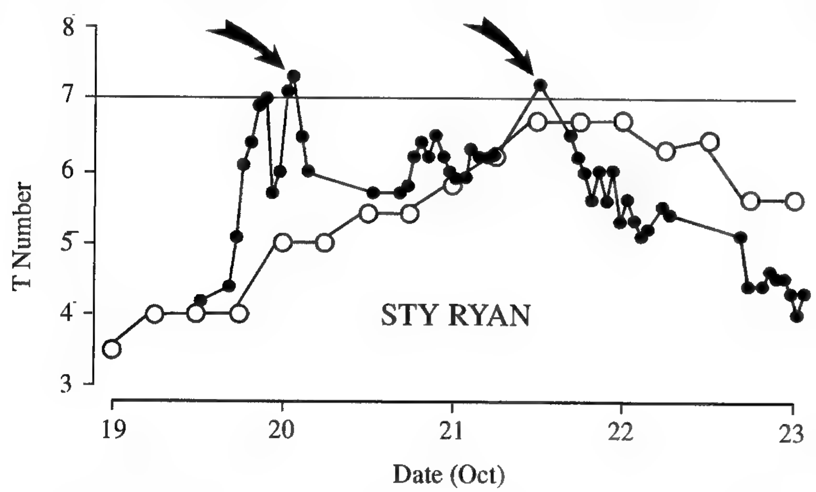

Figure 3-19-2 This comparison of the DD numbers (solid circles) and final best track intensity (open circles) converted to T-numbers for the period 19 to 23 September shows the variation between raw data and the final smoothed product for Ryan. Arrows indicate the two instances where the "digital" values exceeded T7.0.

c. *Rapid fluctuations in Ryan's DD numbers*

During 1995, detailed records of the hourly values of the DD numbers were tabulated for five typhoons: Oscar (17W), Polly (18W), Ryan, Ward (26W), and Angela (29W). (See the more detailed description of the DD numbers in Oscar's (17W) summary.) The time series of the hourly values of the DD numbers for Oscar (17W) was relatively stable, and was in good agreement with the JTWC warning intensity and the final best-track intensity. With Ryan, the time series of the hourly DD numbers underwent some large fluctuations (Figure 3-19-2) that were not in good agreement with the warning intensity or with the final best track intensity. The magnitude of Ryan's DD numbers exceeded T 7.0 — equivalent to an intensity of 140 kt (72 m/sec) maximum sustained wind speed — twice during its life (for

maximum wind and minimum sea-level pressure equivalents to Dvorak's T numbers, see Table 2-2). The first DD of T 7.0 occurred at 192230Z, and reached T 7.3 at 200230Z (see Figure 3-19-3a) before falling back into values in the vicinity of T 6.0. The warning intensity at this time was 90 kt (46 m/sec), and the final best track intensity was 85 kt (44 m/sec) — this intensity is approximately T 5.0 on the Dvorak scale.

After the first DD peak of T 7.3 at 200230Z, the hourly time series of the DD fell back to within a few tenths of T 6.0 for a period of about 30 hours, after which the DD rose once again above T 7.0 at 211230Z (see Figure 3-19-3b). The warning intensity (and final best-track intensity) for Ryan reached a peak of 130 kt (67 m/sec) at this time (211200Z). An intensity of 130 kt lies between a T 6.5 and a T 7.0 on the Dvorak scale. The warning intensity and the DD were in close agreement at this time.

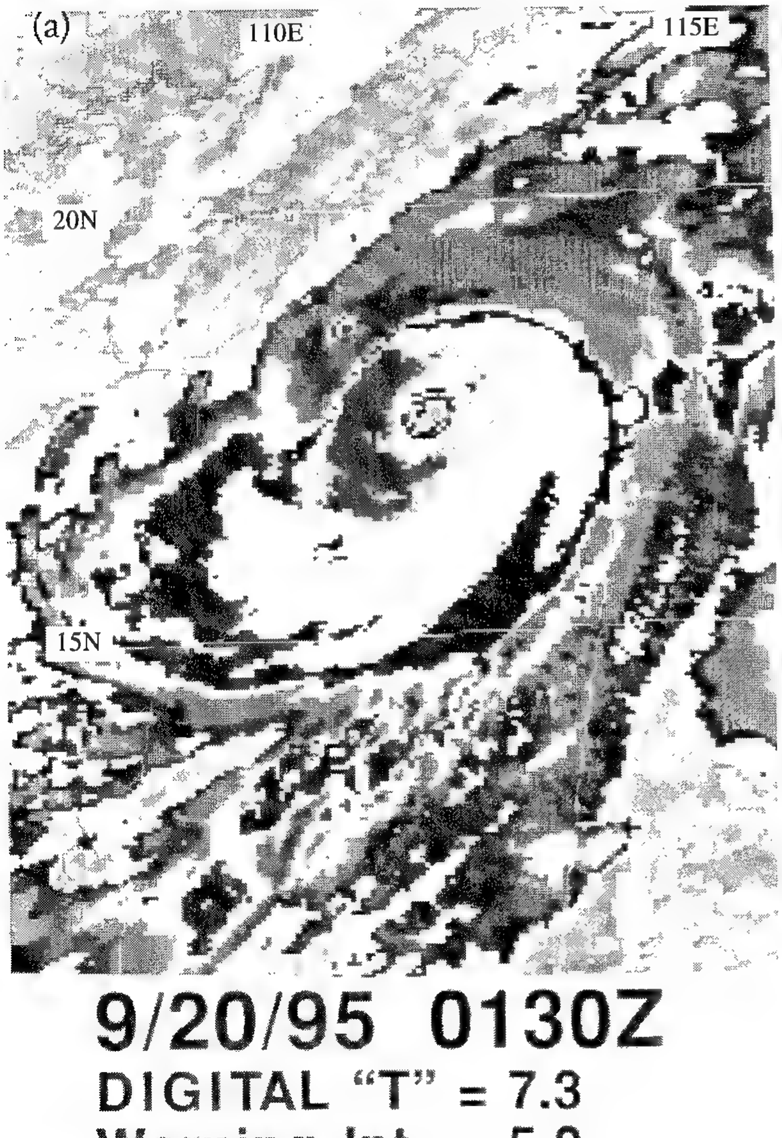

Figure 3-19-3 (a) Ryan reaches a DD number of 7.3 (200130Z September enhanced infrared GMS imagery).

That the warning intensity and best track intensity do not reflect the first rise of the DD to T 7.0 has several explanations. For one, the magnitude of the rise of 2.6 T numbers in five hours (from T 4.4 to T 7.0) exceeds the constraints allowed by Dvorak's technique. For another, given the large fluctuations of the intensity at this time (both up and down), the best-track intensity has been greatly smoothed. In the absence of ground-truth measurements, it will never be known if the intensity of Ryan was actually on the order of 140 kt (72 m/sec) at one, both, or neither of the places along its track where the DD exceeded T 7.0. If the DD numbers truly represented Ryan's intensity, there are two topics for further research: (1) how are the extremely rapid fluctuations of intensity, if they are genuine, to be incorporated into the warning? and, (2) how can the best-tracks, having had these rapid fluctuations removed, be used to study the processes governing what may prove to be real intensity fluctuations of the magnitude indicated by the DD numbers?

d. *Record tying wind gust*

At 220300Z September, Ryan passed near the Taiwanese island of Lanyu (WMO 46762) where a peak wind gust of 166 kt (85.3 m/sec) tied the strongest wind gust ever recorded in a typhoon. The other event occurred at Miyako Jima (WMO 47927) in September 1966 near the eye of Typhoon Cora.

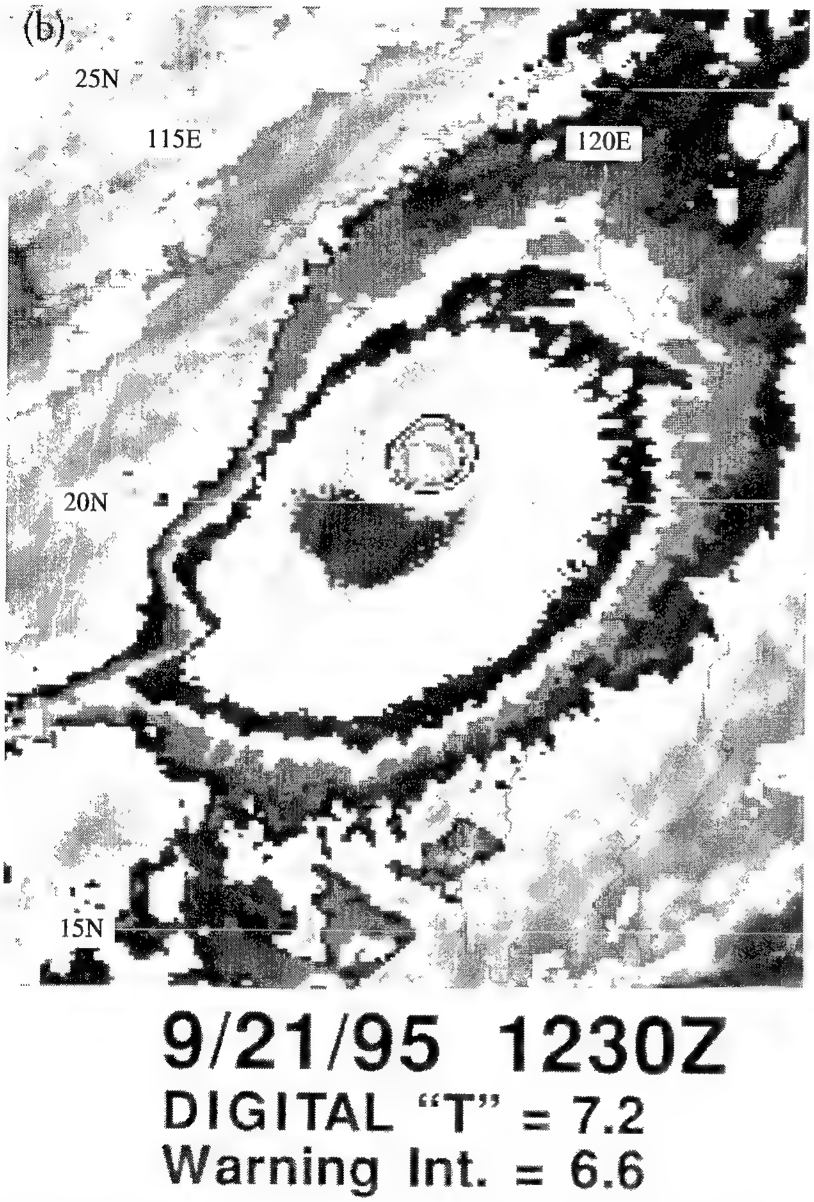

(b) Ryan's DD number once again is greater than 7.0 (211230Z September enhanced infrared GMS imagery).

IV. IMPACT

Ryan affected the Philippines, Taiwan, and Japan. In the northern Philippines, at least three fishermen died when high waves generated by Ryan overturned their boats. Nearly 2,500 people were forced to flee when high surf washed into homes along the coast of Ilocos Norte. A Philippine Navy ship, the Badjao, was reported adrift and listing badly in high seas, and members of the crew of 54 were being rescued. Reports concerning the ultimate fate of this ship were not received by the JTWC. In Taiwan, two people were reported to have died in typhoon-related incidents, and wind damage cut electricity to 4,500 households in the central and southern parts of the island. Rail and air traffic was disrupted. Taipei's financial markets, government offices and schools were closed for one day. In southwestern Japan, heavy rain flooded more than 950 homes and high winds cut off electrical power to about 17,400 homes. More than 1,500 buildings were damaged by heavy rain. Three people were hurt by flying glass in Kagoshima, and two people were injured by flying objects on the southern island of Okinawa. Domestic air and rail service was disrupted. The highest wind gust on the main islands of Japan was 90 kt (46 m/sec) recorded at Hiroshima. Earlier, as Ryan passed through the southern Ryukyu islands, a minimum sea-level pressure of 956.5 mb accompanied by a peak gust of 123 kt (63.5 m/sec) was observed on Ishigaki Shima (WMO 47918).

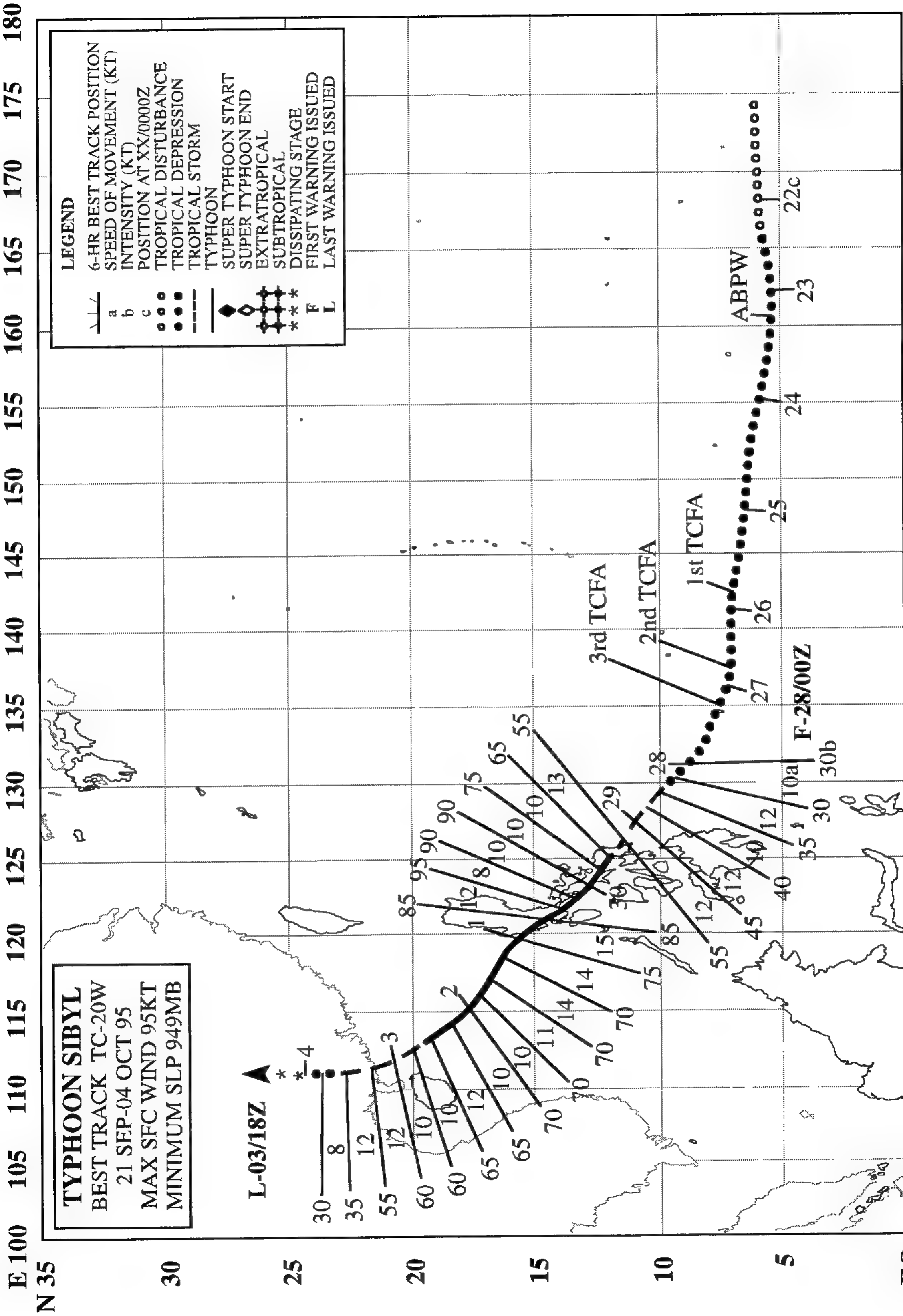
TYPHOON SIBYL
BEST TRACK TC-20W
21 SEP-04 OCT 95
MAX SFC WIND 95KT
MINIMUM SLP 949MB
LEGEND
6-HR BEST TRACK POSITION
SPEED OF MOVEMENT (KT)
INTENSITY (KT)
POSITION AT XX/0000Z
TROPICAL DISTURBANCE
TROPICAL DEPRESSION
TROPICAL STORM
TYPHOON
SUPER TYPHOON START
SUPER TYPHOON END
EXTRATROPICAL
SUBTROPICAL
DISSIPATING STAGE
FIRST WARNING ISSUED
LAST WARNING ISSUED
L-03/18Z
F-28/00Z
1st TCFA
2nd TCFA
3rd TCFA
ABPW
E 100
N 35
EQ

TYPHOON SIBYL (20W)

I. HIGHLIGHTS

Scatterometer data from the ERS-1 satellite played an important role in tracking Sibyl while the system was poorly organized. Sibyl reached its peak intensity of 95 kt (49 m/sec) as it crossed the Visayan islands. Later, it tracked over metro-Manila and entered the South China Sea, where it slowly weakened before making landfall east of the Luichow peninsula in southern China.

II. TRACK AND INTENSITY

The weak tropical disturbance that became Sibyl passed south of Majuro Atoll in the Marshall Islands late on 21 September and just south of Kosrae 24 hours later. Application of Dvorak's technique to the satellite imagery at 221130Z indicated that the system had developed sufficiently to be classified as a T 1.0 (equivalent to an intensity of 25 kt (13m/sec)). Based upon synoptic data and satellite intensity estimates, this tropical disturbance was first mentioned on the 230600Z Significant Tropical Weather Advisory. At 231200Z, the amount and organization of deep convection diminished, and no satellite classifications were made until 251700Z. Nevertheless, synoptic data and satellite imagery did indicate the continued westward movement of the poorly organized disturbance.

When the system began to develop, it did so at a very slow rate, and three Tropical Cyclone Formation Alerts were issued: the first at 252000Z, the second at 262000Z, and the third at 270600Z September. The latter was superseded when the JTWC issued the first warning on Tropical Depression 20W (TD 20W), valid at 280000Z. The slow development from the Marshall Islands to near 130°E is typical of La Niña (cold phase of ENSO) conditions as persistent low-level easterlies prevent the monsoon trough from extending into Micronesia.

Poorly organized convection created working best track problems. For example, from 271800Z until 281130Z, satellite fixes following the deep convection, indicated continued westward movement (the cluster of fixes shown in area A on Figure 3-20-1). However, the low-level wind circulation tracked to the northwest, which was confirmed by two ERS-1 scatterometer passes (note the location of these two fixes on Figure 3-20-1). The differences between the fixes placed within the center of the deep convec-

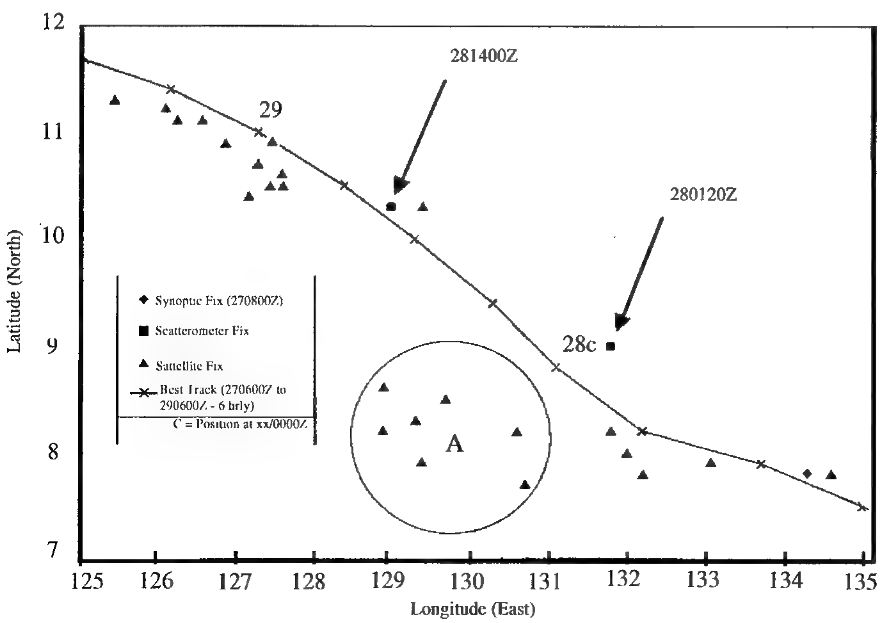

Figure 3-20-1. Display of weather satellite tropical cyclone fixes (triangles), ERS-1 scatterometer fixes (squares), a synoptic fix (diamond), and the best-track positions at 6-hour intervals for the pre-Sibyl tropical disturbance during the period 270600Z to 291200Z September. Note the cluster of satellite fixes in region A (enclosed by a circle) that are well south of the scatterometer fixes and the final best-track positions.

tion versus the wind center fixes based on the scatterometer data were as large as 120 nm (220 km). The 280120Z ERS-1 pass also showed that the system had intensified to 30 kt (15 m/sec) one-minute average (note: the scatterometer winds are considered to be representative of an eight-minute average 10-meter surface wind measurement). The scatterometer data from the ERS-1 pass at 281400Z indicated 35 kt (18 m/sec) maximum marine surface winds in the southeastern quadrant of a well-defined cyclonic circulation (Figure 3-20-2).

Based upon satellite intensity estimates, and scatterometer winds, TD 20W was upgraded to Tropical Storm Sibyl on the warning valid at 281800Z. Sibyl intensified as it neared the Philippines (Figure 3-20-3), and continued to intensify as it moved through the northern Visayan Islands. A minimum sea-level pressure of 977.9 mb was recorded at Tacloban (WMO 98550) at 290900Z. Sibyl attained typhoon intensity three hours later at 291200Z, and reached its peak intensity of 95 kt (49 m/sec) at 301200Z just before moving ashore in Luzon southeast of Manila (Figure 3-20-4). Possible mechanisms for intensification while crossing through an archipelago of high islands are outlined in the discussion section. Surface observations from the Philippines enabled the JTWC to make seven synoptic fixes that aided in tracking Sibyl.

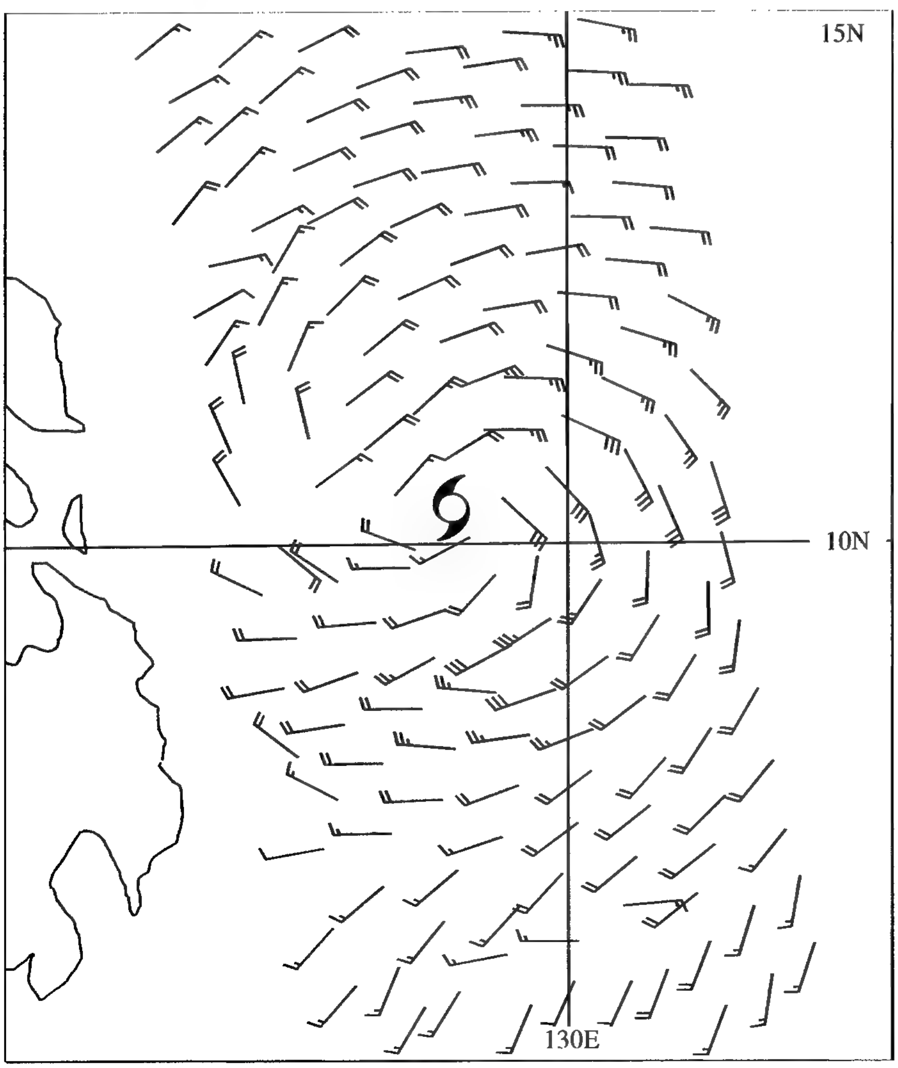

Figure 3-20-2 Scatterometer data from the ERS-1 spacecraft indicate that Sibyl has a well-defined cyclonic circulation in the low-level wind field and a maximum wind speed of 35 kt (17m/sec) (281400Z September ERS-1 scatterometer-derived marine surface winds).

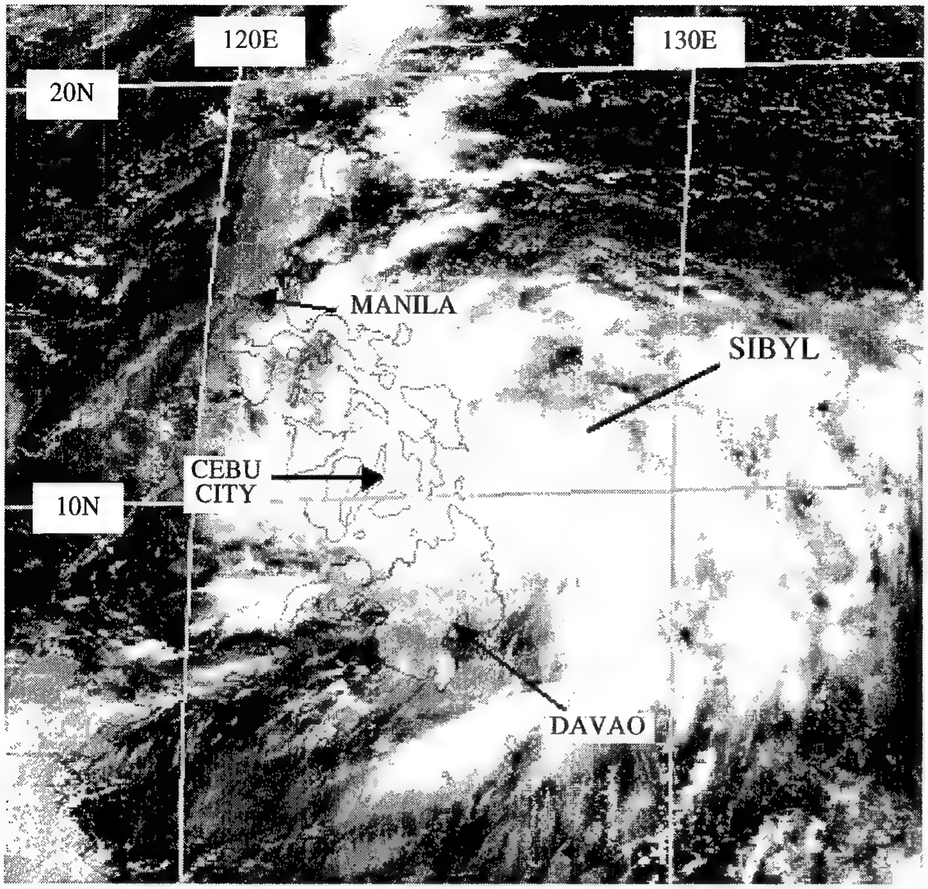

Figure 3-20-3 Sibyl approaches the Philippines with an intensity of 45 kt (23 m/sec) (290031Z September visible GMS imagery).

By 301800Z, Sibyl had crossed most of metropolitan Manila. Data received after-the-fact from the Philippine Atmospheric, Geophysical, and Astronomical Services (PAGASA) indicated that Sangley Point (WMO 98428) recorded maximum 10-minute sustained winds of 65 kt (33 m/sec) at 301655Z. This converts to 75 kt (39 m/sec) 1-minute sustained wind speed. The typhoon exited the Philippines at 010000Z October and entered the South China Sea. Weakening over water in the South China Sea , Sibyl was downgraded to a tropical storm on the warning valid at 021800Z October. Making a gradual turn to the north, Sibyl made landfall at 030400Z about 175 nm (325 km) west-southwest of Hong Kong, where Waglan Island (WMO 45007) measured maximum sustained winds of 58 kt (30 m/sec) (one-minute average) with a peak gust of 62 kt (32 m/sec). Surface synoptic reports in China near Sibyl indicated that the low-level circulation dissipated on the morning of 04 October. The JTWC issued the final warning on Sibyl valid at 031800Z October.

III. DISCUSSION

Intensification while crossing the Philippines

Although tropical cyclones usually weaken over land, those that cross through the Visayan region of the Philippines often intensify. The following discussion offers a hypothetical explanation of this phenomenon. The Visayan region of the Philippines is an archipelago of high islands with more of the area covered by water — very warm water — than by land. A tropical cyclone passing through this region may thus continue to derive energy through air-sea interaction. In addition, the mountainous islands of the archipelago and the southern part of Luzon (which forms a barrier on the northern side of the region) may act — through frictional effects and geographic barrier effects — to shrink the size of a tropical

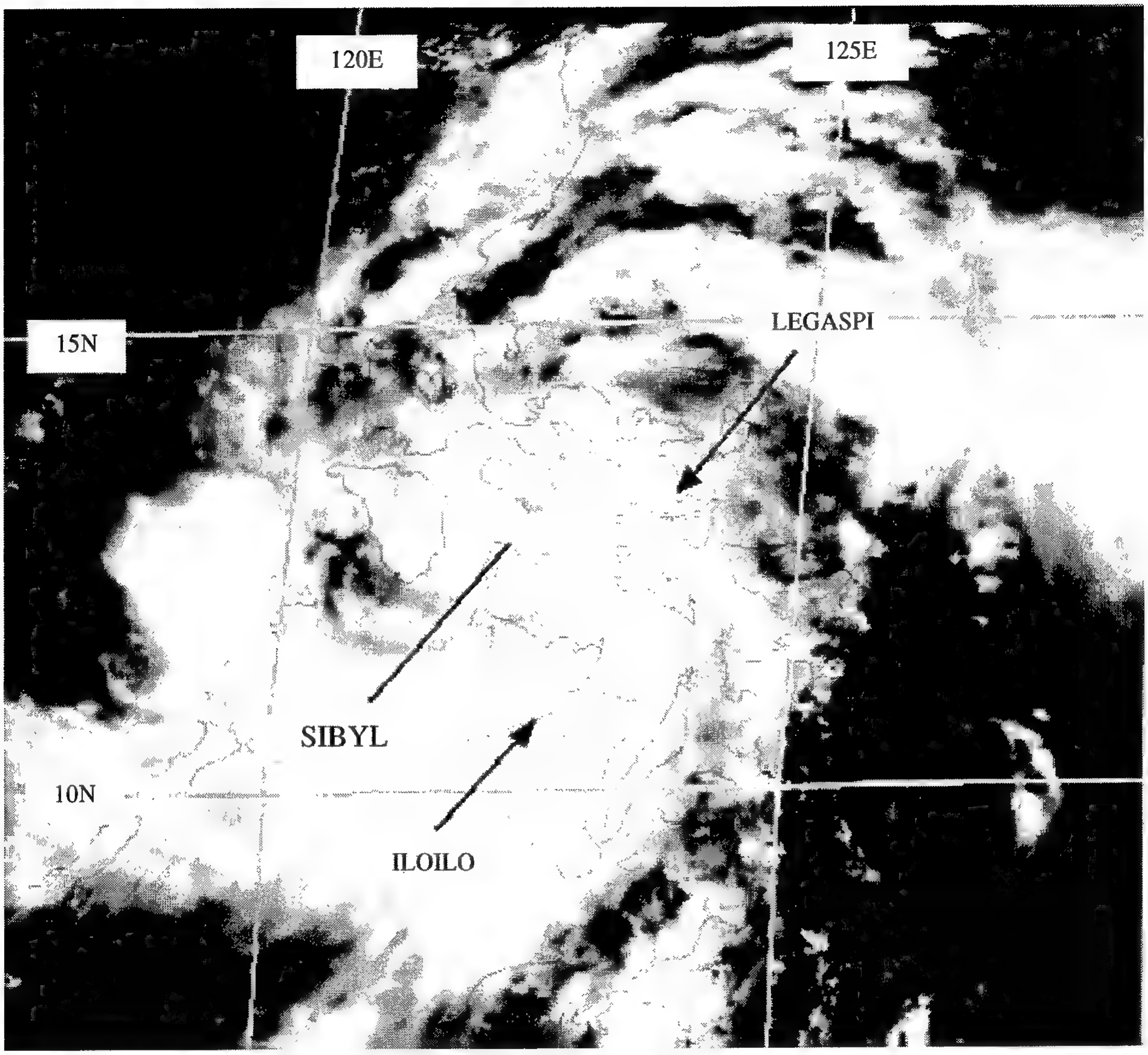

Figure 3-20-4. Typhoon Sibyl a few hours before reaching its peak intensity of 95 kt (49 m/sec) when located about 125 nm (230 km) southeast of Manila (300331Z September visible GMS imagery).

cyclone entering the region. Low-level cyclonic winds are forced to accelerate through channels between the land areas, enhancing the low-level convergence. As long as upper-level flow patterns are favorable for intensification, the increased low-level convergence will lead to greater convection, and, as the wind field shrinks, the vorticity may become more concentrated toward the core or the tropical cyclone. As a result, intensification proceeds as the tropical cyclone passes through the archipelago.

IV. IMPACT

In the Philippines, Sibyl's passage resulted in at least 108 deaths and left 100 people missing. Fifty of the deaths occurred in the town of Cabalantian (50 nm (95 km) north of Manila) from floods and 18-foot high lahars (mudflows) from the slopes of Mount Pinatubo. Storm-related torrential rains and associated landslides caused fatalities and destruction of property as far as 500 nm (925 km) south of Manila. In Manila, power was cut to thousands of people. Damage from Sibyl exceeded 1 billion pesos or US$38.5 million. No reports of damage were received from China.

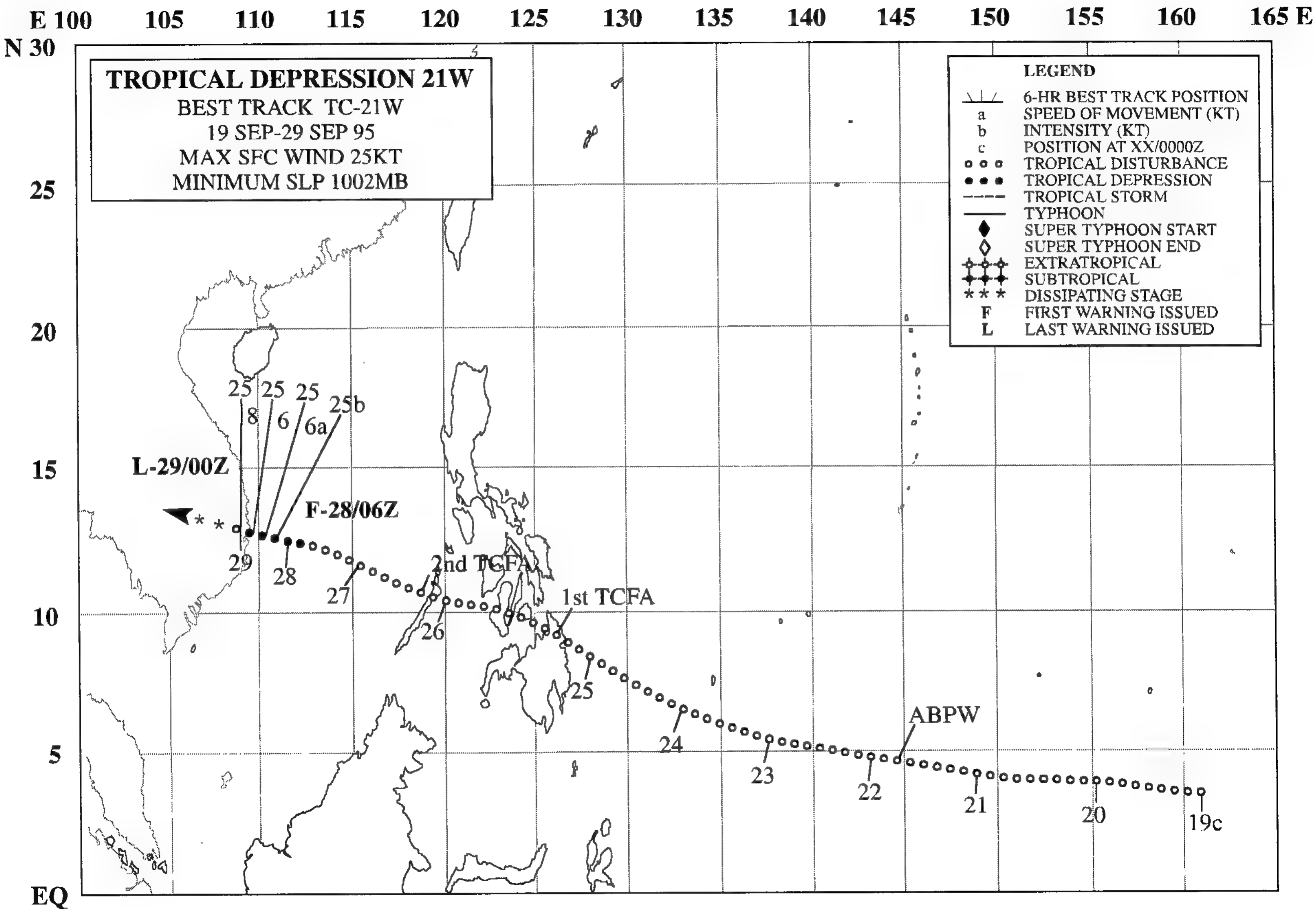

TROPICAL DEPRESSION 21W
BEST TRACK TC-21W
19 SEP-29 SEP 95
MAX SFC WIND 25KT
MINIMUM SLP 1002MB
LEGEND
6-HR BEST TRACK POSITION
a SPEED OF MOVEMENT (KT)
b INTENSITY (KT)
c POSITION AT XX/0000Z
TROPICAL DISTURBANCE
TROPICAL DEPRESSION
TROPICAL STORM
TYPHOON
SUPER TYPHOON START
SUPER TYPHOON END
EXTRATROPICAL
SUBTROPICAL
DISSIPATING STAGE
F FIRST WARNING ISSUED
L LAST WARNING ISSUED
E 100
105
110
115
120
125
130
135
140
145
150
155
160
165 E
N 30
25
20
15
10
5
EQ
L-29/00Z
F-28/06Z
25 8
25 6
25 6a
25b
29
28
27
26
2nd TCFA
1st TCFA
25
24
23
22
ABPW
21
20
19c

TROPICAL DEPRESSION (21W)

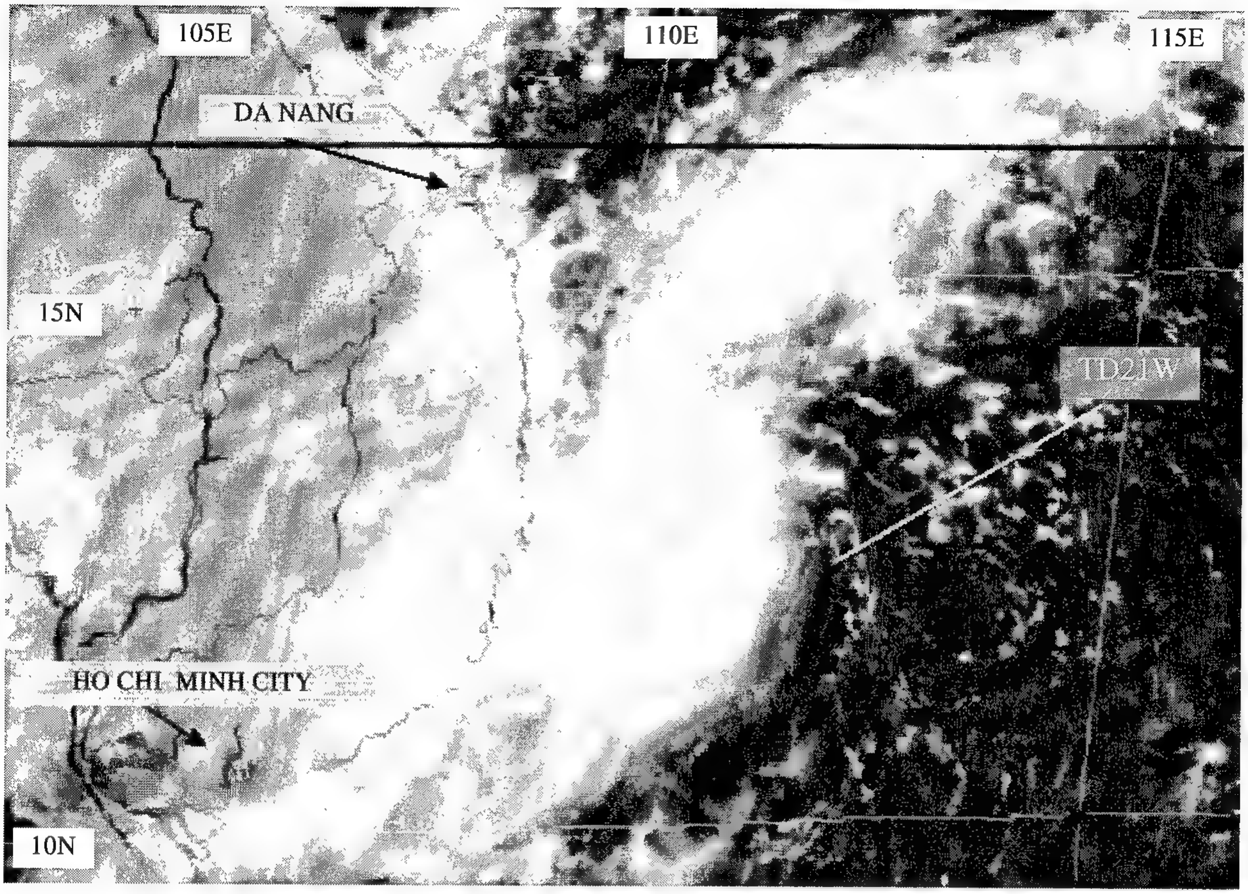

Figure 3-21-1 Tropical Depression 21W reaches its peak intensity of 25 kt (13 m/sec) as it approaches the coast of Vietnam (280231Z September visible GMS imagery).

During the last week of September, amounts of deep convection increased throughout Micronesia. This convection organized into an east-west chain of tropical disturbances. The disturbance that became Tropical Depression 21W was first mentioned on the 211800Z September Significant Tropical Weather Advisory when synoptic data indicated that a weak surface circulation accompanied an area of deep convection south of Chuuk. For three days, this tropical disturbance drifted westward toward the Philippines. On 25 September, satellite imagery indicated that the deep convection and low-level cloud lines accompanying this disturbance had become better organized, prompting the JTWC to issue a Tropical Cyclone Formation Alert (TCFA) at 250500Z. As the disturbance crossed the Philippines, it failed to intensify, and a second TCFA was issued at 260400Z in anticipation of intensification as it moved into the South China Sea. When the system failed to become better organized once in the South China Sea, the second TCFA was canceled at 262130Z. On 28 September, as this tropical disturbance neared the coast of Vietnam, the deep convection consolidated near the low-level circulation center, and its low-level cloud lines became better defined (Figure 3-21-1). The JTWC issued the first warning on Tropical Depression 21W, valid at 280600Z. The final warning was issued, valid at 290000Z, after the system made landfall on the coast of Vietnam and began to dissipate.

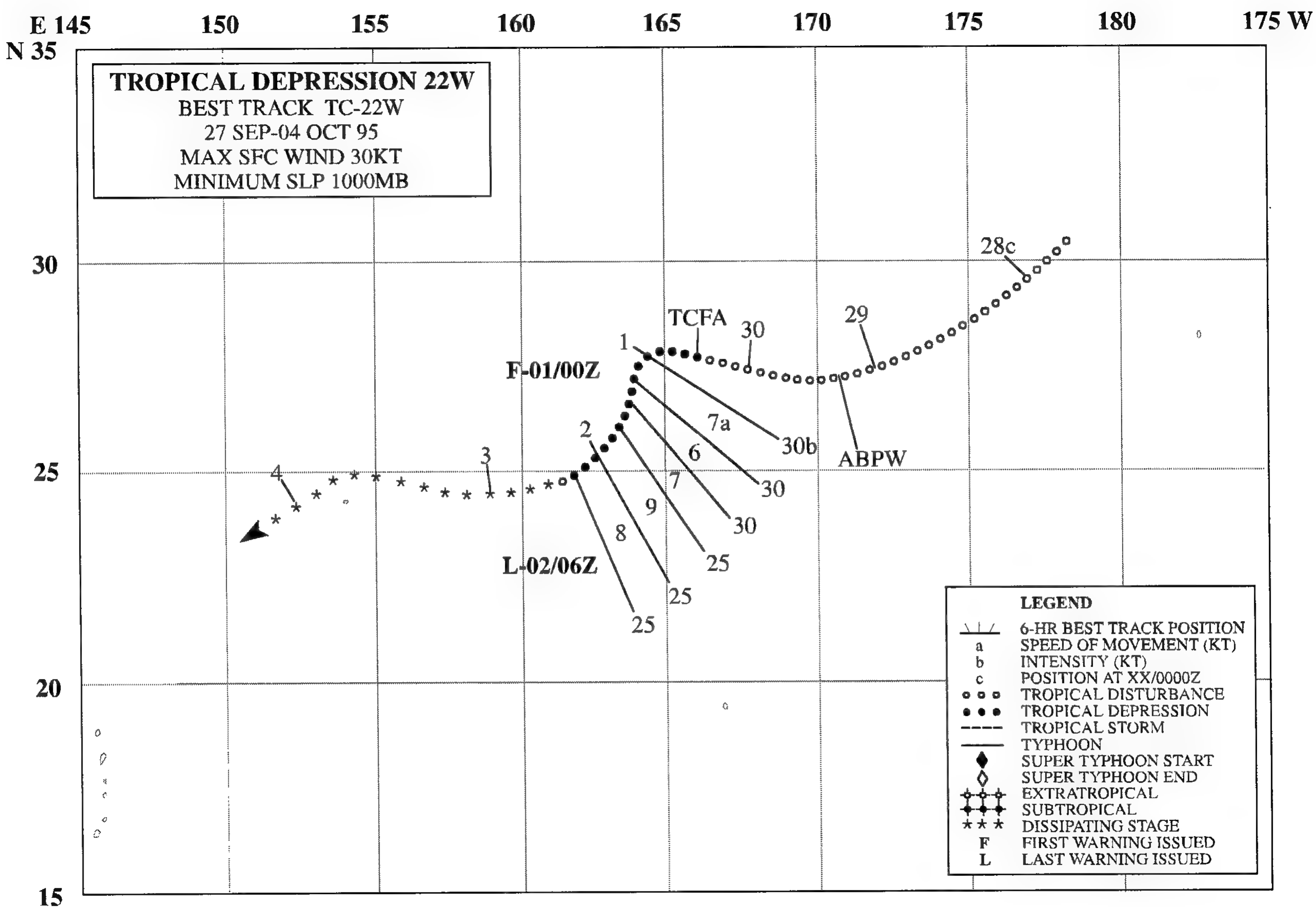

TROPICAL DEPRESSION 22W
BEST TRACK TC-22W
27 SEP-04 OCT 95
MAX SFC WIND 30KT
MINIMUM SLP 1000MB
E 145
150
155
160
165
170
175
180
175 W
N 35
30
25
20
15
TCFA
F-01/00Z
L-02/06Z
ABPW
28c
29
30
30b
7a
6
7
9
8
30
30
25
25
25
1
2
3
4
LEGEND
6-HR BEST TRACK POSITION
a SPEED OF MOVEMENT (KT)
b INTENSITY (KT)
c POSITION AT XX/0000Z
TROPICAL DISTURBANCE
TROPICAL DEPRESSION
TROPICAL STORM
TYPHOON
SUPER TYPHOON START
SUPER TYPHOON END
EXTRATROPICAL
SUBTROPICAL
DISSIPATING STAGE
F FIRST WARNING ISSUED
L LAST WARNING ISSUED

TROPICAL DEPRESSION (22W)

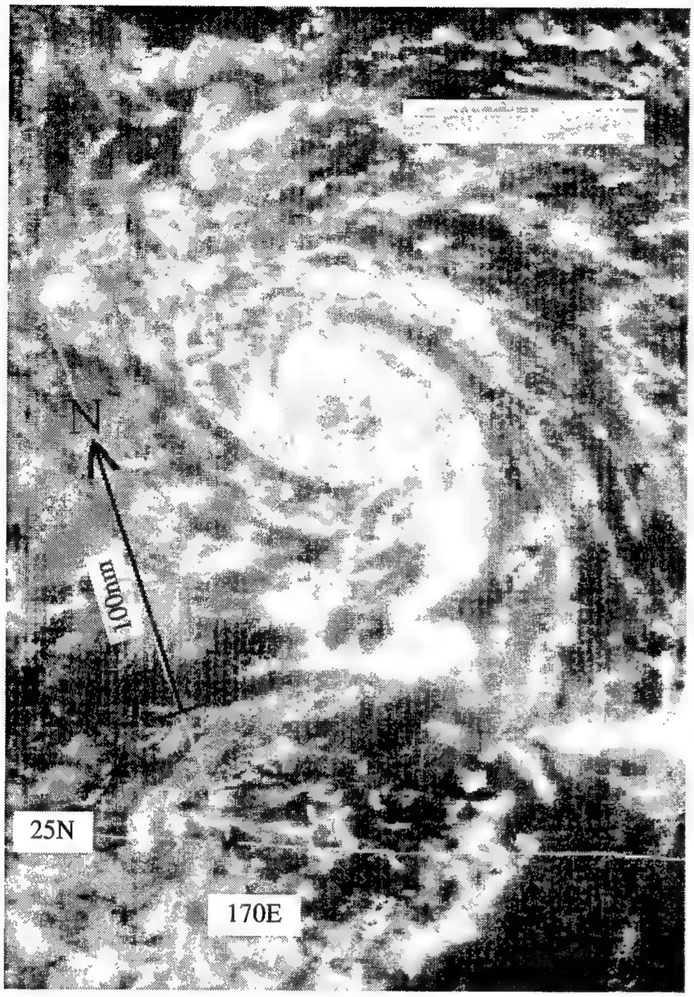

Figure 3-22-1 The low-level vortex that became TD 22W possesses cloud features that mimic those of a mature tropical cyclone: well-defined tightly coiled low-level cloud lines, and a "ring" of low and middle cloud surrounding a relatively cloud-free "eye" (290031Z September visible GMS imagery).

I. HIGHLIGHTS

Forming at a relatively high latitude (30°N) near the international date line, Tropical Depression 22W was a very small tropical cyclone — the smallest tropical cyclone in the western North Pacific warned on by the JTWC during 1995.

II. TRACK AND INTENSITY

On 24 September, a portion of a dissipating cold front (linked to an occluded low-pressure system south of the Aleutian Islands) pushed slowly southward across 30°N between 160° E and the international date line. An area of deep convection formed along this front near the international date line. This convection was most probably associated with an upper-tropospheric low that was in the process of becoming cut-off at approximately 35°N 175°E. On 28 September, a very small well-defined low-level cyclonic vortex formed to the northwest of this area of deep convection. On 29 September, the deep convection in the subtropics (25-30°N) near the international date line subsided, however the very small well-defined low-level vortex remained (Figure 3-22-1) and began to drift toward the west. This low-level vortex was first mentioned on the 290600Z Significant Tropical Weather Advisory. This advisory included the following remarks:

"... A low level circulation is indicated on visible satellite imagery [Figure 3-22-1] ... Scatterometer data [Figure 3-22-2] indicate winds of 20 to 25 knots, however, almost no [deep] convection is associated with this system ..."

For the next several days, this vortex drifted toward the west-southwest while embedded in the east-northeasterly flow south of the axis of the lower tropospheric subtropical ridge. During the night of 29 September, deep convection (on the scale of an individual large thunderstorm) developed near the low-level circulation center of this disturbance (Figure 3-22-3). This deep convection grew and decayed several times until the night of 30 September, when it became more extensive and persistent. Based upon this increase and persistence of deep convection, a Tropical Cyclone Formation Alert was issued at 301200Z. On the morning of 01 October, the amount and organization of the deep convection associat-

ed with this very small vortex increased (Figure 3-22-4), and the first warning, valid at 010000Z, on Tropical Depression 22W was issued. Central deep convection associated with TD 22W persisted for only about 24 hours. On 02 October, the deep convection began to shear away to the east (Figure 3-22-5), and by the afternoon of 02 October the deep convection was lost. As a result, the JTWC issued the final warning, valid at 020600Z on Tropical Depression 22W. Steadily weakening, the low-level vortex continued to track toward the west-southwest, and could be located in the low-cloud field through 04 October.

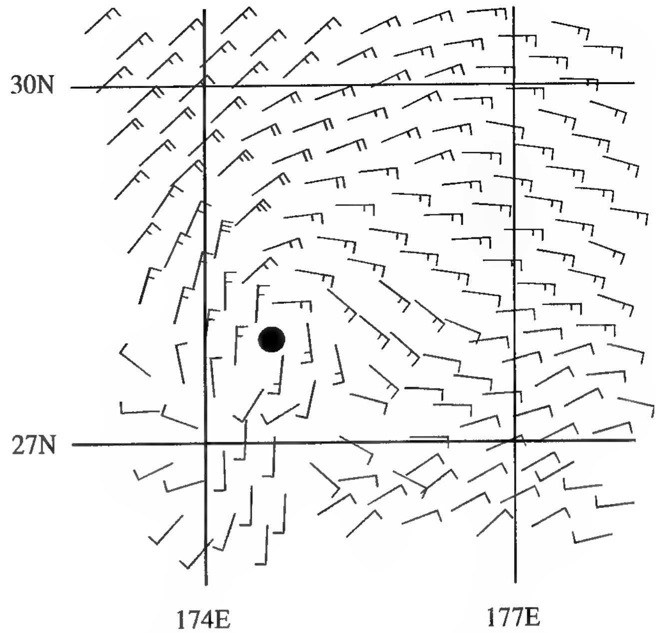

Figure 3-22-2 The surface wind field accompanying the low-level vortex (solid dot) that became TD 22W (281049Z September ERS-1 scatterometer-derived sur-

III. DISCUSSION

How small can a tropical cyclone be?

Tropical Depression 22W was a very small tropical cyclone — easily the smallest tropical cyclone of 1995, and perhaps about as small as a tropical cyclone can be. Although the processes governing the formation of the very small low-level circulation center that became TD 22W are uncertain, it is clear that this tiny vortex later acquired persistent central deep convection, and became a typical tropical cyclone except for its unusually small size. Before it acquired its central deep convection, the diameter of the region occupied by well-defined cyclonically curved lines of low-level clouds was approximately 180 nm (300 km). At one point, a ring of low and middle cloud (with perhaps some low-topped convection) (Figure 3-22-1) surrounded a relatively cloud-free "eye" whose diameter was 20 nm (35 km). Interestingly, the physical dimensions of these central features are typical for the analogous central features in much larger tropical cyclones. What seemed to contribute most to the apparent very small size of Tropical Depression 22W was the absence of peripheral bands of deep convection and extensive curved bands of outflow cirrus.

The very small size of Tropical Depression 22W leads one to ask a fundamental question: how small can a tropical cyclone be? The answer to this question is beyond the scope of this summary, however the nature of the formation and evolution of this tropical cyclone yield some information that may be relevant: (1) the size was established at the time of the genesis of its embryonic vortex, (2) the size was established before it acquired persistent central deep convection, and (3) the size remained unchanged during the brief 24-hour time span during which it possessed central deep convection. A final point to consider is that without remotely sensed imagery and scatterometry, it is doubtful that Tropical Depression 22W would ever have been detected.

IV. IMPACT

No reports of damage or injuries attributable to Tropical Depression 22W were received at the JTWC.

Figure 3-22-3 A lone thunderstorm casting a long shadow in the evening sunlight is the first deep convection to appear near the center of TD 22W (290531Z September visible GMS imagery).

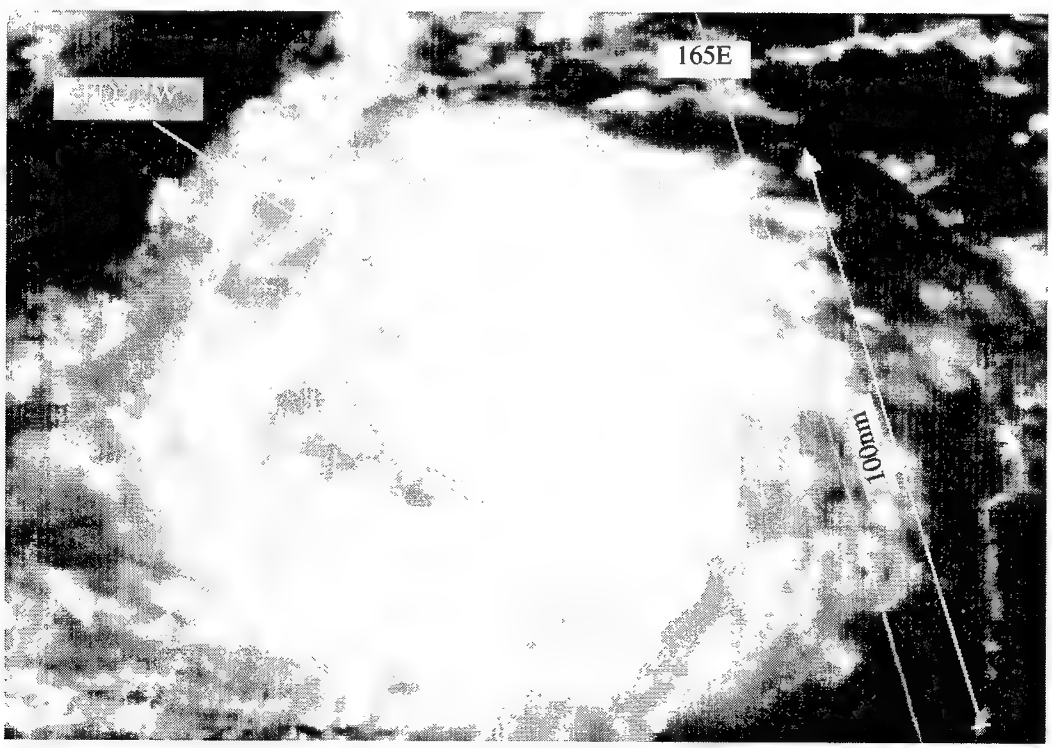

Figure 3-22-4 Deep convection associated with TD 22W reaches a maximum (010131Z October visible GMS imagery).

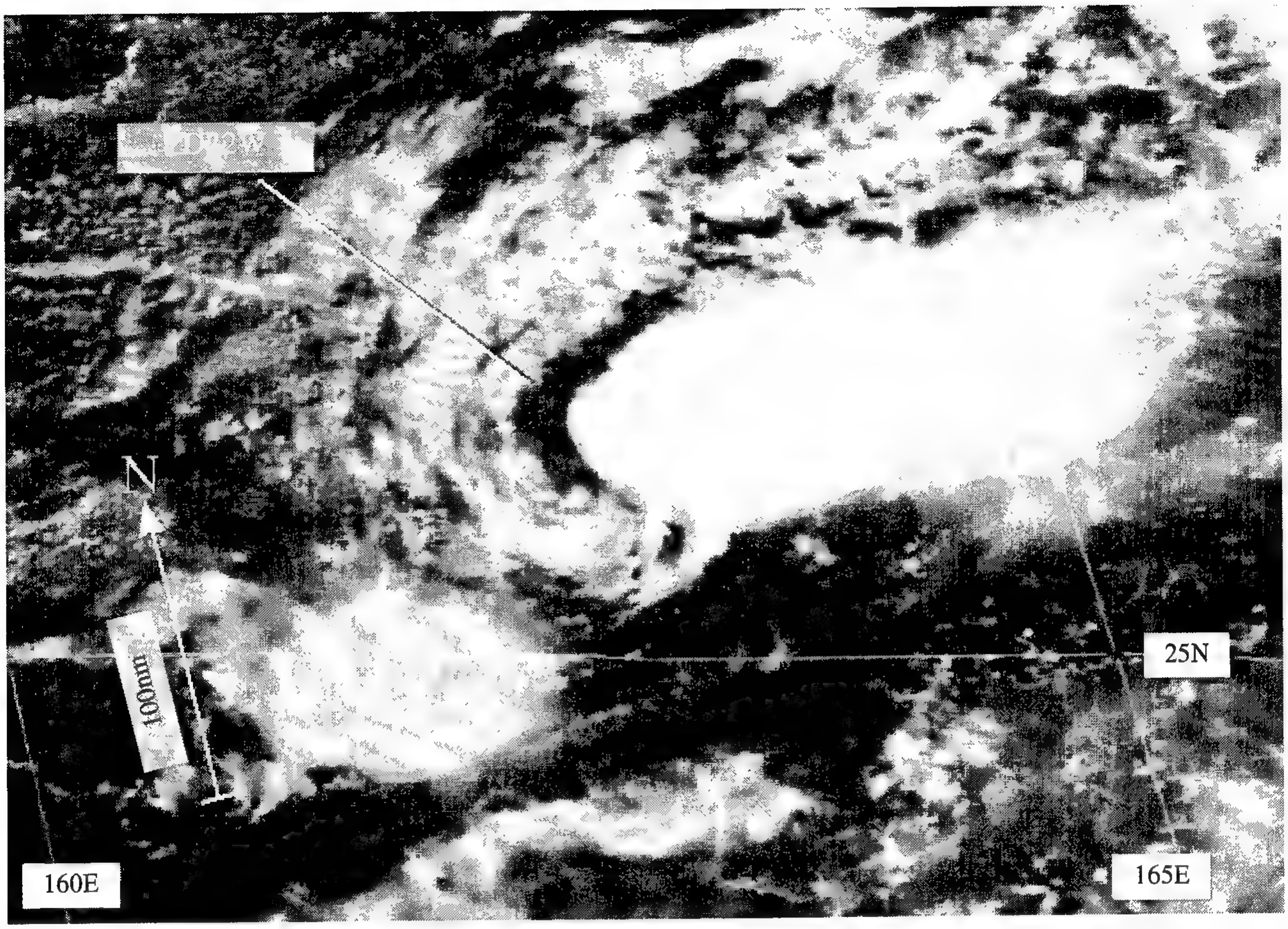

Figure 3-22-5 The central deep convection associated with TD 22W begins to encounter westerly vertical wind shear, and will shortly collapse (012131Z October visible GMS imagery).

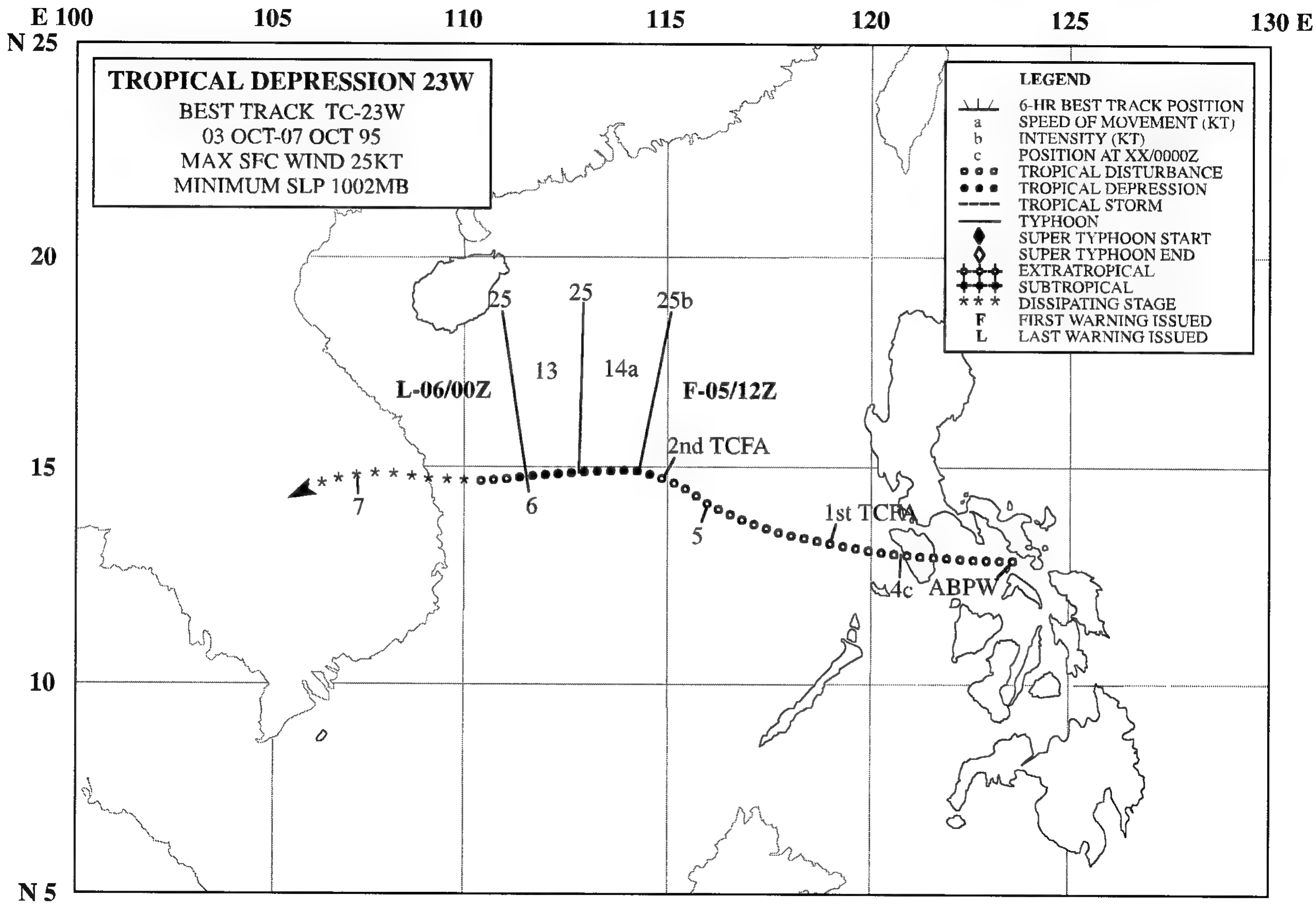
TROPICAL DEPRESSION 23W
BEST TRACK TC-23W
03 OCT-07 OCT 95
MAX SFC WIND 25KT
MINIMUM SLP 1002MB
LEGEND
6-HR BEST TRACK POSITION
a SPEED OF MOVEMENT (KT)
b INTENSITY (KT)
c POSITION AT XX/0000Z
TROPICAL DISTURBANCE
TROPICAL DEPRESSION
TROPICAL STORM
TYPHOON
SUPER TYPHOON START
SUPER TYPHOON END
EXTRATROPICAL
SUBTROPICAL
DISSIPATING STAGE
F FIRST WARNING ISSUED
L LAST WARNING ISSUED
E 100
105
110
115
120
125
130 E
N 25
20
15
10
N 5
L-06/00Z
F-05/12Z
2nd TCFA
1st TCFA
ABPW
25
13
25
14a
25b
7
6
5
4c

TROPICAL DEPRESSION 23W

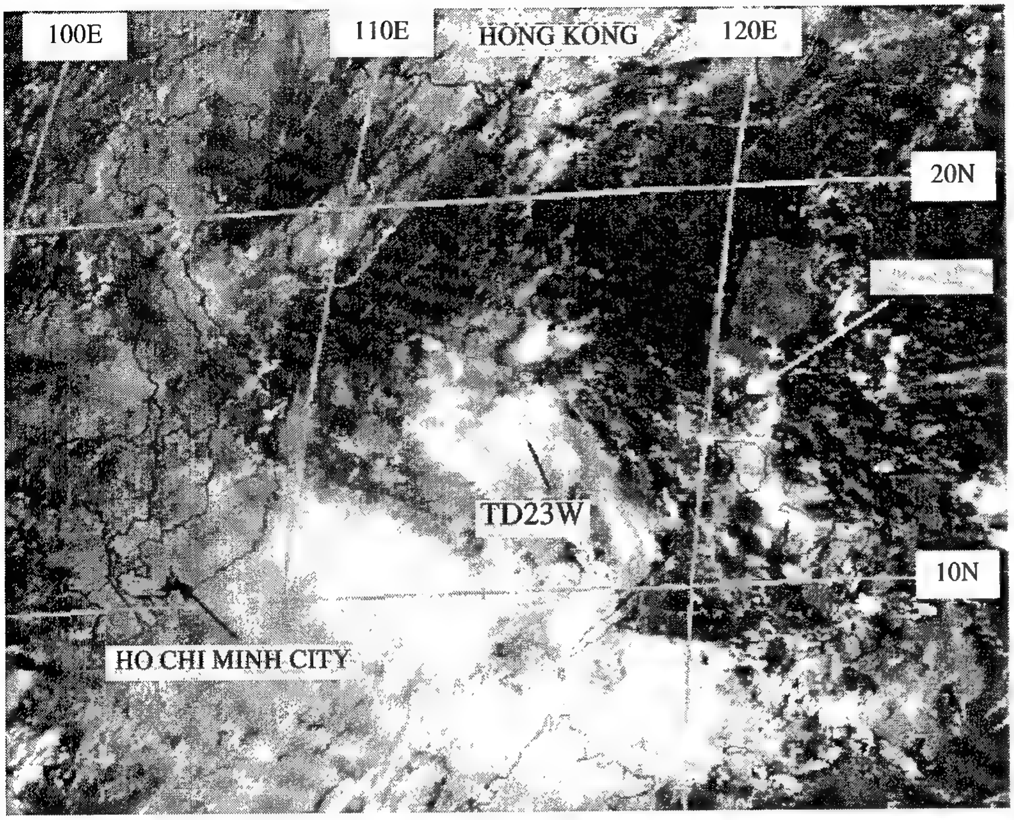

Figure 3-23-1 The tropical disturbance that became Tropical Depression 23W begins to consolidate its deep convection around its low-level circulation center (042331Z October visible GMS imagery).

While Tropical Storm Sibyl (20W) was making landfall in southern China, another tropical disturbance was crossing the central Philippines. Expecting that the environment would become more favorable for development of the tropical disturbance over the Philippines once Sibyl weakened over China (the outflow from Sibyl appeared to be creating northerly shear on this disturbance), the JTWC added it to the Significant Tropical Weather Advisory at 030600Z October. When this disturbance moved into the South China Sea, deep convection increased in areal coverage and organization, prompting the JTWC to issue a Tropical Cyclone Formation Alert (TCFA) at 040800Z. Moving westward in the South China Sea, the disturbance failed to intensify. An exposed low-level circulation center was revealed by visible satellite imagery during the daylight hours of 05 October (Figure 3-23-1). Although the maximum winds in the system were estimated to be only 15 to 20 kt (8 to 10 m/sec), the environment was considered favorable for development, so a second TCFA was issued at 050800Z. At 051200Z, synoptic data, and wind speeds derived from microwave imagery indicated that the wind speeds in the system had increased to 25 kt (13 m/sec). Based on these data, the first warning on Tropical Depression 23W (TD 23W) was issued, valid at 051200Z. TD 23W moved steadily westward toward the coast of Vietnam and, only twelve hours after the first warning, the final warning was issued at 060000Z when satellite imagery indicated weakening. The remnants of TD 23W moved inland over southeast Asia later that day and dissipated.

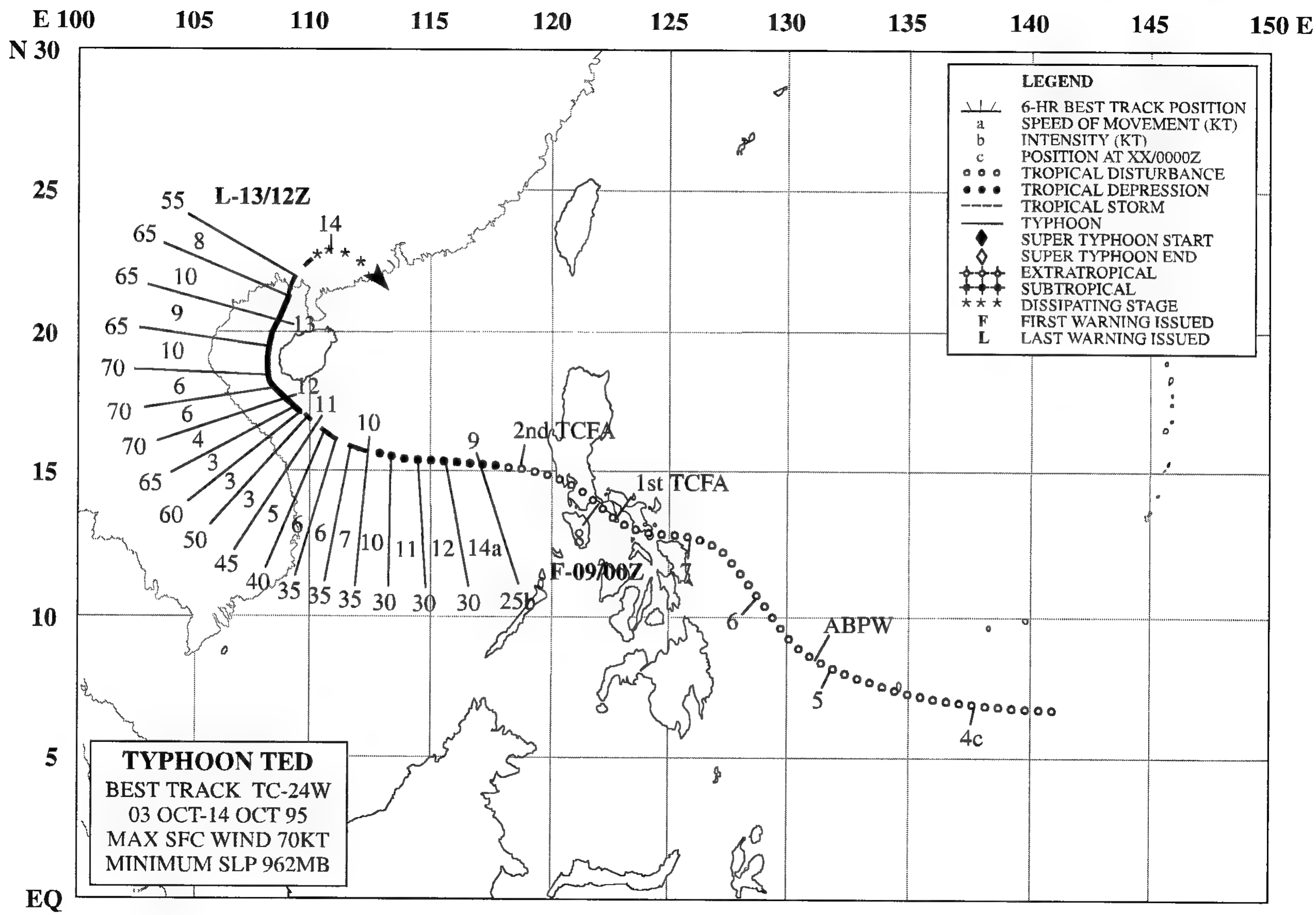
E 100
105
110
115
120
125
130
135
140
145
150 E
N 30
25
20
15
10
5
EQ
LEGEND
6-HR BEST TRACK POSITION
SPEED OF MOVEMENT (KT)
INTENSITY (KT)
POSITION AT XX/0000Z
TROPICAL DISTURBANCE
TROPICAL DEPRESSION
TROPICAL STORM
TYPHOON
SUPER TYPHOON START
SUPER TYPHOON END
EXTRATROPICAL
SUBTROPICAL
DISSIPATING STAGE
FIRST WARNING ISSUED
LAST WARNING ISSUED
L-13/12Z
F-09/00Z
2nd TCFA
1st TCFA
ABPW
TYPHOON TED
BEST TRACK TC-24W
03 OCT-14 OCT 95
MAX SFC WIND 70KT
MINIMUM SLP 962MB

TYPHOON TED (24W)

I. HIGHLIGHTS

Typhoon Ted developed east of the Philippines in the near-equatorial trough. After moving through the islands of the central Philippines as a tropical disturbance, Ted became a typhoon in the South China Sea when south of Hainan Island. As Ted passed into the Gulf of Tonkin, a gust of 111 kt (55 m/sec) was observed at the top (100 m above sea level) of an oil rig, and winds of typhoon force were estimated to have occurred at sea-level by crew members working at the base of the platform. Ted eventually dissipated over the mountains of southern China.

II. TRACK AND INTENSITY

The tropical disturbance that became Ted can be traced back to a flare-up of deep convection approximately 200 nm (370 km) south-southeast of Ulithi Atoll in the western Caroline Islands that occurred at 031200Z October along the axis of a weak near-equatorial trough. This disturbance was slow to develop and wasn't mentioned by the JTWC until the Significant Tropical Weather Advisory was reissued at 050300Z to include it. The first of two Tropical Cyclone Formation Alerts (TCFAs) was issued at 071800Z when the disturbance went ashore in southeastern Luzon near Legaspi. At this time, the upper-tropospheric flow pattern was deemed by forecasters to be favorable for intensification. The system, however, did not intensify as it passed over the many islands in the center of the Philippine archipelago. With the synoptic environment still appearing to favor intensification, a second TCFA was issued at 081800Z as the disturbance entered the South China Sea.

Based on an improved satellite signature and ship reports, the first warning was issued on Tropical Depression 24W (TD 24W), valid at 090000Z. Twenty-four hours later, satellite intensity estimates reached 35 kt (18 m/sec), and TD 24W was upgraded to Tropical Storm Ted on the warning valid at 100000Z. Thereafter, Ted moved westward and continued to intensify (Figure 3-24-1). On 11 October, Ted began to track more northwestward toward the Gulf of Tonkin, and started to intensify at a faster rate.

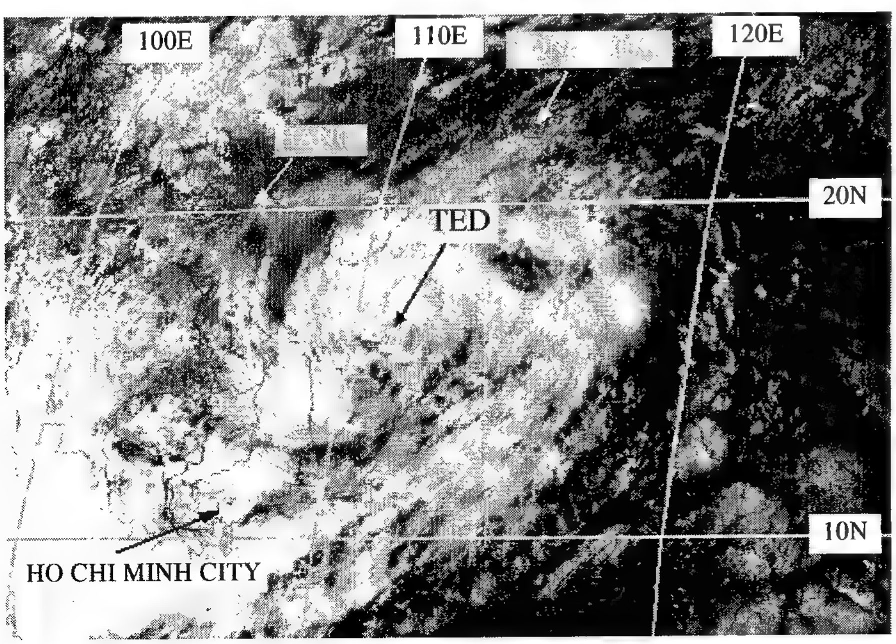

Figure 3-24-1 Ted begins to intensify as it nears Hainan Island (100831Z October visible GMS imagery).

Intensity estimates based upon the application of Dvorak's technique to satellite imagery did not provide an accurate picture of Ted's "true" intensity as determined from synoptic data. All warning intensities on 11 October were at least 20 kt (10 m/sec) too low, and all forecasts indicated a weakening trend. However, observations from an oil rig at approximately 120000Z (that were not received at the JTWC until 120600Z) indicated that Ted most probably reached typhoon intensity late on 11 October (see the discussion of Ted's intensity on 11 and 12 October in the next section).

Typhoon Ted reached its peak intensity of 75 kt (39 m/sec) at 120000Z and maintained this intensity for 18 hours. The typhoon continued to track around the west side of Hainan Island with its eye and eye wall remaining just offshore. Late on 12 October, Ted turned to the north-northeast and made landfall near Beihai in southern China as a minimal typhoon. It dissipated rapidly as it moved inland, and the final warning, valid at 131200Z, was issued.

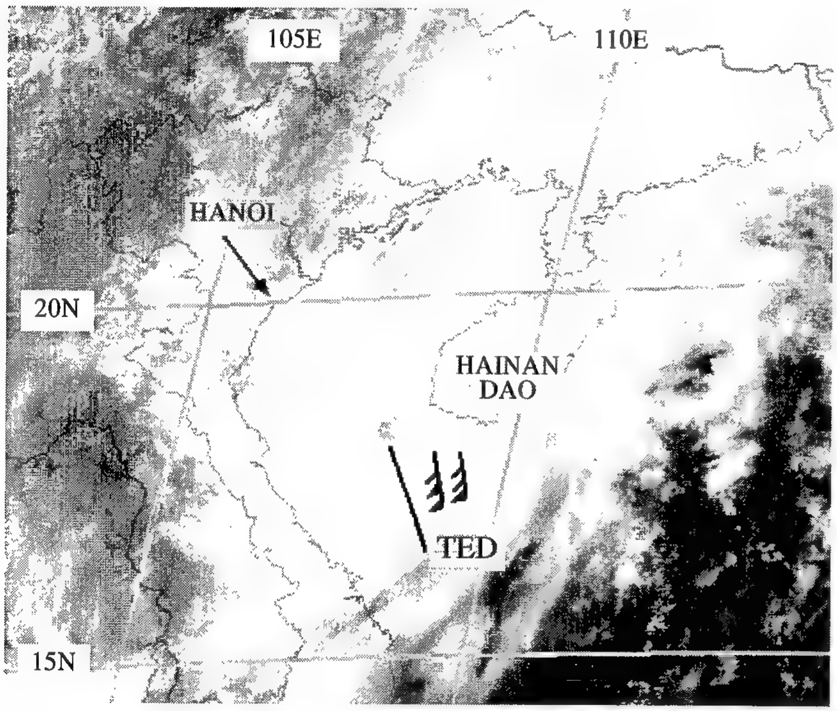

Figure 3-24-2 Typhoon Ted with the observed winds at an oil rig superimposed. The winds (observed at different times) are plotted relative to Ted's center, not the rig location (120331Z October visible GMS imagery). (Wind data courtesy of Nobel Denton Weather Services Ltd, London).

III. DISCUSSION

Typhoon intensity revealed by synoptic data

The peak wind information observed on an oil rig located at 17.9°N 109.7°E (south of Hainan Island) that was passed to the JTWC by Noble Denton Weather Services Ltd. of London, is a good illustration of discrepancies that can occur between surface observations of the winds in a tropical cyclone and the surface wind speed as estimated using currently available satellite techniques. Intensity values yielded by the application of Dvorak's techniques indicated an intensity of 45 kt (23 m/sec) as Ted approached Hainan Dao. Observations from the oil rig, however, indicated that the wind speeds were substantially higher. Wind gusts at the top of the 300 ft (100 m) platform reached a peak of 111 kt (57 m/sec) at 111930Z, while wind speeds near the surface were estimated to be at typhoon force at 120000Z (Figure 3-24-2). Using the reduction scheme for marine observations of Liu et al. (1979) and the gust factors of Atkinson (1974) or Krayer and Marshall (1992), the 111 kt gust at 300 feet yields an estimate of 75 kt (37 m/sec) for the one-minute sustained wind at a height of 10 meters. These synoptic reports were the basis for the upgrade of Ted to typhoon intensity. The graphic in Figure 3-24-3 shows

the influence of synoptic ground truth data on both the warning and the final best track warning intensity.

IV. IMPACT

The disturbance that became Ted caused local flooding as it traversed the Philippines. No reports of damage or injuries in either the Philippines or in China were received at the JTWC.

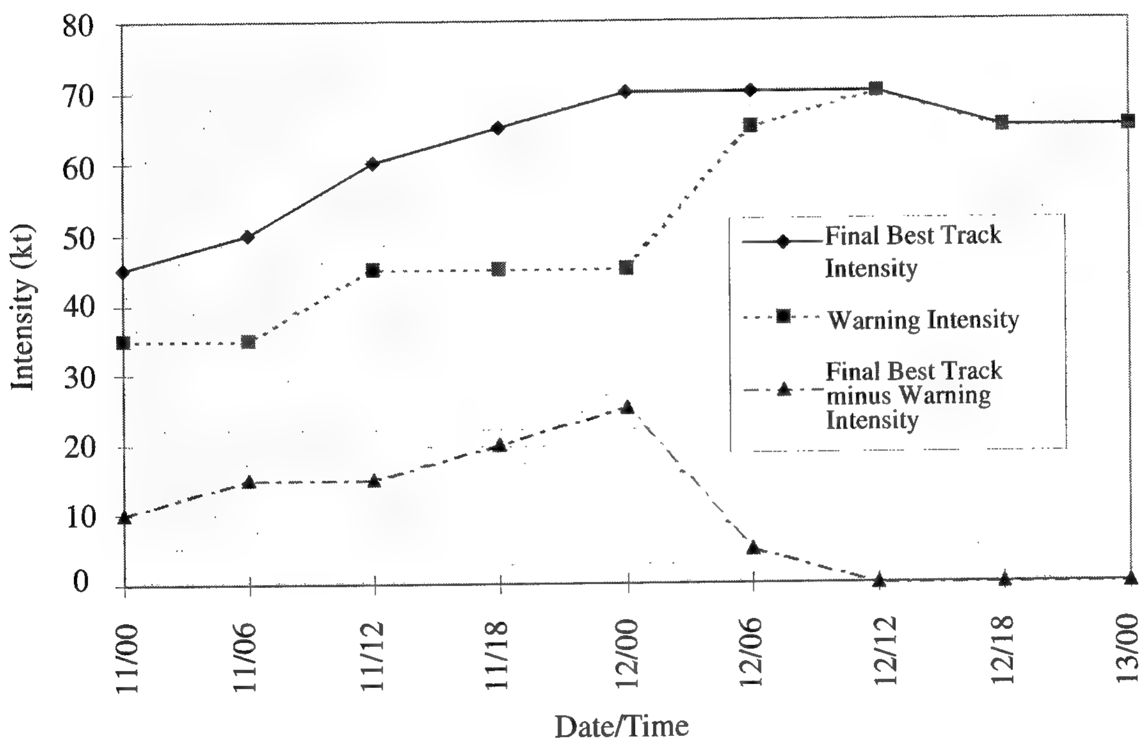

Figure 3-24-3 The influence of ground truth data at 120000Z (12/00Z) October on both the warning and final best track intensity.

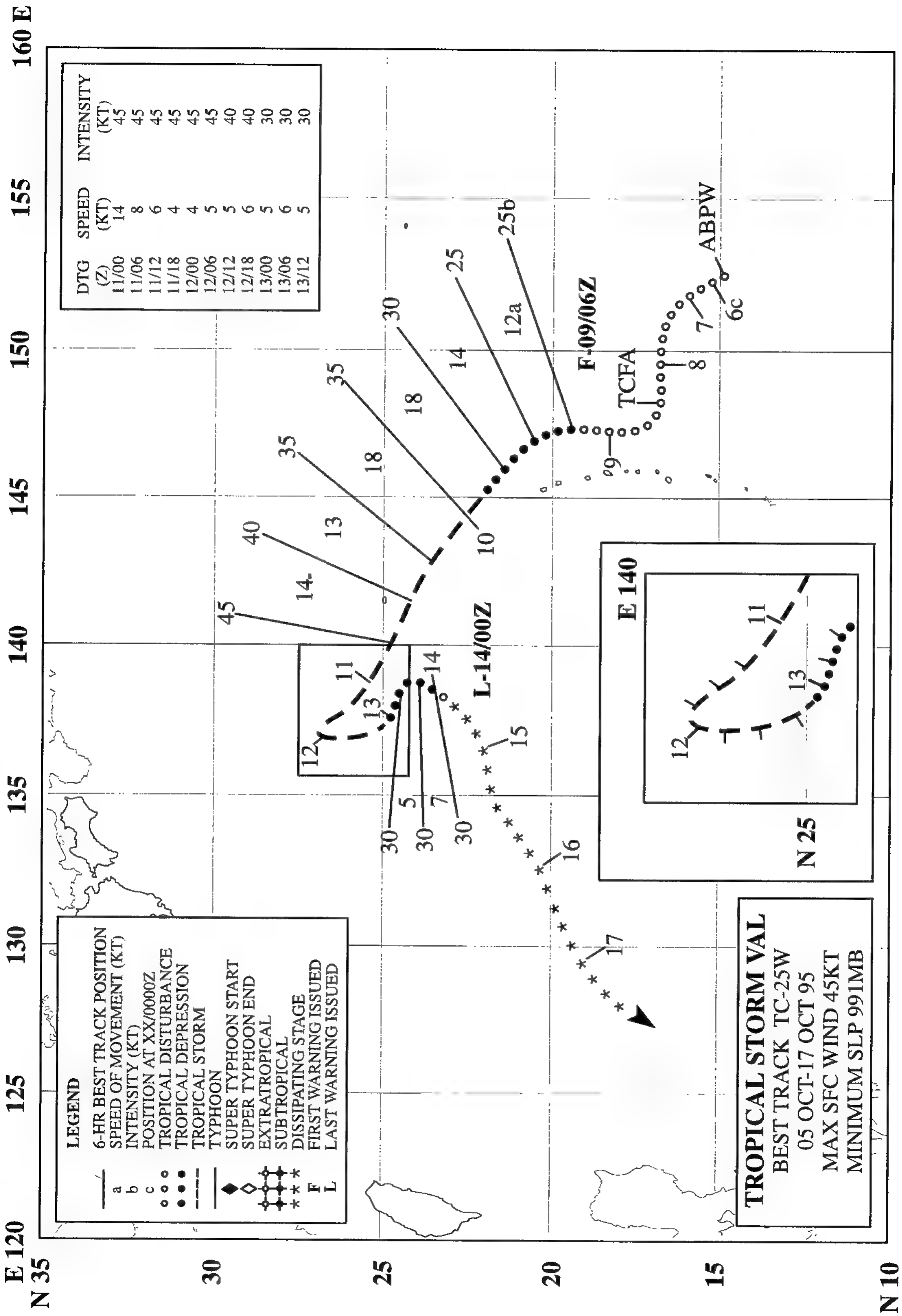
TROPICAL STORM VAL
BEST TRACK TC-25W
05 OCT-17 OCT 95
MAX SFC WIND 45KT
MINIMUM SLP 991MB
LEGEND
6-HR BEST TRACK POSITION
SPEED OF MOVEMENT (KT)
INTENSITY (KT)
POSITION AT XX/0000Z
TROPICAL DISTURBANCE
TROPICAL DEPRESSION
TROPICAL STORM
TYPHOON
SUPER TYPHOON START
SUPER TYPHOON END
EXTRATROPICAL
SUBTROPICAL
DISSIPATING STAGE
FIRST WARNING ISSUED
LAST WARNING ISSUED
DTG (Z) | SPEED (KT) | INTENSITY (KT)
11/00 14 45
11/06 8 45
11/12 6 45
11/18 4 45
12/00 4 45
12/06 5 45
12/12 5 40
12/18 6 40
13/00 5 30
13/06 6 30
13/12 5 30
F-09/06Z
L-14/00Z
TCFA
ABPW
E 140
N 25
E 120
N 35
160 E
N 10

TROPICAL STORM VAL (25W)

I. HIGHLIGHTS

Tropical Storm Val interacted with a monsoon gyre. This interaction coupled with the structural evolution of Val contributed to large track forecast errors.

II. TRACK AND INTENSITY

During the first week of October, an extensive area of deep convection and its associated cirrus debris stretched east-west from Southeast Asia to the Marshall Islands. This zone of maximum cloudiness, associated with a weak monsoon trough and a well-developed TUTT to its north, eventually produced two tropical disturbances that became named tropical cyclones: Typhoon Ted (24W), and Tropical Storm Val.

When Ted (24W) began to consolidate east of the Philippines, the zone of maximum cloudiness had moved northward, and stretched from the Philippines eastward past Guam. This band of deep convection was first mentioned on the 051800Z October Significant Tropical Weather Advisory. Val developed within this area of deep convection, but not until the large-scale low-level wind flow and the large scale pattern of deep convection became organized as a monsoon gyre.

At 080800Z October, a Tropical Cyclone Formation Alert (TCFA) was issued on this tropical disturbance. Remarks on this TCFA included:

"... Satellite imagery and synoptic data indicate that a tropical disturbance located approximately 200 nm [370 km] northeast of Guam is becoming better organized. The area is located beneath an upper level anticyclone and outflow is being enhanced by the presence of an upper-level low (TUTT cell) to the northwest..."

During the daylight hours of 09 October, the tropical disturbance that became Val consolidated into a well-organized area of deep convection to the northeast of Guam. It was embedded in a larger band of deep convection that wrapped around the periphery of a monsoon gyre whose broad center was located north-northwest of Guam and about 450 nm (850 km) west-northwest of the pre-Val tropical disturbance (Figure 3-25-1). Turning northward, as it interacted with the circulation of the monsoon gyre, the tropical disturbance intensified and the JTWC issued the first warning valid at 090600Z October on Tropical Depression 25W.

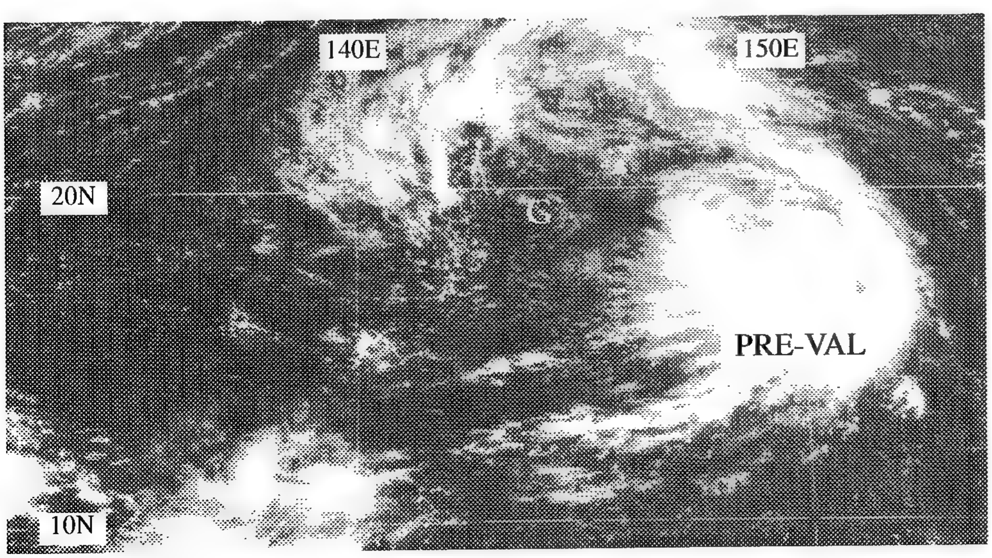

Figure 3-25-1 The tropical disturbance that became Val is located in the eastern side of the circulation of a monsoon gyre whose center is labeled "G" (090031Z October visible GMS imagery).

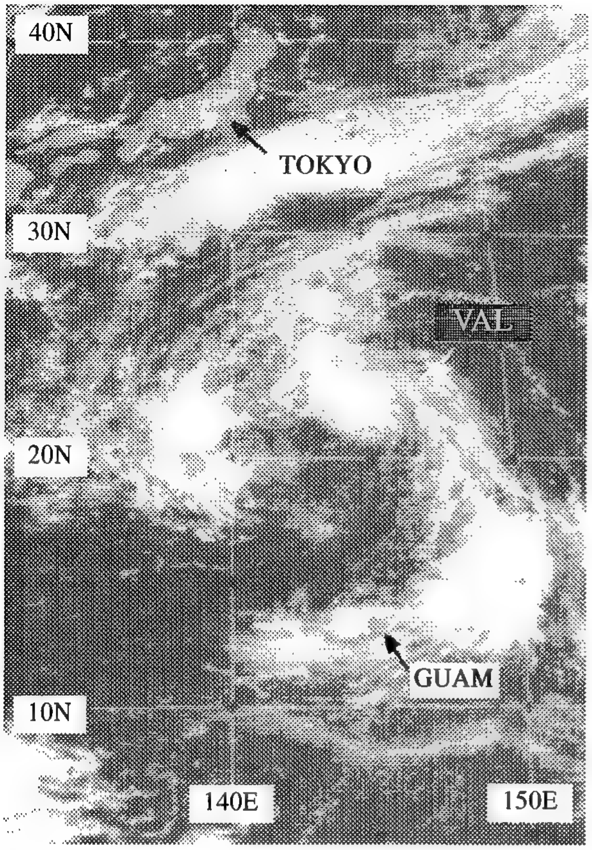

Figure 3-25-2 The CDO of Val is located to the northeast of the center of the monsoon gyre (100131Z October visible GMS imagery).

At 100000Z October, Tropical Depression 25W was upgraded to a tropical storm based upon persistent central deep convection (Figure 3-25-2). Remarks on this warning included:

"... Tropical Depression 25W has been upgraded to Tropical Storm Val . . . Latest Satellite imagery indicates that Val is orbiting around a larger monsoon gyre. Our forecast is for these two systems to merge in the next 24 to 36 hours then move off to the west-northwest. . . ."

By 11 October, Val had orbited from the eastern side of the gyre to its northern side (Figure 3-25-3). While located north of the center of the monsoon gyre, Val stalled and began to undergo vertical shearing from the west. On the morning of 12 October, visible satellite imagery (Figure 3-25-4) indicated that the low-level circulation center of Val was sheared to the west of the deep convection. Earlier during the previous night, the low-level circulation center was thought to have moved to the northeast under the deep convection, leading to a nearly 120 nm (225 km) relocation in the morning (a perfect example of the phenomenon known as the "sunrise surprise"). These diagnostic problems led to some very large forecast track errors (see discussion).

Eventually, all of the deep convection was sheared away, and Val merged with the monsoon gyre; the merged vortex drifted to the west-southwest and slowly dissipated. The final warning valid at 140000Z was issued when all deep convection was lost and only a low-level circulation center remained.

III. DISCUSSION

a. *Tropical cyclone interaction with a monsoon gyre*

A monsoon gyre is one of several patterns of the summer monsoon flow of the western North Pacific. As a monsoon gyre, the low-level circulation of the western North Pacific becomes organized as a large cyclonic vortex associated with a nearly circular 2500-km-wide depression in the contours of the sea-level pressure (e.g., see Figure 3-25-3). Typically, a cyclonically curved band of deep convection rims the southern through eastern periphery of this large vortex — in the case of the October 1995 monsoon gyre, the deep convection wrapped all the way around to the northwestern side of the gyre (see Figure 3-25-2). Also typical of a monsoon gyre is the formation of small or very small tropical cyclones in the peripheral cloud band of the gyre. Historically, most tropical cyclones that interact with a monsoon gyre undergo one of three possible fates (Figure 3-25-5): (1) the tropical cyclone orbits the gyre within the northeast quadrant of the gyre, and then escapes the influence of the gyre and recurves, (2) the tropical cyclone merges with the gyre and the two become one large circulation, and (3) the tropical cyclone, upon reaching the northern side of the gyre continues to move westward, or west-southwestward, in tandem with the gyre or between the gyre and an anticyclone to its northwest. In Val's case, it appeared that upon reaching the north side of the monsoon gyre, that it came very close to recurving. Instead, it

stalled for two days, its convection was sheared away, and the remnant vortex merged with the gyre and then moved to the west-southwest and dissipated near the Philippines.

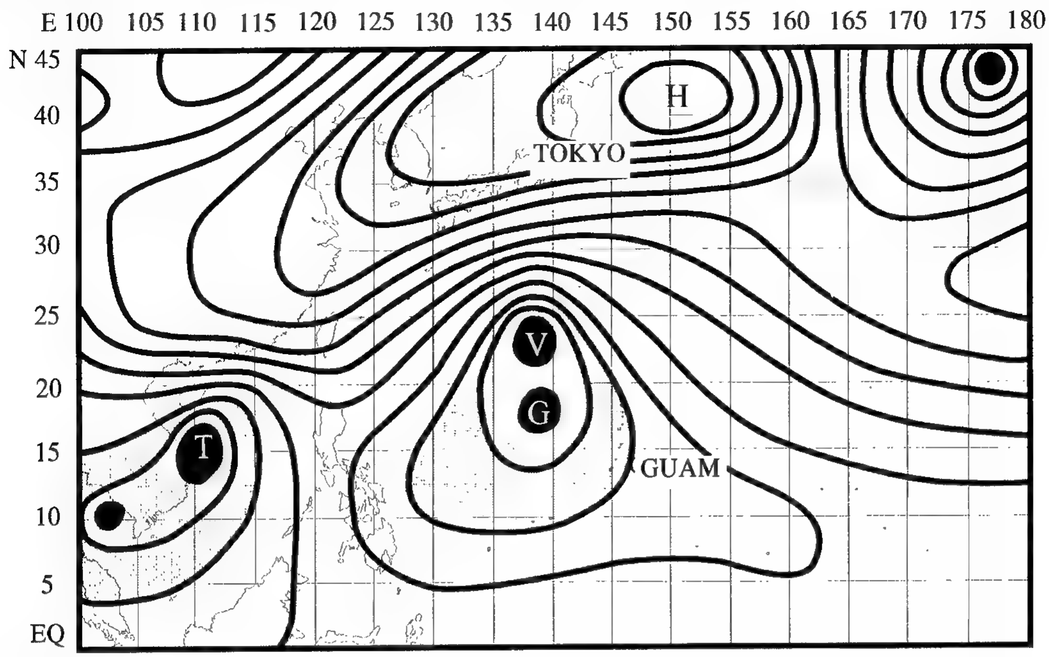

Figure 3-25-3 Contours of sea-level pressure (SLP) (at 2 mb intervals) at 110000Z October showing Val (V) located to the north of the center of the monsoon gyre (G). Another tropical cyclone — Ted (T) — is located in the South China Sea. Shaded region shows area where SLP is 1010 mb or lower; regions of SLP of 1006 mb or lower are black.

b. *Large track errors*

Val had large 48- and 72-hour track forecast errors (Figure 3-25-6). The four forecasts made between 110600Z and 120000Z each exceeded 1000 nm (1850 km) at 72 hours — the largest of these errors was 1386 nm (2550 km). The four forecasts made between 100600Z and 110000Z each exceeded 600 nm (1125 km) at 72 hours as a result of assuming that Val would continue to move steadily westward after rounding the northern side of the monsoon gyre. The largest of all the track forecast errors — those that occurred between 110600Z and 120000Z — resulted from an incorrect anticipation that Val would recurve.

Diagnostic errors during the night hours of 11 October contributed to the erroneous forecasts for Val to recurve. During the night hours of 11 October, the deep convection associated with the low-level circulation center of Val appeared to be moving northward. The satellite fix positions incorrectly followed the convection northward, while in reality, the deep convection was being sheared away from the low-level circulation center. By the first light of the morning of 12 October, the extent of the diagnostic errors became known. Based upon visible satellite imagery (Figure 3-25-4), the low-level circulation center of Val was repositioned approximately 120 nm to the west-southwest of the night infrared position estimate. Also contributing to the nighttime choice of recurvature were some dynamic model indications that Val would recurve.

In retrospect, it is possible that an SSM/I image of Val at 1110005Z October (Figure 3-25-7) could have been used to diagnose the sheared condition of Val, and that this information could have been used by the JTWC to reconsider its forecasts of recurvature before the morning visible satellite imagery revealed the diagnostic error.

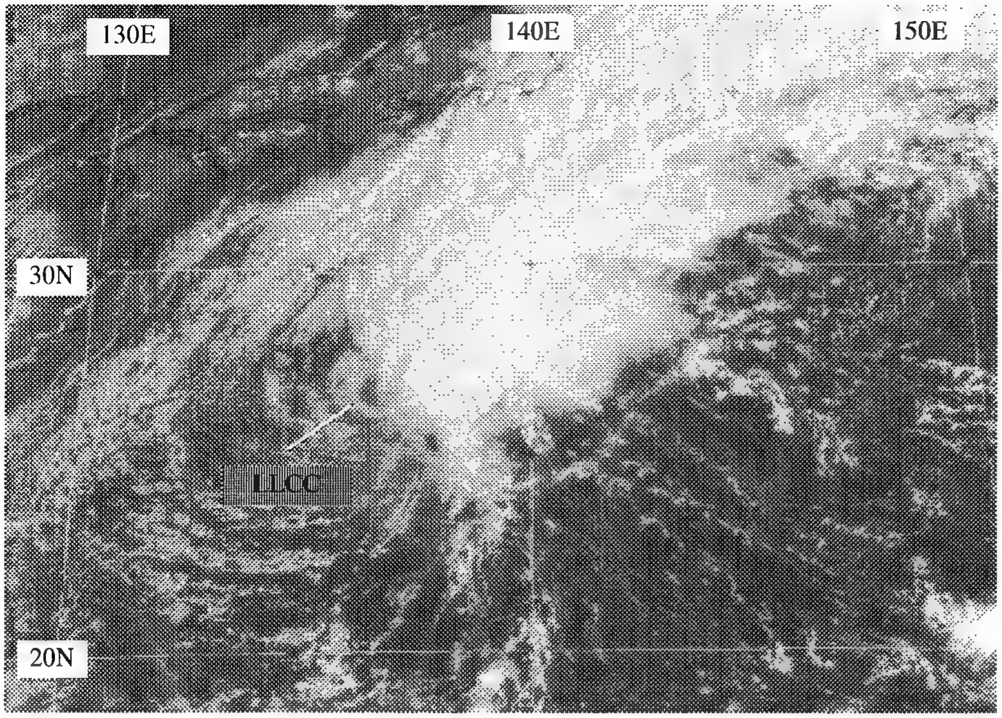

Figure 3-25-4 Val's low-level circulation center (marked LLCC) is located to the west of the deep convection (112224Z October visible GMS imagery).

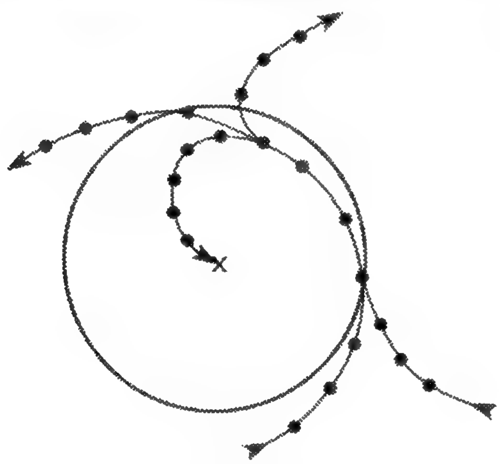

Figure 3-25-5 A schematic illustration of the typical interactions between a tropical cyclone and a monsoon gyre. The circle represents the outermost closed isobar of the monsoon gyre. Possible cyclone tracks are shown with respect to the center of the monsoon gyre.

IV. IMPACT

No reports of damage or injuries were received at the JTWC.

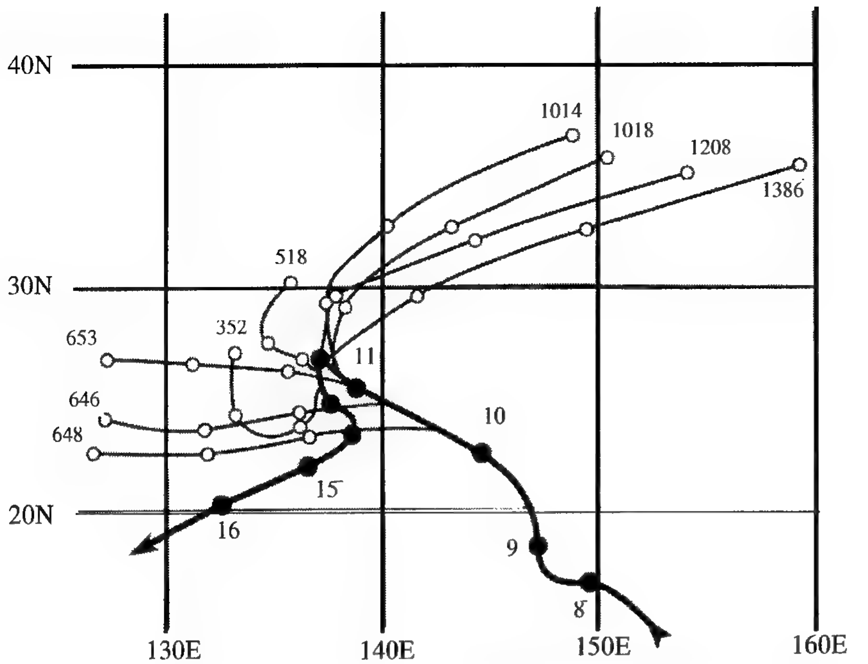

Figure 3-25-6 A schematic illustration of some selected track forecasts made by the JTWC for Val. The track of Val is indicated by the thick black line with black dots indicating the 0000Z positions of the indicated day. Small open circles connected by thin lines are selected JTWC track forecasts. Each track forecast has three open circles indicating the 24-, 48- and 72-hour forecast positions. The small numbers at the 72-hour forecast positions indicate the error associated with that forecast position (units are nm).

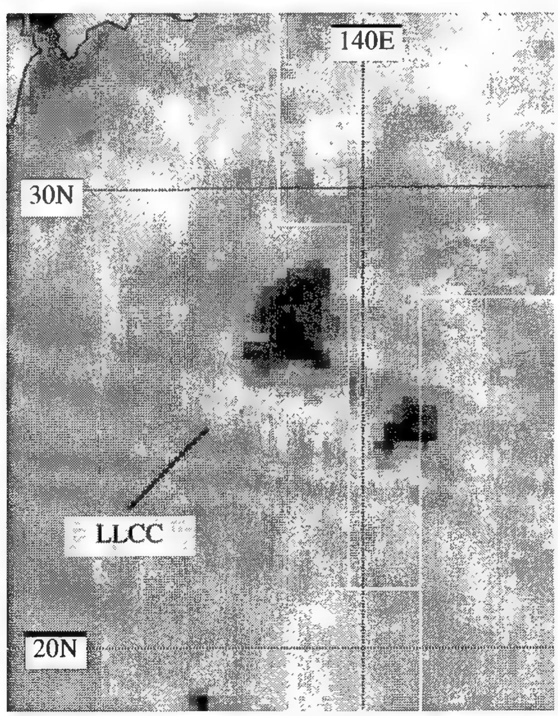

Figure 3-25-7 An 85 GHz (horizontally polarized) microwave image of Val showing that the deep convection is sheared to the northeast of the low-level circulation center (111005Z October SSM/I DMSP imagery).

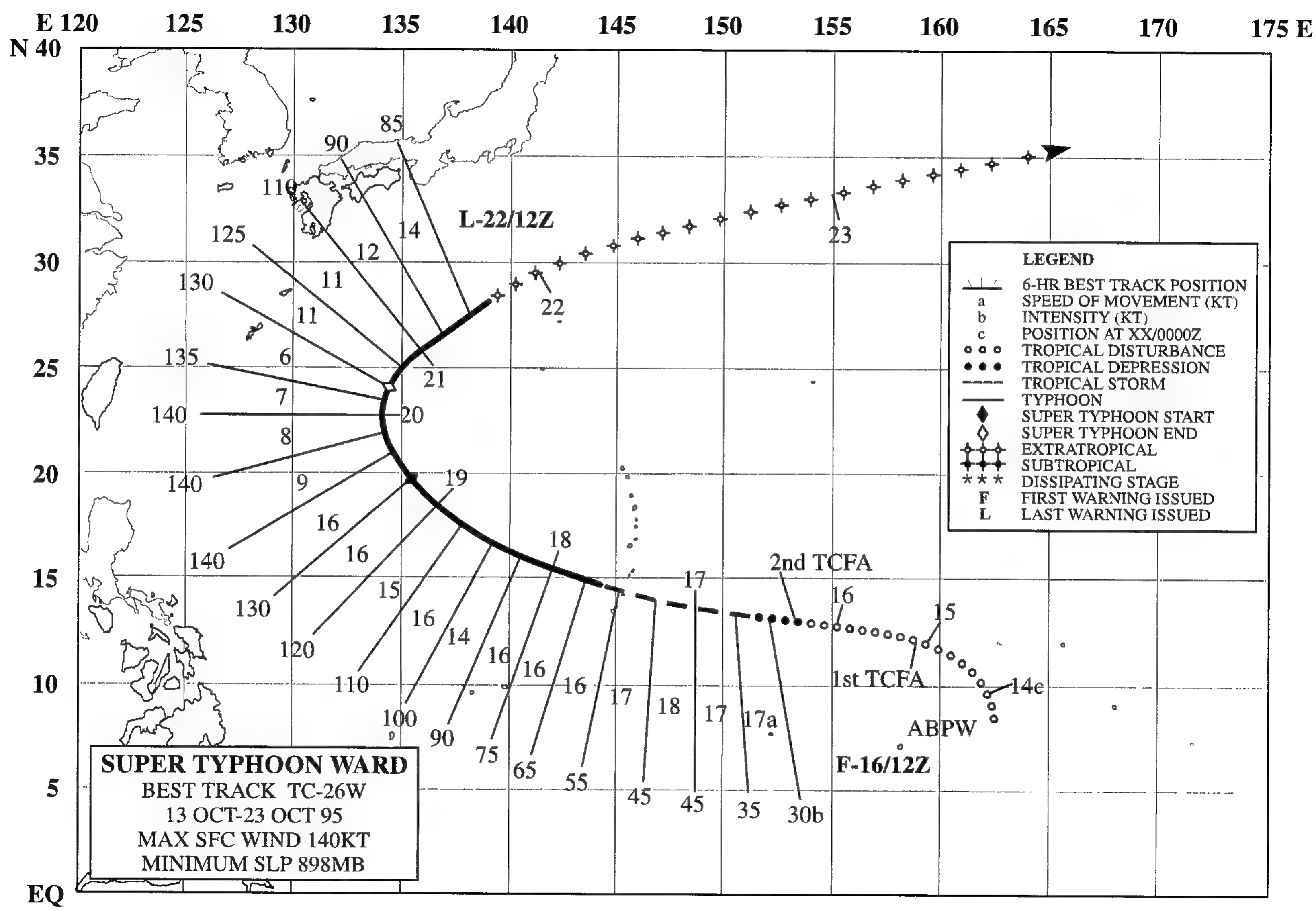

E 120
125
130
135
140
145
150
155
160
165
170
175 E
N 40
35
30
25
20
15
10
5
EQ
LEGEND
6-HR BEST TRACK POSITION
a SPEED OF MOVEMENT (KT)
b INTENSITY (KT)
c POSITION AT XX/0000Z
TROPICAL DISTURBANCE
TROPICAL DEPRESSION
TROPICAL STORM
TYPHOON
SUPER TYPHOON START
SUPER TYPHOON END
EXTRATROPICAL
SUBTROPICAL
DISSIPATING STAGE
F FIRST WARNING ISSUED
L LAST WARNING ISSUED
L-22/12Z
F-16/12Z
2nd TCFA
1st TCFA
ABPW
14e
30b
17a
SUPER TYPHOON WARD
BEST TRACK TC-26W
13 OCT-23 OCT 95
MAX SFC WIND 140KT
MINIMUM SLP 898MB

SUPER TYPHOON WARD (26W)

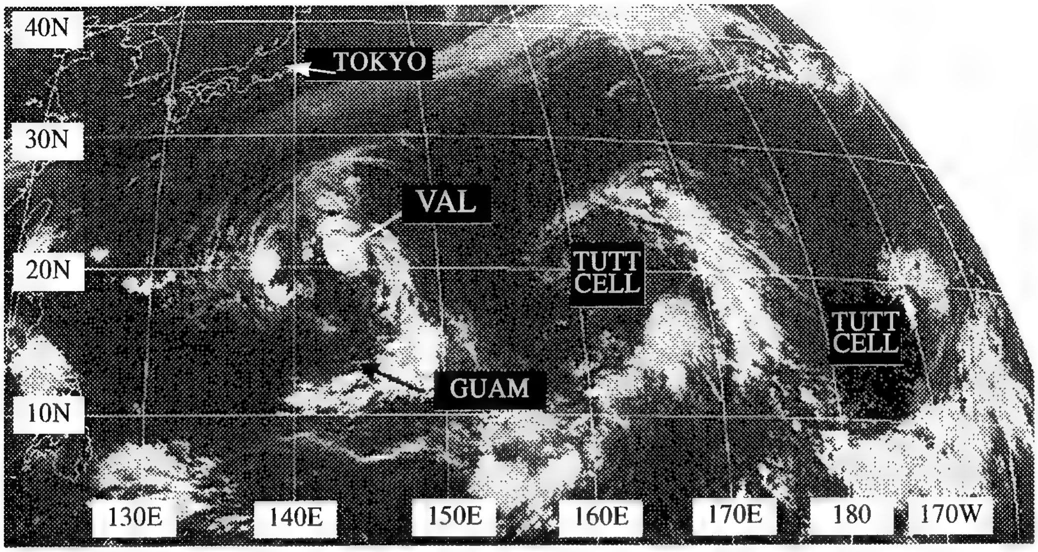

Figure 3-26-1 A chain of three atmospheric vortices with similar satellite signatures is spread across the tropics of the western Pacific: a monsoon gyre with an embedded tropical cyclone — Val (25W), and two TUTT cells centered at the indicated locations (100033Z October infrared GMS imagery).

I. HIGHLIGHTS

The fourth of five super typhoons during 1995, Ward formed as a small tropical cyclone east of Guam. Guam's NEXRAD provided a detailed look at the structure of this small tropical cyclone as it was intensifying and passing through the southern Mariana Islands. Ward's first visible eye was very small; it was later replaced by an average sized eye.

II. TRACK AND INTENSITY

The tropical disturbance that became Ward had it origins in the Marshall Islands where a nearly stationary area of deep convection associated with a chain of TUTT cells was present as early as 10 October (Figure 3-26-1). This area of convection remained poorly organized for the next few days, and was comprised of mesoscale convective systems that grew and decayed. On 14 October, this area of deep convection — located to the south of a well-defined TUTT cell — became more organized (e.g., a cyclonically curved band composed of mesoscale convective systems and anticyclonically curved streamers of outflow cirrus), prompting its first mention on the 131800Z October Significant Tropical Weather Advisory.

While moving westward in tandem with the TUTT cell to its north, the deep convection in this tropical disturbance began to consolidate around a well defined low-level circulation center. This prompted the JTWC to issue a Tropical Cyclone Formation Alert (TCFA) at 150130Z October. At 152330Z, the TCFA was canceled when amounts of deep convection near the center diminished. A second TCFA was issued soon thereafter at 160830Z when persistent deep convection once again consolidated near the low-level circulation center. The JTWC issued the first warning on Tropical Depression 26W valid at 161200Z when it became apparent in satellite imagery that the system was rapidly becoming better

organized. By the morning of 17 October, satellite imagery indicated a significant improvement in the organization of TD 26W, and it was upgraded to Tropical Storm Ward at 170000Z. Moving rather quickly at 17 kt (32 km/hr) toward the west, Ward passed between the islands of Rota and Saipan, or about 70 nm (130 km) to the north of Guam, during the night of 17 October. At 171800Z, Ward was upgraded to a typhoon based upon a maximum inbound velocity of 81 kt (42 m/sec) at 7,000 ft above sea level as depicted by Guam's NEXRAD, and also as corroborated by satellite intensity estimates.

After becoming a typhoon, Ward began to track on a more northwestward direction. Moving towards a "break" (i.e., a col) along the axis of the mid-tropospheric subtropical ridge axis, Ward slowed, turned toward the north and reached its point of recurvature at 200000Z. While approaching its point of recurvature, Ward also intensified, and attained its peak intensity of 140 kt (72 m/sec) at 191200Z (Figure 3-26-2). After passing through the ridge axis, Ward turned sharply toward the northeast, accelerated, and

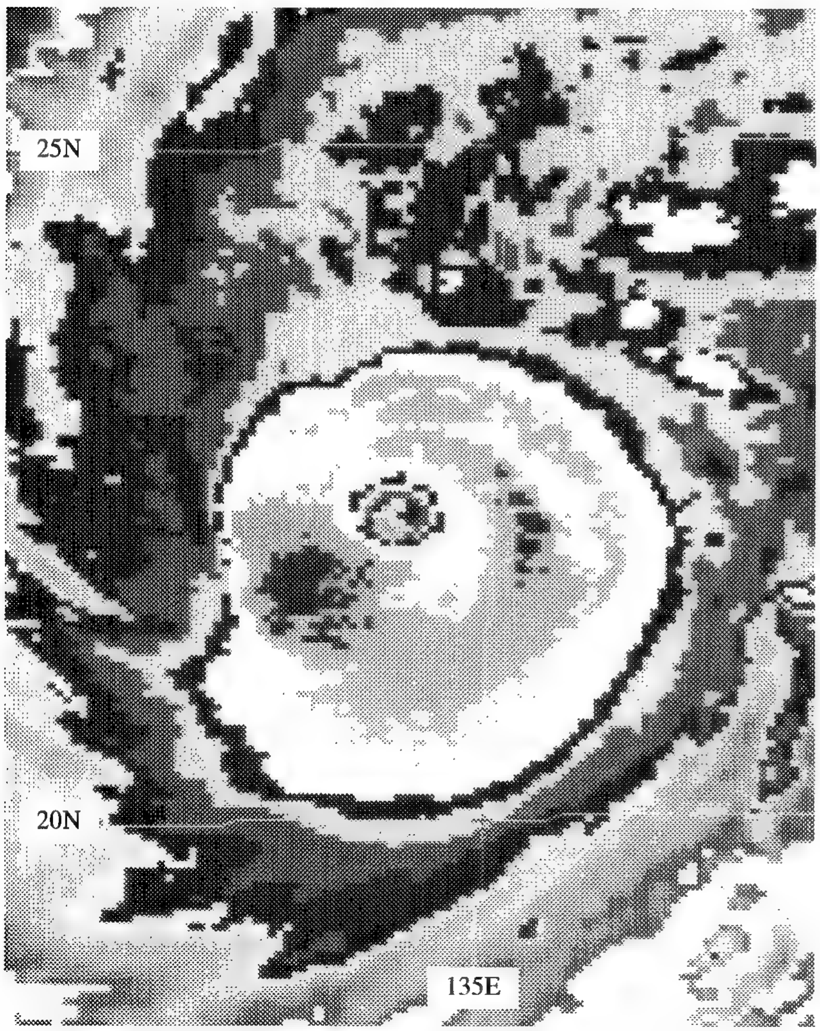

Figure 3-26-2 Ward at peak intensity of 140 kt (72 m/sec) (191931Z October enhanced infrared GMS imagery).

began to weaken as the vertical wind shear in the westerly wind flow north of the subtropical ridge sheared the system. At 220600Z, Ward was downgraded to a tropical storm as the low-level circulation became fully exposed to the southwest of its extensive shield of multi-layered middle and high cloud — a typical appearance of a tropical cyclone undergoing extratropical transition (Figure 3-26-3). Based upon the expected completion of its extratropical transition, the final warning was issued at 221200Z.

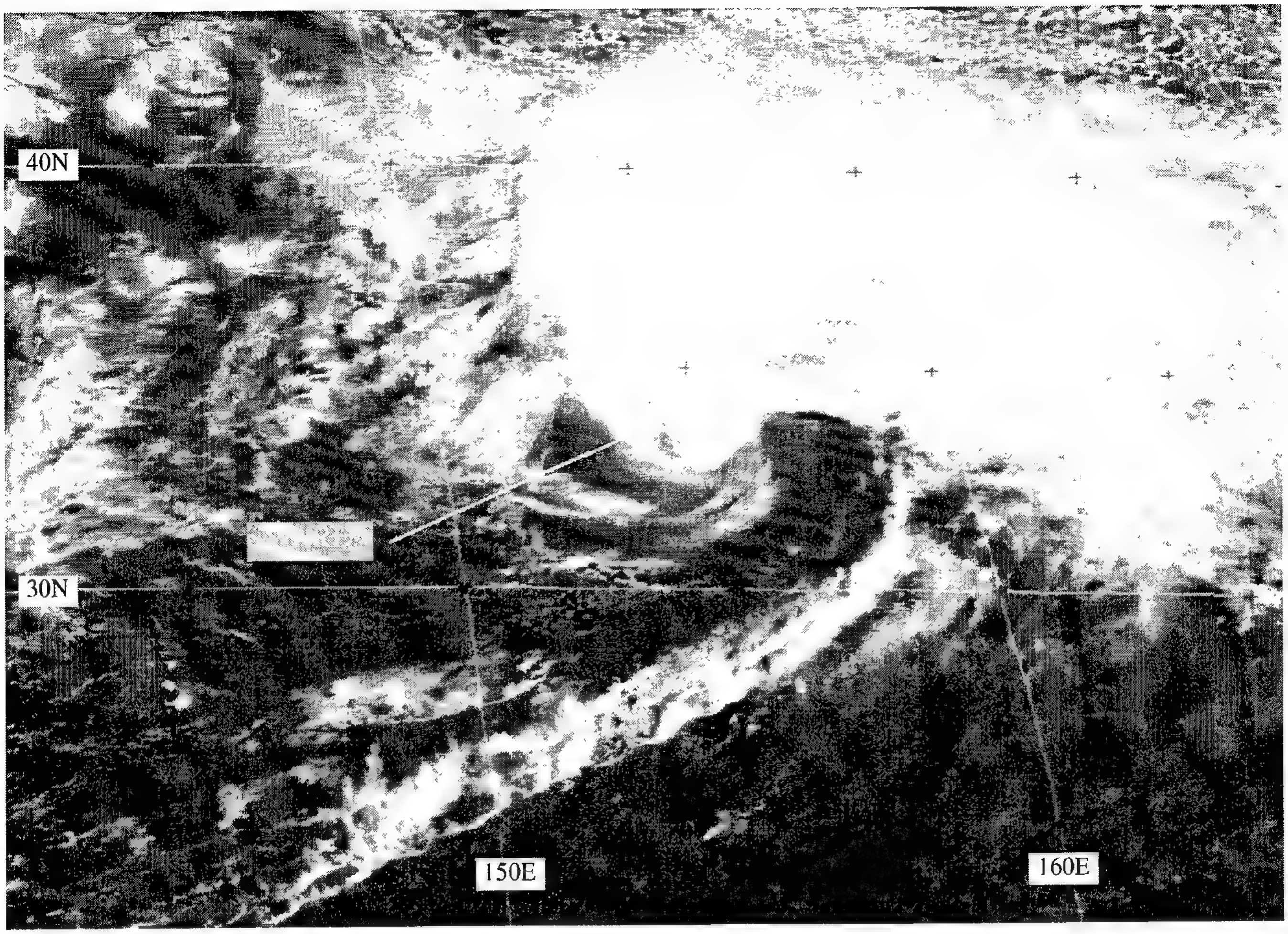

Figure 3-26-3 Ward's extratropical transition is nearly complete (222331Z October visible GMS imagery).

III. DISCUSSION

a. *A NEXRAD view of the early development of Ward*

During the night of 17 October, Ward passed between the islands of Rota and Saipan, or about 70 nm (130 km) to the north of Guam. This placed the small circulation of the intensifying Ward well within the range of Guam's NEXRAD. While within the 124-nm range of the NEXRAD Doppler capability, Ward moved toward the west-northwest at an average translational speed of 17 kt (32 km/hr) and intensified from 45 to 65 kt (23 to 33 m/sec). One aspect of Ward's structure that was well-depicted by the NEXRAD was the nature of the wind asymmetry. The wind asymmetry between the north side and the south side of Ward appeared to be primarily a result of Ward's translation speed. The effect of the translation was almost fully represented. At a translation speed of 17 kt, one would expect the difference in the wind speed between the north side and the south side of Ward to be twice the speed of translation, or approximately 35 kt. As Ward came within the Doppler range, about 120 nm (220 km) to the east-northeast of Guam, a maximum inbound wind of 50 kt (26 m/sec) was present on the north side at the lowest beam altitude of 16,000 ft. On the south side of Ward, the maximum outbound wind was 17 kt (9 m/sec) (also at 16,000 ft). The differential between the inbound and outbound wind was thus 33 kt, or very nearly what would be expected from a full accounting of the speed of translation. Later, as Ward moved due north of the NEXRAD (and thereby placing the asymmetry introduced by the speed of

translation perpendicular to the radar), the inbound and outbound velocities became nearly equal at about 65 kt each way, and both at the lowest beam elevation of 7,000 ft.

This brings us to another structural characteristic of Ward's wind field as revealed by the NEXRAD: the maximum wind speed, whether inbound or outbound, always occurred at the lowest possible beam elevation. In this case, the lowest altitude of beam penetration was 7,000 ft when Ward was at its closest point of approach. That the highest winds in a TC should be at a low level is not a surprising finding, however, in some other TCs that have come even closer to Guam (e.g., Eli (04W) and Verne (1994)), the maximum winds near the center have been observed to occur at elevations as low as 2,000 feet; and again nearly always at the lowest possible viewing altitude of the NEXRAD. Such findings bring into question the conventional tactic of reducing aircraft reconnaissance flight-level wind speed (usually near 10,000 ft) by 80% to estimate the surface wind speed.

Ward was a small-sized tropical cyclone as it passed to the north of Guam. When due north of Guam, the distance between the maximum inbound and outbound winds was only 12 nm (22 km) at 7,000 ft. The diameter of gale-force winds was approximately 40 nm (75 km) at 7,000 ft. The speed of the westerly winds on Guam when Ward passed only 70 nm (130 km) to the north was only 10 kt (5 m/sec). The subsequent growth in size and the large increase of the intensity of this small vortex was a remarkable structural change.

Some additional general structural characteristics of tropical cyclones passing within the range of Guam's NEXRAD are: (1) the maximum wind speed is found at the lowest beam elevation in the most highly reflective and deepest convection, (2) over time scales on the order of tens of minutes, the wind speeds rise and fall as deep convective elements grow and decay, and (3) when deep convection grows in the eye wall, wind speeds increase throughout the depth of the troposphere and become more nearly constant with height (i.e., the deep convection appears to be accelerating the wind velocity, and also to be transporting the momentum to higher altitudes).

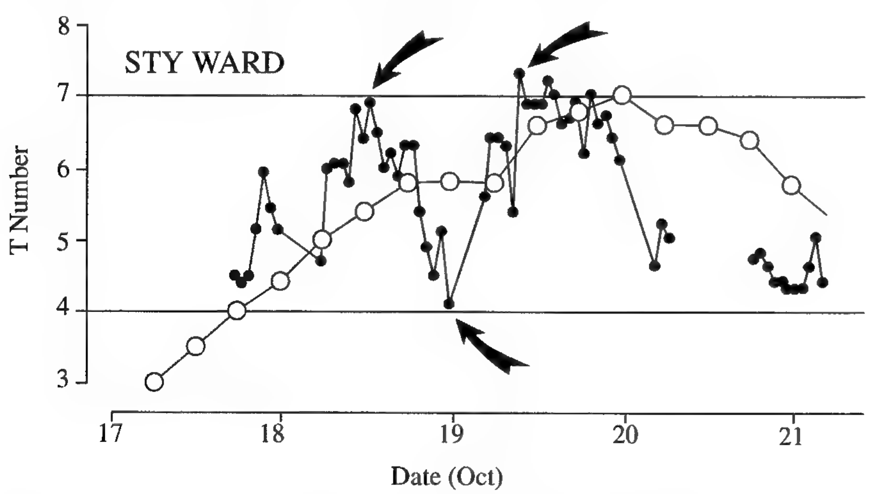

Figure 3-26-4 A time series of Ward's hourly "Digital" Dvorak (DD) intensity estimates (black dots). Also shown is the warning intensity (converted to a T number) (open circles). Arrows indicate two peaks and an intervening minimum in the DD time series.

b. *Evidence of two intensity peaks related to eye structure*

Ward was another of the year's tropical cyclones for which hourly values of the Digital Dvorak (DD) numbers (Figure 3-26-4) were tabulated during much of its life (see Oscar's (17W) summary for a description of the DD algorithm installed on the JTWC's MIDDAS satellite image processing equipment). The time series of Ward's DD (Figure 3-26-4) indicates two peaks of intensity near T 7.0 (equivalent to 140 kt): one near 181200Z and the other 24 hours later at 191200Z. Between these two peaks, the DD indicated that the intensity fell as low as T 4.0 (minimal typhoon intensity) at about 190000Z.

These two intensity peaks are closely related to the evolution of Ward's eye. After first becoming a typhoon, Ward's eye was extremely small (as seen by NEXRAD and later as it appeared on visible satellite imagery). After attaining its first intensity peak at 181200Z with a very small eye (Figure 3-26-5), the eye clouded over (resulting in lower intensity estimates) and then reappeared at a larger size when it attained its second peak intensity at 191200Z (Figure 3-26-2).

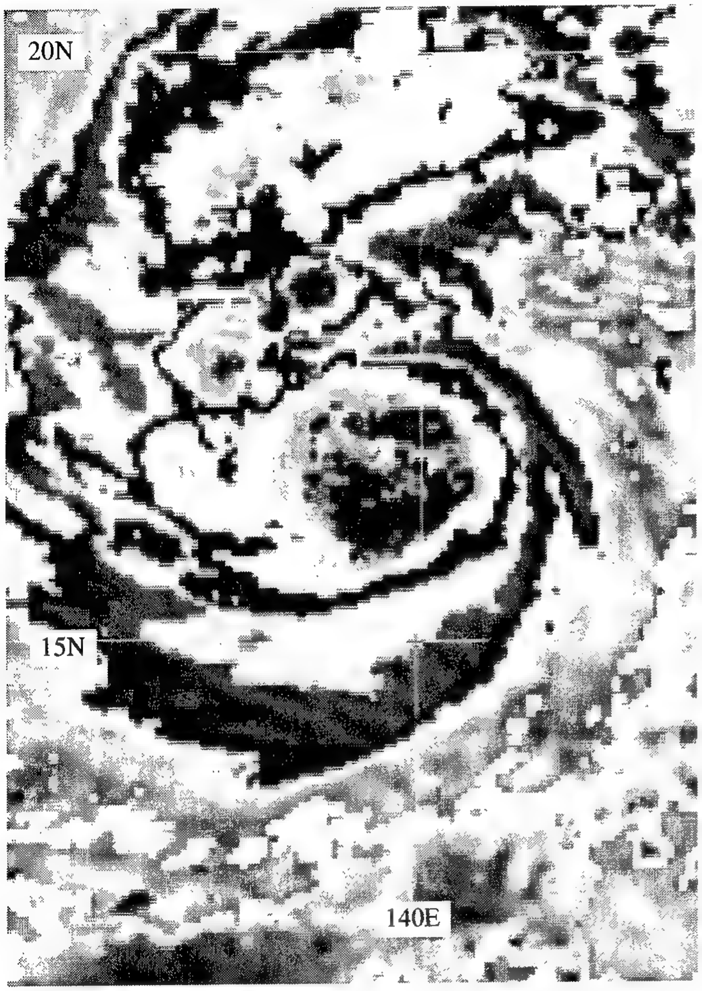

Figure 3-26-5 Ward possesses a very small eye at the time of the first peak on the DD time series (181031Z October enhanced infrared GMS imagery).

Similar to the case with Ryan (19W), the warning intensity and the final best-track intensity do not reflect the first peak of the DD (i.e., DD = 140 kt; final best-track = 100 kt). As the DD rose to its second peak, the warning and final best-track intensity rose to match it (i.e., DD = 140 kt; final best-track intensity = 140 kt). Once again, the DD has revealed extremely large and rapid fluctuations of intensity that were not reflected in the warning intensity or the final best-track intensity. In the absence of ground truth measurements, it is not possible to know in fine detail how Ward's intensity changed. In the case of Ward, there is a clear reason for the rapid changes in the DD intensity: the changes in Ward's eye characteristics. If the DD truly represented Ward's intensity, there are two sobering implications: (1) an extremely rapid increase of intensity occurred that was not reflected in the warning, and (2) the best-track data base, having had these rapid fluctuations removed, can not be used to study the processes governing what may prove to be real intensity fluctuations of the magnitude indicated by the DD.

IV. IMPACT

As Ward passed through the Mariana Islands it affected the islands of Rota, Tinian and Saipan. Heavy rain caused minor flooding on several Saipan streets. On Tinian, gusty winds and heavy rains caused a loss of electrical power to half of the island.

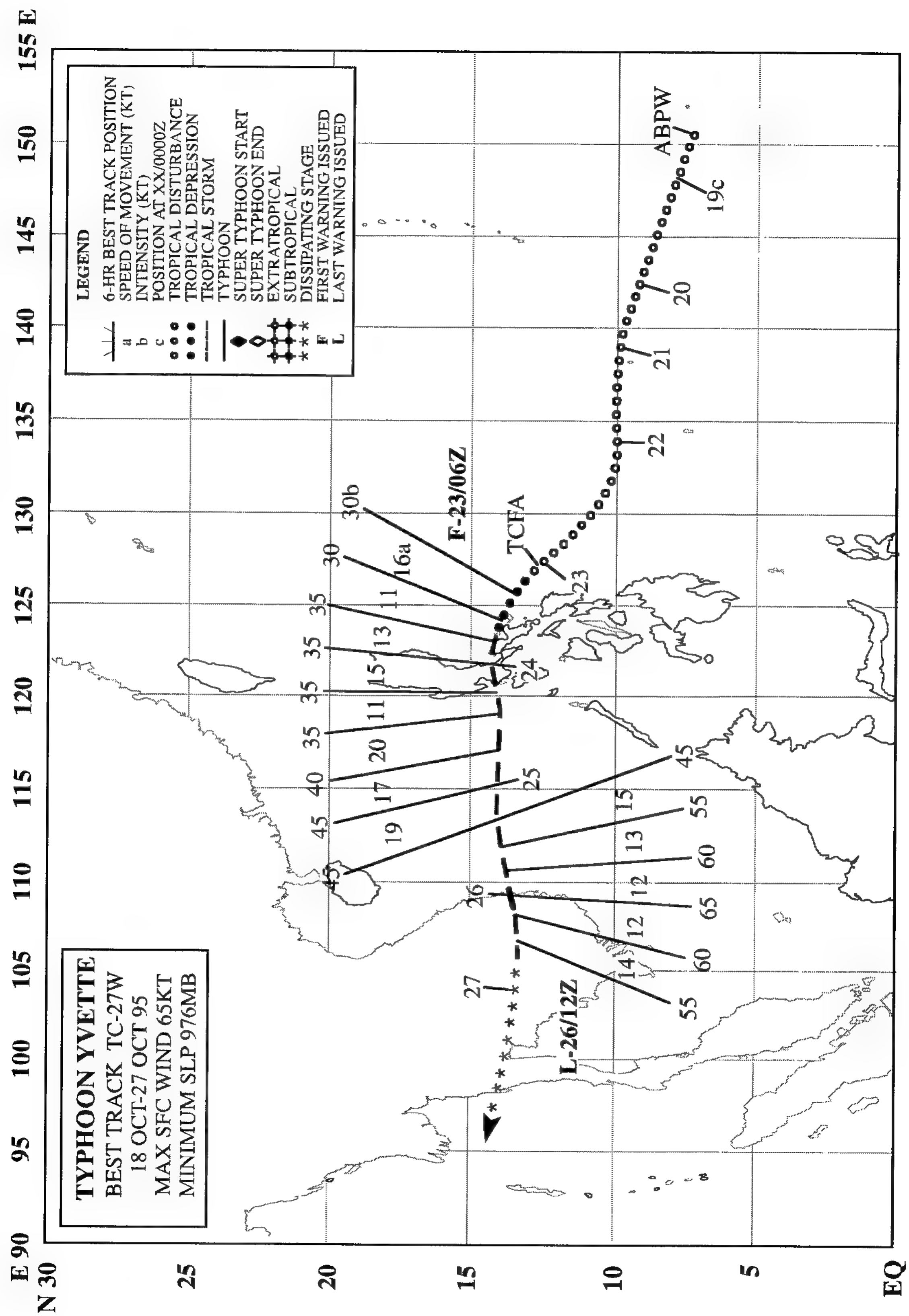

TYPHOON YVETTE
BEST TRACK TC-27W
18 OCT-27 OCT 95
MAX SFC WIND 65KT
MINIMUM SLP 976MB
LEGEND
6-HR BEST TRACK POSITION
SPEED OF MOVEMENT (KT)
INTENSITY (KT)
POSITION AT XX/0000Z
TROPICAL DISTURBANCE
TROPICAL DEPRESSION
TROPICAL STORM
TYPHOON
SUPER TYPHOON START
SUPER TYPHOON END
EXTRATROPICAL
SUBTROPICAL
DISSIPATING STAGE
FIRST WARNING ISSUED
LAST WARNING ISSUED
ABPW
TCFA
F-23/06Z
L-26/12Z

TYPHOON YVETTE (27W)

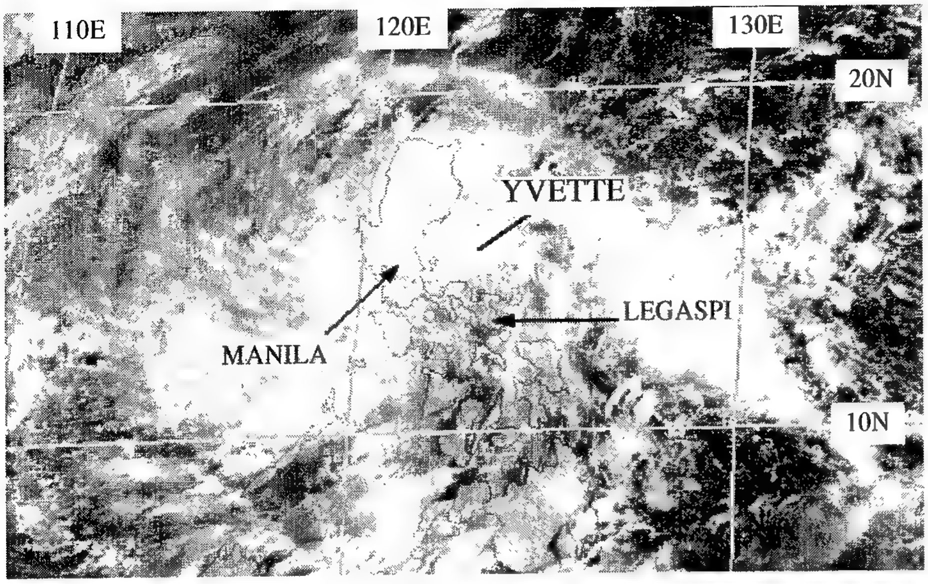

Figure 3-27-1 As the low-level circulation center of Yvette makes landfall on Luzon, bands of deep convection extend well to the east and west, giving Yvette an elongated appearance (232331Z October visible GMS imagery).

I. HIGHLIGHTS

Yvette was one of seven tropical cyclones during 1995 that passed over the Philippines with an intensity of 35 kt (18 m/sec) or greater. Like many other tropical cyclones during 1995, Yvette did not develop significantly until it had tracked westward to near the Philippines. While in the Philippine Sea, Yvette was difficult to track by satellite due to its poor organization.

II. TRACK AND INTENSITY

As Typhoon Ward was beginning its recurvature south of Japan, the tropical disturbance that became Yvette originated west of Chuuk in a weak near-equatorial trough. This disturbance was first mentioned on the 180900Z October Significant Tropical Weather Advisory when an area of deep convection had persisted for 12 hours in association with a weak low-level cyclonic circulation near Chuuk. For over three days, the disturbance moved westward without intensifying. On 23 October, as the disturbance approached the Philippines, satellite imagery indicated that the system had become better organized, and that northeasterly shear on the system was weakening. This prompted the JTWC to issue a Tropical Cyclone Formation Alert, valid at 230100Z. Rapid improvement in the organization of the system was subsequently noted in visible satellite imagery, and the JTWC issued the first warning on Tropical Depression 27W, valid at 230600Z. As Tropical Depression 27W was passing just north of Daet (located on southeastern Luzon), it appeared to be forming a CDO, and was upgraded to Tropical Storm Yvette on the warning valid at 231800Z. However, as Yvette began to cross Luzon, its development was arrested; its cloud bands became elongated in an east-west direction (Figure 3-27-1), and its intensity held steady at 35 kt (18 m/sec) until it entered the South China Sea. Moving westward over the South China Sea, Yvette began to slowly intensify, and reached typhoon intensity (Figure 3-27-2) just before making landfall along the coast of Vietnam at 260000Z. After making landfall, Yvette weakened over the mountains of Vietnam, and dissipated over Kampuchea. The final warning, valid at 261200Z, was issued as the weakening Yvette moved into Kampuchea.

III. DISCUSSION

Large positioning errors and poor guidance

Yvette was often difficult to track with satellite imagery. Average fix errors were 59 nm (109 km) as compared with the 1995 average of 29 nm (54 km). This, and the poor performance of the dynamic model guidance, led to larger than average track forecast errors. CLIPER forecasts were extremely poor, partly due to the initial position errors, and partly due to the fact that climatology favors recurvature for tropical cyclones in the South China Sea during October.

IV. IMPACT

No reports of damage or injuries were received.

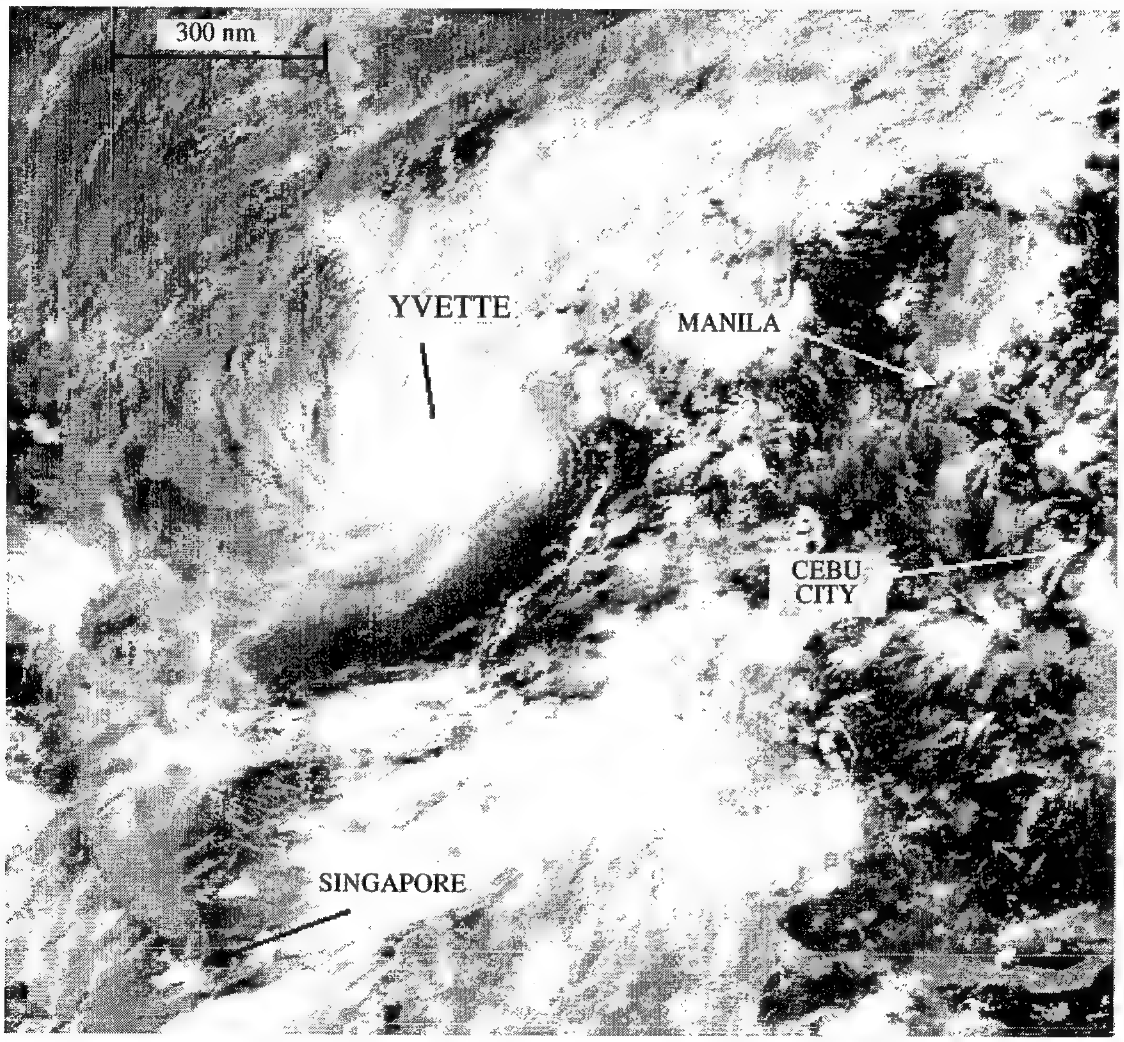

Figure 3-27-2 Yvette briefly attains typhoon intensity just as it makes landfall on the coast of Vietnam (260031Z October visible GMS imagery).

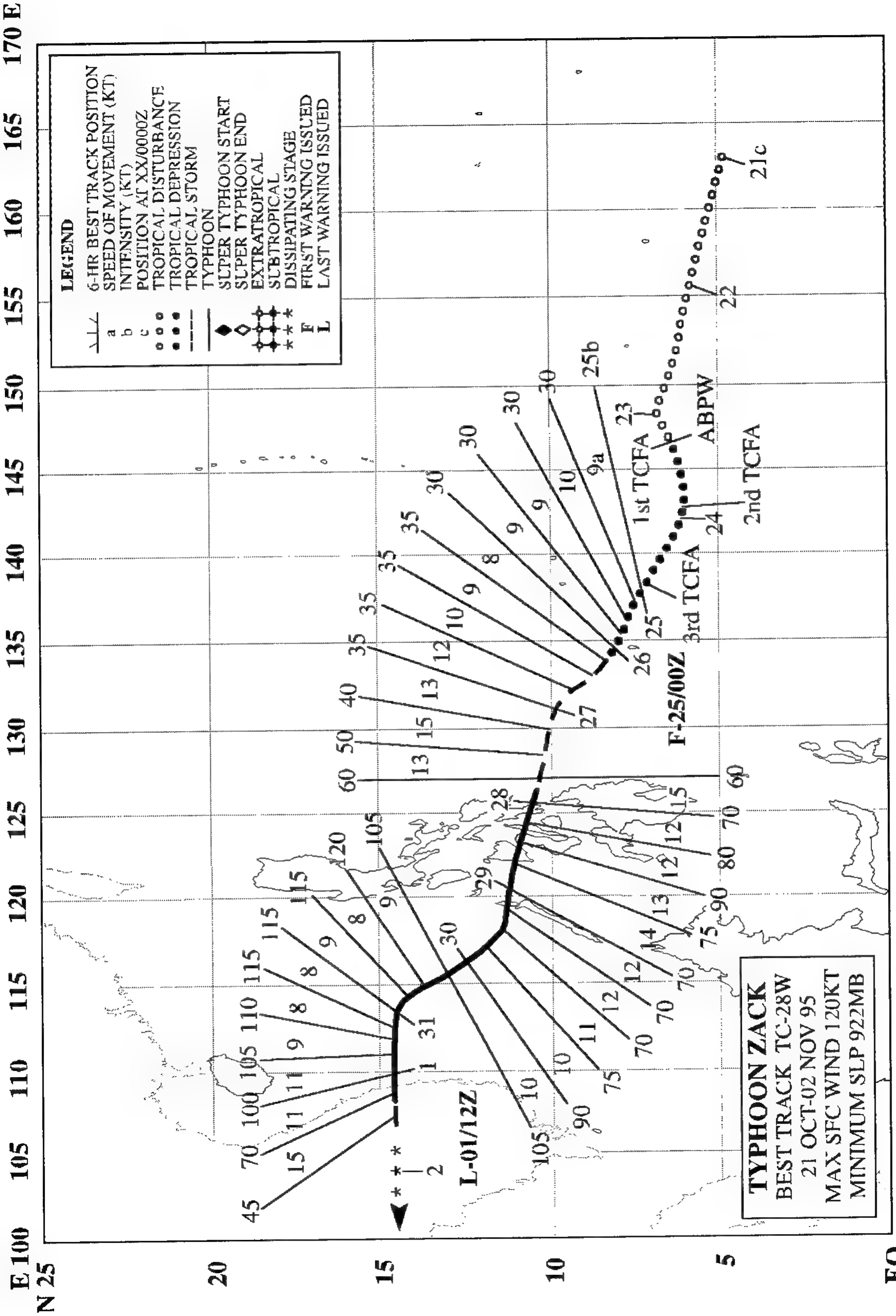
TYPHOON ZACK
BEST TRACK TC-28W
21 OCT-02 NOV 95
MAX SFC WIND 120KT
MINIMUM SLP 922MB
LEGEND
6-HR BEST TRACK POSITION
SPEED OF MOVEMENT (KT)
INTENSITY (KT)
POSITION AT XX/0000Z
TROPICAL DISTURBANCE
TROPICAL DEPRESSION
TROPICAL STORM
TYPHOON
SUPER TYPHOON START
SUPER TYPHOON END
EXTRATROPICAL
SUBTROPICAL
DISSIPATING STAGE
FIRST WARNING ISSUED
LAST WARNING ISSUED
F-25/00Z
L-01/12Z
1st TCFA
2nd TCFA
3rd TCFA
ABPW
E 100
170 E
N 25
EQ

TYPHOON ZACK (28W)

I. HIGHLIGHTS

Originating from a tropical disturbance in the eastern Caroline Islands, Zack did not significantly intensify for nearly six days. As was the case with Sibyl (20W), Zack intensified as it crossed the Visayan islands. But, unlike Sibyl (which weakened over the South China Sea after crossing the Philippines), Zack intensified significantly, peaking at 120 kt (62 m/sec). Zack became one of that region's most intense tropical cyclones (see Ryan's summary for a discussion of very intense tropical cyclones in the South China Sea). Typhoon Zack, along with Super Typhoon Angela (29W) and Tropical Storm Brian (30W), comprised one of only three occasions during 1995 that the JTWC was simultaneously warning on three tropical cyclones in the western North Pacific. Zack made landfall in Vietnam with 100 kt (51 m/sec) maximum sustained winds. It left a path of death and destruction in both the Philippines and Vietnam.

II. TRACK AND INTENSITY

The tropical disturbance that became Zack was first detected on 21 October along the axis of the near-equatorial trough near Kosrae, and was first mentioned on the 230600Z Significant Tropical Weather Advisory. This poorly defined tropical disturbance appeared to have multiple wind circulation centers creating a difficult diagnostic situation. The circulation that became Zack was properly identified at 221200Z when amounts of deep convection increased and became focused around a single low-level circulation center. The tropical disturbance that became Zack, like so many others in 1995, was slow to develop. This slow rate of development contributed to the issuance of three Tropical Cyclone Formation Alerts: the first at 230600Z October, the second at 232030Z, and the third at 242030Z. The latter was superseded when the JTWC issued the first warning on Tropical Depression 28W, valid at 250000Z. The system was upgraded to Tropical Storm Zack 30 hours later on the warning valid at 260600Z.

Zack was difficult to track during the early stages of its development. On 25 October, position estimates of Zack's (then Tropical Depression 28W) low-level circulation center made from satellite imagery (Figure 3-28-1) incorrectly indicated that Zack was moving on a northwest track, vice the west-northwest track of the actual system that is shown in the final best track. As a result, positioning errors were as large as 140 nm (260 km) with respect to the final best track. In retrospect, the Japanese research ship, Tokai Maru (call sign: JBOA), passed just to the west of the low-level circulation center at 250600Z where it recorded a minimum sea-level pressure of 1002 mb. It wasn't until the first visible satellite imagery on the morning of 26 October that the satellite fixes began to track the low-level circulation center that was consistent with synoptic data (e.g., the surface and upper-air data from Koror). Forecasts during the period were heavily weighted toward climatology, and the tropical cyclone was forecast to move toward the central Philippines.

On the afternoon of 27 October, Zack began to intensify at a rate of 10 kt (5 m/sec) every 6 hours as it approached the Visayan Islands of the Philippines. Based upon satellite intensity estimates, Zack was upgraded to a typhoon on the warning valid at 280000Z. At 280200Z, Zack struck Leyte with sustained winds of 70 kt (36 m/sec). The Island capital of Tacloban (WMO 98550) recorded a peak gust of 81 kt (42 m/sec) and the Guian radar site on the island of Samar (WMO 98558) recorded a 1-minute sustained wind of 62 kt (32 m/sec) and a peak gust of 68 kt (35 m/sec). Zack continued to intensify as it crossed the Visayan Islands, reaching a peak intensity of 90 kt (46 m/sec) before striking the large mountainous

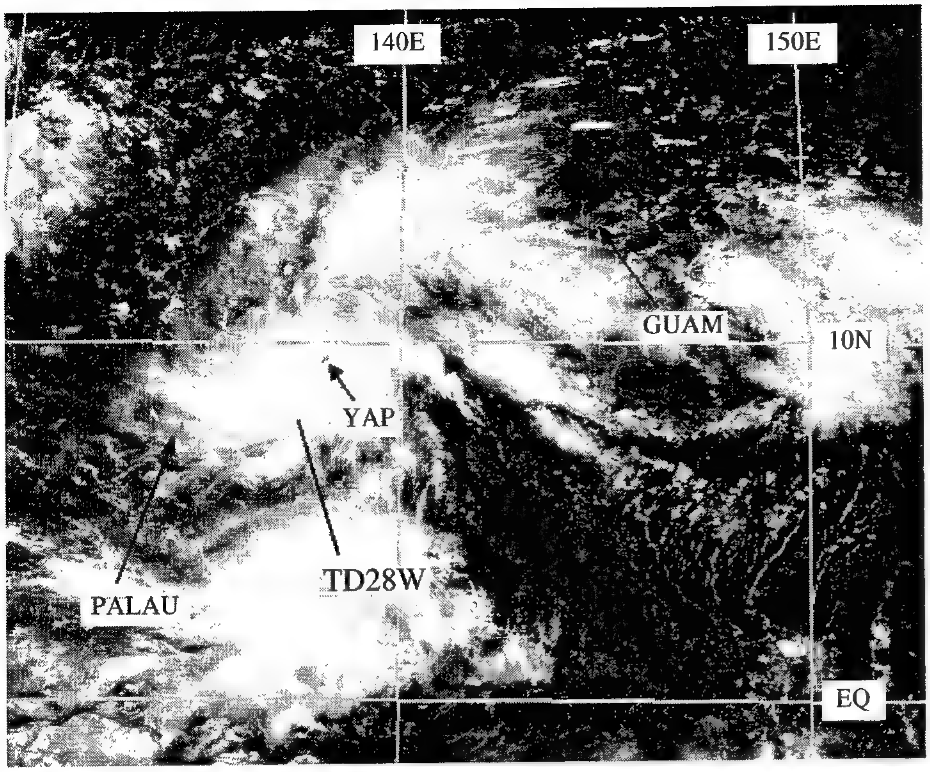

Figure 3-28-1 Tropical Depression 28W is located about 175 nm (325 km) east of Palau. The obvious knot of convection west of Yap was not co-located with the primary low-level circulation center. (250424Z October visible GMS imagery).

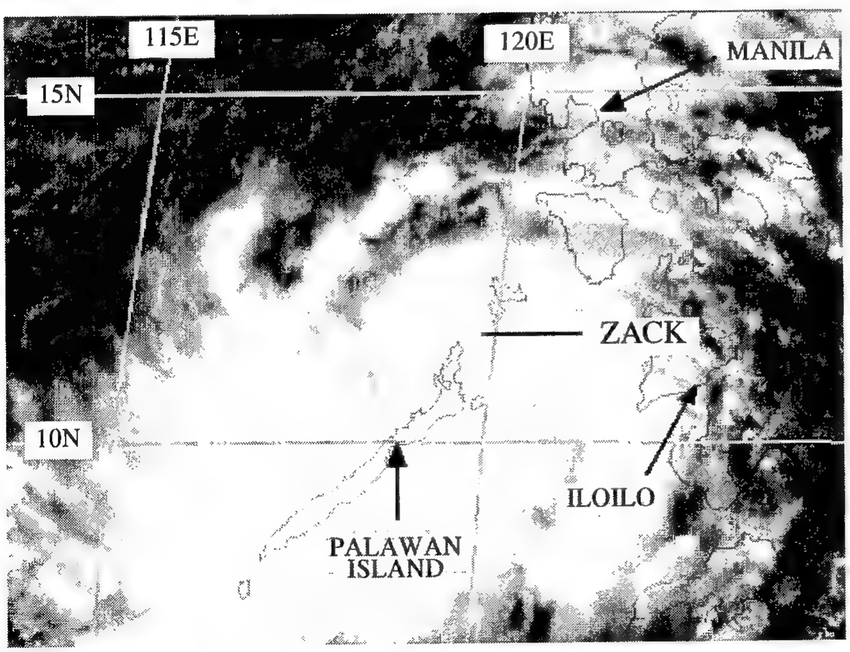

Figure 3-28-2 Typhoon Zack, at an intensity of 70 kt (36 m/sec) enters the South China Sea after passing by the northwest tip of Palawan Island (290531Z October visible GMS imagery).

island of Panay, after which the typhoon weakened (Figure 3-28-2). Both Cuyo Island (WMO 98630) and Iloilo (WMO 98637) measured sustained winds of 62 kt (32 m/sec) as Zack was crossing Panay. Possible mechanisms for intensification while crossing through an archipelago of high islands are outlined in the discussion section of Typhoon Sibyl's (20W) summary — Sibyl (20W) also intensified as it followed a path similar to Zack's through the central Philippines.

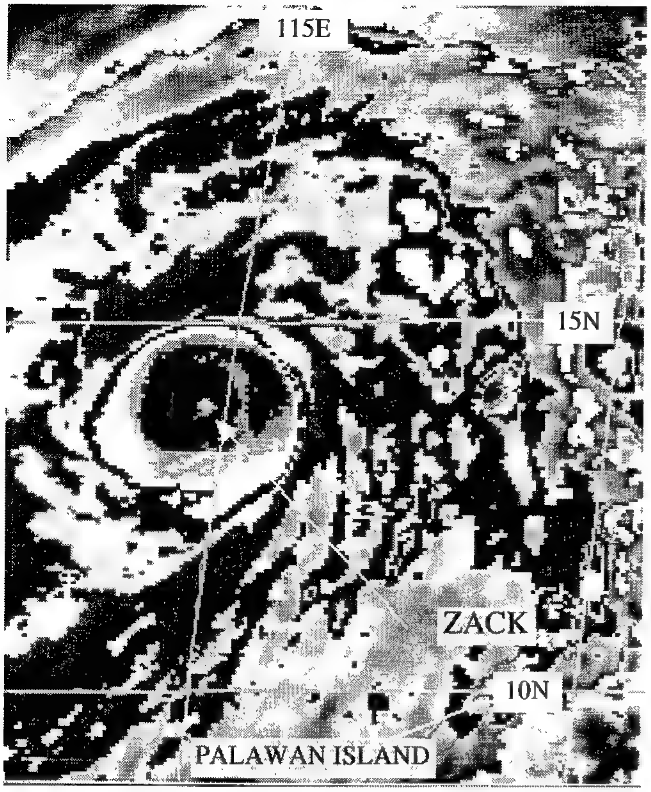

Figure 3-28-3 Typhoon Zack at peak intensity (301231Z October enhanced infrared GMS imagery).

After entering the South China Sea, Zack began to re-intensify. From 291800Z to 301200Z (a period of only 18 hours), Zack intensified 45 kt (23 m/sec) to its peak intensity of 120 kt (62 m/sec) (Figure 3-28-3). The associated rate of decrease of the estimated minimum sea-level pressure of 2.5 mb/hour meets the criterion for explosive deepening (see the discussion section). After peaking, Zack slowly weakened over water as it headed westward toward Vietnam. Zack made landfall in Vietnam at 010300Z November, about 70 nm (130 km) south of Da Nang. The final warning was issued, valid at 011200Z November, as the system entered the highlands of Laos. Complete dissipation occurred 18 hours later over Thailand.

III. DISCUSSION

a. *Intensification while passing over the central Philippines*

Zack, like Sibyl (20W), intensified while tracking across the central Philippines. For a discussion of the possible mechanisms for intensification while crossing through an archipelago of high islands, the reader is referred to the discussion section of Typhoon Sibyl's (20W) summary.

b. *Explosive deepening in the South China Sea*

Zack intensified 45 kt (23 m/sec) over an 18-hour span while over water in the South China Sea. This corresponds to a decrease of minimum sea-level pressure of 2.5 mb/hour which meets the criterion for explosive deepening as described by Dunnavan (1981). Zack reached a peak intensity of 120 kt (62 m/sec) at 301200Z (Figure 3-28-3). It is interesting to note that Zack appears to be totally isolated from its environment as the phase of explosive deepening began (Figure 3-28-4). In a study of the relationship between the cloud pattern and the intensification rate of tropical cyclones, Spratt (1990) found no significant differences in the average intensification rates of tropical cyclones whose cloud patterns resembled a "9", a "6", a two-tailed pattern (resembling the tropical cyclone symbol), or those (like Zack) that were circular.

IV. IMPACT

Zack caused considerable death, destruction, and agricultural losses in the Visayan Islands of the Philippines. Hardest hit of the Visayan Islands were Panay and Negros Occidental. There were over 110 deaths reported, of which 72 occurred in Negros Occidental, 18 in Cebu, and 20 in Iloilo. Flooded rivers and capsized boats claimed most of the victims. More than 30,000 homes were reported destroyed or damaged and preliminary estimates of agricultural losses amounted to US$2 million, primarily sugar cane. Bacolod, a city of 400,000, was without power for several days.

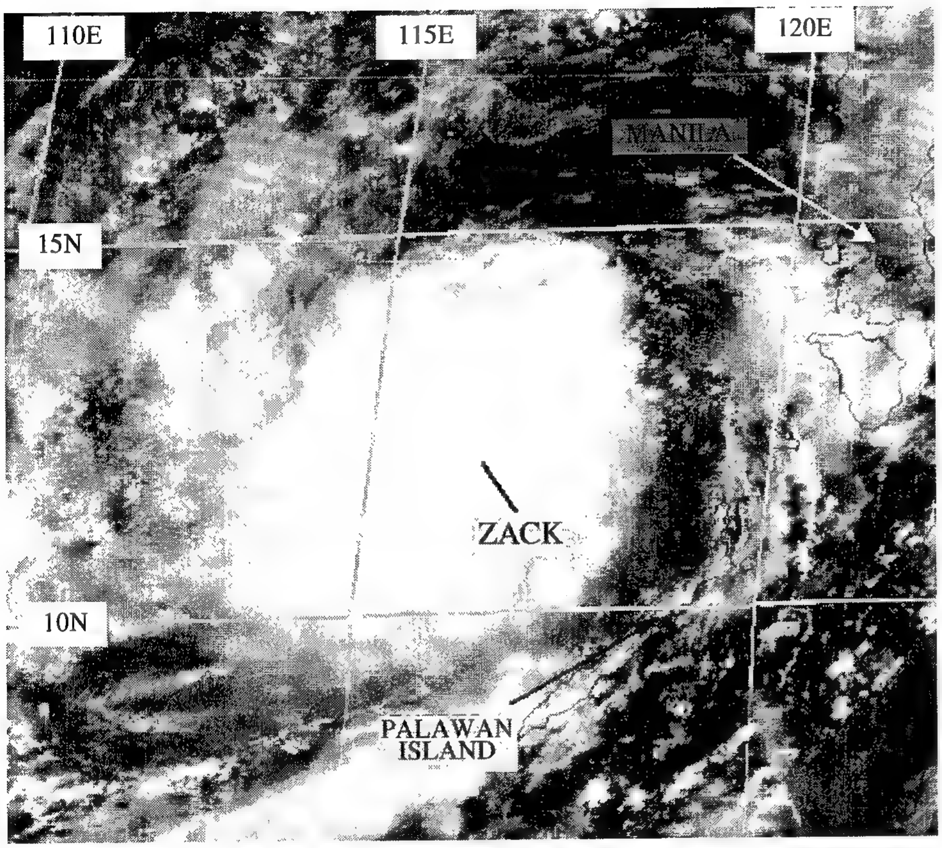

Figure 3-28-4 Zack is undergoing explosive deepening at the time of this picture (300031Z October visible GMS imagery). Note that the system appears to be isolated from its environment.

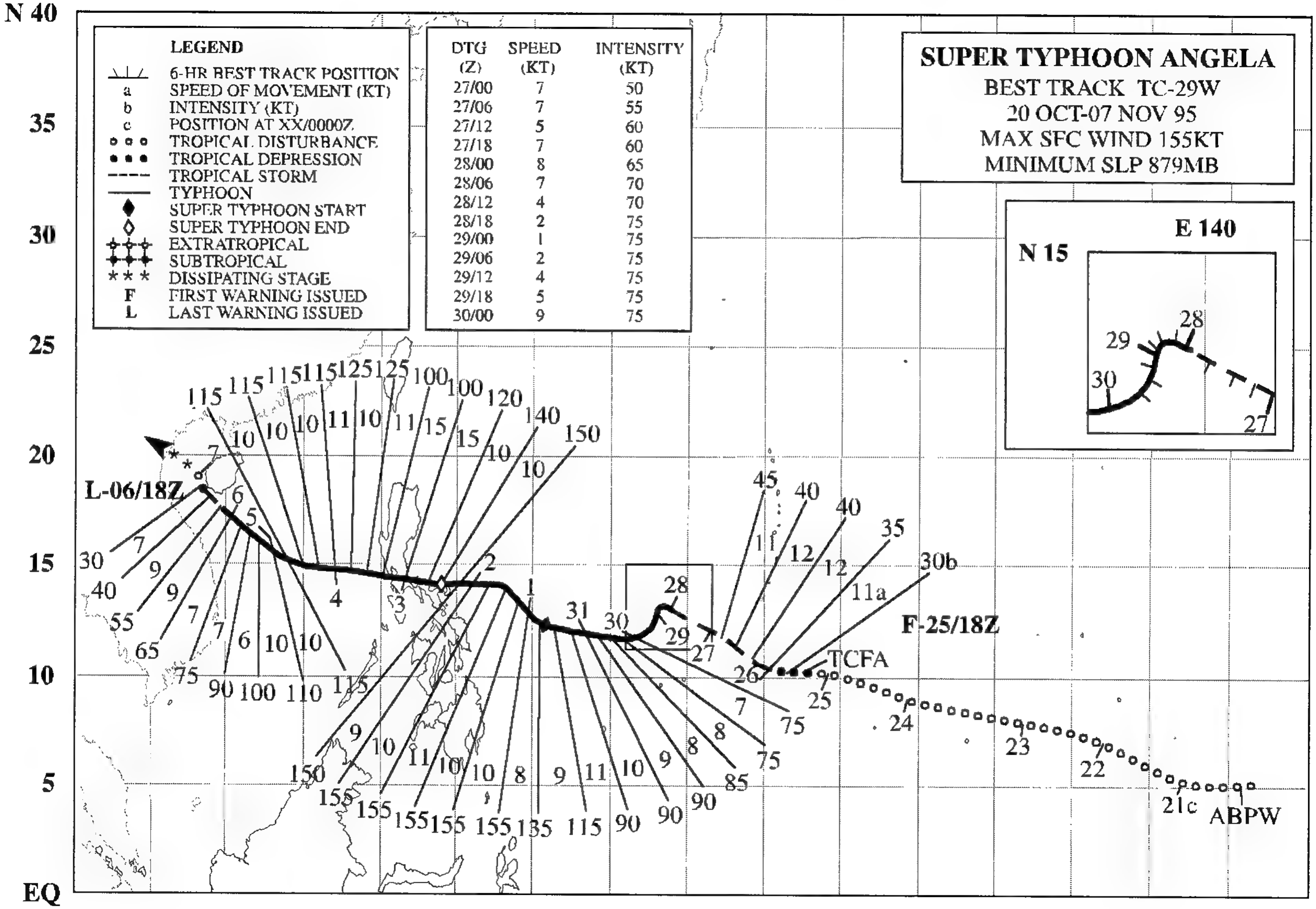
SUPER TYPHOON ANGELA
BEST TRACK TC-29W
20 OCT-07 NOV 95
MAX SFC WIND 155KT
MINIMUM SLP 879MB
LEGEND
6-HR BEST TRACK POSITION
a SPEED OF MOVEMENT (KT)
b INTENSITY (KT)
c POSITION AT XX/0000Z
TROPICAL DISTURBANCE
TROPICAL DEPRESSION
TROPICAL STORM
TYPHOON
SUPER TYPHOON START
SUPER TYPHOON END
EXTRATROPICAL
SUBTROPICAL
DISSIPATING STAGE
F FIRST WARNING ISSUED
L LAST WARNING ISSUED
DTG (Z) SPEED (KT) INTENSITY (KT)
27/00 7 50
27/06 7 55
27/12 5 60
27/18 7 60
28/00 8 65
28/06 7 70
28/12 4 70
28/18 2 75
29/00 1 75
29/06 2 75
29/12 4 75
29/18 5 75
30/00 9 75
N 15
E 140
N 40
35
30
25
20
15
10
5
EQ
L-06/18Z
F-25/18Z
TCFA
ABPW

SUPER TYPHOON ANGELA (29W)

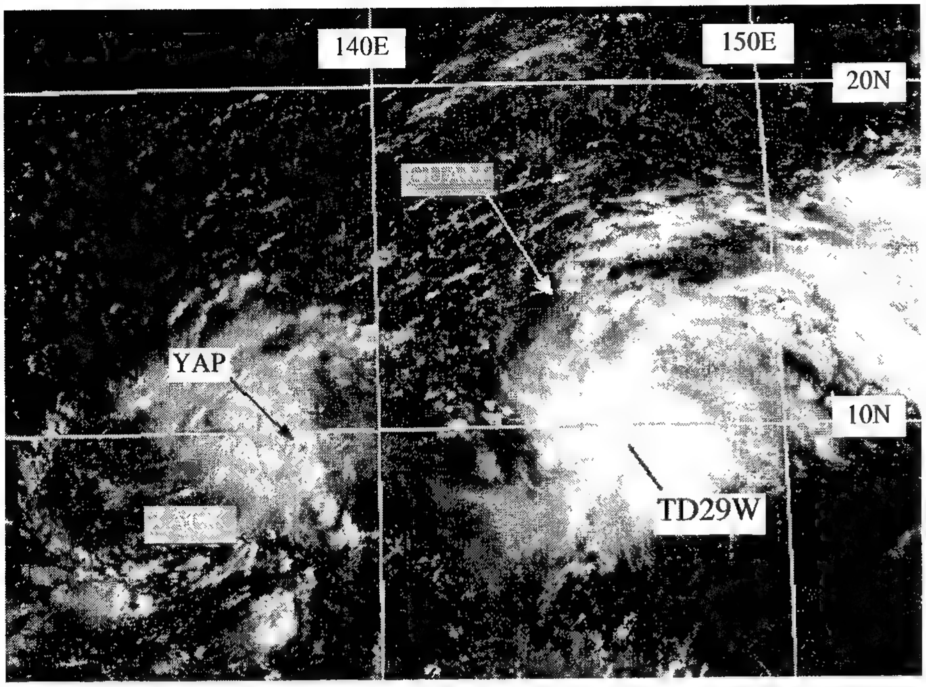

Figure 3-29-1 Tropical Depression 29W at an intensity of 30 kt (15 m/sec). Tropical Storm Zack (28W) is located about 480 nm (890 km) to its west (252131Z October visible GMS imagery).

I. HIGHLIGHTS

Angela was the most intense typhoon to hit the Philippines since Typhoon Joan (1970). First striking southern Luzon, it moved westward and crossed the metro-Manila area. More than 600 people perished in the Philippines as a result of Angela. Angela moved westward in tandem with Typhoon Zack (28W) nearly 4000 nm (7400 km) across the western North Pacific. Like many of the 1995 tropical cyclones, Angela was slow to develop, but ultimately, it became one of the most intense typhoons of the decade, peaking at an intensity of 155 kt (80 m/sec).

II. TRACK AND INTENSITY

In the third week of October, as Ward (26W) was recurving and heading towards its eventual transition into an extratropical cyclone southeast of Japan, the monsoon trough again became active along 10°N, from 130°E to east of the international date line. This trough spawned three tropical cyclones that at one time existed simultaneously: Yvette (27W) in the South China Sea, Angela to the south of Guam, and Zack (28W) in between the two and located northwest of Palau. The earliest stages of Angela can be traced to a tropical disturbance that formed in the Marshall Islands. This disturbance was first mentioned on the 200600Z October Significant Tropical Weather Advisory. It moved toward the west-northwest for more than five days — in tandem with the tropical disturbance that became Zack (28W) — before finally organizing into a tropical depression. A Tropical Cyclone Formation Alert was issued at 251230Z when the disturbance was located 240 nm (450 km) south-southeast of Guam. The system continued to organize during the night hours of 25 October, and the first warning on Tropical Depression 29W (TD 29W) was issued by the JTWC, valid at 251800Z (Figure 3-29-1). Twelve hours later, as the system passed about 145 nm (270 km) to the south of Guam and took a more northwestward course, it was upgraded to a tropical storm. During the next two days, Angela slowly intensified as its

forward motion slowed to an average speed of 7 kt (13 km/hr). On the warning valid at 280000Z, Angela was upgraded to a typhoon. At 281200Z, the typhoon abruptly turned to the south-southwest (an unusual heading for a tropical cyclone). This erratic motion was at first difficult to detect due to the lack of a visible eye and frequently changing size, shape, and cloud-top temperatures of its central deep convection. During the 24-hour period of slow south-southwestward motion Angela maintained a 75 kt (39 m/sec) intensity (Figure 3-29-2).

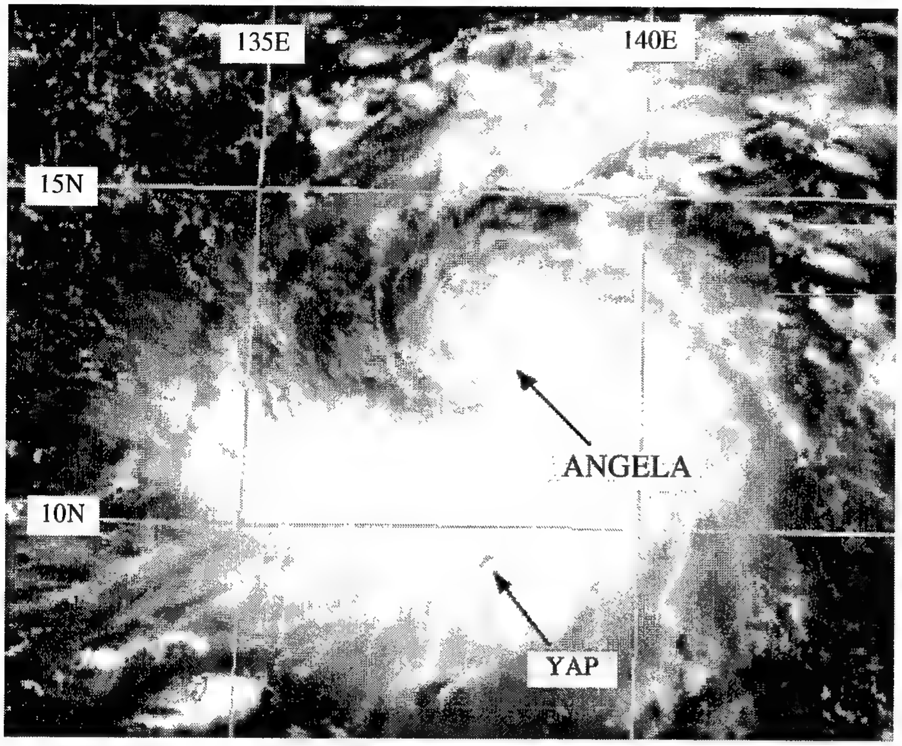

Figure 3-29-2 Typhoon Angela moves slowly south-southwestward as it passes north of Yap (290631Z October visible GMS imagery).

On the morning of 30 October, Angela turned back to the west and accelerated to an average speed of 9 kt (17 km/hr). During the afternoon, the typhoon began to slowly intensify. At 310600Z, with an intensity of 90 kt (46 m/sec), Angela began to rapidly intensify (Figure 3-29-3), and 18 hours later, it reached its maximum intensity of 155 kt (80 m/sec) (Figure 3-29-4). (A more in-depth description of Angela's rapid intensification process, including digital Dvorak (DD) intensity estimates, is found in the Discussion Section).

On the morning of 01 November, Angela moved to the northwest for 18 hours, before heading west along 14°N latitude. Angela maintained its peak intensity for 36 hours before striking the northern Bicol region of southern Luzon. During 31 October through 01 November, Angela passed to the north of a Navy drifting buoy (WMO 52523). The data recorded by this buoy (Figure 3-29-5) were important for defining the radius of 35 kt (18 m/sec) and 50 kt (26 m/sec) winds (see the discussion section). Also, landfall data obtained from PAGASA for postanalysis provided valuable information concerning Angela's peak winds as it approached and crossed Luzon.

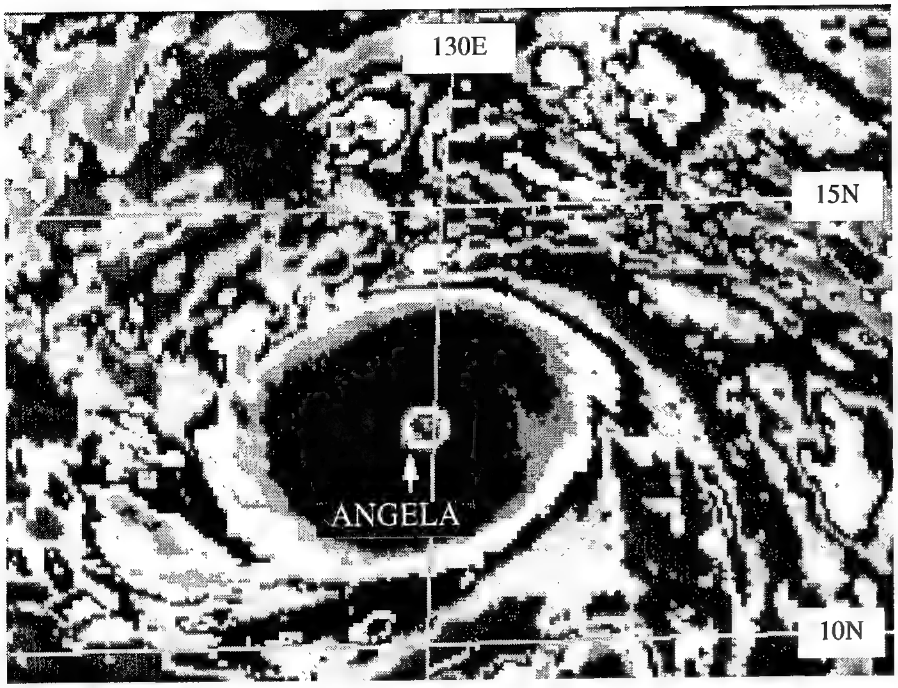

Figure 3-29-3 Angela undergoing explosive deepening. At the time of this picture, its intensity was 140 kt (72 m/sec). The typhoon is located about 420 nm (780 km) northwest of Palau and 50 nm (95 km) east of one of the Navy drifting buoys (312231Z October enhanced infrared GMS imagery).

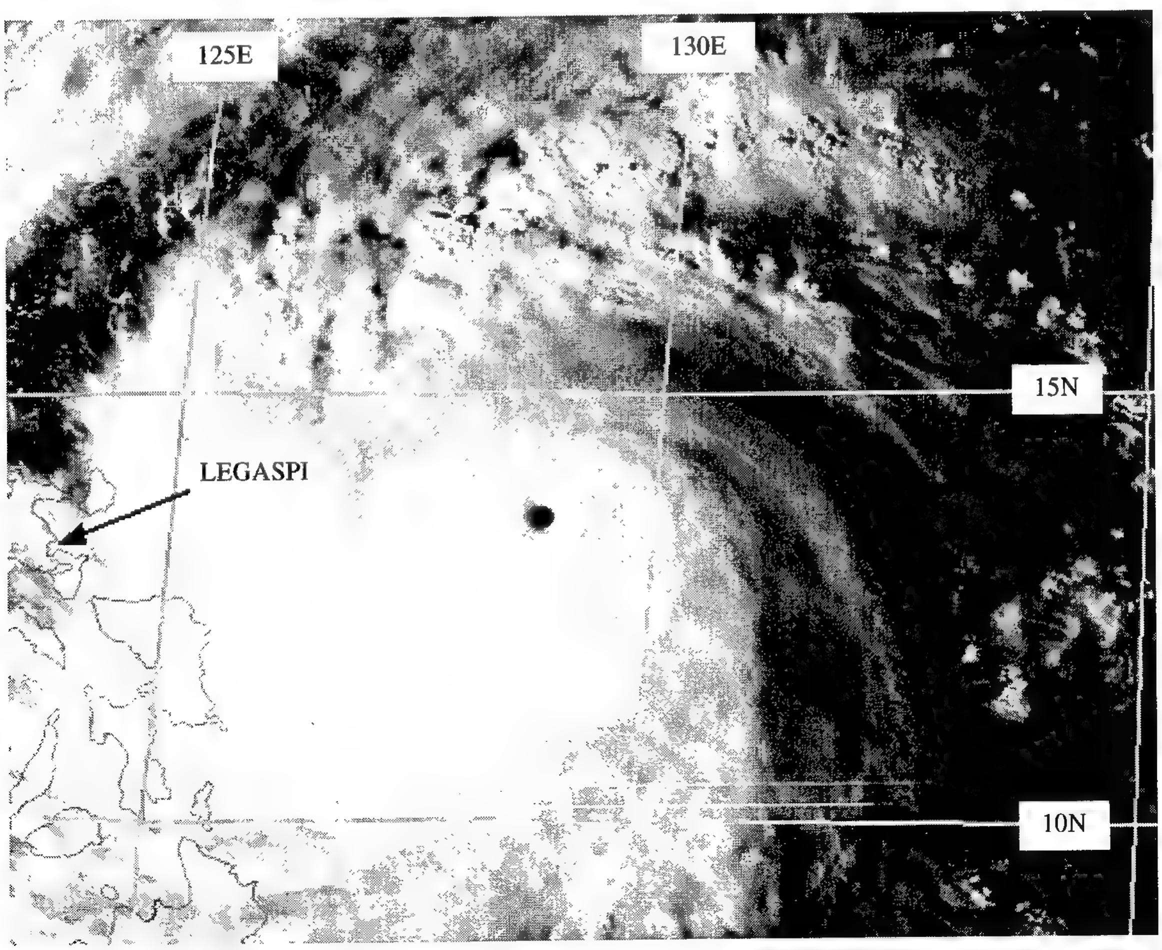

Figure 3-29-4 Angela at peak intensity of 155 kt (80 m/sec) (010731Z November visible GMS imagery).

At 030600Z November, Angela exited the Philippines into the South China Sea with 100 kt (51 m/sec) sustained winds. It re-intensified to a peak of 125 kt (64 m/sec) in the South China Sea, then slowly weakened as it turned to the northwest toward Hanoi (Figure 3-29-6). On the evening of 05 November, Angela weakened further as a result of strong vertical shear imposed on it by the northeast monsoon in the low levels and strong westerlies in the middle and upper levels. The following afternoon, the typhoon was downgraded to a tropical storm. The final warning, valid at 061800Z, was issued as the system dissipated over the Gulf of Tonkin.

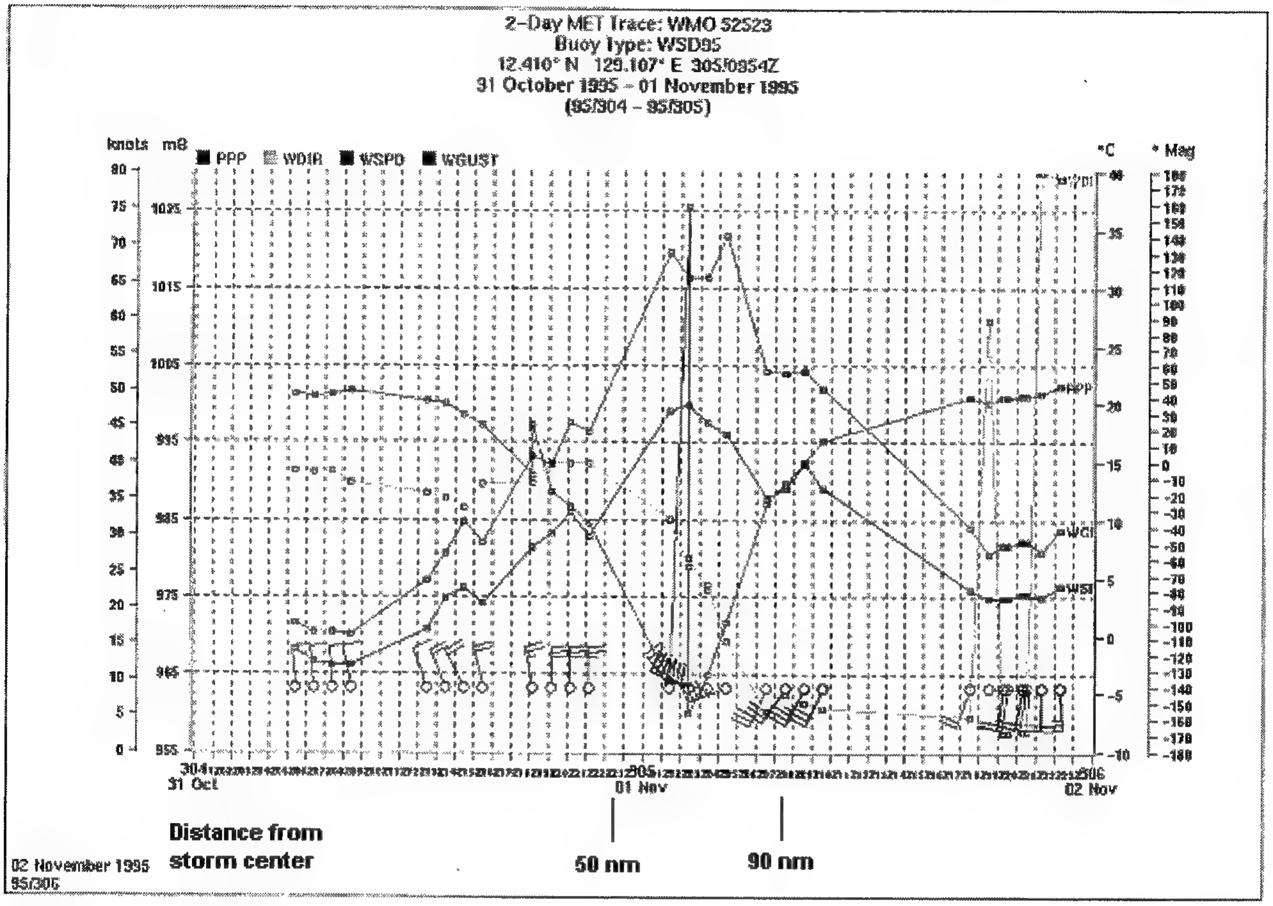

Figure 3-29-5 Two-day (31 October through 01 November) meteorogram from one of the Navy's drifting buoys, designated WMO 52523, as Angela passed by it. Sea-level pressure, 8-minute average wind speed, wind gusts, and wind direction are indicated.

III. DISCUSSION

a. *Erratic movement over the Philippine Sea*

On 28 October, Angela's west-northwestward movement abruptly stopped, and the system moved slowly to the south — about 90 nm (170 km) over 24 hours. By 300000Z, the typhoon had resumed a westward track at 8-10 kt (15-19 km/hr). The sudden change in motion was not predicted. It is hypothesized that Angela was forced to move southward by the building of a subsidence-induced anticyclone between it and Zack (28W). As Zack and Angela moved in tandem to the west, the clouds between the two tropical cyclones rapidly dissipated on 28 October, indicative of subsidence, when the separation distance between the two tropical cyclones was only 540 nm (1000 km). This clearing was very evident on 29 October as Angela was moving slowly southward.

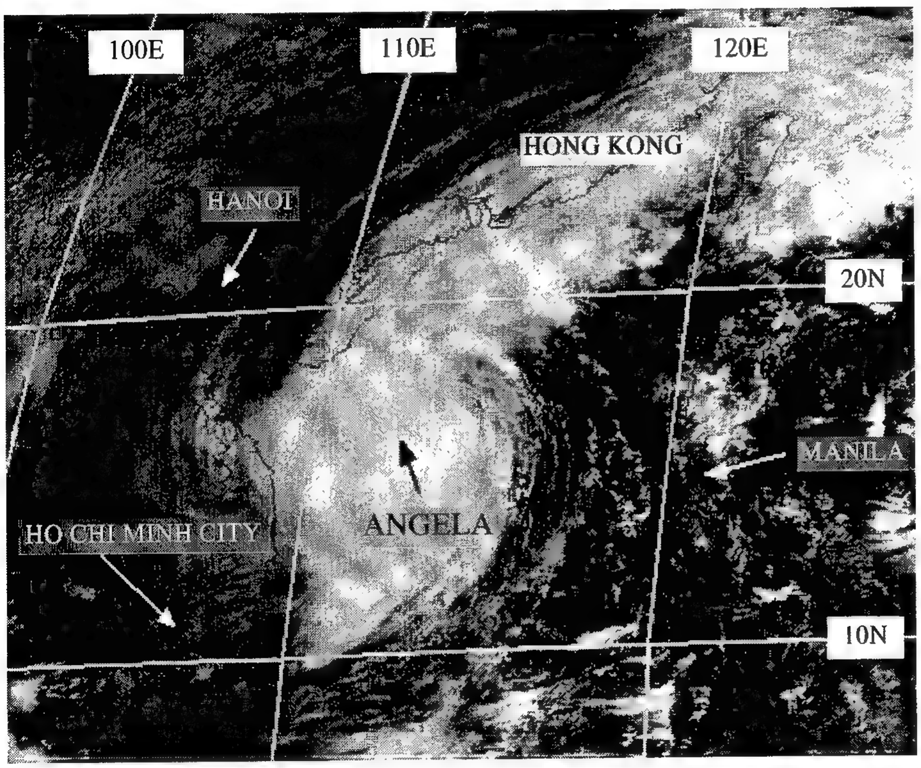

Figure 3-29-6 Angela in the South China Sea (050031Z November visible GMS imagery).

b. *Rapid intensification over the Philippine Sea*

On 31 October, after Angela's intensity had reached 90 kt (46 m/sec), it began to rapidly intensify (Holliday and Thompson 1979). Eighteen hours later, Angela's maximum sustained wind had increased to 155 kt (80 m/sec). The equivalent pressure fall over this eighteen-hour period was 71 mb, and the average rate of fall was 3.94 mb/hr. This meets the criterion for a special case of rapid intensification called explosive deepening (Dunnavan 1981), in which the pressure decrease must exceed 2.5 mb/hr for at least 12 hours. Of interest, satellite imagery does not reveal significant differences between Angela's environment and that of other tropical cyclones that intensify at much slower rates.

At approximately 010200Z November, the center of Angela passed 40 nm (75 km) to the northeast of the Navy's drifting buoy (WMO 52523). Data from this buoy (Figure 3-29-5) helped to define the distribution of 35 kt (18 m/sec) and 50 kt (26 m/sec) winds on the south side of Angela. They depict a small radius of 35 kt (18 m/sec) wind in the southwestern quadrant during the explosive deepening phase of Angela. A peak gust of 72 kt (37 m/sec) and a minimum sea-level pressure of 960 mb was

recorded by the buoy.

c. *Measured winds and pressures as Angela crossed the Philippines*

As Angela approached the Philippines with 155 kt (80 m/sec) maximum sustained 1-minute winds, satellite intensity estimates began to indicate a weakening. Table 3-29-1 shows the T numbers, the current intensity (CI) numbers, DD numbers, and the intensity-based analysis of synoptic observations over the Philippines during the period 020000Z to 030300Z November (see also Figure 3-29-7). While still at peak intensity, Angela moved about 15 nm (28 km) north of the Catanduenas Island radar site (WMO 98446) and 40 nm (75 km) north of Virac, Catanduenas Island (WMO 98447). The radar site recorded gusts to 140 kt (72 m/sec) and Virac had gusts to 111 kt (57 m/sec). Since the radar site appeared to be in the southern eyewall, and the translation speed of Angela was toward the west at 10 kt (19 km/hr), a reasonable estimation of Angela's intensity when it passed to the north of Catanduenas at 021200Z (taking full account of the speed of translation and using a gust factor of 1.2) is 140 kt sustained 1-minute wind with gusts to 170 kt (72G87 m/sec).

Since Angela was not a small tropical cyclone, its wind and pressure would be expected to conform relatively well to the Atkinson and Holliday wind-pressure relationship, which gives a sustained 1-minute wind of 115 kt (59 m/sec) using the 926 mb minimum sea-level pressure recorded at Daet (WMO 98440) at 021900Z. Since the center of Angela's eye passed over Daet, this value — 115 kt with gusts to 140 kt (59G72 m/sec) — must be considered to be a reasonable estimate of Angela's intensity. The peak gust recorded at Daet was 135 kt (69 m/sec).

In the Metro-Manila area, wind and pressure measurements indicate that Angela's sustained winds had weakened to 80-90 kt (41-46 m/sec). The center of Angela appears to have passed near or over the Ninoy Aquino International Airport in Manila (WMO 98429) where a minimum sea-level pressure of 975.6 mb was recorded at 030230Z; the center of Angela also appears to have passed near or over Cubi Point (WMO 98426) where a minimum sea-level pressure of 976.3 mb was recorded at 030330Z.

IV. IMPACT

Angela caused considerable death, destruction, and agricultural losses in the Philippines. More than 600 people perished with and additional 100 reported missing. Over 96,000 homes were destroyed, and an estimated US$70 million in damage was inflicted on roads and bridges. Hardest hit was the northern Bicol region of southern Luzon (located approximately 100-150 nm (185-280 km) southeast of Manila). Catanduenas Island and the Metro-Manila area were also hard hit. There were at least 121 deaths in Calauag, Bicol, primarily from storm surge and a river that flooded when a dam burst. More than 100 perished in the neighboring village of Paracale, primarily from mudslides. Damage to agriculture exceeded US$18 million. Electrical power was lost by one-third of the country.

Table 3-29-1 Intensity Comparison for Angela

Date/time	Average#	CI#	DD#	Synoptic Analysis
020000Z	7.0	7.5	6.9	7.5
020300Z	7.0	7.5	6.9	7.5
020600Z	7.0	7.5	6.8	7.4
020900Z	7.0	7.5	6.3	7.2
021200Z	7.0	7.5	6.0	7.0
021500Z	6.5	7.5	5.5	6.6
021800Z	6.0	7.0	5.8	6.3
022100Z	6.0	7.0		5.8
030000Z	6.0	7.0		5.4
030300Z	6.0	7.0		4.6

Date/time	Intensity (kt)	Intensity (kt)	Intensity (kt)	Synoptic Analysis
020000Z	140	155	138	155
020300Z	140	155	138	155
020600Z	140	155	136	150
020900Z	140	155	124	145
021200Z	140	155	115	140
021500Z	127	155	102	130
021800Z	115	155	110	120
022100Z	115	140		110
030000Z	115	140		100
030300Z	115	140		80

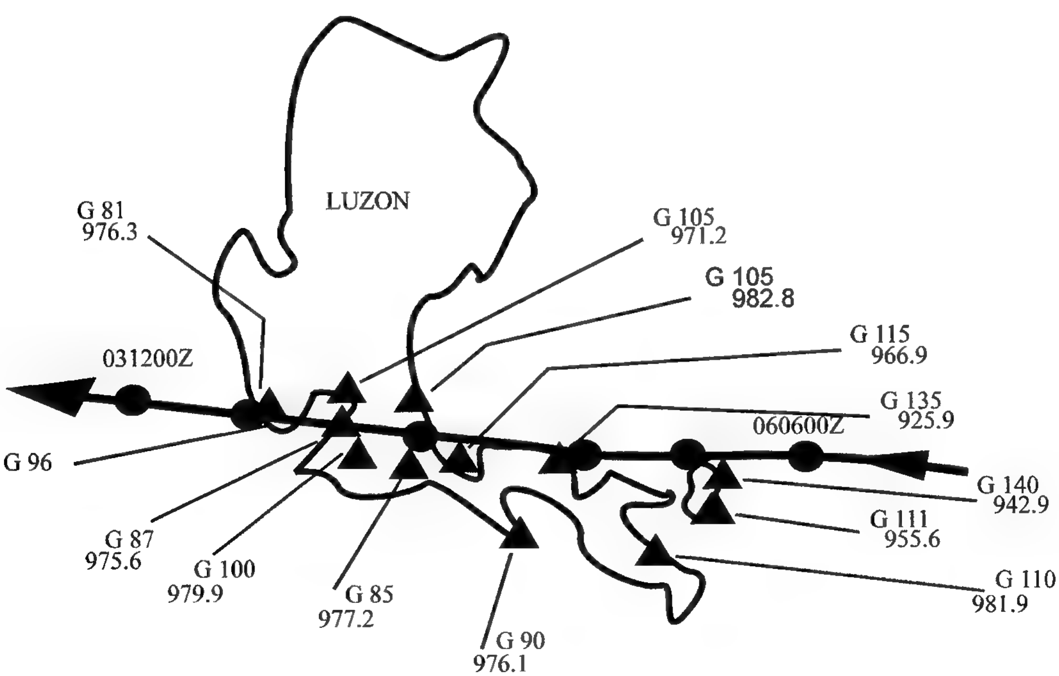

Figure 3-29-7 Peak wind gusts and minimum sea-level pressures recorded at selected observation sites (solid triangles) as Angela crossed the Philippines. Angela's 6-hourly best-track positions are indicated by the black dots connected by the solid line.

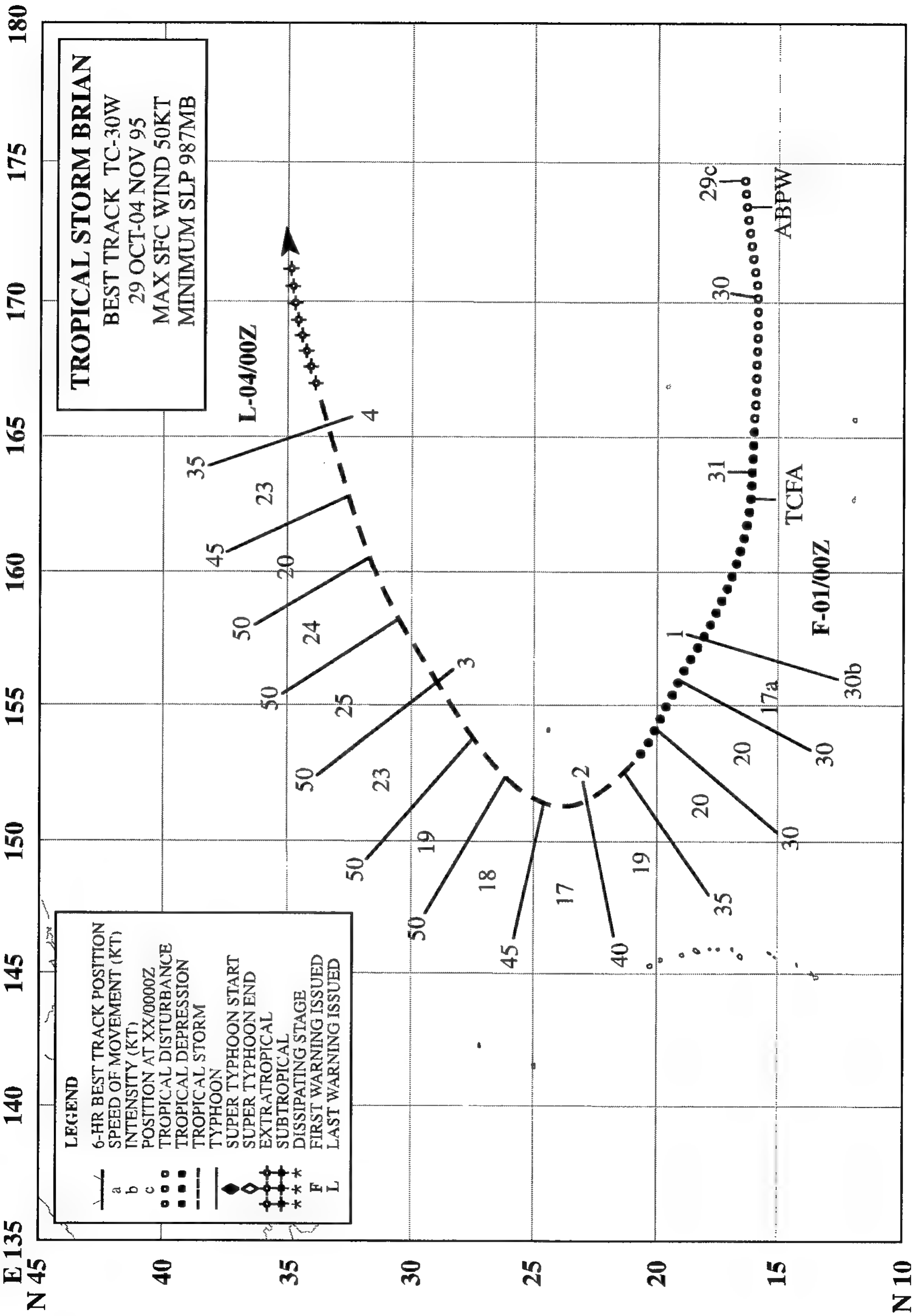
TROPICAL STORM BRIAN
BEST TRACK TC-30W
29 OCT-04 NOV 95
MAX SFC WIND 50KT
MINIMUM SLP 987MB
LEGEND
6-HR BEST TRACK POSITION
SPEED OF MOVEMENT (KT)
INTENSITY (KT)
POSITION AT XX/0000Z
TROPICAL DISTURBANCE
TROPICAL DEPRESSION
TROPICAL STORM
TYPHOON
SUPER TYPHOON START
SUPER TYPHOON END
EXTRATROPICAL
SUBTROPICAL
DISSIPATING STAGE
FIRST WARNING ISSUED
LAST WARNING ISSUED
L-04/00Z
F-01/00Z
TCFA
ABPW
29c
30b
17a
E 135
140
145
150
155
160
165
170
175
180
N 45
40
35
30
25
20
15
N 10

TROPICAL STORM BRIAN (30W)

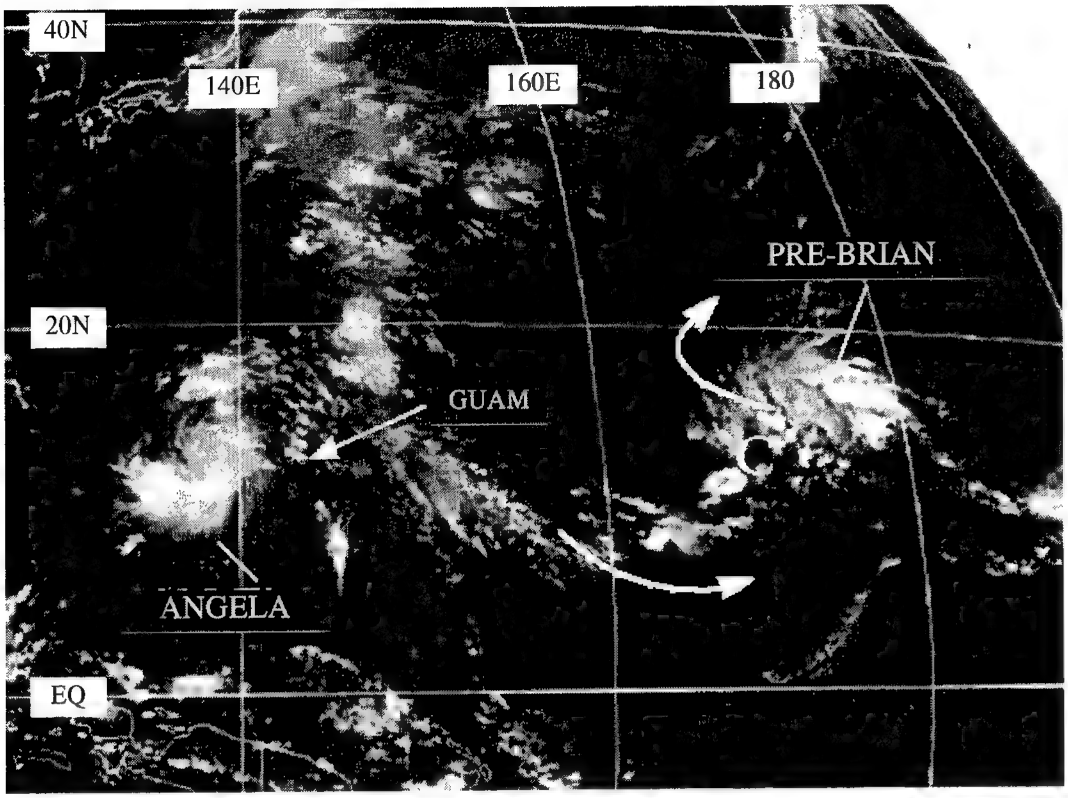

Figure 3-30-1 The indicated area of deep convection located to the northeast of a TUTT cell (labeled, C) that was the precursory tropical disturbance from which Brian developed (290633Z October Infrared GMS imagery).

I. HIGHLIGHTS

Brian formed in direct association with a TUTT cell. Typical of such tropical cyclones, Brian was small and embedded in the easterly wind flow on the southwestern flank of the low-level subtropical ridge. Prior to recurving and becoming absorbed into the cloud band of an advancing cold front, Brian's entire cloud system was isolated within a large relatively cloud-free region south of the polar front and to the north of the convection associated with the tradewind trough.

II. TRACK AND INTENSITY

Based upon over 48 hours of persistence, an area of deep convection that was located to the north of the Marshall Islands was first mentioned on the 290600Z October Significant Tropical Weather Advisory. This area of deep convection (Figure 3-30-1) was associated with a TUTT cell (Figure 3-30-2a,b). On 31 October, the deep convection consolidated to the northeast of the TUTT cell and became better organized (Figure 3-30-3), prompting the JTWC to issue a Tropical Cyclone Formation Alert at 310500Z. By the daylight hours of 01 November, visible satellite imagery indicated that the cloud system had become well-organized, and the first warning on Tropical Depression 30W, valid at 010000Z November, was issued.

In advance of an approaching frontal system (Figure 3-30-4), Tropical Depression 30W turned northward and intensified. It was upgraded to Tropical Storm Brian on the warning valid at 020600Z (post-analysis indicated that tropical storm intensity was reached 12 hours earlier at 011800Z). Brian was at its point of recurvature at this time, and subsequently began to accelerate to the northeast. It continued to intensify following recurvature reaching a peak intensity of 50 kt (26 m/sec) during the period

021200Z to 031200Z. As Brian moved northeast, the frontal system to its west was catching up with it. Overtaken by the frontal system on 04 November, Brian lost its deep convection and merged with the frontal cloud band. The final warning on Tropical Storm Brian was issued valid at 040000Z November when the weakening tropical cyclone began to merge with the frontal cloud band.

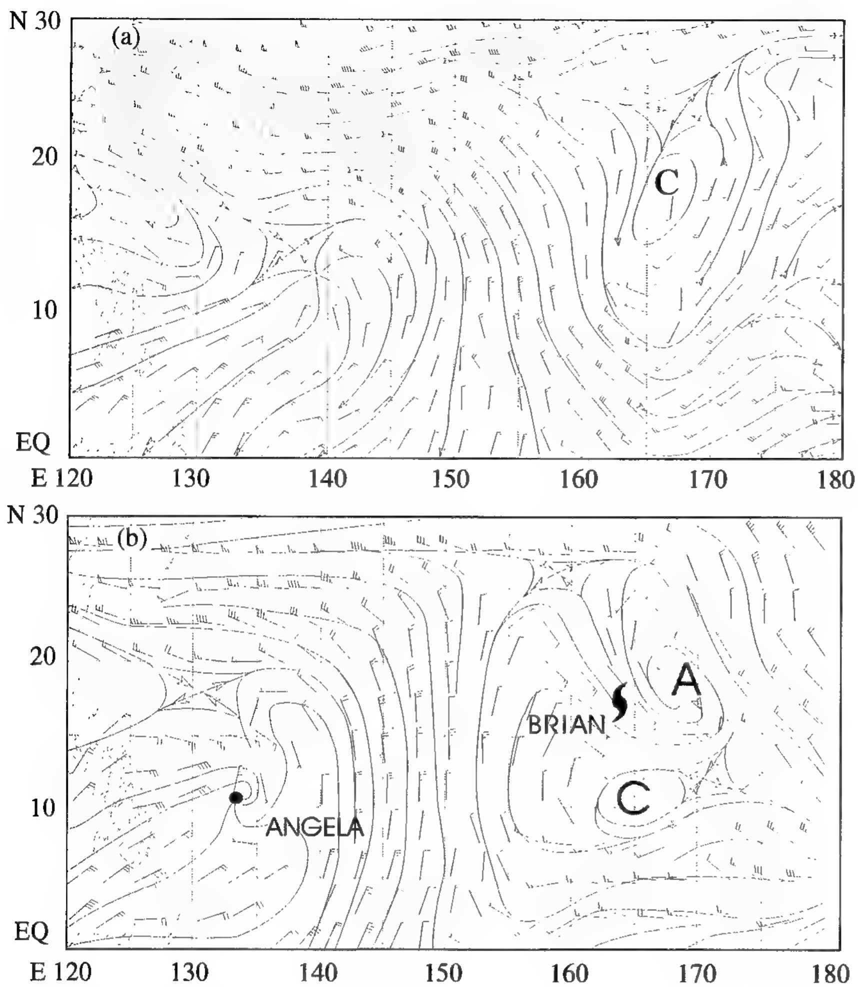

Figure 3-30-2 (a) A TUTT cell (labeled, C) is located north of the Marshall Islands (281200Z October NOGAPS 200-mb windbarbs and streamlines). (b) The TUTT cell (labeled, C) moved southward as diffluent and anticyclonically curved flow became established over the developing Brian (indicated by the tropical cyclone symbol). The center of an anticyclone is labeled, A. (310000Z October NOGAPS 200-mb windbarbs and streamlines).

III. DISCUSSION

Formation in direct association with a TUTT cell

A persistent feature of the upper-tropospheric flow over the tropics of the western North Pacific and North Atlantic oceans during the summer is the tropical upper tropospheric trough (TUTT) (Sadler 1975). In the western North Pacific, the axis of the TUTT overlies low-level easterly flow approximately mid-way between the axis of the subtropical ridge and the axis of the monsoon trough.

In synoptic analyses, the TUTT is commonly observed to consist of a chain of westward moving synoptic-scale cyclonic vortices called "TUTT cells" in the western North Pacific, and, "upper cold lows" in the Atlantic. The typical distribution of clouds associated with a TUTT cell features isolated cumulonimbi and/or small mesoscale convective systems in, or near, its core. Cloudiness to the south and east of a TUTT cell in the western North Pacific is often associated with the monsoon trough, and the TUTT cell (or a chain of TUTT cells) may affect the distribution of cloudiness along the axis of the trough and also of the cirrus outflow from the monsoon cloud band (e.g., see Figure 3-26-1 in Ward's summary).

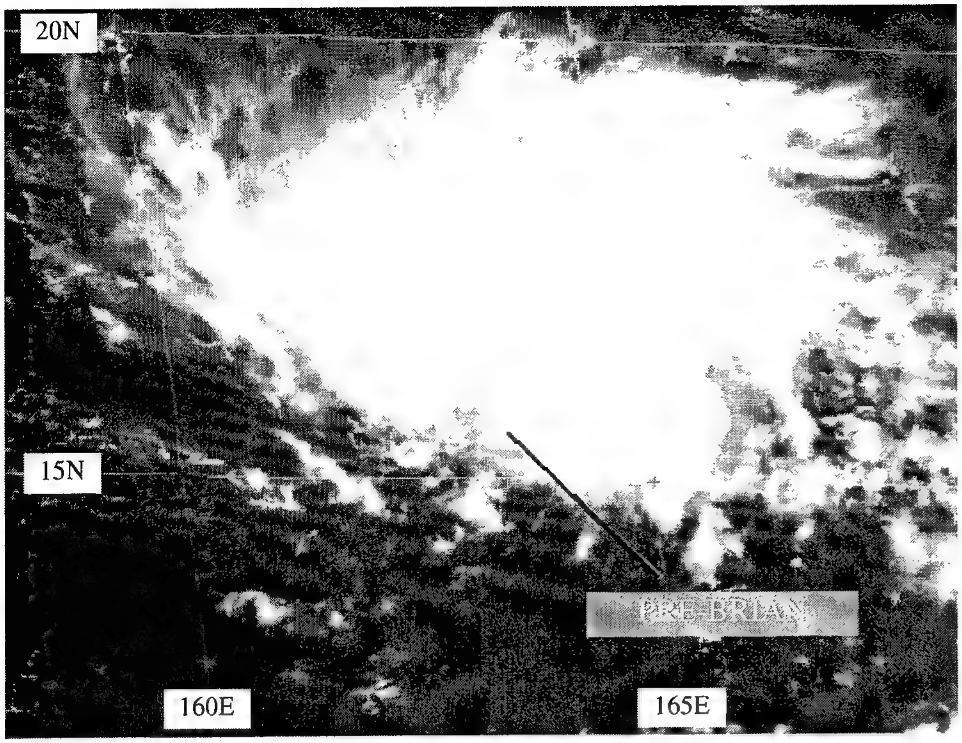

Figure 3-30-3 Cyclonically curved bands of deep convection associated with some poorly defined cyclonically curved low-level cloud lines indicated that the tropical disturbance that became Brian was intensifying (302331Z October visible GMS imagery).

Sadler (1967) proposed that the TUTT (with its embedded TUTT cells) was the primary source for disturbances (e.g., inverted troughs, isolated areas of deep convection, etc.) in the tradewind flow. Sadler (1967) also credits TUTT cells with the capacity to induce tropical cyclogenesis. TUTT-induced tropical cyclogenesis was envisioned by Sadler to be the result of the distal penetration of the TUTT cell's cyclonic circulation into the lower levels, thereby initiating deep convection which, through the release of latent heat, gradually converted the TUTT cell into a warm-core low (i.e., a tropical cyclone). In a later paper (Sadler 1976), the TUTT (and of TUTT cells within it) is hypothesized to contribute to the development of a tropical cyclone by providing an efficient outflow channel for the incipient tropical cyclone. In this scenario, the tropical cyclone is located to the south or southeast of the TUTT, or a TUTT cell.

In our investigations of the role of the TUTT — and in particular, TUTT cells — in tropical cyclone formation, we have observed a process whereby a small tropical cyclone forms (sometimes rapidly) under diffluent and anticyclonically curved flow to the east through north of the TUTT cell. This process is similar to Sadler's (1967) distal mechanism of TUTT cell-induced tropical cyclogenesis. Careful observation has shown that the isolated area of deep convection that forms a tropical cyclone near a TUTT cell, does so not directly in the core of the TUTT cell, but usually 200 to 400 km to the north or northeast of the circulation center of the TUTT cell. Brian was a good example of tropical cyclogenesis in direct association with a TUTT cell. Typical characteristics of direct TUTT-induced tropical cyclones include:

(1) rapid formation;
(2) small size;
(3) isolation in an easterly low-level flow regime;
(4) a relatively cloud free environment;

(5) a relatively high latitude of formation (i.e., near the latitude of the axis of the TUTT — usually at about 20-30°N); and,

(6) initial motion with a component south of west.

IV. IMPACT

No reports of damage or injuries attributable to Tropical Storm Brian were received at the JTWC.

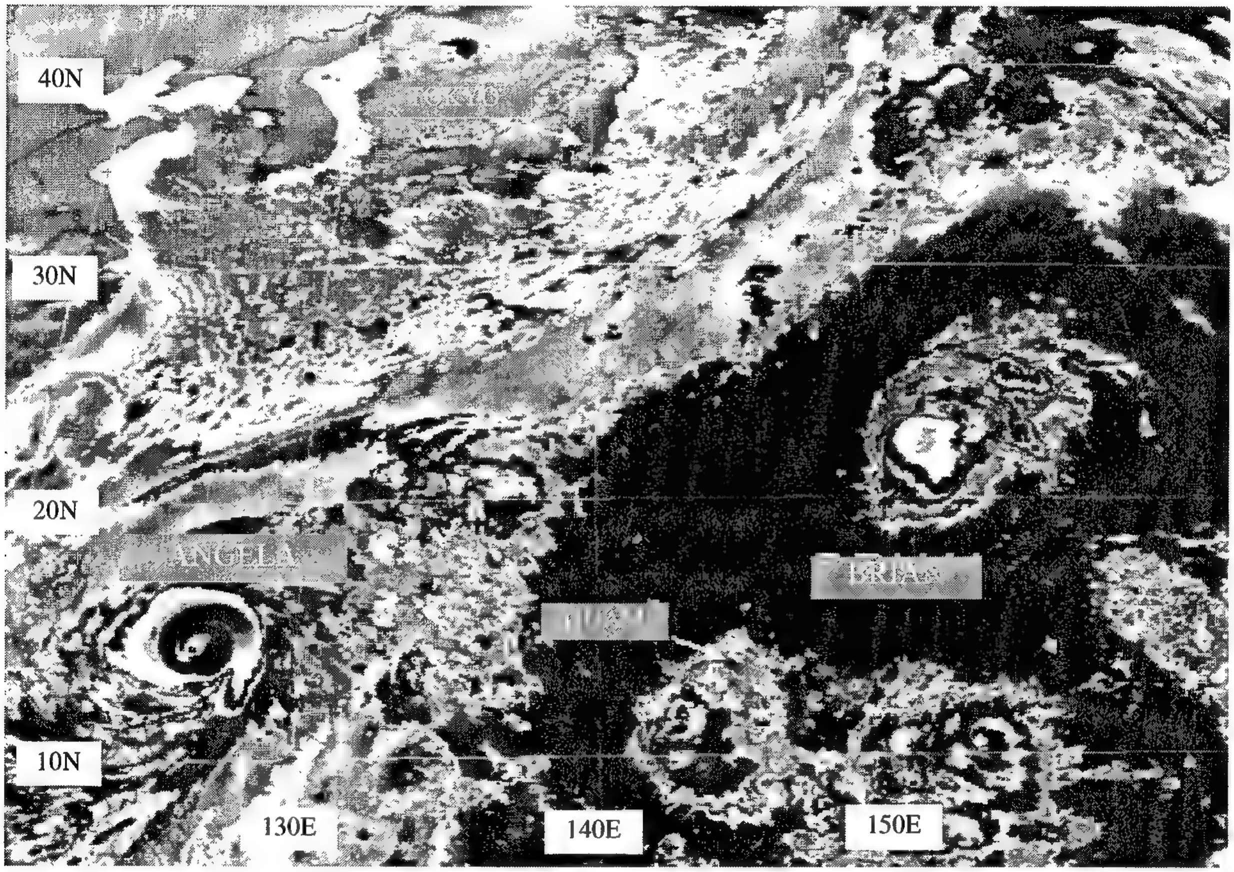

Figure 3-30-4 In advance of an approaching frontal system, Brian recurves and intensifies (012031Z November enhanced infrared GMS imagery).

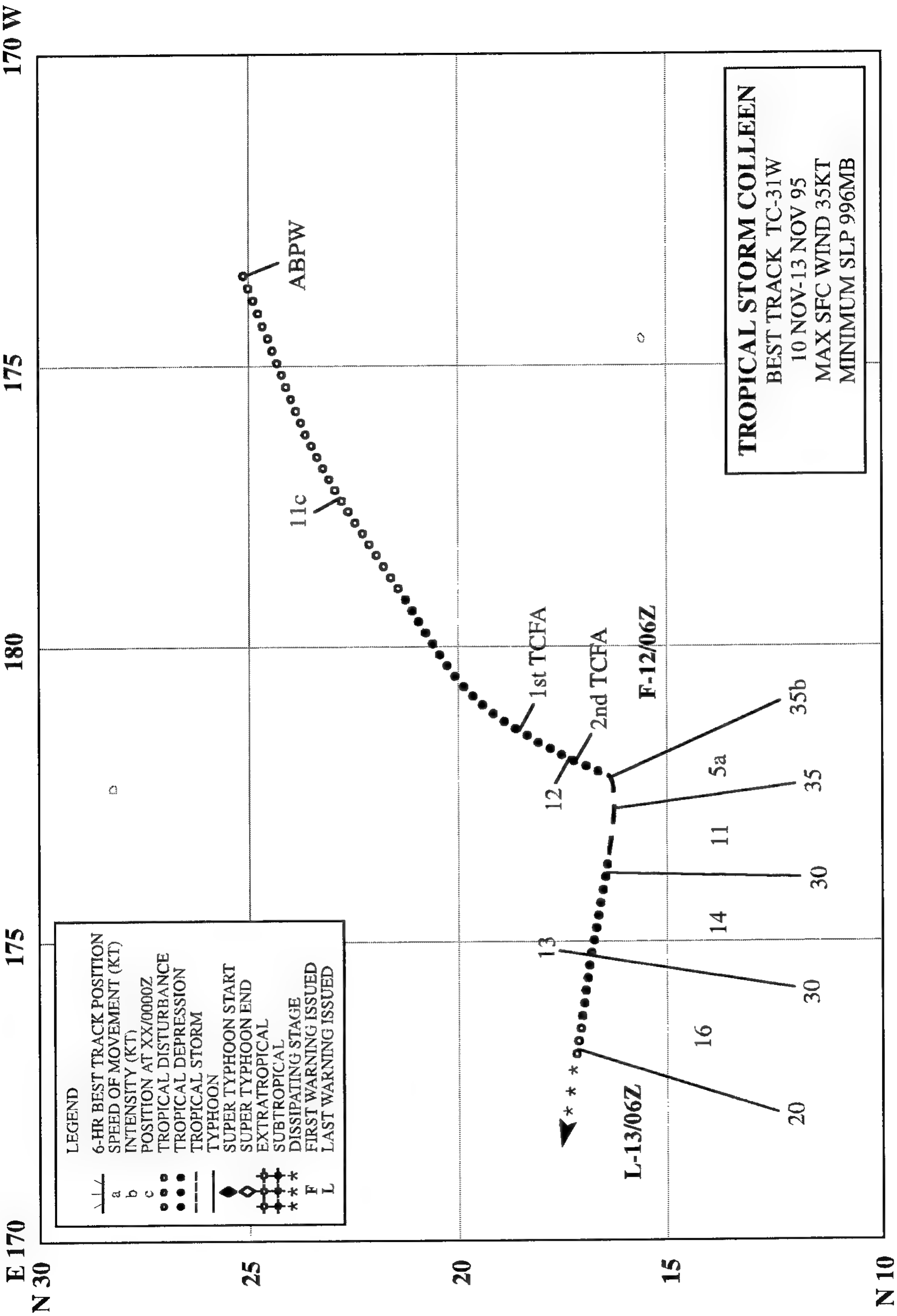
TROPICAL STORM COLLEEN
BEST TRACK TC-31W
10 NOV-13 NOV 95
MAX SFC WIND 35KT
MINIMUM SLP 996MB
LEGEND
a 6-HR BEST TRACK POSITION
b SPEED OF MOVEMENT (KT)
c INTENSITY (KT)
POSITION AT XX/0000Z
TROPICAL DISTURBANCE
TROPICAL DEPRESSION
TROPICAL STORM
TYPHOON
SUPER TYPHOON START
SUPER TYPHOON END
EXTRATROPICAL
SUBTROPICAL
DISSIPATING STAGE
F FIRST WARNING ISSUED
L LAST WARNING ISSUED
ABPW
11c
1st TCFA
2nd TCFA
12
F-12/06Z
35b
5a
35
11
30
14
13
30
16
20
L-13/06Z
E 170
175
180
175
170 W
N 30
25
20
15
N 10

TROPICAL STORM COLLEEN (31W)

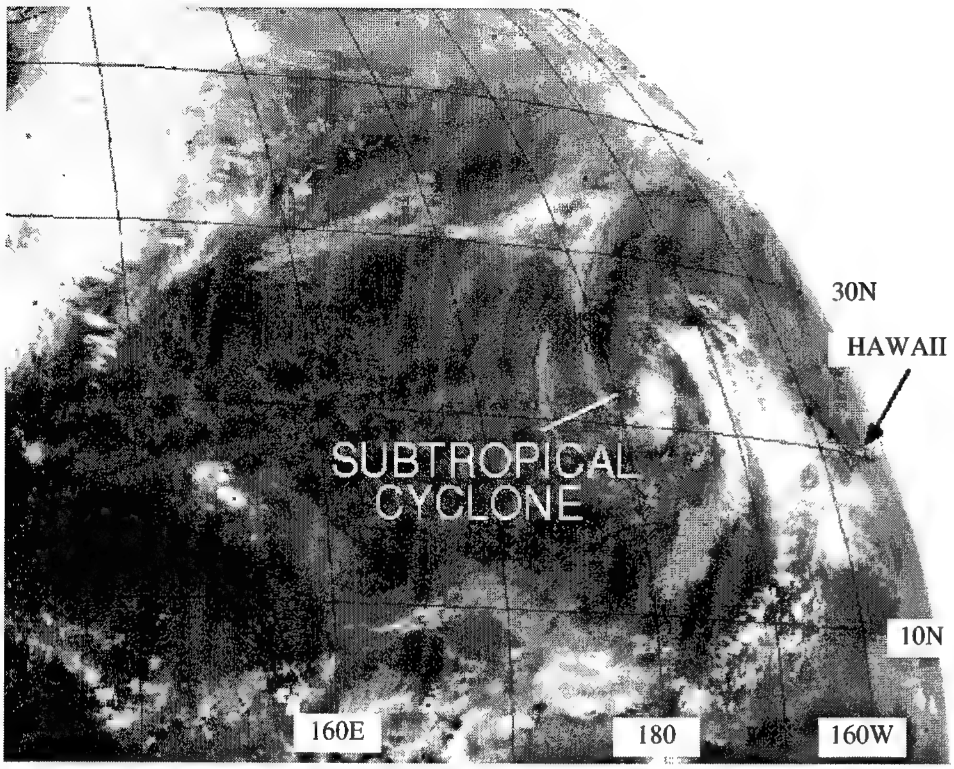

Figure 3-31-1 A "Kona" storm located to the west-northwest of Hawaii has just acquired central deep convection marking the beginning of its transition from a subtropical cyclone to a tropical cyclone (102332Z November infrared GMS imagery).

I. HIGHLIGHTS

Colleen developed in an unusual manner for a tropical cyclone in the western North Pacific. The disturbance that became Colleen was a cut-off low that formed in the subtropics to the northwest of Hawaii — a classic "Kona" low. Drifting toward the southwest, the "Kona" low crossed the international date line into JTWC's area of responsibility, where it acquired persistent central convection and became a tropical storm.

II. TRACK AND INTENSITY

On 09 November, a cold-core low pressure system became cut-off about 600 nm (1100 km) to the northwest of Hawaii. This system possessed the structural characteristics of a subtropical cyclone (Hebert and Poteat 1975). Such systems in the Hawaiian region are called "Kona" storms (Ramage 1971) in reference to their southwesterly winds that blow onshore in the normal leeward, or "Kona", sides of the islands.

After becoming cut-off to the northwest of Hawaii, the subtropical low (or "Kona" storm) that became Colleen began to drift toward the southwest, and on 11 November it crossed the international date line. Prior to crossing the international date line, the amount of deep convection began to increase near the low-level circulation center (Figure 3-31-1), prompting its first mention on the 110600Z Significant Tropical Weather Advisory. Remarks on this advisory included:

". . . A low-level circulation is located near 22°N 179°W. This area is associated with a subtropical low pressure system that has been moving southwest at 15 knots [28 km/hr] over the past 24 hours. Convection has increased, and is sheared to the east and south of the exposed low-level circulation . . ."

The system crossed the international date line at 110900Z. Shortly thereafter, based upon persistent convection near the low-level circulation center, and anticipation that the system would intensify, the first Tropical Cyclone Formation Alert (TCFA) was issued at 111930Z. A second TCFA was issued at 120100Z in order to reposition the alert area. Remarks on this second TCFA included:

". . . A low-level circulation associated with a subtropical low pressure system has continued drifting south-southwest, and is showing signs of developing into a tropical cyclone. Convection is forming closer to the center of the circulation, which is well defined in the low-level cloud lines. . . ."

During the daylight hours of 12 November, it was deemed by the JTWC that the subtropical low had become a tropical storm (Figure 3-31-2), and the first warning on Tropical Storm Colleen valid, at 120600Z was issued. Remarks on this first warning included:

". . . Tropical Storm Colleen (31W) has formed from a subtropical low pressure system located northeast of the Marshall Islands. Colleen has been diving southward over the past twelve hours, but is expected to assume a westward track within 12 to 24 hours . . ."

After becoming a tropical storm, Colleen did indeed assume a westward track. After turning toward the west, however, amounts of deep convection near the low-level circulation center decreased, most-probably as a result of increasing westerly wind shear on the system. By warning number 4 (valid at 130000Z), there was no organized deep convection associated with the system, however microwave imagery indicated that 30 kt (15 m/sec) sustained winds were still associated with the low-level circulation center. Tropical Storm Colleen was downgraded to a tropical depression at this time and, with continued weakening, the JTWC issued a final warning valid at 130600Z.

III. DISCUSSION

Subtropical cyclones, "Kona" storms, and tropical cyclones

Establishing the defining characteristics of a tropical cyclone is a challenging exercise. For purposes of public warning, the nature of tropical cyclones has been simplified to a stratification based upon intensity. In this simplified framework, the first stage toward the development of a tropical cyclone is the tropical disturbance. A tropical disturbance is a discrete system of apparently organized convection, generally 200 to 600 km in diameter, originating in the tropics or subtropics, having a non-frontal, migratory character and having maintained its identity for 12- to 24-hours (Elsberry, et al. 1987). The system may or may not be associated with a detectable perturbation of the low-level wind or pressure field. It is the basic generic designation which, upon acquiring a persistent low-level cyclonic wind field associated with an area of lowered sea-level pressure, becomes a tropical cyclone. In the United States, (TCs) are categorized by their intensity: (1) a tropical depression is a TC with maximum sustained one-minute mean surface winds (V1 Max) of less than 34 kt (17 m/sec); (2) a tropical storm is a TC with a V1 Max in the range of 34 to 63 kt (17 to 32 m/sec); (3) a hurricane (typhoon) is a TC with a V1 Max of 64 kt (33 m/sec) or more. In recent years, a fourth category — the super hurricane (typhoon) — has gained popular acceptance; it is a subset of the hurricane (typhoon) category with a V1 Max of 130 kt (67 m/sec) or greater.

Dvorak (1975, 1984) developed a technique for estimating the intensity of tropical cyclones from satellite imagery. His technique is used worldwide. In the Dvorak classification technique, persistent deep convection must be located within 120 nm (220 km) of the low-level circulation center in order to initiate classification. The intensity of the tropical cyclone is determined by several properties of the deep convection (e.g., the proximity of the low-level circulation center to the deep convection, the size of the central dense overcast, the cloud-top temperatures and horizontal width of the eye wall cloud, the width and extent of peripheral banding features, etc.). The basic tropical cyclone pattern types identi-

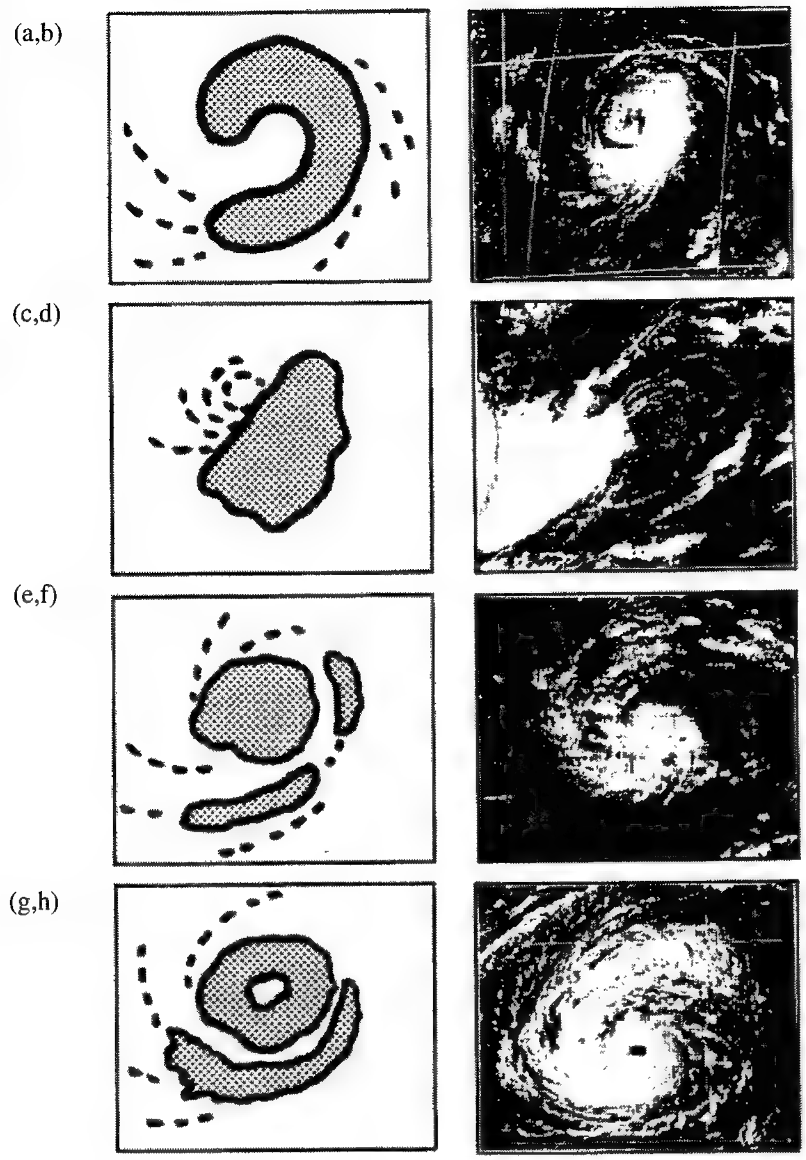

Figure 3-31-2 Schematic illustration (left column) and representative satellite imagery (right column) of Dvorak's (1975) basic tropical cyclone pattern types: (a,b) the "curved band" pattern; (c,d) the "shear" pattern; (e,f) the "central dense overcast" pattern; and, (g,h) the "eye" pattern.

fied by Dvorak are: (1) the "curved band" pattern (Figure 3-31-3a,b); (2) the "shear" pattern (Figure 3-31-3c,d); (3) the "central dense overcast", or "embedded center", pattern (Figure 3-31-3e,f); and, (4) the "eye" pattern (Figure 3-31-3g,h).

Some cyclones possess characteristics of both extra-tropical (ET) cyclones and tropical cyclones. For example, the subtropical cyclone (Hebert and Poteat 1975), the "Kona" storm (Ramage 1971), the arctic hurricane (Businger and Baik 1991), the monsoon depression (Ramage 1971, and JTWC 1993), and the monsoon gyre (Lander 1994, Carr and Elsberry 1994). These types of cyclones have caused diagnostic and forecast problems for decades. Further complicating things is the fact that transitions among some of the types are possible.

Because Dvorak's techniques are not applicable to subtropical (ST) cyclones, Hebert and Poteat (1975) (hereafter referred to as HP75) developed a satellite classification technique for ST cyclones. Their technique provides an intensity estimate (from satellite imagery) of ST cyclones, and provides guidelines for determining the cyclone type (i.e., tropical, ST or ET). The technique was designed so that the intensity estimate would intermesh with the Dvorak technique when the cyclone changed type.

For example, if a subtropical cyclone with an estimated intensity of ST 3.0 became a tropical cyclone, it would then be given a Dvorak "T" number of T 3.0.

HP75 identified three modes of origin for the ST cyclone: (1) high-level origin from an upper cold low; (2) low-level origin from a frontal wave; and (3) low-level origin east of an upper-level trough but not on a front. Determining when a ST cyclone becomes a TC is not clearly defined by HP75, but one of the criteria in Table 3-31-1 would seem to be the most definitive: the ST cyclone cannot have its center under central dense overcast. If it does, it should be classified as tropical.

Colleen developed when an upper cold low that cut-off to the northwest of Hawaii — a "Kona" storm — moved southwestward and acquired persistent central deep convection. "Kona" storms are primarily a feature of the winter weather of Hawaii. Occurring from about late October to mid-April, they rarely become tropical cyclones. The "Kona" storm that became Colleen is a good example of the transition of a subtropical cyclone to a tropical cyclone — a rare event in the North Pacific Ocean.

IV. IMPACT

No reports of damage or injuries attributable to Tropical Storm Colleen were received at the JTWC.

Table 3-31-1. Similarities and differences between the Dvorak technique for tropical cyclones and the technique of Hebert and Poteat (1975) for subtropical cyclones as adapted from Table 3 in HP75.

SIMILARITIES

(1) Uses convective overcast.

(2) Uses distance of the low-level circulation center from the convective overcast.

(3) The ST number features and associated intensities are selected to correspond to observed current intensity numbers so that ST numbers merge to Dvorak's T numbers when the system becomes tropical.

DIFFERENCES

(1) ST technique considers the environment in determining type.

(2) A subtropical cyclone cannot have its low-level circulation center under central dense overcast.

(3) The ST technique adds translation speed excess above 20 kt to cloud feature wind estimate.

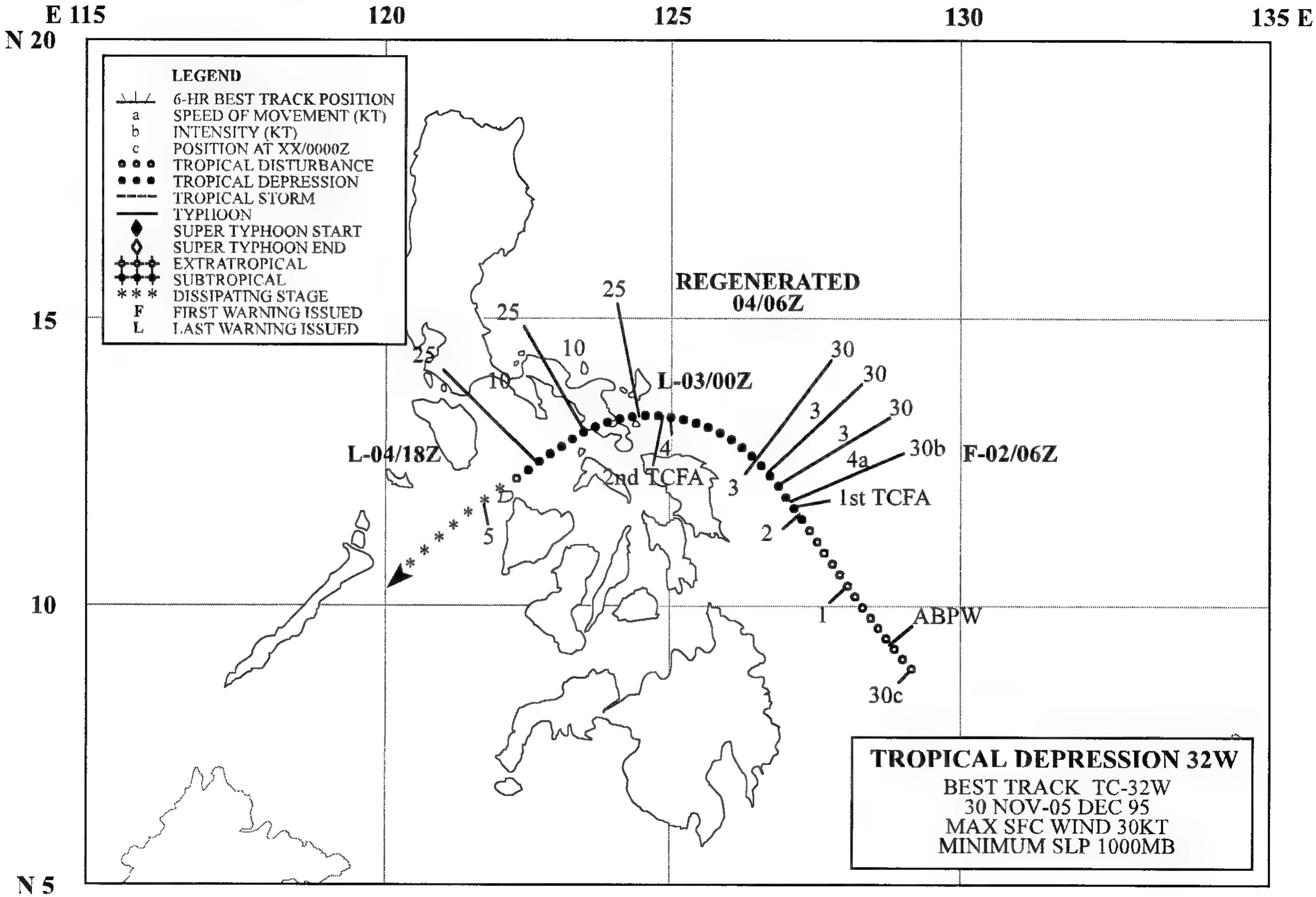
E 115
120
125
130
135 E
N 20
15
10
N 5
LEGEND
6-HR BEST TRACK POSITION
a SPEED OF MOVEMENT (KT)
b INTENSITY (KT)
c POSITION AT XX/0000Z
TROPICAL DISTURBANCE
TROPICAL DEPRESSION
TROPICAL STORM
TYPHOON
SUPER TYPHOON START
SUPER TYPHOON END
EXTRATROPICAL
SUBTROPICAL
DISSIPATING STAGE
F FIRST WARNING ISSUED
L LAST WARNING ISSUED
REGENERATED
04/06Z
L-03/00Z
L-04/18Z
F-02/06Z
1st TCFA
2nd TCFA
ABPW
30c
30b
4a
TROPICAL DEPRESSION 32W
BEST TRACK TC-32W
30 NOV-05 DEC 95
MAX SFC WIND 30KT
MINIMUM SLP 1000MB

TROPICAL DEPRESSION 32W

I. HIGHLIGHTS

Tropical Depression 32W (TD 32W) was originally treated as two separate tropical cyclones by the JTWC — TD 32W and TD 33W. The decision to combine the two tropical cyclones was based on a rigorous postanalysis. It is the first time since 1989, when Tropical Storm Ken and Tropical Storm Lola were designated as Tropical Storm Ken-Lola, that two tropical cyclones that were warned on separately have been subsequently designated as a single tropical cyclone. The after-the-fact designation of TD 32W and TD 33W as one system (i.e., TD 32W) underscores the difficulty that occasionally occurs in warning on poorly organized tropical cyclones. TD 32W developed east of Mindanao, tracked across southeastern Luzon near Legaspi, and dissipated in the Sulu Sea.

II. TRACK AND INTENSITY

The origin of Tropical Depression 32W can be traced to a tropical disturbance that formed on 30 November about 150 nm (280 km) east of Mindanao. The disturbance was first mentioned on the 300600Z November Significant Tropical Weather Advisory. For two days, the low-level circulation center (located on the west side of a 150 nm wide area of deep convection) moved slowly to the north-northwest. On 02 December, the deep convection appeared on satellite imagery to have become better organized and a Tropical Cyclone Formation Alert was issued at 020430Z. The first warning on TD 32W was issued, valid at 020600Z based on a satellite-derived intensity of 30 kt (15 m/sec). A Navy drifting buoy (WMO 52523) — the same one that survived an earlier nearby passage of Angela (29W) — recorded sustained southwest winds of 30 kt (15 m/sec) at 020300Z (Figure 3-32-1). TD 32W was forecast to recurve to the northeast and intensify. As the deep convection moved northward, however, it moved into a deformation zone along the shearline and appeared to split into two parts: one part moved to the northeast and the other part moved to the west (see the Discussion Section). The final warning on TD 32W was issued, valid at 030000Z, as the area of deep convection that was moving to the northeast along the shearline dissipated. In Figure 3-32-1, the track a-b-c shows the original working best track of TD 32W.

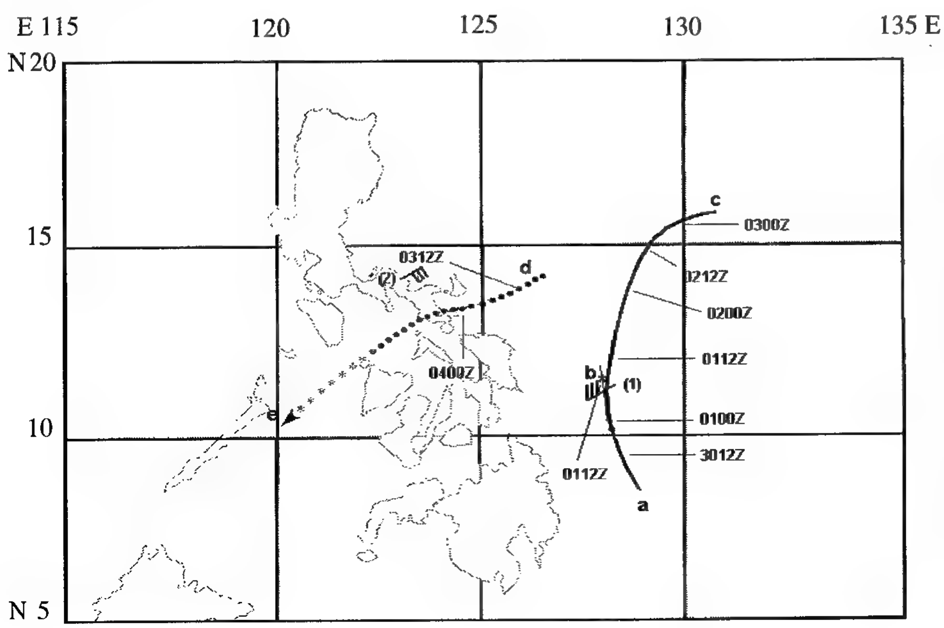

Figure 3-32-1 Working best track of the original TD 32W (indicated by the curved line labeled, a-b-c), and the working best track of the original TD 33W (indicated by the dotted line, d-e) are shown. Supporting synoptic observations shown are: (1) the wind from the Navy drifting buoy (WMO 52523) at 020300Z December, and (2) the wind observed at Daet (WMO 98440) at 040000Z December.

As convection associated with TD 32W dissipated, another area of deep convection was noted to its west and mentioned on the 030600Z December Significant Tropical Weather Advisory. A Tropical Cyclone Formation Alert was issued at 040030Z. The first warning on TD 33W was issued by the JTWC, valid at 040600Z. During the night of 04 December, the low-level circulation center of TD 33W (Figure 3-32-1) passed over the Bicol region of southern Luzon, where, earlier in the day, maximum sustained winds of 30 kt (15 m/sec) were observed at Daet (WMO 98440). The deep convection associated with the system decreased and the final warning was issued by the JTWC, as TD 33W moved into the northern Sulu Sea.

III. DISCUSSION

Rationale for combining TD 32W with TD 33W

Track a-b-c in Figure 3-32-1 was the working best track of the original TD 32W and track d-e was the working best track of the original TD 33W. Figure 3-32-2 illustrates the separation of convection into the two areas (labeled, x and y). Cloud system y (the area of deep convection that moved northeast along the shear line) was initially believed to contain a vertically coupled low-level cyclonic circulation (i.e., TD 32W). When cloud system x (the area of deep convection that moved to the west over the Philippines) showed signs of becoming better organized it was thought to be associated with a new low-level circulation center, and hence was warned on as TD 33W (Figure 3-32-3). A careful reexamination of synoptic data suggests that there was all along only one low-level circulation center throughout the period and that the motion of the masses of convection was not directly associated with the movement of the low-level circulation center.

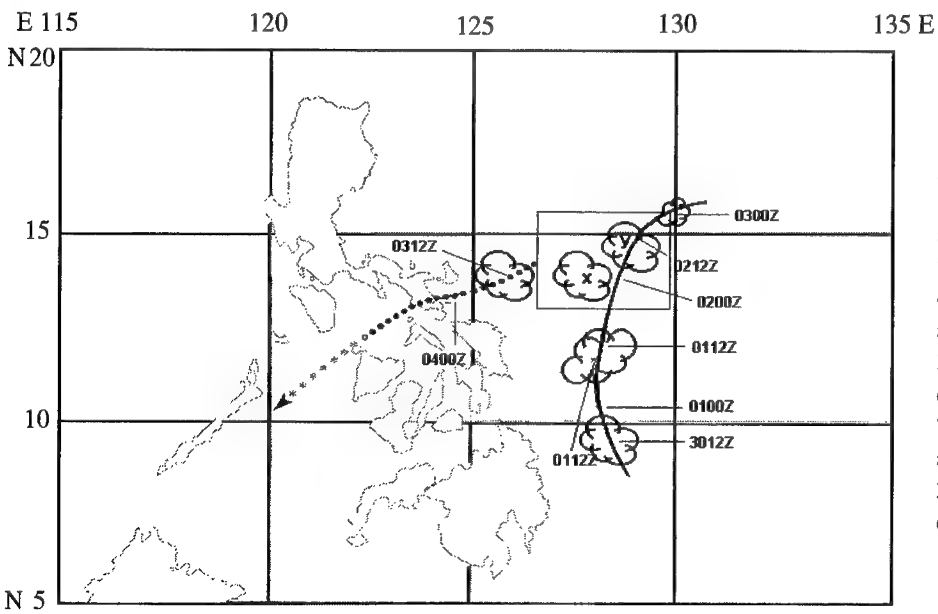

Figure 3-32-2 Schematic illustration of the movement and splitting of the mesoscale convective system (MCS) that was the original TD 32W into elements x and y. MCS "x" became TD 33W (working best track is indicated by the dotted line). MCS "y" was thought to have been associated with a recurving TD 32W (working best track is indicated by the solid line).

IV. IMPACT

At least 14 people were reported killed in floods and landslides in the Philippines. Twelve people were buried in a landslide that occurred at Viga, Catanduenas Island. The two others drowned in flooding at other villages of the Bicol region of southeastern Luzon.

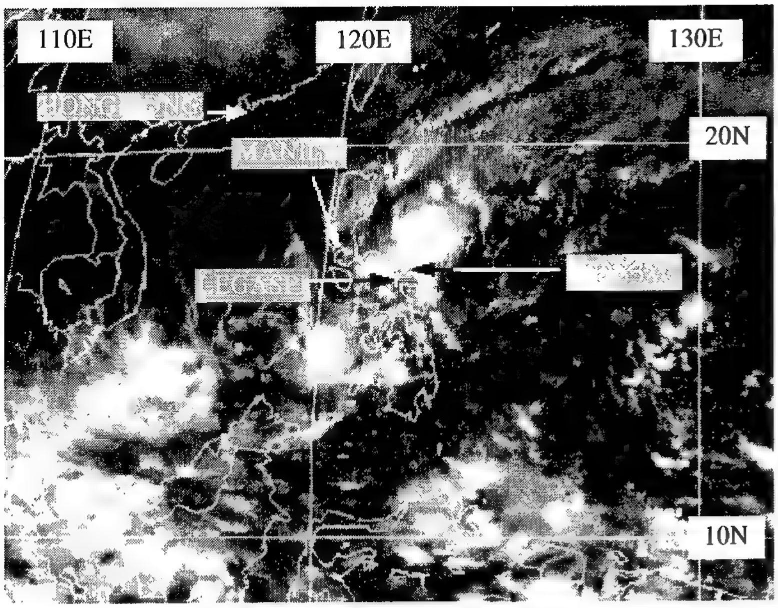

Figure 3-32-3 The deep convection associated with the original TD 33W (later combined with TD 32W) as it passes over southeastern Luzon near Legaspi (041233Z December infrared GMS imagery).

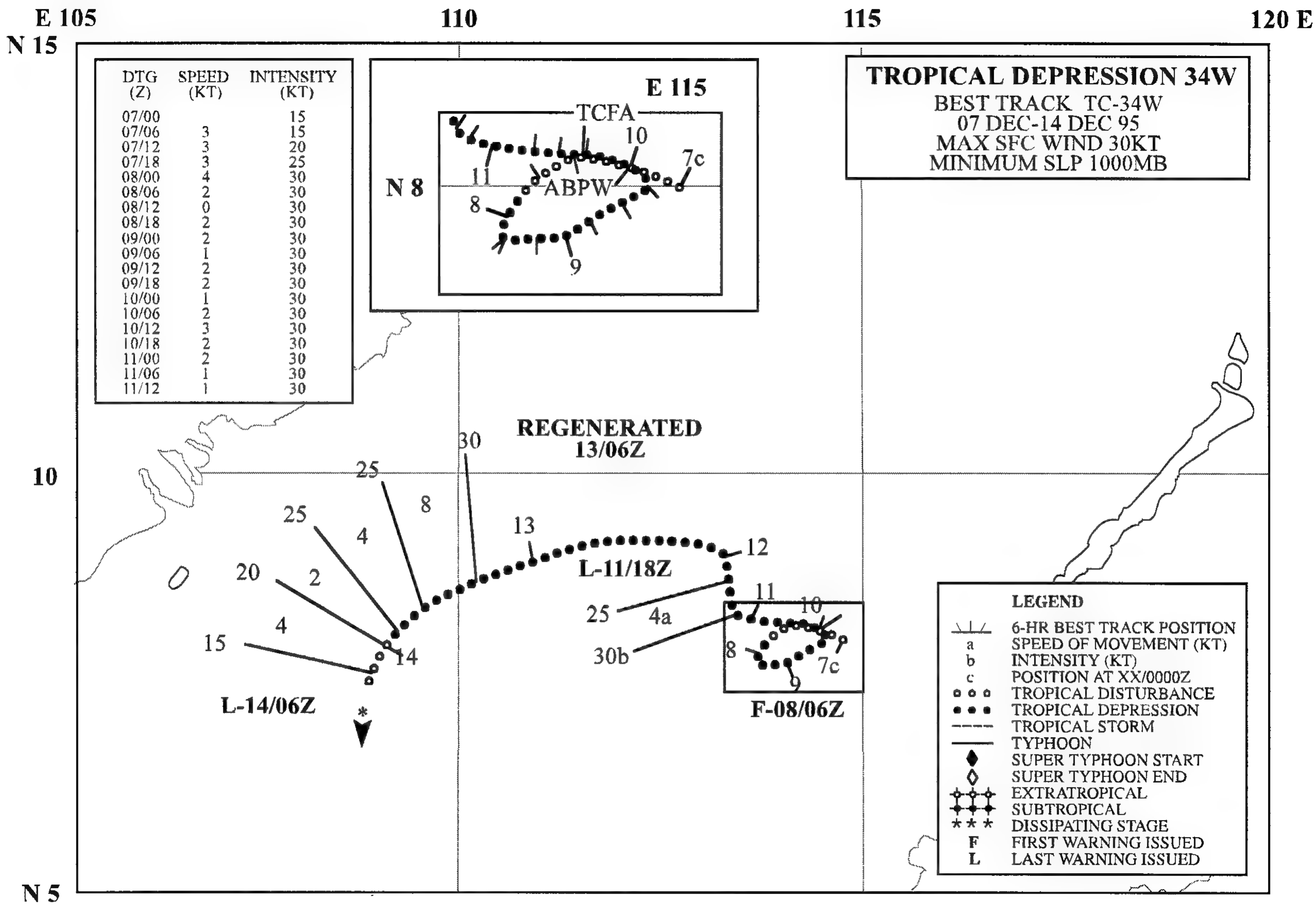

DTG (Z)	SPEED (KT)	INTENSITY (KT)
07/00		15
07/06	3	15
07/12	3	20
07/18	3	25
08/00	4	30
08/06	2	30
08/12	0	30
08/18	2	30
09/00	2	30
09/06	1	30
09/12	2	30
09/18	2	30
10/00	1	30
10/06	2	30
10/12	3	30
10/18	2	30
11/00	2	30
11/06	1	30
11/12	1	30

TROPICAL DEPRESSION 34W

Tropical Depression 34W was the second of three significant tropical cyclones that formed in the western North Pacific during December. It was first mentioned on the 070600Z December Significant Tropical Weather Advisory when satellite imagery and synoptic data showed that a low-level circulation center was associated with an area of persistent deep convection northwest of Borneo. As the deep convection became better organized, the JTWC issued a Tropical Cyclone Formation Alert, valid at 071130Z. Ship reports indicating wind speeds of 30 kt (15 m/sec) near the low-level circulation center prompted the JTWC to issue the first warning on Tropical Depression 34W, valid at 080600Z. Even higher wind speeds of 40 kt (21 m/sec) were occurring throughout much of the South China Sea to the north of TD 34W as a manifestation of a surge in the Northeast Monsoon.

Under normal conditions, a surge in the northeast monsoon flow of winter in the South China Sea accompanies a low-pressure system that becomes anchored off the northwest coast of Borneo — the so-called "Borneo low". Tropical cyclogenesis is not normally expected from a true Borneo low. In the case of TD 34W, however, the low-pressure area that formed to the northwest of Borneo was not a typical Borneo low, but rather, it formed from processes that produce tropical cyclone twins during times of enhanced equatorial westerly winds (Lander 1990). Tropical Depression 34W was the Northern Hemisphere twin to Tropical Cyclone Frank (03S) in the Southern Hemisphere (Figure 3-34-1a,b).

Whereas Frank (03S) recurved into northwestern Australia, TD 34W was constrained by the Northeast Monsoon to remain in the southern portion of the South China Sea for its entire life. For three days (08-11 December), the depression meandered in a small area about one degree of latitude square, centered near 8°N 114°E. During the night of 11 December, convection had subsided, and a "final" warning was issued, valid at 111800Z. The remnant low-level vortex drifted to the west during 12 December, and on 13 December, satellite imagery indicated that the system had regenerated, prompting the JTWC to reissue warnings commencing at 130600Z. The second final warning was issued by the JTWC, valid at 140600Z, as the system dissipated over water near 7°N 109°E.

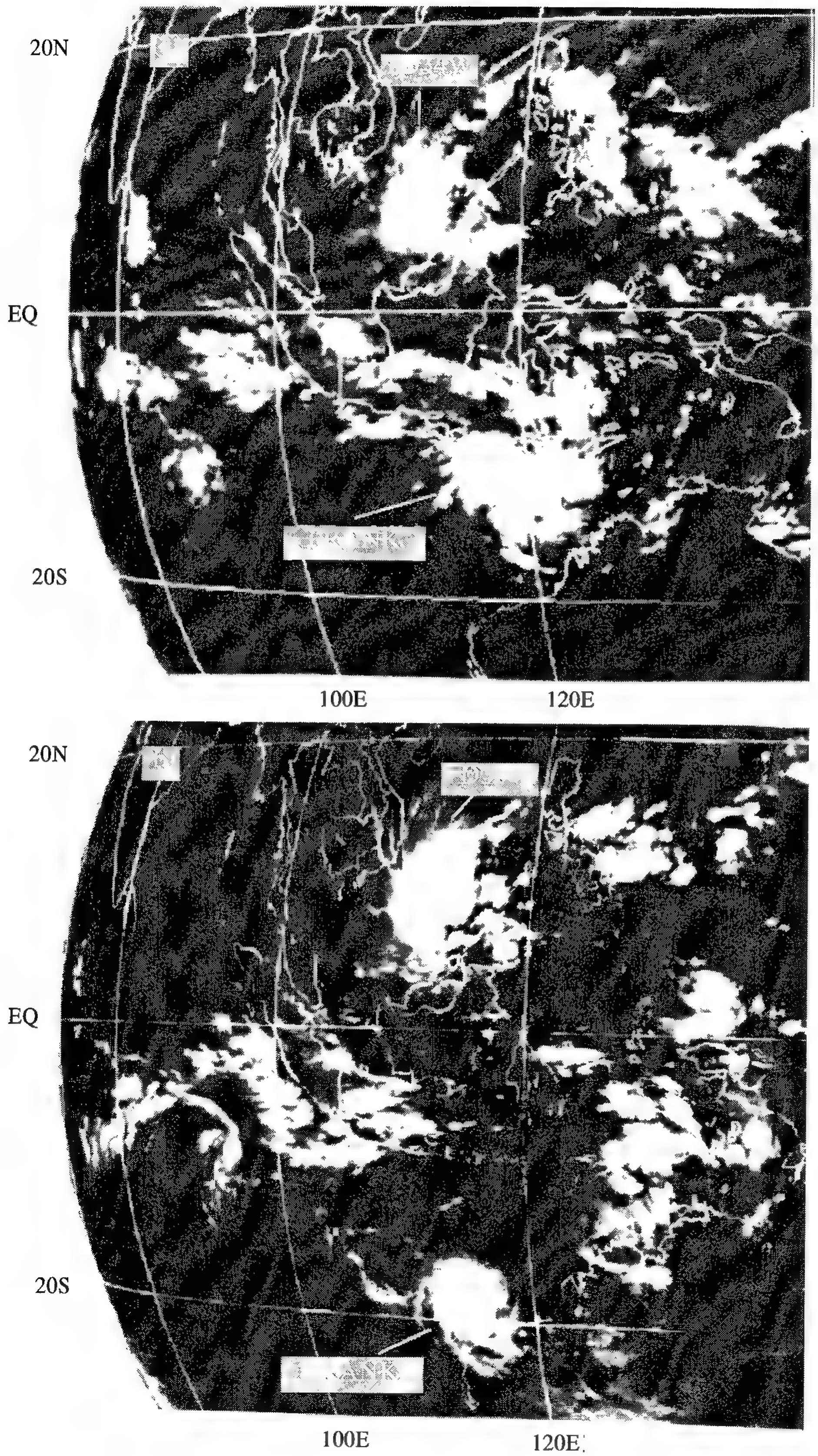

Figure 3-34-1 Tropical Depression 34W, and Tropical Cyclone Frank (03S) developed in tandem as tropical cyclone twins: (a) 070033Z December infrared GMS imagery, and (b) 100033Z December infrared GMS imagery).

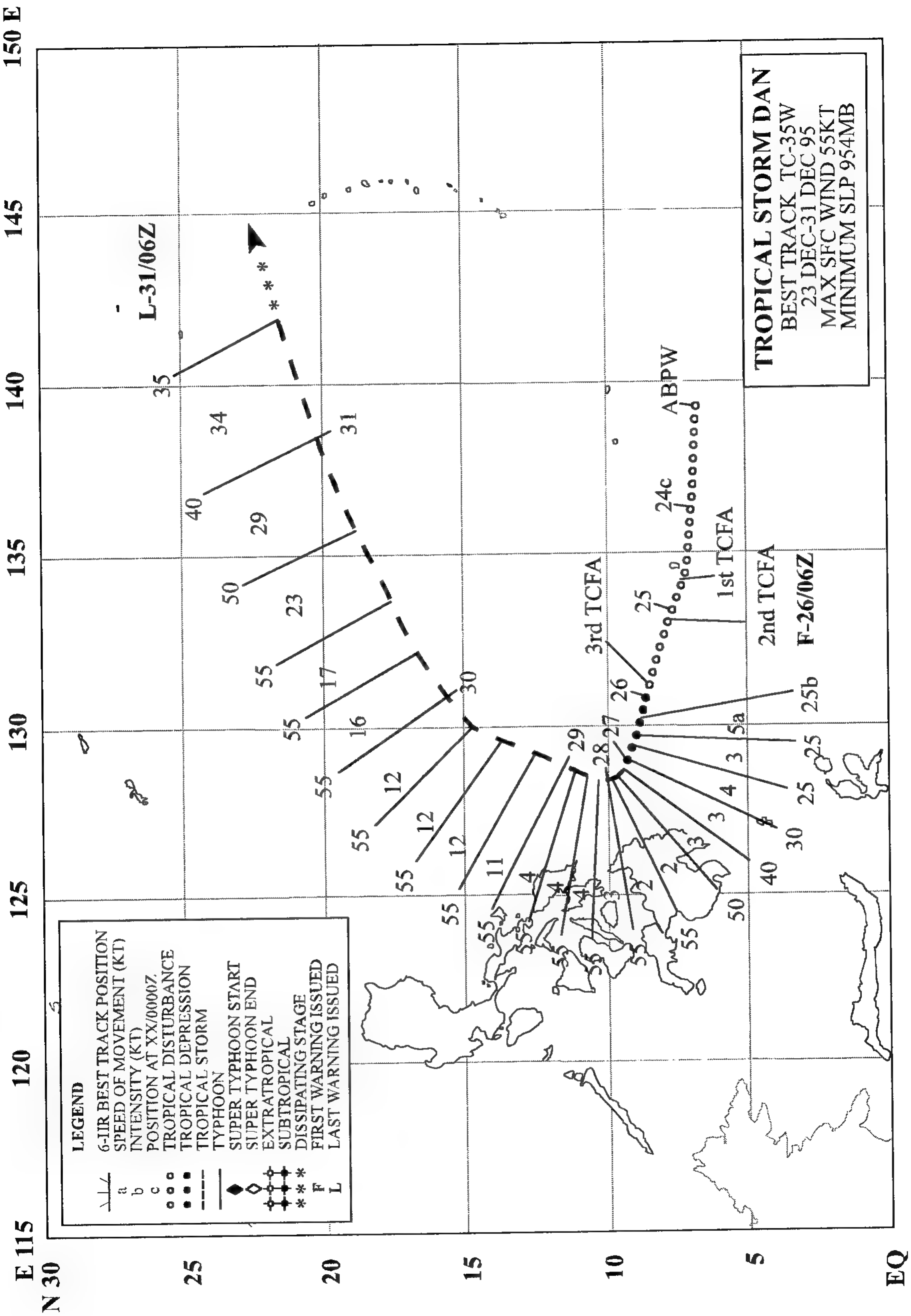

TROPICAL STORM DAN
BEST TRACK TC-35W
23 DEC-31 DEC 95
MAX SFC WIND 55KT
MINIMUM SLP 954MB
LEGEND
6-HR BEST TRACK POSITION
SPEED OF MOVEMENT (KT)
INTENSITY (KT)
POSITION AT XX/0000Z
TROPICAL DISTURBANCE
TROPICAL DEPRESSION
TROPICAL STORM
TYPHOON
SUPER TYPHOON START
SUPER TYPHOON END
EXTRATROPICAL
SUBTROPICAL
DISSIPATING STAGE
FIRST WARNING ISSUED
LAST WARNING ISSUED
L-31/06Z
F-26/06Z
ABPW
1st TCFA
2nd TCFA
3rd TCFA
E 115
120
125
130
135
140
145
150 E
N 30
25
20
15
10
5
EQ

TROPICAL STORM DAN (35W)

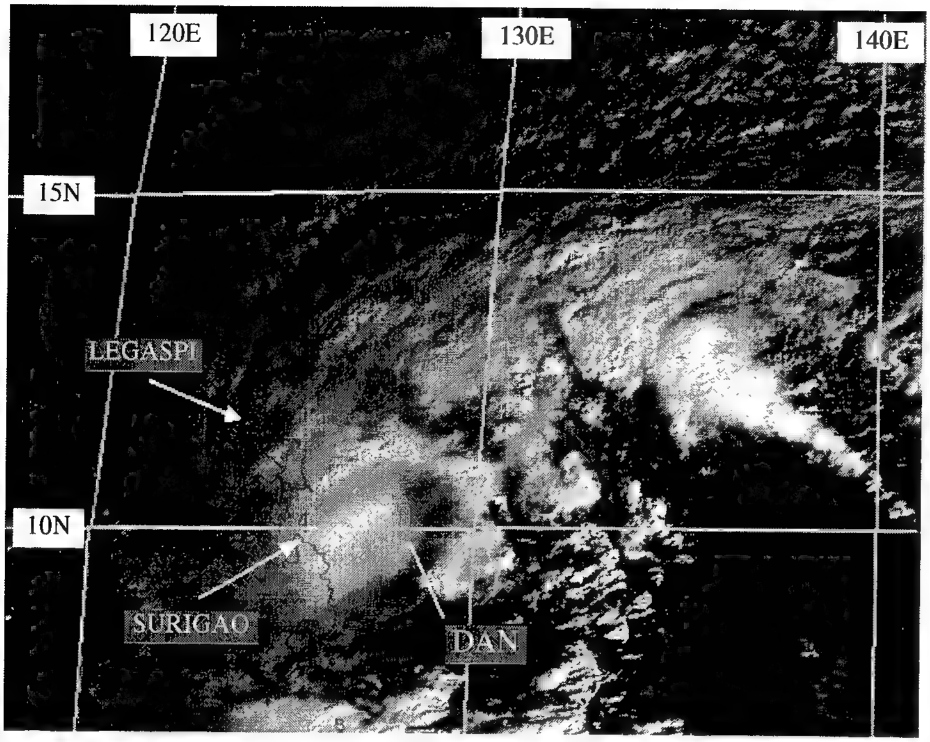

Figure 3-35-1 Tropical Storm Dan at peak intensity of 55 kt (28 m/sec). The low-level circulation center, located on the east side of the CDO, is obscured by dense cirrus (272331Z December visible GMS imagery).

I. HIGHLIGHTS

Dan was the last significant tropical cyclone to occur in the western North Pacific during 1995. Like many other tropical cyclones during 1995, Dan did not develop until it had tracked westward to near the Philippines. Tracking Dan by satellite was difficult because of its large cirrus canopy, obscuring its low-level circulation center. Microwave imagery from a DMSP satellite proved to be important in determining the location and structure of Dan.

II. TRACK AND INTENSITY

During December 1995, strong tradewinds dominated the tropics of the western North Pacific. A persistent tradewind convergence zone developed along 5°N, extending from 170°W to 140°E. Several tropical disturbances formed in the convergence zone and moved across the southern islands of Micronesia. These disturbances, coupled with the penetration of shear lines into low latitudes, produced heavier than normal rainfall across Guam and the Northern Mariana Islands. One of these disturbances, mentioned on the 230600Z December Significant Tropical Weather Advisory, became Tropical Storm Dan. The disturbance moved toward the west, but similar to the evolution of many other tropical cyclones during 1995 remained poorly organized until it moved west of 130°E. Between 241300Z and 260000Z, three Tropical Cyclone Formation Alerts were issued. On 26 December, the amount and organization of deep convection improved, prompting the JTWC to issue the first warning on Tropical Depression 35W (TD 35W), valid at 260600Z. With the development of persistent central deep convection, and extensive bands of deep convection to its north and east, satellite intensity estimates increased, and TD 35W was upgraded to Tropical Storm Dan on the 270600Z warning. Dan reached its peak intensity of 55 kt (28 m/sec) at 271800Z (Figure 3-35-1). At this time, Dan turned toward the north and

maintained its 55 kt (28 m/sec) intensity for the next 60 hours (271800Z to 301200Z). Early on 30 December, Dan began to accelerate toward the northeast. The final warning was issued on Dan, valid at 310600Z, when the system transitioned into an extratropical low and was moving to the northeast in excess of 30 kt (55 km/hr).

III. DISCUSSION

a. *Large positioning errors*

Tracking Dan by satellite was difficult because of its large central dense overcast (CDO), which obscured the low-level circulation center. Dan's low-level circulation center was sheared to the east of the center of its large cirrus canopy, but the amount of shear was not easily determined until the night of 28 December when microwave imagery (Figure 3-35-2) showed the large extent of the shear. The difference between the low-level circulation center inferred from infrared satellite imagery and that revealed beneath the cirrus canopy by microwave imagery at nearly the same time was over 100 nm (185 km). Average fix errors were over 74 nm (137 km) as compared to 29 nm (54 km) for all of 1995. Most of the fixes with large errors were significantly west of the actual location of the low-level circulation center. The large errors of the fixes led to a large average initial position error of 44 nm (82 km), with individual errors as high as 95 nm (176 km). Also, the large positioning errors resulted in larger than normal forecast track errors, especially for forecast periods less than 36 hours.

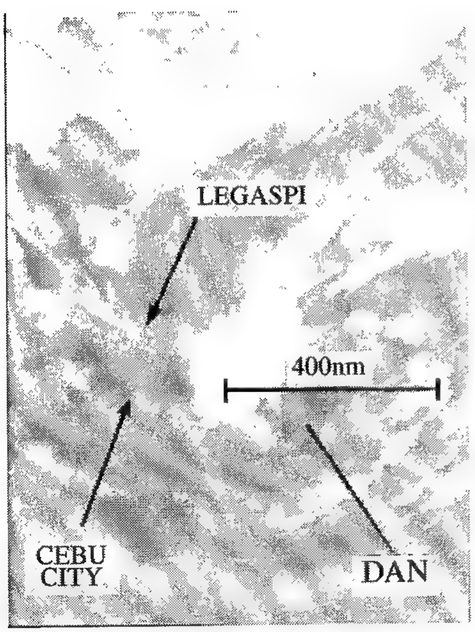

Figure 3-35-2 Microwave imagery acquired from the special sensor microwave/imager (SSM/I) reveals that the low-level circulation center of Dan is displaced to the southeast of the deep convection (281335Z December horizontally polarized 85 GHz microwave DMSP imagery). The low-level center was obscured by dense cirrus in conventional visible and infrared satellite imagery.

b. *Large wind asymmetries*

As Dan reached its closest point of approach to the Philippines and made its sharp turn to the north, a large area of gales formed in the Philippine Sea to Dan's north (Figure 3-35-3). Such large asymmetries are common when late-season tropical cyclones approach the Asian mainland where the sea-level pressure is very high. The high pressure over the Asian mainland is responsible for the northeast monsoon that occupies the South China Sea during the late fall and winter. Similar wind asymmetries were noted in the case of Tropical Depression 34W (see its summary).

IV. IMPACT

Dan caused heavy rain and high surf in northern and eastern Mindanao. Waves as high as 7 feet (2.1 m) destroyed some houses in Cagayan de Oro. Several thousand people in the region were evacuated because of high surf.

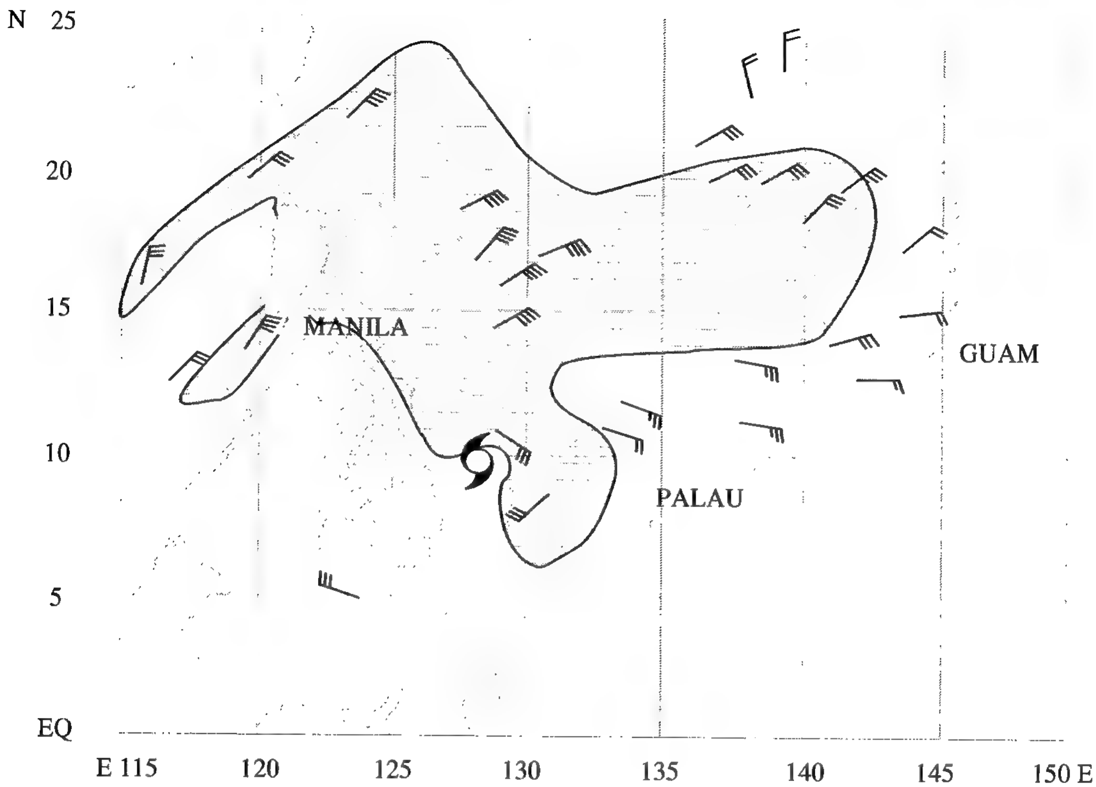

Figure 3-35-3 Ship reports and low-cloud velocities observed between 270600Z to 280000Z December reveal a large area of 30-40-kt (15-21-m/sec) winds (within the shaded area) to the north and northeast of Dan.

3.2 NORTH INDIAN OCEAN TROPICAL CYCLONES

In 1995, four significant tropical cyclones occurred in the North Indian Ocean. Three of these were in the Bay of Bengal and one in the Arabian Sea (Table 3-6). Spring and fall in the North Indian Ocean are periods of transition between major climatic controls, and the most favorable seasons for tropical cyclone activity. There is a tendency for the months of May and June to be less favored than the months of October, November and December (Table 3-7). The distribution in 1995, where all the tropical cyclones occurred in the fall, was unusual. For the 26-year record (1975-1995), this has only been noted in four years: 1980, 1981, 1983 and 1993.

The best track composite for 1995 is shown in Figure 3-14. The two most intense tropical cyclones were in November. They both recurved through the axis of the subtropical ridge.

Table 3-6 NORTH INDIAN OCEAN SIGNIFICANT TROPICAL CYCLONES FOR 1995

TROPICAL CYCLONE	PERIOD OF WARNING	NUMBER OF WARNINGS ISSUED	MAXIMUM SURFACE WINDS-KT (M/SEC)	ESTIMATED MSLP (MB)
01B	16 SEP - 17 SEP	4	45 (23)	991
02A	12 OCT - 17 OCT	22	50 (26)	987
03B	07 NOV - 09 NOV	11	70 (36)	972
04B	21 NOV - 25 NOV	17	105 (54)	938
	TOTAL	54		

The criteria used in Table 3-7 are as follows:

1. If a tropical cyclone was first warned on during the last two days of a particular month and continued into the next month for longer than two days, then that system was attributed to the second month.
2. If a tropical cyclone was warned on prior to the last two days of a month, it was attributed to the first month, regardless of how long the system lasted.
3. If a tropical cyclone began on the last day of the month and ended on the first day of the next month, that system was attributed to the first month. However, if a tropical cyclone began on the last day of the month and continued into the next month for only two days, then it was attributed to the second month.

TABLE 3-7LEGEND

Total for the month/year	4
Typhoons / Tropical Storms / Tropical Depressions	2 2 0

Table 3-7 DISTRIBUTION OF NORTH INDIAN OCEAN TROPICAL CYCLONES FOR 1975-1995

YEAR	JAN	FEB	MAR	APR	MAY	JUN	JUL	AUG	SEP	OCT	NOV	DEC	TOTALS
1975	1	0	0	0	2	0	0	0	0	1	2	0	6
	010	000	000	000	200	000	000	000	000	100	020	000	3 3 0
1976	0	0	0	1	0	1	0	0	1	1	0	1	5
	000	000	000	010	000	010	000	000	010	010	000	010	0 5 0
1977	0	0	0	0	1	1	0	0	0	1	0	2	5
	000	000	000	000	010	010	000	000	000	010	000	110	1 4 0
1978	0	0	0	0	1	0	0	0	0	1	2	0	4
	000	000	000	000	010	000	000	000	000	010	200	000	2 2 0
1979	0	0	0	0	1	1	0	0	2	1	2	0	7
	000	000	000	000	100	010	000	000	011	010	011	000	1 4 2
1980	0	0	0	0	0	0	0	0	0	0	1	1	2
	000	000	000	000	000	000	000	000	000	000	010	010	0 2 0
1981	0	0	0	0	0	0	0	0	1	0	1	1	3
	000	000	000	000	000	000	000	000	010	000	100	100	2 1 0
1982	0	0	0	0	1	1	0	0	0	2	1	0	5
	000	000	000	000	100	010	000	000	000	020	100	000	2 3 0
1983	0	0	0	0	0	0	0	1	0	1	1	0	3
	000	000	000	000	000	000	000	010	000	010	010	000	0 3 0
1984	0	0	0	0	1	0	0	0	0	1	2	0	4
	000	000	000	000	010	000	000	000	000	010	200	000	2 2 0
1985	0	0	0	0	2	0	0	0	0	2	1	1	6
	000	000	000	000	020	000	000	000	000	020	010	010	0 6 0
1986	1	0	0	0	0	0	0	0	0	0	2	0	3
	010	000	000	000	000	000	000	000	000	000	020	000	0 3 0
1987	0	1	0	0	0	2	0	0	0	2	1	2	8
	000	010	000	000	000	020	000	000	000	020	010	020	0 8 0
1988	0	0	0	0	0	1	0	0	0	1	2	1	5
	000	000	000	000	000	010	000	000	000	010	110	010	1 4 0
1989	0	0	0	0	1	1	0	0	0	0	1	0	3
	000	000	000	000	010	010	000	000	000	000	100	000	1 2 0
1990	0	0	0	1	1	0	0	0	0	0	1	1	4
	000	000	000	001	100	000	000	000	000	000	001	010	1 1 2
1991	1	0	0	1	0	1	0	0	0	0	1	0	4
	010	000	000	100	000	010	000	000	000	000	010	000	1 3 0
1992	0	0	0	0	1	2	1	0	1	3	3	2	13
	000	000	000	000	100	020	010	000	001	021	210	020	3 8 2
1993	0	0	0	0	0	0	0	0	0	0	2	0	2
	000	000	000	000	000	000	000	000	000	000	200	000	2 0 0
1994	0	0	1	1	0	1	0	0	0	1	1	0	5
	000	000	010	100	000	010	000	000	000	010	010	000	1 4 0
1995	0	0	0	0	0	0	0	0	1	1	2	0	4
	000	000	000	000	000	000	000	000	010	010	200	000	2 2 0
(1975-1995)													
MEAN	0.2	0.1	0.1	0.2	0.6	0.6	0.1	0.1	0.3	0.9	1.4	0.6	4.8
CASES	3	1	1	4	12	12	1	1	6	19	29	12	101

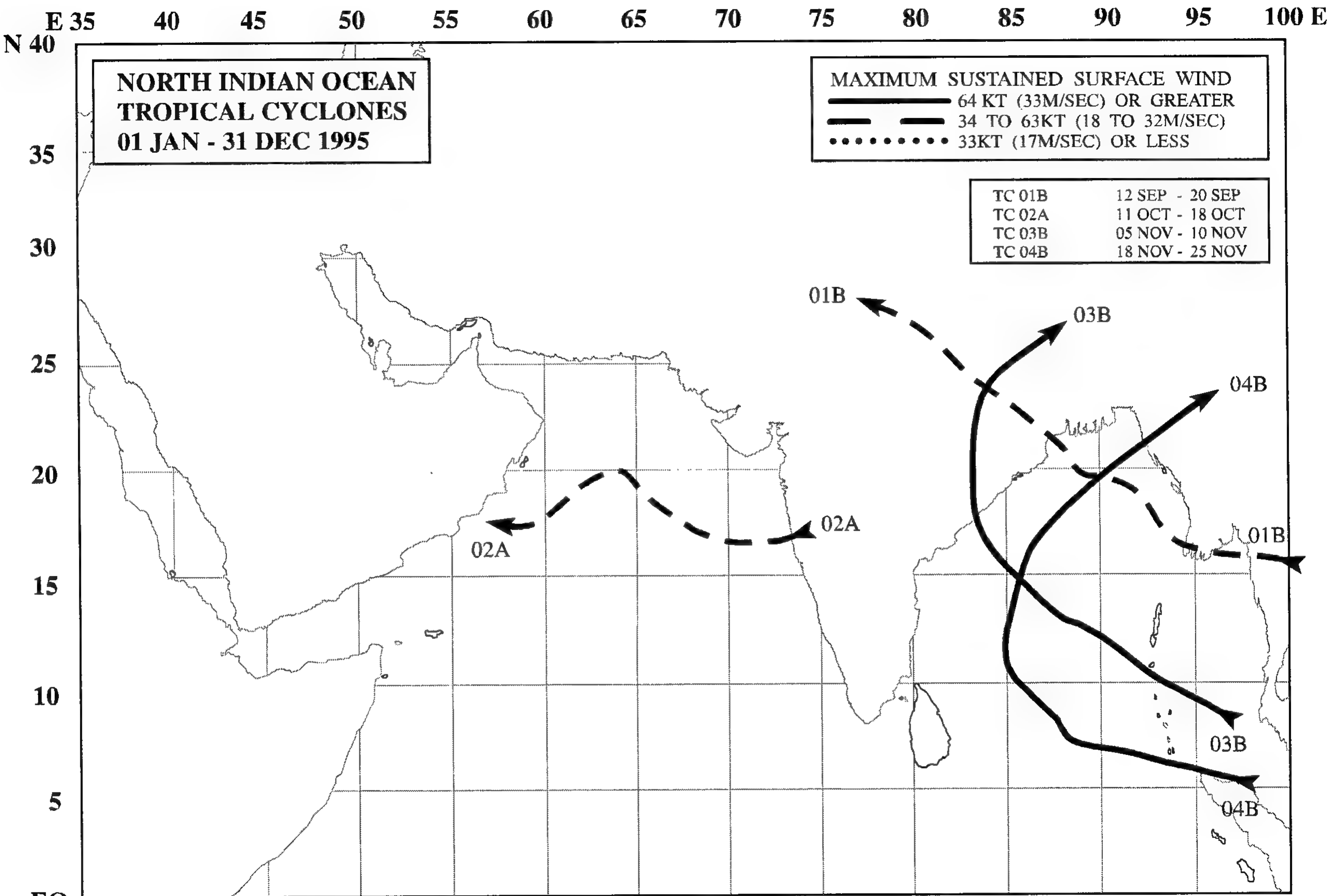

Figure 3-14 Composite of best tracks for North Indian Ocean tropical cyclones for 1995.

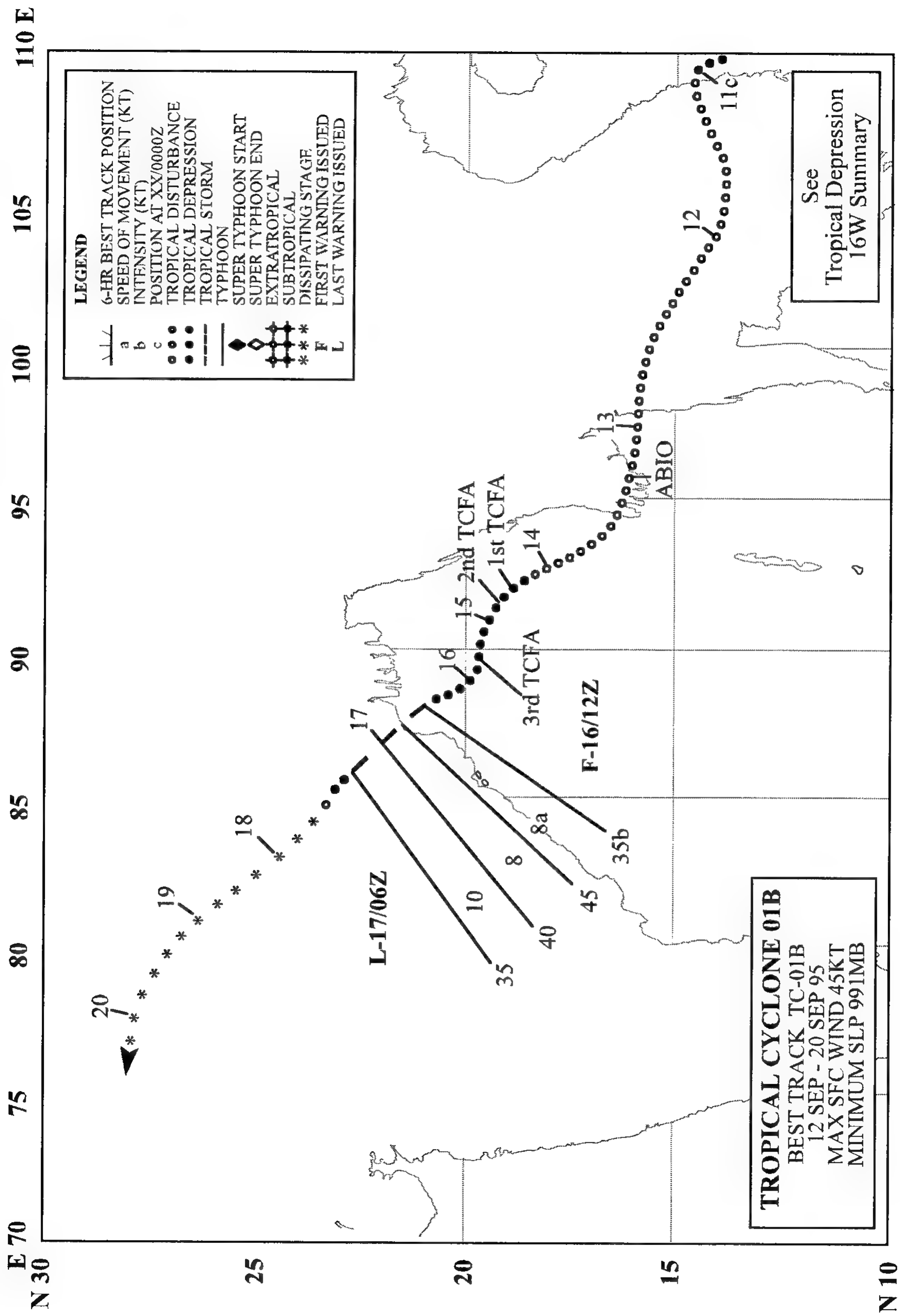
TROPICAL CYCLONE 01B
BEST TRACK TC-01B
12 SEP - 20 SEP 95
MAX SFC WIND 45KT
MINIMUM SLP 991MB
LEGEND
6-HR BEST TRACK POSITION
a SPEED OF MOVEMENT (KT)
b INTENSITY (KT)
c POSITION AT XX/0000Z
TROPICAL DISTURBANCE
TROPICAL DEPRESSION
TROPICAL STORM
TYPHOON
SUPER TYPHOON START
SUPER TYPHOON END
EXTRATROPICAL
SUBTROPICAL
DISSIPATING STAGE
F FIRST WARNING ISSUED
L LAST WARNING ISSUED
See
Tropical Depression
16W Summary
L-17/06Z
F-16/12Z
1st TCFA
2nd TCFA
3rd TCFA
ABIO
E 70
75
80
85
90
95
100
105
110 E
N 30
25
20
15
N 10

TROPICAL CYCLONE 01B

I. HIGHLIGHTS

Forming in September, Tropical Cyclone 01B was the North Indian Ocean's (NIO's) first significant tropical cyclone of 1995. For the second time in the past three years, a significant tropical cyclone did not occur until the fall transition season. Since 1975 this has only happened six times, while climatologically one to two cyclones develop during the April-June spring transition season.

II. TRACK AND INTENSITY

Tropical Cyclone 01B (TC01B) developed from the remnant vortex of Tropical Depression 16W (TD16W), a western North Pacific system that tracked from the South China Sea and across Vietnam and Southeast Asia between 11-13 September. Convection and upper-level divergent winds had been observed over the Andaman Sea and Bay of Bengal over this period — an environment that supported further development once the low-level circulation moved into this area.

The potential for redevelopment was first discussed on the 130600Z September Significant Tropical Weather Advisory when the vortex entered the NIO. As convective activity increased, the first of three Tropical Cyclone Formation Alerts (TCFAs) was issued, valid 140900Z. Two more TCFAs followed, valid at 141600Z and 151600Z, respectively. The system moved slowly northwestward across the Bay of Bengal. The 151600Z TCFA stated, in part: "The cyclonic circulation ... has taken on the appearance of a large monsoon depression and has yet to consolidate...".

The first warning, valid at 161200Z, was issued on TC01B when satellite imagery indicated that convection had concentrated about the low-level circulation center and that the system was intensifying. Six hours later, TC01B peaked in intensity at 45 kt (23 m/sec) — just prior to making landfall on the Indian coast, south of Calcutta (Figure 3-01B-1). The JTWC issued the final warning, valid 170600Z, as the tropical cyclone tracked slowly northwestward. The remnants of TC01B continued to track slowly to the northwest for the next several days before finally dissipating near Delhi on 20 September.

III. IMPACT

No reports of fatalities or significant damage were received at the JTWC.

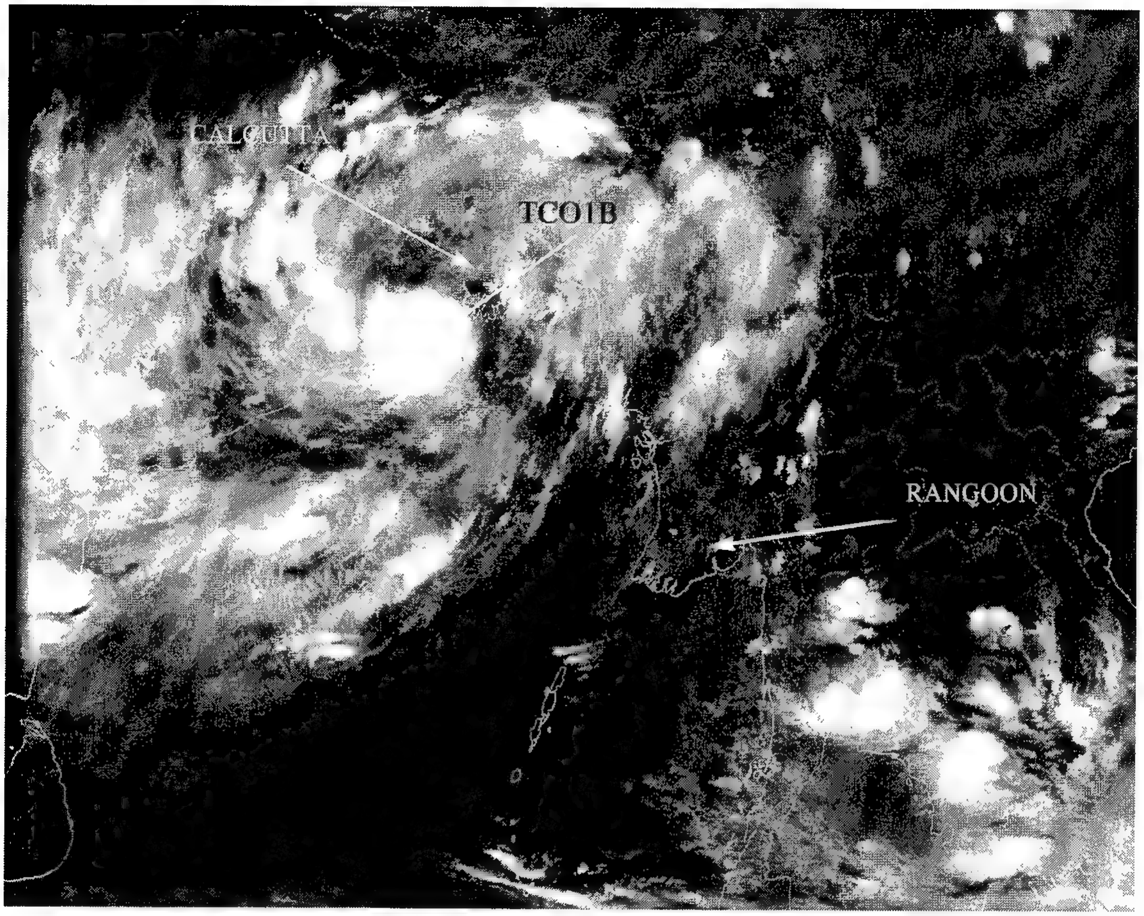

Figure 3-01B-1 Tropical Cyclone 01B at peak intensity of 45 kt (23 m/sec) (161406Z September infrared DMSP imagery).

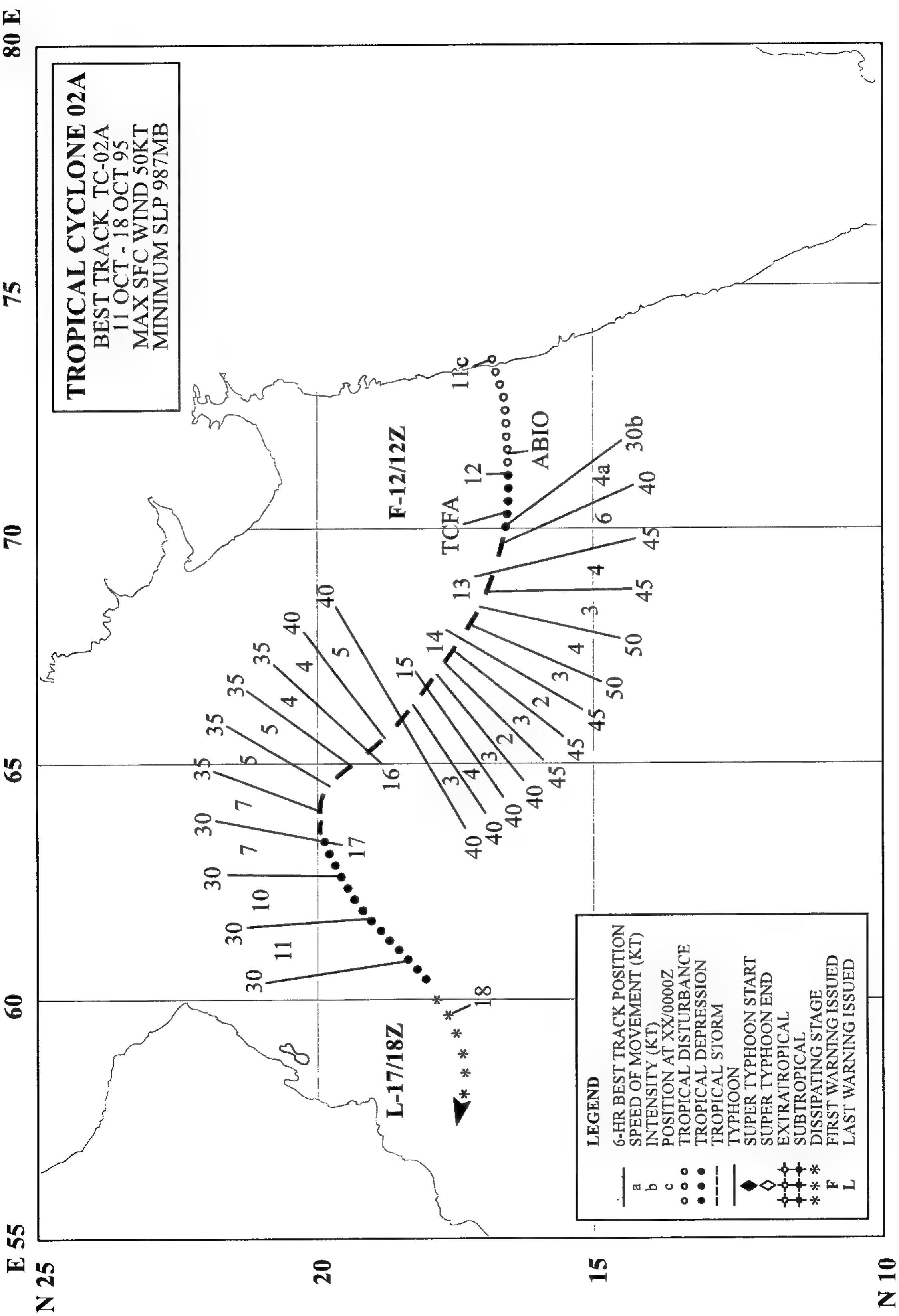
TROPICAL CYCLONE 02A
BEST TRACK TC-02A
11 OCT - 18 OCT 95
MAX SFC WIND 50KT
MINIMUM SLP 987MB
F-12/12Z
L-17/18Z
TCFA
ABIO
LEGEND
6-HR BEST TRACK POSITION
SPEED OF MOVEMENT (KT)
INTENSITY (KT)
POSITION AT XX/0000Z
TROPICAL DISTURBANCE
TROPICAL DEPRESSION
TROPICAL STORM
TYPHOON
SUPER TYPHOON START
SUPER TYPHOON END
EXTRATROPICAL
SUBTROPICAL
DISSIPATING STAGE
FIRST WARNING ISSUED
LAST WARNING ISSUED
N 25
20
15
N 10
E 55
60
65
70
75
80 E

TROPICAL CYCLONE 02A

The disturbance that became Tropical Cyclone 02A was first mentioned on the 111800Z October Significant Tropical Weather Advisory when a persistent surface circulation moved westward from India into the North Arabian Sea where it became better organized. When convective organization improved, a Tropical Cyclone Formation Alert was issued at 120500Z. The first warning followed, valid at 121200Z. The system moved west-northwestward and intensified for the next 36 hours, reaching a maximum intensity of 50 kt (26 m/sec) at 131200Z. The system began to weaken slowly thereafter, maintaining a generally northwestward track through 161200Z. Subjected to strong northeasterly vertical wind shear, the system continued to weaken. After the deep convection was sheared away, the low-level circulation center moved west and then southwest, and the system dissipated over water. The final warning was issued valid at 171800Z.

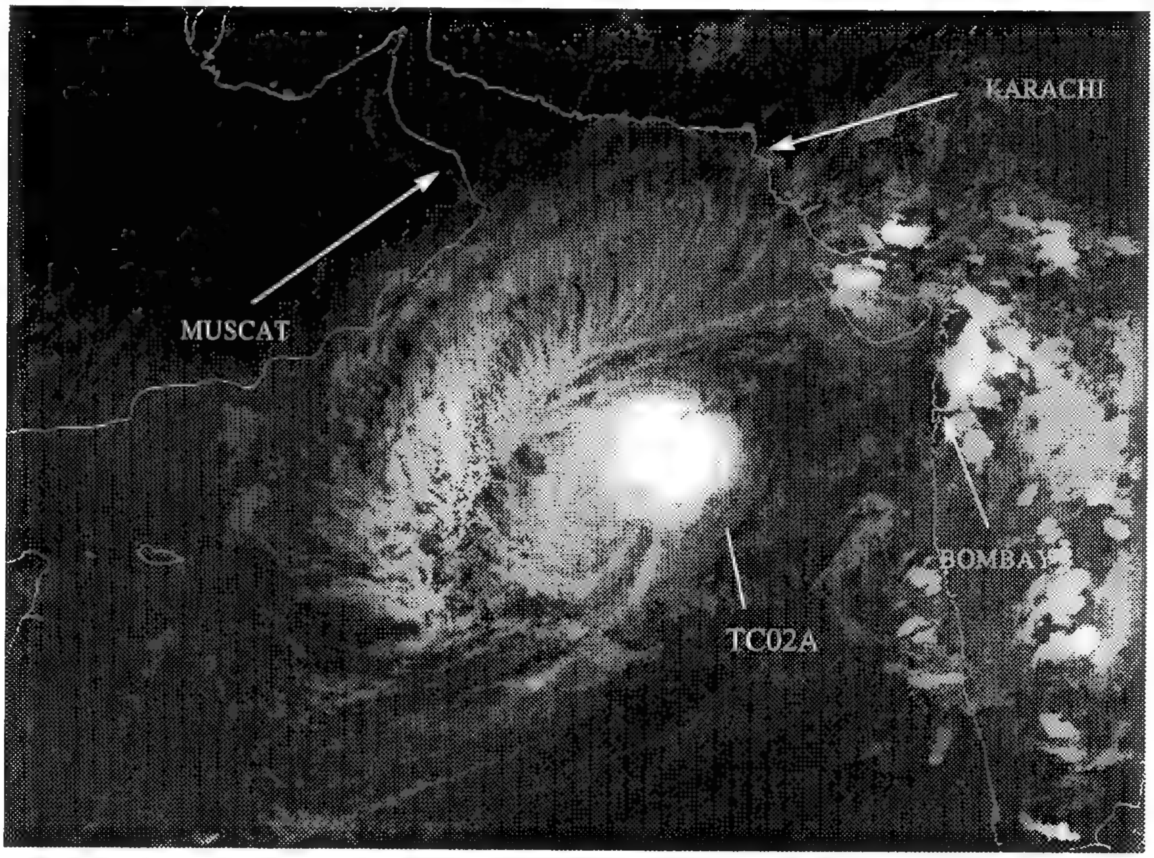

Figure 3-02A-1 Tropical Cyclone 02A at peak intensity of 50 kt (26 m/sec)(131216Z October infrared DMSP imagery).

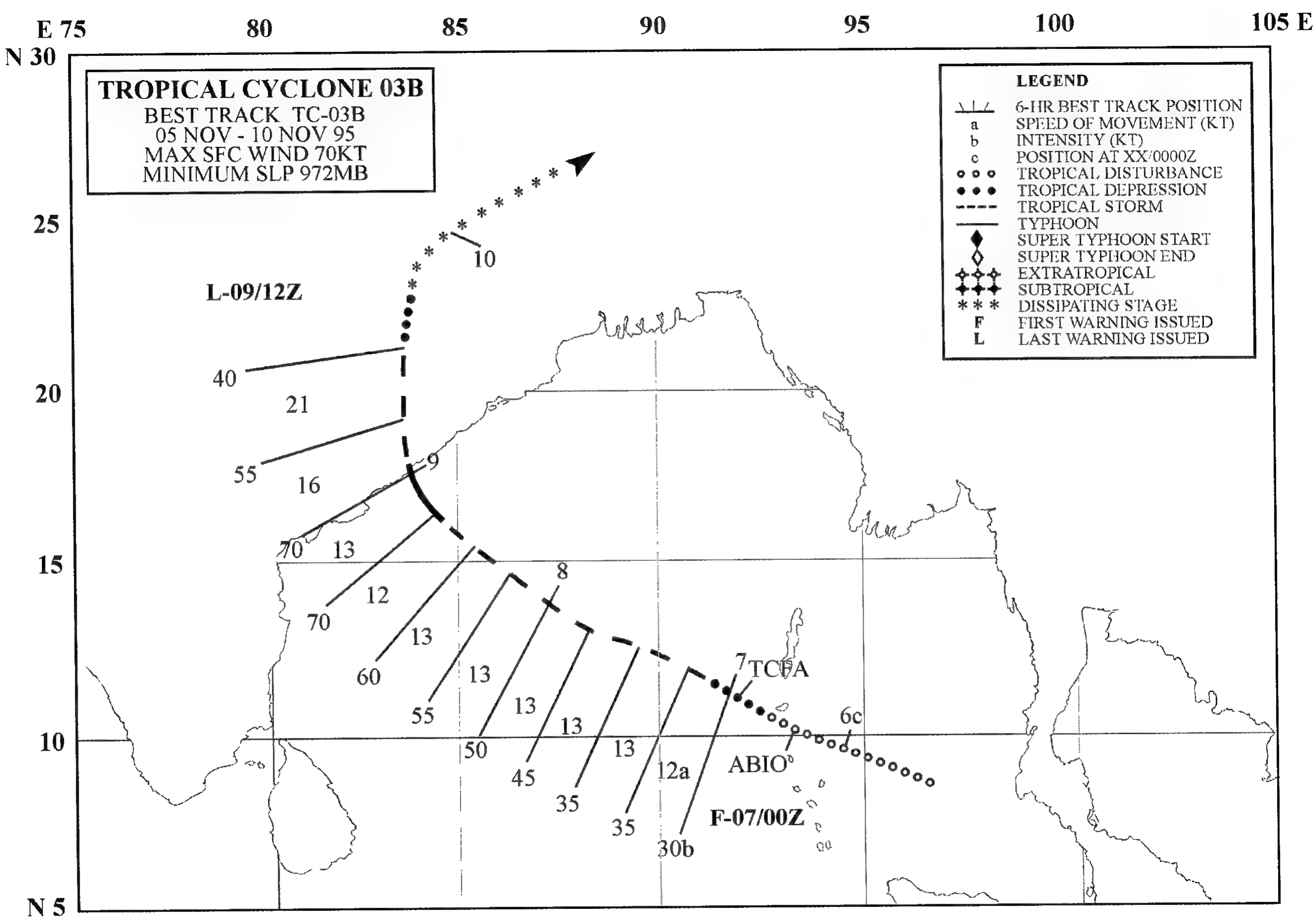

E 75
80
85
90
95
100
105 E
N 30
25
20
15
10
N 5
TROPICAL CYCLONE 03B
BEST TRACK TC-03B
05 NOV - 10 NOV 95
MAX SFC WIND 70KT
MINIMUM SLP 972MB
LEGEND
6-HR BEST TRACK POSITION
a SPEED OF MOVEMENT (KT)
b INTENSITY (KT)
c POSITION AT XX/0000Z
TROPICAL DISTURBANCE
TROPICAL DEPRESSION
TROPICAL STORM
TYPHOON
SUPER TYPHOON START
SUPER TYPHOON END
EXTRATROPICAL
SUBTROPICAL
DISSIPATING STAGE
F FIRST WARNING ISSUED
L LAST WARNING ISSUED
L-09/12Z
10
40
21
55
16
9
70
13
12
70
60
13
55
13
8
50
13
45
13
35
13
35
12a
30b
7
TCFA
6c
ABIO
F-07/00Z

TROPICAL CYCLONE 03B

I. HIGHLIGHTS

Tropical Cyclone 03B originated as a tropical disturbance on 05 November and reached peak intensity just prior to landfall on the east coast of India on 09 November. Its remnants induced heavy snowfall as this moist tropical system ascended the steep slopes of the Himalayan Mountains.

II. TRACK AND INTENSITY

Persistent convection associated with a low-level circulation, an estimated minimum sea-level pressure of 1002 mb, and a surge in the monsoon westerlies led to the re-issuance of the Significant Tropical Weather Advisory for the Indian Ocean at 061230Z November to include the tropical disturbance which developed into Tropical Cyclone 03B. A Tropical Cyclone Formation Alert was issued on this system at 062100Z, and the initial warning, valid at 070000Z, followed. Warnings on Tropical Cyclone 03B commenced while the system was still a tropical depression, but it soon intensified to 35 kt. The tropical cyclone continued to intensify as it tracked northwestward toward India, reaching a maximum intensity of 70 kt (36 m/sec) around 081800Z (Figure 3-03B-01). Minimum sea-level pressure is estimated at 972 mb just before the system made landfall near the city of Vishakhapatnam, India, just after 090000Z November.

Tropical Cyclone 03B weakened to tropical storm intensity as it moved inland and tracked northward. The final warning was issued, valid at 091200Z. The remnants of Tropical Cyclone 03B continued northward, and then northeastward, and moved up the mountain slopes of Nepal, at which point the weak circulation could no longer be tracked with satellite imagery or synoptic observations.

III. IMPACT

Tropical Cyclone 03B brought a fair amount of precipitation and cloud cover across the Bay of Bengal and adjoining land areas, but no significant damage as a result of the cyclone's passage were received at the JTWC. Casualties and property damage remain unknown. Quite evident, however, was the impact the remnants of this cyclone had over the Himalayan Mountains. The moist tropical clouds ascended the slopes, bringing heavy snowfall. At least 62 people were killed in avalanches and landslides along the bases of the mountains along Nepal's Goyko Valley. An additional 418 people were reported rescued from the area by helicopter. Snow accumulation of over 6 feet in eastern Nepal was reported.

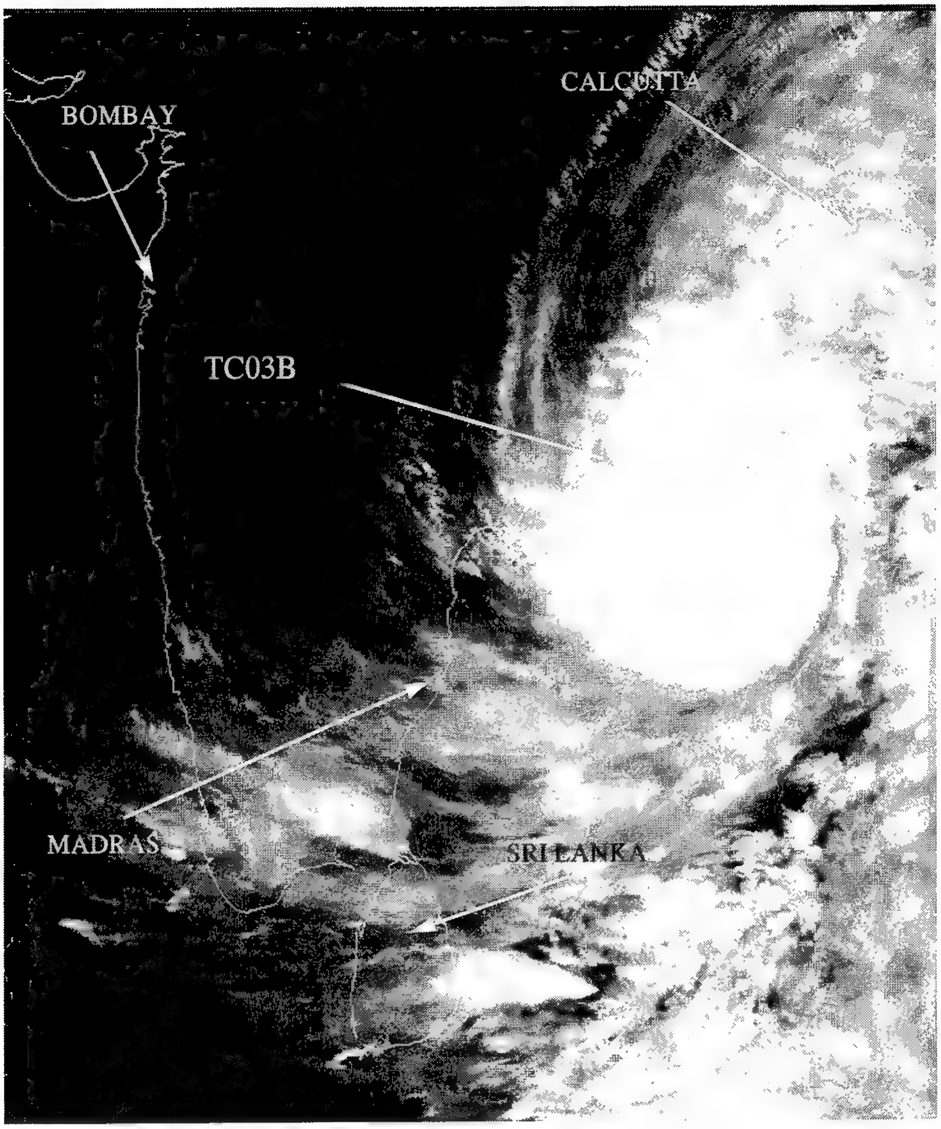

Figure 3-03B-1 Tropical Cyclone 03B heads for the coast of India with an intensity of 70 kt (36 m/sec) (081751Z November infrared DMSP imagery).

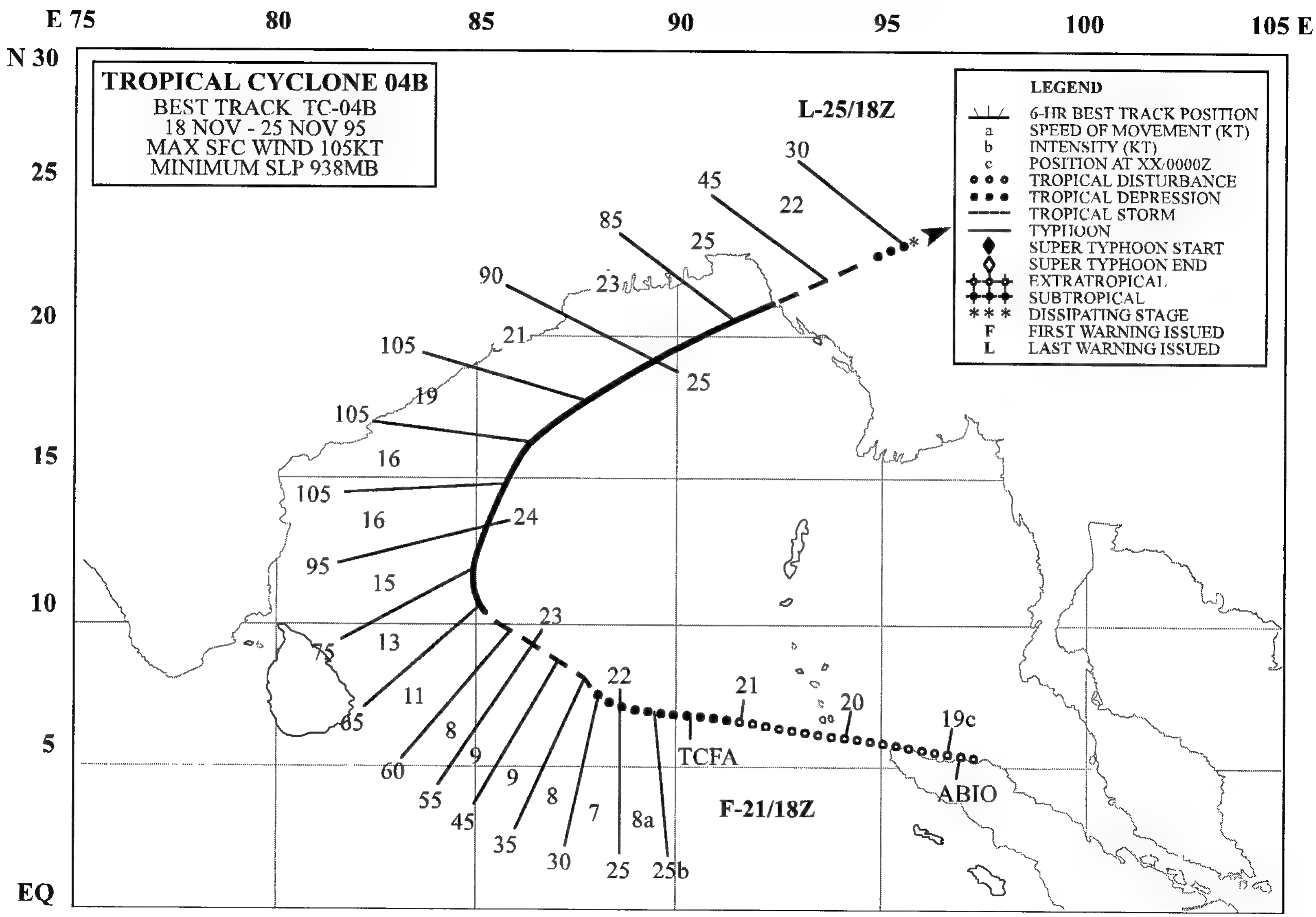

TROPICAL CYCLONE 04B
BEST TRACK TC-04B
18 NOV - 25 NOV 95
MAX SFC WIND 105KT
MINIMUM SLP 938MB
LEGEND
6-HR BEST TRACK POSITION
a SPEED OF MOVEMENT (KT)
b INTENSITY (KT)
c POSITION AT XX/0000Z
TROPICAL DISTURBANCE
TROPICAL DEPRESSION
TROPICAL STORM
TYPHOON
SUPER TYPHOON START
SUPER TYPHOON END
EXTRATROPICAL
SUBTROPICAL
DISSIPATING STAGE
F FIRST WARNING ISSUED
L LAST WARNING ISSUED
L-25/18Z
F-21/18Z
TCFA
ABIO
E 75
80
85
90
95
100
105 E
N 30
25
20
15
10
5
EQ

TROPICAL CYCLONE 04B

I. HIGHLIGHTS

Tropical Cyclone 04B was the most intense tropical cyclone in the North Indian Ocean during 1995. Its path was similar to Tropical Cyclone 02B of 1994, forming north of Sumatra, recurving, and making landfall near Cox's Bazar in Bangladesh.

II. TRACK AND INTENSITY

A flare up in the convection associated with the tropical disturbance that became Tropical Cyclone 04B was the reason for the reissuance of a Significant Tropical Weather Advisory at 182330Z November. A Tropical Cyclone Formation Alert was issued for the area of persistent convection at 211130Z, followed by a first warning, valid 211800Z. The tropical cyclone intensified rapidly, increasing two T-numbers a day from 220000Z [25 kt (13m/sec)] to 230000Z [55 kt (29 m/sec)], then one-and-a-half T-numbers a day from 230000Z to 240000Z [95 kt (49 m/sec)], reaching a maximum intensity of 105 kt (54 m/sec) by 240600Z. The 250600Z intensity prior to landfall was 85 kt (44 m/sec). The JTWC issued a final warning, valid at 251800Z, as Tropical Cyclone 04B's weakening low-level vortex dissipated over land.

III. IMPACT

Cox's Bazar reported 50 kt (26 m/sec) sustained winds and a 989.5 mb pressure at 250600Z — three hours before this cyclone swept across the coast. Press reports indicated nine people were killed and 300 were missing in the area. Monetary figures were not available for property damage incurred.

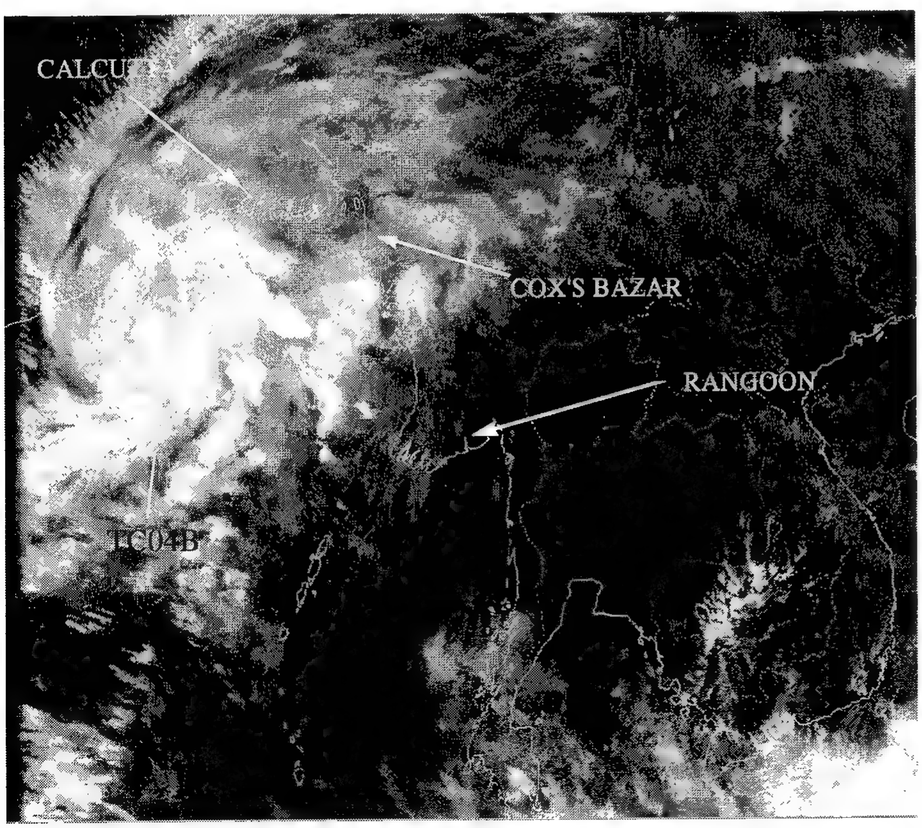

Figure 3-04B-1 The most intense cyclone in the North Indian Ocean in 1995, TC04B churns across the Bay of Bengal towards Bangladesh (241618Z November infrared DMSP imagery).

4. SUMMARY OF SOUTH PACIFIC AND SOUTH INDIAN OCEAN TROPICAL CYCLONES

4.1 GENERAL

On 1 October 1980, JTWC's area of responsibility (AOR) was expanded to include the Southern Hemisphere from 180° east longitude, westward to the coast of Africa. Details on Southern Hemisphere tropical cyclones and JTWC warnings from July 1980 through June 1982 are contained in Diercks et al. (1982) and from July 1982 through June 1984, in Wirfel and Sandgathe (1986). Information on Southern Hemisphere tropical cyclones after June 1984 can be found in the applicable Annual Tropical Cyclone Report.

The NAVPACMETOCCEN, Pearl Harbor, Hawaii issues warnings on tropical cyclones in the South Pacific, east of 180° east longitude. In accordance with CINCPACINST 3140.1W, Southern Hemisphere tropical cyclones are numbered sequentially from 1 July through 30 June. This convention is established to encompass the Southern Hemisphere tropical cyclone season, which primarily occurs from January through April. There are two Southern Hemisphere ocean basins for warning purposes - the South Indian (west of 135° east longitude) and the South Pacific (east of 135° east longitude) - which are identified by appending the suffixes "S" and "P," respectively, to the tropical cyclone number.

Intensity estimates for Southern Hemisphere tropical cyclones are derived from the interpretation of satellite imagery using the Dvorak (1984) technique and, when available, from surface observations and scatterometer data. The Dvorak technique relates specific cloud signatures to maximum sustained one-minute average surface wind speeds. The conversion from maximum sustained winds to minimum sea-level pressure is obtained from Atkinson and Holliday (1977) (Table 4-1).

4.2 SOUTH PACIFIC AND SOUTH INDIAN OCEAN TROPICAL CYCLONES

The total number of significant tropical cyclones during the 1995 season (1 July 1994 - 30 June 1995) (Table 4-2) was 22 which was five less than the overall climatological mean for the past 15 years as shown in Table 4-3. Looking at the annual variation of Southern Hemisphere Tropical Cyclones by ocean basins (Table 4-4), it becomes apparent that tropical cyclone activity was less than normal in all Southern Hemisphere basins in JTWC's AOR.

Table 4-1 MAXIMUN SUSTAINED 1-MINUTE MEAN SURFACE WINDS AND EQUIVALENT MINIMUM SEA LEVEL PRESSURE (ATKINSON AND HOLLIDAY, 1977) RELATIONSHIP

WIND-KT	(M/SEC)		PRESSURE (MB)
30	(15)	....	100
35	(18)	....	997
40	(21)	....	994
45	(23)	....	991
50	(26)	....	987
55	(28)	....	984
60	(31)	....	980
65	(33)	....	976
70	(36)	....	972
75	(39)	....	967
80	(41)	....	963
85	(44)	....	958
90	(46)	....	954
95	(49)	....	948
100	(51)	....	943
105	(54)	....	938
110	(57)	....	933
115	(59)	....	927
120	(62)	....	922
125	(64)	....	916
130	(67)	....	910
135	(69)	....	906
140	(72)	....	898
145	(75)	....	892
150	(77)	....	885
155	(80)	....	879
160	(82)	....	872
165	(85)	....	965
170	(87)	....	858
175	(90)	....	851
180	(93)	....	844

The JTWC was in warning status a total of 107 days, which included 22 days when warnings were issued on two or more Southern Hemisphere tropical cyclones. A chronology of the tropical cyclone activity is provided in Figure 4-1. Composites of the best tracks appear in Figures 4-2 and 4-3.

Table 4-2 SOUTH PACIFIC AND SOUTH INDIAN OCEAN SIGNIFICANT TROPICAL CYCLONES

TROPICAL CYCLONE		PERIOD OF WARNING	NUMBER OF WARNINGS ISSUED	ESTIMATED MAXIMUM SURFACE WINDS KT (M/SEC)	ESTIMATED MSLP (MB)
01P	VANIA	13 NOV - 17 NOV	10	55 (28)	984
02S	ALBERTINE	24 NOV - 01 DEC	17	115 (59)	927
03S	ANNETTE	15 DEC - 19 DEC	9	110 (57)	933
04P*	-----	15 DEC - 16 DEC	4*	35 (18)	997
05P*	WILLIAM	31 DEC - 03 JAN	7*	65 (33)	976
06S	BENTHA	03 JAN - 06 JAN	10	55 (28)	984
07S	CHRISTELLE	06 JAN - 09 JAN	6	40 (21)	994
08S	DORINA	20 JAN - 29 JAN	20	100 (57)	944
09S	FODAH	24 JAN - 26 JAN	6	45 (23)	990
10S	GAIL	05 FEB - 11 FEB	13	75 (39)	967
11S	HEIDA	05 FEB - 07 FEB	5	40 (21)	994
12S	BOBBY	21 FEB - 26 FEB	17	110 (57)	933
13S	INGRID	24 FEB - 01 MAR	12	100 (51)	944
14P	VIOLET	03 MAR - 07 MAR	11	75 (39)	967
15P	WARREN	05 MAR - 06 MAR	4	55 (28)	984
16S	JOSTA	07 MAR - 12 MAR	11	65 (33)	976
17S	KYLIE	07 MAR - 14 MAR	16	85 (44)	958
18P*	-----	16 MAR - 17 MAR	2*	30 (15)	1000
19S	MARLENE	30 MAR - 10 APR	36	125 (64)	916
20S	-----	03 APR - 05 APR	7	25 (13)	1002
21S	CHLOE	05 APR - 08 APR	14	125 (64)	916
22P	AGNES	17 APR - 22 APR	21	110 (57)	933
JTWC total			245		
Issued by NPMOC			13*		
Grand total			258		

* Warnings issued by NAVPACMETOCCEN (NPMOC)

Table 4-3 MONTHLY DISTRIBUTION OF SOUTH PACIFIC AND SOUTH INDIAN OCEAN TROPICAL CYCLONES

YEAR	JUL	AUG	SEP	OCT	NOV	DEC	JAN	FEB	MAR	APR	MAY	JUN	TOTAL
(1959-1978) AVERAGE*	-	-	-	0.4	1.5	3.6	6.1	5.8	4.7	2.1	0.5	-	24.7
1981	0	0	0	1	3	2	6	5	3	3	1	0	24
1982	1	0	0	1	1	3	9	4	2	3	1	0	25
1983	1	0	0	1	1	3	5	6	3	5	0	0	25
1984	1	0	0	1	2	5	5	10	4	2	0	0	30
1985	0	0	0	0	1	7	9	9	6	3	0	0	35
1986	0	0	1	0	1	1	9	9	6	4	2	0	33
1987	0	1	0	0	1	3	6	8	3	4	1	1	28
1988	0	0	0	0	2	3	5	5	3	1	2	0	21
1989	0	0	0	0	2	1	5	8	6	4	2	0	28
1990	2	0	1	1	2	2	4	4	10	2	1	0	29
1991	0	0	1	1	1	3	2	5	5	2	1	1	22
1992	0	0	1	1	2	5	4	11	3	2	1	0	30
1993	0	0	1	1	0	5	7	7	2	2	2	0	27
1994	0	0	0	0	2	4	8	4	9	3	0	0	30
1995	0	0	0	0	2	2	5	4	5	4	0	0	22
TOTAL	5	1	5	8	23	49	89	99	70	44	14	2	409
(1981-1995) AVERAGE	0.3	0.1	0.3	0.5	1.5	3.3	5.9	6.6	4.7	2.9	0.9	0.1	27.3

* (GRAY, 1979)

Table 4-4 ANNUAL VARIATION OF SOUTHERN HEMISPHERE TROPICAL CYCLONES BY OCEAN BASINS

YEAR	SOUTH INDIAN (WEST OF 105°E)	AUSTRALIAN (105°E - 165°E)	SOUTH PACIFIC (EAST OF 165°E)	TOTAL
(1959-1978) AVERAGE*	8.4	10.3	5.9	24.6
1981	13	8	3	24
1982	12	11	2	25
1983	7	6	12	25
1984	14	14	2	30
1985	14	15	6	35
1986	14	16	3	33
1987	9	8	11	28
1988	14	2	5	21
1989	12	9	7	28
1990	18	8	3	29
1991	11	10	1	22
1992	11	6	13	30
1993	10	16	1	27
1994	16	10	4	30
1995	11	7	4	22
TOTAL (1981-1995)	186	146	77	409
AVERAGE	12.4	9.7	5.1	27.3

* (GRAY,1979)

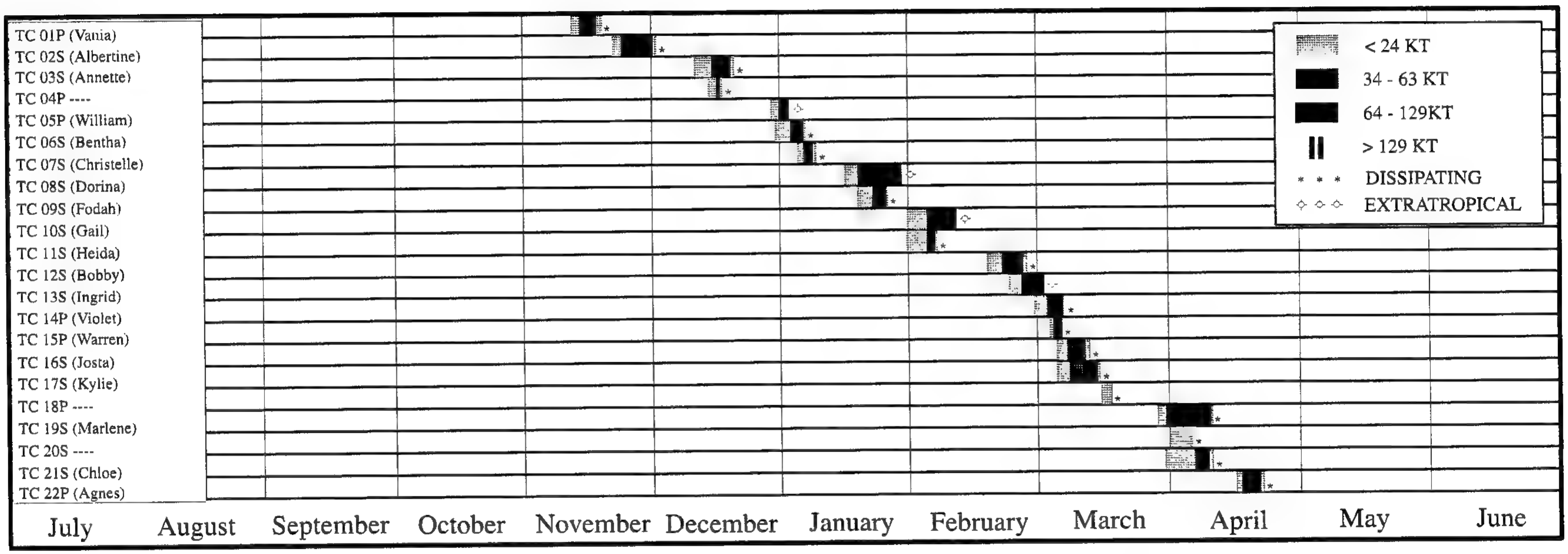

Figure 4-1 Chronology of South Pacific and South Indian Ocean tropical cyclones for 1995 (1 July 1994 - 30 June 1995).

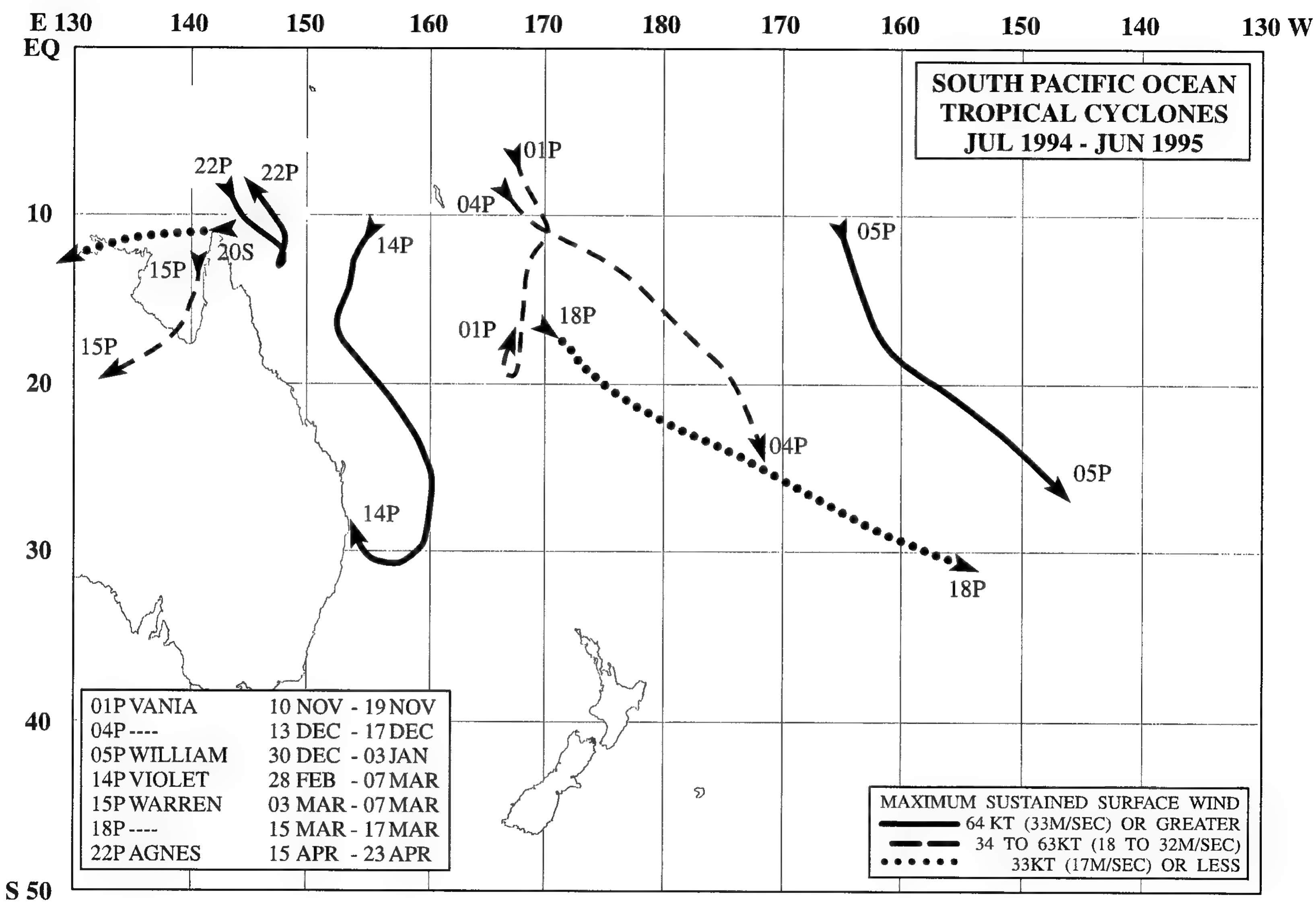

Figure 4-2 Tropical cyclone best tracks east of 130° east longitude.

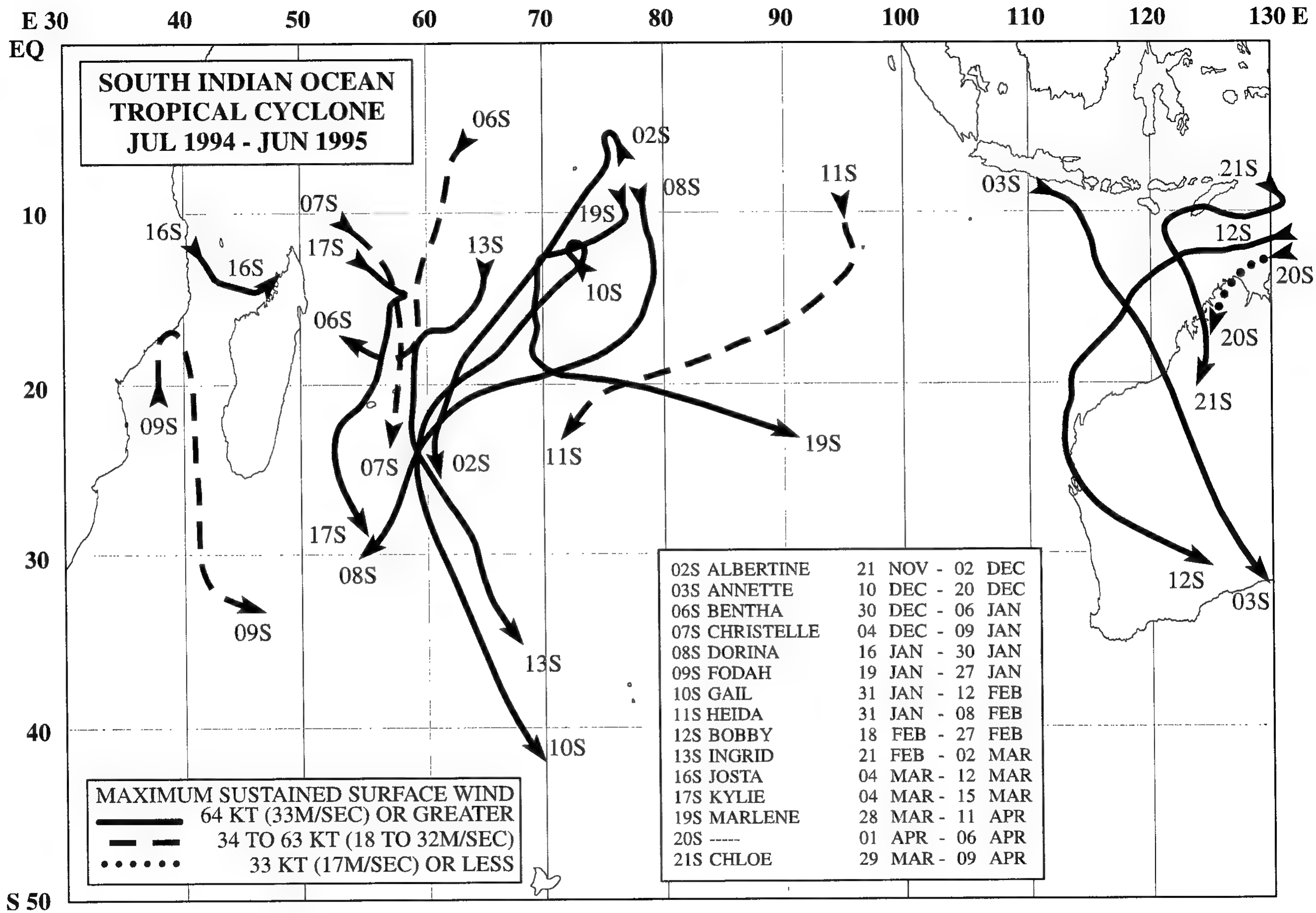

Figure 4-3 Tropical cyclone best tracks west of 130° east longitude.

5. SUMMARY OF FORECAST VERIFICATION

5.1 ANNUAL FORECAST VERIFICATION

Verification of warning positions and intensities at initial, 24-, 48- and 72-hour forecast periods was made against the final best track. The (scalar) track forecast, along-track and cross-track errors (illustrated in Figure 5-1) were calculated for each verifying JTWC forecast. These data, in addition to a detailed summary for each tropical cyclone, are included as Chapter 6. This section summarizes verification data for 1995 and contrasts it with annual verification statistics from previous years.

5.1.1 NORTHWEST PACIFIC OCEAN — The frequency distributions of errors for initial warning positions and 12-, 24-, 36-, 48- and 72-hour forecasts are presented in Figures 5-2a through 5-2f. Table 5-1 includes mean track, along-track and cross-track errors for 1978-1994. Figure 5-3 shows mean track errors and a 5-year running mean of track errors at 24-, 48- and 72-hours for the past 20 years. Table 5-2 lists annual mean track errors from 1959, when the JTWC was founded, until the present.

5.1.2 NORTH INDIAN OCEAN — The frequency distributions of errors for warning positions and 12-, 24-, 36-, 48- and 72-hour forecasts are presented in Figures 5-4a through 5-4f, respectively. Table 5-3 includes mean track, along-track and cross-track errors for 1978-1995. Figure 5-5 shows mean track errors and a 5-year running mean of track errors at 24-, 48- and 72-hours for the past 20 years.

5.1.3 SOUTH PACIFIC AND SOUTH INDIAN OCEANS — The frequency distributions of errors for warning positions and 12-, 24-, 36-, 48- and 72-hour forecasts are presented in Figures 5-6a through 5-6f, respectively. Table 5-4 includes mean track, along-track and cross-track errors for 1981-1995. Figure 5-7 shows mean track errors and a 5-year running mean of track errors at 24-, 48-, and 72-hours for the 15 years that the JTWC has issued warnings in the region.

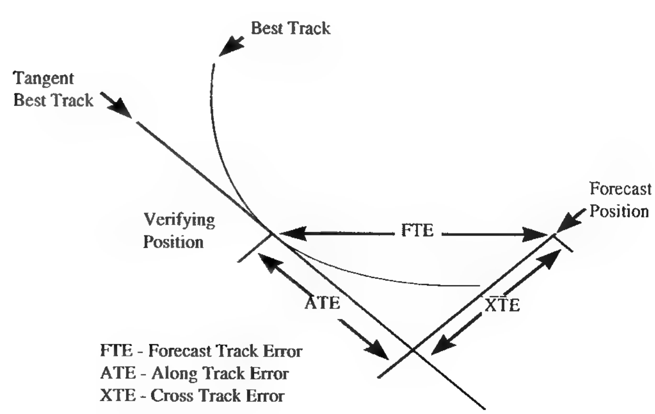

Figure 5-1 Definition of cross-track error (XTE), along-track error (ATE) and forecast track error (FTE). In this example, the XTE is positive (to the right of the best track) and the ATE is negative (behind or slower than the best track).

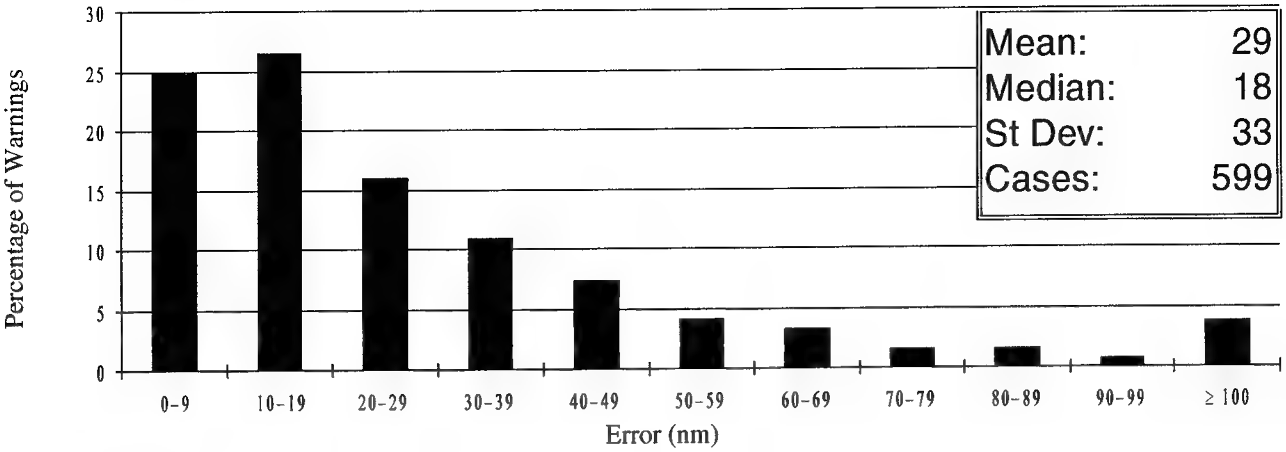

Figure 5-2a Frequency distribution of initial warning position errors (10-nm increments) for western North Pacific Ocean tropical cyclones in 1995. The largest error, 279 nm, occured on Tropical Depression 32W.

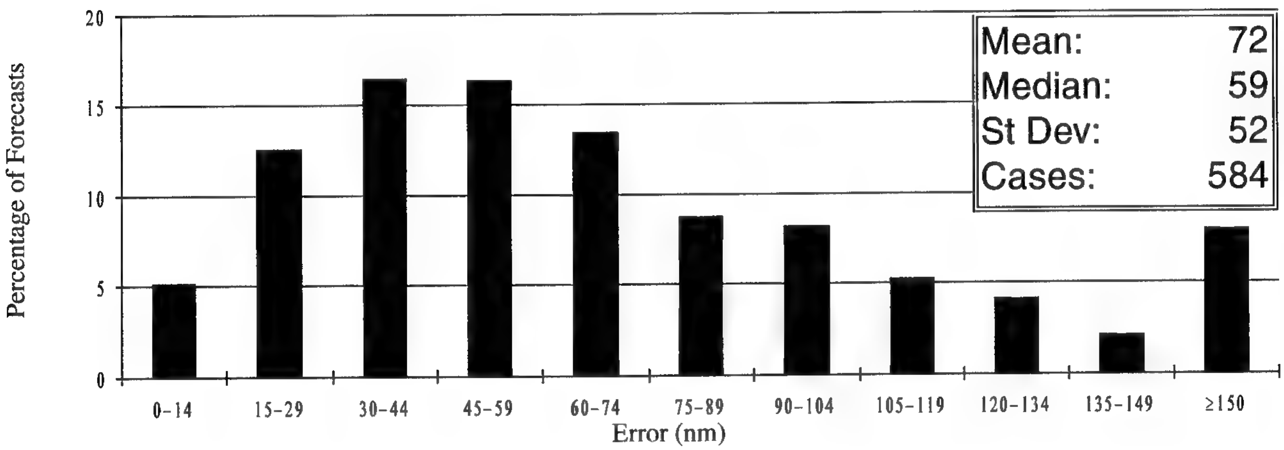

Figure 5-2b Frequency distribution of 12-hour track forecast errors (15-nm increments) for western North Pacific Ocean tropical cyclones in 1995. The largest error, 460 nm, occurred on Tropical Depression 32W.

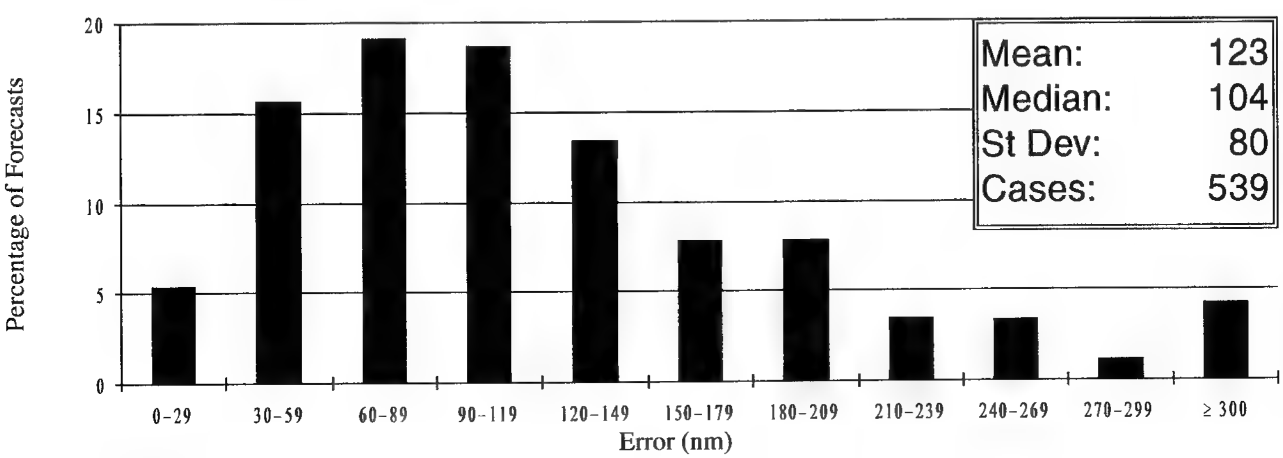

Figure 5-2c Frequency distribution of 24-hour track forecast errors (30-nm increments) for western North Pacific Ocean tropical cyclones in 1995. The largest error, 618 nm, occurred on Tropical Storm Deanna (03W).

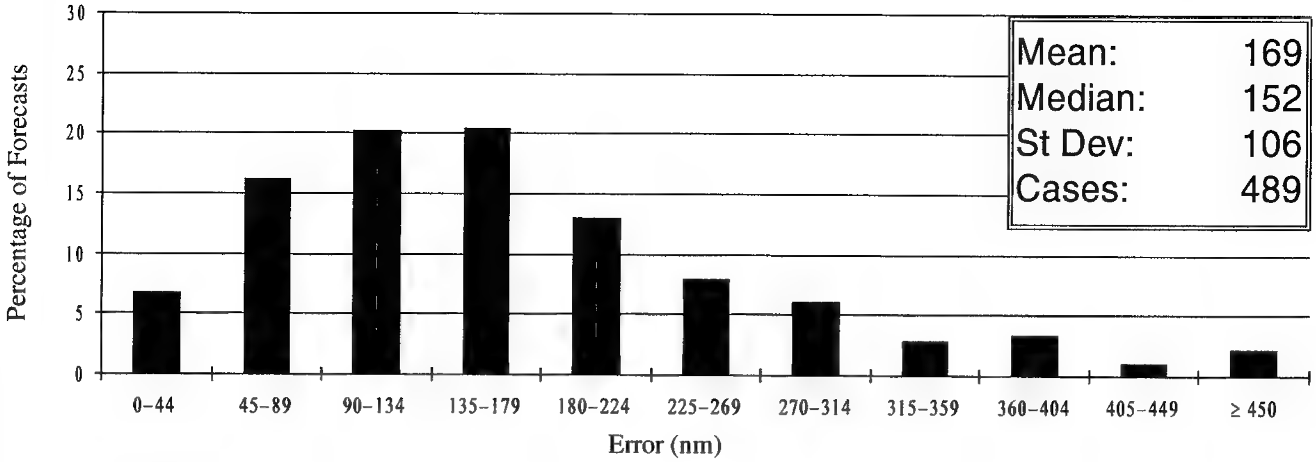

Figure 5-2d Frequency distribution of 36-hour track forecast errors (45-nm increments) for western North Pacific Ocean tropical cyclones in 1995. The largest error, 743 nm, occurred on Super Typhoon Ward (26W).

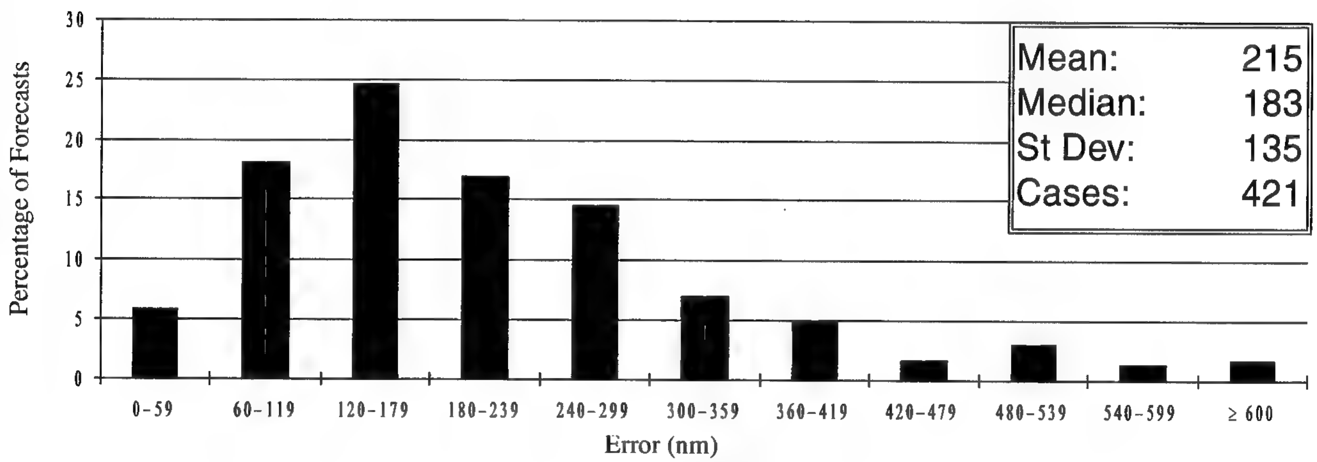

Figure 5-2e Frequency distribution of 48-hour track forecast errors (60-nm increments) for western North Pacific Ocean tropical cyclones in 1995. The largest error, 760 nm, occurred on Tropical Storm Val (25W).

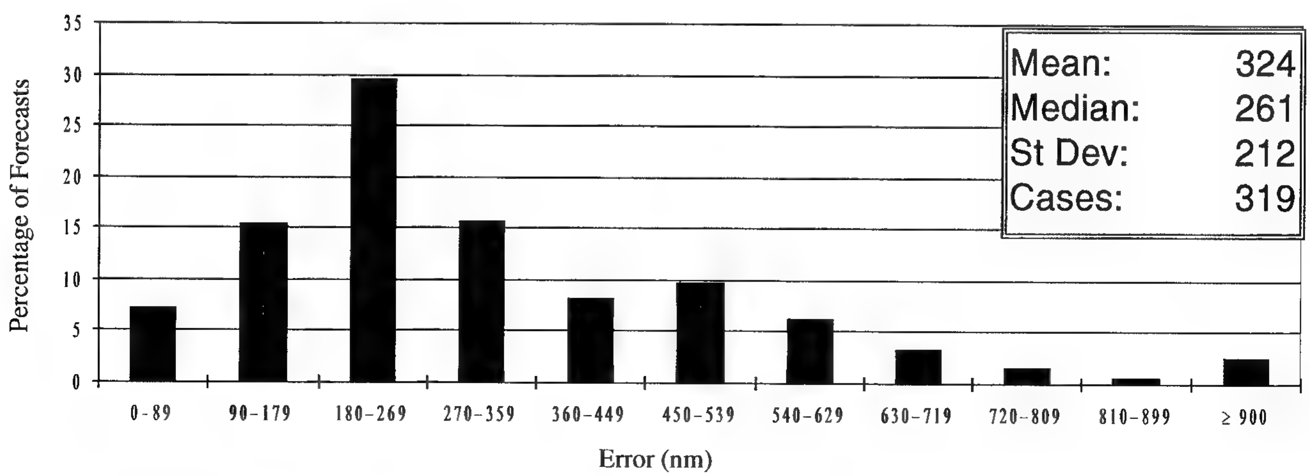

Figure 5-2f Frequency distribution of 72-hour track forecast errors (90-nm increments) for western North Pacific Ocean tropical cyclones in 1995. The largest error, 1386 nm, occurred on Tropical Storm Val (25W).

Table 5-1 INITIAL ~~WARNING POSITION AND FORECAST ERRORS (NM)~~ FOR THE WESTERN NORTH PACIFIC FOR 1981-1995.

	NUMBER OF	INITIAL	NUMBER OF	24-HOUR			NUMBER OF	48-HOUR			NUMBER OF	72-HOUR		
YEAR	WARNINGS	POSITION	FORECASTS	TRACK	ALONG	CROSS	FORECASTS	TRACK	ALONG	CROSS	FORECASTS	TRACK	ALONG	CROSS
1981	584	25	466	124	80	77	348	221	146	131	246	334	206	219
1982	786	19	666	113	74	70	532	238	162	142	425	342	223	211
1983	445	16	342	117	76	73	253	260	169	164	184	407	259	263
1984	611	22	492	117	84	64	378	232	163	131	286	363	238	216
1985	592	18	477	117	80	68	336	231	153	138	241	367	230	227
1986	743	21	645	126	85	70	535	261	183	151	412	394	276	227
1987	657	18	563	107	71	64	465	204	134	127	389	303	198	186
1988	465	23	373	114	85	58	262	216	170	103	183	315	244	159
1989	710	20	625	120	83	69	481	231	162	127	363	350	265	177
1990	794	21	658	103	72	60	525	203	148	110	432	310	225	168
1991	835	22	733	96	69	53	599	185	137	97	484	287	229	146
1992	941	25	841	107	77	59	687	205	143	116	568	305	210	172
1993	853	26	725	112	79	63	570	212	151	117	437	321	226	173
1994	1058	24	932	98	85	62	753	176	158	105	608	242	218	144
1995	599	29	539	123	89	67	421	215	159	117	319	325	240	167
15-YEAR AVERAGE														
1981-1995	709	22	605	113	79	65	466	219	162	125	372	331	232	190

Note: Cross-track and along -track errors were adopted by the JTWC in 1986. Right-angle errors (used prior to 1986) were recomputed as cross-track and along-track errors after-the-fact to extend the data base. See Figure 5-1 for the definitions of cross-track and along-track errors.

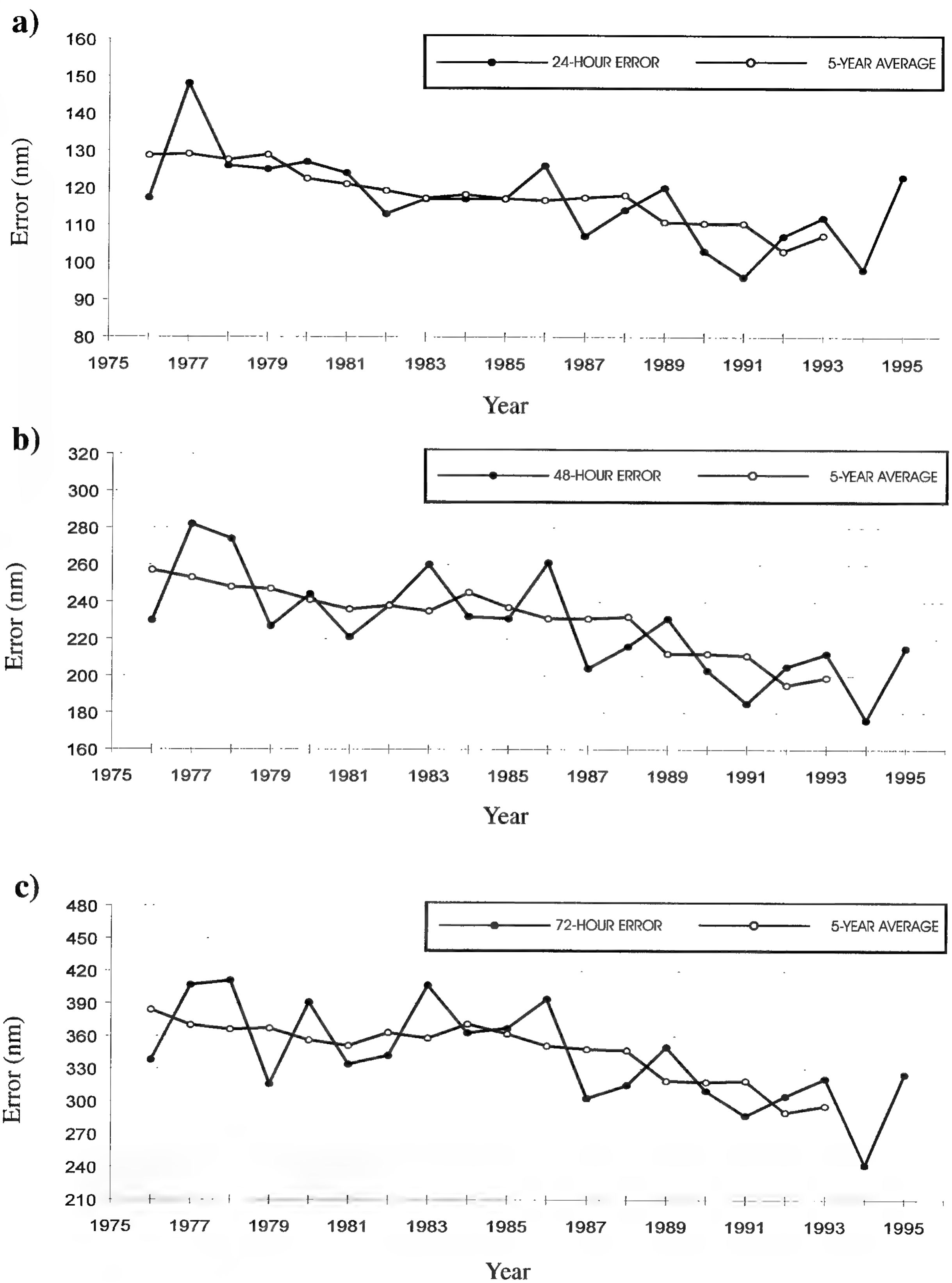

Figure 5-3 Mean track forecast error (nm) and 5-year running mean for a) 24 hours, b) 48 hours and c) 72 hours for western North Pacific Ocean tropical cyclones for the period 1976 to 1995.

Table 5-2

MEAN FORECAST TRACK ERRORS (NM) FOR WESTERN NORTH PACIFIC TROPICAL CYCLONES FOR 1959-1995

	24-HOUR				48-HOUR				72-HOUR			
YEAR	TY[1]	TC	CROSS TRACK[2]	ALONG TRACK[2]	TY[1]	TC	CROSS TRACK[2]	ALONG TRACK[2]	TY[1]	TC	CROSS TRACK[2]	ALONG TRACK[2]
1959	117*				267*							
1960	177*				354*							
1961	136				274							
1962	144				287				476			
1963	127				246				374			
1964	133				284				429			
1965	151				303				418			
1966	136				280				432			
1967	125				276				414			
1968	105				229				337			
1969	111				237				349			
1970	98	104			181	190			272	279		
1971	99	111	64		203	212	118		308	317	177	
1972	116	117	72		245	245	146		382	381	210	
1973	102	108	74		193	197	134		245	253	162	
1974	114	120	78		218	226	157		357	348	245	
1975	129	138	84		279	288	181		442	450	290	
1976	117	117	71		232	230	132		336	338	202	
1977	140	148	83		266	283	157		390	407	228	
1978	120	127	71	87	241	271	151	194	459	410	218	296
1979	113	124	76	81	219	226	138	146	319	316	182	214
1980	116	126	76	86	221	243	147	165	362	389	230	266
1981	117	123	77	80	215	220	131	146	342	334	219	206
1982	114	113	70	74	229	237	142	162	337	341	211	223
1983	110	117	73	76	247	259	164	169	384	405	263	259
1984	110	117	64	84	228	233	131	163	361	363	216	238
1985	112	117	68	80	228	231	138	153	355	367	227	230
1986	117	121	70	85	261	261	151	183	403	394	227	276
1987	101	107	64	71	211	204	127	134	318	303	186	198
1988	107	114	58	85	222	216	103	170	327	315	159	244
1989	107	120	69	83	214	231	127	162	325	350	177	265
1990	98	103	70	81	191	203	138	162	299	310	211	242
1991	93	96	53	69	187	185	97	137	298	286	146	229
1992	97	107	59	77	194	205	116	143	295	305	172	210
1993	102	112	63	79	205	212	117	151	320	321	173	226
1994	96	98	53	71	172	176	101	123	244	242	146	163
1995	105	123	89	67	200	215	159	117	311	325	240	167

1. Forecasts were verified for typhoons when intensities were at least 35kt (18m/sec).

2. Cross-track and along-track errors were adopted by the JTWC in 1986. Right angle errors (used prior to 1986) were recomputed as cross-track errors after-the-fact to extend the data base. See Figure 5-1 for the definitions of cross-track and along-track.

* Forecast positions north of 35^0 north latitude were not verified.

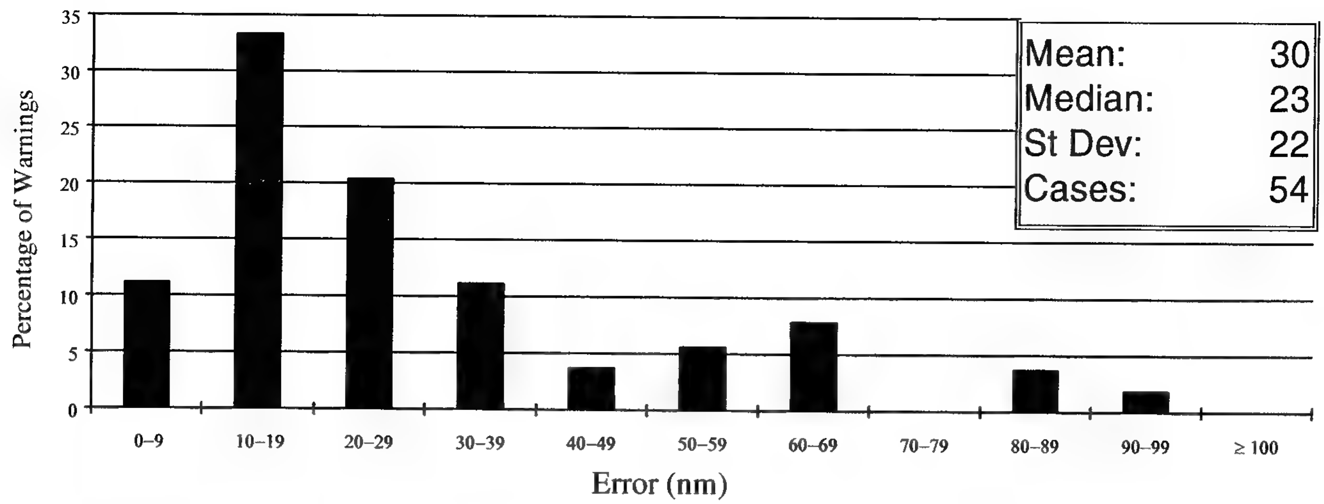

Figure 5-4a Frequency distribution of initial warning position errors (10-nm increments) for North Indian Ocean tropical cyclones in 1995. The largest error, 91nm, was on TC02A.

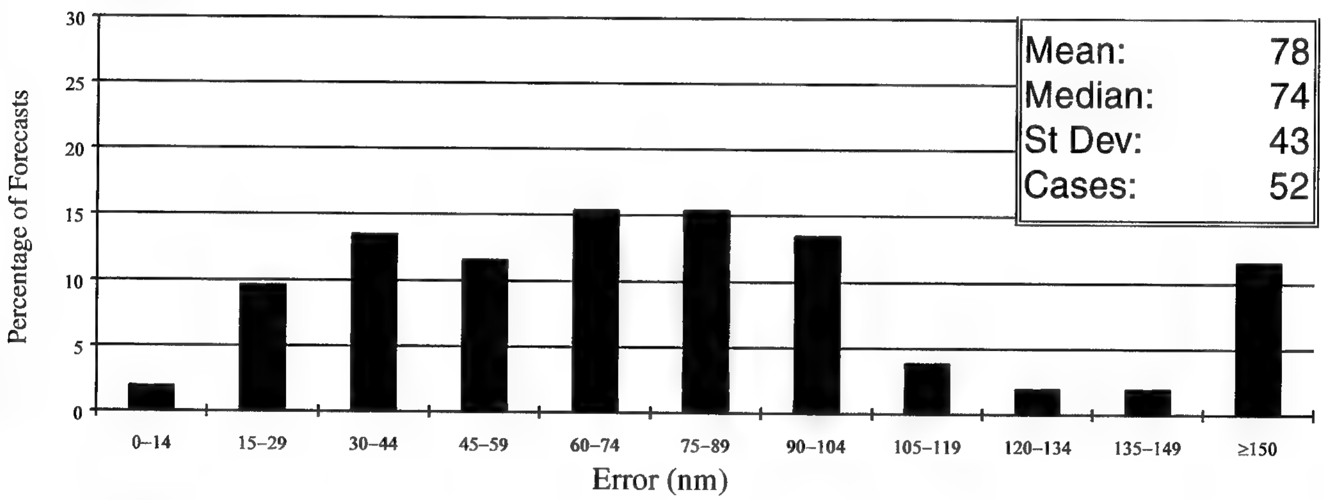

Figure 5-4b Frequency distribution of 12-hour track forecast errors (15-nm increments) for North Indian Ocean tropical cyclones in 1995. The largest error, 181nm, was on TC04B.

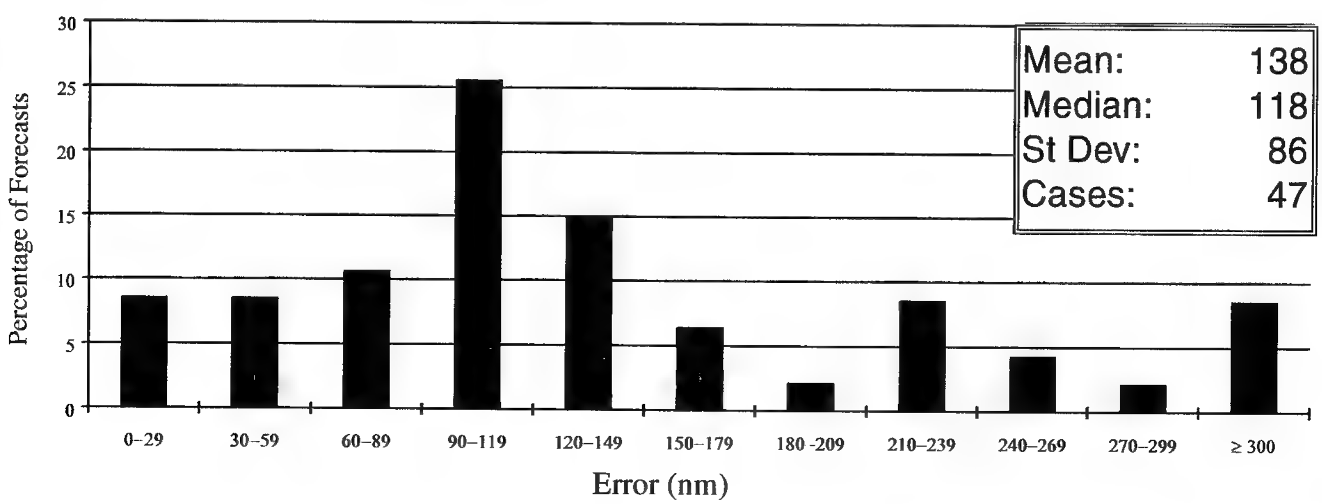

Figure 5-4c Frequency distribution of 24-hour track forecast errors (30-nm increments) for North Indian Ocean tropical cyclones in 1995. The largest error, 326 nm, was on TC02A.

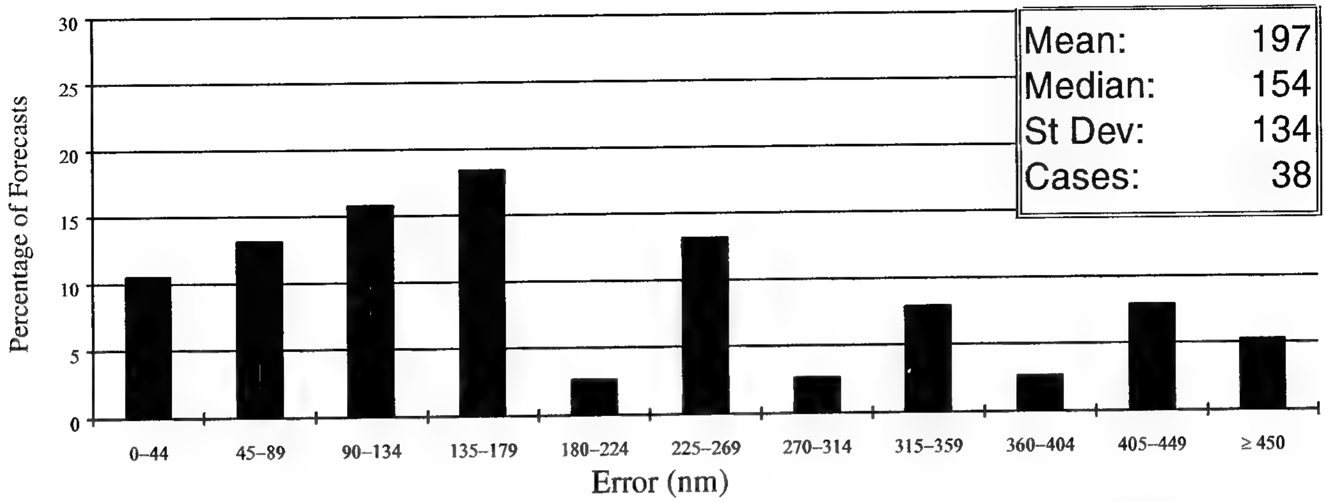

Figure 5-4d Frequency distribution of 36-hour track forecast errors (45-nm increments) for North Indian Ocean tropical cyclones in 1995. The largest error, 502 nm, was on TC04B.

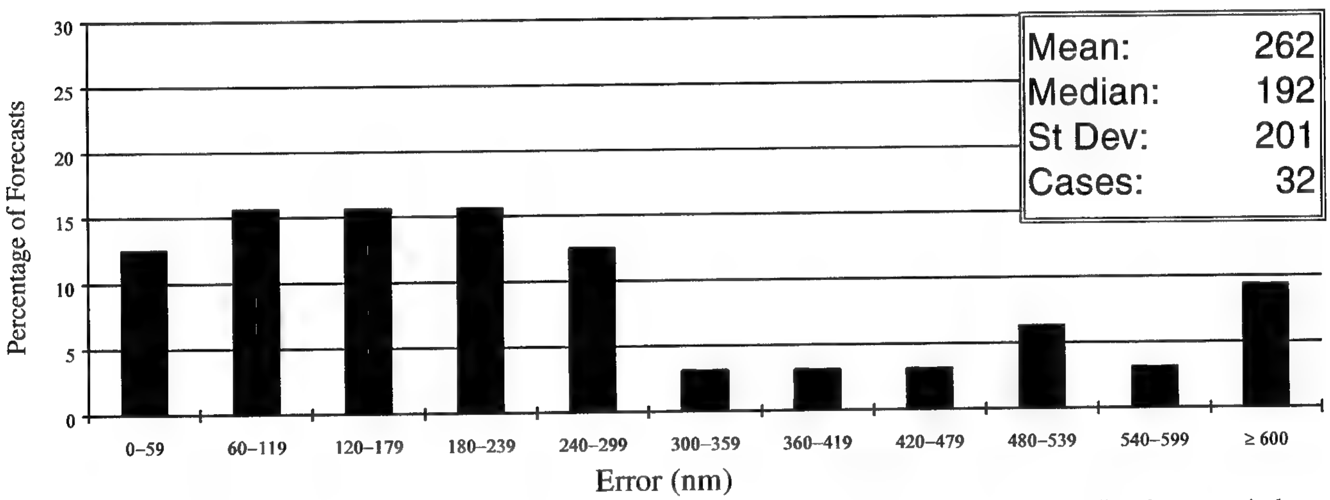

Figure 5-4e Frequency distribution of 48-hour track forecast errors (60-nm increments) for North Indian Ocean tropical cyclones in 1995. The largest error, 728 nm, was on TC04B.

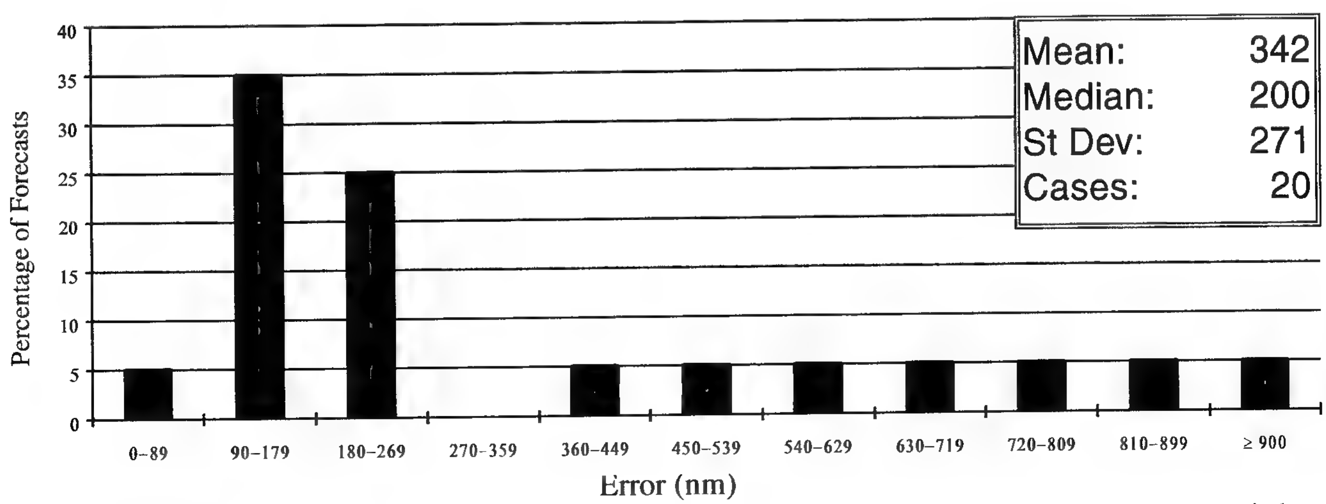

Figure 5-4f Frequency distribution of 72-hour track forecast errors (90-nm increments) for North Indian Ocean tropical cyclones in 1995. The largest error, 924 nm, was on TC04B.

Table 5-3

INITIAL POSITION AND FORECAST POSITION ERRORS (NM) FOR THE NORTH INDIAN OCEAN FOR 1981-1995

				24-HOUR				48-HOUR				72-HOUR		
YEAR	NUMBER OF WARNINGS	INITIAL POSITION	NUMBER OF FORECASTS	TRACK	ALONG	CROSS	NUMBER OF FORECASTS	TRACK	ALONG	CROSS	NUMBER OF FORECASTS	TRACK	ALONG	CROSS
1981	41	28	29	109	76	63	2	176	120	109	5	197	150	111
1982	55	35	37	138	110	68	17	368	292	209	7	762	653	332
1983	18	38	7	117	90	50	18	153	137	53	0			
1984	67	33	42	154	124	67	20	274	217	139	16	388	339	121
1985	53	31	30	122	102	53	8	242	119	194	0			
1986	28	52	16	134	118	53	7	168	131	80	5	269	189	180
1987	83	42	54	144	97	100	25	205	125	140	21	305	219	188
1988	44	34	30	120	89	63	18	219	112	176	12	409	227	303
1989	44	19	33	88	62	50	17	146	94	86	12	216	164	111
1990	46	31	36	101	85	43	24	146	117	67	17	185	130	104
1991	56	38	43	129	107	54	27	235	200	89	14	450	356	178
1992	191	35	149	128	73	86	100	244	141	166	62	398	276	218
1993	36	27	28	125	87	79	20	198	171	74	12	231	176	116
1994	60	25	44	97	80	44	28	153	124	63	13	213	177	92
1995	54	30	47	138	119	58	32	262	247	77	20	342	304	109
15 YEAR AVERAGE														
1981-1995	58	33	42	123	94	62	24	213	156	115	14	336	258	166

Cross-track and along-track errors were adopted by the JTWC in 1986. Right angle errors (used prior to 1986) were recomputed as cross-track and along-track errors after-the-fact to extend the data base. See Figure 5-1 for the definitions of cross-track and along-track errrors.

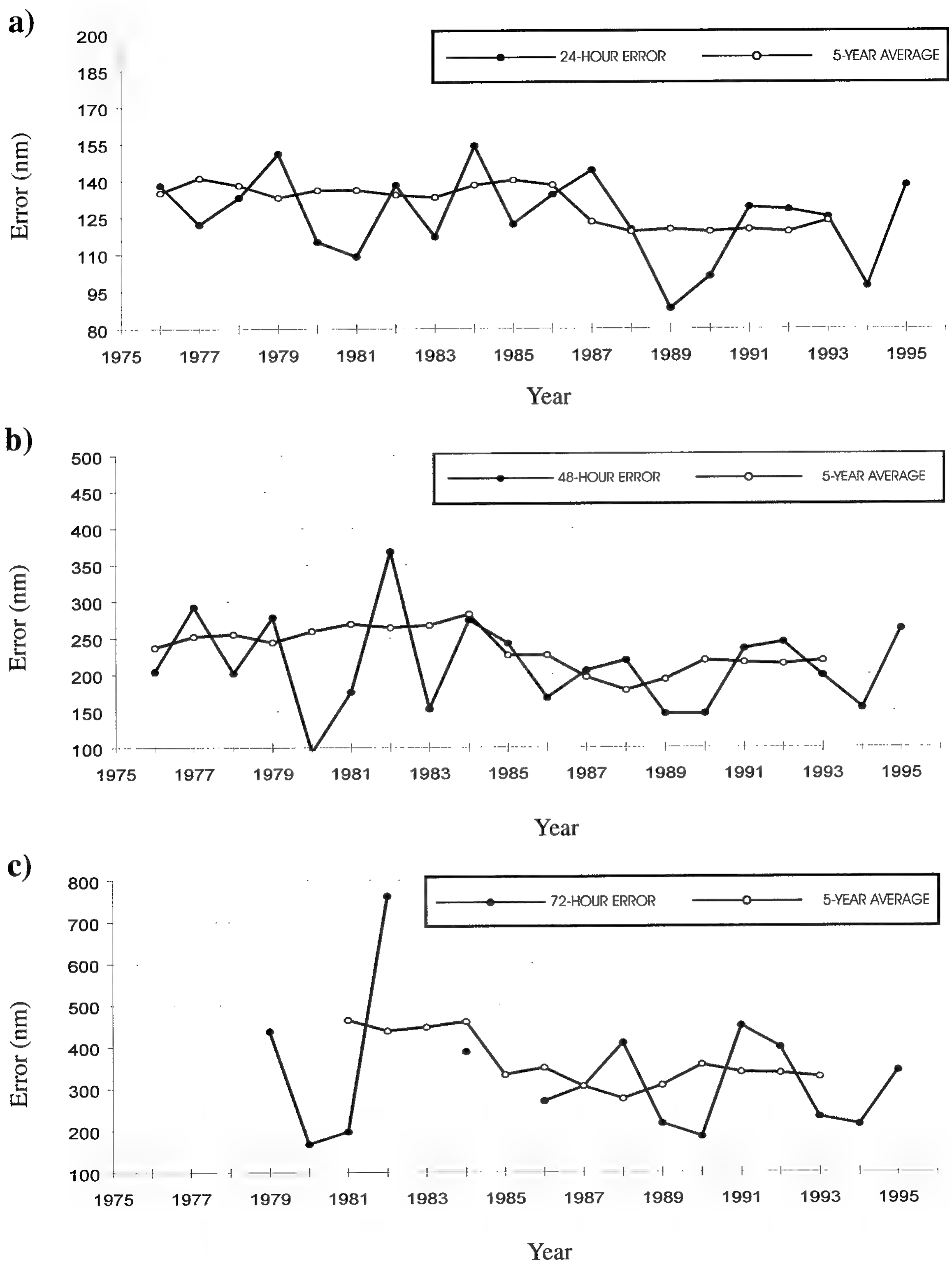

Figure 5-5 Mean track forecast error (nm) and 5-year running mean for a) 24 hours, b) 48 hours and c) 72 hours for North Indian Ocean tropical cyclones for the period 1976 to 1995.

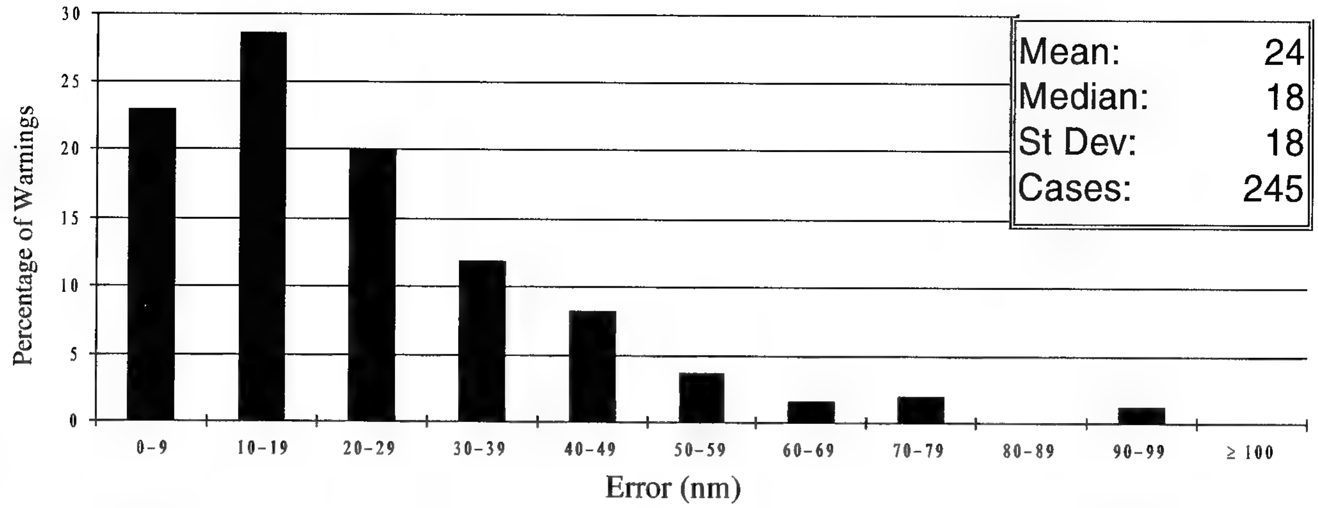

Figure 5-6a Frequency distribution of initial warning position errors (10-nm increments) for South Pacific and South Indian Ocean tropical cyclones in 1995. The largest error, 243 nm, occurred on Tropical Cyclone 05P (William).

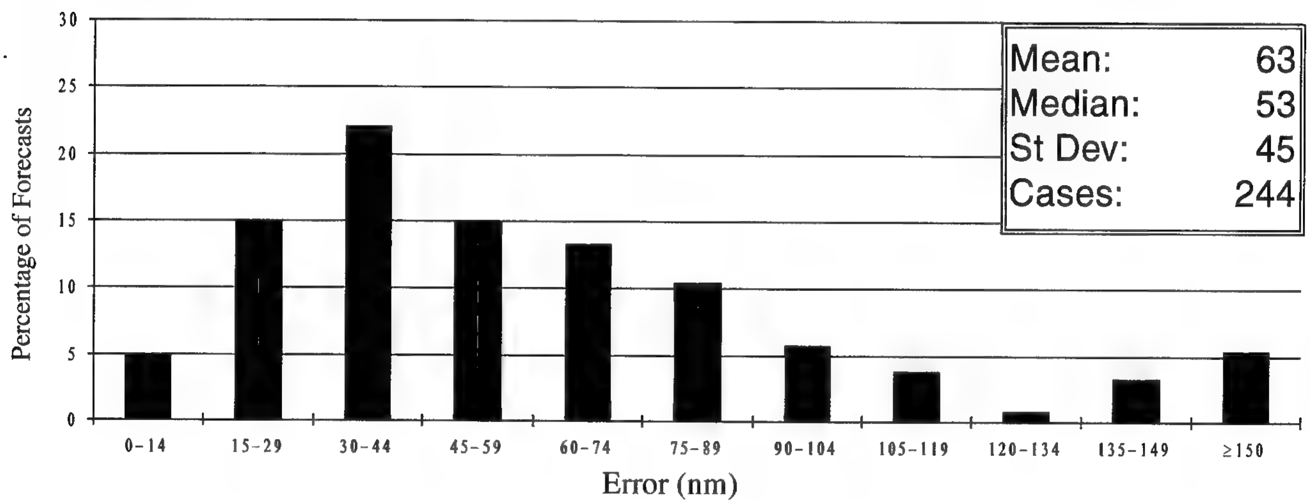

Figure 5-6b Frequency distribution of 12-hour track forecast errors (15-nm increments) for South Pacific and South Indian Ocean tropical cyclones in 1995. The largest error, 341 nm, occurred on Tropical Cyclone 05P (William).

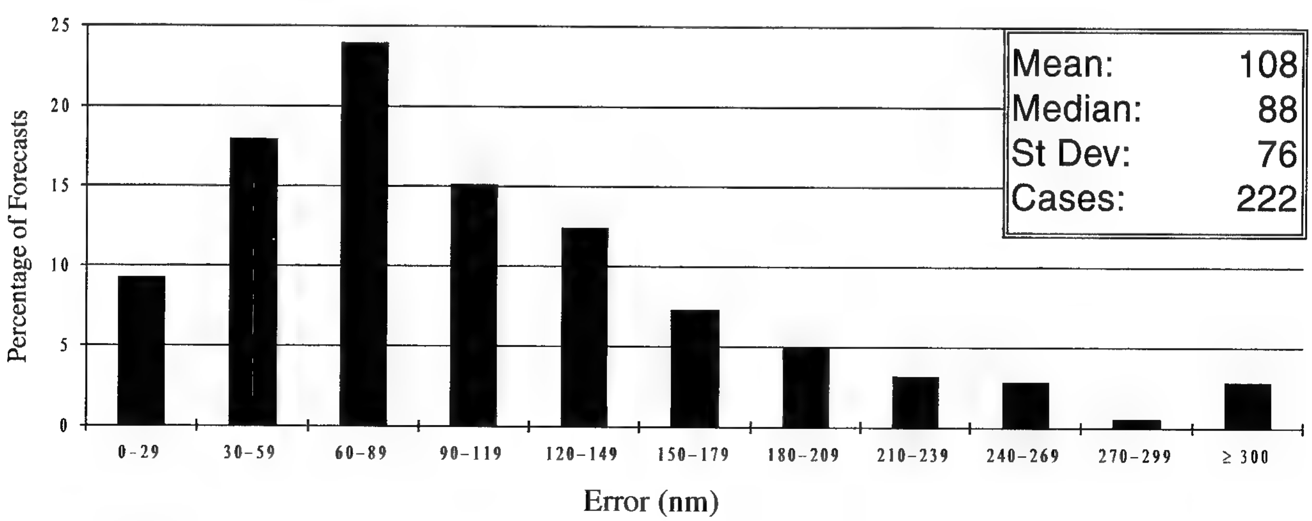

Figure 5-6c Frequency distribution of 24-hour track forecast errors (30-nm increments) for South Pacific and South Indian Ocean tropical cyclones in 1995. The largest error, 492 nm, occurred on Tropical Cyclone 14P (Violet).

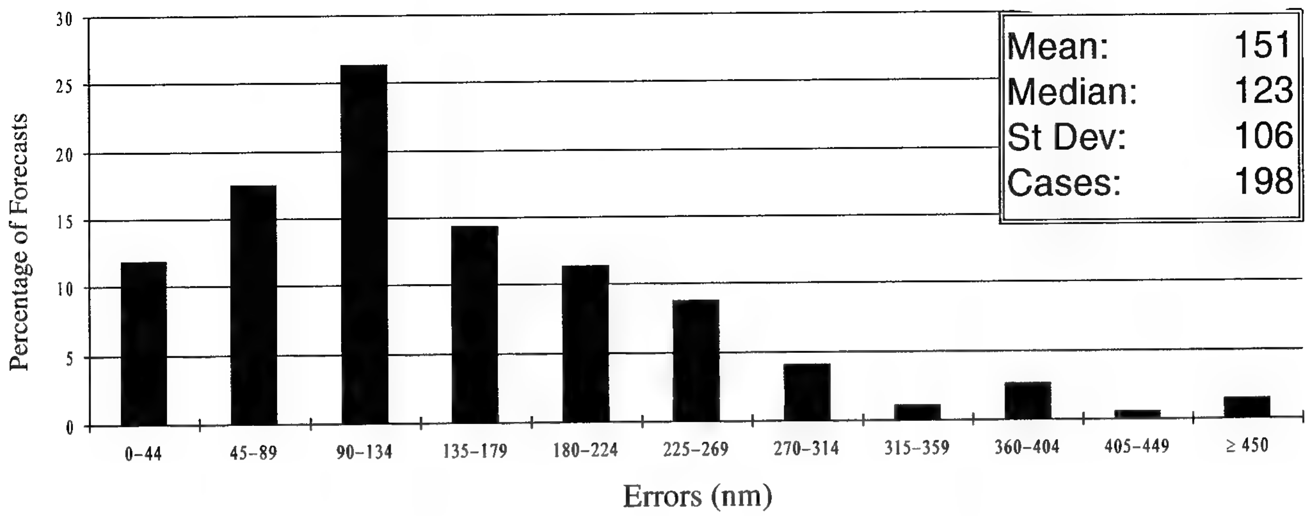

Figure 5-6d Frequency distribution of 36-hour track forecast errors (45-nm increments) for in the South Pacific and South Indian Ocean tropical cyclones in 1995. The largest error, 757 nm, occurred on Tropical Cyclone 14P (Violet).

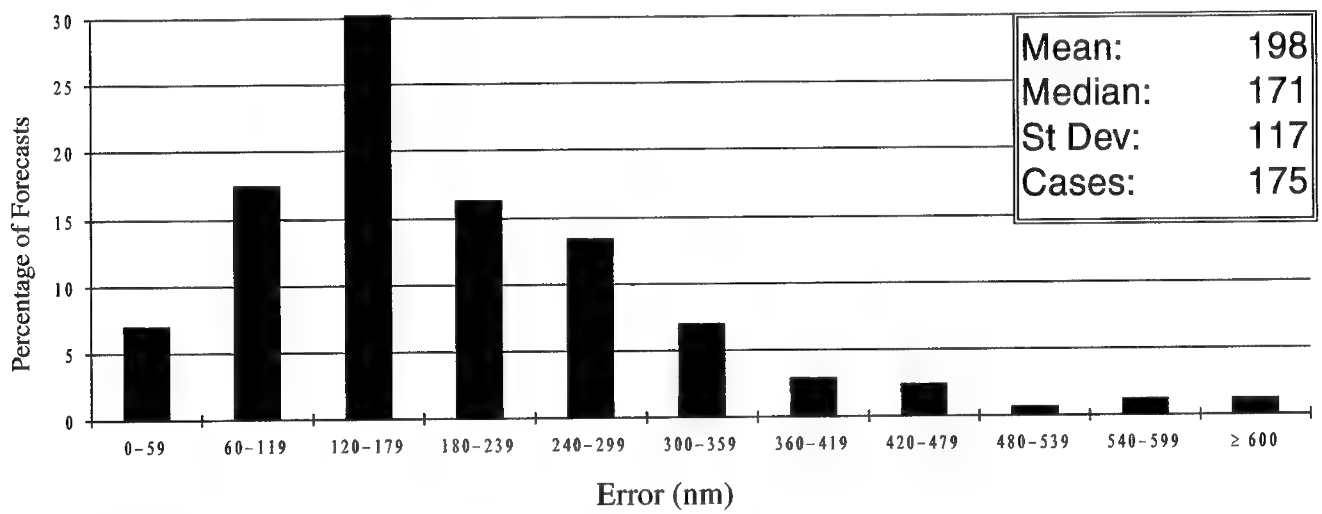

Figure 5-6e Frequency distribution of 48-hour track forecast errors (60-nm increments) for in the South Pacific and South Indian Ocean tropical cyclones in 1995. The largest error, 622 nm, occurred on Tropical Cyclone 19S (Marlene).

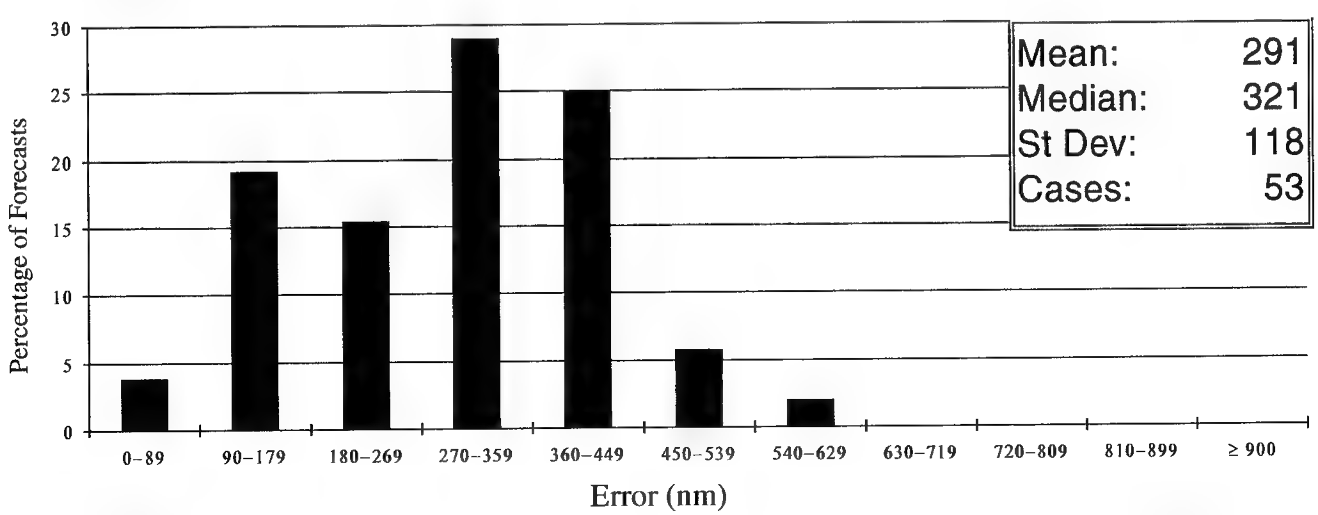

Figure 5-6f Frequency distribution of 72-hour track forecast errors (120-nm increments) for in the South Pacific and South Indian Ocean tropical cyclones in 1995. The largest error, 565 nm, occurred on Tropical Cyclone 22P (Agnes).

Table 5-4

INITIAL POSITION AND FORECAST POSITION ERRORS (NM) FOR THE SOUTHERN HEMISPHERE FOR 1981-1995

				24-HOUR				48-HOUR				72-HOUR		
YEAR	NUMBER OF WARNINGS	INITIAL POSITION	NUMBER OF FORECASTS	TRACK	ALONG	CROSS	NUMBER OF FORECASTS	TRACK	ALONG	CROSS	NUMBER OF FORECASTS	TRACK	ALONG	CROSS
1981	226	48	190	165	103	106	140	315	204	201				
1982	275	38	238	144	98	86	176	274	188	164				
1983*	191	35	163	130	88	77	126	241	158	145				
1984	301	36	252	133	90	79	191	231	159	134				
1985*	306	36	257	134	92	79	193	236	169	132				
1986*	279	40	227	129	86	77	171	262	169	164				
1987*	189	46	138	145	94	90	101	280	153	138				
1988*	204	34	99	146	98	83	48	290	246	144				
1989*	287	31	242	124	84	73	186	240	166	136				
1990*	272	27	228	143	105	74	177	263	178	152				
1991*	264	24	231	115	75	69	185	220	152	129				
1992*	267	28	230	124	91	64	208	240	177	129				
1993*	257	21	225	102	74	57	176	199	142	114				
1994*	386	28	345	115	77	68	282	224	147	134				
1995**	245	24	222	108	82	55	175	198	144	108	53	291	169	190
AVERAGE														
1981-1995	263	33	219	130	89	76	169	248	170	142	53	291	169	190

* These stastics are for JTWC forecasts only. NPMOC statistics are not included.

** JTWC began publishing 72-hour forecast verification in 1995.

Cross-track and along-track errors were adopted by the JTWC in 1986. Right-angle (used prior to 1986) were recomputed as cross-track and along-track errors after-the-fact to extend the data base.

See Figure 5-1 for the definitions of cross-track and along-track errors.

a)

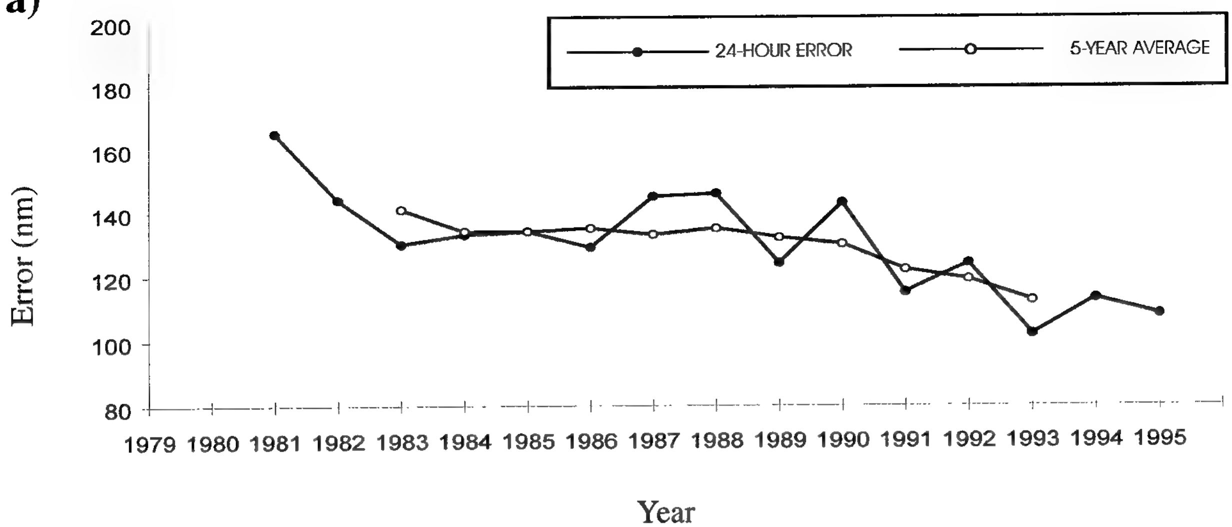

b)

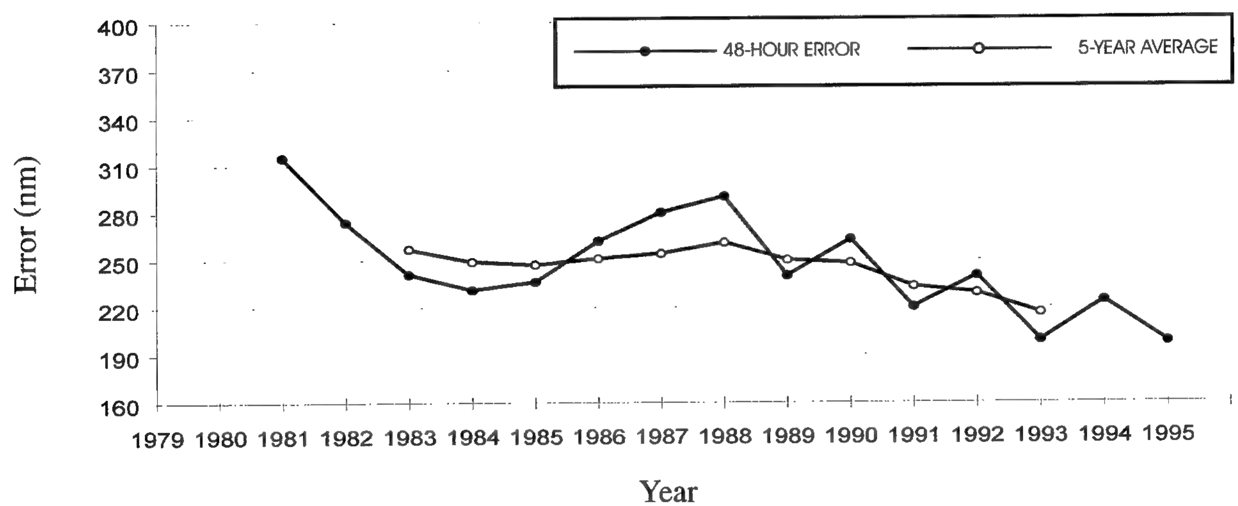

Figure 5-7 Mean track forecast errors (nm) and 5-year running mean for a) 24 hours and b) 48 hours for South Pacific and South Indian Ocean tropical cyclones for the period 1981 to 1995.

5.2 COMPARISON OF OBJECTIVE TECHNIQUES

JTWC uses a variety of objective techniques for guidance in the warning preparation process. Multiple techniques are required, because each technique has particular strengths and weaknesses which vary by basin, numerical model initialization, time of year, synoptic situation and forecast period. The accuracy of objective aid forecasts depends on both the specified position and the past motion of the tropical cyclone as determined by the working best track. JTWC initializes its objective techniques using an extrapolated working best track position so that the output of the techniques will start at the valid time of the next warning initial position.

Unless stated otherwise, all the objective techniques discussed below run in all basins covered by JTWC's AOR and provide forecast positions at 12-, 24-, 36-, 48-, and 72-hours unless the technique aborts prematurely during computations. The techniques can be divided into six general categories: extrapolation, climatology and analogs, statistical, dynamic, hybrids, and empirical or analytical.

5.2.1 EXTRAPOLATION (XTRP) — Past speed and direction are computed using the rhumb line distance between the current and 12-hour old positions of the tropical cyclone. Extrapolation from the current warning position is used to compute forecast positions.

5.2.2 CLIMATOLOGY and ANALOGS

5.2.2.1 CLIMATOLOGY (CLIM) — Employs time and location windows relative to the current position of the tropical cyclone to determine which historical storms will be used to compute the forecast. The historical data base is 1945-1981 for the Northwest Pacific, and 1900 to 1990 for the rest of JTWC's AOR. Objective intensity forecasts are available from these data bases. Scatter diagrams of expected tropical cyclone motion at bifurcation points are also available from these data bases.

5.2.2.2 ANALOG — A revised Typhoon Analog 1993 (TYAN93) picks the top matches with the basin climatology of tropical cyclone best tracks. Matches are based upon the differences between the direction and speed of the superimposed best track positions and the past direction and speed of the cyclone. Specifically, the directions and speeds are calculated from the 12-hour old position to the "fix" position and the 24-hr old position to the "fix" position. Separate comparisons are made for climatology cyclone tracks classified as "straight", "recurver" and "other". There is also a "total" group, that includes the top matches without regard to classification of tracks.

TYAN93 works the same in all basins. The time-window is +/- 35 days from the "fix." The space-window is +/- 2.5 degrees latitude and +/- 5 degrees longitude from the "fix" position on the first pass of each forecast. The maximum-wind-speed window is as follows (for basins with climatology wind speeds): a. If "fix" wind speed is <= 25 kt, climatology cyclone wind speed must be <= 30 kt. b. If "fix" wind speed is 30 kt, climatology cyclone wind speed must be in range from 25 to 35 kt. c. If "fix" wind speed is >= 35 kt, climatology cyclone wind speed must be at least 35 kt. Matching is based upon weighted direction and speed errors. Forecasting is based upon "straight" and "recurver" type climatology tropical cyclones, where the 12-hour and 24-hour best "straight" ("recurver") matches are combined into one set of best matches for "straight" ("recurver").

5.2.3 STATISTICAL

5.2.3.1 CLIMATOLOGY AND PERSISTENCE (CLIPER or CLIP) — A statistical regression technique that is based on climatology, current position and 12-hour and 24-hour past move-

ment. This technique is used as a crude baseline against which to measure the forecast skill of other, more sophisticated techniques. CLIP in the western North Pacific uses third-order regression equations, and is based on the work of Xu and Neumann (1985). CLIPER has been available outside this basin since mid-1990, with regression coefficients recently recomputed by FNMOC based on the updated 1900-1989 data base.

5.2.3.2 COLORADO STATE UNIVERSITY MODEL (CSUM) — A statistical-dynamical technique based on the work of Matsumoto (1984). Predictor parameters include the current and 24-hr old position of the storm, heights from the current and 24-hr old NOGAPS 500-mb analyses, and heights from the 24-hr and 48-hr NOGAPS 500-mb prognoses. Height values from 200-mb fields are substituted for storms that have an intensity exceeding 90 kt and are located north of the subtropical ridge. Three distinct sets of regression equations are used depending on whether the storm's direction of motion falls into "below," "on," or "above" the subtropical ridge categories. During the development of the regression equation coefficients for CSUM, the so-called "perfect prog" approach was used, in which verifying analyses were substituted for the numerical prognoses that are used when CSUM is run operationally. Thus, CSUM was not "tuned" to any particular version of NOGAPS, and in fact, the performance of CSUM should presumably improve as new versions of NOGAPS improve. CSUM runs only in the western North Pacific, South China Sea, and North Indian Ocean basins.

5.2.3.3 JTWC92 or JT92 - JTWC92 is a statistical-dynamical model for the western North Pacific Ocean basin which forecasts tropical cyclone positions at 12-hour intervals to 72 hours. The model uses the deep-layer mean height field derived from the NOGAPS forecast fields. These deep-layer mean height fields are spectrally truncated to wave numbers 0 through 18 prior to use in JTWC92. Separate forecasts are made for each position. That is, the forecast 24-hour position is not a 12-hour forecast from the forecasted 12-hour position.

JTWC92 uses five internal sub-models which are blended and iterated to produce the final forecasts. The first sub-model is a statistical blend of climatology and persistence, known as CLIPER. The second sub-model is an analysis mode predictor, which only uses the "analysis" field. The third sub-model is the forecast mode predictor, which uses only the forecast fields. The fourth sub-model is a combination of 1 and 2 to produce a "first guess" of the 12-hourly forecast positions. The fifth sub-model uses the output of the "first guess" combined with 1,2, and 3 to produce the forecasts. The iteration is accomplished by using the output of sub-model 5 as though it were the output from sub-model 4. The optimum number of iterations has been determined to be three.

When JTWC92 is used in the operational mode, all the NOGAPS fields are forecast fields. The 00Z and 12Z tropical forecasts are based upon the previous 12-hour old synoptic time NOGAPS forecasts. The 06Z and 18Z tropical forecasts are based on the previous 00Z and 12Z NOGAPS forecasts, respectively. Therefore, operationally, the second sub-model uses forecast fields and not analysis fields.

5.2.4 DYNAMIC

5.2.4.1 NOGAPS VORTEX TRACKING ROUTINE(NGPS/X)—Tropical cyclone vortices are tracked at FNMOC by converting the 1000-mb u and v wind component fields into isogons. The intersection of isogons are either the center of a cyclonic or anticyclonic circulation, or a col. The tracking program starts at the last known location of the cyclone - a warning position. Based on this position and the last known speed and direction of movement, the

program hunts for the next cyclonic center representing the tropical cyclone. Confidence factors are generated within the program and are modified, as required, by a quality control program that formats the data for transmission.

5.2.4.2 ONE-WAY (INTERACTIVE) TROPICAL CYCLONE MODEL (OTCM) — This technique is a coarse resolution (205-km grid), three layer, primitive equation model with a horizontal domain of 6400 x 4700 km. OTCM is initialized using 6-hour or 12-hour prognostic fields from the latest NOGAPS run, and the initial fields are smoothed and adjusted in the vicinity of the storm to induce a persistence bias into OTCM's forecast. A symmetric bogus vortex is then inserted, and the boundaries updated every 12 hours by NOGAPS fields as the integration proceeds. The bogus vortex is maintained against frictional dissipation by an analytical heating function. The forecast positions are based on the movement of the vortex in the lowest layer of the model (effectively 850-mb).

5.2.4.3 FNOC BETA AND ADVECTION MODEL (FBAM) — This model is an adaptation of the Beta and Advection model used by NCEP. The forecast motion results from a calculation of environmental steering and an empirical correction for the observed vector difference between that steering and the 12-hour old storm motion. The steering is computed from the NOGAPS Deep Layer Mean (DLM) wind fields which are a weighted average of the wind fields computed for the 1000-mb to 100-mb levels. The difference between past storm motion and the DLM steering is treated as if the storm were a Rossby wave with an "effective radius" propagating in response to the horizontal gradient of the coriolis parameter, beta. The forecast proceeds in one-hour steps, recomputing the effective radius as beta changes with storm latitude, and blending in a persistence bias for the first 12 hours.

5.2.5 HYBRIDS

5.2.5.1 HALF PERSISTENCE AND CLIMATOLOGY (HPAC) — Forecast positions generated by equally weighting the forecasts given by XTRP and CLIM.

5.2.5.2 BLENDED (BLND) —A simple average of JTWC's six primary forecast aids: OTCM, CSUM, FBAM, JT92, CLIP, and HPAC.

5.2.5.3 WEIGHTED (WGTD) — A weighted average of the forecast guidance used to compute BLND: OTCM (29%), CSUM (22%), FBAM (14%), JT92 (14%), HPAC (14%), and CLIP (7%).

5.2.5.4 DYNAMIC AVERAGE (DAVE) — A simple average of all dynamic forecast aids: NOGAPS (NGPS), Bracknell (EGRR), Japanese Typhoon Model (JTYM), JT92, FBAM, OTCM and CSUM.

5.2.6 EMPIRICAL OR ANALYTICAL

5.2.6.1 DVORAK — An estimation of a tropical cyclone's current and 24-hour forecast intensity is made from the interpretation of satellite imagery (Dvorak, 1984). These intensity estimates are used with other intensity related data and trends to forecast short-term tropical cyclone intensity.

5.2.6.2 MARTIN/HOLLAND — The technique adapts an earlier work (Holland, 1980) and specifically addresses the need for realistic 35-, 50- and 100-kt (18-,26- and 51-m/sec) wind radii around tropical cyclones. It solves equations for basic gradient wind relations within the tropical cyclone area, using input parameters obtained from enhanced infrared satellite imagery. The diagnosis also includes an asymmetric area of winds caused by tropical cyclone

movement. Satellite-derived size and intensity parameters are also used to diagnose internal steering components of tropical cyclone motion known collectively as "beta-drift".

5.2.6.3 TYPHOON ACCELERATION PREDICTION TECHNIQUE (TAPT) — This technique (Weir, 1982) utilizes upper-tropospheric and surface wind fields to estimate acceleration associated with the tropical cyclone's interaction with the mid-latitude westerlies. It includes guidelines for the duration of acceleration, upper limits and probable path of the cyclone.

5.3 TESTING AND RESULTS

A comparison of selected techniques is included in Table 5-5 for all western North Pacific tropical cyclones, Table 5-6 for all North Indian Ocean tropical cyclones and Table 5-7 for the Southern Hemisphere. For example, in Table 5-5 for the 12-hour mean forecast error, 687 cases available for a (homogeneous) comparison, the average forecast error at 12 hours was 92 nm (170 km) for CLIP and 89 nm (165 km) for FBAM. The difference of 3 nm (6 km) is shown in the lower right. (Differences are not always exact, due to computational round-off which occurs for each of the cases available for comparison).

TABLE 5-5 1995 ERROR STATISTICS FOR SELECTED OBJECTIVE TECHNIQUES IN THE NORTHWEST PACIFIC (1 JAN 1995 - 31 DEC 1995)

12-HOUR MEAN FORECAST ERROR (NM)

Number of Cases	X-Axis Technique Error
Y-Axis Technique Error	Error Difference (Y-X)

	JTWC		DAVE		NGPS		OTCM		CSUM		FBAM		CLIP		JT92	
JTWC	584	72														
	72	0														
DAVE	511	71	601	92												
	77	6	92	0												
NGPS	430	64	393	70	447	131										
	126	62	130	60	131	0										
OTCM	553	70	584	92	429	125	683	92								
	84	14	87	-5	80	-45	92	0								
CSUM	564	71	596	92	432	126	681	92	694	98						
	82	11	92	0	76	-50	98	6	98	0						
FBAM	557	71	589	92	430	125	674	92	686	98	687	89				
	81	10	85	-7	75	-50	88	-4	89	-9	89	0				
CLIP	567	71	597	92	434	125	683	92	694	98	687	89	697	92		
	84	13	89	-3	78	-47	91	-1	92	-6	92	3	92	0		
JT92	564	71	596	92	432	126	680	92	693	97	685	89	693	92	693	164
	84	13	130	38	72	-54	165	73	164	67	165	76	164	72	164	0

24-HOUR MEAN FORECAST ERROR (NM)

	JTWC		DAVE		NGPS		OTCM		CSUM		FBAM		CLIP		JT92	
JTWC	539	123														
	123	0														
DAVE	474	123	569	137												
	117	-6	137	0												
NGPS	393	113	363	111	414	146										
	140	27	141	30	146	0										
OTCM	505	119	542	132	391	137	637	147								
	139	20	142	10	134	-3	147	0								
CSUM	527	122	566	137	402	141	635	147	662	168						
	141	19	162	25	133	-8	159	12	168	0						
FBAM	522	123	561	137	400	140	630	147	656	169	657	135				
	125	2	131	-6	121	-19	131	-16	135	-34	135	0				
CLIP	530	122	567	137	403	141	637	147	662	168	657	135	665	151		
	144	22	149	12	135	-6	147	0	151	-17	151	16	151	0		
JT92	527	122	566	137	402	141	634	147	661	168	655	135	661	151	661	187
	126	4	168	31	118	-23	171	24	187	19	188	53	187	36	187	0

Table 5-5 (CONTINUED) 1995 ERROR STATISTICS FOR SELECTED OBJECTIVE TECHNIQUES IN THE NORTHWESTERN PACIFIC (1 JAN 1995 - 31 DEC 1995)

36-HOUR MEAN FORECAST ERROR (NM)

	JTWC		DAVE		NGPS		OTCM		CSUM		FBAM		CLIP		JT92	
JTWC	489	170														
	170	0														
DAVE	435	171	529	168												
	160	-11	168	0												
NGPS	333	157	309	151	354	195										
	188	31	187	36	195	0										
OTCM	455	163	499	164	333	185	586	200								
	195	32	199	35	190	5	200	0								
CSUM	481	170	524	166	345	189	582	200	612	209						
	198	28	209	43	187	-2	200	0	209	0						
FBAM	476	171	520	168	342	189	579	201	606	209	610	185				
	176	5	181	13	171	-18	180	-21	184	-25	185	0				
CLIP	483	170	526	168	345	189	586	200	612	209	610	185	617	212		
	206	36	210	42	188	-1	202	2	210	1	212	27	212	0		
JT92	481	170	525	168	345	189	583	201	611	209	608	185	614	212	614	232
	176	6	202	34	161	-28	218	17	214	5	232	47	232	20	232	0

48-HOUR MEAN FORECAST ERROR (NM)

	JTWC		DAVE		NGPS		OTCM		CSUM		FBAM		CLIP		JT92	
JTWC	421	215														
	215	0														
DAVE	374	215	488	216												
	208	-7	216	0												
NGPS	283	201	267	202	305	259										
	254	53	256	54	259	0										
OTCM	390	207	459	213	288	254	540	260								
	256	49	260	47	259	5	260	0								
CSUM	414	215	484	216	296	254	538	260	568	259						
	263	48	264	48	245	-9	250	-10	259	0						
FBAM	410	216	479	216	293	253	533	261	562	259	563	245				
	235	19	241	25	241	-12	237	-24	245	-14	245	0				
CLIP	416	215	485	216	296	254	540	260	568	259	563	245	570	273		
	275	60	273	57	245	-9	260	0	273	14	273	28	273	0		
JT92	414	215	484	216	296	254	537	260	567	259	561	245	567	273	567	284
	238	23	264	48	225	-29	261	1	284	25	283	38	284	11	284	0

72-HOUR MEAN FORECAST ERROR (NM)

	JTWC		DAVE		NGPS		OTCM		CSUM		FBAM		CLIP		JT92	
JTWC	319	325														
	325	0														
DAVE	280	326	393	331												
	333	7	331	0												
NGPS	207	315	199	339	234	383										
	382	67	384	45	383	0										
OTCM	284	316	354	323	207	376	422	386								
	387	71	392	69	412	36	386	0								
CSUM	314	324	390	330	227	379	422	386	466	366						
	380	56	378	48	386	7	347	-39	366	0						
FBAM	313	324	387	329	225	378	418	387	462	366	463	375				
	368	44	372	43	408	30	359	-28	376	10	375	0				
CLIP	316	324	391	329	227	379	422	386	464	367	461	373	466	384		
	407	83	391	62	376	-3	367	-19	384	17	385	12	384	0		
JT92	313	324	389	330	226	378	420	387	463	367	460	376	462	384	463	383
	358	34	379	49	343	-35	363	-24	383	16	383	7	381	-3	383	0

TABLE 5-6 1995 ERROR STATISTICS FOR SELECTED OBJECTIVE TECHNIQUES IN THE NORTH INDIAN OCEAN (1 JAN 1995 - 31 DEC 1995)

12-HOUR MEAN FORECAST ERROR (NM)

	JTWC		NGPS		OTCM		CSUM		FBAM		CLIP		HPAC		WGTD	
JTWC	52	78														
	78	0														
NGPS	40	78	40	114												
	114	36	114	0												
OTCM	45	77	39	111	46	118										
	118	41	122	11	118	0										
CSUM	46	78	40	114	46	118	47	123								
	124	46	124	10	122	4	123	0								
FBAM	46	78	40	114	46	118	47	123	47	88						
	90	12	89	-25	87	-31	88	-35	88	0						
CLIP	46	78	40	114	46	118	47	123	47	88	47	92				
	93	15	94	-20	91	-27	92	-31	92	4	92	0				
HPAC	46	78	40	114	46	118	47	123	47	88	47	92	47	95		
	97	19	99	-15	95	-23	95	-28	95	7	95	3	95	0		
WGTD	32	78	27	124	32	125	33	122	33	88	33	91	33	95	33	101
	103	25	107	-17	101	-24	101	-21	101	13	101	10	101	6	101	0

24-HOUR MEAN FORECAST ERROR (NM)

	JTWC		NGPS		OTCM		CSUM		FBAM		CLIP		HPAC		WGTD	
JTWC	47	138														
	138	0														
NGPS	38	143	38	169												
	169	26	169	0												
OTCM	38	129	32	165	39	229										
	229	100	242	77	229	0										
CSUM	44	139	38	169	39	229	45	288								
	288	149	289	120	290	61	288	0								
FBAM	44	139	38	169	39	229	45	288	45	147						
	149	10	150	-19	135	-94	147	-141	147	0						
CLIP	44	139	38	169	39	229	45	288	45	147	45	161				
	163	24	168	-1	146	-83	161	-127	161	14	161	0				
HPAC	44	139	38	169	39	229	45	288	45	147	45	161	45	167		
	170	31	178	9	151	-78	167	-121	167	20	167	6	167	0		
WGTD	30	135	25	176	26	231	31	279	31	149	31	161	31	163	31	184
	188	53	201	25	161	-70	184	-95	184	35	184	23	184	21	184	0

36-HOUR MEAN FORECAST ERROR (NM)

	JTWC		NGPS		OTCM		CSUM		FBAM		CLIP		HPAC		WGTD	
JTWC	38	197														
	197	0														
NGPS	33	207	33	208												
	208	1	208	0												
OTCM	29	171	25	177	30	321										
	320	149	335	158	321	0										
CSUM	37	199	33	208	30	321	38	459								
	458	259	454	246	469	148	459	0								
FBAM	37	199	33	208	30	321	38	459	38	213						
	215	16	219	11	189	-132	213	-246	213	0						
CLIP	37	199	33	208	30	321	38	459	38	213	38	235				
	238	39	250	42	191	-130	235	-224	235	22	235	0				
HPAC	37	199	33	208	30	321	38	459	38	213	38	235	38	239		
	243	44	255	47	191	-130	239	-220	239	26	239	4	239	0		
WGTD	27	200	23	217	21	325	28	453	28	213	28	241	28	247	28	263
	269	69	291	74	210	-115	263	-190	263	50	263	22	263	16	263	0

TABLE 5-6 (CONTINUED) 1995 ERROR STATISTICS FOR SELECTED OBJECTIVE TECHNIQUES IN THE NORTH INDIAN OCEAN (1 JAN 1995 - 31 DEC 1995)

48-HOUR MEAN FORECAST ERROR (NM)

	JTWC		NGPS		OTCM		CSUM		FBAM		CLIP		HPAC		WGTD	
JTWC	32	262														
	262	0														
NGPS	25	282	25	285												
	285	3	285	0												
OTCM	25	218	19	245	26	389										
	388	170	415	170	389	0										
CSUM	31	265	25	285	26	389	32	620								
	617	352	584	299	634	245	620	0								
FBAM	31	265	25	285	26	389	32	620	32	256						
	257	-8	255	-30	230	-159	256	-364	256	0						
CLIP	31	265	25	285	26	389	32	620	32	256	32	301				
	304	39	318	33	238	-151	301	-319	301	45	301	0				
HPAC	31	265	25	285	26	389	32	620	32	256	32	301	32	298		
	303	38	316	31	233	-156	298	-322	298	42	298	-3	298	0		
WGTD	23	267	18	285	19	397	24	626	24	255	24	319	24	313	24	315
	325	58	352	67	249	-148	315	-311	315	60	315	-4	315	2	315	0

72-HOUR MEAN FORECAST ERROR (NM)

	JTWC		NGPS		OTCM		CSUM		FBAM		CLIP		HPAC		WGTD	
JTWC	20	342														
	342	0														
NGPS	14	358	14	326												
	326	-32	326	0												
OTCM	17	324	12	260	18	504										
	484	160	473	213	504	0										
CSUM	19	351	14	326	18	504	20	866								
	856	505	810	484	875	371	866	0								
FBAM	19	351	14	326	18	504	20	866	20	297						
	302	-49	298	-28	288	-216	297	-569	297	0						
CLIP	19	351	14	326	18	504	20	866	20	297	20	397				
	388	37	399	73	370	-134	397	-469	397	100	397	0				
HPAC	19	351	14	326	18	504	20	866	20	297	20	397	20	388		
	383	32	387	61	357	-147	388	-478	388	91	388	-9	388	0		
WGTD	16	388	11	374	15	566	17	905	17	302	17	444	17	438	17	384
	386	-2	405	31	359	-207	384	-521	384	82	384	-60	384	-54	384	0

TABLE 5-7 1995 ERROR STATISTICS FOR SELECTED OBJECTIVE TECHNIQUES IN THE SOUTHERN HEMISPHERE (1 JUL 1994 - 30 JUN 1995)

12-HOUR MEAN FORECAST ERROR (NM)

	JTWC		NGPS		OTCM		FBAM		CLIP		HPAC		WGTD		CLIM	
JTWC	244	63														
	63	0														
NGPS	172	63	262	83												
	85	22	83	0												
OTCM	226	62	205	86	321	79										
	77	15	78	-8	79	0										
FBAM	224	64	205	87	316	79	319	67								
	64	0	67	-20	65	-14	67	0								
CLIP	229	64	208	86	321	79	319	67	324	86						
	83	19	84	-2	83	4	86	19	86	0						
HPAC	229	64	208	86	321	79	319	67	324	86	324	77				
	75	11	77	-9	75	-4	77	10	77	-9	77	0				
WGTD	189	62	176	87	263	79	261	66	266	83	266	76	266	74		
	73	11	75	-12	72	-7	75	9	74	-9	74	-2	74	0		
CLIM	228	64	208	86	319	79	317	67	322	86	322	77	266	74	322	86
	86	22	87	1	84	5	86	19	86	0	86	9	84	10	86	0

24-HOUR MEAN FORECAST ERROR (NM)

	JTWC		NGPS		OTCM		FBAM		CLIP		HPAC		WGTD		CLIM	
JTWC	222	108														
	108	0														
NGPS	160	112	246	125												
	125	13	125	0												
OTCM	202	103	189	121	292	131										
	130	27	129	8	131	0										
FBAM	206	109	191	126	288	132	298	107								
	106	-3	115	-11	104	-28	107	0								
CLIP	210	109	194	125	292	131	298	107	302	151						
	149	40	151	26	146	15	152	45	151	0						
HPAC	210	109	194	125	292	131	298	107	302	151	302	130				
	132	23	134	9	125	-6	130	23	130	-21	130	0				
WGTD	172	103	163	125	240	130	244	105	248	146	248	126	248	121		
	123	20	125	0	115	-15	122	17	121	-25	121	-5	121	0		
CLIM	209	109	194	125	290	131	296	107	300	151	300	130	248	121	300	158
	162	53	164	39	152	21	159	52	158	7	158	28	151	30	158	0

36-HOUR MEAN FORECAST ERROR (NM)

	JTWC		NGPS		OTCM		FBAM		CLIP		HPAC		WGTD		CLIM	
JTWC	198	151														
	151	0														
NGPS	133	153	209	179												
	166	13	179	0												
OTCM	175	147	156	168	261	186										
	181	34	181	13	186	0										
FBAM	184	151	165	178	258	187	278	159								
	153	2	170	-8	154	-33	159	0								
CLIP	187	151	168	176	261	186	278	159	281	210						
	200	49	204	28	200	14	211	52	210	0						
HPAC	187	151	168	176	261	186	278	159	281	210	281	182				
	178	27	184	8	177	-9	183	24	182	-28	182	0				
WGTD	154	144	142	175	214	183	229	152	232	203	232	176	232	168		
	163	19	172	-3	161	-22	169	17	168	-35	168	-8	168	0		
CLIM	186	151	168	176	259	186	276	159	279	210	279	182	232	168	279	219
	221	70	224	48	217	31	221	62	219	9	219	37	209	41	219	0

TABLE 5-7 (CONTINUED) 1995 ERROR STATISTICS FOR SELECTED OBJECTIVE TECHNIQUES IN THE SOUTHERN HEMISPHERE (1 JUL 1994 - 30 JUN 1995)

48-HOUR MEAN FORECAST ERROR (NM)

	JTWC	NGPS	OTCM	FBAM	CLIP	HPAC	WGTD	CLIM
JTWC	175 198							
	198 0							
NGPS	109 191	174 229						
	203 12	229 0						
OTCM	156 198	131 201	238 254					
	257 59	238 37	254 0					
FBAM	161 197	136 223	235 255	253 209				
	195 -2	220 -3	201 -54	209 0				
CLIP	164 197	139 222	238 254	253 209	256 270			
	256 59	250 28	259 5	271 62	270 0			
HPAC	164 197	139 222	238 254	253 209	256 270	256 238		
	233 36	240 18	232 -22	239 30	238 -32	238 0		
WGTD	136 194	117 218	194 249	207 197	210 260	210 230	210 218	
	219 25	224 6	212 -37	219 22	218 -42	218 -12	218 0	
CLIM	163 196	139 222	236 253	251 209	254 269	254 238	210 218	254 280
	276 80	288 66	274 21	281 72	280 11	280 42	263 45	280 0

72-HOUR MEAN FORECAST ERROR (NM)

	CLIP	JTWC	NGPS	OTCM	FBAM	HPAC	CLIM
CLIP	203 405						
	405 0						
JTWC	50 427	53 291					
	287 -140	291 0					
NGPS	102 360	38 287	124 341				
	340 -20	387 100	341 0				
OTCM	187 398	47 281	98 261	187 405			
	405 7	381 100	387 126	405 0			
FBAM	200 406	49 286	99 336	184 406	200 313		
	313 -93	258 -28	310 -26	308 -98	313 0		
HPAC	203 405	50 287	102 340	187 405	200 313	203 347	
	347 -58	349 62	331 -9	344 -61	348 35	347 0	
CLIM	201 404	50 287	102 340	185 405	198 313	201 348	201 384
	384 -20	405 118	383 43	380 -25	386 73	384 36	384 0

6. TROPICAL CYCLONE WARNING VERIFICATION STATISTICS

6.1 GENERAL

Due to the rapid growth of microcomputers in the meteorological community, tropical cyclone track data (with best track, initial warning, 12-, 24-, 36-, 48-, and 72-hour JTWC forecasts) and fix data (satellite, aircraft, radar and synoptic) are now available as computer files separately upon request. The data will be in ASCII format and can be copied to 3.5 inch diskettes, and will fill two diskettes (or one high density diskette). These data include the western North Pacific Ocean (1 January - 31 December 1995) on one and North Indian Ocean (1 January - 31 December 1995), and western South Pacific and South Indian Oceans (1 July 1994 - 30 June 1995) on the other. Agencies or individuals desiring these data sets should send the appropriate number of diskettes to NAVPACMETOCCEN WEST/JTWC Guam with their request. When the request and your diskettes are received, the data will be copied onto your diskettes and returned with an explanation of the data formats.

6.2 WARNING VERIFICATION STATISTICS

6.2.1 WESTERN NORTH PACIFIC — This section includes verification statistics for each JTWC tropical cyclone warning in the western North Pacific Ocean during 1995.

JTWC BEST TRACK, FORECAST TRACK AND INTENSITY ERRORS BY WARNING

TROPICAL DEPRESSION 01W

DTG	WRN NO.	BEST TRACK LAT	LONG	WIND (KT)	POSITION ERRORS(NM) 00	12	24	36	48	72	WIND ERRORS(KT) 00	12	24	36	48	72
95010412		3.9N	171.0W	20												
95010418		4.2N	171.7W	20												
95010500		4.7N	172.4W	25												
95010506		5.0N	173.0W	25												
95010512		5.2N	173.6W	25												
95010518		5.4N	174.4W	20												
95010600		5.6N	175.4W	20												
95010606		5.8N	176.4W	20												
95010612		6.0N	177.5W	25												
95010618		6.2N	178.5W	25												
95010700		6.4N	179.5W	25												
95010706		6.7N	179.5E	25												
95010712		7.0N	178.5E	25												
95010718		7.4N	177.6E	30												
95010800		7.9N	176.6E	30												
95010806	1	8.6N	175.6E	30	21	48	50				0	10	20			
95010812	2	9.3N	174.6E	25	31	38					0	10				
95010818	3	9.9N	173.4E	20	26	95					5	10				
95010806		8.6N	175.6E	30												
95010812		9.3N	174.6E	25												
95010818		9.9N	173.4E	20												
95010900		10.2N	172.1E	15												
95010906		10.3N	170.9E	15												
			AVERAGE		27	61	50				2	10	20			
			# CASES		3	3	1				3	3	1			

TROPICAL STORM CHUCK (02W)

DTG	WRN NO.	BEST TRACK LAT	LONG	WIND (KT)	POSITION ERRORS(NM) 00	12	24	36	48	72	WIND ERRORS(KT) 00	12	24	36	48	72
95042300		5.5N	169.0E	15												
95042306		5.5N	168.9E	15												
95042312		5.5N	168.8E	15												
95042318		5.5N	168.7E	15												
95042400		5.4N	168.6E	15												
95042406		5.4N	168.5E	15												
95042412		5.4N	168.4E	15												
95042418		5.3N	168.3E	15												
95042500		5.3N	168.2E	15												
95042506		5.3N	168.0E	15												
95042512		5.2N	167.8E	15												
95042518		5.2N	167.6E	15												
95042600		5.2N	167.4E	20												
95042606		5.1N	167.0E	20												
95042612		5.0N	166.7E	20												
95042618		5.0N	166.3E	20												
95042700		5.1N	165.8E	25												
95042706		5.1N	165.3E	25												
95042712		5.2N	164.7E	25												
95042718		5.3N	164.4E	25												
95042800		5.4N	164.2E	25												
95042806	1	5.4N	164.0E	25	124	155	182	194	201	211	5	5	5	15	25	40
95042812	2	5.5N	163.8E	25	168	193	202	212	222	182	5	0	10	20	30	45
95042818	3	5.6N	163.6E	30	192	228	245	258	269	219	0	-5	0	10	25	45
95042900	4	5.7N	163.4E	35	161	157	180	210	245	234	0	0	5	15	25	40
95042906	5	5.7N	163.2E	35	148	176	219	266	295	313	0	0	5	15	25	40
95042912	6	5.8N	163.1E	35	148	157	177	200	207	251	0	0	10	20	25	35
95042918	7	5.8N	162.9E	35	176	186	199	191	155	131	0	0	10	20	25	35
95043000	8	5.9N	162.7E	35	37	43	60	80	146	262	0	5	10	15	20	30
95043006	9	5.9N	162.5E	35	41	43	36	85	163		0	5	10	10	15	
95043012	10	6.0N	162.3E	30	35	26	26	108	192		0	10	10	10	15	
95043018	11	6.0N	162.1E	30	24	13	83	174	247		0	10	10	10	15	
95050100	12	6.2N	161.8E	25	47	127					0	-5				
95050506		13.9N	149.3E	20												
95050512		14.3N	147.8E	20												
95050518		14.7N	146.1E	15												
95050600		15.0N	144.2E	15												
			AVERAGE		109	126	147	180	213	226	1	4	8	15	22	39
			# CASES		12	12	11	11	11	8	12	12	11	11	11	8

TROPICAL STORM DEANNA (03W)

DTG	WRN NO.	BEST TRACK LAT	LONG	WIND (KT)	POSITION ERRORS(NM) 00	12	24	36	48	72	WIND ERRORS(KT) 00	12	24	36	48	72
95052800		7.3N	149.8E	15												
95052806		8.2N	148.8E	20												
95052812		8.8N	147.8E	20												
95052818		9.1N	146.6E	20												
95052900		9.5N	145.4E	20												
95052906		9.7N	144.3E	20												
95052912		9.8N	142.8E	20												
95052918		9.7N	141.4E	20												
95053000		9.5N	139.7E	20												
95053006		9.3N	138.4E	20												
95053012		9.0N	137.1E	20												
95053018		8.8N	135.8E	20												
95053100		8.6N	134.3E	20												
95053106		8.8N	132.9E	20												
95053112		9.1N	131.2E	20												
95053118		9.3N	130.0E	20												
95060100		9.8N	128.8E	25												
95060106		10.2N	127.7E	25												
95060112		10.7N	126.8E	25												
95060118	1	11.5N	125.3E	25	46	62	76	47	41	441	0	-5	-15	-25	-20	-15
95060200	2	12.2N	123.9E	30	26	37	41	25	88	405	0	-5	-15	-20	-15	-15
95060206	3	12.7N	122.8E	30	42	114	180	236	337	513	0	-5	-5	0	5	-15
95060212	4	13.1N	121.8E	35	21	64	114	133	240	376	0	-5	-5	5	5	5
95060218	5	13.4N	120.7E	40	37	74	77	74	182	234	-5	-15	-10	0	0	0
95060300	6	13.7N	119.8E	45	0	26	80	227	258	258	-10	-10	0	0	0	0

TROPICAL STORM DEANNA (03W) (CONTINUED)

DTG	WRN NO.	LAT	LONG	WIND (KT)	00	12	24	36	48	72	00	12	24	36	48	72
95060306	7	13.9N	119.1E	50	11	18	161	278	258	233	-10	-5	5	10	5	5
95060312	8	14.2N	118.5E	50	5	90	269	309	262	196	-5	5	10	10	10	5
95060318	9	14.9N	118.0E	50	37	183	318	284	239	185	-5	5	10	5	5	0
95060400	10	16.0N	118.1E	45	71	219	239	176	174	183	0	5	10	10	5	0
95060406	11	17.4N	118.8E	45	8	45	58	178	303	452	0	5	5	5	0	-5
95060412	12	18.7N	119.5E	45	12	48	189	328	499	667	0	5	10	5	0	-5
95060418	13	19.4N	119.9E	45	18	107	238	373	508	635	0	5	5	0	-5	-5
95060500	14	19.2N	120.1E	45	8	134	245	398	493	544	0	10	10	5	0	0
95060506	15	19.1N	119.6E	45	8	86	197	323	383	448	0	10	10	10	5	0
95060512	16	18.9N	119.3E	40	24	95	223	311	352	372	5	10	10	10	5	0
95060518	17	18.7N	119.1E	40	107	167	246	252	312	258	5	10	10	10	10	0
95060600	18	18.5N	118.9E	40	17	70	87	82	86	73	0	5	5	5	0	-10
95060606	19	18.4N	118.5E	40	12	54	40	28	39	304	0	5	5	10	0	-10
95060612	20	18.3N	118.0E	40	53	63	48	47	88	525	0	0	5	10	5	0
95060618	21	18.6N	117.6E	40	22	43	92	161	298	973	0	0	0	0	0	-5
95060700	22	19.1N	117.6E	40	28	43	105	199	332		0	0	5	5	0	
95060706	23	19.7N	117.8E	40	6	45	95	227	471		0	5	5	5	-5	
95060712	24	20.3N	118.0E	40	21	82	183	353	617		-5	0	-5	-5	-10	
95060718	25	21.0N	118.3E	35	5	27	57	283	538		0	0	-5	-10	-10	
95060800	26	21.8N	118.8E	35	12	47	185	458			-5	-5	-5	-10		
95060806	27	22.7N	119.2E	35	5	99	347	650			-5	-5	-5	-10		
95060812	28	23.7N	120.6E	35	30	190	457				-5	-10	-15			
95060818	29	24.7N	122.0E	35	84	326	618				-5	-15	-15			
95060900	30	26.2N	124.4E	35	10	89					-10	-15				
95060906		28.0N	127.7E	35												
95060912		29.2N	130.9E	35												
95060918		30.3N	135.5E	35												
			AVERAGE		27	92	182	239	296	395	3	6	8	7	5	5
			# CASES		30	30	29	27	25	21	30	30	29	27	25	21

TROPICAL STORM ELI (04W)

	WRN	BEST TRACK			POSITION ERRORS(NM)						WIND ERRORS(KT)					
DTG	NO.	LAT	LONG	WIND (KT)	00	12	24	36	48	72	00	12	24	36	48	72
95053000		5.2N	155.5E	15												
95053006		5.5N	155.4E	15												
95053012		5.8N	155.3E	15												
95053018		6.1N	155.2E	15												
95053100		6.4N	154.9E	15												
95053106		6.6N	154.5E	15												
95053112		6.7N	154.0E	15												
95053118		6.7N	153.4E	15												
95060100		6.8N	152.8E	15												
95060106		6.9N	152.2E	15												
95060112		7.1N	151.5E	20												
95060118		7.4N	150.9E	20												
95060200		8.0N	150.3E	20												
95060206		8.7N	149.9E	20												
95060212		9.5N	149.5E	20												
95060218		10.3N	148.9E	20												
95060300		11.0N	148.2E	20												
95060306		11.7N	147.5E	25												
95060312		12.2N	146.6E	25												
95060318		12.6N	145.7E	30												
95060400		13.0N	144.8E	35												
95060406	1	13.3N	143.8E	40	61	99	145	169			-10	-10	-5	-5		
95060412		13.5N	142.8E	40												
95060418	2	13.7N	141.8E	40	102	181	233	252			-10	-5	-5	-5		
95060500		14.0N	140.8E	40												
95060506	3	14.4N	139.8E	35	55	69	145	243			-5	-5	-5	-5		
95060512		14.9N	138.9E	35												
95060518	4	15.6N	138.1E	35	45	12	28	41			-5	-5	-5	-5		
95060600		16.4N	137.6E	35												
95060606	5	17.2N	137.3E	35	24	53	111	147	166	429	-5	0	5	10	10	10
95060612	6	17.8N	137.2E	35	64	87	124	138	114		-5	0	5	15	10	
95060618	7	18.3N	137.2E	35	36	62	66	36	54		-5	-5	0	5	5	
95060700	8	18.8N	137.3E	35	11	21	37	108	252		0	0	10	15	15	
95060706	9	19.2N	137.3E	35	12	24	71	180	380		0	0	10	15	15	
95060712	10	19.6N	137.3E	35	24	55	102	218			0	10	10	10		
95060718	11	20.1N	137.2E	35	30	62	116	252			0	5	0	5		
95060800	12	20.8N	137.2E	30	42	115	258				0	0	0			
95060806	13	21.7N	137.3E	30	16	18					0	5				
95060812		22.8N	137.7E	30												

TROPICAL STORM ELI (04W) (CONTINUED)

DTG	WRN NO.	LAT	LONG	WIND (KT)	00	12	24	36	48	72	00	12	24	36	48	72
95060818		24.1N	138.5E	30												
95060900		25.7N	139.7E	30												
95060906		27.9N	141.5E	25												
		AVERAGE			41	66	120	163	194	429	3	4	5	9	11	10
		# CASES			13	13	12	11	5	1	13	13	12	11	5	1

TYPHOON FAYE (05W)

	WRN	BEST TRACK			POSITION ERRORS(NM)						WIND ERRORS(KT)					
DTG	NO.	LAT	LONG	WIND (KT)	00	12	24	36	48	72	00	12	24	36	48	72
95071206		6.2N	155.5E	15												
95071212		6.0N	154.5E	15												
95071218		5.9N	153.4E	15												
95071300		5.9N	152.2E	15												
95071306		6.0N	150.9E	15												
95071312		6.4N	149.6E	20												
95071318		7.0N	148.5E	20												
95071400		7.6N	147.3E	20												
95071406		8.3N	146.2E	20												
95071412		9.2N	145.1E	20												
95071418		10.1N	144.2E	20												
95071500		11.1N	143.5E	25												
95071506		12.2N	142.8E	25												
95071512		13.0N	142.3E	25												
95071518		14.0N	142.0E	25												
95071600	1	14.9N	141.8E	25	5	47	58	65	92	49	0	-5	-5	-10	-10	-30
95071606	2	16.0N	141.6E	25	11	16	30	30	39	76	0	-5	-5	-10	-15	-30
95071612	3	16.7N	141.4E	30	12	37	65	94	156	351	-5	-5	-5	-10	-25	-45
95071618	4	17.3N	141.0E	30	31	64	71	126	222	433	0	0	0	-10	-30	-50
95071700	5	17.7N	140.5E	35	16	37	49	104	147	284	-5	-5	-5	-15	-20	-35
95071706	6	18.0N	139.9E	35	26	37	62	112	152	296	0	-5	-5	-10	-15	-40
95071712	7	18.2N	139.5E	40	21	49	108	168	230	398	-5	-5	-10	-15	-20	-45
95071718	8	18.5N	139.1E	40	24	79	148	189	263	447	0	-5	-10	-10	-20	-45
95071800	9	18.8N	138.5E	45	8	59	73	98	156	298	0	0	-5	-5	-10	-20
95071806	10	19.2N	137.6E	50	24	36	42	43	82	171	5	0	5	0	-10	-20
95071812	11	19.4N	136.7E	55	23	36	66	105	153	214	0	0	5	-5	-10	-25
95071818	12	19.7N	135.9E	60	39	49	82	153	211	239	-5	0	-5	-10	-10	-20
95071900	13	19.9N	135.2E	65	17	18	42	89	137	197	-5	-5	-10	-15	-15	-20
95071906	14	20.2N	134.6E	65	5	28	90	115	164	159	-5	-10	-20	-20	-25	-25
95071912	15	20.6N	133.6E	70	20	45	78	103	133	170	-5	-10	-15	-15	-20	-20
95071918	16	21.0N	132.8E	75	17	65	95	132	153	234	-10	-15	-15	-20	-20	-20
95072000	17	21.6N	131.8E	80	21	69	98	107	132	343	-10	-20	-20	-25	-20	-20
95072006	18	22.3N	130.6E	85	13	26	42	39	65	383	-5	-5	-15	-15	-15	-10
95072012	19	22.9N	129.7E	90	0	29	34	66	133	475	-15	-15	-20	-15	-25	-5
95072018	20	23.6N	128.8E	90	8	29	31	65	177	527	-15	-20	-20	-20	-25	5
95072100	21	24.2N	128.0E	95	8	16	32	118	247	619	-20	-25	-20	-20	-25	10
95072106	22	24.9N	127.2E	100	0	29	89	164	253	514	-25	-25	-25	-20	-20	15
95072112	23	25.4N	126.8E	105	12	22	113	202	318	579	-15	-5	-10	-20	5	15
95072118	24	26.3N	126.3E	105	8	37	133	212	288	542	-15	-10	-25	-20	0	0
95072200	25	27.2N	126.2E	105	0	58	116	217	304	510	-10	-5	-5	20	15	15
95072206	26	28.1N	126.5E	105	6	59	164	243	331	528	-10	-10	-15	10	10	10
95072212	27	29.3N	127.1E	105	23	136	325	412	439		-10	-20	10	15	20	
95072218	28	30.7N	127.6E	105	0	69	138	156	193		-15	-10	20	25	20	
95072300	29	32.3N	127.8E	105	0	59	88	137	173		-15	15	25	30	25	
95072306	30	34.5N	127.9E	95	4	31	67	166	274		-10	20	25	20	10	
95072312	31	36.3N	128.0E	70	33	44	146	310			10	15	20	15		
95072318	32	37.9N	128.9E	60	48	37	126	304			5	10	5	10		
95072400	33	39.4N	130.9E	55	61	42	31				0	5	0			
95072406	34	40.6N	133.2E	45	11	51	148				0	-5	-5			
95072412	35	41.7N	135.7E	40	39	148					0	0				
95072418	36	42.6N	138.5E	40	105	142					-10					
95072500		43.2N	141.3E	35												
95072506		43.9N	144.7E	30												
		AVERAGE			20	51	91	146	194	348	7	9	12	15	17	23
		# CASES			36	36	34	32	30	26	36	36	34	32	30	26

TROPICAL STORM 06W

DTG	WRN NO.	BEST TRACK LAT	LONG	WIND (KT)	POSITION ERRORS(NM) 00	12	24	36	48	72	WIND ERRORS(KT) 00	12	24	36	48	72
95072506		15.1N	133.2E	20												
95072512		15.5N	132.3E	20												
95072518		15.8N	131.3E	20												
95072600		16.3N	129.3E	20												
95072606		16.3N	127.6E	20												
95072612		16.3N	125.8E	20												
95072618	1	16.3N	124.4E	25	43	36	169	321			0	0	-10	-10		
95072700		16.5N	123.5E	25												
95072706	2	16.6N	121.8E	25	29	103	241	339	393		0	-5	-10	0	10	
95072712	3	16.7N	121.7E	30	17	47	85	78			0	-5	-5	5		
95072718	4	17.0N	122.1E	30	34	86	88	66			0	-5	0	10		
95072800	5	17.3N	122.4E	35	34	8	29				-5	-5	0			
95072806	6	17.6N	122.7E	35	5	16	56				-5	0	5			
95072812	7	18.0N	122.7E	35	16	51					-5	0				
95072818	8	18.5N	122.5E	30	24	63					0	5				
95072900	9	18.8N	122.2E	30	0						0					
95072906	10	18.9N	121.7E	25	0						-5					
			AVERAGE		21	52	112	202	393		2	3	5	6	10	
			# CASES		10	8	6	4	1		10	8	6	4	1	

TYPHOON GARY (07W)

DTG	WRN NO.	BEST TRACK LAT	LONG	WIND (KT)	POSITION ERRORS(NM) 00	12	24	36	48	72	WIND ERRORS(KT) 00	12	24	36	48	72
95072706		18.5N	120.0E	20												
95072712		18.5N	120.0E	20												
95072718		18.5N	120.0E	25												
95072800		18.2N	120.0E	30												
95072806		18.2N	119.7E	30												
95072812		18.3N	119.5E	35												
95072818		18.3N	119.3E	35												
95072900	1	18.3N	119.1E	40	46	30	45	64			-15	-20	-30	-35		
95072906	2	18.6N	118.6E	45	42	47	50	17	102		-15	-20	-20	-10	10	
95072912	3	18.8N	118.3E	50	16	34	23	98	156		-10	-15	-10	0	30	
95072918	4	19.0N	118.0E	55	6	24	23	108	159		-15	-20	-10	10	45	
95073000	5	19.1N	117.7E	60	12	34	126	194			-15	-15	-10	25		
95073006	6	19.5N	117.5E	65	18	96	207	244			-15	-10	10	40		
95073012	7	20.2N	117.4E	65	28	103	110				-15	-10	25			
95073018	8	21.2N	117.3E	65	0	49	81				-10	10	15			
95073100	9	22.8N	117.0E	65	24	34					-5	5				
95073106	10	23.9N	116.9E	55	13	68					0	10				
95073112	11	24.8N	116.9E	40	60						0					
95073118	12	25.8N	116.9E	25	66						10					
			AVERAGE		28	52	84	121	140		10	14	16	20	28	
			# CASES		12	10	8	6	3		12	10	8	6	3	

TYPHOON HELEN (08W)

DTG	WRN NO.	BEST TRACK LAT	LONG	WIND (KT)	POSITION ERRORS(NM) 00	12	24	36	48	72	WIND ERRORS(KT) 00	12	24	36	48	72
95080300		12.0N	145.3E	15												
95080306		12.2N	144.6E	15												
95080312		12.4N	143.9E	15												
95080318		12.6N	143.3E	20												
95080400		12.9N	142.8E	20												
95080406		13.1N	142.2E	15												
95080412		13.2N	141.6E	15												
95080418		13.3N	141.0E	15												
95080500		13.4N	140.4E	15												
95080506		13.5N	139.8E	15												
95080512		13.6N	139.0E	15												
95080518		13.8N	138.4E	20												
95080600		14.0N	137.6E	20												
95080606		14.1N	136.8E	20												
95080612		14.3N	135.7E	20												
95080618		14.5N	134.5E	20												
95080700	1	14.6N	133.2E	25	84	83	74	154			0	-5	-5	0		

TYPHOON HELEN (08W) (CONTINUED)

DTG	WRN NO.	LAT	LONG	WIND (KT)	00	12	24	36	48	72	00	12	24	36	48	72
95080706	2	14.7N	131.8E	25	34	112	216	247	229	121	0	-5	0	5	10	10
95080712	3	15.1N	130.3E	30	54	157	241	224	212	82	-5	0	10	15	25	20
95080718	4	16.0N	129.1E	30	118	220	243	224	180	18	0	5	15	20	20	30
95080800	5	17.2N	128.2E	30	170	268	273	294	247	185	0	5	5	10	15	0
95080806	6	18.3N	127.3E	30	29	62	133	166	210	200	0	0	0	0	0	-5
95080812	7	19.0N	125.9E	30	52	85	140	169	179	74	0	-5	0	0	0	-5
95080818	8	19.1N	124.8E	30	73	152	185	206	218	108	0	0	-5	-5	-5	-10
95080900	9	19.1N	123.5E	35	24	75	122	150	139	12	0	0	0	0	-5	-15
95080906	10	19.1N	121.7E	35	18	49	106	156	139	99	5	0	0	0	-5	-10
95080912	11	19.1N	120.4E	35	18	55	93	87	102	216	5	5	5	0	0	10
95080918	12	18.9N	119.4E	40	12	62	98	79	83	166	0	-5	-5	-10	-10	0
95081000	13	18.5N	118.4E	40	42	88	103	112	117		0	-5	-10	-10	-40	
95081006	14	18.3N	117.8E	45	55	70	111	185	213		-5	-5	-15	-15	-20	
95081012	15	18.2N	117.2E	45	11	43	135	206	285		0	-10	-15	-20	15	
95081018	16	18.3N	116.4E	50	8	75	98	102	107		-5	-10	-15	5	0	
95081100	17	19.0N	115.9E	55	6	20	28	32	86		-5	-5	-15	-5	-5	
95081106	18	19.8N	115.5E	60	16	45	60	48			0	0	-5	0		
95081112	19	20.7N	115.1E	60	5	18	30	30			0	-5	10	5		
95081118	20	21.6N	114.8E	65	8	22	44				-5	-5	5			
95081200	21	22.4N	114.6E	70	8	13	32				-10	10	10			
95081206	22	23.3N	114.5E	50	12	30					-5	0				
95081212	23	24.2N	114.5E	35	8	57					0	0				
95081218		25.1N	114.7E	30												
95081300		26.0N	115.2E	25												
			AVERAGE		38	81	123	152	172	117	2	4	7	7	11	10
			# CASES		23	23	21	19	16	11	23	23	21	19	16	11

TROPICAL STORM IRVING (09W)

DTG	WRN NO.	BEST TRACK LAT	LONG	WIND (KT)	POSITION ERRORS(NM) 00	12	24	36	48	72	WIND ERRORS(KT) 00	12	24	36	48	72
95081306		11.6N	124.0E	15												
95081312		12.0N	123.3E	15												
95081318		12.4N	122.5E	15												
95081400		12.7N	121.5E	15												
95081406		12.8N	120.4E	15												
95081412		12.9N	119.5E	15												
95081418		13.0N	118.7E	15												
95081500		13.1N	118.0E	15												
95081506		13.2N	117.4E	15												
95081512		13.3N	116.8E	15												
95081518		13.4N	116.2E	15												
95081600		13.6N	115.5E	15												
95081606		14.0N	114.8E	15												
95081612		14.5N	114.1E	15												
95081618		15.0N	113.5E	20												
95081700		15.6N	113.0E	25												
95081706	1	16.2N	112.7E	30	56	103	154	185	193	261	-5	-10	-10	-10	-10	20
95081712	2	16.8N	112.5E	35	18	32	33	43	20	68	0	5	5	-5	0	20
95081718	3	17.4N	112.4E	35	21	29	34	80	133	165	0	0	0	-5	5	5
95081800	4	17.9N	112.3E	40	11	16	54	108	139	153	-5	-5	-5	0	10	10
95081806	5	18.4N	112.2E	45	5	24	82	145	181		0	0	0	15	0	
95081812	6	18.8N	112.1E	50	12	46	104	151	170		0	-5	5	5	-10	
95081818	7	19.2N	111.9E	55	18	70	132	157	171		0	0	15	10	-5	
95081900	8	19.5N	111.5E	60	18	52	84	94	104		0	10	15	10	0	
95081906	9	19.8N	111.0E	60	12	28	45	71			0	5	5	5		
95081912	10	20.1N	110.4E	55	17	41	71	123			0	5	5	10		
95081918	11	20.5N	109.8E	50	13	43	69				0	0	5			
95082000	12	21.0N	109.3E	45	11	39	62				0	0	0			
95082006	13	21.6N	108.9E	40	61	137					0	0				
95082012	14	22.2N	108.5E	35	37	65					0	5				
95082018	15	22.9N	108.1E	30	44						0					
95082100		23.7N	107.7E	25												
			AVERAGE		24	52	77	116	140	162	1	4	6	8	5	14
			# CASES		15	14	12	10	8	4	15	14	12	10	8	4

TROPICAL STORM JANIS (10W)

DTG	WRN NO.	BEST TRACK LAT	LONG	WIND (KT)	POSITION ERRORS(NM) 00	12	24	36	48	72	WIND ERRORS(KT) 00	12	24	36	48	72
95081700		12.0N	144.0E	15												
95081706		14.3N	143.7E	15												
95081712		15.9N	143.1E	15												
95081718		17.1N	142.3E	15												
95081800		18.0N	141.2E	15												
95081806		18.5N	140.2E	15												
95081812		18.8N	139.0E	15												
95081818		19.2N	137.8E	15												
95081900		19.6N	136.5E	20												
95081906		19.9N	135.3E	20												
95081912		20.2N	133.9E	20												
95081918		20.4N	132.8E	20												
95082000		20.6N	131.7E	20												
95082006		20.5N	130.6E	25												
95082012		20.5N	130.0E	25												
95082018		20.4N	129.5E	25												
95082100		20.2N	129.1E	30												
95082106		20.2N	129.5E	30												
95082112	1	20.2N	129.9E	35	11	73	114	117	158	154	-10	-10	0	10	30	35
95082118	2	20.3N	130.3E	40	41	96	81	112	129	185	-5	0	10	25	35	45
95082200	3	20.6N	130.6E	45	22	65	82	162	160	226	-5	5	15	35	35	50
95082206	4	21.2N	130.5E	45	30	76	207	243	240	264	0	10	25	30	40	55
95082212	5	21.8N	130.1E	45	79	228	385	390	365	312	0	10	30	30	35	70
95082218	6	22.4N	129.1E	45	97	231	279	275	293	272	0	15	25	25	35	70
95082300	7	23.5N	127.8E	45	0	78	92	108	149	144	-5	10	5	0	15	35
95082306	8	24.5N	126.2E	40	26	41	49	70	99	247	0	5	0	0	20	20
95082312	9	25.4N	124.9E	35	49	41	56	95	84	150	5	0	0	15	30	15
95082318	10	25.9N	124.2E	40	28	6	28	31	13	218	5	5	10	20	30	25
95082400	11	26.3N	123.4E	45	8	52	82	95	117	306	0	-10	-15	-5	-10	-10
95082406	12	26.9N	122.7E	50	24	73	82	66	156	349	-5	-5	-5	0	-15	-10
95082412	13	27.5N	122.1E	55	17	48	102	171	243	372	0	15	30	20	5	5
95082418	14	28.0N	121.4E	55	36	42	50	115	129	266	-5	0	5	-5	-5	-10
95082500	15	28.8N	121.0E	50	24	59	95	135	94	189	-5	5	-5	-15	-5	-15
95082506	16	29.8N	120.8E	45	5	38	84	108	119	274	-5	5	-10	-5	-10	-15
95082512	17	31.1N	121.0E	35	30	67	117	91	91	218	5	0	-15	-5	-10	-15
95082518	18	32.4N	121.4E	35	43	102	73	66	60		5	-5	-5	-10	-10	
95082600	19	34.1N	122.4E	40	11	35	103	169	135		5	-5	0	-5	-10	
95082606	20	35.7N	123.7E	45	39	55	118	97	83		5	5	0	-5	-10	
95082612	21	36.9N	125.7E	50	23	84	163	113	140		0	5	0	-5	-10	
95082618	22	37.7N	127.6E	40	27	99	78	68			0	0	-5	-5		
95082700		38.2N	129.7E	40												
95082706		38.3N	132.5E	40												
95082712		38.9N	135.6E	40												
95082718		39.9N	138.6E	40												
95082800		40.7N	141.8E	40												
95082806		40.9N	145.9E	40												
95082812		41.1N	151.4E	40												
95082818		41.0N	157.0E	40												
95082900		41.1N	162.4E	35												
95082906		42.0N	167.0E	35												
95082912		42.8N	171.3E	35												
95082918		44.0N	174.0E	35												
95083000		45.0N	176.0E	30												
			AVERAGE		31	77	115	132	146	244	3	6	10	13	19	29
			# CASES		22	22	22	22	21	17	22	22	22	22	21	17

TROPICAL DEPRESSION 11W

DTG	WRN NO.	BEST TRACK LAT	LONG	WIND (KT)	POSITION ERRORS(NM) 00	12	24	36	48	72	WIND ERRORS(KT) 00	12	24	36	48	72
95082100		23.2N	130.1E	15												
95082106		23.4N	129.0E	15												
95082112		23.8N	128.0E	20												
95082118		24.2N	127.1E	20												
95082200		24.6N	126.2E	25												
95082206		24.9N	125.6E	25												
95082212		25.2N	125.0E	25												
95082218		25.0N	124.3E	25												
95082300		23.5N	125.9E	20												

TROPICAL DEPRESSION 11W (CONTINUED)

95082306		24.5N	126.2E	20												
95082212	1	25.2N	125.0E	25	6	121					0	5				
95082218		25.0N	124.3E	25												
95082300	2	23.5N	125.9E	20	112						5					
95082306		24.5N	126.2E	20												
				AVERAGE	59	121					3	5				
				# CASES	2	1					2	1				

SUPER TYPHOON KENT (12W)

DTG	WRN NO.	BEST TRACK LAT	LONG	WIND (KT)	POSITION ERRORS(NM) 00	12	24	36	48	72	WIND ERRORS(KT) 00	12	24	36	48	72
95082400		9.6N	133.7E	15												
95082406		9.8N	133.1E	15												
95082412		10.2N	132.6E	20												
95082418		10.8N	131.9E	20												
95082500		11.5N	131.3E	20												
95082506		12.4N	130.8E	20												
95082512		13.1N	130.3E	20												
95082518		13.9N	129.7E	30												
95082600	1	14.7N	128.9E	35	72	81	106	157			-10	-30	-35	-35		
95082606		15.3N	128.1E	45												
95082612	2	15.7N	127.3E	55	50	51	97	150	191	214	-15	-15	-15	-20	-20	-70
95082618	3	16.1N	126.8E	60	39	71	103	129	142	147	-10	-5	-5	0	10	-40
95082700	4	16.6N	126.6E	60	17	71	134	193	220	194	-5	-5	-10	0	-10	-35
95082706	5	16.9N	126.5E	65	24	86	144	193	234	217	-10	-5	0	5	-15	-40
95082712	6	17.1N	126.4E	65	29	74	107	133	177	229	-5	-10	0	-5	-40	-35
95082718	7	17.3N	126.4E	70	29	52	61	69	102	244	-5	-5	-5	-20	-40	-20
95082800	8	17.5N	126.3E	75	12	12	26	76	151	409	-10	-5	-15	-45	-30	0
95082806	9	17.8N	126.2E	75	6	33	99	165	244	442	-5	0	-15	-30	-15	10
95082812	10	18.0N	126.0E	75	18	54	90	123	191	323	0	0	-30	-20	-10	15
95082818	11	18.2N	125.6E	80	26	62	82	127	181	308	-5	-20	-35	-20	-20	-5
95082900	12	18.5N	125.1E	90	12	16	57	95	140	267	-15	-55	-40	-30	-15	15
95082906	13	18.7N	124.6E	105	8	45	97	142	186	350	-20	-40	-20	0	15	30
95082912	14	19.1N	124.0E	130	6	53	104	160	211	430	0	10	25	35	65	65
95082918	15	19.6N	123.2E	130	20	79	130	188	269	590	0	10	20	35	45	50
95083000	16	20.2N	122.1E	125	8	30	85	149	262		5	15	25	35	30	
95083006	17	20.6N	121.0E	120	5	16	55	121	203		10	20	25	15	15	
95083012	18	21.1N	119.6E	115	6	18	63	158	231		15	25	25	20	10	
95083018	19	21.6N	118.3E	110	5	33	126	223	306		20	15	20	15	10	
95083100	20	22.1N	116.7E	105	16	36	104	185			20	20	30	10		
95083106	21	22.6N	115.2E	95	5	67	134	206			10	10	5	5		
95083112	22	23.2N	113.5E	75	8	57	121				5	10	5			
95083118	23	23.9N	111.4E	55	32	106	161				10	5	0			
95090100	24	24.5N	109.4E	35	36	39					0	0				
95090106		24.9N	107.4E	30												
95090112		25.3N	105.6E	25												
95090118		25.3N	103.7E	20												
				AVERAGE	21	52	100	150	203	312	9	14	18	19	23	31
				# CASES	24	24	23	21	18	14	24	24	23	21	18	14

TYPHOON LOIS (13W)

DTG	WRN NO.	BEST TRACK LAT	LONG	WIND (KT)	POSITION ERRORS(NM) 00	12	24	36	48	72	WIND ERRORS(KT) 00	12	24	36	48	72
95082106		15.6N	114.8E	10												
95082112		15.8N	114.8E	10												
95082118		16.0N	114.7E	10												
95082200		16.2N	114.7E	10												
95082206		16.4N	114.7E	15												
95082212		16.5N	114.7E	15												
95082218		16.6N	114.7E	15												
95082300		16.7N	114.7E	20												
95082306		16.8N	114.7E	20												
95082312		16.9N	114.8E	20												
95082318		16.9N	114.8E	20												
95082400		16.9N	114.9E	20												
95082406		17.0N	115.1E	20												
95082412		17.1N	115.2E	20												
95082418		17.2N	115.3E	20												
95082500		17.3N	115.3E	20												
95082506		17.3N	115.3E	20												

TYPHOON LOIS (13W) (CONTINUED)

DTG	WRN NO.	LAT	LONG	WIND (KT)	00	12	24	36	48	72	00	12	24	36	48	72
95082512		17.4N	115.3E	20												
95082518		17.6N	115.0E	25												
95082600	1	17.7N	114.6E	30	51	87	168	223	251	276	-5	-10	-10	-25	-20	-10
95082606	2	17.6N	114.2E	30	37	83	112	132	132	171	0	0	-10	-5	0	0
95082612	3	17.6N	113.9E	35	41	95	128	137	140	164	-5	-5	-15	-10	0	0
95082618	4	17.3N	113.2E	35	74	99	133	147	144	192	0	-20	-15	-10	0	0
95082700	5	17.3N	112.7E	40	12	67	125	159	178	277	5	-10	-10	-5	0	20
95082706	6	17.5N	112.0E	55	8	6	18	8	8	200	0	5	5	0	5	15
95082712	7	17.7N	111.3E	60	13	34	42	50	61	256	-5	0	5	5	0	15
95082718	8	18.0N	110.6E	60	38	30	37	53	86	367	0	5	10	10	5	30
95082800	9	18.3N	110.0E	65	8	33	52	50	41		0	-10	0	0	-15	
95082806	10	18.6N	109.5E	65	8	11	5	28	139		0	-5	0	5	-5	
95082812	11	18.7N	108.9E	65	8	16	22	102	238		0	0	5	25	10	
95082818	12	18.9N	108.4E	65	6	21	45	164	293		0	0	5	10	5	
95082900	13	19.1N	107.8E	65	12	39	135	277	396		0	0	10	15	10	
95082906	14	19.3N	107.1E	65	0	46	167	284			0	0	5	10		
95082912	15	19.3N	106.4E	65	12	98	251	389			0	0	10	10		
95082918	16	19.2N	105.3E	65	29	151	265				0	5	15			
95083000	17	18.8N	103.9E	50	43	186	331				0	5	0			
95083006	18	18.4N	102.2E	40	18	123					0	10				
95083012		18.2N	100.3E	30												
95083018		18.2N	98.9E	20												
95083100		18.2N	96.7E	20												
			AVERAGE		24	69	120	147	162	238	1	5	8	10	6	11
			# CASES		18	18	17	15	13	8	18	18	17	15	13	8

TYPHOON MARK (14W)

DTG	WRN NO.	BEST TRACK LAT	LONG	WIND (KT)	POSITION ERRORS(NM) 00	12	24	36	48	72	WIND ERRORS(KT) 00	12	24	36	48	72
95082806		24.0N	151.2E	20												
95082812		24.1N	151.0E	20												
95082818		24.3N	150.8E	20												
95082900		24.8N	150.8E	20												
95082906		25.2N	150.8E	20												
95082912		26.0N	151.0E	20												
95082918		27.0N	151.2E	25												
95083000	1	28.3N	151.9E	30	27	38	76	116	130	475	0	-5	-20	-25	-45	-55
95083006	2	29.1N	152.8E	35	12	23	63	72	74	453	0	-15	-25	-35	-65	-40
95083012	3	29.6N	153.5E	40	28	52	110	112	121	486	5	-15	-25	-45	-65	-20
95083018	4	30.1N	154.2E	55	0	11	46	115	176	323	0	-10	-25	-60	-65	-20
95083100	5	30.5N	155.1E	60	7	15	54	167	297		-5	-10	-35	-60	-50	
95083106	6	31.0N	156.1E	65	13	7	45	194	357		0	-5	-40	-50	-30	
95083112	7	31.5N	157.1E	65	6	54	190	326	417		0	-15	-40	-35	-10	
95083118	8	32.4N	158.0E	70	28	133	301	478	596		-5	-30	-40	-20	-10	
95090100	9	33.4N	159.0E	80	11	146	302	449			-5	-20	-15	0		
95090106	10	34.9N	160.8E	95	15	93	199	271			-10	-20	0	5		
95090112	11	36.4N	163.4E	95	14	59	114				-10	-5	20			
95090118	12	37.9N	166.0E	95	53	91	100				-20	0	10			
95090200	13	39.3N	169.1E	80	44	111					-5	20				
95090206	14	40.3N	172.6E	65	54	122					-15	0				
95090212	15	40.7N	176.0E	45	41						0					
95090218		41.0N	179.2E	45												
			AVERAGE		24	69	134	230	272	435	5	12	25	34	43	34
			# CASES		15	14	12	10	8	4	15	14	12	10	8	4

TROPICAL STORM NINA (15W)

DTG	WRN NO.	BEST TRACK LAT	LONG	WIND (KT)	POSITION ERRORS(NM) 00	12	24	36	48	72	WIND ERRORS(KT) 00	12	24	36	48	72
95090100		8.2N	139.3E	20												
95090106		9.0N	137.9E	25												
95090112		9.7N	136.0E	25												
95090118		10.4N	134.2E	25												
95090200		11.1N	132.4E	25												
95090206		11.6N	130.9E	25												
95090212		12.0N	129.4E	25												
95090218	1	12.6N	127.9E	30	26	90	151	145	112	51	0	0	0	0	-5	5
95090300	2	13.6N	126.7E	35	26	119	122	64	59	78	0	0	0	-5	0	0
95090306	3	14.7N	125.8E	35	33	98	112	129	113	79	0	0	0	-5	0	0
95090312	4	15.8N	124.9E	35	13	81	201	313	342		0	-5	-10	-10	-15	

TROPICAL STORM NINA (15W) (CONTINUED)

95090318	5	16.5N	123.6E	35	74	186	303	376			0	-10	-10	-10		
95090400	6	16.9N	122.2E	35	25	131	174	199	178	231	0	-10	-10	-5	-5	-5
95090406	7	17.1N	120.8E	35	53	51	99	87	51	192	-10	-10	-5	0	-5	0
95090412	8	17.1N	119.5E	35	80	113	155	152	120	86	0	5	10	10	10	5
95090418	9	17.0N	118.2E	35	12	53	75	59	61	205	0	0	5	0	0	10
95090500	10	16.8N	117.2E	35	49	96	93	59	55	196	0	0	0	5	0	20
95090506	11	16.7N	116.4E	35	12	42	95	179	277		0	5	0	0	5	
95090512	12	16.7N	115.7E	35	8	46	120	224	336		0	0	0	0	5	
95090518	13	16.9N	115.0E	35	33	26	102	178	224		0	0	-5	5	10	
95090600	14	17.4N	114.2E	40	8	64	145	237	292		-5	0	-5	5	25	
95090606	15	18.1N	113.5E	40	24	85	171	258			0	-5	0	15		
95090612	16	19.0N	112.7E	40	47	112	196	260			0	0	5	25		
95090618	17	19.9N	111.9E	45	49	103	182				0	5	10			
95090700	18	20.9N	110.8E	45	13	93	204				0	-5	10			
95090706	19	21.8N	109.5E	40	60	98					5	5				
95090712	20	22.6N	107.9E	40	21	150					0	10				
95090718		22.9N	106.1E	30												
95090800		22.9N	104.1E	20												
			AVERAGE		34	92	150	183	171	140	1	4	5	6	7	6
			# CASES		20	20	18	16	13	8	20	20	18	16	13	8

TROPICAL DEPRESION 16W

DTG	WRN NO.	BEST TRACK LAT	LONG	WIND (KT)	POSITION ERRORS(NM) 00	12	24	36	48	72	WIND ERRORS(KT) 00	12	24	36	48	72
95090312		4.5N	144.1E	15												
95090318		4.7N	143.1E	15												
95090400		5.0N	141.8E	15												
95090406		5.3N	140.6E	15												
95090412		5.5N	139.2E	15												
95090418		5.9N	138.2E	20												
95090500		6.2N	137.0E	20												
95090506		6.4N	136.0E	20												
95090512		6.7N	134.8E	20												
95090518		6.9N	133.8E	20												
95090600		7.3N	132.2E	20												
95090606		7.6N	131.2E	20												
95090612		8.0N	129.9E	20												
95090618		8.2N	128.6E	20												
95090700		8.5N	127.2E	20												
95090706		9.0N	125.8E	15												
95090712		9.5N	124.3E	15												
95090718		9.9N	122.8E	15												
95090800		10.4N	121.0E	20												
95090806		11.3N	119.2E	20												
95090812		11.7N	117.2E	25												
95090818		12.0N	115.4E	25												
95090900		12.4N	113.7E	20												
95090906		12.9N	112.4E	20												
95090912		13.3N	111.4E	20												
95090918	1	13.5N	110.7E	20	24	163	279				5	-10	-5			
95091000		13.6N	110.3E	25												
95091006	2	13.9N	110.0E	30	13	50	83				-5	0	-5			
95091012		14.0N	109.7E	30												
95091018	3	14.3N	109.5E	25	29	52					0	0				
95091100		14.6N	109.4E	25												
95091106	4	14.9N	108.9E	20	29						0					
95091112		14.9N	107.7E	15												
95091118		14.6N	105.6E	15												
			AVERAGE		24	89	182				3	3	5			
			# CASES		4	3	2				4	3	2			

SUPER TYPHOON OSCAR (17W)

DTG	WRN NO.	BEST TRACK LAT	LONG	WIND (KT)	POSITION ERRORS(NM) 00	12	24	36	48	72	WIND ERRORS(KT) 00	12	24	36	48	72
95090706		8.5N	161.2E	15												
95090712		8.9N	160.0E	15												
95090718		9.3N	158.9E	15												
95090800		9.6N	157.8E	15												
95090806		10.0N	156.5E	15												

SUPER TYPHOON OSCAR (17W) (CONTINUED)

DTG	WRN NO.	LAT	LONG	WIND (KT)	00	12	24	36	48	72	00	12	24	36	48	72
95090812		10.3N	155.3E	20												
95090818		10.6N	154.3E	20												
95090900		10.8N	153.5E	20												
95090906		11.0N	152.9E	20												
95090912		11.3N	152.5E	20												
95090918		11.6N	152.1E	20												
95091000		11.9N	151.7E	20												
95091006		12.3N	151.2E	20												
95091012		12.8N	150.6E	20												
95091018		13.4N	150.0E	20												
95091100		13.9N	149.5E	20												
95091106		14.4N	148.9E	20												
95091112		14.9N	148.2E	25												
95091118	1	15.3N	147.7E	25	21	59	83	91	69	103	5	5	0	-10	-10	-50
95091200	2	15.8N	147.2E	30	17	28	54	82	122	130	0	0	0	-10	-10	-35
95091206	3	16.4N	146.8E	30	18	36	58	78	98	99	0	0	-5	-5	-20	-40
95091212	4	16.9N	146.4E	35	6	21	29	84	144	179	0	0	-10	-10	-35	-40
95091218	5	17.5N	145.8E	40	21	41	59	112	136	210	0	-5	-5	-20	-35	-40
95091300	6	18.0N	145.1E	45	51	77	150	161	192	223	0	-10	-10	-35	-35	-40
95091306	7	18.6N	144.4E	55	80	131	199	211	217	236	0	0	-15	-25	-40	-40
95091312	8	19.1N	143.6E	65	46	95	143	184	211	171	-10	-10	-35	-40	-50	-50
95091318	9	19.7N	142.5E	65	5	28	25	32	81	106	10	-5	-20	-35	-35	-50
95091400	10	20.4N	141.2E	75	8	47	68	74	76	58	0	-25	-30	-35	-35	-25
95091406	11	21.0N	140.1E	90	5	22	60	46	31	111	0	-15	-30	-25	-25	5
95091412	12	21.5N	139.2E	110	6	37	57	37	16	317	0	-5	-15	-15	-25	5
95091418	13	22.3N	138.5E	115	6	18	49	71	78	354	-5	-25	-25	-25	-35	15
95091500	14	23.1N	137.9E	125	6	22	29	33	74	552	-5	-15	-10	-10	-5	35
95091506	15	24.1N	137.4E	140	0	13	31	42	120	552	-5	0	0	-5	20	45
95091512	16	25.0N	137.0E	140	0	12	40	119	359	662	0	5	0	10	25	55
95091518	17	26.0N	136.6E	140	6	41	85	243	481		0	0	0	25	45	
95091600	18	27.1N	136.5E	140	6	46	57	218	372		0	0	0	0	15	
95091606	19	28.4N	136.7E	140	13	52	187	317	569		0	-10	10	10	15	
95091612	20	29.7N	137.3E	140	0	58	247	429	657		0	5	20	25	25	
95091618	21	31.2N	138.3E	140	5	143	344	541			0	20	40	30		
95091700	22	33.3N	139.9E	125	12	173	322	556			0	10	30	20		
95091706	23	36.4N	142.9E	110	0	84	228				0	15	20			
95091712	24	39.7N	146.3E	100	0	96	387				0	20	20			
95091718	25	42.4N	150.4E	80	32	169					0	5				
95091800	26	44.4N	155.4E	65	22	225					0	20				
95091806		45.2N	161.3E	55												
95091812		45.4N	167.3E	45												
			AVERAGE		15	69	125	171	206	254	2	9	15	19	27	36
			# CASES		26	26	24	22	20	16	26	26	24	22	20	16

TYPHOON POLLY (18W)

DTG	WRN NO.	BEST TRACK LAT	LONG	WIND (KT)	POSITION ERRORS(NM) 00	12	24	36	48	72	WIND ERRORS(KT) 00	12	24	36	48	72
95090900		8.1N	141.8E	15												
95090906		8.4N	140.8E	15												
95090912		9.0N	140.1E	15												
95090918		10.1N	139.6E	20												
95091000		10.8N	138.9E	20												
95091006		11.5N	137.5E	20												
95091012		11.6N	135.4E	20												
95091018		11.7N	133.0E	20												
95091100		11.9N	130.3E	20												
95091106		12.4N	128.4E	20												
95091112		13.0N	126.3E	20												
95091118		13.6N	124.4E	20												
95091200		13.8N	124.1E	20												
95091206		14.0N	123.4E	20												
95091212		14.3N	122.9E	20												
95091218		14.7N	122.7E	20												
95091300		15.1N	122.6E	20												
95091306		15.6N	122.7E	20												
95091312		16.1N	122.9E	20												
95091318		16.5N	123.1E	20												
95091400		16.7N	123.3E	25												
95091406	1	16.9N	123.5E	30	53	48	50	132	278	645	0	0	5	10	15	25
95091412	2	17.0N	123.7E	30	6	18	64	193	312	574	0	0	5	5	15	20
95091418	3	17.1N	124.0E	35	11	40	144	271	398	530	0	5	5	10	20	15
95091500	4	17.3N	124.4E	35	8	22	134	253	394	452	0	0	0	10	20	5

TYPHOON POLLY (18W) (CONTINUED)

DTG	WRN NO.	LAT	LONG	WIND (KT)	POS 00	POS 12	POS 24	POS 36	POS 48	POS 72	WIND 00	WIND 12	WIND 24	WIND 36	WIND 48	WIND 72
95091506	5	17.4N	124.8E	35	8	80	194	318	463	422	0	-5	0	10	20	-5
95091512	6	17.6N	125.7E	35	22	133	229	364	408	321	0	-5	0	10	15	-15
95091518	7	18.0N	127.1E	40	52	127	210	311	266	175	-5	-5	0	10	5	-15
95091600	8	18.3N	128.6E	45	59	115	215	231	134	53	0	0	15	20	10	-10
95091606	9	18.6N	130.0E	45	67	109	170	104	30	106	0	0	15	10	0	-10
95091612	10	18.8N	131.5E	45	65	130	129	66	71	123	0	0	10	0	-10	-10
95091618	11	19.0N	133.2E	45	17	87	197	271	368	461	0	10	0	-10	-10	-10
95091700	12	19.2N	135.1E	45	11	90	216	299	415	582	0	0	-15	-25	-20	-20
95091706	13	19.3N	136.7E	45	16	156	232	273	305	300	0	-10	-25	-25	-20	-20
95091712	14	19.6N	137.3E	50	40	112	160	214	242	255	5	-15	-30	-25	-20	-20
95091718	15	20.1N	137.5E	60	33	72	121	179	198	183	-5	-25	-30	-30	-25	-20
95091800	16	20.9N	137.6E	70	13	29	102	168	225	325	-5	-20	-15	0	0	-10
95091806	17	22.0N	137.7E	80	12	63	135	259	379	500	-15	-20	-15	0	0	-10
95091812	18	23.0N	137.9E	90	0	62	133	186	268	283	-10	0	10	10	0	0
95091818	19	24.0N	138.0E	90	8	43	109	165	228	205	0	0	10	10	5	10
95091900	20	24.8N	138.3E	90	17	105	179	229	281	279	0	5	10	5	5	15
95091906	21	25.7N	139.0E	90	0	65	85	137	120	44	0	5	0	-5	-15	10
95091912	22	26.6N	140.1E	90	13	44	43	31	18	116	-5	0	-5	-10	-15	15
95091918	23	27.8N	141.3E	90	0	24	78	118	156	348	0	-5	-5	-10	-5	20
95092000	24	28.9N	142.5E	90	6	56	111	142	155		0	-5	-5	-5	0	
95092006	25	29.8N	143.9E	90	11	37	60	99	138		0	0	-5	5	15	
95092012	26	30.8N	145.6E	90	13	57	104	156	128		0	0	-5	0	15	
95092018	27	31.9N	147.6E	85	13	66	114	114	64		0	-10	-5	5	15	
95092100	28	33.2N	149.7E	85	32	98	96	124	187		0	-5	0	25	20	
95092106	29	34.8N	152.3E	85	11	50	82	106	230		0	5	15	25	25	
95092112	30	36.3N	155.0E	80	20	58	49	165	359		-5	0	20	20	25	
95092118	31	38.1N	158.0E	70	37	51	115	303			-5	10	20	20		
95092200		39.8N	161.0E	65												
95092206		41.1N	164.1E	50												
95092212		41.9N	167.2E	40												
95092218		42.2N	170.2E	35												
95092300		42.1N	172.9E	35												
95092306		41.7N	175.6E	30												
95092312		41.6N	178.3E	25												
95092318		41.6N	178.8W	25												
95092400		42.3N	176.0W	25												
				AVERAGE	22	73	132	193	241	317	2	5	10	12	13	13
				# CASES	31	31	31	31	30	23	31	31	31	31	30	23

SUPER TYPHOON RYAN (19W)

DTG	WRN NO.	BEST TRACK LAT	LONG	WIND (KT)	POSITION ERRORS(NM) 00	12	24	36	48	72	WIND ERRORS(KT) 00	12	24	36	48	72
95091412		13.7N	114.8E	20												
95091418		13.7N	114.7E	20												
95091500		13.8N	114.6E	25												
95091506		13.8N	114.6E	25												
95091512	1	13.8N	114.5E	30	144	171	200	242			0	0	-5	-5		
95091518		16.9N	114.5E	30												
95091600	2	14.0N	114.5E	30	5	41	57	41	104	294	5	0	5	5	5	5
95091606	3	14.1N	114.6E	35	18	60	81	58	30	124	5	5	10	0	-5	-10
95091612	4	14.2N	114.7E	35	47	81	52	32	122	231	10	10	10	0	0	-15
95091618	5	14.2N	114.7E	35	18	30	48	41	57	238	10	10	5	-5	-5	-20
95091700	6	14.3N	114.7E	35	24	43	30	45	141	201	10	5	0	-5	-5	-30
95091706	7	14.4N	114.7E	35	18	47	108	191	253	303	0	-5	-5	-10	-10	-40
95091712	8	14.6N	114.5E	40	18	63	121	199	244	315	5	-5	-5	-10	-15	-45
95091718	9	14.7N	114.2E	45	47	117	195	270	333	329	0	-10	-10	-15	-20	-50
95091800	10	14.7N	113.9E	50	40	83	147	179	221	197	-5	-10	-5	-15	-25	-55
95091806	11	14.8N	113.5E	55	8	36	58	96	119	60	0	5	0	0	-20	-35
95091812	12	14.8N	113.2E	55	23	55	62	91	97	24	0	5	-5	-10	-25	-40
95091818	13	14.8N	112.9E	60	23	37	72	72	53	162	-5	0	-10	-20	-30	-45
95091900	14	15.0N	112.6E	60	23	85	129	180	238	340	-5	-5	-20	-25	-40	-55
95091906	15	15.7N	112.6E	65	13	56	88	141	225	345	0	-5	-20	-25	-35	-40
95091912	16	16.3N	112.6E	70	40	86	108	90	110	189	-5	-15	-25	-35	-40	-55
95091918	17	16.9N	112.6E	75	8	18	82	153	201	277	-10	-20	-25	-40	-55	-50
95092000	18	17.5N	112.8E	85	12	79	179	237	279	369	5	0	-5	-15	-30	-20
95092006	19	17.9N	113.2E	95	8	62	130	191	244	378	-5	-5	-10	-20	-30	-25
95092012	20	18.3N	113.9E	100	5	51	101	146	194	322	-5	-10	-15	-15	-40	-20
95092018	21	18.7N	114.9E	105	5	17	32	77	123	351	-10	-15	-25	-45	-40	-20
95092100	22	19.2N	116.2E	115	0	0	24	69	136	471	-15	-20	-25	-45	-35	-10
95092106	23	19.7N	117.4E	120	0	5	58	113	179	525	-5	-5	-5	-5	-10	5
95092112	24	20.3N	118.6E	125	16	32	85	149	216	681	5	10	10	15	10	35
95092118	25	20.9N	119.7E	130	8	32	88	153	295	874	0	10	25	20	20	45

SUPER TYPHOON RYAN (19W) (CONTINUED)

DTG	WRN NO.	LAT	LONG	WIND (KT)	POS 00	POS 12	POS 24	POS 36	POS 48	POS 72	WIND 00	WIND 12	WIND 24	WIND 36	WIND 48	WIND 72
95092200	26	21.5N	120.9E	130	8	32	96	199	364		0	0	20	15	20	
95092206	27	22.3N	122.2E	130	11	12	77	235	492		-10	5	0	0	5	
95092212	28	23.6N	123.5E	130	5	50	158	386	679		-5	10	5	15	15	
95092218	29	25.0N	124.8E	115	5	39	210	466	753		-10	-5	0	25	25	
95092300	30	26.6N	126.1E	110	16	64	133	243			-5	0	-5	5		
95092306	31	28.5N	127.6E	105	7	67	143	281			0	0	-5	0		
95092312	32	30.9N	129.5E	100	35	109	244				0	15	5			
95092318	33	33.5N	131.8E	90	19	88	178				-5	5	10			
95092400	34	36.9N	134.4E	75	12	60					-10	0				
95092406	35	39.8N	138.3E	65	15	206					-5	5				
95092412	36	41.9N	143.5E	55	46						-5					
95092418		42.3N	149.7E	45												
				AVERAGE	21	61	109	164	233	317	5	7	10	15	22	32
				# CASES	36	35	33	31	28	24	36	35	33	31	28	24

TYPHOON SIBYL (20W)

DTG	WRN NO.	BEST TRACK LAT	LONG	WIND (KT)	POSITION ERRORS(NM) 00	12	24	36	48	72	WIND ERRORS(KT) 00	12	24	36	48	72
95092106		6.0N	174.1E	15												
95092112		6.0N	172.0E	15												
95092118		6.0N	169.8E	15												
95092200		5.9N	167.9E	15												
95092206		5.8N	166.6E	20												
95092212		5.7N	165.4E	25												
95092218		5.4N	163.9E	25												
95092300		5.3N	162.1E	25												
95092306		5.3N	160.5E	25												
95092312		5.4N	158.8E	20												
95092318		5.6N	157.0E	15												
95092400		5.8N	155.2E	15												
95092406		6.0N	153.4E	20												
95092412		6.2N	151.6E	20												
95092418		6.3N	149.7E	20												
95092500		6.5N	147.7E	20												
95092506		6.6N	145.7E	20												
95092512		6.8N	144.1E	20												
95092518		7.0N	142.5E	20												
95092600		7.1N	141.2E	20												
95092606		7.1N	140.0E	25												
95092612		7.0N	138.7E	25												
95092618		7.0N	137.4E	25												
95092700		7.3N	136.3E	25												
95092706		7.5N	135.0E	25												
95092712		7.9N	133.7E	25												
95092718		8.2N	132.2E	30												
95092800	1	8.8N	131.1E	30	41	102	147	164	174	249	-5	-5	-10	-35	-55	-30
95092806	2	9.4N	130.3E	30	84	117	125	120	144	234	0	-5	-20	-35	-45	-15
95092812	3	10.0N	129.3E	35	91	126	132	156	174	258	-5	-10	-30	-55	-55	-15
95092818	4	10.5N	128.4E	40	76	84	65	65	81	75	-5	-10	-30	-40	-30	5
95092900	5	11.0N	127.3E	45	32	92	139	143	189	191	0	-15	-35	-40	-15	5
95092906	6	11.4N	126.2E	55	50	110	151	174	219	219	0	-15	-25	-15	5	35
95092912	7	11.7N	124.9E	65	37	41	29	88	129	177	0	-20	-20	5	30	45
95092918	8	12.2N	124.0E	75	5	13	79	79	61	102	-5	-15	-5	20	30	60
95093000	9	12.7N	123.1E	90	16	35	72	71	66	84	-5	0	30	45	55	60
95093006	10	13.2N	122.2E	90	13	54	78	61	77	146	0	10	35	45	60	65
95093012	11	13.8N	121.7E	95	29	96	104	85	87	177	5	35	45	50	60	85
95093018	12	14.8N	121.0E	85	32	69	80	62	63	38	-10	20	30	45	55	30
95100100	13	15.8N	119.8E	75	13	75	112	133	119	126	0	20	30	45	40	35
95100106	14	16.4N	118.5E	70	5	39	66	84	101	141	5	10	25	30	-5	10
95100112	15	16.9N	117.1E	70	12	30	54	90	92	219	5	10	25	15	5	5
95100118	16	17.2N	116.0E	70	0	8	17	48	116		5	15	30	20	30	
95100200	17	17.8N	115.1E	70	11	30	60	156	234		5	15	30	40	50	
95100206	18	18.4N	114.2E	65	6	20	66	154	233		10	20	30	45	30	
95100212	19	19.2N	113.2E	65	18	11	95	182	279		10	15	40	50	35	
95100218	20	19.9N	112.5E	60	28	45	162	259			0	-5	15	15		
95100300	21	20.7N	111.9E	60	11	66	133	189			0	15	5	5		
95100306	22	21.7N	111.2E	55	11	80	154				5	10	0			
95100312	23	22.9N	111.1E	35	28	82					15	10				
95100318	24	23.7N	111.0E	30	47	85					10					
95100400		24.4N	110.9E	25												
95100406		25.0N	111.0E	20												
95100412		25.6N	111.1E	15												

TYPHOON SIBYL (20W) (CONTINUED)

DTG	WRN NO.	LAT	LONG	WIND (KT)	POS 00	12	24	36	48	72	WIND 00	12	24	36	48	72
		AVERAGE			30	63	97	123	139	163	5	13	25	33	36	33
		# CASES			24	24	22	21	19	15	24	24	22	21	19	15

TROPICAL DEPRESSION 21W

DTG	WRN NO.	BEST TRACK LAT	LONG	WIND (KT)	POSITION ERRORS(NM) 00	12	24	36	48	72	WIND ERRORS(KT) 00	12	24	36	48	72
95091900		3.5N	161.0E	15												
95091906		3.6N	159.6E	15												
95091912		3.6N	158.1E	15												
95091918		3.8N	156.5E	15												
95092000		3.9N	155.1E	15												
95092006		3.9N	153.5E	15												
95092012		4.0N	152.0E	15												
95092018		4.0N	150.5E	15												
95092100		4.2N	149.1E	15												
95092106		4.4N	147.7E	15												
95092112		4.5N	146.3E	15												
95092118		4.7N	144.9E	15												
95092200		4.8N	143.4E	15												
95092206		5.0N	141.9E	15												
95092212		5.1N	140.5E	15												
95092218		5.3N	139.0E	15												
95092300		5.4N	137.7E	15												
95092306		5.6N	136.4E	15												
95092312		5.9N	135.2E	15												
95092318		6.3N	134.1E	15												
95092400		6.6N	133.0E	15												
95092406		6.9N	132.0E	15												
95092412		7.3N	130.6E	15												
95092418		7.9N	129.0E	15												
95092500		8.5N	127.7E	20												
95092506		9.2N	126.2E	25												
95092512		9.8N	124.0E	25												
95092518		10.2N	121.7E	25												
95092600		10.4N	120.0E	20												
95092606		10.7N	118.8E	20												
95092612		11.0N	117.7E	20												
95092618		11.3N	116.7E	20												
95092700		11.6N	115.7E	20												
95092706		11.9N	114.7E	20												
95092712		12.1N	113.7E	20												
95092718		12.3N	112.6E	25												
95092800		12.4N	111.7E	25												
95092806	1	12.5N	110.9E	25	29	8					0	0				
95092812	2	12.6N	110.3E	25	52	47					0	-5				
95092818		12.8N	109.7E	25												
95092900	3	12.9N	108.9E	25	11						0					
		AVERAGE			31	28					0	3				
		# CASES			3	2					3	2				

TROPICAL DEPRESSION 22W

DTG	WRN NO.	BEST TRACK LAT	LONG	WIND (KT)	POSITION ERRORS(NM) 00	12	24	36	48	72	WIND ERRORS(KT) 00	12	24	36	48	72
95092718		30.4N	178.2E	15												
95092800		29.6N	177.0E	15												
95092806		28.9N	175.8E	15												
95092812		28.3N	174.5E	15												
95092818		27.8N	173.1E	15												
95092900		27.4N	171.8E	15												
95092906		27.2N	170.6E	20												
95092912		27.1N	169.5E	20												
95092918		27.3N	168.5E	20												
95093000		27.4N	167.7E	20												
95093006		27.5N	166.8E	20												
95093012		27.7N	165.8E	25												
95093018		27.8N	164.9E	25												
95100100	1	27.8N	164.2E	30	35	112	201	237	253	221	0	5	15	25	25	20
95100106	2	27.2N	163.7E	30	49	158	208	244	217	251	0	10	15	25	25	25
95100112	3	26.6N	163.6E	30	67	128	146	154	147		0	5	10	15	20	
95100118	4	26.0N	163.2E	25	68	137	153	186	240		0	0	10	10	15	

TROPICAL DEPRESSION 22W (CONTINUED)

DTG	WRN NO.	LAT	LONG	WIND (KT)	POS 00	POS 12	POS 24	POS 36	POS 48	POS 72	WIND 00	WIND 12	WIND 24	WIND 36	WIND 48	WIND 72
95100200	5	25.3N	162.5E	25	18	29	59	132	207		0	5	10	10	15	
95100206	6	25.0N	161.7E	25	32	93	107				0	5	0			
95100212		24.7N	160.9E	20												
95100218		24.4N	160.0E	20												
95100300		24.3N	158.8E	20												
95100306		24.5N	157.3E	20												
95100312		24.8N	155.6E	20												
95100318		24.9N	153.9E	20												
95100400		24.2N	152.5E	20												
95100406		23.7N	151.1E	15												
			AVERAGE		45	110	146	191	213	237	0	5	10	17	20	23
			# CASES		6	6	6	5	5	2	6	6	6	5	5	2

TROPICAL DEPRESSION 23W

DTG	WRN NO.	BEST TRACK LAT	LONG	WIND (KT)	POSITION ERRORS(NM) 00	12	24	36	48	72	WIND ERRORS(KT) 00	12	24	36	48	72
95100306		12.9N	123.6E	15												
95100312		12.9N	123.0E	15												
95100318		12.9N	122.1E	15												
95100400		13.0N	120.8E	15												
95100406		13.2N	119.6E	15												
95100412		13.4N	118.4E	20												
95100418		13.7N	117.2E	20												
95100500		14.2N	116.1E	20												
95100506		14.7N	115.3E	20												
95100512	1	15.0N	114.3E	25	8	70	132	96			0	5	10	15		
95100518		15.0N	112.8E	25												
95100600	2	14.8N	111.5E	25	18	34					0	0				
95100606		14.7N	109.7E	25												
95100612		14.9N	108.5E	20												
95100618		14.9N	108.0E	20												
95100700		14.8N	107.3E	15												
95100706		14.7N	106.6E	10												
95100712		14.5N	105.9E	10												
			AVERAGE		13	53	132	96			0	3	10	15		
			# CASES		2	2	1	1			2	2	1	1		

TYPHOON TED (24W)

DTG	WRN NO.	BEST TRACK LAT	LONG	WIND (KT)	POSITION ERRORS(NM) 00	12	24	36	48	72	WIND ERRORS(KT) 00	12	24	36	48	72
95100312		6.7N	140.9E	15												
95100318		6.8N	139.3E	15												
95100400		6.9N	137.7E	15												
95100406		7.1N	136.1E	15												
95100412		7.4N	134.5E	15												
95100418		7.8N	133.0E	15												
95100500		8.2N	131.7E	15												
95100506		8.8N	130.6E	15												
95100512		9.4N	129.8E	15												
95100518		10.0N	129.2E	15												
95100600		10.7N	128.6E	15												
95100606		11.4N	128.1E	15												
95100612		12.1N	127.5E	15												
95100618		12.6N	126.8E	20												
95100700		12.8N	125.8E	20												
95100706		13.0N	124.8E	20												
95100712		13.2N	123.7E	20												
95100718		13.4N	122.7E	20												
95100800		14.0N	122.0E	20												
95100806		14.5N	121.3E	20												
95100812		15.1N	120.2E	20												
95100818		15.3N	118.7E	20												
95100900	1	15.5N	117.0E	25	120	171	199	164	122	72	5	0	0	0	-5	-30
95100906	2	15.6N	115.6E	30	26	21	29	63	125	234	0	5	5	5	0	-50
95100912	3	15.6N	114.4E	30	78	93	119	179	238		0	0	0	-20	-45	
95100918	4	15.7N	113.3E	30	73	102	152	221			0	0	-15	-35		
95101000	5	15.9N	112.3E	35	17	62	143	254			0	-5	-20	-45		
95101006	6	16.1N	111.6E	35	41	114	194	295			0	-10	-25	-50		
95101012	7	16.3N	111.0E	40	50	132	207	293			-5	-15	-35	-55		

TYPHOON TED (24W) (CONTINUED)

DTG	WRN NO.	LAT	LONG	WIND (KT)	00	12	24	36	48	72	00	12	24	36	48	72
95101018	8	16.6N	110.5E	45	64	132	204				-10	-25	-50			
95101100	9	16.9N	110.1E	50	42	62	87	121	268		-15	-30	-40	-45	-45	
95101106	10	17.1N	109.8E	55	34	64	87	119	165		-20	-35	-40	-40	-45	
95101112	11	17.3N	109.5E	65	67	133	138	123	114		-20	-30	-35	-35	-35	
95101118	12	17.5N	109.2E	70	69	96	118	179			-25	-35	-40	-45		
95101200	13	17.8N	108.9E	75	61	54	112	158			-30	-35	-30	-35		
95101206	14	18.1N	108.4E	75	29	37	110	152	183		-10	-5	-5	20	0	
95101212	15	18.6N	108.0E	75	13	58	112	144	164		-5	0	5	30	5	
95101218	16	19.6N	108.2E	70	29	112	159	166			-5	-5	20	15		
95101300	17	20.5N	108.5E	65	36	42					0	-5				
95101306	18	21.4N	109.0E	65	34	56					0	15				
95101312	19	22.2N	109.3E	55	12	61					0	5				
95101318		22.8N	110.1E	35												
95101400		23 0N	110.8E	25												
95101406		22.9N	111.6E	25												
95101412		22.4N	112.2E	20												
			AVERAGE		48	85	136	176	173	153	8	14	23	32	23	40
			# CASES		19	19	16	15	8	2	19	19	16	15	8	2

TROPICAL STORM VAL (25W)

	WRN	BEST TRACK			POSITION ERRORS(NM)						WIND ERRORS(KT)					
DTG	NO.	LAT	LONG	WIND (KT)	00	12	24	36	48	72	00	12	24	36	48	72
95100518		14.9N	152.5E	15												
95100600		15.1N	152.4E	15												
95100606		15.3N	152.3E	15												
95100612		15.6N	152.1E	15												
95100618		15.9N	151.9E	15												
95100700		16.1N	151.7E	15												
95100706		16.4N	151.5E	15												
95100712		16.6N	151.2E	15												
95100718		16.8N	150.4E	20												
95100800		16.9N	149.6E	20												
95100806		16.8N	148.7E	20												
95100812		16.9N	148.0E	20												
95100818		17.3N	147.4E	20												
95100900		18.3N	147.2E	20												
95100906	1	19.4N	147.4E	25	41	12	126	187			0	-5	-5	-15		
95100912		20.5N	147.0E	25												
95100918	2	21.5N	146.0E	30	45	154	208	234	197	170	0	0	-5	0	5	20
95101000	3	22.6N	144.5E	35	24	102	199	272	321	503	0	0	-5	0	10	45
95101006	4	23.6N	142.9E	35	17	62	184	316	374	648	0	-5	-5	0	10	45
95101012	5	24.2N	141.6E	40	10	68	120	206	277	638	-5	-5	0	5	20	45
95101018	6	24.8N	140.2E	45	32	73	157	213	311	646	0	5	10	20	35	60
95101100	7	25.4N	138.8E	45	13	74	137	230	367	653	0	5	10	25	45	60
95101106	8	25.9N	138.1E	45	34	56	175	355	527	1014	0	10	10	10	10	10
95101112	9	26.4N	137.7E	45	8	41	206	378	545	1018	0	10	15	20	10	10
95101118	10	26.8N	137.5E	45	36	171	352	523	760	1386	0	0	5	5	0	5
95101200	11	26.8N	137.0E	45	37	134	282	388	598	1208	0	5	10	5	0	5
95101206	12	26.3N	136.9E	45	12	97	172	261	334	518	0	5	15	15	30	35
95101212	13	25.8N	137.0E	40	35	45	148	205	276	352	0	10	10	10	25	30
95101218	14	25.2N	137.2E	40	20	90	170	188	244	396	0	10	10	20	25	30
95101300	15	24.8N	137.6E	30	37	45	32	24	71	240	0	0	5	20	25	25
95101306	16	24.6N	138.2E	30	45	73	182	226	337	533	0	0	15	20	25	30
95101312	17	24.5N	138.7E	30	20	119	234	366	496	755	0	0	15	20	25	35
95101318	18	24.0N	138.9E	30	53	179	244	395	518	828	0	10	10	15	25	35
95101400	19	23.4N	138.5E	30	16	30					-5	0				
95101406		22.8N	137.9E	20												
95101412		22.6N	137.9E	20												
95101418		22.4N	137.3E	20												
95101500		22.0N	136.5E	20												
95101506		21.7N	134.8E	20												
95101512		21.2N	134.1E	20												
95101518		20.7N	133.3E	20												
95101600		20.3N	132.5E	20												
95101606		20.0N	131.7E	20												
95101612		19.8N	131.0E	20												
95101618		19.5N	130.2E	20												
95101700		19.0N	129.4E	20												
95101706		18.6N	128.7E	15												
95101712		17.9N	128.0E	15												

TROPICAL STORM VAL (25W) (CONTINUED)

				AVERAGE	29	86	185	276	386	677	1	4	9	13	19	31
				# CASES	19	19	18	18	17	17	19	19	18	18	17	17

SUPER TYPHOON WARD (26W)

DTG	WRN NO.	BEST TRACK LAT	LONG	WIND (KT)	POSITION ERRORS(NM) 00	12	24	36	48	72	WIND ERRORS(KT) 00	12	24	36	48	72
95101318		8.4N	162.5E	15												
95101400		9.3N	162.3E	20												
95101406		10.1N	162.0E	20												
95101412		10.8N	161.5E	20												
95101418		11.3N	160.6E	20												
95101500		11.8N	159.6E	20												
95101506		12.2N	158.5E	20												
95101512		12.5N	157.4E	20												
95101518		12.7N	156.3E	20												
95101600		12.9N	155.0E	20												
95101606		13.1N	153.7E	25												
95101612	1	13.2N	152.2E	30	5	39	99	138	176	284	0	0	-15	-30	-45	-70
95101618	2	13.3N	150.5E	45	13	58	100	349	171	256	-15	-10	-25	-45	-55	-70
95101700	3	13.6N	148.8E	35	5	11	18	34	72	241	0	-10	-25	-45	-55	-65
95101706	4	14.1N	147.0E	45	21	58	67	80	87	261	0	-15	-30	-45	-60	-60
95101712	5	14.5N	145.3E	55	0	6	8	45	132	308	0	-10	-35	-40	-50	-30
95101718	6	14.9N	143.7E	65	0	21	62	116	200	414	0	-15	-25	-35	-35	-15
95101800	7	15.4N	142.1E	75	5	37	69	154	229	457	0	-20	-30	-40	-30	0
95101806	8	16.0N	140.6E	90	5	32	97	181	258	476	0	-5	-15	-15	0	45
95101812	9	16.7N	139.3E	100	12	48	140	210	273	557	0	-5	-10	0	10	45
95101818	10	17.5N	137.9E	110	5	34	94	167	237	418	0	-10	-10	5	0	35
95101900	11	18.4N	136.7E	120	8	66	130	192	295	545	-10	-20	-15	0	15	35
95101906	12	19.6N	135.6E	130	8	58	134	207	331	740	-20	-20	-10	5	35	45
95101912	13	21.0N	134.7E	140	11	22	49	150	284	793	-10	-10	0	10	25	55
95101918	14	21.9N	134.4E	140	20	61	111	241	392	1022	-5	-5	5	30	35	60
95102000	15	22.7N	134.4E	140	11	42	52	109	172	650	0	0	10	25	20	25
95102006	16	23.4N	134.4E	135	36	60	96	118	192	725	-5	-5	20	20	20	15
95102012	17	24.0N	134.5E	130	34	52	108	158	314	790	0	10	25	25	30	15
95102018	18	25.0N	135.0E	125	8	79	122	215	397		0	25	25	30	30	
95102100	19	25.8N	135.9E	110	12	48	99	243	460		0	10	10	15	5	
95102106	20	26.5N	137.0E	90	8	43	163	397	666		5	-5	-5	0	-10	
95102112	21	27.4N	138.2E	85	11	62	187	370	587		0	0	5	0	-10	
95102118	22	28.4N	139.5E	75	18	99	255	420			0	0	10	-5		
95102200	23	29.5N	141.4E	70	42	220	452	743			-5	5	0	-10		
95102206	24	30.5N	144.0E	60	26	133	332				0	5	-10			
95102212	25	31.4N	147.4E	50	16	54	96				0	5	-10			
95102218		32.3N	151.1E	45												
95102300		33.2N	155.0E	45												
95102306		34.1N	159.3E	50												
95102312		35.1N	164.1E	50												
				AVERAGE	14	58	126	219	283	526	3	9	15	21	27	40
				# CASES	25	25	25	23	21	17	25	25	25	23	21	17

TYPHOON YVETTE (27W)

DTG	WRN NO.	BEST TRACK LAT	LONG	WIND (KT)	POSITION ERRORS(NM) 00	12	24	36	48	72	WIND ERRORS(KT) 00	12	24	36	48	72
95101812		7.5N	150.0E	15												
95101818		7.8N	148.7E	15												
95101900		8.1N	147.5E	15												
95101906		8.4N	146.2E	15												
95101912		8.7N	144.9E	15												
95101918		8.9N	143.8E	15												
95102000		9.1N	142.7E	15												
95102006		9.3N	141.9E	15												
95102012		9.5N	140.9E	15												
95102018		9.7N	139.9E	15												
95102100		9.9N	138.9E	15												
95102106		10.0N	137.7E	15												
95102112		10.0N	136.4E	15												
95102118		10.0N	135.1E	15												
95102200		10.0N	133.7E	15												
95102206		10.0N	132.4E	15												
95102212		10.3N	130.9E	15												
95102218		11.1N	129.1E	15												

TYPHOON YVETTE (27W) (CONTINUED)

95102300		12.4N	127.5E	20												
95102306	1	13.4N	125.6E	30	8	5	46	96	183	308	0	10	15	20	25	20
95102312	2	14.0N	124.1E	30	31	29	61	151	240	340	0	10	15	15	15	25
95102318	3	14.1N	123.0E	35	13	18	71	164	224	305	0	10	15	20	15	35
95102400	4	14.2N	121.7E	35	37	61	100	172	213	331	0	10	10	10	10	50
95102406	5	14.1N	120.2E	35	47	85	172	225	264	396	0	-5	0	-5	5	50
95102412	6	14.0N	119.1E	35	61	180	267	297	320	496	0	-10	-10	-10	10	55
95102418	7	14.0N	117.0E	40	112	220	274	314	355	547	-5	-10	-15	-10	10	35
95102500	8	14.0N	115.2E	45	29	29	63	84	146		0	-10	-10	-15	0	
95102506	9	14.1N	113.2E	45	5	29	62	97	193		0	-15	-15	-15	-5	
95102512	10	13.9N	111.7E	55	8	42	65	47	63		0	-10	-15	0	0	
95102518	11	13.8N	110.4E	60	29	67	87	78			-5	-20	-15	-5		
95102600	12	13.6N	109.2E	65	13	59	134				-5	-20	-10			
95102606	13	13.4N	108.0E	60	35	118	258				0	-10	-5			
95102612	14	13.3N	106.6E	55	58	140	269				0	10	0			
95102618		13.3N	105.3E	45												
95102700		13.4N	103.4E	30												
95102706		13.6N	101.5E	25												
95102712		13.8N	99.6E	20												
95102718		14.1N	97.8E	20												
			AVERAGE		35	78	138	157	221	390	1	11	11	11	10	39
			# CASES		14	14	14	11	10	7	14	14	14	11	10	7

TYPHOON ZACK (28W)

DTG	WRN NO.	BEST TRACK LAT	LONG	WIND (KT)	POSITION ERRORS(NM) 00	12	24	36	48	72	WIND ERRORS(KT) 00	12	24	36	48	72
95102100		4.8N	163.2E	15												
95102106		5.0N	161.6E	15												
95102112		5.2N	160.0E	15												
95102118		5.5N	158.0E	15												
95102200		5.7N	156.0E	15												
95102206		5.9N	154.0E	15												
95102212		6.1N	152.0E	20												
95102218		6.4N	150.0E	20												
95102300		6.8N	148.1E	20												
95102306		6.5N	146.6E	20												
95102312		6.2N	145.1E	25												
95102318		6.0N	143.6E	25												
95102400		6.2N	142.2E	25												
95102406		6.3N	141.1E	25												
95102412		6.6N	140.1E	25												
95102418		6.9N	139.1E	25												
95102500	1	7.2N	138.1E	25	55	90	132	152	143	103	0	0	5	10	15	-5
95102506	2	7.4N	137.2E	30	90	123	150	156	135	101	-5	0	0	10	10	-15
95102512	3	7.7N	136.2E	30	88	131	140	142	187	203	5	10	10	15	5	-25
95102518	4	7.8N	135.3E	30	131	141	117	117	149	224	5	5	10	10	-5	-10
95102600	5	8.0N	134.4E	30	18	42	81	75	123	239	5	0	5	-5	-20	-20
95102606	6	8.3N	133.7E	35	13	67	104	126	187	276	0	0	0	-15	-30	-20
95102612	7	8.7N	132.9E	35	11	41	74	124	155	284	0	0	-10	-25	-40	-15
95102618	8	9.2N	132.0E	35	8	67	147	224	282	398	0	-5	-20	-35	-25	-20
95102700	9	9.8N	131.0E	35	16	94	194	271	371	499	0	-15	-30	-45	-20	-35
95102706	10	10.0N	129.7E	40	21	74	119	162	242	309	0	-15	-25	-25	-20	-60
95102712	11	10.2N	128.2E	50	17	73	110	171	234	256	-5	-20	-35	-20	-20	-75
95102718	12	10.3N	126.9E	60	5	30	83	145	185	195	0	-10	0	5	-5	-55
95102800	13	10.5N	125.4E	70	6	18	88	129	171	252	-5	-20	5	5	-20	-55
95102806	14	10.8N	124.2E	80	6	29	58	95	140	213	-15	-10	-10	-5	-30	-35
95102812	15	10.9N	123.0E	90	0	53	102	129	139	203	-25	-5	-5	-20	-45	-30
95102818	16	11.0N	121.7E	75	0	31	82	115	129	186	-10	5	0	-20	-30	-10
95102900	17	11.2N	120.3E	70	13	21	47	75	104	144	-5	5	-15	-35	-30	-5
95102906	18	11.3N	119.1E	70	5	5	49	90	83	97	5	0	-20	-25	-20	25
95102912	19	11.4N	117.9E	70	5	36	90	92	67	180	5	-15	-55	-50	-45	20
95102918	20	11.9N	116.9E	75	8	36	60	53	42	199	0	-30	-40	-50	-40	25
95103000	21	12.4N	116.0E	90	18	67	61	34	21	244	-15	-45	-30	-25	-25	30
95103006	22	13.1N	115.3E	105	11	25	8	18	52	293	-15	-25	-30	-20	5	40
95103012	23	13.8N	114.7E	120	16	67	95	126	179		5	10	15	10	50	
95103018	24	14.3N	114.0E	115	11	43	75	93	162		0	0	10	40	45	
95103100	25	14.6N	113.1E	115	30	72	94	125	201		0	5	10	55	20	
95103106	26	14.7N	112.3E	115	6	5	52	157	234		0	10	40	15	10	
95103112	27	14.7N	111.5E	110	8	18	44	148			5	15	15	10		
95103118	28	14.7N	110.6E	105	0	18	97				5	0	10			
95110100	29	14.7N	109.5E	100	18	99	203				0	5	15			
95110106	30	14.7N	108.4E	70	13	128	261				20	10	10			

TYPHOON ZACK (28W) (CONTINUED)

95110112	31	14.6N	106.9E	45	21	87					20	15				
95110118		14 6N	105.4E	30												
95110200		14.5N	103.8E	25												
95110206		14.5N	102.2E	15												
			AVERAGE		22	60	101	124	159	232	6	10	16	22	24	29
			# CASES		31	31	30	27	26	22	31	31	30	27	26	22

SUPER TYPHOON ANGELA (29W)

	WRN	BEST TRACK			POSITION ERRORS(NM)						WIND ERRORS(KT)					
DTG	NO.	LAT	LONG	WIND (KT)	00	12	24	36	48	72	00	12	24	36	48	72
95102006		5.0N	176.5E	15												
95102012		5.0N	175.1E	15												
95102018		5.0N	173.5E	15												
95102100		5.2N	172.0E	15												
95102106		5.6N	170.7E	15												
95102112		6.1N	169.4E	15												
95102118		6.5N	168.3E	15												
95102200		7.0N	167.0E	15												
95102206		7.3N	165.7E	15												
95102212		7.5N	164.5E	15												
95102218		7.7N	163.4E	15												
95102300		7.9N	161.9E	15												
95102306		8.1N	160.2E	15												
95102312		8.4N	158.3E	15												
95102318		8.7N	156.3E	15												
95102400		9.0N	154.5E	15												
95102406		9.3N	152.9E	20												
95102412		9.7N	151.4E	20												
95102418		10.0N	150.0E	20												
95102500		10.1N	149.0E	20												
95102506		10.2N	148.2E	20												
95102512		10.2N	147.5E	25												
95102518	1	10.2N	146.5E	30	8	13	45	97	147	326	0	-10	-10	-15	-15	-20
95102600	2	10.4N	145.4E	35	18	49	48	88	144	383	-5	-5	0	5	10	15
95102606	3	10.9N	144.3E	40	21	54	131	211	275	548	-5	-5	0	5	5	20
95102612	4	11.4N	143.2E	40	42	88	158	194	285	547	0	0	5	10	15	20
95102618	5	11.8N	142.2E	45	23	68	106	151	270	534	0	-5	5	5	10	20
95102700	6	12.1N	141.6E	50	18	42	85	185	306	484	5	0	0	5	15	25
95102706	7	12.3N	140.9E	55	11	29	88	187	310	553	5	0	-5	0	15	25
95102712	8	12.5N	140.4E	60	0	24	49	151	285	530	0	0	5	10	20	15
95102718	9	12.8N	139.7E	60	13	52	79	178	339	592	0	-5	0	10	20	-5
95102800	10	13.0N	138.9E	65	21	83	156	267	372	568	0	5	10	10	20	5
95102806	11	13.1N	138.2E	70	29	103	211	338	432	576	-5	0	10	10	20	5
95102812	12	12.9N	137.9E	70	26	118	213	278	355	553	0	0	10	10	10	-20
95102818	13	12.7N	137.9E	75	52	107	184	218	267	454	0	0	10	10	5	-40
95102900	14	12.7N	138.0E	75	26	67	102	126	153	256	0	0	10	0	0	-60
95102906	15	12.5N	138.0E	75	30	71	104	133	176	243	0	0	10	-5	0	-60
95102912	16	12.1N	137.9E	75	8	95	153	184	230	268	0	0	-5	-5	-30	-70
95102918	17	11.8N	137.5E	75	30	67	92	140	196	218	0	0	-10	-5	-50	-70
95103000	18	11.7N	136.6E	75	30	58	110	165	187	256	0	-10	-10	-30	-70	-70
95103006	19	11.7N	135.9E	75	13	13	18	68	81	176	0	-15	-10	-50	-70	-65
95103012	20	11.7N	135.1E	85	21	59	78	87	101	201	5	10	-5	-30	-30	-15
95103018	21	11.8N	134.3E	90	13	41	71	40	40	133	0	10	-25	-30	-30	5
95103100	22	11.9N	133.4E	90	17	52	64	58	96	199	0	-15	-45	-30	-30	25
95103106	23	12.0N	132.4E	90	17	24	24	46	79	200	0	-35	-45	-30	-25	25
95103112	24	12.2N	131.3E	115	11	18	18	34	87	205	-25	-55	-40	-30	-15	-5
95103118	25	12.4N	130.4E	135	11	33	46	35	64	109	-35	-40	-30	-15	20	0
95110100	26	12.7N	129.6E	155	13	66	45	8	44	112	0	10	10	15	50	0
95110106	27	13.4N	128.9E	155	11	29	45	82	125	175	0	5	10	35	30	-25
95110112	28	14.0N	128.1E	155	6	68	115	145	173	223	0	5	20	55	5	-15
95110118	29	14.3N	127.0E	155	11	47	79	93	113	182	0	5	30	30	-20	-25
95110200	30	14.2N	126.0E	155	13	45	61	104	149	219	0	15	45	5	-10	-20
95110206	31	14.2N	125.1E	150	5	13	92	95	109	159	5	35	45	-20	-10	-10
95110212	32	14.1N	124.1E	140	11	58	104	105	114	100	15	45	-20	-10	0	0
95110218	33	14.1N	123.1E	120	5	72	93	100	104	58	20	15	-20	-5	0	15
95110300	34	14.3N	121.6E	100	24	58	64	70	78	61	40	-15	-5	5	5	25
95110306	35	14.5N	120.1E	100	13	47	52	54	52	132	20	-5	15	5	10	35
95110312	36	14.6N	119.0E	125	5	18	39	52	99	180	0	15	15	10	10	25
95110318	37	14.7N	118.0E	125	0	8	8	18	63	146	0	15	15	20	25	35
95110400	38	14.8N	116.9E	115	8	21	37	60	93	194	5	5	0	10	25	45
95110406	39	14.9N	115.9E	115	8	18	39	60	96	219	0	0	10	20	25	50
95110412	40	15.0N	114.9E	115	6	18	31	82	114	189	0	5	20	30	30	25

SUPER TYPHOON ANGELA (29W) (CONTINUED)

95110418	41	15.2N	113.9E	115	5	37	54	106	140		0	15	25	10	0	
95110500	42	15.6N	112.9E	110	12	37	62	90	167		0	15	35	35	15	
95110506	43	16.1N	112.0E	100	23	63	71	103	175		0	15	20	35	20	
95110512	44	16.4N	111.5E	90	25	38	12	53	71		0	10	25	35	30	
95110518	45	16.8N	110.9E	75	5	29	58	102			0	10	25	30		
95110600	46	17.2N	110.3E	65	8	33	49	66			5	20	30	25		
95110606	47	17.6N	109.5E	55	5	24	75				-5	15	25			
95110612	48	18.1N	108.7E	40	24	77	102				5	20	25			
95110618	49	18.6N	108.2E	30	18	75					0	10				
95110700		19.2N	108.0E	20												
95110706		19.8N	107.5E	15												
95110712		19.8N	106.8E	15												
			AVERAGE		16	50	80	116	168	287	4	11	17	18	20	26
			# CASES		49	49	48	46	44	40	49	49	48	46	44	40

TROPICAL STORM BRIAN (30W)

DTG	WRN NO.	BEST TRACK LAT	LONG	WIND (KT)	POSITION ERRORS(NM) 00	12	24	36	48	72	WIND ERRORS(NM) 00	12	24	36	48	72
95102900		16.5N	174.2E	15												
95102906		16.4N	173.1E	20												
95102912		16.3N	172.1E	20												
95102918		16.1N	171.1E	20												
95103000		16.0N	170.1E	20												
95103006		16.0N	169.0E	20												
95103012		16.0N	167.2E	25												
95103018		16.1N	165.1E	25												
95103100		16.2N	163.4E	25												
95103106		16.3N	161.9E	25												
95103112		16.5N	160.6E	25												
95103118		17.3N	159.0E	25												
95110100	1	18.1N	157.4E	30	16	78	163	257	481	1003	0	0	-10	-15	-10	10
95110106	2	19.1N	155.9E	30	29	74	178	319	472	717	0	-5	-15	-15	-10	10
95110112	3	20.0N	154.0E	30	5	75	186	328	429	339	0	-10	-10	-10	-15	-10
95110118	4	21.2N	152.3E	35	34	150	306	477	495	358	-5	-10	-5	-5	-5	-10
95110200	5	22.9N	151.4E	40	13	137	310	454	527		-10	-15	-5	-5	5	
95110206	6	24.6N	151.2E	45	24	158	313	407	415		-10	-15	-5	-5	-5	
95110212	7	26.1N	152.2E	50	20	95	162	165	142		0	15	15	15	0	
95110218	8	27.5N	153.7E	50	24	83	112	130	146		0	15	10	10	-5	
95110300	9	28.9N	155.8E	50	31	36	42	158			0	0	5	-5		
95110306	10	30.5N	158.0E	50	40	134	222	382			0	0	0	-10		
95110312	11	31.7N	160.4E	50	20	108	217				0	10	0			
95110318	12	32.5N	162.6E	45	5	48	142				0	0	-10			
95110400	13	33.3N	165.2E	35	10	20					0	-5				
95110406		34.1N	167.5E	35												
95110412		34.6N	169.5E	35												
95110418		34.9N	171.3E	35												
			AVERAGE		21	92	197	308	389	605	2	8	8	10	7	10
			# CASES		13	13	12	10	8	4	13	13	12	10	8	4

TROPICAL STORM COLLEEN (31W)

DTG	WRN NO.	BEST TRACK LAT	LONG	WIND (KT)	POSITION ERRORS(NM) 00	12	24	36	48	72	WIND ERRORS(KT) 00	12	24	36	48	72
95111006		25.1N	173.8W	20												
95111012		24.4N	175.1W	20												
95111018		23.6N	176.4W	20												
95111100		22.8N	177.5W	20												
95111106		21.3N	179.1W	25												
95111112		20.0N	179.4E	25												
95111118		18.6N	178.6E	25												
95111200		17.3N	178.1E	30												
95111206	1	16.3N	177.8E	35	13	149	238				0	5	15			
95111212	2	16.2N	177.3E	35	21	108					0	5				
95111218	3	16.4N	176.2E	30	23	71					5	15				
95111300	4	16.8N	174.8E	30	30						0					
95111306	5	17.1N	173.2E	20	18						5					
			AVERAGE		21	110	238				2	8	15			
			# CASES		5	3	1				5	3	1			

TROPICAL DEPRESSION 32W

DTG	WRN NO.	BEST TRACK LAT	LONG	WIND (KT)	POSITION ERRORS(NM) 00	12	24	36	48	72	WIND ERRORS(KT) 00	12	24	36	48	72
95113000		8.9N	129.1E	15												
95113006		9.3N	128.7E	15												
95113012		9.7N	128.4E	15												
95113018		10.1N	128.1E	15												
95120100		10.4N	127.9E	15												
95120106		10.7N	127.7E	15												
95120112		11.0N	127.5E	20												
95120118		11.3N	127.3E	20												
95120200		11.6N	127.1E	25												
95120206	1	11.8N	127.0E	30	170	189	206	250	313	588	0	10	20	25	35	40
95120212	2	12.1N	126.8E	30	204	248	304	404	567	1048	0	10	20	25	35	40
95120218	3	12.3N	126.6E	30	234	293	386	516	737		0	0	5	15	20	
95120300	4	12.5N	126.4E	30	279	354	472				0	-5	-10			
95120306		12.8N	126.1E	30												
95120312		13.0N	125.8E	30												
95120318		13.2N	125.4E	30												
95120400		13.3N	124.9E	30												
95120406	5	13.4N	124.4E	25	33	105	184				0	0	10			
95120412		13.0N	123.5E	25												
95120418	6	12.5N	122.6E	25	261	460					0	10				
95120500		11.9N	121.8E	20												
95120506		11.2N	121.1E	15												
95120512		10.6N	120.4E	15												
			AVERAGE		197	275	311	390	539	819	0	6	13	22	30	40
			# CASES		6	6	5	3	3	2	6	6	5	3	3	2

TROPICAL DEPRESSION 34W

DTG	WRN NO.	BEST TRACK LAT	LONG	WIND (KT)	POSITION ERRORS(NM) 00	12	24	36	48	72	WIND ERRORS(KT) 00	12	24	36	48	72
95120700		8.0N	114.8E	15												
95120706		8.1N	114.5E	15												
95120712		8.2N	114.2E	20												
95120718		8.1N	113.9E	25												
95120800		7.8N	113.7E	30												
95120806	1	7.6N	113.7E	30	11	61	109	165			0	0	0	0		
95120812		7.6N	113.7E	30												
95120818	2	7.7N	113.9E	30	34	90	149	177			-5	-5	-5	-5		
95120900		7.7N	114.1E	30												
95120906	3	7.8N	114.2E	30	36	95	121	139			0	0	0	-5		
95120912		7.9N	114.4E	30												
95120918		8.0N	114.6E	30												
95121000	4	8.1N	114.5E	30	18	5	23	26			0	0	0	-5		
95121006	5	8.2N	114.3E	30	39	69	90	82			0	0	0	5		
95121012		8.2N	114.0E	30												
95121018	6	8.2N	113.8E	30	8	16	61	112			0	0	5	5		
95121100		8.2N	113.6E	30												
95121106	7	8.2N	113.5E	30	0	35	75	123			0	5	0	0		
95121112		8.3N	113.4E	30												
95121118	8	8.7N	113.3E	25	18	59	141				0	0	-5			
95121200		9.0N	113.3E	25												
95121206		9.2N	112.8E	25												
95121212		9.2N	112.0E	20												
95121218		9.1N	111.4E	25												
95121300		8.9N	110.9E	30												
95121306	9	8.7N	110.2E	30	37	77	97				0	0	10			
95121312		8.4N	109.5E	25												
95121318	10	8.1N	109.2E	25	64	163					0	10				
95121400		7.9N	109.1E	20												
95121406	11	7.6N	108.9E	15	64						5					
95121412		7.3N	108.8E	10												
			AVERAGE		30	68	97	118			1	2	3	4		
			# CASES		11	10	9	7			11	10	9	7		

TROPICAL STORM DAN (35W)

DTG	WRN NO.	BEST TRACK LAT	LONG	WIND (KT)	POSITION ERRORS(NM) 00	12	24	36	48	72	WIND ERRORS(KT) 00	12	24	36	48	72
95122306		6.9N	139.2E	15												
95122312		7.0N	138.3E	15												
95122318		7.0N	137.2E	20												
95122400		7.1N	136.3E	20												
95122406		7.2N	135.4E	20												
95122412		7.3N	134.4E	20												
95122418		7.5N	133.9E	20												
95122500		7.7N	133.3E	20												
95122506		8.0N	132.8E	20												
95122512		8.2N	132.2E	20												
95122518		8.5N	131.5E	20												
95122600		8.7N	130.8E	25												
95122606	1	8.9N	130.2E	25	5	41	71	124			0	0	-10	-25		
95122612		9.1N	129.7E	25												
95122618	2	9.2N	129.4E	25	36	83	154	220			0	-15	-25	-25		
95122700	3	9.4N	129.0E	30	25	47	101	170	222	437	0	-15	-15	-10	-10	-5
95122706	4	9.5N	128.7E	40	39	77	133	193	258	519	-5	-15	-10	-5	0	0
95122712	5	9.7N	128.5E	50	56	97	138	179	268	491	-5	-5	0	0	5	0
95122718	6	9.9N	128.4E	55	54	95	131	139	163	328	-5	-5	0	5	0	-5
95122800	7	10.1N	128.4E	55	88	130	136	165	198	422	0	0	5	10	-5	0
95122806	8	10.4N	128.4E	55	78	76	58	87	157	495	0	5	-5	-10	-15	-5
95122812	9	10.8N	128.5E	55	95	105	60	79	163		0	5	-5	-10	-15	
95122818	10	11.2N	128.7E	55	84	67	16	23	41		0	0	-5	-10	-15	
95122900	11	11.6N	128.8E	55	5	53	90	131	294		0	0	0	0	5	
95122906	12	12.6N	129.2E	55	43	116	168	286	517		0	5	0	5	5	
95122912	13	13.7N	129.6E	55	24	56	145	304			0	-10	-15	-5		
95122918	14	14.8N	130.0E	55	0	75	173	375			0	0	-5	0		
95123000	15	15.7N	130.8E	55	17	110	293				0	0	5			
95123006	16	16.7N	132.1E	55	40	119	314				0	0	5			
95123012	17	17.6N	133.6E	55	62	149					0	5				
95123018	18	18.8N	135.7E	50	81	134					5	10				
95123100	19	20.2N	138.4E	40	25						0					
95123106	20	21.5N	141.8E	35	5						-10					
			AVERAGE		44	91	137	177	229	449	2	5	7	9	8	3
			# CASES		20	18	16	14	10	6	20	18	16	14	10	6

6.2.2 NORTH INDIAN OCEAN — This section includes verification statistics for each warning in the North Indian Ocean during 1995.

JTWC BEST TRACK, FORECAST TRACK AND INTENSITY ERRORS BY WARNING

TROPICAL CYCLONE 01B

DTG	WRN NO.	BEST TRACK LAT	LONG	WIND (KT)	POSITION ERRORS(NM) 00	12	24	36	48	72	WIND ERRORS(KT) 00	12	24	36	48	72
95091200		14.2N	103.7E	15												
95091206		14.9N	102.2E	15												
95091212		15.6N	100.7E	15												
95091218		15.9N	99.0E	15												
95091300		16.0N	97.3E	15												
95091306		16.2N	95.8E	20												
95091312		16.5N	94.2E	20												
95091318		17.4N	93.2E	20												
95091400		18.2N	92.7E	20												
95091406		18.7N	92.2E	25												
95091412		19.1N	91.8E	25												
95091418		19.3N	91.4E	30												
95091500		19.5N	91.0E	30												
95091506		19.6N	90.5E	30												
95091512		19.7N	90.1E	30												
95091518		19.7N	89.6E	25												

TROPICAL CYCLONE 01B (CONTINUED)

95091600		19.8N	89.1E	25												
95091606		20.3N	88.5E	30												
95091612		21.1N	88.1E	35												
95091618		21.6N	87.4E	45												
95091700	1	22.1N	86.7E	40	36	60	93				0	5	5			
95091706	2	22.7N	85.9E	35	53	67					0	5				
95091712		23.2N	85.2E	30												
95091718		23.7N	84.4E	25												
95091800		24.2N	83.5E	25												
95091806		24.9N	82.7E	20												
95091812		25.5N	82.2E	15												
95091818		26.0N	81.6E	15												
95091900		26.4N	81.1E	15												
95091906		26.8N	80.4E	15												
95091912		27.2N	79.7E	15												
95091918		27.5N	78.9E	15												
95092000		27.8N	78.0E	15												
			AVERAGE		45	64	93				0	5	5			
			# CASES		2	2	1				2	2	1			

TROPICAL CYCLONE 02A

	WRN	BEST TRACK			POSITION ERRORS(NM)						WIND ERRORS(KT)					
DTG	NO.	LAT	LONG	WIND (KT)	00	12	24	36	48	72	00	12	24	36	48	72
95101100		16.9N	73.5E	20												
95101106		16.7N	72.7E	20												
95101112		16.6N	72.1E	20												
95101118		16.6N	71.5E	25												
95101200		16.6N	71.0E	25												
95101206		16.6N	70.5E	25												
95101212	1	16.6N	70.0E	30	69	100	128	153	197	213	0	0	10	25	35	50
95101218	2	16.7N	69.6E	40	57	74	98	132	161	189	0	5	10	25	40	50
95101300	3	16.9N	69.0E	45	63	91	110	138	166	177	0	0	15	25	40	55
95101306	4	17.0N	68.6E	45	87	98	126	155	166	175	0	0	10	20	30	45
95101312	5	17.1N	68.3E	50	91	115	149	172	183	192	0	5	10	20	30	45
95101318	6	17.3N	67.9E	50	20	49	83	101	119	164	0	5	15	20	25	35
95101400	7	17.5N	67.6E	45	24	41	64	77	100	120	0	5	15	20	30	40
95101406	8	17.6N	67.4E	45	38	67	72	81	102	89	0	10	15	20	30	40
95101412	9	17.8N	67.1E	45	49	77	85	99	112	101	0	10	15	25	30	40
95101418	10	17.9N	66.9E	40	6	18	29	16	12	151	5	10	15	25	25	35
95101500	11	18.1N	66.6E	40	33	40	34	38	39	208	0	0	5	10	15	25
95101506	12	18.3N	66.2E	40	12	29	63	76	50	155	0	0	5	10	15	25
95101512	13	18.5N	65.9E	40	6	11	32	11	61	231	0	5	5	15	15	30
95101518	14	18.8N	65.5E	40	16	23	24	28	125		0	5	5	15	15	
95101600	15	19.1N	65.2E	35	5	26	17	78	199		5	5	10	10	15	
95101606	16	19.4N	64.9E	35	17	30	41	140	235		0	0	5	5	5	
95101612	17	19.8N	64.5E	35	32	56	127	226	295		0	5	5	5	5	
95101618	18	20.0N	64.0E	35	43	88	173	272			0	5	5	5		
95101700	19	19.9N	63.3E	30	63	171	326	415			5	0	5	5		
95101706	20	19.6N	62.6E	30	69	174	280				0	0	0			
95101712	21	19.1N	61.7E	30	21	82	116				0	5	5			
95101718	22	18.4N	60.8E	30	82	69					0	0				
95101800		17.6N	59.8E	25												
95101806		17.4N	58.8E	25												
95101812		17.5N	57.8E	20												
			AVERAGE		42	70	104	127	137	167	1	4	9	16	24	40
			# CASES		22	22	21	19	17	13	22	22	21	19	17	13

TROPICAL CYCLONE 03B

	WRN	BEST TRACK			POSITION ERRORS(NM)						WIND ERRORS(KT)					
DTG	NO.	LAT	LONG	WIND (KT)	00	12	24	36	48	72	00	12	24	36	48	72
95110512		8.6N	96.4E	15												
95110518		9.1N	95.3E	15												
95110600		9.6N	94.3E	20												
95110606		9.9N	93.6E	20												
95110612		10.2N	92.9E	20												
95110618		10.6N	92.2E	25												
95110700	1	11.3N	91.4E	30	24	88	134	154	187	541	0	5	-5	-5	-5	65
95110706	2	12.0N	90.4E	35	64	108	108	102	41	383	0	0	0	-15	-20	-5
95110712	3	12.6N	89.2E	35	16	26	28	82	279		0	-5	-5	-25	-10	

TROPICAL CYCLONE 03B (CONTINUED)

95110718	4	13.0N	87.9E	45	11	53	117	263	514		0	0	-5	10	15	
95110800	5	13.8N	86.9E	50	25	98	192	409	650		-5	-5	-5	5	5	
95110806	6	14.7N	86.0E	55	24	42	122	333	495		0	-5	10	15	5	
95110812	7	15.6N	85.1E	60	36	60	220	417			-5	-5	15	15		
95110818	8	16.5N	84.2E	70	8	55	220	333			-10	0	10	5		
95110900	9	17.6N	83.5E	70	16	156	301				0	15	15			
95110906	10	19.2N	83.4E	55	16	158	229				5	5	0			
95110912	11	21.3N	83.4E	40	18	45					-5	0				
95110918		23.3N	83.7E	30												
95111000		24.7N	84.8E	25												
95111006		25.4N	85.9E	25												
95111012		26.0N	86.8E	15												
95111018		26.5N	87.6E	15												
			AVERAGE		24	81	168	262	361	462	3	4	7	12	10	35
			# CASES		11	11	10	8	6	2	11	11	10	8	6	2

TROPICAL CYCLONE 04B

DTG	WRN NO.	BEST TRACK LAT	LONG	WIND (KT)	POSITION ERRORS(NM) 00	12	24	36	48	72	WIND ERRORS(KT) 00	12	24	36	48	72
95111818		5.4N	97.2E	20												
95111900		5.5N	96.6E	20												
95111906		5.6N	96.0E	20												
95111912		5.8N	95.4E	20												
95111918		6.0N	94.7E	20												
95112000		6.1N	94.0E	20												
95112006		6.2N	93.3E	20												
95112012		6.4N	92.6E	20												
95112018		6.5N	92.0E	20												
95112100		6.6N	91.5E	20												
95112106		6.8N	90.9E	25												
95112112		6.9N	90.2E	25												
95112118	1	7.0N	89.3E	25	26	75	93	114	145	500	0	0	-10	-15	-20	-30
95112200	2	7.2N	88.5E	25	26	61	109	138	261	711	0	-5	-25	-25	-45	-25
95112206	3	7.5N	87.9E	30	18	87	106	190	348	838	0	-15	-25	-30	-50	-20
95112212	4	8.2N	87.6E	35	35	74	119	242	395	924	5	-10	-10	-30	-30	40
95112218	5	8.9N	87.0E	45	5	38	33	133	295	776	-5	-15	-20	-40	-30	55
95112300	6	9.4N	86.3E	55	18	37	100	235	434		0	0	-20	-20	5	
95112306	7	9.9N	85.7E	60	11	98	237	382	597		0	-10	-30	-20	10	
95112312	8	10.8N	85.0E	65	24	150	314	502	728		-5	-30	-25	0	50	
95112318	9	12.1N	84.9E	75	52	187	319	479	678		-10	-25	-15	5	45	
95112400	10	13.6N	85.1E	95	8	37	118	239			-20	-20	5	50		
95112406	11	15.1N	85.7E	105	13	47	179	322			-5	10	40	70		
95112412	12	16.6N	86.3E	105	12	96	244				0	25	75			
95112418	13	18.1N	87.6E	105	28	140	264				0	30	60			
95112500	14	19.5N	89.3E	90	12	93					5	40				
95112506	15	20.9N	91.3E	85	21	132					0	20				
95112512	16	22.4N	93.5E	45	12						0					
95112518	17	23.6N	95.5E	30	16						0					
			AVERAGE		20	91	172	271	432	751	3	17	28	28	32	34
			# CASES		17	15	13	11	9	5	17	15	13	11	9	5

7. TROPICAL CYCLONE SUPPORT SUMMARY

7.1 SCATTEROMETER APPLICATIONS FOR TROPICAL CYCLONES

J.D. Hawkins
Naval Research Laboratory
Monterey, CA 93943

R.T. Edson
Joint Typhoon Warning Center,Guam

P.S. Chang
NOAA/NESDIS
Camp Springs, MD 20746

Surface wind vectors from the scatterometer aboard the European Remote Sensing Satellite (ERS-1) are playing an increasingly important role to the JTWC. These remotely sensed wind vectors serve to fill a data void at the surface over much of JTWC's area of responsibility (AOR). In addition, as these data became more readily available in near real time during 1995, they increasingly served to supplement the existing reconnaissance platforms with tropical cyclone (TC) vortex locations and the depiction of gale force winds (35 kt (17m/sec)). As the year went on, much of this information became available in time to support the current JTWC warning.

The scatterometer houses an active radar and it records the change in radar reflectivity of the sea due to the perturbation of small ripples (capillary waves) by the wind close to the surface. The radar backscatter returned to the satellite is modified by wind-driven ripples on the ocean surface and, since the energy in these ripples increases with wind velocity, backscatter increases with wind velocity. Wind vector data have shown to be extremely reliable between the range of 3-50 kt (1-25 m/sec) with a root-mean-square (rms) error of 1-2m/sec and a wind directional accuracy of 15-20 degrees rms. Horizontal data resolution is depicted at up to 25km. Although the sensor is subject to a 180 degree directional bias, the trained analyst can readily identify the true direction of the wind vector. As an active radar, the scatterometer is less sensitive to rain attenuation as compared to passive microwave sensors such as the SSM/I . The primary handicap of the scatterometer remains its fairly narrow, 500 km, swath-width as it flies aboard the sun synchronous ERS satellite.

Prior to the 1995 season, use of scatterometer data was a hit or miss proposition. In addition to its narrow swath, data, when available, was generally received anywhere from 8-24 hours after data time. During 1995, arrangements were made through NOAA/NESDIS and NRL-Monterey to receive the data in a more systematic, quicker manner. After NOAA/NESDIS received the data from the European Space Agency (ESA), the data were quickly remapped into specifically requested boxes covering the JTWC AOR. The images were transferred in Tagged Image File Format (TIFF) via File Transfer Protocol (FTP) to JTWC and NRL, usually within 3 to 8 hours of data time. By late 1995, these images became available even quicker via the Internet/World Wide Web. A large scale depiction of the entire globe became available with all current swaths. The user may now further request a 25km resolution blow up over an area of interest. Data over the entire globe are now available within 2 to 4 hours of fly-over. Additionally, toward the end of 1995, the Naval Oceanographic Office (NAVOCEANO) also came on line with a global scatterometer view of the ERS data set, available on the Internet, giving the JTWC a second source to access this valuable data.

Scatterometer wind vectors played a crucial role in depicting "closed circulations" and enabling the TDO to more accurately analyze

both the location and the organization of a developing TC. This information proved to be especially important for those systems that had yet to show a good cloud signature in either the infrared or visual imagery and were used several times in 1995 to relocate poorly defined systems. Once developed, the wind swaths were regularly used to depict both the size and asymmetrical character of the 35 kt (17 m/sec) wind radii. Scatterometer winds are now also routinely incorporated into the TDO's overall synoptic analysis by attaching the individual wind swaths to the daily gradient-level wind chart. This has proved invaluable in filling large data gaps and in aiding the TDO in interpreting the often complex wind flow over the AOR.

Future efforts will focus on the inclusion of two new scatterometer platforms. Full use of the new ERS-2 will begin in the spring of 1996 and will eventually replace the ERS-1 scatterometer. In addition, the NASA Scatterometer (NSCAT) is expected to be launched on the Japanese Advanced Earth Observing Satellite (ADEOS) in August 1996 and has more than twice the swath width (1200km) of the current ERS instruments.

7.2 WATER VAPOR TRACKED WINDS FOR TROPICAL CYCLONE APPLICATIONS

J.D. Hawkins
Naval Research Laboratory
Monterey, CA 93943

T.L. Olander
S.T. Wanzong
C.S. Velden
Cooperative Institute for Meteorological Satellite Studies, University of Wisconsin
Madison, Wisconsin

R.T. Edson
Joint Typhoon Warning Center, Guam

Upper-level wind vectors over the western North Pacific and eastern Indian Ocean are now routinely being derived from GMS-5 water vapor imagery. Water vapor tracked winds, using a set of three half-hourly water vapor images, are created at 00Z and 12Z to map the upper-level wind field from 150-500 mb. These wind vectors, superimposed on a GMS-5 water vapor image, are color coded to represent wind data within three layers of the upper atmosphere: 150-250 mb, 250-350 mb and 350-500mb. These data are an excellent supplement to the more traditional cloud track winds due to the fact that they do not require clouds to be present.

Areas in the tropics with high moisture levels (e.g., areas near active intense convection) typically produce wind vectors at levels from 150-250 mb while drier, cooler regions permit retrievals closer to levels between 350-500 mb. This vertical distribution of water vapor tracked winds (WVTW) has provided a wealth of information of the large scale three-dimensional flow within the Joint Typhoon Warning Center's (JTWC) area of responsibility (AOR). The transmitted images are now routinely attached to the back of the 200-mb (upper-level) wind analysis charts in order to supplement the existing data. This has proven crucial in defining the synoptic patterns of ridges, troughs, TUTTS, cut-off lows, etc., that can be difficult to map in the relatively data void oceanic regions of the western Pacific and Indian Oceans. In addition, the added data have been used qualitatively to determine individual tropical cyclone track and intensity tendencies. Initial results during the fall of 1995 with Typhoons Ward and Angela were very promising.

The GMS-5 data are accessed via Australia and transferred via File Transfer Protocol (FTP) to the Cooperative Institute for Meteorological Satellite Studies (CIMSS) at the University of Wisconsin. These data are then processed to create the wind data sets and the final product is transferred in Tagged Image File Format (TIFF)

via FTP to JTWC and Naval Research Laboratory, Monterey (NRL-MRY) within two hours of the image time. Reliable FTP capabilities at all sites has been the largest obstacle to date.

Considerable attention has been given to the quality of the retrievals. Upper-level wind data from radiosonde island and mainland stations have been collocated with the WVTWs to produce statistical comparisons. Over 15,000 RAOBS have now been matched in time and space with WVTWs and indicate the root mean square error (RMSE) is ~ 7 m/sec (14 kts). This is comparable to the values for cloud tracked winds.

Quality control includes extensive buddy checks with neighboring observations and comparisons with a first guess field, and ensures that vertical consistency is maintained. Results over the last 6 months have shown that very few poor vectors have been produced. Tests continue, refining height assignments which now have an error near 50 mb.

Demonstrations in early 1996 indicated that WVTW retrievals in the Southern Hemisphere are feasible. NRL-MRY and CIMSS are planning to produce data in this area for the next season.

7.3 SSM/I DERIVED STRUCTURE AND INTENSITIES FOR TROPICAL CYCLONES

J.D. Hawkins
Naval Research Laboratory
Monterey, CA 93943

J.C. Sandidge
R.J. Holyer and D. May
Naval Research Laboratory
Stennis Space Center, MS 39529

M. Helveston
Analysis & Technology
Bay St. Louis, MS 39520

Passive microwave digital data from the DMSP Special Sensor Microwave/Imager (SSM/I) is being studied to extract information on the structure and intensity of tropical cyclones. SSM/I data can penetrate many of the higher cloud decks that hinder the analyst's ability to see the low-mid level cloud organization that is crucial in determining tropical cyclone (TC) structure and intensity. The SSM/I's capability to depict the rainbands, eyewall, eye and other pertinent features is being studied and compared with visible and infrared imagery, best track data, and aircraft reconnaissance data.

Over 350 SSM/I passes over TCs ranging in intensity from tropical depressions to super typhoons have been processed. Data have been collected from all major basins, with the main emphasis on the western Pacific (to support the Joint Typhoon Warning Center, JTWC) and the Atlantic basin (to compare with aircraft radar and intensity estimates). This joint Naval Research Laboratory (NRL) effort has taken advantage of the real time global receiving abilities at Stennis Space Center and the full digital archive at NRL-DC (Washington D.C.). In addition, we are coordinating with the Hurricane Research Division, Miami in order to compare P-3 Orion aircraft Doppler radar data with the SSM/I data set.

Initial efforts were directed at qualitatively comparing SSM/I 85-GHz imagery to coincident infrared (IR) data from the Operational Linescan System (OLS). The advantages the passive microwave data has in seeing through much of the upper level cirrus clouds was readily noticed. TC structure in the 85-GHz imagery was clearly evident despite the upper-level cloudiness and the 12-15 km resolution of the microwave data. An analysis of the 85-GHz data for a given TC's evolution readily depicted structural changes in the rainbands, eyewall and eye, including eyewall cycles (Willoughby). Early results show a surprising increase in frequency of eyewall cycles as seen in the microwave data as compared to the previously

used aircraft radar data.

Next, a more quantitative Neural Network (NN) approach was begun by looking at intensity changes from 85 GHz TC structure characteristics. The NN approach was initially selected by using approximately 130 85-GHz images to develop the NN and 30 cases to test the accuracy. This was done by using Empirical Orthogonal Functions (EOFs) to represent the structure in the 85-GHz image data set, extracting the top five coefficients (explaining > 40% of the variance) and inputting this information into the NN along with the best track intensities.

Initial results as compared to official best track data were poor. Next, a training set using "past" intensity values in the form of either 12 or 6 hour old best track intensities was included into the NN along with the 5 EOF coefficients. These results showed an improvement slightly better than persistence. An effort is now underway to eliminate the best track data and to produce a new NN intensity estimate earlier in the life of a TC (e.g. as a tropical depression) and then use this value as input to the NN along with the 5 coefficients. This may permit the NN to "learn" as the storm progresses. In addition, the data set has been expanded by a factor of two (~350) and is continually being upgraded. Particular emphasis is now being placed on processing SSM/I data coincident with 1995 Atlantic storms that have extensive aircraft reconnaissance fixes.

The NN results suggest that valuable information is contained in the SSM/I data and improvements over persistence are obtainable.

7.4 JTWC'S 120-HOUR OUTLOOK

E. J. Trehubenko
Joint Typhoon Warning Center, Guam

JTWC now provides a 120-hour "outlook" on tropical cyclone position and intensity — 48 hours beyond the 72-hour period covered by JTWC's Tropical Cyclone Warnings. The 96- and 120-hour outlooks are realized through the Horizontal Weather Depiction (HWD) products produced by the Operations Department of the NPMOCW, Guam. The TDO provides specific input to the Forecast Supervisor at NPMOCW regarding the development potential of existing tropical disturbances, as well as position and intensity estimates through 120 hours. For tropical cyclones in a warning status, 96- and 120-hour position and intensity estimates are provided, along with the latest 72-hour warning for the respective system. Within the JTWC, the 120-hour outlook is entered as an objective aid, the J120. Tools available to the TDO to support the J120 include NOGAPS (NGPX), the Bracknell Model (EGRR), and the new R120 objective aid. The J120 sample size for 1995 was small (50) but results from the initial test year show promise when compared to guidance provided by the dynamic models and climatology.

7.5 THE R120 OBJECTIVE AID

J.A. Rupp
Joint Typhoon Warning Center, Guam

The R120 objective forecast aid was created to address the absence of climatological guidance in the extended forecast period past 72 hours. The R120 aid was created by Capt John Rupp, USAF. This new objective aid was tested during the 1995 in the western North Pacific. The R120 is a Cliper model that uses the 48 and 72 hour forecast points from the JTWC forecast to project a Cliper forecast to the 96 and 120 hour. It was designed to answer the question of where would climatology take the system if it were to follow the first 72 hours of the forecast track (the currently available clipper model only runs out to 72 hours). The advantage of adding the Cliper guidance to the end of the JTWC warning is that it can benefit from the proven skill at 72 hours and hence outperform a Cliper model initialized from only initial conditions.

The results from the initial test year show promise in having competitive skill with other dynamic aids.

7.6 MONSOONAL INFLUENCES ON TROPICAL CYCLONE MOTION AND STRUCTURE

M.A. Lander
ONR-sponsored research at the
University of Guam
Mangilao, Guam

The low-level summer monsoon circulation of the tropical western North Pacific can appear in the form of a trough or a large gyre. These two broad categories of the monsoon circulation have important implications for the site of genesis, size, and subsequent motion of TCs which form in them.

Lander (1995) focused upon the flow pattern of a monsoon gyre which formed during August 1991. This monsoon gyre had a long (20-day) life and was associated with the genesis of six TCs. The August 1991 monsoon gyre was representative of a distinct pattern type of the monsoon circulation of the WNP which repeats roughly once every other typhoon season at some time during July through mid-October. A monsoon gyre is associated with TCs of extremely small and extremely large size. Only a few studies have been written which have focused on TC size (e.g., Arakawa 1952; Brand 1972; and Merrill 1984). Further understanding of the mechanisms governing TC size may well arise from a close study of the monsoon gyre.

Lander (1996) describes the reverse-oriented monsoon trough and its association with north-oriented TC motion. In its simplest description, the large-scale low-level circulation of summer over the WNP can be described in terms of low-latitude southwesterlies, a monsoon trough and a subtropical ridge. The axis of the summer monsoon trough of the WNP usually emerges from East Asia at about 20° N to 25°N, and extends southeastward to a terminus southeast of Guam (13° ; 145°E). Most of the TCs which develop in the WNP form in the monsoon trough. When the axis of the monsoon trough is in its normal orientation (NW-SE), TCs tend to move northwestward on tracks close to those expected from climatology. As an episodic event, the axis of the monsoon trough becomes displaced to the north of its usual location and takes on a reverse (SW-NE) orientation. When the monsoon trough acquires a reverse orientation, TCs within it tend to exhibit unusual motion, including: northeastward motion at low latitude; long meandering northward tracks; and binary interactions with other TCs along the trough axis. A TC track type, defined as the "S" track, appears to be primarily associated with reverse-orientation of the monsoon trough.

7.7 A TECHNIQUE FOR ESTIMATING RECURRENCE INTERVALS OF TROPICAL CYCLONE RELATED HIGH WINDS IN THE TROPICS: RESULTS FOR GUAM

J.A. Rupp
Joint Typhoon Warning Center
and
M.A. Lander
ONR-sponsored typhoon research at the
University of Guam
Mangilao, Guam

Rupp and Lander (1996) developed a technique that applies existing analytical models of the radial profile of the wind in tropical cyclones to the historical best-track data-base of tropical cyclones in a particular region in order to estimate the wind (at one-hour intervals) experienced at any selected location in the region for any or all of the historical tropical cyclones. Focusing on Guam, we produced a time series of the maximum wind there for each

tropical cyclone in the Guam region during the period 1945 to 1993. The purpose of the technique was to produce a time series of tropical-cyclone related winds that could be used to compute recurrence intervals for extreme wind speeds at any selected tropical location. We condensed the original time series of the estimated wind speeds (at one-hour time steps) for each historical tropical cyclone to a time series of the highest annual tropical-cyclone related wind. Extreme value analysis was applied to the time series of annual peak wind to estimate the recurrence intervals for threshold values of extreme wind speeds. The island of Guam was selected as the site for testing the technique. Guam has excellent historical measurements of wind, from which an independent estimate of the recurrence intervals of selected threshold high wind speeds can be computed. In addition, the wind traces during the passage of several major typhoons which affected Guam were used to assess the ability of the technique to reproduce the wind trace (at hourly intervals) experienced there during the passage of these typhoons. The recurrence intervals computed from our technique match the recurrence intervals computed from the wind measurements. The technique also reproduces a reasonable wind trace for the major typhoons affecting Guam. We believe that our technique can be used to make useful estimates of the recurrence intervals for tropical cyclone related high wind speeds at any tropical location where an historical best-track archive of tropical cyclones exists.

7.8 A SAFFIR-SIMPSON-LIKE HURRICANE DAMAGE POTENTIAL SCALE FOR THE TROPICAL WESTERN PACIFIC OCEAN REGION

C.P. Guard and M.A. Lander
ONR-sponsored typhoon research at the
University of Guam
Mangilao, Guam

The Saffir-Simpson Hurricane Scale (Simpson 1974) commonly used in the Atlantic to relate potential damage to maximum wind speed, has been adapted for use in the tropical western Pacific (hereafter, the Tropical Saffir-Simpson Tropical Cyclone (TSS TC Scale). The TSS TC Scale employs the basic model of the Saffir-Simpson Hurricane Scale which has been used for many years along the Atlantic and Gulf of Mexico coastal areas of the United States. After five years of modification and testing, the TSS TC Scale has been fine-tuned and implemented for use in the western North Pacific. The TSS TC Scale incorporates the basic Saffir-Simpson Scale, but modifies it for tropical building materials and building practices; considers the detrimental effects of termites, wood rot, and airborne sea salt; and it relates the wind speed to specific levels of damage to tropical vegetation and agriculture. Special consideration is given to the oceanic inundation that can be expected from tropical cyclone-related high surf and elevated tidal levels on the various structures (e.g., fringing coral reefs) common to the coasts of tropical Pacific Islands. Because many of the islands of the tropical Pacific contain crops and shelters that are highly susceptible to damage by sub-hurricane-force winds, the TSS TC Scale addresses the potential damage from the winds and seas associated with tropical depressions and tropical storms as well as with typhoons. With minor changes, the TSS TC Scale should be applicable in the global tropics.

7.9 DEVELOPMENT OF A HIGH-CONFIDENCE TROPICAL CYCLONE INTENSITY DATA BASE

C.P. Guard and M.A. Lander
ONR-sponsored research at the
University of Guam
Mangilao, Guam

A close investigation of the tropical cyclone intensity data bases of JTWC and of other warning centers around the world reveals that the quality of the data bases may not be sufficient for tropical cyclone intensity studies and validation of remote-sensing algorithms. Work on a "high-confidence" intensity data base, that reevaluates the raw data, makes changes to intensity data bases (where they are warranted), then places a confidence level on the intensity depending on the quality of the raw data on which the near-surface intensity was based, is continuing. Weighting values are developed for the confidence levels. An important input to the reevaluation is the maximum intensity (e.g., peak gusts and minimum sea-level pressure) measured near the centers of landfalling tropical cyclones. These data are not routinely available to warning centers outside the country of occurrence. In conjunction with this initiative is the acquisition from as many countries as possible (e.g., Taiwan, Japan, Philippines, Hong Kong, Australia, India) of maximum intensity data for landfalling tropical cyclones.

7.10 AN INITIAL LOOK AT WIND DISTRIBUTION FORECAST CAPABILITIES AT THE JOINT TYPHOON WARNING CENTER

C.P. Guard and M.A. Lander
ONR-sponsored research at the
University of Guam
Mangilao, Guam

A study was conducted to ascertain JTWC's ability to predict the gale (>34 kt) and storm force (>48 kt) wind distribution (WD). A primary stratification was made where each tropical cyclone was divided into its strong sector (i.e., right semicircle with respect to the translation in the Northern Hemisphere) and weak sector (i.e., the left side). Forecasts were compared to the appropriate analyses, where data were sufficient to identify the radial extent of gales and storm-force winds in the strong and weak sectors. Of 26 selected tropical cyclones with a total of 586 warnings, there were 122 strong sector gale WD verifications, 73 gale WD weak sector verifications, 38 strong sector storm-force WD verifications, and 29 weak sector storm-force WD verifications. Characteristics of the data availability, absolute errors, and error biases were presented by the author at the 1996 MGPACOM Typhoon Conference and at the 50th Interdepartmental Hurricane Conference. An example of the bias was an under-forecast of the strong sector gale and storm-Force WD, and an over-forecast of the weak sector gale and storm-force WD.

7.11 THE NATURAL VARIATION IN THE RELATIONSHIP BETWEEN THE MAXIMUM WIND AND MINIMUM CENTRAL PRESSURE IN TROPICAL CYCLONES

M.A. Lander and C.P. Guard
ONR-sponsored typhoon research at the
University of Guam
Mangilao, Guam

A four-year investigation of the relationships between the maximum wind and the minimum sea-level pressure in tropical cyclones is nearing completion. The study reveals the physical parameters that contribute to the wind-pressure relationships (WPR), and weights the importance of the various parameters. The radius of maximum wind (RMW) (closely related to eye size) and the rate of "fall-off" of the winds between the RMW and the environmental

flow (closely related to the size of the tropical cyclone) are found to be the most important parameters. The natural variability between observed maximum wind speed and minimum sea-level pressure is explained in terms of the identified parameters. A set of universal, basin-independent WPRs is proposed.

7.12 A STUDY OF THE CHARACTERISTICS OF VERY SMALL (MIDGET) TROPICAL CYCLONES

C.P. Guard and M.A. Lander
ONR-sponsored typhoon research at the
University of Guam
Mangilao, Guam

A special case of the study of the relationship between the maximum wind and minimum central pressure in tropical cyclones addresses the "midget" or very small tropical cyclone (TC) in which the minimum sea-level pressure is observed to be 20 mb higher for a specific maximum sustained wind speed than is the case for large TCs. The study identifies the unique characteristics of these cyclones and presents some proposed mechanisms for their development and commencement of rapid intensification at lower-than-normal threshold intensities. A basin-independent wind-pressure relationship is derived for midget TCs.

7.13 A STUDY OF RAPID INTENSITY FLUCTUATIONS OF TROPICAL CYCLONES USING THE DIGITAL DVORAK ALGORITHM

M.A. Lander
ONR-sponsored typhoon research at the
University of Guam
Mangilao, Guam

One of the utilities installed in the JTWC's MIDDAS satellite image processing equipment is an automated routine for computing Dvorak "T" numbers for tropical cyclones that possess eyes. The routine, developed by Zehr (personal communication), adapts the rules of the Dvorak technique as subjectively applied to enhanced infrared imagery (Dvorak 1984) in order to arrive at an objective T number, or "digital Dvorak" T number (hereafter referred to as DD numbers). Infrared imagery is available hourly from the GMS satellite, and hourly DD numbers were calculated for several of the typhoons of 1995.

The DD numbers presented are experimental, and methods for incorporating them into operational practice are being explored. In some cases, the DD numbers differ substantially from the warning intensity and also from the subjectively determined T numbers obtained from application of Dvorak's technique. The output of the DD algorithm, when performed hourly, often undergoes rapid and large fluctuations. The fluctuations of the DD numbers may lay the ground work for future modifications to the current methods of estimating tropical-cyclone intensity from satellite imagery. The discussion of the behavior of the time series of the DD numbers for some of the typhoons of 1995 (e.g., see the summaries of Oscar (17W), Polly (18W), Ryan (19W), Ward (26W), and Angela (29W)), is intended to highlight certain aspects of the DD time series that may prove to have important research and/or warning implications.

If the DD numbers truly represented rapid (on the order of 3 to 6 hours) intensity fluctuations with magnitudes (30-40 kt) as large as seen with some typhoons, there are two topics for further research: (1) how are the extremely rapid fluctuations of intensity, if they are genuine, to be incorporated into the warning? and, (2) how can the best tracks, having had these rapid fluctuations removed, be used to study the processes governing what may prove to be real intensity fluctuations of the magnitude indicated by the DD numbers?

7.14 ON THE INTERANNUAL VARIATIONS IN GLOBAL TROPICAL CYCLONE ACTIVITY

M.A. Lander and C.P. Guard
ONR-sponsored typhoon research at the
University of Guam
Mangilao, Guam

During 1995, there was a well-publicized near-record tropical cyclone (TC) activity in the Atlantic. This activity fueled speculation that it marked a tangible signal of global climate change. Although the Atlantic was very active during 1995, activity in other worldwide basins was generally below normal. An ongoing study of the global TC distribution by the authors has led to the following preliminary conclusions:

(1) The global annual average number of TCs is 88/year, ranging from the low 70s to the low 100s.

(2) There are global "jackpot" years (> 100 TCs) and "meager" years (< 80 TCs); the TC activity in each ocean basin also features "jackpot" years and "meager" years (Table 7-1).

(3) There is an ENSO connection to the global number of TCs — the global average is low during both the warm (i.e., El Niño) years and the cold (i.e., La Niña) years.

(4) Global "jackpot" years occur during normal (i.e., non-El Niño, non-La Niña) years.

(5) There are some weak, but statistically significant positive correlations between the annual number of TCs in the western North Pacific and the annual number of TCs in the eastern North Pacific, and between the annual numbers of TCs in the Southern Hemisphere and the annual numbers of TCs in the Western North Pacific. There were no statistically significant correlations found to exist between the Atlantic basin and any other TC basin.

Table 7-1 TROPICAL CYCLONE DISTRIBUTION

Basin	1995	long-term average	"jackpot" years
WNP	26	28	1994
SH	22	28	1986, 1992
ENP	10	17	1992
NIO	4	5	1992
NAT	19	10	1995

BIBLIOGRAPHY

Arakawa, H., 1952: Mame Taifu or midget typhoon (small storms of typhoon intensity). *Geophysical Magazine*, **24**, pp 463-474.

Atkinson, G.D., 1974: Investigation of gust factors in tropical cyclones. FLEWEACEN Tech. Note: JTWC 74-1. Photocopy available from: JTWC, COMNAVMAR, PSC 489, Box 17, FPO AP 96536-0051.

Atkinson, G. D. and C. R. Holliday, 1977: Tropical cyclone minimum sea-level pressure and maximum sustained wind relationship for the western North Pacific. *Mon. Wea. Rev.*, **105**, No. 4, pp 421-427 (also Fleet Weather Central/JTWC Technical Note 75-1).

Australian Bureau of Meteorology, 1995: Monthly 850-mb wind anomalies. Darwin Tropical Diagnostic Statements, Jan. through Dec. The Regional Director, Bureau of Meteorology, GPO Box 735, Darwin, Northern Territory 0801, Austalia.

Bartels, D.L., and R.A. Maddox, 1990: Midlevel cyclonic vortices generated by mesoscale convective systems. Mon. Wea. Rev., **119**, pp **104**. **118**.

Bister, M., and K.A. Emanuel, 1995: On tropical cyclogenesis from mesoscale convective systems: a model study of a mechanism suggested by observations in TEXMEX. Preprints. 21st Conference on Hurricanes and Tropical Meteorology. American Meteorological Society, Boston, MA, 660 pp.

Brand, S., 1970: Interaction of binary tropical cyclones in the western North Pacific Ocean. *J. Appl. Meteor.*, **9**, pp 433-441.

Brand, S., 1972: Very large and very small typhoons of the western North Pacific Ocean. *J. Meteor. Soc. Japan*, **50**, pp 332-341.

Businger, S., and Baik, J-J., 1991: An arctic hurricane over the Bering Sea. *Mon. Wea. Rev.*, **119**, pp 2293-2322.

Carr, L.E. , and R.L. Elsberry, 1994: Monsoonal interactions leading to sudden tropical cyclone track changes. *Mon. Wea. Rev.*, **123**, pp 265-289.

Carr, L.E., and R.L. Elsberry, 1994: Systematic and integrated approach to tropical cyclone track forecasting, Part I: Description of basic approach. Naval Postgraduate School publication NPS-MR-002. Naval Postgraduate School, Monterey, CA 93943. 65 pp. plus figs. and append.

Carr, L.E., M.A. Boothe, S.R. White, C.S. Kent, and R.L. Elsberry, 1995: Systematic and integrated approach to tropical cyclone track forecasting. Part II: Climatology reproducibility, and refinement of meteorological knowledge base. Naval Postgraduate School publication NPS-MR-95-001. Naval Postgraduate School, Monterey, CA 93943, 96 pp.

Climate Analysis Center, 1994: Monthly 850-mb and 200-mb wind anomalies. *Climate Diagnostics Bulletin.* U.S. Prediction Center Dept of Commerce, Washington, D.C. month by bulletins.

Diercks, J. M., R. C. Weir and M. K. Kopper, 1982: Forecast verification and reconnaissance data for Southern Hemisphere tropical cyclones (July 1980 through June 1982). NOCC/JTWC Technical Note 82-1, 77 pp.

Dong, K. and C. J. Neumann, 1983: On the relative motion of binary tropical cyclones. *Mon. Wea. Rev.*, **111**, pp 945-953.

Dunnavan, G. M., 1981: Forecasting intense tropical cyclones using 700-mb equivalent potential temperature and central sea-level pressure. NOCC/JTWC Technical Note 81-1, 12 pp.

Dvorak, V. F., 1975: TC intensity analysis and forecasting from satellite imagery. *Mon. Wea. Rev.*, **103**, No. 5, pp 420-430.

Dvorak, V. F., 1984: Tropical cyclone intensity analysis using satellite data. NOAA Technical Report NESDIS 11, 46 pp.

Elsberry, R.L., W.M. Frank, G.J. Holland, J.D. Jarrell, and R.L. Southern, 1987: A global view of tropical cyclones. Limited edition publication sponsored by the U.S. Navy, Office of Naval Research, Washington DC, 185 pp.

Emanuel, K.A., 1992: The physics of tropical cyclogenesis in the eastern Pacific. Presentation at the International Symposium on Tropical Cyclone Disasters, Beijing, China, 12-16 October.

Frank, W.M., and S. Chen, 1991: Simulations of vortex formation in convective weather systems. Preprints, 19th Conference on Hurricanes and Tropical Meteorology. American Meteorological Society, Boston, MA.

Fujiwhara, S., 1921: The natural tendency towards symmetry, etc. *Quart. J. Roy. Meteor. Soc.*, **47**, pp 287-293.

Fujiwhara, S., 1923: On the growth and decay of vortical systems. *Quart. J. Roy. Meteor. Soc.*, **49**, pp 75-104.

Fujiwhara, S., 1931: Short note on the behavior of two vortices. *Proc. Phys. Math. Soc. Japan*, Ser. 3, **13**, pp 106-110.

Glass, M., and G.W. Felde, 1990: Tropical storm structure analysis using SSM/I and OLS data. 5th Intl. Conf. on Interactive and Info. Processing Systems for Meteor., Oceanogr. and Hydrol., Aneheim, CA, Amer. Meteor. Soc., 432-437.

Gray, W.M., 1968: Global view of the origin of tropical disturbances and storms. *Mon. Wea. Rev.*, **96**, pp 669-700.

Guard, C.P., 1983: A Study of western North Pacific tropical storms and typhoons that intensify after recurvature. First Weather Wing Technical Note-83/002, 28 pp.

Harr, P.A., and R.L. Elsberry, 1991: Tropical cyclone track characteristics as a function of large-scale circulation anomalies. *Mon. Wea. Rev.*, **119**, pp 1448-1468.

Harr, P.A., and R.L. Elsberry, 1995: Large-scale circulation variability over the tropical western North Pacific. Part I: Spatial patterns and tropical cyclone characteristics. *Mon. Wea. Rev.* **123**, pp 1225-1246.

Hawkins, H.F., and D.T. Rubsam, 1967: Hurricane Inez -- a classic "micro-hurricane". *Mariners Weather Log*, **11**, pp 157-160.

Hebert, P.J., 1973: Subtropical cyclones. *Mariners Weather Log*, **4**, pp 203-207.

Herbert, P. H. and K. O. Poteat, 1975: A satellite classification technique for subtropical cyclones. NOAA Technical Memorandum NWS SR-83, 25 pp.

Holland, G. J., 1980: An analytical model of wind and pressure profiles in hurricanes, **108**, No. 8, pp 1212-1218.

Holland, G.J., 1987: [Tropical cyclone] mature structure and structure change. A Global View of Tropical Cyclones. R.L. Elsberry, Ed. [Limited edition publication sponsored by the U.S. Navy, Office of Naval Research].

Holliday, C. R. and A. H. Thompson, 1979: Climatological characteristics of rapidly intensifying typhoons. *Mon. Wea. Rev.*, **107**, No 8, pp 1022-1034.

JMA, 1976: The north-oriented track type. Forecasting Manual for Typhoons, [English version], Available in English or Japanese from the Japan Meteorological Agency, 1-3-4 Ote-machi, Chiyoda-ku, Tokyo, Japan, pp 194-197.

JTWC, 1993: Illustration of the cloud distribution in a monsoon depression. 1993 Annual Tropical Cyclone Report, JTWC, p 130.. [NTIS AD A285097].

Keen, R.A. 1982: The role of cross-equatorial tropical cyclone pairs in the Southern Oscillation. **110**, pp 1405-1416.

Kepert, J.D., 1993: Research rapporteur report on oceanography and air-sea interaction. Annex to Topic Rapporteur Reports of the Third WMO/ICSU International Workshop on Tropical Cyclones (JTWC-III), Huatulco, Santa Cruz, Mexico, 22 November -1 December 1993. WMO/TD No. 573. Secretariat of the WMO, Geneva, Switzerland.

Krayer, W.R., and R.D. Marshall, 1992: Gust factors applied to hurricane winds. *Bull. Amer. Meteor.* Soc., **73**, pp 613-617.

Kurihara, Y., 1992: Surface conditions in tropical cyclone models. In Modeling Severe Weather: Papers presented at the Fourth BMRC Modeling Workshop.Bureau of Meteorology Research Centre, Melbourne, Australia.

Lander, M. A., 1990: Evolution of the cloud pattern during the formation of tropical cyclone twins symmetrical with respect to the equator. *Mon. Wea. Rev.*, **118**, No. 5, pp 1194-1202.

Lander, M.A., and G.J. Holland, 1993: On the interaction of tropical-cyclone scale vortices. I: Observations. *Quart. J. Roy. Meteor. Soc.*, **119**, pp 1347 - 1361.

Lander, M.A., 1994a: Description of a monsoon gyre and its effects on the tropical cyclones in the western North Pacific during August 1991. *Weather and Forecasting*, **9**, pp 640-654.

Lander, M.A., 1994b: An exploration of the relationships between tropical storm formation in the Western North Pacific and ENSO, *Mon. Wea. Rev.*, **122**, No. 4, pp 636-651.

Lander, M.A., 1995a: Specific tropical cyclone track types and unusual tropical cyclone motions associated with a reverse-oriented monsoon trough in the western North Pacific. *Weather and Forecasting*, **11**, No. 2. pp 170-186.

Lander, M.A., 1995b: The merger of two tropical cyclones. (Submitted to *Mon. Wea. Rev.*)

Lander, M.A., 1996: Specific tropical cyclone track types and unusual tropical cyclone motions associated with a reverse-oriented monsoon trough in the western North Pacific. *Weather and Forecasting*, **11**, No. 2, pp 170-186.

Liu, W.T., K.B. Katsaros, and J.A. Businger, 1979: Bulk parameterizations of air-sea exchanges of heat and water vapor including the molecular constraints at the interface. *J. Atmos. Sci.*, **36**, pp 1722-1735.

Luther, D.S., D.E. Harrison and R.A. Knox, 1983: Zonal winds in the Central Equatorial Pacific and El Niño.*Science*, **222**, pp 327-330.

Matsumoto, C. R., 1984: A statistical method for one- to three-day tropical cyclone track prediction. Colorado State University Department of Atmospheric Science, Paper 379, 201 pp.

Mckinley, E.J., and R.L. Elsberry, 1993: Observations during TCM 92 of the role of tropical mesoscale convective systems in tropical cyclogenesis. Preprints, 20th Conference on Hurricanes and Tropical Meteorology. American Meteorological Society, Boston, MA. 623 pp. plus 64 joint pages.

Merrill, R.T., 1982: The comparison of large and small tropical cyclones. Colorado State University Department of Atmospheric Science, Paper 352, 75 pp.

Mundell, D.B., 1990: Prediction of tropical cyclone rapid intensification events. Thesis for fulfillment of Master's degree submitted to Colorado State University, 186 pp.

OFCM, 1993: National Hurricane Operations Plan, U.S. Dept. of Commerce, Washington, D.C., p E-1.

Price, J.F., 1981: Upper ocean response to a hurricane. J. Phys. Oceanogr., **11**, 153-175.

Ramage, C.S., 1986: El Nino. *Scientific American*, May Issue, pp 77-84.

Ramage, C.S., 1971: Monsoon Meteorology. Academic Press, 296 pp.

Rupp, J.A., and M.A. Lander, 1996: A technique for estimating recurrence intervals of tropical cyclone-related high winds in the the tropics: results for Guam. *J. Appl. Meteorol.*, **35**, pp 627-637.

Sadler, J.C., 1975: The upper circulation over the global tropics. UHMET Pub. 75-05. Dept. of Meteor., Univ. of Hawaii, Honolulu, HI 96822.

Sadler, J.C., 1967: The tropical upper tropospheric trough as a secondary source of typhoons and a primary source of trade wind disturbances. Final Report, contract No. AF 19(628)-3860, HIG Report 67-12, Hawaii Institute of Geophysics, University of Hawaii, Honolulu, HI, 44 pp.

Sadler, J.C., 1976: A role of the tropical upper tropospheric trough in early season typhoon development. *Mon. Wea. Rev.*, **104**, pp 1266-1278.

Sadler, J.C., M.A. Lander, A.M. Hori, and L.K. Oda, 1987: Tropical marine climatic Atlas, Vol II, Pacific Ocean. UHMET 87-02, University of Hawaii, Department of Meteorology, 14 pp.

Sadler, J.C., 1979: Tropical cyclone initiation of the tropical upper-tropospheric trough. Naval Environmental Prediction Research Facility Paper No. 2-76, 103 pp.

Sandgathe, S. A., 1987: Opportunities for tropical cyclone motion research in the Northwest Pacific region. Technical Report NPS 63-87-006, Naval Postgraduate School, Monterey, CA 93943, 36 pp.

Shoemaker, D.N., 1991: Characteristics of tropical cyclones affecting the Philippine Islands. NOCC/JTWC Technical Note 91-01, 35 pp.

Simpson, R.H., 1974: The hurricane disaster potential scale. *Weatherwise*, **27**, pp 169-186.

Spratt, S.M., 1990: Tropical cyclone cloud patterns: climatology and relationships to intensity changes. Master's Thesis. Department of Meteorology, University of Hawaii, 2525 Correa Rd., Honolulu, HI 96822.

Weatherford, C.L. and W.M. Gray, 1985: Typhoon Structural Variability. Colorado State University Department of Atmospheric Science, Paper No. 391, 77 pp.

Weir, R. C., 1982: Predicting the acceleration of northward-moving tropical cyclones using upper-tropospheric winds. NOCC/JTWC Technical Note 82-2, 40 pp.

Willoughby, H.E., J.A. Clos, and M.G., 1982: Concentric eye walls, secondary wind maxima, and the evolution of the hurricane vortex. *J. Atmos. Sci.*, **39**, pp 395-411.

Willoughby, H.E., 1990: Temporal changes in the primary circulation in tropical cyclones. *J. Atmos. Sci.*, **47**, pp 242-264.

Wirfel, W. P. and S. A. Sandgathe, 1986: Forecast verification and reconnaissance data for Southern Hemisphere tropical cyclones (July 1982 through June 1984). NOCC/JTWC Technical Note 86-1, 102 pp.

Xu, Y. and C. J. Neumann, 1985: A statistical model for the prediction of western North Pacific tropical cyclone motion. NOAA Technical Memorandum NWS NHC 28, 30 pp.

Zehr, R.M., 1992: Tropical cyclogenesis in the western North Pacific. NOAA Technical Report, NESDIS 61, U.S. Dept. of Commerce, Washington DC, 181 pp.

APPENDIX A
DEFINITIONS

BEST TRACK - A subjectively smoothed path, versus a precise and very erratic fix-to-fix path, used to represent tropical cyclone movement, and based on an assessment of all available data.

BINARY INTERACTION - Binary interaction is a mutual cyclonic orbit of two tropical cyclones around their centroid. Lander and Holland (1993) showed that the behavior of most binary tropical cyclones consists of an approach, sudden capture, then a period of steady cyclonic orbit followed by a sudden escape or (less frequently) a merger (see Figure A-1).

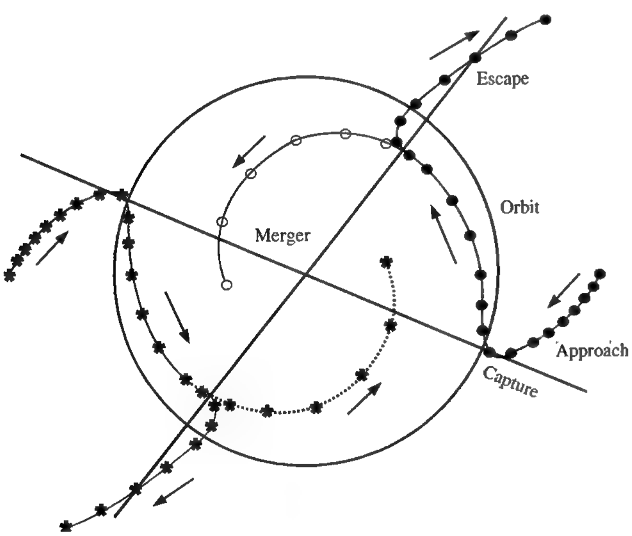

Figure A-1 Model of binary interation of two tropical cyclones that contain the major elements of approach and capture, followed by mutual orbit, then escape, or merger.

CENTER - The vertical axis or core of a tropical cyclone. Usually determined by cloud vorticity patterns, wind and/or pressure distribution.

EPHEMERIS - Position of a body (satellite) in space as a function of time; used for gridding satellite imagery. Since ephemeris gridding is based solely on the predicted position of the satellite, it is susceptible to errors from vehicle wobble, orbital eccentricity, the oblateness of the Earth, and variation in vehicle speed.

EXPLOSIVE DEEPENING - A decrease in the minimum sea-level pressure of a tropical cyclone of 2.5 mb/hr for at least 12 hours or 5 mb/hr for at least six hours (Dunnavan, 1981).

EXTRATROPICAL - A term used in warnings and tropical summaries to indicate that a cyclone has lost its "tropical" characteristics. The term implies both poleward displacement from the tropics and the conversion of the cyclone's primary energy source from the release of latent heat of condensation to baroclinic processes. It is important to note that cyclones can become extratropical and still maintain winds of typhoon or storm force.

EYE - The central area of a tropical cyclone when it is more than half surrounded by wall cloud.

INTENSITY - The maximum sustained 1-minute mean surface wind speed, typically within one degree of the center of a tropical cyclone.

MAXIMUM SUSTAINED WIND - The highest surface wind speed averaged over a 1-minute period of time. (Peak gusts over water average 20 to 25 percent higher than sustained winds).

MEI-YU FRONT - The Term "mei-yu" is the Chinese expression for "plum rains". The mei-yu front is a persistant east-west zone of disturbed weather during spring which is quasi - stationary and stretches from the east China coast, across Taiwan, and eastward into the Pacific south of Japan.

MONSOON DEPRESSION - A tropical cyclonic vortex characterized by: 1) its large size, the outer-most closed isobar may have a diameter on the order of 600 nm (1000 km); 2) a loosely organized cluster of deep convective elements; 3) a low-level wind distribution which features a 100-nm (200-km) diameter light-wind core which may be partially surrounded by a band of gales; and, 4) a lack of a distinct cloud system center. Note: most monsoon depressions which form in the western North Pacific eventually acquire persistent central convection and accelerated core winds marking its transition into a conventional tropical cyclone.

MONSOON GYRE - A mode of the summer monsoon circulation of the western North Pacific characterized by: 1) a very large nearly circular low-level cyclonic vortex that has an outer-most closed isobar with diameter on the order of 1200 nm (2500 km); 2) a cloud band rimming the southern through eastern periphery of the vortex/surface low; 3) a relatively long (two week) life span - initially, a subsident regime exists in its core and western and northwestern quadrants with light winds and scattered low cumulus clouds; later, the area within the outer closed isobar may fill with deep convective cloud and become a monsoon depression or tropical cyclone; and, 4) the large vortex cannot be the result of the expanding wind field of a preexisting monsoon depression or tropical cyclone. Note: a series of small or very small tropical cyclones may emerge from the "head" or leading edge of the peripheral cloud band of a monsoon gyre (JTWC, 1993; Lander,1994a).

RAPID DEEPENING - A decrease in the minimum sea-level pressure of a tropical cyclone of 1.75 mb/hr or 42 mb for 24-hours (Holliday and Thompson, 1979).

RECURVATURE - The turning of a tropical cyclone from an initial path toward the west and poleward to east and poleward, after moving poleward of the mid-tropospheric subtropical ridge axis.

REVERSE-ORIENTED MONSOON TROUGH - The distinguishing characteristics of a reverse-oriented monsoon trough are a SW-NE (i.e., reverse) orientation of the trough axis with respect to the normal NW-SE orientation of the trough axis, and the penetration of the trough axis into subtropical areas normally the province of easterly flow.

SIGNIFICANT TROPICAL CYCLONE - A tropical cyclone becomes "significant" with the issuance of the first numbered warning by the responsible warning agency.

SIZE - The areal extent of a tropical cyclone, usually measured radially outward from the center to the outer-most closed isobar. Based on an average radius of the outer-most closed isobar, size categories in degrees of latitude follow: $< 2°$ = very small, 2° to 3° = small, 3° to 6° = medium (average), 6° to 8° = large, and 8° or greater = very large (Brand, 1972 and a modification of Merrill, 1982).

STRENGTH - The average wind speed of the surrounding low-level wind flow, usually measured within one to three degrees of the center of a tropical cyclone (Weatherford and Gray, 1985).

SUBTROPICAL CYCLONE - A low pressure system that forms over the ocean in the subtropics and has some characteristics of a tropical circulation, but not a central dense overcast. Although of upper cold low or low-level baroclinic origins, the system can transition to a tropical cyclone.

SUPER TYPHOON - A typhoon with maximum sustained 1-minute mean surface winds of 130 kt (67 m/sec) or greater.

TROPICAL CYCLONE - A non-frontal, migratory low-pressure system, usually of synoptic scale, originating over tropical or subtropical waters and having a definite organized circulation.

TROPICAL DEPRESSION - A tropical cyclone with maximum sustained 1-minute mean surface winds of 33 kt (17 m/sec) or less.

TROPICAL DISTURBANCE - A discrete system of apparently organized convection, generally 100 to 300 nm (185 to 555 km) in diameter, originating in the tropics or subtropics, having a non-frontal, migratory character and having maintained its identity for 12- to 24-hours. The system may or may not be associated with a detectable perturbation of the low-level wind or pressure field. It is the basic generic designation which, in successive stages of development, may be classified as a tropical depression, tropical storm, typhoon or super typhoon.

TROPICAL STORM - A tropical cyclone with maximum 1-minute mean sustained surface winds in the range of 34 to 63 kt (18 to 32 m/sec), inclusive.

TROPICAL UPPER-TROPOSPHERIC TROUGH (TUTT) - A dominant climatological system and a daily upper-level synoptic feature of the summer season, over the tropical North Atlantic, North Pacific and South Pacific Oceans (Sadler, 1979). Cold core lows in the TUTT are referred to as cells, or TUTT cells.

TYPHOON (HURRICANE) - A tropical cyclone with maximum sustained 1-minute mean surface winds of 64 to 129 kt (33 to 66 m/sec). West of 180° E longitude they are called typhoons and east of 180° E longitude hurricanes.

WALL CLOUD - An organized band of deep cumuliform clouds that immediately surrounds the central area of a tropical cyclone. The wall cloud may entirely enclose or partially surround the center.

WESTERLY WIND BURST - A short-duration low-level westerly wind event along and near the equator in the western Pacific Ocean (and sometimes in the Indian Ocean) (Luther et al. 1983). Typically, a westerly wind burst (WWB) lasts several days and has westerly winds of at least 10 kt (5 m/sec) (Keen 1988). Most WWBs occur during the monsoon transition months of April-May, and November-December. They show some relationship to the ENSO phenomenon (Luther et al. 1983; Ramage 1986). Some WWBs are even more energetic, with wind speeds of 30 kt (15 m/sec) observed during well-developed systems. These intense WWBs are associated with a large cluster of deep-convective cloud along the equator. An intense WWB is a necessary precursor to the formation of tropical cyclone twins symmetrical with respect to the equator (Keen 1982; Lander 1990).

APPENDIX B

NAMES FOR TROPICAL CYCLONES IN THE WESTERN NORTH PACIFIC OCEAN AND SOUTH CHINA SEA

Column 1		Column 2		Column 3		Column 4	
ANN	*AN*	**ABEL**	*A-bel*	**AMBER**	*AM-ber*	**ALEX**	*AL-x*
BART	*BART*	**BETH**	*BETH*	**BING**	*BING*	**BABS**	*BABS*
CAM	*KAM*	**CARLO**	*KAR-lo*	**CASS**	*KASS*	**CHIP**	*CHIP*
DAN	*DAN*	**DALE**	*DAY-l*	**DAVID**	*DAY-vid*	**DAWN**	*DAWN*
EVE	*EEV*	**ERNIE**	*ER-nee*	**ELLA**	*EL-la*	**ELVIS**	*EL-vis*
FRANKIE	*FRANK-ee*	**FERN**	*FERN*	**FRITZ**	*FRITZ*	**FAITH**	*FAITH*
GLORIA	*GLOR-ee-uh*	**GREG**	*GREG*	**GINGER**	*JIN-jer*	**GIL**	*GIL*
HERB	*HERB*	**HANNAH**	*HAN-nah*	**HANK**	*HANGK*	**HILDA**	*HIL-dah*
IAN	*EE-an*	**ISA**	*EE-sah*	**IVAN**	*I-van*	**IRIS**	*I-ris*
JOY	*JOY*	**JIMMY**	*JIM-ee*	**JOAN**	*JONE*	**JACOB**	*JAY-kob*
KIRK	*KIRK*	**KELLY**	*KEL-lee*	**KEITH**	*KEETH*	**KATE**	*KATE*
LISA	*LEE-sah*	**LEVI**	*LEEV-eye*	**LINDA**	*LIN-dah*	**LEO**	*LEE-o*
MARTY	*MAR-tee*	**MARIE**	*mah-REE*	**MORT**	*MORT*	**MAGGIE**	*MAG-gee*
NIKI	*NI-kee*	**NESTOR**	*NES-tor*	**NICHOLE**	*nik-KOL*	**NEIL**	*NEEL*
ORSON	*OR-son*	**OPAL**	*O-pel*	**OTTO**	*OT-tow*	**OLGA**	*OL-gah*
PIPER	*PI-per*	**PETER**	*PEE-ter*	**PENNY**	*PEN-nee*	**PAUL**	*PAUL*
RICK	*RICK*	**ROSIE**	*RO-zee*	**REX**	*REX*	**RACHEL**	*RAY-chel*
SALLY	*SAL-lee*	**SCOTT**	*SKOT*	**STELLA**	*STEL-lah*	**SAM**	*SAM*
TOM	*TOM*	**TINA**	*TEE-nah*	**TODD**	*TOD*	**TANYA**	*TAHN-yah*
VIOLET	*VI-uh-let*	**VICTOR**	*vik-TOR*	**VICKI**	*VIK-kee*	**VIRGIL**	*VER-jil*
WILLIE	*WIL-lee*	**WINNIE**	*WIN-nee*	**WALDO**	*WAL-do*	**WENDY**	*WEN-dee*
YATES	*YATES*	**YULE**	YOU-le	**YANNI**	*YAN-ni*	**YORK**	*YORK*
ZANE	*ZANE*	**ZITA**	*ZEE-tah*	**ZEB**	*ZEB*	**ZIA**	*ZEE-uh*

NOTE 1: Assign names in rotation, alphabetically, starting with (ANN) for first tropical cyclone of 1996. When the last name in Column 4 (ZIA) has been used, the sequence will begin again with the first name in Column 1 (ANN).

NOTE 2: Pronunciation guide for names is italicized.

SOURCE: CINCPACINST 3140.1W

APPENDIX C
CONTRACTIONS

AB	Air Base
ABW	Air Base Wing
ABIO	Significant Tropical Weather Advisory for the Indian Ocean
ABPW	Significant Tropical Weather Advisory for the Western Pacific Ocean
ACCS	Air Control Center Squadron
ACFT	Aircraft
ADP	Automated Data Processing
AFB	Air Force Base
AFDIS	Air Force Dial-In System
AFGWC	Air Force Global Weather Central
AIREP	Aircraft (Weather) Report
AJTWC	Alternate Joint Typhoon Warning Center
AMOS	Automatic Meteorological Observing Station
AOR	Area of Responsibility
ARC	Automated Remote Collection (system)
ARGOS	(International Service for Drifting Buoys)
ARQ	Automatic Response to Query
ATCF	Automated Tropical Cyclone Forecast (system)
ATCR	Annual Tropical Cyclone Report
AUTODIN	Automated Digital Network
AWDS	Automated Weather Distribution System
AWN	Automated Weather Network
BLND	Blended (Hybrid Aid)
CDO	Central Dense Overcast
CI	Current Intensity
CIMSS	Cooperative Institue for Meterological Satellite Studies
CIV	Civilian
CLD	Cloud
CLIM	Climatology
CLIP or **CLIPER**	Climatology and Persistence Technique
CM	Centimeter(s)
C-MAN	Coastal-Marine Automated Network
CMOD	Compact Meteorological and Oceanographic Drifter
COMNAVMETOCCOM or CNMOC	Commander Naval Meteorology and Oceanography Comm-and
CPA	Closest Point of Approach
CPHC	Central Pacific Hurricane Center
CSC	Cloud System Center
CSUM	Colorado State University Model
DAVE	Name of a Hybrid Aid
DD	Digital Dvorak
DDN	Defense Data Network
DEG	Degree(s)
DFS	Digital Facsimile System
DISN	Defense Information Systems Network
DMS	Defense Messaging System
DMSP	Defense Meteorological Satellite Program
DOD	Department of Defense
DSN	Defense Switched Network
DTG	Date Time Group
EGRR	Bracknell Model
ENSO	El Niño-Southern Oscillation
ERS	European Space Agency (ESA) Remote Sensing Satellite
FBAM	FNOC Beta and Advection Model
FI	Forecast Intensity (Dvorak)

FLENUMETOCCEN	Fleet Numerical Meteorology and Oceanography Center
FT	Foot/Feet
FTP	File Transfer Protocol
GCA	Great Circle Arc
GMS	Geostationary Meteorological Satellite
GMT	Greenwich Mean Time
GOES	Geostationary Operational Environmental Satellite
GSRS	Geostationary Satellite Receiving System
GTS	Global Telecommun-ications System
hPa	Hectopascal
HPAC	Mean of XTRP and CLIM Techniques (Half Persistence and Climatology)
HF	High Frequency
HR	Hour(s)
HRPT	High Resolution Picture Transmission
ICAO	International Civil Aviation Organization
INIT	Initial
INST	Instruction
IP	Internet Protocol
IR	Infrared
JTWC	Joint Typhoon Warning Center
JTWC92 or JT92	Statistical-Dynamical Objective Technique
JTYM	Japanese Typhoon Model
KM	Kilometer(s)
KT	Knot(s)
LAN	Local Area Network
LAT	Latitude
LLCC	Low-Level Circulation Center
LONG	Longitude
LUT	Local User Terminal
LVL	Level
M	Meter(s)
MAX	Maximum
MB	Millibar(s)
MBAM	Medium Beta and Advection Model
MCAS	Marine Corps Air Station
MCS	Mesoscale Convective System
MET	Meteorological
MIDDAS	Meteorological Imagery, Data Display, and Analysis System
MIN	Minimum
MINI-MET	Mini-Meteorological
MISTIC	Mission Sensor Tactical Imaging Computer
MM	Millimeter(s)
MOVG	Moving
MSLP	Minimum Sea-level Pressure
NARDAC	Naval Regional Data Automation Center
NAS	Naval Air Station
NASA	National Aeronautics and Space Administration
NAVPACMETOCCEN	Naval Pacific Meteorology and Oceanography Center (Hawaii)
NAVPACMETOCCEN WEST	Naval Pacific Meteorology and Oceanography Center (Guam)
NCEP	National Centers for Environmental Prediction
NEDN	Naval Environmental Data Network
NESDIS	National Environmental Satellite, Data, and information Service
NESN	Naval Environmental Satellite Network
NEXRAD	Next Generation (Doppler Weather) Radar
NHC	National Hurricane Center
NIPRNET	Non-secure Internet Protocol Router Network
NM	Nautical Mile(s)
NMC	National Meteorological Center

NOAA	National Oceanic and Atmospheric Administration
NODDES	Naval Environmental Data Network Oceanographic Data Distribution and Expansion System
NOGAPS or NGPS	Navy Operational Global Atmospheric Prediction System
NODDS	Naval Oceanography Data Distribution Systems
NPS	Naval Postgraduate School
NR	Number
NRL	Naval Research Laboratory
NRL-MRY	Naval Research Laboratory at Monterey, CA
NRPS or NORAPS	Navy Operational Regional Atmospheric Prediction System
NSCAT	NASA Scatterometer
NSDS-G	Naval Satellite Display System - Geostationary
NTWP	Naval Telecommunications Area Master Station, Western Pacific
SIPRNET	Secret Internet Protocol Router Network
NWP	Northwest Pacific
NWS	National Weather Service
OBS	Observations
OLS	Operational Linescan System
ONR	Office of Naval Research
OSS	Operations Support Squadron
OSB	Ocean Sciences Branch
OTCM	One-Way (Interactive) Tropical Cyclone Model
PACAF	Pacific Air Force
PACMEDS	PacificMeteorological Data System
PACOM	Pacific Command
PAGASA	Philippine Atmospheric, Geophysical Astronomical Services Administation
PC	Personal Computer
PCN	Position Code Number
PDN	Public Data Network
PIREP	Pilot Weather Report(s)
RADOB	Radar Observation
RECON	Reconnaissance
RECR	Recurve (Forecast Aid)
RMSE	Root mean Square Error
ROCI	Radius of outer-most closed isobar
SAT	Satellite
SEC	Second(s)
SDHS	Satellite Data Handling System
SFC	Surface
SGDB	Satellite Global Data Base
SIPRNET	Secret Internet Protocol Router Network
SLP	Sea-Level Pressure
SPAWRSYSCOM	Space and Naval Warfare Systems Command
SSM/I	Special Sensor Microwave/Imager
SST	Sea Surface Temperature
ST	Subtropical
STNRY	Stationary
STR	Subtropical Ridge
STRT	Straight (Forecast Aid)
STY	Super Typhoon
TAPT	Typhoon Acceleration Prediction Technique
TC	Tropical Cyclone
TCFA	Tropical Cyclone Formation Alert
TD	Tropical Depression
TDA	Typhoon Duty Assistant
TDO	Typhoon Duty Officer
TELEFAX	Telephone Facsimile
TESS	Tactical Environmental Support System
TIFF	Tagged Image File Format
TIROS-N	Television Infrared Observational Satellite-Next Generation
TOGA	Tropical Ocean Global Atmosphere
TOVS	TIROS Operational Vertical Sounder

TS	Tropical Storm
TUTT	Tropical Upper-Tropospheric Trough
TY	Typhoon
TYAN	Typhoon Analog (Forecast Aid)
ULCC	Upper-Level Circulation Center
US	United States
USAF	United States Air Force
USCINCPAC	Commander-in-Chief Pacific (AF - Air Force, FLT - Fleet)
USN	United States Navy
VIS	Visual
WAN	Wide Area Network
WESTPAC	Western (North) Pacific
WGTD	Weighted (Hybrid Aid)
WMO	World Meteorological Organization
WNP	Western North Pacific
WRN or WRNG	Warning(s)
WSD	Wind Speed and Direction
WSR-88D	Weather surveillance Radar - 1988 Doppler
WVTW	Water Vapor Tracked Winds
WWW	World Wide Web
XTRP	Extrapolation
Z	Zulu time (Greenwich Mean Time/Universal Coordinated Time)

APPENDIX D

PAST ANNUAL TROPICAL CYCLONE REPORTS

Copies of the past Annual Tropical Cyclone Reports for DOD agencies or contractors can be obtained through:

Defense Technical Information Center
ATTN:FDAC
Cameron Station
Alexandria, VA 22304-6145

Phone: (703)-767-8274
Fax: (703)-767-9070

Copies for non-DOD agencies or users can be obtained from:

National Technical Information Service
5285 Port Royal Road
Springfield, VA 22161

Phone: (703)-487-4650
Fax: (703)-321-8547

Refer to the following numbers when ordering:

Year	Acquisition Number	Year	Acquisition Number	Year	Acquisition Number
1959	AD 786147	1971	AD 768333	1983	AD A137836
1960	AD 786148	1972	AD 768334	1984	AD A153395
1961	AD 786149	1973	AD 777093	1985	AD A168284
1962	AD 786128	1974	AD 010271	1986	AD A184082
1963	AD 786208	1975	AD A023601	1987	AD A191883
1964	AD 786209	1976	AD A038484	1988	AD A207206
1965	AD 786210	1977	AD A055512	1989	AD A232469
1966	AD 785891	1978	AD A070904	1990	AD A239910
1967	AD 785344	1979	AD A082071	1991	AD A251952
1968	AD 785251	1980	AD A094668	1992	AD A274464
1969	AD 785178	1981	AD A112002	1993	AD A285097
1970	AD 785252	1982	AD A124860	1994	AD A301618

APPENDIX E
DISTRIBUTION LIST

1 COPY

ACCU-WEATHER, INC.
AMERICAN EMBASSY, NEW DEHLI
ANALYSIS & PROCESSING CENTER, INDONESIA
ARNOLD ASSOCIATES
ASIAN DISASTER PREPAREDNESS CENTER, BANGKOK, THAILAND
ATMOSPHERIC DIV LIBRARY, NEW ZEALAND
BARRETT CONSULTING GROUP
BRUNEI SHELL PETROLEUM CO
CATHOLIC UNIVERSITY OF AMERICA
CAF WEATHER CENTRAL, TAIWAN
CENTRAL MET OBSERVATORY, BEIJING
CENTRAL METEOROLOGICAL OFFICE, SEOUL
CHULALONGKORN UNIVERSITY, BANGKOK
CHUNG CHENG INSTITUTE, TAIWAN
CITY POLYTECHNIC OF HONG KONG
CIUDAD UNIVERSITARIA, MEXICO
CIVIL DEFENSE, CHUUK
CIVIL DEFENSE, MAJURO
CIVIL DEFENSE, PALAU
CIVIL DEFENSE, POHNPEI
CIVIL DEFENSE, SAIPAN
CIVIL DEFENSE, YAP
CINCPACFLT
CNN, ATLANTA, GA
CNO, WASHINGTON, D.C.
COMNAVMETOCCOM
COLORADO STATE UNIVERSITY LIBRARY
COMMONWEALTH NORTHERN MARIANA ISLANDS
COMNAVMAR
COMNAVSURFPAC, SAN DIEGO
COMPHIBGRU ONE
COMSCWESTPAC GU
COMSEVENTHFLT
COMSPAWARSYSCOM
COMSUBGRU SEVEN
COMTHIRDFLT
COMUSNAVCENT
CONGRESSIONAL INFORMATION SERVICE, MD
DCA GUAM
DET 2, 5WS CAMP HUMPHREYS, KOREA
DET 3, 5WS CAMP CASEY, KOREA
DISASTER CONTROL OFFICE, SAIPAN
ECONOMIC COUNCIL SAIPAN
EDMUNDS COLLEGE SOCIAL SCIENCE DEPT
ENVIRONMENTAL QUALITY PROTECTION BOARD, PALAU
FEDERAL EMERGENCY MANAGEMENT AGENCY, GUAM
FIJI METEOROLOGICAL SERVICE
GEOLOGICAL FLUID DYNAMICS LAB, PRINCETON, NJ
GEOLOGICAL SURVEY, GUAM
GEOPHYSICS LAB/LYS
GIFU METEOROLOGICAL OFFICE, JAPAN
GODDARD SPACE FLIGHT CENTER
GUAM COMMUNITY COLLEGE
GUAM POWER AUTHORITY
GUAM PUBLIC LIBRARY
HORIZON MARINE, INC
HQ AIR COMBAT COMMAND/OSW
HQ AMC TACC/WXC
HQ AWS
HQ US STRATCOM/J3615
HQ USAF/XOWO
INDIA METEOROLOGICAL DEPT.
INDIAN INSTITUTE OF TROPICAL MET
INSTITUO DE GEOFISICA, MEXICO
INTERNATIONAL CENTER FOR DISASTER MITIGATION, TOKYO
JAPAN AIR LINES
JCS ENV SERVICES DIV, PENTAGON
JET PROPULSION LAB, PASADENA
KOREAN METEOROLOGICAL ADMIN FORECAST BUREAU
LEND FOUNDATION
LISD CAMP SPRINGS CENTER, MD
LOS ANGELES PUBLIC LIBRARY
MARATHON OIL CO, TX
MAURITIUS METEOROLOGICAL SERVICE
MASS INST OF TECH
MCAS FUTENMA
MCAS IWAKUNI
MCAS KANEOHE BAY, HI
MERCANTILE AND GENERAL REINSURANCE, AUSTRALIA
METEOROLOGICAL DEPARTMENT, PAKISTAN
METEOROLOGICAL OFFICE, BRACKNELL
METEOROLOGICAL SERVICE, MADAGASCAR
METEOROLOGICAL SERVICE, MAURITIUS
METEOROLOGICAL SERVICE, NEW ZEALAND
METEOROLOGICAL SERVICE, REUNION
MIL ASST ENV SCI (R & AT / E &LS)
MOBIL OIL GUAM, INC
NASA
NATIONAL CLIMATIC DATA CENTER LIBRARY, ASHEVILLE,NC
NATIONAL METEOROLOGICAL CENTER
NATIONAL METEOROLOGICAL LIBRARY, BRACKNELL, UK

NATIONAL TAIWAN UNIVERSITY
NATIONAL TECHNICAL INFORMATION SERVICE
NATIONAL WEATHER SERVICE, CHUUK
NATIONAL WEATHER SERVICE, MAJURO
NATIONAL WEATHER SERVICE, PALAU
NATIONAL WEATHER SERVICE, PAPUA NEW GUINEA
NATIONAL WEATHER SERVICE, POHNPEI
NATIONAL WEATHER SERVICE, SAIPAN
NATIONAL WEATHER SERVICE, YAP
NAVAL CIVIL ENG LAB PORT HUENENE, CA
NAVAL POSTGRADUATE SCHOOL LIBRARY
NAVAL RESEARCH LAB
NAVEURMETOCCEN, ROTA
NAVHISTCEN
NAVICECEN, SUITLAND
NAVLANTMETOCCEN, NORFOLK
NAVLANTMETOCDET, ASHEVILLE
NAVLANTMETOCFAC, JACKSONVILLE
NAVOCEANO
NAVPACMETOCDET, ATSUGI
NAVPACMETOCDET, BAHRAIN
NAVPACMETOCDET, KADENA
NAVPACMETOCDET, SASEBO
NAVPACMETOCFAC, SAN DIEGO
NAVPACMETOCFAC, YOKOSUKA
NAVTRAMETOCDET, NEWPORT
NEW ZEALAND INSURANCE
NOAA/ACQUISITION SECTION, ROCKVILLE, MD
NOAA/AOML, HRD, MIAMI, FL
NOAA/HYDROMETEOROLOGY BR, SILVER SPRINGS, MD
NOAA/NESDIS, HONOLULU, HI
NOAA/PMEL, SEATTLE, WA
NOAA ENVIRONMENTAL RESEARCH LAB
NOAA LIBRARY, SEATTLE, WA
NOBEL DENTON
NRL ATMOSPHERIC DIRECTORATE
OCEANROUTES, INC, JOLIMENT, WEST AUSTRALIA
OCEANROUTES, INC, SINGAPORE
OCEANROUTES, INC, SUNNYVALE, CA
OCEANWEATHER, INC
OFFICE OF FEDERAL COORDINATOR MET
OFFICE OF NAVAL RESEARCH
OFFICE OF THE NAVAL DEPUTY, NOAA
ONR
PACIFIC STARS & STRIPES
PACNAVFACENGCOM
PAGASA FORECAST SECTION
PAGASA LIBRARY
PENNSYLVANIA STATE UNIVERSITY
QUEENS COLLEGE, DEPT OF GEOLOGY
REUNION METEOROLOGICAL SERVICE
RUCH WEATHER SERVICE, INC
SAINT LOUIS UNIVERSITY
SAT APPL LAB, NOAA/NESDIS, WASHINGTON, DC
SHANGHAI TYPHOON INSTITUTE
SOUTHSIDE WEATHER SERVICE AUSTRALIA
SRI LANKA METEOROLOGICAL SOCIETY
SRI LIBRARY
TAO PROJECT OFFICE
TEXAS A & M UNIVERSITY
UNIV OF COLORADO, ATMOS SCIENCE
UNIVERSITY OF CHICAGO
UNIVERSITY OF GUAM, BIOLOGY DEPT
UNIVERSITY OF HAWAII LIBRARY
UNIVERSITY OF WASHINGTON
USAFETAC/DN
USCINCPAC
USCINCPAC REP GUAM
USNA (OCEANOGRAPHY DEPT/LIBRARY)
USS AMERICA (CV 66)
USS BLUE RIDGE (LCC 19)
USS CARL VINSON (CVN 70)
USS CONSTELLATION (CV 64)
USS EISENHOWER (CVN 69)
USS INDEPENDENCE (CV 62)
USS J. F. KENNEDY (CV 67)
USS KITTY HAWK (CV 63)
USS NEW ORLEANS (LPH 11)
USS NIMITZ (CVN 68)
USS PELELIU (LHA 5)
USS TARAWA (LHA 1)
USS ESSEX (LHA-2)
USS BELLEAU WOOD (LHA-3)
USS TRIPOLI (LPH 10)
USS T. ROOSEVELT (CVN 71)
USS WASP (LHD 1)
VANUATU METEOROLOGICAL SERVICE
WORLD DATA CENTER B1, MOSCOW
AFGWC/WFM
607WS WS/CC YONGSAN AIN KOREA
5 WS
8 0SS/OSW KUNSAN AB, KOREA
15 OSS/OSW
18 OSS/OSW KADENA AB, JAPAN
35 OSS/OSW
36 ABW
36 OSS/OSW
53 WRS
77 OSS/OSW MCCLELLAN AFB, CA
334 TTS/TTMV KEESLER AFB, MS
374 OSS/DOW YOKOTA AB, JAPAN
375 OG/WXF SCOTT AFB, IL
432 OSS/OSW MISAWA AB, JAPAN
603 ACCENS/WE OSAN AB, KOREA
633 OSS/OSW ANDERSEN AFB, GU

815 WS (AFRES), KEESLER AFB, MS

2 COPIES

AEROMET INC., KWAJALEIN
AFGWC/WFMP
AWS TECH LIBRARY
BUREAU OF METEOROLOGY, BRISBANE
BUREAU OF METEOROLOGY, DARWIN
BUREAU OF METEOROLOGY LIBRARIAN, MELBOURNE
BUREAU OF METEOROLOGY, PERTH
BUREAU OF PLANNING, GUAM
CIVIL DEFENSE, GUAM
DEFENSE TECHNICAL INFORMATION CENTER
DEPARTMENT OF COMMERCE
ECMWF, BERKSHIRE, UK
ESCAP LIBRARY, BANGKOK
FLENUMETOCCEN MONTEREY
FLORIDA STATE UNIVERSITY
HQ AWS GROUP, ATC & WX WING JASDF, TOKYO
INSTITUTE OF PHYSICS, TAIWAN
MARINERS WEATHER LOG
MET RESEARCH INST LIBRARY, TOKYO
MICRONESIAN RESEARCH CENTER UOG, GUAM
NATIONAL CLIMATIC DATA CENTER
NATIONAL DATA BUOY CENTER
NATIONAL HURRICANE CENTER, MIAMI
NATIONAL WEATHER SERVICE, HONOLULU
NAVPACMETOCCEN
NAVPACMETOCDET DIEGO GARCIA
NAVPACMETOCDET MISAWA
NOAA GUAM
NORA 1570 DALLAS, TX
OKINAWA METEOROLOGY OBSERVATORY
SAT APPL LAB, NOAA/NESDIS, CAMP SPRINGS, MD
TYPHOON COMMITTEE SECRATARIAT, MANILA
UNIVERSITY OF PHILIPPINES
US ARMY, FORT SHAFTER
WORLD DATA CENTER A, NOAA
73 WEATHER GROUP, ROK AF

3 COPIES

BUREAU OF METEOROLOGY, DIRECTOR, MELBOURNE, AUSTRALIA
CENTRAL WEATHER BUREAU, TAIWAN
INDIA METEOROLOGICAL DEPT
INOSHAC, DDGM (WF)
JAPAN METEOROLOGICAL AGENCY
KOREAN METEOROLOGY ADMINISTRATION PLANNING BUREAU
NAVPGSCOL DEPT OF METEOROLOGY
NOAA CORAL GABLES LIBRARY
PACAF/DOW
UNIVERSITY OF HAWAII, METEOROLOGY DEPT
WEATHER CENTRAL, CAF
COLORADO STATE UNIVERSITY
METEOROLOGY DEPT, BANGKOK
R & D UNIT, NHC, MIAMI
ROYAL OBSERVATORY HONG KONG
NRL WEST
NATIONAL WEATHER ASSOCIATION

REPORT DOCUMENTATION PAGE

Form Approved
OMB No. 0704-0188

1A. REPORT SECURITY CLASSIFICATION UNCLASSIFIED	1b. RESTRICTIVE MARKINGS
2a. SECURITY CLASSIFICATION AUTHORITY	3. DISTRIBUTION/AVAILABILITY OF REPORT AS IT APPEARS IN THE REPORT/ DISTRIBUTION UNLIMITED
2a. SECURITY CLASSIFICATION AUTHORITY	
4. PERFORMING ORGANIZATION REPORT NUMBER(S)	5. MONITORING ORGANIZATION REPORT NUMBER(S)
6a. NAME OF PERFORMING ORGANIZATION NAVPACMETOCCENWEST/JTWC 6b. OFFICE SYMBOL (If applicable)	7a. NAME OF MONITORING ORGANIZATION NAVPACMETOCCENWEST/JTWC
6c. ADDRESS (City, State and Zip Code) PSC 489, BOX 12 FPO AP 96536-0051	7b. ADDRESS (City, State and Zip Code) PSC 489, BOX 12 FPO AP 96536-0051
8a. NAME OF FUNDING/SPONSORING ORGANIZATION NAVPACMETOCCENWEST/JTWC 8b. OFFICE SYMBOL (If applicable)	9. PROCUREMENT INSTRUMENT IDENIFICATION NUMBER
8c. ADDRESS (City, State and Zip Code) PSC 489, BOX 12 FPO AP 96536-0051	10. SOURCE OF FUNDING NUMBERS PROGRAM ELEMENT N0. / PROJECT NO. / TASK NO. / WORK UNIT ACCESSION NO.

11. TITLE (Include Security Classification)

1995 ANNUAL TROPICAL CYCLONE REPORT

12. PERSONAL AUTHOR(S)

13a. TYPE OF REPORT	13b. TIME COVERED	14. DATE OF REPORT(Year, Month, Day)	15. PAGE COUNT
ANNUAL	FROM JAN 95 TO DEC 95	1995	289 plus i - vi

16. SUPPLEMENTARY NOTATION

17. COSATI CODES

FIELD	GROUP	SUB-GROUP
04	02	

18. SUBJECT TERMS (Continued on reverse if necessary and identify by block number)
TROPICAL CYCLONES; TROPICAL STORMS; TROPICAL DEPRESSIONS; TYPHOONS/SUPER TYPHOONS; TROPICAL CYCLONE RESEARCH; METEOROLOGICAL SATELLITES

19. ABSTRACT (Continued on reverse if necessary and identify by block number)

ANNUAL PUBLICATION SUMMARIZING TROPICAL CYCLONE ACTIVITY IN THE WESTERN NORTH PACIFIC, BAY OF BENGAL, ARABIAN SEA, WESTERN SOUTH PACIFIC AND SOUTH INDIAN OCEANS. A BEST TRACK IS PROVIDED FOR EACH SIGNIFICANT TROPICAL CYCLONE. A BRIEF NARRATIVE IS GIVEN FOR ALL TROPICAL CYCLONES IN THE WESTERN NORTH PACIFIC AND NORTH INDIAN OCEANS. ALL FIX DATA USED TO CONSTRUCT THE BEST TRACKS ARE PROVIDED UPON REQUEST ON DISKETTES. FORECAST VERIFICATION DATA AND STATISTICS FOR THE JOINT TYPHOON WARNING CENTER (JTWC) ARE SUBMITTED.

20. DISTRIBUTION/AVAILABILITY OF ABSTRACT [x] UNCLASSIFIED/UNLIMITED [x] SAME AS RPT. [ ] DTIC USERS	21. ABSTRACT SECURITY CLASSIFICATION UNCLASSIFIED
22a. NAME OF RESPONSIBLE INIVIDUAL FRANK H. WELLS	22b. TELEPHONE (Include Area Code) (671) 349-5286 — 22c. OFFICE SYMBOL JTWC

BLOCK 18 (CONTINUED)

RADAR
AUTOMATIC METEOROLOGICAL OBSERVING STATIONS
SYNOPTIC DATA
TROPICAL CYCLONE INTENSITY
TROPICAL CYCLONE BEST TRACK
TROPICAL CYCLONE FORECASTING
TROPICAL CYCLONE RECONNAISSANCE
TROPICAL CYCLONE STEERING MODELS
OBJECTIVE FORECASTING TECHNIQUES
TROPICAL CYCLONE FIX DATA
MICROWAVE IMAGERY
DRIFTING BUOYS

BACK COVER: From its location on Guam, JTWC monitors an area of responsibility that stretches from 180° east longitude westward across the Western Pacific and Indian Oceans to the eastern coast of Africa.

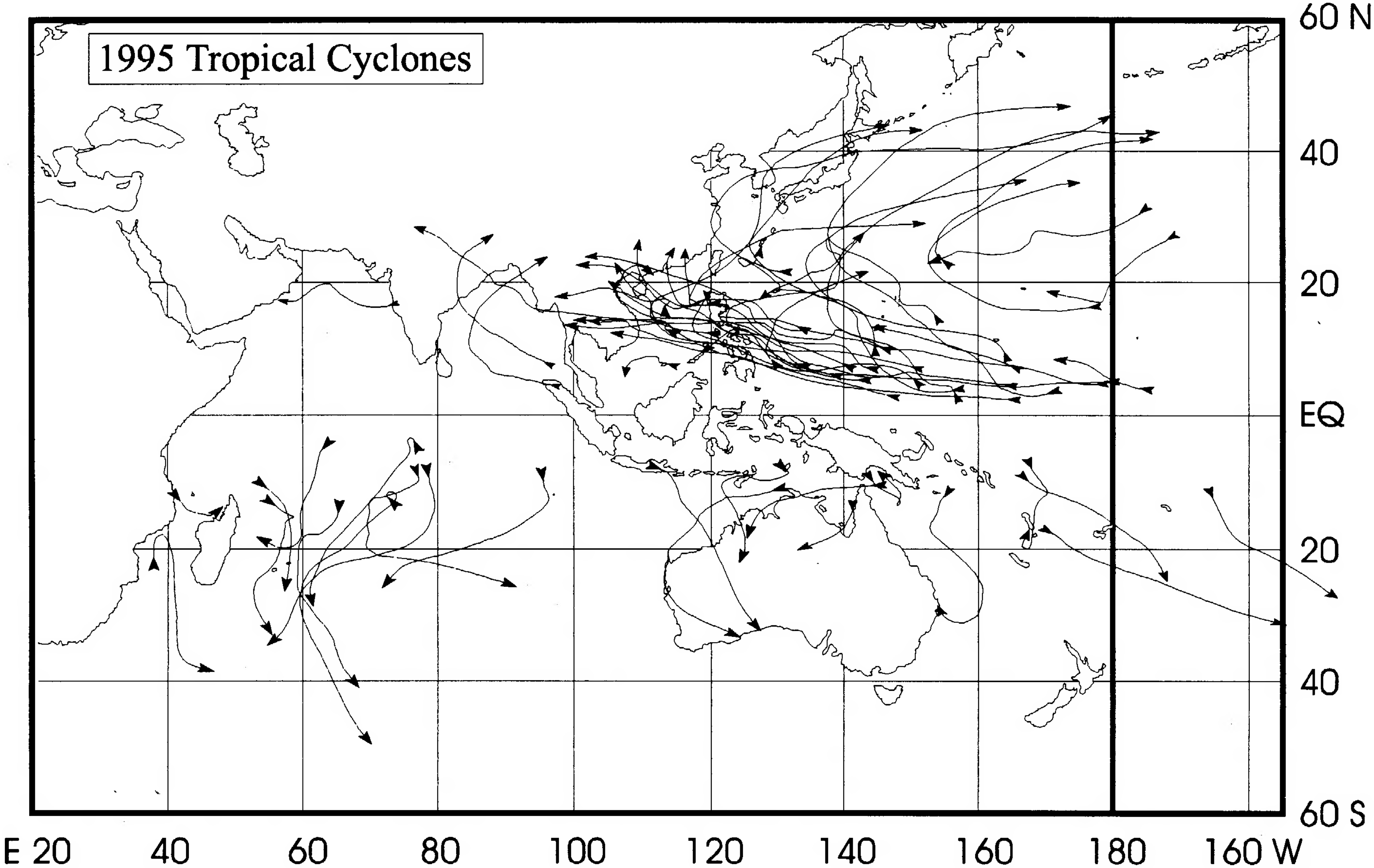
1995 Tropical Cyclones
60 N
40
20
EQ
20
40
60 S
E 20
40
60
80
100
120
140
160
180
160 W